UNIVERSITY OF ALBERTA

A Numerical/Empirical Technique for History Matching and Predicting Cyclic Steam Performance in Canadian Oil Sands Reservoirs

by

Theodore Henry Leshchyshyn ©

A THESIS
SUBMITTED TO THE FACULTY OF GRADUATE STUDIES AND RESEARCH
IN PARTIAL FULFILLMENT OF THE REQUIREMENTS FOR THE DEGREE
OF

Doctor of Philosophy
In
Petroleum Engineering

Department of Civil and Environmental Engineering

Edmonton, Alberta
Fall 1999

National Library
of Canada

Acquisitions and
Bibliographic Services

395 Wellington Street
Ottawa ON K1A 0N4
Canada

Bibliothèque nationale
du Canada

Acquisitions et
services bibliographiques

395, rue Wellington
Ottawa ON K1A 0N4
Canada

Your file Votre référence

Our file Notre référence

The author has granted a non-exclusive licence allowing the National Library of Canada to reproduce, loan, distribute or sell copies of this thesis in microform, paper or electronic formats.

L'auteur a accordé une licence non exclusive permettant à la Bibliothèque nationale du Canada de reproduire, prêter, distribuer ou vendre des copies de cette thèse sous la forme de microfiche/film, de reproduction sur papier ou sur format électronique.

The author retains ownership of the copyright in this thesis. Neither the thesis nor substantial extracts from it may be printed or otherwise reproduced without the author's permission.

L'auteur conserve la propriété du droit d'auteur qui protège cette thèse. Ni la thèse ni des extraits substantiels de celle-ci ne doivent être imprimés ou autrement reproduits sans son autorisation.

0-612-46873-9

Canada

UNIVERSITY OF ALBERTA

LIBRARY RELEASE FORM

Name of Author:	THEODORE H. LESHCHYSHYN
Title of Thesis:	A NUMERICAL/EMPIRICAL TECHNIQUE FOR HISTORY MATCHING AND PREDICTING CYCLIC STEAM PERFORMANCE IN CANADIAN OIL SANDS RESERVOIRS
Degree for which Thesis Was Presented:	DOCTOR OF PHILOSOPHY
Year this Degree Granted:	1999

Permission is hereby granted to THE UNIVERSITY OF ALBERTA LIBRARY to reproduce single copies of this thesis and to lend or sell such copies for private, scholarly or scientific research purposes only.

The author reserves other publication rights, and neither the thesis nor extensive extracts from it may be printed or otherwise reproduced without the author's written permission.

(SIGNED) Ted Leshchyshyn

PERMANENT ADDRESS:

5616 - 134 Ave
Edmonton, Alberta
T5A 0L2

DATED Sept 30/99

Theory don't work in practice.

_ T. Leshchyshyn, presentation of technical
paper for Society of Petroleum Engineers,
Calgary, 1996

Do your homework,
Don't sell your soul.

_ T. Leshchyshyn, in lecture to University of
Alberta Petroleum Engineering students
from1995 onwards

UNIVERSITY OF ALBERTA

FACULTY OF GRADUATE STUDIES AND RESEARCH

The undersigned certify that they have read, and recommend to the Faculty of Graduate Studies and Research, for acceptance, a thesis entitled A Numerical/Empirical Technique for History Matching and Predicting Cyclic Steam Performance in Canadian Oil Sand Reservoirs submitted by Theodore Leshchyshyn in partial fulfillment of the requirements for the degree of Doctor of Philosophy in Petroleum Engineering.

Professor S.M. Farouq Ali (Supervisor)

Professor Q.T. Doan (Co-Supervisor)

Professor R. Chalaturnyk

Professor B. Lepski (Chair of Committee)

Ben Rostron

Professor B. Rostron

R G Moore

Professor R.G. Moore (External Examiner)

Date September 30/99

To my father, Theodore H. Sr., who never got to see me graduate, and to my mother, Mary, who appreciated the value of an education by housing and feeding many university students over the last 30 years.

ABSTRACT

The ***oil sands*** of Alberta contain some one trillion barrels of bitumen-in-place, most contained in the ***McMurray, Wabiskaw, Clearwater, and Grand Rapids*** formations. Depth of burial is 0 - 550 m, 10% of which is surface mineable, the rest recoverable by ***in-situ*** technology-driven enhanced oil recovery schemes. To date, significant commercial recovery has been attributed to ***Cyclic Steam Stimulation*** (CSS) using vertical wellbores. Other techniques, such as Steam Assisted Gravity Drainage (SAGD) are proving superior to other recovery methods for increasing early oil production but at initial higher development and/or operating costs. Successful optimization of bitumen production rates from the entire reservoir is ultimately decided by the operator's understanding of the reservoir in its original state and, the positive and negative changes which occur in oil sands and heavy oil deposits upon heat stimulation. ***Reservoir description*** is the single most important factor in attaining satisfactory history matches and forecasts for optimized production of the commercially-operated processes. Reservoir characterization which lacks understanding can destroy a project. For example, incorrect assumptions in the geological model for the Wolf Lake Project in northeast Alberta resulted in only about one-half of the predicted recovery by the original field process. It will be shown here why the presence of thin ***calcite streaks*** within oil sands can determine the success or failure of a commercial cyclic steam project.

A vast amount of field data, mostly from the ***Primrose Heavy Oil Project*** (PHOP) near Cold Lake, Alberta, enabled the development a simple set of ***correlation curves*** for

predicting bitumen production using CSS. A previously calibtrated ***thermal numerical simulation*** model was used in its simplist form, that is, a single layer, radial grid blocks, "***fingering***" or "***dilation***" adjusted ***permeability curves***, and no simulated fracture, to generate the first cycle production correlation curves. The key reservoir property used to develop a specific curve was to vary the initial ***mobile water saturation***. Individual pilot wells were then history-matched using these correlation curves, adjusting for ***thermal net pay*** using ***perforation height*** and a fundamentally derived "net pay factor". Operating days (injection plus production) were required to complete the history matching calculations. Subsequent cycles were then history-matched by applying an ***Efficiency Multiplication Factor*** (EMF) to the original first cycle prediction method as well as selecting the proper correlation curve for the specific cycle under analysis by using the appropriate steam injection rates and slug sizes.

History matches were performed on eight PHOP wells (two back-to-back, five-spot patterns) completed in the Wabiskaw and, three single-well tests completed just below in the McMurray Formation. ***Predictions*** for the PHOP Wabiskaw Formation first cycle bitumen production averaged within 1% of the actual pilot total. Bitumen recovery from individual wells for second cycle onwards, was within 20% of actual values. For testing the correlations, matching was also performed on cyclic steam data from British Petroleum's Wolf Lake Project, the Esso Cold Lake Project, and the PCEJ Fort McMurray Pilot, a joint venture of Petro-Canada, Cities Services (Canadian Occidental), Esso, and Japan-Canada Oil Sands with reasonable results.

ACKNOWLEDGEMENTS

I wish to express sincere appreciation for the interest, guidance, encouragement, caring and patience conveyed by my mentor, supervisor, and old friend, Dr. S.M. Farouq Ali, who gave me the opportunity to return to school and complete a dream started many years ago. As a graduate student advisor, Dr. Farouq Ali has tirelessly shaped a generation of petroleum engineers and I am honoured to be one of his many students.

Also, special thanks goes to fellow graduate student, and now professor at the University of Alberta, Dr. Quang Doan, who was always willing to help solve the many technical and university life problems I faced.

I am indebted to my companion and colleague, Kris Beadall for her faith, professional critique, and tolerance of the many moods of a practical minded, older graduate student. Kris was also the thesis technical editor.

Tamara and Jason, my two children, received fewer hours of attention than they deserved, please forgive me.

Grateful acknowledgement goes to all other professors at the University of Alberta, and the University of Calgary, fellow students, family and friends who supported me through my endeavours.

Thanks to Judy Leshchyshyn, Tamara Leshchyshyn and Jason Leshchyshyn for computerizing the pilot data.

To my sister, Carol, and brotrhers Roy, and Allan who shouldered my family responsibilities while I studied.

Finally, thanks to Petro-Canada Resources for the extensive PHOP (Primrose Heavy Oil Project) data and also to the PCEJ business partners (Petro-Canada, Canadian Occidental, ESSO, and JACOS, Japan-Canada Oil Sands), who supplied further data for this thesis, I thank them for their assistance in completing the study. The major conclusions could not have been drawn without real data.

TABLE OF CONTENTS

ABSTRACT

ACKNOWLEDGEMENTS

LIST OF TABLES

LIST OF FIGURES

NOMENCLATURE

Chapters	**Page**
1. Introduction	1
1.1 Primrose Heavy Oil Pilot (PHOP) Project, Location and Well Spacing	5
2. Literature Review	13
2.1 Discussion	31
3. Statement of the Problem	34
4. PHOP Injection Data	37
4.1 Injection Data Provided	37
4.2 Accuracy of Injection Data	38
5. PHOP Project Production Data	43
5.1 Production Data Provided	43

5.2 Accuracy of Production Data 45

6. Validation of PHOP Project Injection and Production Data 47

6.1 Injection Data Validation 47

6.1.1 Geomechanical Theory 49

6.1.2 Reservoir Flow Theory 56

6.1.3 Conventional Reservoir Theory with Modification for Geomechanical Shear Dilation 57

6.2 Production Data Validation 58

6.3 Summary 59

7. Effect of Well Completion on Production 60

7.1 Perforations 61

7.2 Wire Wrapped Screens 62

8. Shear Fracturing or Dilation 65

8.1 Process of Shear Parting 65

9. Numerical Simulator 74

9.1 Model Equations and Unknowns 74

9.2 Representation of Gas Solubilities in Oil using K-Values 78

9.3 Components and Phases 79

9.4 Specific Volume 82

9.5 Viscosities 83

9.6 Temperature Dependency 84

10. Simulator Input Data 86

10.1 Wellbore Heat Losses 86

10.2 Reservoir Description and Well Completion 95

10.3 Relative Permeability Curves 106

10.4 Viscosity Calculations with Temperature 111

11. Development of the Semi-Analytical/Correlative Model 113

11.1 Summary of Correlation Curves Development 113

11.2 Introduction to Correlation Curve Model Development 118

11.3 Reservoir Characterization 119

11.3.1 Definitions of Thermal Pay, Net Pay, and Gross Pay 120

11.3.2 Fracturing Through Shale 121

11.3.3 Fracturing Through Calcite, and other Lithologies 122

11.3.4 Effect of Fracture Height Growth and Perforation Height on Bitumen Production 125

11.3.5 Measuring the Restricted Height Growth 125

11.3.6 Effect of Initial Water Saturation on Bitumen Production 126

12. Running the Numerical Simulator to Generate the Correlation Curves 138

12.1 Simulator Grid Sizing by Varying Number of Layers and Lateral Ring Size 138

12.1.1 Interpretation of the Sensitivity Runs 149

12.2 Detailed Analysis of Production Data from the Simulation Model 149

12.2.1 Slug Size of 3,000 m^3 149

a) Rate at 66.7 m^3/d 150

b) Rate at 110 m^3/d 150

c) Rate at 200 m^3/d 156

d) General Comments on Layering 156

12.2.2 Slug Size of 5,000 m^3 159

12.2.3 Slug Size of 7,000 m^3 166

12.2.4 Comparing 3,000 m^3, 5,000 m^3, and 7,000 m^3 Slug Sizes 166

12.2.5 Effect of Radial Grid Size on 3,000 m^3, 5,000 m^3, and 7,000 m^3 Slug Sizes 166

a) Slug Size of 3,000 m^3 174

b) Slug Size of 5,000 m^3 176

c) Slug Size of 7,000 m^3 176

12.2.6 Conclusions on Layering and Ring Size 176

12.3 Building the Correlation Curves 177

12.3.1 Varying Initial Water Saturation 177

12.3.2 Determining Optimum Slug Size for the Correlation Curve 178

12.3.3 Plotting the Correlation Curves 178

13. First Cycle Prediction of Bitumen Production 194

13.1 Step-by-step Method for Estimating First Cycle Bitumen Production 194

13.2 Example Calculations for PHOP Well IP2 197

13.3 Calculation of Bitumen Production for Remainder of PHOP IP Wells 199

13.4 Related Comments on Bitumen Production for the PHOP IP Wells 201

13.5 Calculation of Bitumen Production for PHOP Single-Well Tests 202

14. Multi-cycle History match and Prediction for the PHOP IP Wells and SWT's 206

14.1 Method 1 for Estimating Multi-cycle Bitumen Production 206

14.2 Method 2 for Estimating Multi-cycle Bitumen Production 207

14.3 Summary of Prediction Method for First-cycle Bitumen Production 207

14.4 Calculation of Multiple Cycles of PHOP Bitumen Production using Method 1 218

  14.4.1 Example Prediction of Second-cycle IP5 Bitumen Production using Method 1 218

14.5 Calculation of Multiple Cycles of PHOP Bitumen Production using Method 2 219

  14.5.1 Example Prediction of Second-cycle IP5 Bitumen Production using Method 2 219

14.6 Summary of Multiple Cycles of PHOP Bitumen Production and Associated Errors 220

14.7 The Utility of Predictions after Successful History Matching 222

15. Multiple-cycles of Other Oil Sands Reservoirs in Alberta 224

15.1 Descriptions for Various Oil Sands Reservoirs 224

  15.1.1 Comparison of Average Reservoir Properties 224

  15.1.2 Comparison of Average Bitumen Properties 231

  15.1.3 Comparison of Steam Injection and Fracture Properties 233

15.2 History-matching Other Reservoirs using the PHOP Production Correlation Curves 237

  15.2.1 History-matching of the Wolf Lake-Clearwater Average Well Simulation 237

15.2.2 History-matching of an ESSO Cold Lake-Clearwater Average Well Simulation 241

15.2.3 Comparison of History-matching of the Various Reservoirs 243

16. Discussion 257

17. Conclusions 260

REFERENCES 262

APPENDIX A: PHOP Pilot and Single Well Tests Summary of Injection and Production Data 273

APPENDIX B: PHOP Pilot, Wells IP2 and IP8 and Single Well Test 10-34 Daily Injection Data 280

APPENDIX C: : PHOP Pilot, Wells IP2 and IP8 and Single Well Test 10-34 Daily Production Data 302

APPENDIX D: Example of Correlation of Weight Percent Bitumen Between Logs and Cores, PCEJ Area 1, McMurray Formation 403

APPENDIX E: Effects of Various Parameters on Creation of Multiple Fractures and Fracture Length 415

APPENDIX F: Rule of Eight Derivation 418

APPENDIX G: Mandel-Volek Steam Volume Calculations for PHOP Wells IP4 and IP5 420

APPENDIX H: Letter of Permission from Petro-Canada to use PHOP and PCEJ data 431

LIST OF TABLES

Table **Page**

10.1: Example of Input Data File for the Numerical Simulator Therm 87

10.2.1: PHOP Reservoir Description, Well IP1 96

10.2.2: PHOP Reservoir Description, Well IP2 97

10.2.3: PHOP Reservoir Description, Well IP3 98

10.2.4: PHOP Reservoir Description, Well IP4 99

10.2.5: PHOP Reservoir Description, Well IP5 100

10.2.6: PHOP Reservoir Description, Well IP6 101

10.2.7: PHOP Reservoir Description, Well IP7 102

10.2.8: PHOP Reservoir Description, Well IP8 103

10.2.9: PHOP Reservoir Description, General Well 104

12.1.1: Operating Conditions Single Layer Model; Optimization of Injection Rates and Slug Size, Initial Water Saturation, Swi = 0.50, 1 Layer, 8 rings 139

12.1.2: Operating Conditions Varied Layer Model; Optimization of Injection Rates and Slug Size, Initial Water Saturation, Swi = 0.50, 1, 5, and 10 layers, 8 and 15 rings 142

12.2.1: Operating Conditions Varied Layer Model; Optimization of Injection Rates and Slug Size, Initial Water Saturation, Swi = 0.50, 1, 5, and 10 layers, 8 and 15 rings 153

12.3.1.1: Operating Conditions Single Layer Model;Varying Initial Water Saturation, Sensitivities for Runs 5A, 7A, and 1A 179

13.3.1: 1st Cycle Primrose Pilot Prediction of Produced Oil, Wells IP1 - IP8, Vs Actual Production 200

13.5.1: 1st Cycle MITS (Single Well Tests); Prediction of Produced Oil Vs Actual 203

14.6.1a: 2nd Cycle PHOP; Prediction of Produced Oil, Wells IP1 - IP8, Vs Actual 208

14.6.1b: 2nd Cycle Single well Tests; Prediction of Produced Oil Vs Actual 210

14.6.2a: 3rd Cycle PHOP; Prediction of Produced Oil, Wells IP1 - IP8 excl. IP6, Vs Actual 211

14.6.2b: 3rd Cycle Single well Tests; Prediction of Produced Oil Vs Actual 212

14.6.3a: 4th Cycle PHOP; Prediction of Produced Oil, Wells IP1 - IP8 excl. IP6 Vs Actual 213

14.6.3b: 4th Cycle Single Well Tests; Prediction of Produced oil Vs Actual 214

14.6.4a: 5th Cycle PHOP; Prediction of Produced Oil, Wells IP1, IP2, IP7, and IP8, Vs Actual 215

14.6.5a: 6th Cycle PHOP; Prediction of Produced Oil, Well IP1 216

14.6.6a: 7th Cycle PHOP; Prediction of Produced Oil, Well IP1 217

14.6.7: Summary of PHOP Pilot and Single Well Tests Predicted Oil Production using both Methods and Associated Error (by Well,by cycle) 221

15.1.1.1: Comparison of Average Reservoir Properties for Various Oil Sands Reservoirs 225

15.1.1.2: Comparison of Average Mineral Constituents for Various Oil Sands Reservoirs 226

15.1.1.3: Reservoir Model of Wolf Lake Project average Well (Well 4G) 227

15.1.2.1: Comparison of Average Bitumen Properties for Various Oil Sands Reservoirs 228

15.2.1.1: Wolf Lake Comparison of Correlation Curve and Simulated Production, PCI Simulation similar to OP. Strategy as in Case (7) of BP Study No. 640, Average Well 4G, 250 m^3/d 229

15.1.3.1: Fracture Parameters Compared between Athabasca (McMurray) and Cold Lake (Clearwater and Lower Grand Rapids) 230

15.2.1: PHOP Well IP8 Comparison of Type Curve and Simulated Production 238

15.2.1.1: Wolf Lake Comparison of Correlation Curve and Simulated Production, PCI Simulation similar to OP. Strategy as in Case (7) of BP Study No. 640, Average Well 4G, 250 m^3/d 239

15.2.1.2: Wolf Lake Comparison of Correlation Curve and Simulated Production, PCI Simulation similar to OP. Strategy as in Case (7) of BP Study No. 640, Average Well 4G, 160 m^3/d 240

15.2.2.1: ESSO Cold Lake Comparison of Correlation Curve and Simulated Production, ERCB Application Phases III & IV, March, 1984 242

15.2.3.1: PCEJ Well 13-27-84-11W4 Comparison of Correlation Curve and Simulated Production, Vs Actual 244

15.2.3.2: PHOP Well McMurray Comparison of Correlation Curve and Simulated Production, PCI August, 1983, Vs Actual 245

Appendix A

A1.1a: Summary of Injection & Production Data by Well for PHOP Pilot, Wells IP1 - IP8 274

A1.1b: Summary of Injection & Production Data and Depletion Index by Well for PHOP Pilot, Wells IP1 - IP8 275

A1.1c: Summary of Injection & Production Data, WOR, PDOR, CDOR, and SOR by Well for the PHOP Pilot, Wells IP1 - IP8 276

A1.2: Summary of 11-10 Single W[illegible]est Injection & Production Data as of February 28, 1985 277

A1.3: Summary of 10-34 Single Well Test Injection & Production Data as of February 28, 1985 278

A1.4: Summary of 11-21 Single Well Test Injection & Production Data as of February 28, 1985 279

Appendix B

BIP2IC1 to BIP2IC5: Daily Injection Data for PHOP Pilot Well IP2, by Cycle 281

BIP8IC1 to BIP8IC5: Daily Injection Data for PHOP Pilot Wells IP8, by Cycle 289

BW1034IC1 to BW1034IC4: Daily Injection Data for Single Well Test 10-34, by Cycle 295

Appendix C

CIP2PC1 to CIP2PC5: Daily Production Data for PHOP Pilot Well IP2, by Cycle 303

CIP8PC1 to CIP8PC5: Daily Production Data for PHOP Pilot Wells IP8, by Cycle 337

CW1034PC1 to CW1034PC4: Daily Production Data for Single Well Test 10-34, by Cycle 370

Appendix D

AD 1: PCEJ Area 1 - Core and Log Analysis, Well 13-27-84-11W4 413

AD 2: PCEJ Area 1 - Core and Log Analysis, Well 16-28-84-11W4 414

Appendix E

E1: Factors Affecting Multiple Fracture Generation 416

E2: Factors Affecting Fracture Length Growth 417

Appendix G

AG1 IP4 Steam Volume Calculations - Summary of Results 427

AG2 IP5 Steam Volume Calculations - Summary of Results 427

LIST OF FIGURES

Figure **Page**

1.1.1: Location map of cyclic steam oil sands projects in Alberta, Canada, with fracture trend and rock stress directions 6

1.1.2: Primrose Heavy Oil Project (PHOP) Pilot well spacing 7

1.1.3: PHOP Pilot well IP1 log correlations 8

1.1.4: Fundamental lithological unit for the PHOP Pilot area in the Wabiskaw formation 10

1.1.5: Fence diagram, PHOP Pilot 11

1.1.6: Stratigraphic columns for the Wabiskaw, Athabasca, and Cold Lake deposits and their correlation 12

3.1: Flow diagram for developing correlation curves to history match and predict bitumen production from cyclic steaming of oil sands 36

6.1.1: PHOP Pilot wells steam injection rates (CWE) Vs casing pressure, Cycle1, by well 48

6.1.2: PHOP Pilot wells steam injection rates (CWE) Vs casing pressure, Cycle 1, by well with slopes 50

6.1.3: PHOP Pilot wells steam injection rates (CWE) Vs casing pressure, Cycle 1 51

6.1.4: PHOP Pilot wells steam injection rates (CWE) Vs casing pressure, Cycle 2 52

6.1.5: PHOP Pilot wells steam injection rates (CWE) Vs casing pressure, Cycle 3 53

6.1.1.1: Measured increase in Stress with increase in Pore Pressure, PCEJ Pilot 55

8.1.1: Stress - strain relationship for rock 66

8.1.2: Creation of a dilated zone near the wellbore 68

8.1.3: Well test analysis of dilation in the McMurray oil sands using a 2-zone composite model 72

10.1.1: Estimated bottomhole steam quality assuming 80% wellhead quality Vs steam injection rate 94

10.3.1: Water - Oil Rock Types 1 - 3, PHOP Relative Permeability Data 107

10.3.2: Water - Oil Rock Type 4, PHOP Relative Permeability Data 108

10.3.3: Gas - Oil Rock Types 1 - 3, PHOP Relative Permeability Data 109

10.3.4: Gas - Oil Rock Type 4, PHOP Relative Permeability Data 110

11.1.1: PCEJ McMurray oil sands residual oil saturation Vs temperature for a hotwater/steamflood 116

11.1.2: PHOP Wabiskaw & McMurray plus PCEJ and GLISP oil sands residual oil saturation with temperature for a hotwater/steamflood 117

11.3.6.4: PCEJ cut-off curve, McMurray oil sands 132

11.3.6.5: Bulk Volume Water (BVW) and Porosity Vs Wt% Bitumen for PCEJ 137

12.1.1: Spacing for 8 and 15 ring grids, radial numerical model 141

12.1.1.1a: RUN NO's 1A, 2A, and 3A Oil production for Sw = 0.50, injection rate = 66.7 m^3/d, slug sizes = 3000, 5000, and 7000 m^3, 0.2 BHQ 143

12.1.1.1b: RUN NO's 1A, 2A, and 3A Water production for Sw = 0.50, injection rate = 66.7 m^3/d, slug sizes = 3000, 5000, and 7000 m^3, 0.2 BHQ 144

12.1.1.2a: RUN NO's 4A, 5A, and 6A Oil production for Sw = 0.50, injection rate = 110 m^3/d, slug sizes = 3000, 5000, and 7000 m^3, 0.425 BHQ 145

12.1.1.2b: RUN NO's 4A, 5A, and 6A Water production for Sw = 0.50, injection rate = 110 m^3/d, slug sizes = 3000, 5000, and 7000 m^3, 0.425 BHQ 146

12.1.1.3a: RUN NO's 7A, 8A, and 9A Oil production for Sw = 0.50, injection rate = 200 m^3/d, slug sizes = 3000, 5000, and 7000 m^3, 0.5 BHQ 147

12.1.1.3b: RUN NO's 7A, 8A, and 9A Water production for Sw = 0.50, injection rate = 200 m^3/d, slug sizes = 3000, 5000, and 7000 m^3, 0.5 BHQ 148

12.2.1.1a: RUN NO's 1A and 1B Oil production for Sw = 0.50, injection rate = 66.7 m^3/d, slug size = 3000 m^3, 1 and 10 layers 151

12.2.1.1b: RUN NO's 1A and 1B Water production for Sw = 0.50, 152 injection rate = 66.7 m^3/d, slug size = 3000 m^3, 1 and 10 layers

12.2.1.2a: RUN NO's 4A, 4B, 4C and 4D Oil production for Sw = 0.50, injection rate = 110 m^3/d, slug size = 3000 m^3, 1,5, and 10 layers 154

12.2.1.2b: RUN NO's 4A, 4B, 4C and 4D Water production for Sw = 0.50, injection rate = 110 m^3/d, slug size = 3000 m^3, 1,5, and 10 layers 155

12.2.1.3a: RUN NO's 7A and 7B Oil production for Sw = 0.50, injection rate = 200 m^3/d, slug size = 3000 m^3, 1 and 10 layers 157

12.2.1.3b: RUN NO's 7A and 7B Water production for Sw = 0.50, injection rate = 200 m^3/d, slug size = 3000 m^3, 1 and 10 layers 158

12.2.2.1a: RUN NO's 2A, 2B, and 2C Oil production for Sw = 0.50, injection rate = 66.7 m^3/d, slug size = 5000 m^3, 1,5, and 10 layers 160

12.2.2.1b: RUN NO's 2A, 2B, and 2C Water production for Sw = 0.50, injection rate = 66.7 m^3/d, slug size = 5000 m^3, 1,5, and 10 layers 161

12.2.2.2a: RUN NO's 5A, 5B, 5C, and 5D Oil production for Sw = 0.50, injection rate = 110 m^3/d, slug size = 5000 m^3, 1,5, and 10 layers 162

12.2.2.2b: RUN NO's 5A, 5B, 5C, and 5D Water production for Sw = 0.50, injection rate = 110 m^3/d, slug size = 5000 m^3, 1,5, and 10 layers 163

12.2.2.3a: RUN NO's 8A and 8B Oil production for Sw = 0.50, injection rate = 200 m^3/d, slug size = 5000 m^3, 1 and 10 layers 164

12.2.2.3b: RUN NO's 8A and 8B Water production for Sw = 0.50, injection rate = 200 m^3/d, slug size = 5000 m^3, 1 and 10 layers 165

12.2.3.1a: RUN NO's 6A, 6B, and 6D Oil production for Sw = 0.50, injection rate = 110 m^3/d, slug size = 7000 m^3, 1,5 and 10 layers 167

12.2.3.1b: RUN NO's 6A, 6B, and 6D Water production for Sw = 0.50, injection rate = 110 m^3/d, slug size = 7000 m^3, 1,5 and 10 layers 168

12.2.3.2a: RUN NO's 9A and 9B Oil production for Sw = 0.50, injection rate = 200 m^3/d, slug size = 7000 m^3, 1 and 10 layers 169

12.2.3.2b: RUN NO's 9A and 9B Water production for Sw = 0.50, injection rate = 200 m^3/d, slug size = 7000 m^3, 1 and 10 layers 170

12.2.5.2a: RUN NO's 4D, 5D, and 6D Oil production for Sw = 0.50, injection rate = 110 m^3/d, slug size = 3000,5000, and 7000 m^3, 5 layers, 15 rings 171

12.2.5.2b: RUN NO's 4D, 5D, and 6D Water production for Sw = 0.50, injection rate = 110 m^3/d, slug size = 3000,5000, 172 and 7000 m^3, 5 layers, 15 rings

12.2.5.3: Effect on lost oil by varying layer number and grid size
using 110-200 m3/d injection rates 175

12.3.1.1: RUN NO's 13, 14, and 15 Bottomhole injection pressure
for Sw = 0.40, 0.45, and 0.50, injection rate = 110 m^3/d,
slug sizes = 3000,5000, and 7000 m^3, 1 layer, 8 rings 180

12.3.1.2: RUN NO's 13, 14, 15, and 16 Oil production
for Sw = 0.35, 0.40, 0.45, and 0.50, injection rate = 110 m^3/d,
slug sizes = 3000 or 5000 m^3, 1 layer, 8 rings 181

12.3.1.3: RUN NO's 17, 18, and 19 Oil production
for Sw = 0.40, 0.45, and 0.50, injection rate = 200 m^3/d,
slug sizes = 3000 or 5000 m^3, 1 layer, 8 rings 182

12.3.1.4: RUN NO's 1A (20), and 21 (history match 1st cycle IP6)
Oil production for Sw = 0.45, and 0.50, injection rate = 66.7 m^3/d,
slug size = 3000 m^3, 1 layer, 8 rings 183

12.3.2.1: RUN NO's 1A, 2A, and 3A Optimization of well performance
at 60 days production, Sw = 0.50, injection rate = 66.7 m^3/d,
slug sizes = 3000, 5000, and 7000 m^3, 1 layer, 8 rings 184

12.3.2.2: RUN NO's 4A, 5A, and 6A Optimization of well performance
at 60 days production, Sw = 0.50, injection rate = 110 m^3/d,
slug sizes = 3000, 5000, and 7000 m^3, 1 layer, 8 rings 185

12.3.2.3: RUN NO's 7A, 8A, and 9A Optimization of well performance
at 60 days production, Sw = 0.50, injection rate = 200 m^3/d,
slug sizes = 3000, 5000, and 7000 m^3, 1 layer, 8 rings 186

12.3.2.4: RUN NO's 1A to 9B Summary of well performance
at 60 days production, Sw = 0.50, injection rate = 66.7, 110, and 200 m^3/d,
slug sizes = 3000, 5000, and 7000 m^3, 1, 5, and 10 layers, 8 and 15 rings 187

12.3.2.5: RUN NO's 1A to 9A Heat injected Vs oil produced,
Sw = 0.50, injection rate = 66.7, 110, and 200 m^3/d,
slug sizes = 3000, 5000, and 7000 m^3, 1 layer, 8 rings 188

12.3.3.1: Correlation curves for PHOP 1st cycle steam stimulation 189

12.3.3.2: Net pay factor to account for production of bitumen
above and below perforations 191

13.1.1: Net pay factor to account for production of bitumen above
and below Perforations 196

15.1.1.1: Comparison of sieve analysis from cores of various oil sands formations 232

15.1.2.1: Viscosity of heavy crudes as a function of temperature (Buckles, 1979) 234

15.1.3.2: Comparison of fracture lengths versus cumulative steam injected in the Cold Lake-Clearwater and Fort McMurray-McMurray oil sands formations (Leshchyshyn, 1991) 236

15.2.3.1a: Multicycle efficiency factors for various reservoirs versus cycle number 247

15.2.3.1b: Multicycle efficiency factors for various reservoirs versus cumulative steam injection 248

15.2.3.2a: Production/injection days for various reservoirs versus cycle number 249

15.2.3.2b: Production/injection days for various reservoirs versus cumulative steam injected 250

15.2.3.2c: Cumulative production/injection days for various reservoirs versus cumulative steam injected 251

15.2.3.4a: Bitumen production for various reservoirs versus cycle number 253

15.2.3.4b: Bitumen production/cycle for various reservoirs versus cumulative steam injection 254

15.2.3.4c: Bitumen production for various reservoirs versus cumulative steam injected 255

Appendix G

AG1: Mandel-Volek Function F_3 as a function of t_D 428

AG2: Mandl-Volek steam front, radial mode, 3 cycles 429

AG3: Mandl-Volek steam front, elipse, a = 1/5b, 3 cycles 430

NOMENCLATURE

a	constant based on rock texture for Archie's equation for water saturation, dimensionless
C_I	compressibility of component I, vol/vol kPa
C_T	coefficient of thermal expansion, vol/vol °C
c	constant for calculation of fracture length, derived from the Carter fracture length equation
c_t	total compressibility, kPa^{-1}, $[1/ML^{-1}t^{-2}]$
D	diffusion coefficient, m^2s^{-1}, $[L^2t^{-1}]$
Ep	energy of phase p, J $kmol^{-1}$, $[ML^2t^{-2}]$
Fi	empirical drainage radius factor
f	fraction of well associated with the well block
f_g	geometrical factor
f_h	layer thickness factor
g	gravity constant = 9.81 $m.s^{-2}$, $[Lt^{-2}]$
H_p	Enthalpy of phase p, J $kmol^{-1}$, $[ML^2t^{-2}]$
h	layer thickness, m, [L]
I	components, 1 = water, 2 = heavy oil, 3 = gas
i	steam injection rate (CWE) for calculating fracture length from Carter's fracture length equation, m^3/d, $[L^3t^{-1}]$
J	phases, 1 = liquid water, 2 = oil, 3 = gas
J	productivity index, m^3 s^{-1} Pa^{-1}, $[m^{-1}L^4 t]$
J'	constant portion of productivity index
$J_{i,j,k}$	layer productivity/injectivity of phase i, layer j, well k, m^3 s^{-1} Pa^{-1}, $[m^{-1}L^4t]$
K	consistency constant in rheological model, $kg.m^{-1}s^{n-1}$, $[mL^{-1}t^{n-1}]$
K	equilibrium constant for PVT calculations = y/x mole fractions
K	thermocouple type
k	absolute permeability, m^2, $[L^2]$
k_h	horizontal permeability, md
k_r	relative permeability, dimensionless
$Krwro$	end point relative permeability to water at irreducible oil saturation

K_{vip}	equilibrium ratio of component i in phase p
Kv	equilibrium gas solubility values, dimensionless
k_v	vertical permeability, md
$Kv1$ - $Kv5$	solubility constants for calculating equilibrium K-values
l	characteristic length in rheological model, m, [L]
L	total moles in the liquid phase
Lf	half fracture length, m
m	non-newtonian fluid parameter
mKB	meters depth from rig Kelly Bushing, m
Mf	volumetric heat capacity of the reservoir matrix, J m^{-3} rock K^{-1}, $[M^{-2}L^{2}t^{-2}\theta^{-1}]$
n	total number of moles present in both liquid and gas phase
n	number of grid layer layers
n	previous time step, reservoir PVT data known
$n+1$	next time step, reservoir PVT data unknown, to be calculated by model
nm^3	normal or standard cubic metres at atmospheric pressure and 15 °C
Nc	number of components
Np	number of phases
P	pressure, kPa, Pa, $[ML^{-1}t^{-2}]$
$Pcgo$	capillary pressure in a gas/oil system, Pa, $[ML^{-1}t^{-2}]$
$Pcow$	capillary pressure in an oil/water system, Pa, $[ML^{-1}t^{-2}]$
Pg	pressure of gas phase, Pa, $[ML^{-1}t^{-2}]$
Po	pressure of oil phase, Pa, $[ML^{-1}t^{-2}]$
Pw	pressure of water phase, Pa, $[ML^{-1}t^{-2}]$
p	rheological model fitting parameter
p_e	average grid block pressure in which wellbore is located, Pa $[ML^{-1}t^{2}]$
p_{wf}	flowing bottomhole pressure at the perforations, Pa, $[ML^{-1}\,t^{-2}]$
q	production rate, $m^3\,s^{-1}$, $[L^3\,t^{-1}]$
q	energy source/sink, J s^{-1}, $[ML^{2}t^{-3}]$
$\tilde{q}$	production rate per unit reservoir volume, kmol $s^{-1}\,m^{-3}$
$\tilde{q}$	energy source/sink per unit reservoir volume, J $s^{-1}\,m^{-3}$

q_i	production rate of component i from grid block, kmol s^{-1}, [L^{3}t^{-1}]
Q	steam injection rate (CWE), m^3/d
R_t	log formation resistivity, ohm-m^3/m^2
Rt	measured resistivity of the formation at a given depth for Archie's equation, same as R_t
Rw	resistivity at 100% water saturation for Archie's equation for water saturation
r	radius, m
S	saturation, fraction
So init	SORG
Swc	connate water saturation, fraction
Swi	initial water saturation = Swc, fraction
Swir	end point irreducible water saturation, relative permeability to water equals zero, fraction
s	skin damage (+) or improvement (-) near wellbore
t	time, days, hours, minutes, or seconds
t	steam injection time for Carter equation, days
t_p	equivalent time in well test analysis = total injected volume/final injection rate, minutes or hours
T	temperature, °C
T	fluid flow transmissibility, m^3 Pa^{-1} s^{-1}, [M^{-1} L^4 t]
TX	x-direction transmissibilities, Rm^3-mPa.s/day-kPa
TY	y-direction transmissibilities, Rm^3-mPa.s/day-kPa
TZ	z-direction transmissibilities, Rm^3-mPa.s/day-kPa
V	total moles in the vapour phase
V_b	bulk volume, m^3, [L^3]
V_f	volume of fines, fraction
V_{IJ}	partial volume of component I in phase J
V_J	specific volume of liquid phase J, m^3/mole
X	mole fraction
X_I	mole fraction of component I in the component's master phase
x	mole fraction
x	mole fraction of the component in the oil phase

y	mole fraction of the component in the gas phase
z	space coordinate for areal model, depth, positive downwards, m, [L]

SUBSCRIPTS

cl	closure
D	density
e	effective
f	fines
g	gas
$I=1$	water component
$I=2$	heavy oil component
$I=3$	gaseous component
i	grid in x direction
J	thermocouple type
$J=1$	liquid water phase
$J=2$	oil phase
$J=3$	gas phase
j	grid in y direction
k	grid in z direction
N	neutron
o	oil
p	phase
ref	reference
SH	shale
T	thermal expansion
T	total
t	time
t	total
w	water
w	wellbore

SUPERSCRIPTS

m	cementation exponent for Archie's equation, dimensionless
n	saturation exponent for Archie's equation, dimensionless

SYMBOLS

ρ	density, gm/cc [M/L^3]
ρ_p	density of phase p, kg m^{-3}, [ML^{-3}]
ρ_{rw}	relative density to water, dimensionless
μ	viscosity, cp, mPa.sec
μp	viscosity of phase p, Pa..s, [ML^{-1}t^{-1}]
$\varnothing$	porosity, fraction, m^3/m^3, [L^3/L^3]
$\varnothing_D$	log density porosity, fraction, m^3/m^3, [L^3/L^3]
$\varnothing_e$	log effective porosity, fraction, m^3/m^3, [L^3/L^3]
$\varnothing_N$	log neutron porosity, fraction, m^3/m^3, [L^3/L^3]
$\varnothing_{SH}$	log shale porosity, fraction, m^3/m^3, [L^3/L^3]
$\varnothing_T$	log total porosity, fraction, m^3/m^3, [L^3/L^3]
σ_1	maximum stress (for vertical fractures = weight of overburden), kPa, [ML^{-1}t^{-2}]
σ_2	intermediate stress (for vertical fractures = maximum horizontal stress, kPa, [M L^{-1}t^{-2}]
σ_3	minimum stress (for vertical fractures = minimum horizontal stress, kPa, [M L^{-1}t^{-2}]
γ	constant of liquid density gradient, kPa/m
λ	mobility, Pa^{-1}.s^{-1}, [M^{-1} Lt]
λc	thermal conductivity, J s^{-1} m^{-1} K^{-1}, [MLt$^{-3}\theta^{-1}$]
α	constant for shifting temperature dependent permeabilities
θ	temperature, K, θ

OPERATORS

δu	$u_{n+1} - u_n$, time
Δu	$u_1 - u_2$, space
$\nabla \bullet u$	divergence of vector u
∇u	gradient of scalar u

ABREVIATIONS/MODEL INPUT KEYWORDS

ABC	AOSTRA ,Bow Valley Cold Lake Project
AEUB	Alberta Energy Utilities Board, formerly ERCB
AOSTRA	Alberta Oil Sands Technology and Research Authority
AVIS	constant "a" for calculating liquid viscosity at any temperature
BHP	bottom hole pressure
BHP	model limiting bottomhole pressure at layer KBHP, kPa
BHQ	bottom hole steam injection quality, fraction
BOUND	boundary grids for values, i-i,j-j,k-k
BP	British Petroleum plc.
BQ	Basal Quartz formation
BVIS	constant "b" for calculating liquid viscosity at any temperature
BVW	bulk volume water in rock , BVW = Øe*Sw
CANMET	Canada Centre for Mineral and Energy Technology
CDOR	calendar day oil rate, m^3/d
COMP	compressibility, kPa^{-1}
CON	constant value
CP1,CP2,CP3	first, second, and third coefficient in the ideal gas state, specific heat equation, KJ/kg.K, CP2 = CP3 = 0
CPOB	overburden heat capacity, $kJ/m^3.°C$
CPR	reservoir rock heat capacity, kJ/m^3 rock. °C
CPUB	underburden heat capacity, $kJ/m^3.°C$
CR	rock compressibilty, 1/MPa
CSS	cyclic steam stimulation
CT	thermal expansion coefficient for liquids, vol/vol °C
CWE	cold water equivalent of steam volume, m^3

DENST	density at stock tank conditions, kg/m^3
DI	depletion index, oil plus water produced/steam injected, vol/vol, dimensionless
DPITN	maximum allowable pressure change per iteration, kPa
DPMAX	maximum allowable pressure change per time step, kPa
DSITN	maximum allowable saturation change per iteration, fraction
DSMAX	maximum allowable saturation change per time step, fraction
DSWCDT	temperature dependency on relative permeability data, increase in connate water saturation with temperature, fraction/ °C
DSWIRDT	temperature dependency on relative permeability data, increase in irreducible water saturation with temperature, fraction/ °C
DSORWDT	temperature dependency on relative permeability data, decrease in irreducible oil saturation with temperature, fraction/ °C
DSORGDT	temperature dependency on relative permeability data, decrease in irreducible oil saturation with temperature in a gas system, fraction/ °C
DTHET	θ-direction grid block increments, CON = constant, angle °
DTITN	maximun allowable temperature change per iteration, °C
DTMAX	maximum allowable temperature change per time step
DTMIN	minimum allowable temperature change per time step
DTPMAX	desired temperature change per time step, °C
DXITN	maximum allowable mole fraction change per iteration, fraction
DXMAX	maximum mole fraction change per time step, fraction
DZ	ZVAR = Variable z-direction grid block dimensions
EMF	efficiency multiplication factor
EQUIL	equilibration data to follow, eg. reservoir pressure, temperature, Sw, So, Sg
EOS	equation-of-state
ERCB	Energy Resources Conservation Board, now AEUB
FMS	formation scanner log to see in situ fractures in open hole
FMULT	pattern scale multiplier for production performance for 1/2, 1/4, or 1/8 th well

GDK	Gertsma-DeKlerk fracture model, elliptic along fracture length (short fat fracture)
GLISP	Gregoire Lake Steam Pilot
GOR	gas/oil ratio, nm^3/m^3
Gravg	API log value for zone of interest, API units
GRmax	API log value at 100% shale content, API units
GRmin	API log value at 0% shale content, API units
HH	hydrostatic head (weight), kPa for groundwater well testing, the value is in metres
HTOP	depth to top of grid blocks, m
HVAP	heat of vaporization coefficient, KJ/kg
ID	identification number
INJ	defines a well as a fluid injector
IP well	injection and production from same well
IPV	inaccessible pore volume
IRATE	component injection rates for a fluid injection well using water/steam, oil, or gas
ISIP	instantaneous shut-in pressure (surface pressure required to propagate a fracture, no wellbore or perforation friction included) usually obtained immediately after shut-in during an injection operation
ITNPC	iteration summary print control
KBHP	layer number to which BHP applies
KHL	well productivity or injectivity index
KOB	overburden thermal conductivity, kJ/day.m.°C
KR	R-direction permeability, md
KRG	relative permeability to gas in the presence of oil at connate water saturation, fraction
KRGRO	relative permeability to gas at $Sg = 1 - Swc - So$ init
KROCW	relative permeability to oil at connate water saturation, fraction
KROG	relative permeability to oil in the presence of gas at irreducible water saturation, fraction

KROW	relative permeability to oil in the presence of water, curve, fraction
KRW	relative permeability to water in presence of oil, curve, fraction
KRWRO	relative Permeability to Water at residual oil saturation
KT	rock thermal conductivity, kJ/day.m.°C
KTHET	EQUALS KR = θ-direction permeability, md
KUB	underburden thermal conductivity, kJ/day.m.°C
KV1- KV5	coefficients in the equation for equilibrium k-values
KZ	z-direction permeability, md
LPC	linear water-oil capillary pressure curve to be calculated, first and last value, kPa
MAXITN	maximum number of iterations per time step
MINITN	minimum number of iterations per time step
MITS	PHOP single well tests
MOD	modify specific grids by location, i-i,j-j,k-k value
MW	molecular weight, kg/kmole
NGAS	component number for gas
NPF	net pay factor, multiplication factor for extra thermal pay above and below perforations contributing to oil production, dimensionless
NR	number of grids in r-direction
NTHET	number of grid blocks in the θ-direction
NZ	number of grid blocks in the z-direction
OD	operating days (injection plus production, not shut-in and/or downtime)
OOIP	original oil-in-place
OPCI	oil production capability index, $m^3/OD/m_{perf}$
OSR	oil/steam ratio
PC pump	progressive cavity screw pump
PCEJ	Petro-Canada, Canadian Occidental Petroleum Ltd., Esso Imperial Oil, JACOS (Japan Canada Oil Sands Ltd.)
PCI	production capability index, = OPCI, $m^3/OD/m$ perf
PCRIT	critical pressure, kPa
PDOR	producing day oil rate, m^3/d

PERF	specifies which layer is perforated, well# layer#-layer#
PHI	VALUE = #grids*porosity, fraction
PHI	sand grain size from seive analysis, dimensionless
PHOP	Primrose Heavy Oil Project
PINIT	initial pressure at depth, kPa
PINJ	injection pressure for a fluid injection well, kPa
PKN	Perkins-Kern fracture model, elliptic along fracture height (long fracture)
PMAX	upper pressure limit in internally generated viscosity tables, °C
PMIN	lower pressure limit in internally generated viscosity tables, °C
PRATE	desired or target production fluid rate, m3/d
PREF	reference pressure, atmospheric, 101.35 kPa
PRESKV	pressures at which to calculate k-values, kPa
PROD	defines well as a producer
PRUNITS	production well units, = STBLIQ = Nm^3/day
PVOL	partial volume at reference temperature and presssure, m^3/kg
PVT	properties of fluids at a specific pressure, volume, and temperature
QUAL	quality of injected steam for a fluid injection well, mass fraction
R	R-direction grid block outer radii, m
RGRD	average gamma ray deflection for zone of interest divided by maximum gamma ray deflection
ROCK TYPE	oil, water, and gas relative permeability curves for a specific physical event
RTD	resistance type device thermocouple
RTYPE	rock type, set of permeability curves
RTZ	cylindrical grid system
RUN	recurrent data to follow
Run	simulation sensitivity study
RVAR	variable grib block radii
RW	wellbore radius, mm
SAGD	steam assisted gravity drainage
SGR	residual gas saturation

SH	reservoir description for calcite, a mixture of shale and carbonate
SI	steam injectivity index
SEM	scanning electron microscope
SGAS	initial gas saturation, fraction
SLIQ	liquid saturation, connate water saturation plus oil saturation, fraction
SOIL	initial oil saturation, fraction
SOLUTION	DIRECT = Gaussian elimination with D4 ordering ITER = implicit iterative method
SOR	steam/oil ratio
SORG	residual oil saturation to gas, fraction
SORMIN	irreducible oil saturation
SORW	residual oil saturation to water, fraction
SPM	shots per meter
STONE 1	oil relative permeability in three phase system without using krw and krg
STONE 2	oil relative permeability in three phase system using krw and krg
Sw	water saturation of zone
SW	water saturation, x-axis relative permeability curve, fraction
SWATER	initial water saturation, fraction
SWIR	irreducible water saturation
SWT	single well test
T_0	initial reservoir temperature, °C
TCRIT	critical temperature, °C
TDC	Todd,Dietrich,Chase report to Petro-Canada, PHOP well IP1
TEMPKV	temperatures at which to calculate k-values, °C
TIME	time to make changes in well control, days
TINIT	initial temperature at depth
TINJ	temperature of the well injection stream, °C
TMAX	upper temperature limit in internally generated viscosity tables, °C
TMIN	lower temperature limit in internally generated viscosity tables, °C
TOIL	cumulative oil production, m^3

TREF	reference temperature, 15.56 °C
t_{pay}	effective thermal pay, m
WELL	direction of grid block flow from wellbore, I = x-direction, J = y-direction
WMULT	multiplicative factor for printing full well rates
WT%BIT	weight% bitumen = wt oil/ (wt oil + wt water + wt sand)*100
X	initial concentrations of components in their respective master phase, mole fraction
XRD	quantitative analysis using X-ray defraction for determination of clays
5PT	five-point finite-difference formulation

GLOSSARY

calcite streak	layer of calcareous/shale mixture, more difficult to fracture through than shale
capillary pressure	imbibition, water or oil pressure when flowing into a core, kPa
capillary pressure	drainage, water or oil pressure when flowing out of a core, kPa
closure gradient	minimum in situ stress divided by depth, kPa/m
compaction	reverse of dilation during production
condensation	cooling or increasing pressure to change phases from gas(K) to liquid (I,J)
conduction	flow of heat in reservoir through heat transfer across rock
convection	flow of heat in reservoir through fluid/gas flow
conventional	light oil and gas reservoirs
cryogenic	liquid nitrogen temperatures
cycle	one event of steam injection or oil production
cyclic steam	steam injection and bitumen production from same well
dead oil viscosity	viscosity of oil measured at surface conditions, gas removed, cp
deviated well bore	well bore drilled at some angle off vertical
dilation	shearing of rock near wellbore or tensile hydraulic fracture during fluid/steam injection resulting in an average matrix permeability and porosity increase

equal volume	grid blocks of equal volume, not geometrically spaced
formulation, direct	calculation of rate at n+1 time step using a direct equation, no iteration
formulation, implicit	calculation of rate at n+1 time step using an iterative method
five-spot	double-inverted-back-to-back pattern with wells on four corners of rectangle with additional well in pattern center
fill-up volume	steam zone size at end of cyclic steam production cycle
fingering	alternate word used to describe dilation
finite-difference	mathematical solution using slopes of very small intervals
flow, bilinear	flow along fracture then into formation radially
flow, linear	flow along fracture length or perpendicular to fracture
flow, radial	well bore flow equally in a lateral direction
flow, spherical	wellbore flow equally in all directions
fluid level	level of fluid above perforations, m
fracture gradient	bottomhole injection pressure divided by depth of overburden, kPa/m
flashing	heating or lowering pressure to change phases from liquid (I,J) to gas(K)
fracture closure	bottomhole pressure at minimum horizontal stress, kPa
fracture stimulation	fractures created in conventional reservoirs, usually propped, to increase oil and gas production or water injection
fracture trend	NE/SW direction of vertical fractures in Alberta
fully implicit	all calculations are fully analytical (exact) with no approximations
geometric	logarithmic equal spacing for grid blocks
grain weight oil	weight oil/weight sand (water not included)
gravity drainage	separation in reservoir of oil/water/gas by density with production at bottom of pay
gross pay	total thickness of oil pay in a formation including shale layers, m
Hall plot	plot of cummulative bottomhole pressure versus cummulative injection rate, a slope change signifies a change in mobility
harmonic decline	one of three types of production rate decline analysis
hydraulic diffusivity	$k/\phi\mu c_t$, a constant of the diffusity equation

hydrostatic pressure	weight of water from surface to perforations = 9.81 kPa/m
in situ combustion	injection of air or oxygen into an ignited reservoir to drive and/or lower production fluid viscosities
jet charge	gun powder discharge pressure concentrated to a point to blow a hole through the well bore casing and cement into the reservoir (one perforation about 10 mm in diameter)
joint	one length of pipe = 9 m
latent heat	steam energy as a liquid
layer	oil sands thermal pay zone divided into number of layers of certain thickness
lean oil sand	oil sand with porosity < 30%, and Sw of 45 - 60%
lost oil	movement of oil from a hot grid block to a cold grid block, the final viscosity being too low to flow, back-calculated as extra steam zone volume
micro-channeling	another word for dilation
mini-frac test	injection of fluid into a well to determine ISIP, minimum formation stress, leak-off coefficient, and permeability
mobile water	displaceable water, connate water saturation minus irreducible water saturation, fraction
multicycle factor	multiplication factor decreasing with increasing cycle number used to predict bitumen production, dimensionless
net pay	reservoir thickness containing hydrocarbons, above some net pay cut-off, m
net pay cut-off	minimum value criteria used to select net pay
net pay factor	multiplying factor used to determine extra thermal pay above and below perforations, dimensionless
non-linear permeability	pressure-dependent permeability
oil-in-water emulsions	1-2 micron sized oil particles suspended in water
oil sands	formation sands which contain bitumen
overburden	sedimentary layers and formations above heated zone
perforations	blowing holes through the wellbore casing and/or into the reservoir using explosives to provide fluid or gas communication between the wellbore and the reservoir

permeability	conductivity/(reservoir thickness or fracture width)
phasing, 60°	perforations rotating downwards at 60 ° intervals around wellbore casing
Poisson's ratio	strain/stress (sometimes refered to as squish/squash), dimensionless
proppant	material used to prop fracture open
relative permeability	fractional flow to oil, water or gas in the presence of oil,water and/or gas
rich oil sand	oil sand with porosity > 30%, Sw of 30 - 50%
ring	boundary between cylindrical grid blocks
seismic cloud	seismic noise indicating multiple fractures spread over wide area near wellbore, upon injection of fluid
sensible heat	steam energy as a flashed gas
shallow reservoirs	reservoirs at less than 700 m depth
shear angle	angle of cohesion, about 35° angle from strain face
shear parting	breaking of formation rock by bending
skin, negative	well testing calculation of improved flow around the wellbore, dimensionless
skin, positive	well testing calculation of damaged flow around the wellbore, dimensionless
slippage, rock	slippage between fracture faces
slippage, formation	slippage between formation interfaces
slug size	cumulative steam volume (CWE) injection/ cycle, m^3
soak time	shut-in time immediately following steam injection, no flow-back
solution gas drive	production due to gas pushing the fluid
special core analysis	analysis of core other than Sw or So
steam flood	steam injection towards a production well
steam override	steam rise
steam quality	ratio of steam gas/condensed water (by CWE volume)
steam rise	segregation of steam upwards due to density differences
steam soak	another word for cyclic steam, or sometimes refered to as shut-in time between steam injection and production
steam zone	heated volume in reservoir occupied by steam as a gas

super heat	"dry" steam, with no condensed water
T-fracture	vertical fracture communicating with horizontal fracture above
tensile fracture	hydraulic fracture
thermal pay	productive pay from a steam injection process
tiltmeter	instrument used to measure formation tilt from vertical, micro-radians
tortuosity	resistance to flow caused by a sharp turn along a vertical fracture, usually towards a fracture trend
type curve matching	dimensionless curves in well testing fited over pressure data to determine permeability and skin
upstream weighting	interblock weighting of enthalpy for phase J to account for a hot water zone in front of the steam zone
underburden	sedimentary layers and formations below heated zone
water-in-oil emulsion	free water trapped in bitumen
weight% bitumen	weight bitumen/(weight oil + weight water +weight sand)
well cell	numerically converting the wellbore grid block into well casing (anulus)
wormholes	small flow channels created in oil sands due to formation sand production from bubbly viscous flow

Chapter 1

Introduction

The production response of an in situ oil sands reservoir to cyclic steam stimulation (*CSS*) is a strong function of the quality of the steam generated, the amount of heat injected, and the placement of the heat relative to the producing wellbore. Actual placement of heat where it is required is particularly difficult in the case of cold reservoirs containing bitumen with a viscosity of millions of centipoises (dead oil), as opposed to warmer California-type reservoirs with initial viscosities of less than 1000 cp. Amounts of heat injected are normally controlled by daily injection rates, measured as a cold water equivalent (*CWE*), through displacement in a piston pump at the front end of a boiler. Placing the heat economically at the wellbore perforations in a reasonable amount of time requires management of pressure drops and heat losses, which typically involves optimizing surface steam quality for the downhole completion.

Larger volumes of oil are produced by injected steam than by hot water injection (steam provides latent heat plus gas drive). The higher recovery by steam injection implies that superheated steam will produce more oil than lower quality steam. Several experiments were performed at the Alberta Research Council (1975-1981) using superheated steam on in situ oil sands and it was found that, for cyclic steam flood, superheated steam produced more bitumen than saturated steam. Most commercial oil field boilers cannot operate efficiently and deposit-free past eighty percent steam quality, thus actual bottomhole values can vary between zero and seventy percent, depending on wellbore heat losses when injecting through production tubing, the annulus, or manifolded through both tubulars. The only superheated steam field pilot the author is aware of is the ABC Pilot at Cold Lake, Alberta (about 1985). Superheated steam was made by dropping steam pressure at 80% quality into a heated separator, the resulting superheated steam was then injected down the insulated wellbore into the oil sands formation.

The most important parameter for successful production is the volume of bitumen that has been heated sufficiently to flow towards the production wellbore, and the distance the bitumen must travel to reach this wellbore. The volume of steam injected and bitumen heated is controlled by the heterogeneous flow and/or fracture characteristics of the reservoir, coupled with wellbore completion practices and the characteristic rapid rise of steam towards the top of the reservoir as time progresses.

Successful optimization of bitumen production rates from the total reservoir is ultimately decided by the operator's understanding of the reservoir in its original state and the positive and negative changes that occur in the reservoir upon heat stimulation. That is, reservoir characterization is the single most critical factor in attaining successful history matches and forecasts for optimization of the commercially operated processes. A poor description can terminate even the best-laid plans. The Wolf Lake project near Cold Lake, Alberta is a case in point. The project did not meet anticipated production capacities and was shut down due to an original overestimate of the exploitable oil-in-place. This problem was compounded by the failure to adequately account for the effect of formation heterogeneities (such as impermeable calcite streaks) on bitumen recovery.

A close analysis of the McMurray Formation near Fort McMurray, Alberta, has led to the conclusion that multiple shear fracturing plays a major role in steam placement (Leshchyshyn et al., 1994b). This theory is also confirmed for the Clearwater Formation near Cold Lake (Kry et al., 1989), with the suggestion the formation is fractured as a cigar shape with extensive shear fracturing adjacent to the single vertical tensile fracture. Shear fracturing, when subjected to well test analysis, identified itself as a "composite" reservoir with radial flow appearances (Leshchyshyn et al., 1994b). This has since been supported by well test analyses in other conventional oil reservoirs (Leshchyshyn et al., 1996).

Numerical modeling of steam injection into the Clearwater and McMurray formation reservoirs has changed over the years. Initially fixed vertical fractures with flow directly into the undisturbed reservoir were used (Todd, Dietrich, and Chase, 1979).

Later, vertical climbing fractures with formation compaction were included (in-house modeling performed by Petro-Canada, about 1990).

The general tendency is to use a radial flow representation (or an ellipse with a:b ratio less than 1:5), with the steam zone portion of the composite reservoir accounted for by increased porosity and/or permeability as a function of pressure. Previously, fracturing was accounted for by arbitrary upward modification of oil/water relative permeability curves. These curves have not been duplicated in lab tests on recovered cores. The upward shift was attributed to "fingering" (Dietrich et al., 1981).

This thesis will also use numerical modeling without inserted fractures but with radial flow to history match an eight-well in situ oil sands pilot (Primrose Heavy Oil Pilot: PHOP) to seven cycles of steam injection and production. The basic assumption is that steam placement into the oil sands reservoir is mostly radial, due to multiple shear fracturing away from the main tensile fracture.

Throughout this thesis, two types of fracturing will be discussed. Most people are familiar with hydraulic or tensile fracturing where a fluid, like water is pressured higher than the minimum stress of the rock causing it to part and propagate away from the wellbore (Howard and Fast, 1957). The other type of fracture is shear. All shear fractures are created dry, caused by bending of the rock and may be newly created from hydraulic fracturing, or may have been created thousands or millions of years ago as natural fractures and may be filled with any combination of fluids, gases or solid deposits. Hydraulic fluids can widen these shear fractures, making them act similar to hydraulic fractures with the possibility of fracture length extension.

At best, fracturing of any rock, shallow or deep-basin, is extremely complicated and beyond the analytical mathematics available today. As mine-backs of hydraulically-fractured rocks increase, more variations of multiple fractures are physically identified, and amazingly, not one mine-back has seen a "single" propagated fracture, upon which most rock mechanic theories are based (Warpinski et al., 1993). Even with the ability to identify such phenomena as dilation and multiple hydraulic fractures, theory will be constructed around the "bulk" nature of the rock rather than the individual crack properties and interactions in-between. As such, well testing will play an increasingly more important role in supplying reservoir data for reservoir modeling, especially numerical modeling, where bulk anomalies are much easier to integrate into the model in space and time.

This thesis is concerned with the practical aspects of fracturing and identifying the bulk nature of fracturing because it is not possible to make an exact model. To build a complete micro-scale numerical model would require the input of a team of experts dedicated to statistically solving the frequency, orientation, and azimuth of multiple individual fractures propagating from individual wells in individual reservoirs containing multiple heterogeneities in all three dimensions. The model must also contain the proper elastoplastic deformation theory such that residual, or permanent dilation, is accounted for and matched to actual field data. Such a model could then be used for conventional oil and gas fracture stimulation at least to depths of 2200 m. Experience indicates that below this depth additional theory is required to determine why fracture widths appear to be substantially reduced. One possibility is the fracture near the wellbore reduces in width, i.e., "***pinching***", while far field the fracture width is greater due to large forces on a plastic rock. The fluid flow models reported to date couple with a geomechanical model through pressure (water), temperature, and porosity. Porosity changes need to be identified as permeability changes but not in the conventional matrix sense since small fractures with high conductivity have been created (***pressure dependent leak-off***). Leshchyshyn et al. (1994) performed field tests in the McMurray oil sands which indicated the dilated zone permeability to water had increased from 1 md to 300 md with an approximate increase in porosity from 0.33 to 0.34 - 0.36. Also, total compressibility in the dilated zone increases by 1000 times. Settari et al. (1989) used pressure dependent permeabilities in his mathematical model to handle the above changes, but this function can and has been performed without coupling to a geomechanical model. The term "***compaction***" has been widely used in thermal models but is really "***reverse dilation***", as observed at Lake Maracibo in Venezuela (Farouq Ali, 1993).

Missing from all models to date is formation "***creep***". Similar to the movement of a lava river, it is possible, with long injection times, that the unconsolidated oil sands formation as a whole actually moves horizontally with permanent rock shearing at the upper and lower boundaries of the affected pay. Near Fort McMurray the measured formation shift was as much as 6 inches resulting in vertical wellbores being completely sheared. This leads to the conclusion that a single fracture may have a width greater than 6 inches. A combination of shear movement and dilation could eventually cause the entire overburden to collapse around the wellbore. Leshchyshyn et al. (1999) witnessed dilation in well test analyses and tiltmeters while performing massive sand disposal into the Mannville formation in 1996 near Lloydminster, Alberta. At the recent Fracturing Workshop in Houston, Texas in September 1997, it was experimentally shown that conventional reservoirs were exhibiting signs of creep during fracture stimulation jobs, therefore creep or residual fracture width, should be considered for even short injection times.

Considering all of the above mechanical factors, and assembling all the theory into a single model, one may find, in the end, that the older thermal reservoir models matched the end condition of the reservoir by incorporating "***fingering adjusted***" relative permeability curves, then accounting for all of the above discussed complications by using a bulk "***pseudo***" permeability curve.

1.1 Primrose Heavy Oil Pilot (PHOP) Project, Location and Well Spacing

The Primrose Heavy Oil Project (PHOP) is located in north-eastern Alberta at the north-west corner of the Cold Lake bombing range (Figure 1.1.1). The Project consists of 8 pilot wells arranged in a double inverted 5-spot pattern with 0.485 hectare (1.2 acre) spacing (Figure 1.1.2). A detailed log suite for PHOP pilot well IP1 is presented (Figure 1.1.3). The density-porosity log shows the oil sand coarsens upwards. A major calcite streak (general oilfield term used to describe shale containing calcarious type cementation or imbedment) is located just below the third set of perforations. A temperature log run after first cycle (shown at the far right) indicates that steam was trapped below the calcite streak. Only the two lower perforations accepted steam.

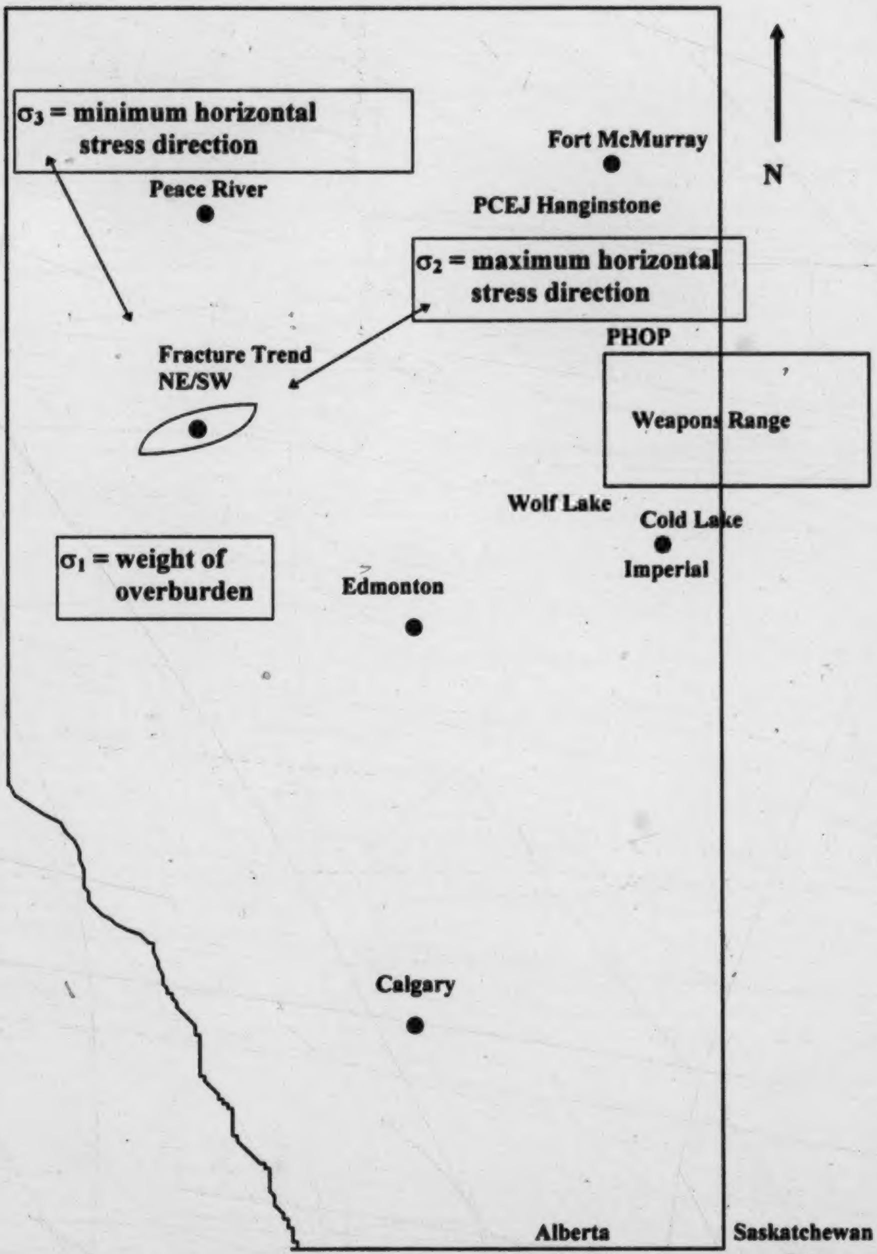
σ₃ = minimum horizontal stress direction
Fort McMurray
N
Peace River
PCEJ Hanginstone
σ₂ = maximum horizontal stress direction
PHOP
Fracture Trend NE/SW
Weapons Range
Wolf Lake
Cold Lake
Imperial
σ₁ = weight of overburden
Edmonton
Calgary
Alberta
Saskatchewan

Figure 1.1.1: Location of cyclic steam oil sands projects in Alberta, Canada, with fracture trend and rock stress directions

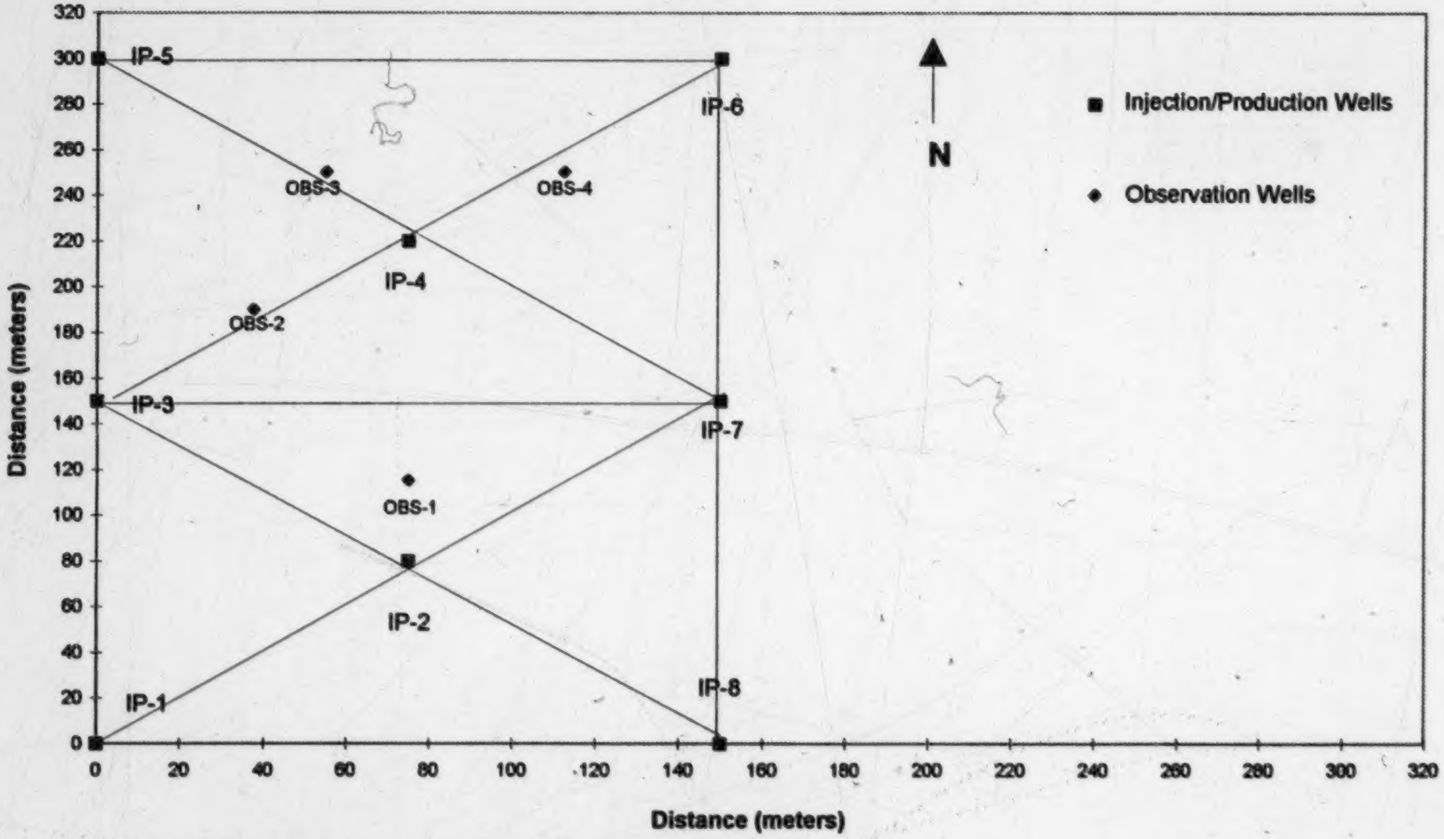

Figure 1.1.2: Primrose Heavy Oil Project (PHOP) Pilot well spacing

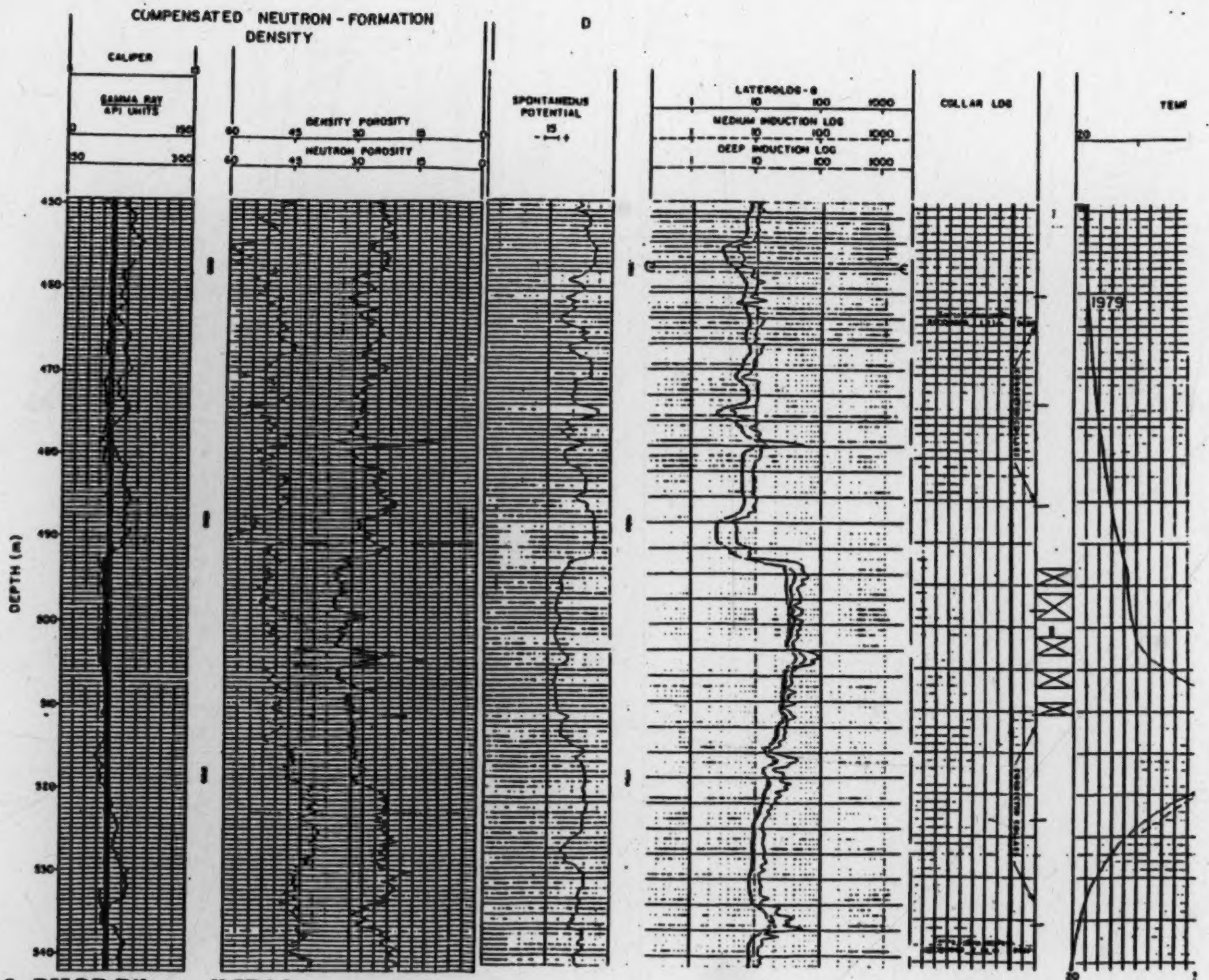

Figure 1.1.3: PHOP Pilot well IP1 log correlations

after first cycle (shown at the far right) indicates that steam was trapped below the calcite streak. Only the two lower perforations accepted steam.

The fundamental lithological unit for a typical well at the PHOP pilot, completed in the Wabiskaw formation contains oil sand separated by an indurated, impermeable shale or calcite layer (Figure 1.1.4). Discontinous shale streaks are also evident.

A fence diagram representing with reasonable acurracy, the relative location and number of shale and calcite layers within the boundaries of the Wabiskaw net pay, depict the complexity of the reservoir (Figure 1.1.5). The perforations for all wells except for IP1 were below the main continuous streak located near the center of the thermal pay.

The Wabiskaw Formation is stratigraphically a part of the Mannville Group from the early Cretaceous period. The other oil sands formations studied in this thesis are within the same group (Figure 1.1.6). The Wabiskaw Formation, a shallow marine environment, is underlain by the McMurray Formation, a deltaic fresh water environment, and is overlain by the Clearwater Formation, also a marine environment.

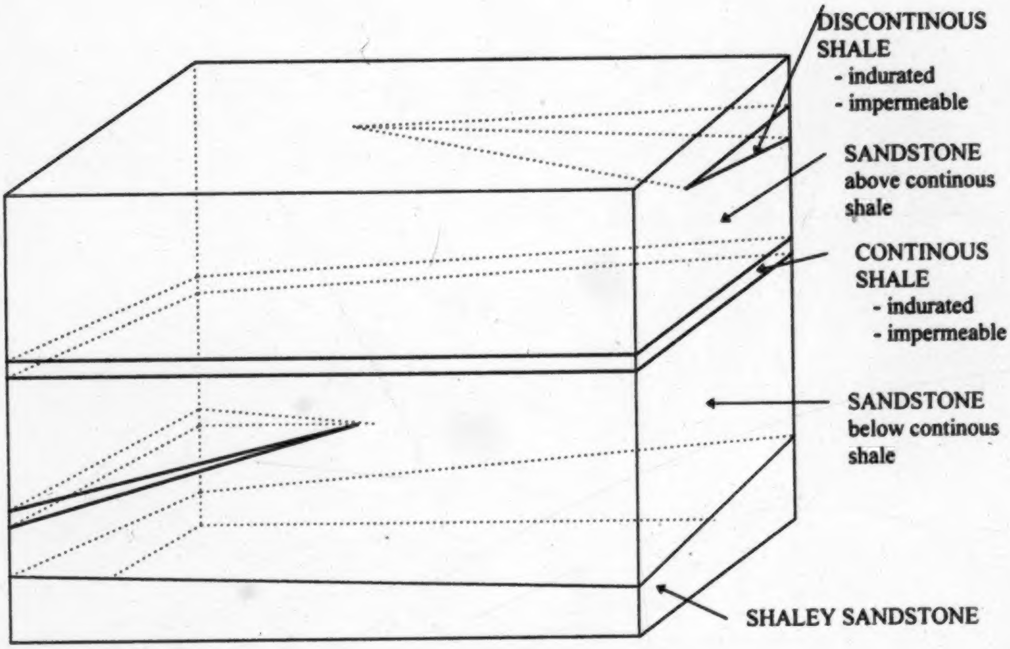
DISCONTINOUS
SHALE
- indurated
- impermeable
SANDSTONE
above continous
shale
CONTINOUS
SHALE
- indurated
- impermeable
SANDSTONE
below continous
shale
SHALEY SANDSTONE

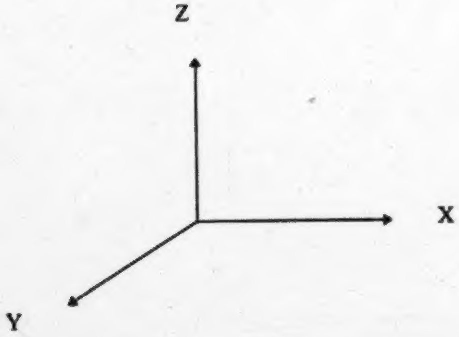

Figure 1.1.4: Fundamental lithological unit for the PHOP Pilot area in the Wabiskaw Formation (after Beadall, 1982, pers. comm.)

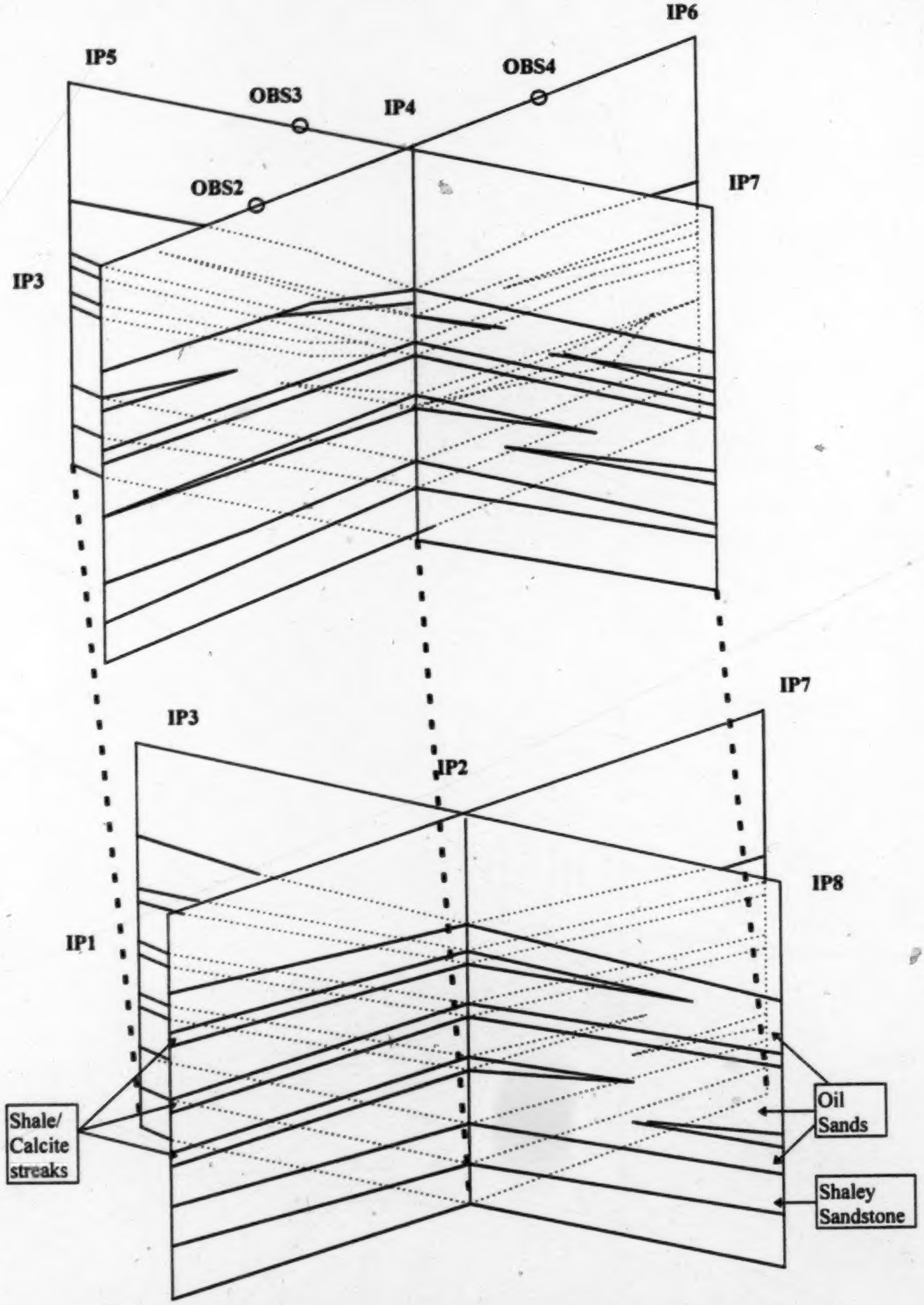
IP6
IP5
OBS4
OBS3
IP4
OBS2
IP7
IP3
IP7
IP3
IP2
IP8
IP1
Shale/
Calcite
streaks
Oil
Sands
Shaley
Sandstone

Figure 1.1.5: Fence Diagram PHOP Pilot (after Beadall, 1982, pers. comm.)

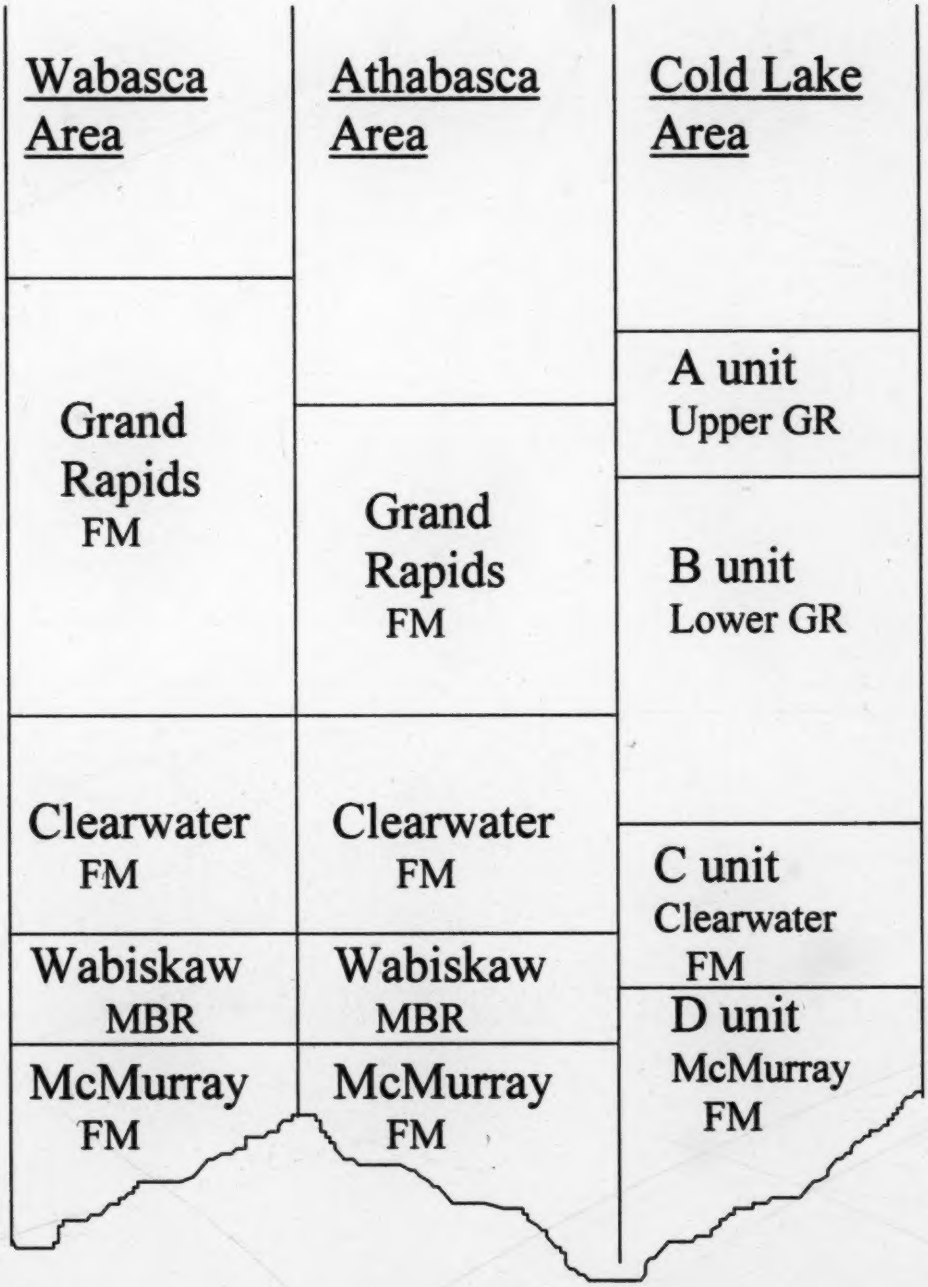
Wabasca Area
Athabasca Area
Cold Lake Area
Grand Rapids FM
Grand Rapids FM
A unit
Upper GR
B unit
Lower GR
Clearwater FM
Clearwater FM
C unit
Clearwater FM
Wabiskaw MBR
Wabiskaw MBR
D unit
McMurray FM
McMurray FM
McMurray FM

Figure 1.1.6: Stratigraphic columns for Wabasca, Athabasca, and Cold Lake deposits of the Lower Cretaceous Mannville Group, ref. Mossop et al, 1981.

Chapter 2

Literature Review

Review of the literature is centered around applications to cyclic steaming or steamflooding of oil sands using basic material balance calculations. Information is presented by year, as a historical compilation. Also reviewed here are the author's papers as a summary of his related work.

Literature on steam stimulation dates back to the 1950's. Matthews et al. (1956) introduced the concept of gravity drainage in depleted reservoirs. He modified the Darcy equation using density and gravity. As early as 1959, steam zone volumes assuming a radial heat balance were calculated by Marx and Langenheim. Migration and growth of the steam zone were limited by vertical losses and the steam injection rate.

Boberg and Lantz et al. (1966) considered oil recovery from a cylindrical reservoir based upon piston-like steam displacement to irreducible oil. Oil production was a function of average reservoir temperatures and gravity drainage was neglected.

Towson and Boberg et al. (1967) reported a model for gravity flow in cyclic steam stimulation where gravity drainage production rates were calculated as a function of steam zone size. To match field performance, they used the larger of the radial flow rate or the gravity drainage rate plus an adjustment in permeability.

Thermal efficiency was considered in 1969 by Mandl and Volek et al.. After vertical heat losses, extra steam becomes available to advance a condensation front. A heat front is then created ahead of the condensate zone.

Seba and Perry et al. (1969), studied a radial composite reservoir with flow from the outer partially-heated layer(s) including the steam zone. Oil production was represented by harmonic decline.

Haan et al. (1969) found that steam drive production from Venezuela oil sand was controlled by solution gas drive and compaction. He assumed a vertical steam front and suppressed compaction drive in the rest of the reservoir.

Wheeler et al. (1969) developed a heat transfer model for fractures that accounted for convection of energy in the fracture, conduction and convection in the pay sand, and conduction in the overburden. It was found that steam migrated out to about 40% distance along a fracture, the tip being at reservoir temperature.

Hearn et al. (1969) investigated the effects of both latent heat and sensible heat in saturated steam using the heat transfer theory of Marx and Langenheim.

In 1970 Kuo et al. solved for production by applying finite-difference simulation to Darcy's law for fluid flow in porous media.

Whitsitt et al. (1970) studied the effect of temperature on conventional fracture stimulation design. In hot reservoirs, cross-linked fluids used for fracturing would not be unstable during the stimulation job since most of the fracture fluid would be at temperatures much lower than the reservoir. Temperature transients away from the fracture face were developed.

Sinclair et al. (1971) identified that slow heat transfer effects permitted the use of low temperature rated fracture fluids as viscosities remained high. He suggested a pre-cooling operation before stimulating. By assigning friction loss over the fracture length, a pressure differential is created between the wellbore and the fracture tip.

Van Der Ploeg et al. (1971) presented equations for elliptical reservoir flow with a well located anywhere within its boundaries.

Abraham de Swaan O et al. (1972) introduced a simple numerical model to predict steam-soak (cyclic steam) production which considers heat losses in all directions. History-matching was done by adjusting the percentage of pay interval steamed. For gravity drainage reservoirs only, the entire pay thickness is considered. Optimum recovery was achieved using soak times above 800 days, which is impractical.

Calculations for rise of steam to the top of the reservoir was introduced by Neuman et al. (1975).

Williamson et al. (1975) showed an isothermal reservoir simulator could be used on steam soak processes. He criticized the use of a thermal numerical model for obtaining production correlation curves because the understanding of the process from the correlation is minimal. Instead, it was better to divide the reservoir into a near-well hot zone and far-well cold zone. The cold zone uses a standard black oil model consisting of one grid block (tank type, radial). The hot zone wellbore model is placed centrally inside this single grid block. Production is determined from the hot zone only once the distance to the boundary has been established.

Dietrich et al. (1976) compared the oil relative permeabilities of Stone I and Stone II three-phase flow models to core tests. Stone I is preferred for $k^0_{ro} < 0.3$, otherwise the use of Stone II is recommended.

Jones et al. (1977) presented a cyclic steam model useful for heavy oil gravity drainage reservoirs. Empirical equations were derived to increase oil production extra to gravity drainage.

Patel et al. (1977) designed a three-phase, one dimensional numerical model with radial flow. Well productivity indices (WPI) were used for the first grid block. Heat was transferred to the overburden and underburden.

Dykstra et al. (1978) provides an historical account of gravity drainage (e.g. discussions of Katz in 1942 and improvements on the studies of Cardwell and Parson, 1949). Results showed that high recoveries could be obtained where gravity was an important part of production.

Prats et al. (1978) stated cyclic steam injection has both elements of stimulation (water replaces oil) and recovery processes (reduced viscosity). A table of the effects of various parameters is presented.

Buckles et al. (1979) introduced findings from fifteen years of steam stimulation at ESSO's Cold Lake cyclic steam project. He stated fractures were created by steam injection and were oriented in the northeast-southwest direction as determined by interwell communications. The fracture gradient is about 17 kPa/m indicating initial vertical fractures. He also describes the Clearwater Formation as being 75% non-quartz, thereby differentiating from the McMurray which is 85-95% quartz. Flow problems due to migration of fines or clay swelling were not observed, most likely due to the high permeabilities to water. It was also noted, that because of the presence of significant amounts of feldspar, chert, volcanic and other minerals, core analysis for bitumen content was far more accurate than log analysis. The net pay cut-off was 6% bitumen. About 12-15 m of the average 45 m thickness is perforated. The average life of a well is six or seven years with 20% recovery of 1.6 hectares (4 acre) spacing.

Grabowski et al.(1979) developed a general-purpose finite-difference model for in situ combustion and steam flooding that was fully-implicit and had finite difference solutions. Upstream weighting was used to improve the shape and movement of the condensate bank.

Grant et al. (1979) looked at the compressibility and hydraulic diffusivity of water-steam flow. He derived a total compressibility equation that included flashing of steam.

Settari et al. (1979) investigated early fracture theory as it related to fracture initiation, orientation, and propagation in oil sands. A Geertsma and de Klerk orientation is assumed. Elastic properties of the rock determined the fracture width. The fracture model and reservoir model are coupled using mass balance equations for single-phase flow only.

Shepherd et al. (1979) made empirical plots of ESSO Cold Lake data by finding best fits of calendar day oil rate (CDOR) versus cumulative oil at mid-cycle. Three types of wells were identified: (a) Type I, a regular well leading to 5m^3/d rate at 30,000 m^3 bitumen production. The reservoir is clean and perforations are low in the reservoir; (b) Type II, some tight streaks are present or the perforations are high, production decline is steeper; and (c) Type III, interwell communication is involved. Shepherd observed that CDOR increases with increasing steam cycle size, the oil rate declines to a common point, and data scatter is significant.

Gomaa et al. (1980) produced correlations for predicting oil recovery by steamflood. He used a 4-layer numerical model to generate graphs of oil recovered versus heat injected, steam quality, reservoir thickness, net/gross ratio, and initial mobile oil saturation.

Vinsome et al. (1980) derived a simple 2-parameter method (p, q) for calculating a temperature profile in the overburden and underburden. Data required for the computation are the temperature at the interface and the thermal diffusivity of the rock.

Mar and Leshchyshyn et al. (1980) used large scale lab tests on cyclic steaming of oil sands with various additives in the steam to demonstrate that emulsions do not form in the reservoir during steaming. It was shown that all the previous emulsion samples taken during lab testing were created after the production control valve where steam was flashed. Visual and physical samples taken before the valve showed separate phases of clear water and bitumen. With the aid of tracer analysis, "condensed steam" was found only in the bitumen (as a result of diffusion and solubility). A true emulsion of oil-in-water was produced only after introducing significant caustic with the steam. Temporary emulsions were formed when surfactants were used as steam additives.

From 1981- 85, Butler et al. modeled the physical and analytical character of gravity drainage in horizontal wells. Directional well placement, when practically applied, increased bitumen recovery from 20% in conventional cyclic steaming to 40-55% using horizontal well pairs. This method, like most analytical methods, employed an empirical constant necessary for history-matching production. As the equations were improved, the value of the constant approached unity.

Through thermal numerical simulation, Dietrich et al. (1981) determined that K_{rw} curves used in history matching are much lower than those derived in lab tests. Also, K_{rw} is higher on injection than production due to micro-fracturing, which results when effective stresses decrease due to formation dilation. The lower K_{rw} effect on production can also be attributed to free gas which partially blocks water permeability.

Meldau et al. (1981) provided field data from a California reservoir that indicated injecting air down the tubing to mix with injected steam doubled oil production during three cyclic steam stimulations.

Rubin et al. (1981) presented analytical solutions for fracture length and width. The flow velocity of fluid penetrating the formation is determined as part of the solution rather than being specified as an input coefficient to the classical fluid leak-off model. This treatment increases the fracture length and reduces fracture width.

Settari et al. (1981) built a 2-phase model for fracture analysis. The idea of T-fractures was supported by his theory. Fractures were aligned on the NE-SW fracture trend existing in Alberta. Field data show most fractures are vertical. The model could represent a single vertical fracture, two perpendicular vertical fractures, or a horizontal fracture. However, dilation could not be handled.

Walsh et al. (1981) developed a thermal injection well fall-off testing method from conventional buildup analysis, to determine the conductivity and volume of a steam swept zone. Slopes from Cartesian and semi-log plots were used to determine permeability-thickness, swept pore volume, and swept bulk volume. The steam-zone compressibility is also calculated. It was assumed that due to the high mobility contrast between the steamed zone and the rest of the reservoir, the steam front behaves as an impermeable boundary.

Ershaghi et al. (1983) used graphical methods to estimate cumulative production as a straight line using a log-log plot of cumulative oil production versus cumulative steam injected. The technique described is equivalent to a plot of cumulative heat injected versus cumulative oil production. Unfortunately, these graphs assume the production cycle is carried to its logical end, where all the heated bitumen returns to the wellbore, disregarding wells shut-in due to interwell communication, sand plugging of pumps, or steam lost to the overburden.

Mehrotra and Svrcek et al. (1982) developed correlations for solubilities of gases in bitumen (CO_2, CH_4, N_2), with temperature. Steam injection with gas additives can increase oil production by as much as 100%.

Pang et al. (1982) applied the hysteresis effect for the mobile water zone to model cyclic steaming. No fracturing was involved. The hysteresis was correlated to an increase in capillary pressure and pore size due to pressure increases. Without hysteresis, oil production was too low and water cuts too high. It was found the contact angle of the wetting phase was two times larger during injection (imbibition) for two-phase flow in a capillary tube.

Schmidt and Leshchyshyn et al. (1982) measured the diffusion of CO_2 into bitumen to determine the importance of the diffusion process in numerical simulation. The author performed such experiments in the lab at room temperature and 200 °C. Results indicated that after one month, the CO_2 had diffused about 15 cm into the bitumen and the concentration versus depth was a function of the molecular concentration of CO_2 at the surface of the bitumen, being less at higher temperatures. Because diffusion was so slow, its effects were omitted in numerical simulation of lab tests, which were mostly of one day duration, or even in the field where steam injection normally lasted about one month.

Smith-Gowan et al. (1982) provided data and equations for the specific heats of sand and bitumen with temperature.

Svercek and Mehrotra et al. (1982) tabulated viscosity and density data with the gas solubilities for Athabasca bitumen.

Ayelotte et al. (1983) presented a more detailed heat balance by dividing the reservoir laterally into six regions at the steam front.

Van Lookeren et al. (1983) analyzed linear and radial flow with steam override.

Gontijo et al. (1983) developed a cyclic steam model comparable to Jones' (1977), which includes most of the heat losses plus production due to pressure drop and gravity drainage. This method also incorporates an empirical constant in the rate calculations.

Ito et al. (1984) discussed micro-channeling (sand deformation) and its application to the numerical simulator. Micro-channeling was open on injection and closed on production. He also noted an increase in pore pressure during second cycle injection due to bitumen plugging. A similar observation is made by the author in this thesis. Ito used four parameters to model the micro-channeling: 1) a mobility multiplication factor (pressure dependent leak-off); 2) energy dispersion (super upstream weighting factor); 3) non-linear porosity change (pressure dependent); and 4) inaccessible pore volume (***IPV***), resulting from poor contact between the injected and produced water.

Ben-Naceur et al. (1985) developed models for heat transfer in hydraulic fracturing. He divided the fracture length into elements with temperature change along the fracture then calculated a 2-D temperature distribution

In 1985, the team of AOSTRA and BP evaluated the commercial feasibility of the Wolf Lake area. The concept of grain weight oil was used to construct net pay contours and bitumen reserves. Agreement between logs and cores appeared good. Unfortunately, the lower range of grain weight was not correlated properly with actual lithological layers and shale accounted for as much as 30% of reserves. The errors leading to overestimation of recoverable reserves is discussed later in this thesis. A seven-cycle steam injection-production forecast was also presented.

Chew and Leshchyshyn et al. (1985) designed a method for using capillary pressure from multiple core analysis to determine an average ***SWIR*** for numerical simulation permeability curves. Data was first adjusted from lab conditions to field conditions using shifted J-functions, correcting for interfacial tension, wetting angle, permeability to the flowing phase, and porosity. Because the ΔP for capillary pressure in the model is fixed for each layer at ± 1 psi (total 15.6 kPa) with the model layer thickness not exceeding 4 m, the ***SWIR*** must be selected from the adjusted capillary curve at the 1 psi value on the y-axis. The result is a general shift of ***SWIR*** to the right on the x-axis. This moves the entire ***KRW*** permeability curve to the right, making it more difficult to inject and produce water, which is consistent with field results.

Miller et al. (1985) introduced a simple gravity override model for steam drive. The model uses an "effective" steam condensate zone size to predict oil production. Recognizing the component of heat loss to the overburden and underburden as postulated by Mandl and Volek et al. (1969), steam rate is optimized by applying just enough steam to sustain these vertical conduction losses plus an extra amount for expanding the steam zone laterally. The steam zone does not move in this model as 100% areal coverage from the gravity overide is assumed starting from some lag time.

Dietrich et al. (1986) performed numerical thermal modeling of both horizontal and vertically fractured reservoirs using a fully-implicit, finite-difference representation. He concluded that the important mechanisms during fluid loading and unloading of induced fractures are thermal expansion of tar oil, counter-current imbibition of water and oil caused by capillary pressure effects, and fracture compressibility. Dilation of the formation was introduced as "thin zones or micro-channels of highly-permeable, unconsolidated elastic material formed by pressure parting".

Kumar et al. (1986) modified the Miller and Leung gravity override model to match ESSO Cold Lake data. This variation involved top-down steam heating by conduction. A time lag was necessary for the first year, likely for the development of the steam zone, and a factor of 1.2 was applied to the permeability. A capture factor for spacing of 0.7 was also required. This model was in good agreement with ESSO's numerical simulator results.

Nakornthap et al. (1986) investigated temperature-dependent relative permeabilities. It was found that as ***SWIR*** increases and ***SOR*** decreases with temperature, the reservoir becomes more water-wet. He further concluded that the absolute permeability to water decreases with temperature.

Arthur et al. (1987) represented a fracture by an elliptical formulation. Heat was transferred across the fracture face into the reservoir, first by the frontal advance of a condensate, then by steam. Stored energy from the previous steam injection cycles were added to the next cycle. The energy accumulation showed no significant improvement over analyzing each cycle on a stand-alone basis. Arthur did not include any dilation in the steam zone. The model was designed to operate on BP's standard numerical simulation model as a subroutine.

Biot et al. (1987) developed a graphical relationship for the convective temperature distribution from a fracture having crack growth leak-off. He generated a plot to estimate the temperature at any distance along the created fracture length. The graph shows the last

40% of fracture length is usually at reservoir temperature if a lower temperature fluid is injected through the wellbore.

Chhina et al. (1987) studied hot gelled water and coloured cement grout as a fracturing fluid in the McMurray Formation near Fort McMurray, Alberta, at 300 m depth to determine fracture geometry. The gelled fluid injection created a vertical fracture. The first grout fracture appeared vertical and the second was observed possibly horizontal. With a 19.5 kPa/m frac gradient measured, and the weight of overburden at 22.5 kPa/m, the latter was likely still vertical. Post fracture cores were drilled. The cement-filled fractures were near vertical at about 85 degrees. The grout bypassed small clay breccia rather than fracturing through them. In addition, small hairline shear fractures were seen but contained no grout. Chhina also postulated some of the fractures might have been in the form of fingers.

McGee et al. (1987) formulated an analytical method for cyclic steam stimulation through vertical fractures, an extension of Wheeler's and Carter's model. The program assumed that all steam was produced during each cycle and leak-off was inversely proportional to the square-root of time.

Meyer et al. (1987) provided an analytical means to calculate heat transfer from the fracture face into the reservoir as well as along the fracture.

Mehrotra and Svrcek et al. (1988) framed their estimation of gas solubility in bitumen around the Peng-Robinson Equation-of-State (***EOS***), then compared the calculated data to lab results. Gas-mixture derived from the ***EOS***-based model were only slightly higher than information obtained in the lab.

Mukherjee and Economides et al. (1988) compared the productivity of horizontal and vertical wells. They concluded that horizontal wells do not outperform a vertical well with vertical fractures. However, horizontal wells are better for fractured formations.

Pethrick et al. (1988) discussed numerical modeling of cyclic steaming in Wolf Lake Clearwater Formation oil sands. A single permeability curve and the same fracture length was used for all cycles. High transmissibilities were assigned on the fracture trend.

Bitter and Leshchyshyn et al. (1989) re-worked a method for the Wolf Lake Project that Leshchyshyn previously developed for the PCEJ project and presented as a technical paper in 1991. Cyclic steam injection was analyzed in real time to determine fracture growth and interwell communication. Only one of the two graphs generated was shown here. Entitled "***Fracture Growth***", the plot was derived from a calculation of fracture length using a modified Carter equation. The correlation of fracture length versus cumulative steam injected enabled the identification of fill-up, relative fracture length, rate of fracture growth, and interwell communication. Some good examples of interwell communication were noted in the Wolf Lake data.

Leshchyshyn et al. (1989) modified a standard temperature logging tool for improved response in sticky bitumen conditions. A procedure measured stabilized temperatures at specific depths using stationary stops. Importantly, the system proved that during cyclic steam stimulation, fracturing and hence heat was contained by thin layers of shales or calcite streaks within the pay zone. Previously, logging tools recorded data while moving slowly in or out of the hole and "smeared" the results, giving the impression that steam really had fractured past the impermeable streaks.

Svrcek and Mehrotra et al. (1988) established a one-parameter generalized correlation with less than 6% deviation for estimating bitumen viscosity at various temperatures. Only the value of the constant, b_1, required a change to characterize different reservoirs.

Settari et al. (1989) introduced dilation in his fracture model. He developed non-linear compressibility and flow properties as a function of pressure, stress, and temperature. Shear failure occurred which affected porosity. A failure zone extended along the fracture face and for a few meters into the reservoir.

Souza et al. (1989) calculated heat losses to the overburden using a composite analytical-numerical method.

Tortike and Farouq Ali et al. (1989) derived functional correlations of saturated steam properties which met the accuracy requirements of fully-implicit thermal simulation. The properties included viscosity, thermal conductivity, density, and specific enthalpy. All values are accurate only within the steam-saturation envelope.

Gajdica et al. (1990) presented a semi-analytical thermal model for linear steam drive. Although the model is 1-D, a steam zone, water zone, and oil zone are accounted for. Pressure drop calculations at the well and through the steam zone were presented. Good matches to thermal numerical models were possible except for length to height ratios less than unity. The FORTRAN program is available from Gajdica.

Fialka et al. (1990) looked at changes in mineral composition in post-steam cores taken from the Wabiskaw formation near Primrose, Alberta. There appeared to be an overall reduction in horizontal permeability. Dissolution of feldspar contributed to an increase in clay content. Kaolinite was converted to smectite and illite. Calcite layers prevented the rise of steam to upper or lower layers.

Leshchyshyn et al. (1990) presented and described examples for estimating effective permeability to water in the Athabasca oil sands using well test analyses. He designed and used a simple bottomhole shut-in tool that removed most of the wellbore storage and allowed better type-curve fitting. Mini-frac design and analysis was also introduced. It was found that while the Nolte analysis gave reasonable values for leak-off, fracture length and width when compared to Settari's model, neither the model nor the Nolte calculation agreed with the actual fracture closure time. It is suggested that fingering, now related to shear dilation, can occur above hydrostatic pressure but below fracture closure pressure or minimum horizontal stress.

Reis et al. (1990) studied fractures induced during cyclic steam injection in California formations. Multiple fractures were generated horizontally in shallow, unconsolidated sands up to 600 feet and vertically in deeper wells up to 1100 feet, but fewer in number. If injection pumps went down, a new fracture was usually initiated in a different direction. A band of a given width, normally about 4 feet, of a production interval through the wellbore and into the reservoir, was used for history matching.

Soliman et al. (1990) conducted field mini-frac tests to show deviated wellbores generate fractures in steps with rough edges as the fracture initiates perpendicular to the wellbore, then turns into the fracture trend.

Beattie et al. (1991) used numerical simulation with dilation and history-dependent recompaction, along with water-oil relative permeability hysteresis to history-match Cold Lake Clearwater cyclic steam production. He succeeded in using actual lab-derived permeability curves for imbibition and drainage as the boundary limits for curve shifting.

Boone et al. (1991) showed that poroelastic effects could increase formation stresses by 1-2 MPa by comparing field microfrac tests' instantaneous shut-in pressures (***ISIP***), to those measured after high-rate injection. This characteristic behavior is the operating basis for Cold Lake's "mega-rows" which bring reservoirs from a state of vertical fracturing to a state of horizontal fracturing before steam is injected into the adjacent row of wells. Production performance is thereby enhanced.

Denbina et al. (1991) stated that the key reservoir drive mechanisms in the early cycles of steam stimulation at Cold Lake is mostly formation compaction, followed a distant second by solution gas drive and fluid expansion. Gravity drainage accounted for very little of the oil produced in the first two cycles but increased in importance in subsequent cycles. The author of this thesis has observed similar results which warrant use of a single layer numerical model. Denbina's modeling required both relative permeability hysteresis and deformation to history-match. Kumar (1992) concluded that up to 15% less oil is produced due to near-wellbore gravity segregation. There is both a heat and mass redistribution.

Leshchyshyn et al. (1991, JCPT 1994) used post core analyses from core samples surrounding a cyclic single well test near Fort McMurray and completed in the McMurray formation, to determine the steam flow path. For the first time, shear fractures were identified which appeared to be plugged with bitumen, possibly on oil-wet rock. Clay analysis indicated most of the bitumen was produced from the shaley oil sands above the net pay, suggesting a climbing vertical fracture from the perforations at a 45° angle, then a possible horizontal component just below the shale-oil sand interface. The geometry and orientation are indicative of a T-frac. Resaturation of cores with bitumen is evident. An FMS log run open-hole during the drilling of the coreholes that showed vertical fractures along the wellbore up to 10 m high. Most of these fractures were discounted by the author as being attributed to the drilling mud since vertical fractures were not seen in the cores. This did show nonetheless that vertical fractures may be created in a heat-stressed environment. Production samples and cores were analyzed using cryogenic SEM (Munoz/CANMET 1990); very few oil-in-water emulsions were seen, and of those none were observed as true emulsions. In situ surfactants were identified. The production sample was characterized as a water-in-oil emulsion with free water. All analyses were compared to the temperature logging which underlined the need for multiple analysis procedures to ascertain where the steam and bitumen has gone.

Leshchyshyn et al. (1991) introduced the "Hall" plot and the "fracture growth analysis" plot with application to the PCEJ cyclic steam process in the McMurray oil sands. The Hall plot is cumulative steam injection pressure versus cumulative steam injection rate, cold water equivalent (CWE). Changes in permeability or leak-off are represented by changes in slope. The point of intersection of the two straight lines corresponds to the steam "fill-up volume" prior to fracturing the oil sand, starting with cycle two. This fill-up volume increases with cycle number. The fracture growth plot is calculated fracture length versus cumulative steam injection rate (cumulative ***CWE*** volume). Fracture length begins at the "***fill-up volume***" and increases to the end of the injection period. Further discussion of this procedure is presented later in the thesis. A direct correlation was shown between the "***fill-up volume***" and the cumulative depletion index (DI) for the various steam injection/production cycles. The Hall fracture slope or the fracture growth slope and the oil/steam ratio (***OSR***), also followed a direct relationship. The longer the fracture, the larger the ***OSR***, to a maximum. An upper limit however, was not seen in the data. Simulated fracture lengths for Wolf Lake could be matched exactly for various steam injection rates and slug sizes using only the simple fracture length calculation introduced here.

Scott et al. (1991) geomechanically tested oil sands cores to determine how permeability is affected by pore pressure, shear stress, and temperature. He found that increases in pore pressures decrease the effective confining stress and cause an unloading of the reservoir. Hence shear fractures result in a net increase in reservoir pore volume and permeability. The volume expansion is higher at lower confining stresses, associated with shallower reservoirs. Permeability increases more rapidly from pore pressure increase than from less stress, at shallower depths. Permeability increases with temperature at shallow depths but the relative change diminishes at increasing depth.

Tortike and Farouq Ali et al. (1991, AOSTRA 1987) developed a numerical model with geomechanical capability for steaming of oil sands. Shear parting or dilation was accounted for using combined elastic plus plastic strain. A difficult task, the model coupled the reservoir to the fracture model. A comparative study of the Athabasca and Cold Lake reservoirs indicated that the Athabasca oil sands was more stiff and displayed dilatant behavior while the Cold Lake oil sands were softer and had contractile characteristics. The pore pressure of the Cold Lake oil sand remained fairly constant during geomechanical testing; the Athabasca oil sands showed a substantial pore pressure reduction. Behaving more like shale, the Cold Lake oil sands had a higher Poisson's ratio.

Van Wunnik et al. (1992) created a gravity drainage model for a reservoir undergoing top-down steam injection through the gas cap. Calculations included mixing of the steam and hydrocarbon gas, temperature distribution in the cap rock and reservoir, plus oil production by thermal expansion and gravity drainage. The model was designed for a densely fractured chalk dome.

Vogel et al. (1992) compared the concepts of steam-drive versus gravity drainage. Under steam-drive, a reservoir yields most of it's production prior to heat breakthrough. The opposite occurs during gravity drainage whereby most oil produced is after heat breakthrough.

Closmann et al. (1993) presented a simplified gravity drainage oil production model for mature steam-drives. The steam completely overlies the reservoir like a hot gas cap. As the interface moves downwards, the location and velocity of the boundary is calculated which then determines production rates. Absolute permeability is adjusted for history-matching. Accuracy is within an order of magnitude.

Gallant et al. (1993) derived a graphical method used by ESSO Cold Lake steam injection operators to determine when, during multiple cycles, fill-up has occurred and the reservoir has started fracturing. A knowledge of timing is important since most oil is produced from fracturing and not fill-up, therefore substantial fracturing must occur during each injection cycle. The “***Steam Injectivity Index***” $SI = (P/9300 + 6Q)$, has a value of unity when fracturing occurs. This thesis has presented two different methods for the same purpose. In a study of the PCEJ Project (see Leshchyshyn et al., 1991), the two curves were denoted “***Hall***” and “***Fracture Growth***”, plotted on the same graph. All the above methods were used to identify interwell communication. Gallant also discusses the work of Vittoratos and his in situ emulsion model.

Leshchyshyn et al. (1994) applied well testing to estimate the amount of dilation from fall-off data in a hydraulically-fractured McMurray oil sands well. An isolated newly drilled well was tested both below and at fracture pressure to determine the distance to the edge of the dilated zone. Permeabilites of 400 md and 0.91md in the dilated and original zone, respectively, were used to back-calculate the storage capacity or $\varnothing c_t$ product in the dilated zone. Distance to the boundary was computed using three different methods that gave a value of 5-8 m. A material balance calculation for increase in porosity due to dilation yielded a value of 0.2-2%, depending on whether the true fracture height was 16 m or 8 m. Of interest, thermal numerical modelers used a value of about 3% or less to match bitumen production and close to 300 md in the dilated zone. The minimum stress in the Settari fracture model, was initiated to the closure value of the shear fractures to obtain a proper fall-off pressure match. The closure gradient was at 13.8 kPa/m, lower than the expected value of 15 kPa/m for a single tensile vertical fracture. The picked value for the tensile fracture closure gradient was 15.1 kPa/m. These values were selected before the author of this thesis had gained the sandstone fracturing experience he has now and before semi-log derivative plots were used in commercial well test software packages. Rework of the data using the software packages have affirmed his previous analyses.

Miller et al. (1994) questioned Unitar's definition of immobile bitumen as being oils having viscosities greater than 10,000 mPa.s at reservoir temperature. He states a number of Canadian oils with higher viscosities can be economically cold-produced. Horizontal wells have increased cold production in Saskatchewan and south-eastern Alberta. The requirements for cold production are: 1) sufficient oil mobility for cold production from rod-pumped vertical wells; 2) enough solution gas for beneficial bubbly flow; 3) sufficient geological data to develop an accurate drilling strategy; 4) no extensive tight streaks; 5) a large enough pay zone to ensure the well is drilled on target without going into under/overburden; and 6) oil properties on the light end of the heavy oil spectrum. Progressive cavity (***PC***) pumps have been modified to produce up to 50-60% sand cuts and 1000 m^3 sand volume. ***PC*** pumps can produce foamy oil. Large-hole perforations are used with no sand control. Oil production is supposedly through "wormholes" created when the sand is produced.

Leshchyshyn et al. (1995) attempted to calculate the correct $\varnothing c_t$ product of a formation for reasonable estimations of distances to boundaries and for improving model studies. With greater confidence, he could use this correct value of $\varnothing c_t$ as a starting point for back-calculating a new value for $\varnothing c_t$ in a dilated zone around the wellbore. This was accomplished by providing a coupled well test analysis technique for obtaining better accuracy in permeability values and using type-curve matching of dimensionless time to back-calculate $\varnothing c_t$. The true r_w is unknown, but provided the same value for r_w and permeability is used in subsequent calculations for the same test on the same well, it is inconsequential. Furthermore, should the reservoir pressure be known before well testing, a pressure value at time, t_p, at infinity will assist in type-curve matching.

Tamim et al. (1995) used a single fracture for steam injection with elliptical heat distribution and linear flow of oil to the wellbore.

Leshchyshyn et al. (1996) showed through well test analysis of minifracs in sandstone reservoirs throughout Alberta (especially reservoirs in the Mannville Group), that dilation can occur at any depth and can affect conventional oil and gas fracture stimulations. Hence oil sands fracture theory could be extended to any sandstone reservoir that is mostly quartz. This statement is supported by work done in the geothermal sector over the last 50 years, and more recently by the progress of geomechanics understanding as told by Narayan (1998).

Leshchyshyn et al. (1997) compared the fracturing of a vertical, deviated, and horizontal gas well in the Glauconite Formation of central Alberta. The wells were directionally drilled into a pool around and under a lake. Multiple fractures were reported as being created in the deviated and horizontal wellbores. The observation has not been investigated by the author insofar as determining the effects of cyclic steam stimulation of deviated wellbores in oil sands, but he believes the same phenomena would occur. This suggests that a fractured deviated or horizontal wellbore should produce more bitumen than a vertical one. Also, it is believed most fractures develop perpendicular to the deviated or horizontal wellbore, then turn into the fracture trend. This sharp turn can cause sand-off in conventional fracture treatments. It has been found from field practice that to wear down the bend, a 100 kg/m^3 concentration of proppant must be mixed throughout the pad, before the main proppant ramp to 600 kg/m^3 plus a 600 kg/m^3 hold stage. Such a design has been 100% successful to date, the required proppant being placed without sanding-off.

Narayan et al. (1998) explains shear dilation from the perspective of the geothermal community of the world and applies the developed theory to oil fields in the U.S. and Japan. Not suprisingly, observations made on geothermal sands are very similar to those made on the McMurray oil sands, the reason being that quartz is the major mineral in all the reservoirs discussed. Noteworthy is the statement that shear fracturing or dilation can occur at pressures below the minimum in situ stress. Narayan includes a discourse on mathematics which thus far appears most relevant to dilation propagation. Seismic clouds reveal that a fracture test in situ can initiate 100 to 20,000 events, a magnitude not normally encountered in a single tensile fracture. In addition, seismicity does not generally occur in an already stimulated zone until the reservoir volume of the previous injection is exceeded. The lack of seismic activity is caused by rock slippage creating an effective, permanently open fracture. The harder the rock, the greater the roughness of the fracture walls, and the greater the dilation. Less pressure is required to initiate a shear fracture as the difference between the minimum and maximum horizontal stresses increases. The larger the shear dilation angle the greater is the increase in permeability.

Farouq Ali et al. (1998) provides a comprehensive summary of cyclic steaming at the international level. He explains that the ratio of applied energy between sensible and latent heat makes a difference to recovery and, that dilation, associated with spongy rock, as well as trend-steaming are critical factors in steam recovery processes. He asserts that there is an outstanding 80% of the oil reserves left to recover, so the extraction problem is still not solved.

Leshchyshyn et al. (1999) analyzed work performed in 1996 and 1997 in La Habra, California and near Lloydminster, Alberta which disposed of waste sand by fracturing into permeable reservoirs, mostly water sands having a permeability of up to 1000 md to water. Sand volumes as high as 200 m^3/day were placed daily in a single well, to total volumes of 30,000 m^3. Major dilation of the Mannville Group formations in Alberta was identified by well test analysis and tiltmeters. The process was difficult to history-match using 3-D fracture modeling. It is possible that the small size of the waste sand (average 100 mesh), plus the tendency of fines less than 100 mesh to plug pores and reduce fracture leak-off, contributed to the placement of the large volumes of sand.

2.1 Discussion:

The semi-empirical model proposed for this thesis is predicated on a set of correlation curves generated from a sophisticated numerical thermal simulator with scope of application to the first cycle only and without capability for gravity drainage. A single layer with radial grids or rings is the chosen grid system. A detailed reservoir description is used, which for the pilot project under study, does not render 100% vertical efficiency. The performance of the remaining cycles is derived from the same correlation curves coupled with a graphical multiplication factor that is applied to production empirically based on field data from various reservoirs.

With the exception of Tamim (1995), none of the methods outlined above have the capability for directly analyzing steam entry into the formation through fractures or fracture systems. The accuracy of these models is not affected by omission of fracture mechanisms. Rather, this thesis will indicate that combined tensile and shear fracturing can be accurately described with the same radial geometry which incorporates an empirical modification to old relative permeability curves.

While knowledge and experience with the geomechanical character of the McMurray and Wabiskaw oil sands has been enhanced by the work of Scott et al. (University of Alberta, 1989), there are some questions regarding the conclusions drawn from this study. Geomechanical properties have been generated by Scott from actual oil sand cores supplied through affiliation with PCEJ. Although the samples were considered relatively competent, they were subjected to gas expansion with associated cracking of the rock, on the trip out of the hole. Also, the samples represented a mere 10% of the total vertical reservoir. These were the only consolidated core of the total length of core taken, able to fit the test apparatus used. The more unconsolidated core, which represented the reservoir actually contacted by steam taking the path of least resistance, was too shear-fractured to collect properly, contained too many shale streaks, or was too varied for consideration as a homogeneous sample, and was therefore not used. Poisson's ratio was estimated at 0.33 from well test analysis and 0.40 from open hole stress log analysis (dipole sonic), but was only 0.25 as measured by Scott. Although a confined, homogeneous, quartz sandstone core anywhere in Alberta below 800 m will give a Poisson's ratio close to 0.25, it is believed the higher values are more accurate due to the unconsolidated and hence, unconfined nature of the bulk of the oil sands. Such heterogeneity and variable consolidation of the samples are considered to have altered the bulk properties of the oil sand, and hence the orientation, azimuth, and amount of dilation of the actual reservoir. The study conducted by Agar et al. (1986) supports the above conclusions and affirms that sample disturbance can have large affects on rock properties. Due to unconsolidation in the reservoir, it is believed that the calcite and shale streaks acting with the vertical sand-shale interfaces and shale overburden play a role in increasing Poisson's ratio over the bulk of the reservoir.

Even such measurements as fresh core permeabilities to water have been erroneously read as compared to actual well tests at the same intervals (PCEJ, 1988-91). While the core results give averaged effective permeabilities of 250 md to water (1500 md absolute permeability to water), applying conventional well testing procedures in the field tests would give only 1 md (Leshchyshyn et al., 1990). One must account for the fact that hot or cold bitumen near a wellbore is pushing against cold bitumen away from the wellbore, not a thin screen and air at room temperature as conventional special core analysis dictates. The reservoir must be analyzed as a total in-situ, reactive entity rather than an aggregate formed of individual lab properties.

Chapter 3

Statement of the Problem

The objective is to postulate, develop, apply, and validate a methodology for predicting the performance of a given steam cycle in Cold Lake oil sands or other zones bearing oil of similar viscosity, using correlation curves.

The purpose goes beyond simply outlining a step-wise procedure for achieving the desired outcome. Rather, the study aims to:

i) establish, by analyzing field data, the physical nature of the recovery mechanisms;

ii) evaluate the formulation and underlying assumptions of existing reservoir and fracture simulation models as a means of extending relevant principles to the theoretical development of the proposed prediction method;

iii) determine the scope of application for these traditional models, in particular their limitations when failing to predict cyclic steam stimulation (CSS) performance;

iv) examine formation geomechanics and the relationship such processes have on petroleum production; and

v) advance a new technique based on field experience, extraction theory, and reservoir simulation to accurately predict bitumen production.

Procedures for accomplishing the above objectives include the following:

Maintain the premise that reservoir description is more important for production history-matching and forecasting than the best simulators in the petroleum industry. A highly realistic simulator will produce the wrong results if the reservoir description is poorly-constructed or incorrect.

1. Investigate model geometry options in order to establish that a single-layer thermal model without fracturing or compaction can reliably predict steam fracturing production from an oil sands reservoir. Essentially, this model uses radial instead of linear flow and a single layer instead of multiple layers (5 or 10). Gravity drainage is minimal for the early life of the well. Emphasize the value of using a proper reservoir description as irreducible water saturation, connate water saturation, perforation height, and impermeable calcite streaks play a very important role in reservoir production forecasting.
2. For the first cycle, a multi-layer model with gravity drainage can be replaced by a single-layer model with no gravity drainage. The gravity drainage flow is still in effect but has no multiple vertical layers for gas to migrate up into or for liquid to drain down into.
3. Construct correlation curves to match the first cycle of an eight-well pilot. Further correlations are then used to match up to seven cycles of pilot production.
4. For assessing the range of applicability, test the method on other oil sands reservoirs: the Wabiskaw Formation at PHOP, the McMurray Formations at PHOP and PCEJ, the Clearwater Formations at Wolf Lake and Esso Cold Lake, and the Grand Rapids Formation at Wolf Lake.

A flow diagram (Figure 3.1) depicts the order of performing the study.

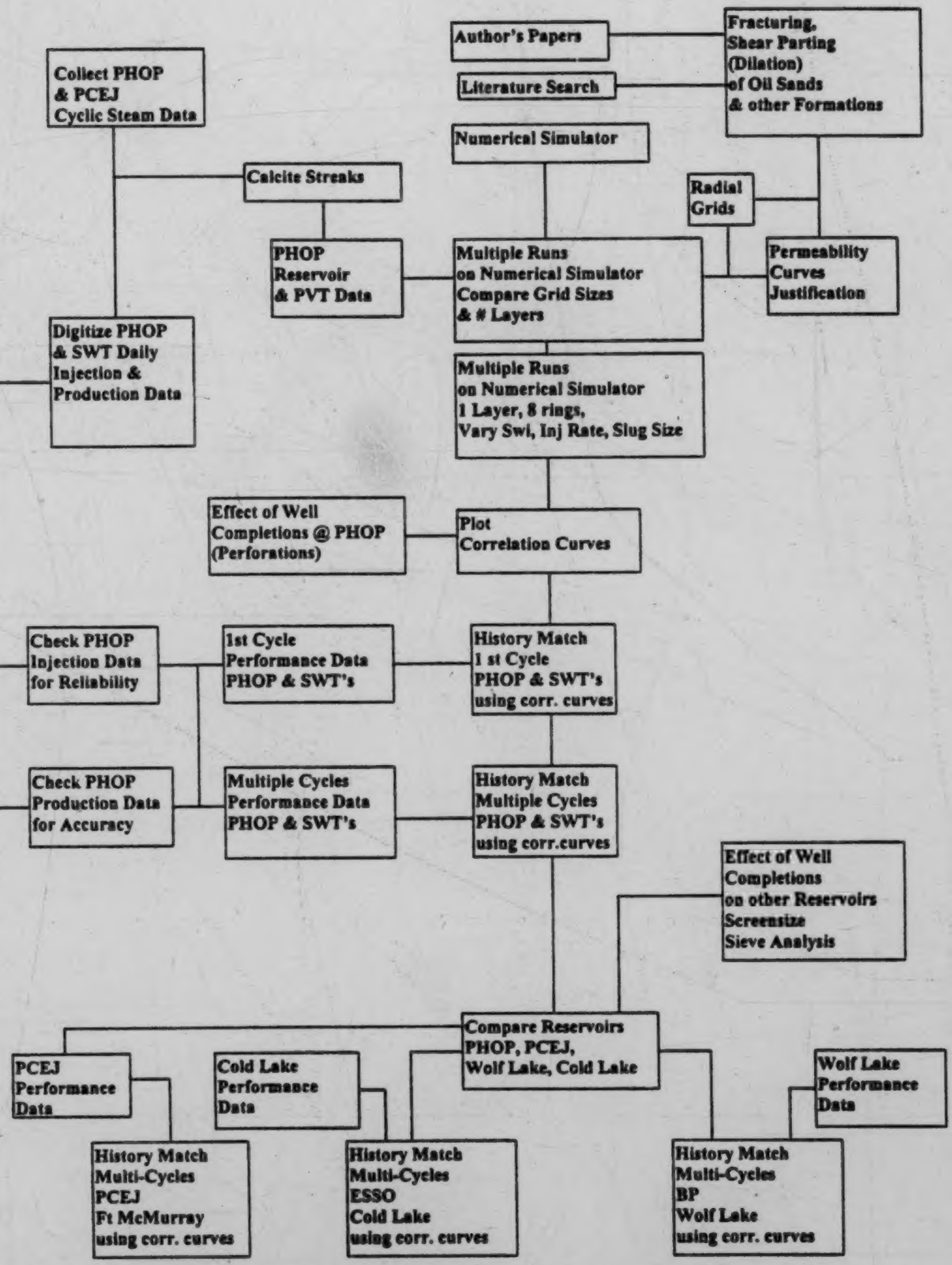
Author's Papers
Literature Search
Fracturing, Shear Parting (Dilation) of Oil Sands & other Formations
Collect PHOP & PCEJ Cyclic Steam Data
Numerical Simulator
Calcite Streaks
Radial Grids
PHOP Reservoir & PVT Data
Multiple Runs on Numerical Simulator Compare Grid Sizes & # Layers
Permeability Curves Justification
Digitize PHOP & SWT Daily Injection & Production Data
Multiple Runs on Numerical Simulator 1 Layer, 8 rings, Vary Swi, Inj Rate, Slug Size
Effect of Well Completions @ PHOP (Perforations)
Plot Correlation Curves
Check PHOP Injection Data for Reliability
1st Cycle Performance Data PHOP & SWT's
History Match 1 st Cycle PHOP & SWT's using corr. curves
Check PHOP Production Data for Accuracy
Multiple Cycles Performance Data PHOP & SWT's
History Match Multiple Cycles PHOP & SWT's using corr.curves
Effect of Well Completions on other Reservoirs Screensize Sieve Analysis
Compare Reservoirs PHOP, PCEJ, Wolf Lake, Cold Lake
PCEJ Performance Data
Cold Lake Performance Data
Wolf Lake Performance Data
History Match Multi-Cycles PCEJ Ft McMurray using corr. curves
History Match Multi-Cycles ESSO Cold Lake using corr. curves
History Match Multi-Cycles BP Wolf Lake using corr. curves

Figure 3.1: Flow Diagram for developing correlation curves to history match and predict bitumen production from cyclic steaming of oil sands

Chapter 4

PHOP Project Injection Data

The chapter reviews injection data made available for this thesis, and evaluates the quality of the information both inherent and systematic error.

To use and comprehend and discuss the significance of collected field data, one must first have an appreciation for the sort of data collected, where and how it is gathered, and the errors associated with the various measurement techniques and readings. Assumptions are always made when estimating bottomhole conditions from surface values, usually resulting in increased error over actually measuring bottomhole pressures. It is most important to understand the accuracy and limitation of the data in order to correctly interpret what is occuring in the reservoir. Included here are data ranges over which error can be assessed from instrumentation quality along with specific examples of improper device locations, the cause of variance.

4.1 Injection Data Provided

Injection data generated from the field tests are voluminous, therefore, only information required for a given subject of interest will be referred to or reported.

Injection data have been obtained from the Province of Alberta's Energy and Utilities Board (AEUB, formerly ERCB) progress reports numbered 1 to 7 entitled " Approval No. 3482, Primrose Heavy Oil Pilot". Permission was granted by Petro-Canada Resources to use the pilot data for thesis support (see Appendix H, Letter of Permission).

Data have been arranged on a per-cycle basis for each well. A daily report would include:

- Well Identification
- Cycle Number
- Date of Injection
- Hours Well is on Injection
- Rate of Injection, m^3/d
- Wellhead Casing Pressure, kPa
- Wellhead tubing temperature, deg C
- Boiler steam quality (upstream of manifold)

Summary data for the eight pilot wells (IP1 to IP8) are supplied in Appendix A, Tables A1.1a to A1.1c. Summary injection data for the Single Well Test (SWT) wells 10-11, 10-34, and 11-21 are presented in Tables A1.2, A1.3, and A1.4, respectively. As examples, daily injection data for the PHOP Pilot individual wells, IP2 and IP8 and SWT 10-34 are supplied in Appendix B.

4.2 Accuracy of Injection Data

Typical accuracy of the data is as follows:

a) Temperature ± 1 or 2 degrees C for "J" or "K" thermocouples.

± 0.5 degrees C for resistance type temperature device (RTD)

± 10 degrees C for thermowells (metal expansion strips)

b) Pressure ± 10 kPa for Marsh bourdon tube gauges using on-site dead weight calibration.

± 500 kPa for new "off-the-shelf", uncalibrated Marsh type gauges (15,000-25,000 kPa full scale).

c) Flow Rates ± 1 m^3 for tank level calculated rates.

± 10 m^3/d for orifice measured rates not calibrated from daily tank levels (i.e. boiler feed-water rates).

± 10 m^3/d for steam manifold split rates (downstream of manifold.

d) Steam Quality ± 1 percentage point at the boiler (before manifold).

± 5 percentage points at the wellhead (for manifolded, multi-well steam injection).

± 20 percentage points at bottomhole conditions.

Most process control and data acquisition systems are designed and installed by facilities engineers who normally have a process responsibility for surface equipment and facilities but are usually not mindfull of the accuracy required for interpretation of data for reservoir purposes. Hence, an unstandardized approach leads to large variations in accuracy. Another source of data error is lack of scheduled maintenance or inspection of measuring devices by operations personnel over the life of the project. It is imperative that the reservoir engineer add to the design stage a mandate for how data is to be measured and reported, what accuracy is required, and maintenance to ensure quality.

Keeping all the above in mind, it is not surprising the measured wellhead temperatures and pressures at saturated steam conditions do not agree. For example, in the first cycle of injection on well IP2, the average temperature is 303.2°C and the average pressure is 10,237 kPa. From steam tables, a saturated temperature of 303.2°C corresponds to a pressure of 9,000 kPa, a difference of well over 1,000 kPa. Alternatively, a saturated pressure of 10,237 kPa corresponds to a temperature of 313°C, a difference of 10°C. Here, the difference is attributed not only to faulty gauges but also to the temperature being measured in the tubing while the pressure is being taken at a distance in the casing. The values for pressure can vary, depending upon whether the steam was injected down the tubing, or down the annulus, or down both simultaneously. If steam is injected concurrently down the tubing and the annulus, as is assumed for this pilot, then the casing pressure and wellhead tubing temperature should agree, provided all inlet valves are fully open.

Bottomhole pressures can be estimated from the casing pressure. For example, at 310°C, a fluid density of 690 kg/m^3 and a vapor density of 54.75 kg/m^3 will result in a head of 1,350 kPa at 65% quality steam (80% at surface and 50% bottomhole), for a well depth of 500 m. Adding this head to a casing pressure of 10,000 kPa yields a bottomhole pressure of 11,350 kPa. Friction pressure drops down the tubing increase steam quality but at lower temperatures, plus wellbore heat losses reduce steam quality. The overall result should be a slight drop in pressure and temperature with a more significant drop in steam quality. Actual bottomhole pressures or temperatures were not measured.

To further complicate the validity of measurement, injection data can show an excessive increase in casing pressure with increasing injection rate, not totally consistent with fractured wells. Values as high as 1.6 times the weight of overburden were noted in the PCEJ McMurray pilot. Cold water injection into the same well would give pressures close to 0.6 times the weight of overburden, normal for vertical fractures. It is possible to create horizontal fractures at 1.6 times the weight of overburden, but if there is a sudden drop to 0.6 times the weight of overburden, it is impossible to keep a horizontal fracture open.

For the PHOP Pilot, a decision was made to let the thermal numerical simulator arrive at the final bottomhole injection pressures, since formation fracturing was not accounted for by the model. Thus no modelling control was available. The simulator gave final injection pressures of about 10,000 kPa for 66 m^3/d , 11,500 kPa for 110 m^3/d, and 12,000 kPa for 200 m^3/d injection rates, respectively. This scenario was equivalent to 0.94, 1.08, and 1.13 times the weight of overburden, respectively. It is reasonable to assume that injection pressure increases with rate, as the first three injection cycles for the PHOP pilot show (data from 8 wells combined), on a plot of rate vs casing pressure (see Chapter 6, Figures 6.1.1 to 6.1.3), giving slopes of 10.8, 6.2, and 4.6 kPa/m^3 respectively. Bottomhole steam quality used in the simulator was 0.25, 0.425, and 0.5 for the respective increasing rates.

If the average bottomhole injection pressure for first cycle injection is 12,000 kPa, and the weight of overburden is 0.94 psi/ft (10,650 kPa total weight), injection is at 1.13 times the weight of overburden, suggesting creation of horizontal fractures. To the contrary, temperature logs pointed to vertical fractures. Very recently, conventional fracturing field data obtained by Stimlab and the University of Oklahoma, suggests that horizontal fractures occur at above 1.4 times the weight of overburden. The geomechanical phenomenom postulated in this thesis are based on vertical fractures with a significant amount of lateral dilation (shear fracturing), resulting in a semi-radial or elliptical distribution of heat and pressure. Because of the shallow depths, literature draws attention to the possibility of either horizontal or vertical fractures. These concepts are discussed to greater length in chapter 6.

Steam quality is difficult to measure at the wellhead or bottomhole so values are normally calculated from chloride concentrations in the water trap at the outlet of the steam generator prior to manifolding to split streams. Boiler capacities were 25 MM or 50 MM BTU/hr. The manifold is assumed to operate at 100% efficiency and split the fluid content evenly among the streams. Traveling down the wellbore, an expected drop in steam quality is 30-50% as injection rates fall from 200 m^3/d to 80 m^3/d, though could be as low as 20% if an aquifer of 100-meter thickness is present between the surface and the oil sands reservoir. At a steam quality below 20% the operation becomes hot water injection.

The best that can be hoped for is that comparing injection data within the project itself will minimize the effects of measurement errors. For example, plots of rate versus pressure (See Chapter 6, Figures 6.1.4 and 6.1.5) for all cycles and wells will still show the relative trends, even though the data measurement is not exact. Further comments on the above plots can be found in Chapter 6.

Chapter 5

PHOP Project Production Data

This chapter provides information pertaining to the production data supporting this thesis and notes the associated errors.

Field production data are far more complicated to manage than injection data. While only steam is injected, steam, bitumen, water, sand, and gas are produced. Separation of bitumen, water, and sand using large knock-out separators and treaters gives only an aggregate measurement for all wells producing at the time. The combined production itself can be difficult to quantify due to residence times in the large vessels plus the inability to accurately determine the water-oil interface levels. Individual well production must be tested in specially-designed test tanks and even here, uncertainties arise in obtaining proper cuts due to separation problems. Performing a production test of four hours duration in order to represent a well producing for 24 hours can have misleading results due to slugging of bitumen. Proration of production rates to storage tanks and trucking is a must and required by government reporting agencies like the AEUB (formerly ERCB).

5.1 Production Data Provided

Production data generated from the field tests are voluminous so only data as required for the particular subject at hand will be referred to or reported. More data and detail are available for future studies by future students.

Production data has been obtained from the Government of Alberta's Energy Resources and Conservation Board (ERCB) progress reports numbered 1 to 7 entitled " Approval No. 3482, Primrose Heavy Oil Pilot". Permission was granted by Petro-Canada Resources to use the pilot data for thesis support (see appendix E, Letter of Permission).

Data have been arranged on a per cycle basis for each well. A daily report would include:

- Well ID Identification (ID)
- Cycle Number
- Date of Production
- Hours on Production
- Produced Fluid, m^3
- Oil Produced, m^3
- Water Produced, m^3
- Fluid Level, joints of tubing from surface to fluid level
- Wellhead Casing Pressure, kPa
- Wellhead tubing temperature, °C

No measurements were taken for gas production as it was vented through the annulus at the wellhead and out the top of the treating and storage tanks. However, the initial reservoir GOR estimate of about 5 m^3/m^3 was determined through analogy to reservoir pressure at Shell's Peace River Project. Sand production is normally listed as sand cut of total fluids. For this pilot, data was recorded only when major sand production had occurred.

Summary data for the eight pilot wells (IP1 to IP8) are supplied in Appendix A, Tables A1.1a to A1.1c. Summary production data for the Single Well Test (SWT) wells 10-11, 10-34, and 11-21 are presented in Tables A1.2, A1.3, and A1.4, respectively. As examples, daily production data for the PHOP Pilot individual wells, IP2 and IP8 and SWT 10-34 are supplied in Appendix C.

Total fluids and oil production per well are normally tested each day by sampling 1 to 4 hours of total production into a test tank of 1 to 3 m^3 capacity diluted with 5 gallons of diesel. Vertically spaced stopcocks locate the oil-water contact, and along with sample centrifugation, oil and sand cuts are determined. At the end of each month, daily production is prorated to trucked sales. These revised values, as tabled here, are then reported to the ERCB.

5.2 Accuracy of Production Data

Typical accuracy of the data is as follows :

a) Temperature	± 1 or 2 °C for "J" or "K" thermocouples.
	± 0.5 degrees for RTD's (resistivity temperature device)
	± 10 °C for thermowells (metal expansion strips).
b) Pressure	± 10 kPa for Marsh type bourdon gauges using on-site dead weight calibration.
	± 50 kPa for new "off the shelf" Marsh type gauges (1,000 kPa full scale).
c) Flow Rates	± 1 m^3 for tank level calculated rates.
	± 10 m^3/d/well for orifice measured rates not calibrated from daily tank levels.
d) Fluid Levels	± 1 joint of tubing where one joint equals 9 m (30 ft)

Production measurements are considered to have better accuracy than injection data because pressures and temperatures are lower, and gauges for production use smaller full scales. Five percent error for a 1,000 kPa full scale gauge is 50 kPa as compared to 750 kPa for a 25,000 kPa gauge.

Oil production rates are typically the most accurate since values must be balanced against shipment invoices , tank storage inventory, and the Alberta Energy and Utilities Board (AEUB) S1 and S2 accounting sheets.

Water production rates are reasonable if balanced against trucking but can be +/- 5 m^3/d/well if metered at the water disposal well.

Bottomhole production pressures (BHP) are best estimated from fluid levels (i.e. joints of fluid from surface), with an expected error of +/- 100 kPa. More accuracy is obtained (+/- 6 inches fluid level or +/- 0.2 kPa) if transit times are measured on the echometer logs rather than counting tubing collars. BHP is calculated as follows:

BHP = height of the water column in the wellbore, h, times the gravitational constant, g, times the relative density of the fluid as compared to water, ρ_{fw}.

$= \rho_{fw} g h$

$= ((1050 \text{ kg/m}^3 \text{ fluid})/(1000 \text{ kg/m}^3\ H_2O))*(9.81 \text{ m/sec}^2)$
*(number of joints corresponding to fluid level in well x 9 meters/joint)

$= (1.05)*(9.81)*(9)*(\#\text{ joints})$

$= 88.29 * \#\text{ joints (kPa)}$

The calculation of hydrostatic head assumes zero gauge pressure above the water column. The density of the bitumen is very close to that of water, even at 100-200°C.

Sand production is generally measured as a percent cut of total daily fluid produced or as joints of tubing from a bailed well during a workover. Values can vary from 0 to 10% and are normally in the range of 1 to 2 %.

Chapter 6

Validation of PHOP Project Injection and Production Data

This chapter deals with the validity of the injection and production data. Plots are made of surface wellhead injection pressures versus injection rates by cycle to determine whether trends exist, such as increasing pressures with increasing rates and cycle number. Should the correlation be found, an assumption is warranted regarding consistency in the data measurements. Confidence is also raised in the ability to interpret reservoir behavior on the basis of identified trends or patterns. Significant interwell interference and injected steam lost to the overburden can complicate any interpretation attempts. Fortunately few inconsistencies were encountered with the field data from the PHOP Pilot. Hall and fracture growth plots (Leshchyshyn et al., 1991) were not generated from the injection data because the undertaking translates to an addition of, at minimum, 11 separate plots tieing 11 wells through 5-7 cycles each.

Injection and production data were obtained from the Government of Alberta's Energy and Conservation Board (ERCB) progress reports Nos. 1 to 7, entitled "Approval No. 3482, Primrose Heavy Oil Pilot".

Information for the eight PHOP pilot wells, IP1 to IP8, arranged in a double, inverted, five-spot configuration (see Chapter 1, Figure 1.1.2) were checked for consistency to decide whether subsequent cycles showed any general trends applicable to cyclic steam bitumen production.

6.1 Injection Data Validation

1st cycle data for all eight PHOP wells were plotted as steam injection pressure versus steam injection rate (Figure 6.1.1). The data appears to be clustered but well behaved (trends are easily apparent). Best fit slopes for individual wells were drawn

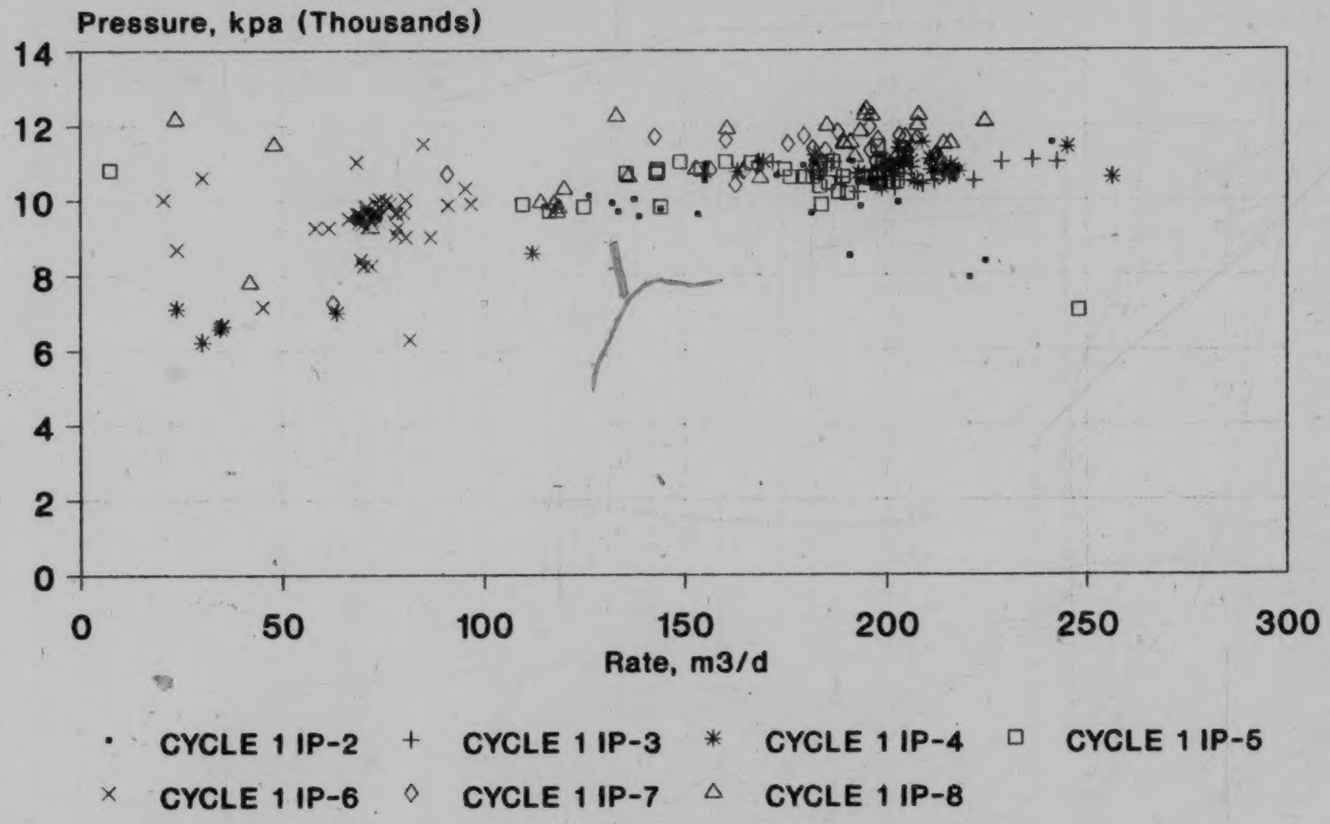

Figure 6.1.1: PHOP Pilot wells steam injection rates (CWE) Vs Casing Pressure, Cycle 1, by well

(Figure 6.1.2). This showed some variations in slopes but generally agreed with a standard step rate test showing dual slope with the earlier slopes being steeper, indicating a possible ***ISIP*** at 10 MPa. Assuming a maximum net pressure of 3 MPa, this would give a minimum horizontal stress (σ_3) of 7 MPa or 15.5 kPa/m gradient, which is as expected for most sandstone reservoirs in Alberta.

The quality of the injection data was investigated by performing a linear regression plot of pressure versus daily injection rate for each of the first three cycles (all wells combined), obtaining a linear equation, intercept, $\boldsymbol{R^2}$, and slope (Figures 6.1.3 to 6.1.5). The values of $\boldsymbol{R^2}$ as shown in the figures indicate the data is less scattered for cycle 1 than for cycle 2 than for cycle 3, suggesting the initial fracturing is more controlled and stress distribution is more consistent for cycle 1. After 1st cycle, repressuring a previous fracture during the start of the next cycle requires more pressure, possibly because an oil bank has formed on the outside edge of the steam zone. Newly created fractures, off the outer edge of the steam zone, that is, extensions after the void space or dilated zone is filled, should be propagated at slightly lower pressures due to less bitumen plugging of the fractures. In comparison, new fractures generated from the wellbore, should be at lower propagation pressures than the above fractures, close to initial first cycle injection pressures as there is no void space between to create a pressure drop. Hence the wide variations in fracture propagation pressures as cycle numbers increase.

For the second cycle, injection pressures have increased by approximately 1,000 kPa plus another 1,000 kPa for cycle three. Different explanations for the difference in injection pressures are plausible.

6.1.1 Geomechanical Theory (supported by Kry, Gronseth, Ito)

The increase in pressures can be accounted for by the fact that after each cycle there is more fluid left in the reservoir, that is, the cumulative depletion index, (***DI***) is less than 1.0. This index can be calculated from the following expression:

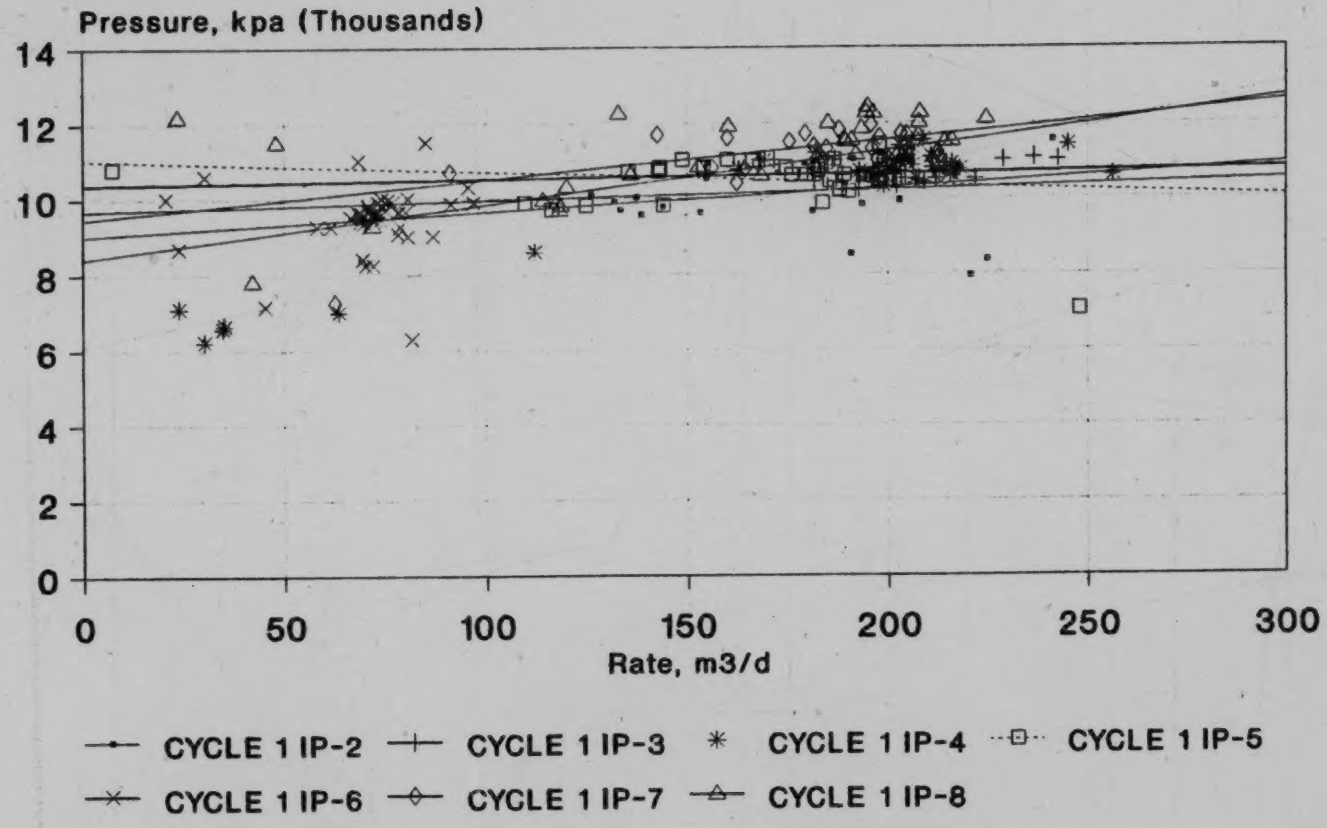

Figure 6.1.2: PHOP Pilot wells steam injection rates (CWE) Vs Casing Pressure, Cycle 1, by cycle with slopes

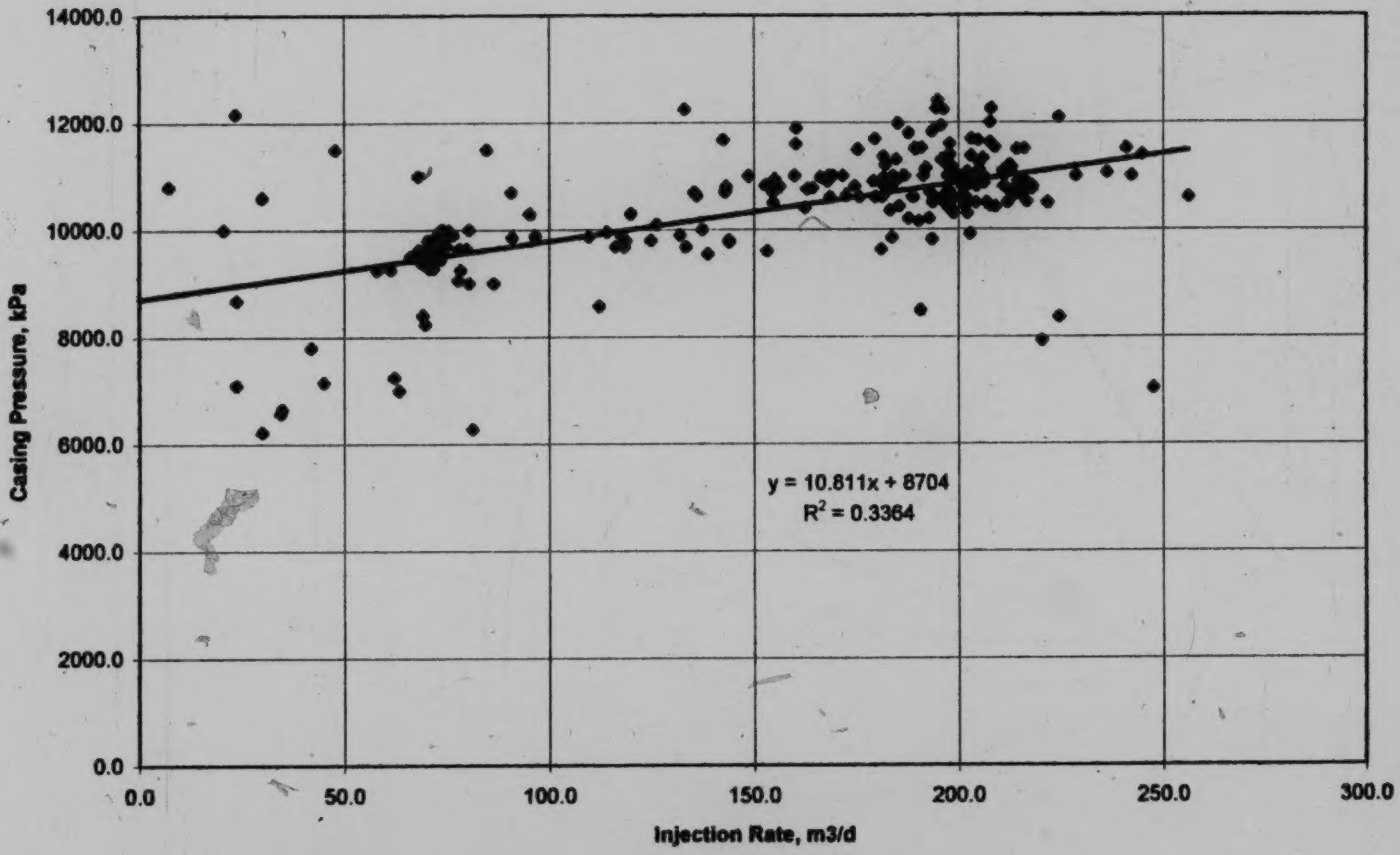

Figure 6.1.3: PHOP Pilot wells steam injection rates (CWE) Vs Casing Pressure, Cycle 1

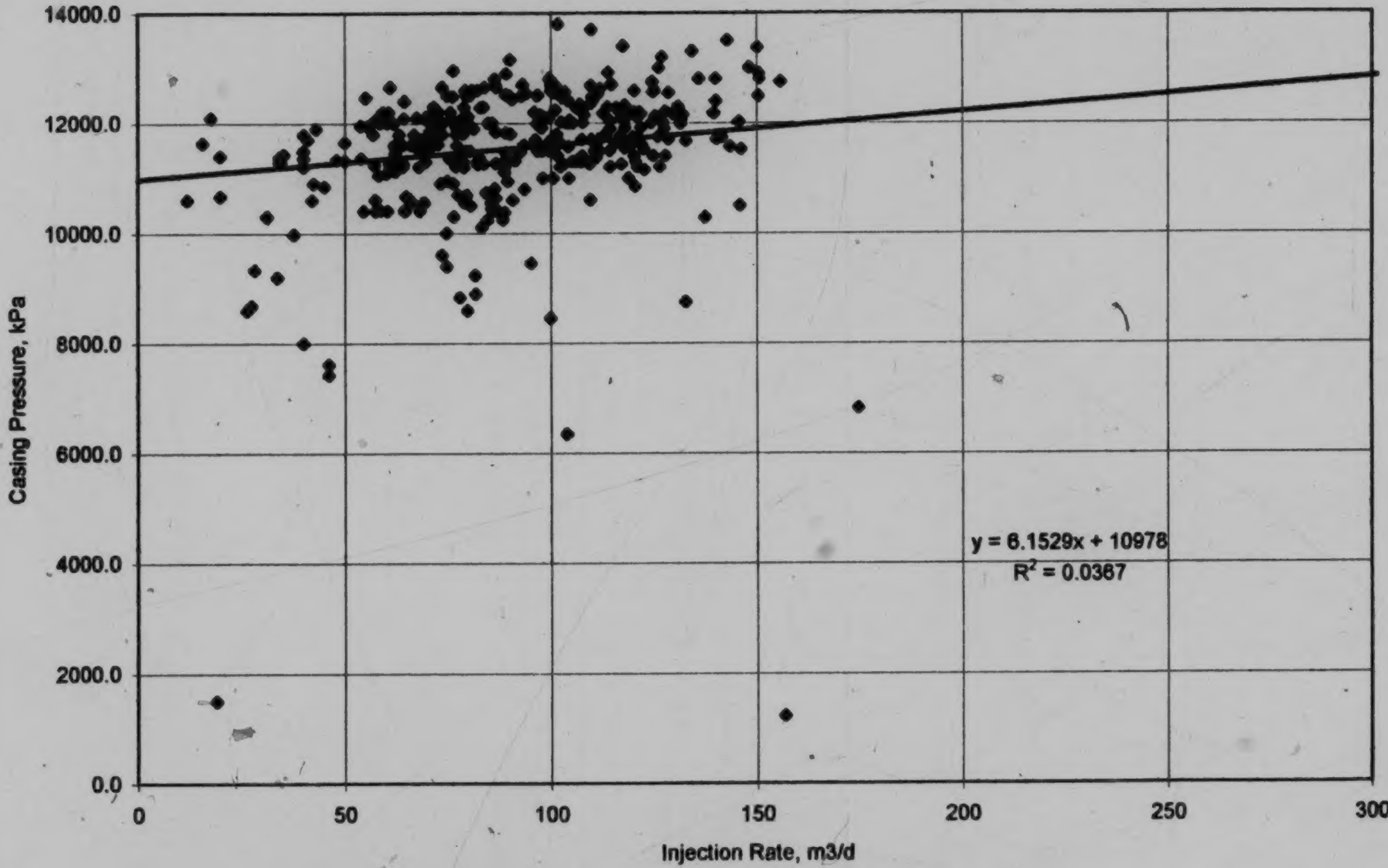

Figure 6.1.4: PHOP Pilot wells steam injection rates (CWE) Vs Casing Pressure, Cycle 2

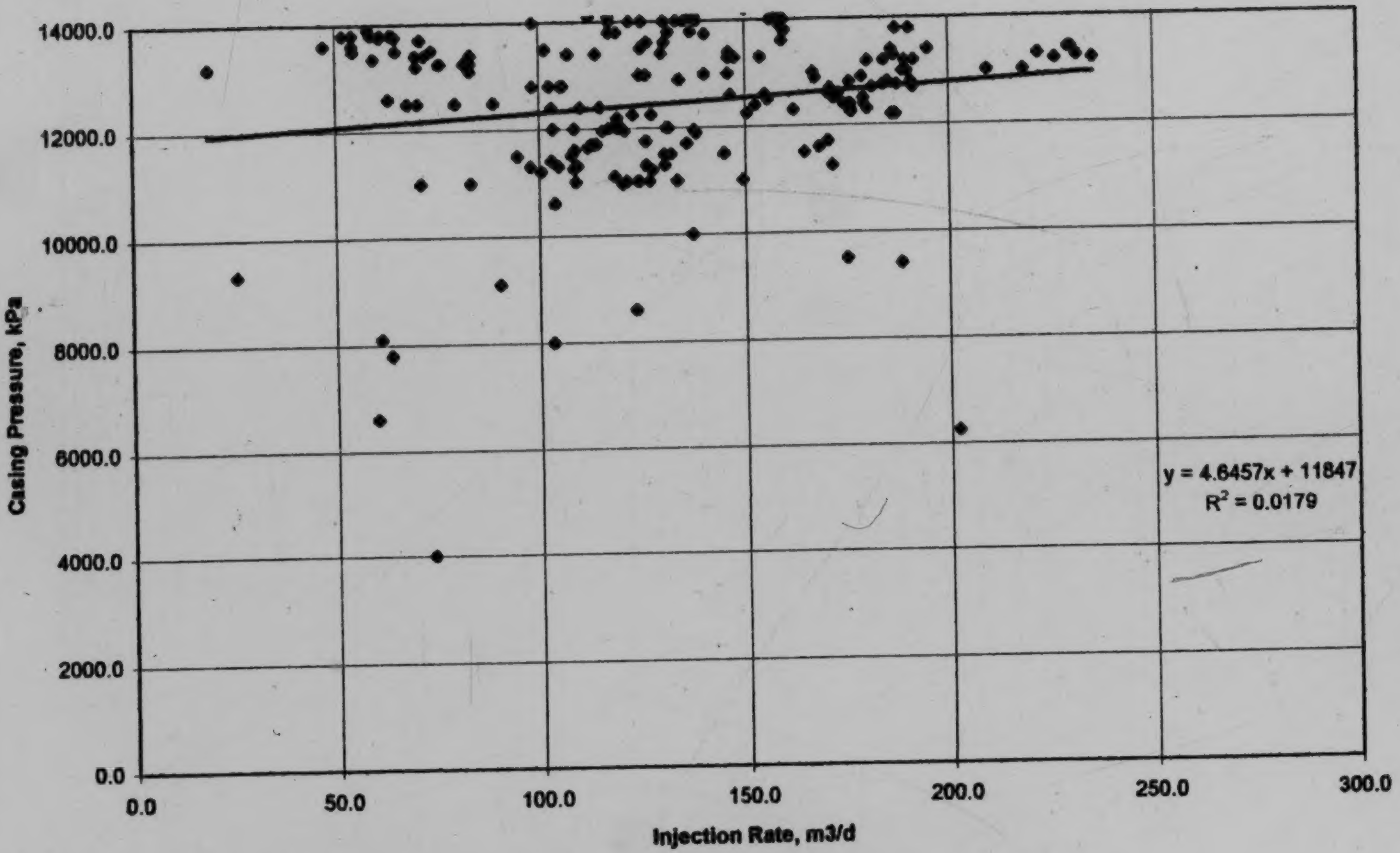

Figure 6.1.5: PHOP Pilot wells steam injection rates (CWE) Vs Casing Pressure, Cycle 3

Depletion index,

$$DI = (m^3\ \text{Oil produced} + m^3\ \text{Water produced})/(m^3\ \text{Steam injected,CWE})$$

From the pilot injection and production summary given in Table A1.1b, it is evident that the cumulative depletion index after the third cycle is about 0.35 to 0.45, corresponding to a total of about 50,000 m^3 of fluid left in the reservoir and not recovered. A total of 80,000 m^3 of fluid remained in the reservoir at the end of the pilot operations. These volumes are high enough to raise the average reservoir pressure in the vicinity of the pilot substantially. Based on an area of 250 m x 400 m = 10 ha, the reservoir has about 130,000 m^3 water initially in ten metres of pay. If the total reservoir compressibility is about 1E-5 kPa^{-1}, just 20,000 m^3 of fluid injected will give a rise in pressure of 2,000 kPa. Here, 10 ha x 10 m x 1E-5/kPa x 2,000 kPa = 20,000 m^3. In the absence of "no flow" boundaries, a volume of 50,000 m^3 in a "***leaky***" reservoir is a possibility. There is also the real possibility of lifting the overburden up to one metre, as measured by surface monuments at the Esso Cold Lake Project. The phenomena is known as "***dilation***" during injection and "***compaction***" during production.

An example of fluid injection causing an increase in stress is shown in Figure 6.1.1.1. These data were collected at the PCEJ pilot at Fort McMurray in the McMurray oil sands. The recovery strategy called for one row of wells being steamed prior to applying steam to the adjacent row. The latter is the row upon which the stress tests were conducted over time. An operational goal was to increase in situ stresses sufficiently high in the next row to create horizontal fractures when steam injection was commenced. About 30,000 m^3 of steam were injected using this pattern to increase the minimum horizontal stress from 5 MPa to 7 MPa. The slope of the curve shows that the stress has increased about 2 MPa for every 1 MPa increase in reservoir pore pressure.

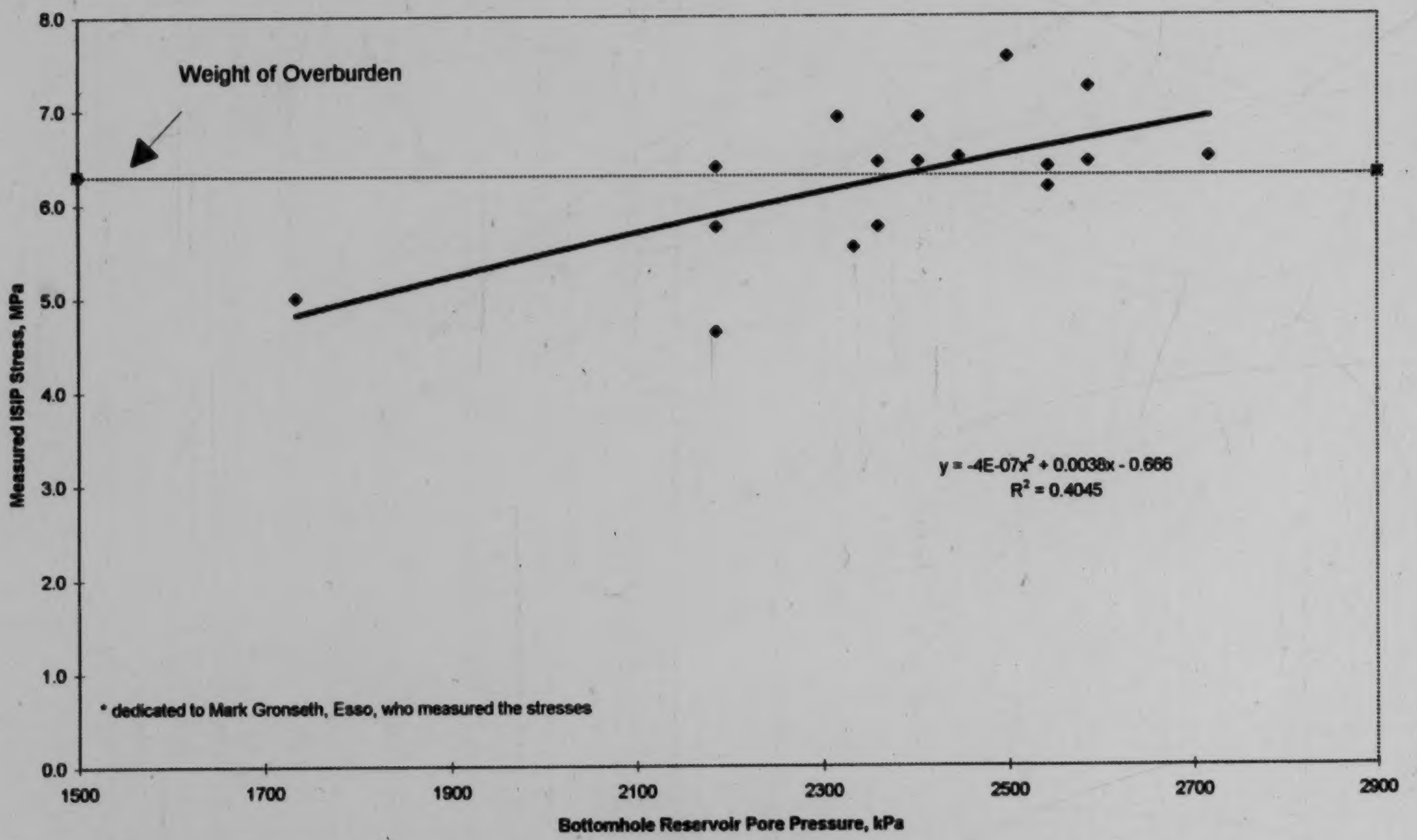

* dedicated to Mark Gronseth, Esso, who measured the stresses

Figure 6.1.1.1: Measured Increase in Stress* with Increase in Pore Pressure, PCEJ Pilot

Conventional reservoir fracturing theory places this value closer to 0.75 to 1.00 MPa/ MPa, suggesting possible thermal expansion effects are also at work.

Although the final stresses in this plot were about 1.1 times the weight of overburden, vertical fractures were still created. This situation is understandable in the light of similar conclusions from Stimlab of Oklahoma on the propagation of horizontal fractures at 1.4 times the weight of overburden.

Esso, at Cold Lake had implemented the same procedure earlier to increase their bitumen production by mega-row steaming.

This theory agrees with a successively larger injection pressure with each cycle as the total fluid in the reservoir increases with time. The increasing cumulative depletion index for the PHOP pilot failed to approach total recovery of the fluid injected into the reservoir, that is, the ***DI*** would have to be > 1 in later individual cycles for an extended period for the event to occur.

6.1.2 Reservoir Flow Theory (supported by Ito et al. and Takamura et al.)

Injection pressure increases may be attributed to reservoir phenomena rather than geomechanical behavior. Injected steam travels radially or elliptically for aspect ratios less than 1:5, through the interconnected smaller water-filled pores not occupied by viscous bitumen. During first cycle production, heated bitumen at much lower viscosity enters these small channels and, upon cooling, plugs the pore throats either directly or by displacement of kaolinite plates (Takamura et al., 1983). During second cycle, injection begins at a low pressure because voidage is being replaced by a combination of unproduced solution gas from the original steam volume and steam vapour being condensed as the pressure increases above the steam saturation pressure. The void space is finally pressured up but to a higher value due to the cooler bitumen plugging the edges of the once empty pores. As more bitumen is produced in subsequent cycles and the reservoir continues to be heated, water saturation in the pores increase, and heat improves flow through the smaller pores. Beyond cycle 2 or 3, injection pressures can therefore decrease with increasing cycle number. From the PHOP injection data it appears that the injected water remaining in the reservoir has more effect than deletion of the bitumen. This most likely is because the steam/oil ratio (***SOR***) has been higher than the expected value of 4 or less (see Table A1.1c).

6.1.3 Conventional Reservoir Theory with Modification for Geomechanical Shear Dilation Theory (supported by Kry et al., Leshchyshyn et al., and Deitrich et al.)

Developing the concept of a dilated fracture within the body of traditional reservoir theory can be recharacterized by the principles for fluid flow. To begin, a tensile, vertical fracture is created at the perforations, causing major local shear fracturing and subsequent opening of shear fractures as injection pressures increase. These phenomena are collectively known as "***dilation***" or "***pressure-dependent leak-off***". Leak-off of fluid or gas is largely through these shear fractures with secondary leak-off from the shear fractures into the reservoir matrix. If enough fluid is injected, a sizeable "***shear zone***" is developed to a few meters radius from the wellbore. In well test analysis, the shear zone is labelled as the "***inner reservoir***" of ***a "radial composite system***". This inner zone then leaks-off, equivalent to a tank full of holes, into the small rock matrix pores filled with water located in the outer reservoir. Compaction of the matrix from the removal of bitumen, water, and gas from the wellbore, along with gas drive, causes cooler bitumen to be forced towards the wellbore. This affects a plugging of the narrow shear fractures and smaller pore throats. Second cycle injection pressure is increased due to lower fluid leak-off and injection through the more resistant shear fractures. It is also suggested here that the fracture Instantaneous Shut-In Pressure (***ISIP***), and the closure pressure (P_{cl}) of the shear fractures are lower than that of the propagating tensile fracture. Thus, the tensile fracture closes first. This is contrary to the belief that shear fracturing occurs at pressures between the minimum and maximum horizontal stress. This reasoning is supported by the author's experience at the PCEJ pilot where it was indicated that the formation can be broken down below fracture propagation pressures (***ISIP***).

Sections 6.1.2 and 6.1.3 correspond when looking at the macroscopic effects occurring in the reservoir. For instance, the pressures and temperatures obtained from a massively fractured (dilated) steam zone model can appear similar to those produced by a radial steam zone model. In the case of analyzing a pressure fall-off from a steamed injection well using standard well test analysis techniques, the exact process involved in forming the steam zone is unknown. Walsh (1981) estimated steam zone volume plus distance to a steamed boundary based on a "***composite reservoir***". The permeability increase in the steamed zone, by a factor of 400 times, is either the result of extensive fingering or extensive shearing. It is known that fracture fluids with low viscosities create more shear fracturing, as these increase pore pressure at some value above reservoir or fracture closure pressure, to some distance from the main tensile fracture (Aud et al., 1993). Further, an example of dilation severity by way of a well test semi-log derivative plot was shown by Leshchyshyn et al. (1996). Well test Figure 8.1.2 in Chapter 8 shows extensive radial fracture behavior. It is also reported that there is but one way to match the rapid-to-slow fall-off data using a hydraulic fracture simulator and that is to employ pressure-dependant permeability hysteresis. This solution was first introduced by Coates et al. (1979), although he did not fully understand the reasoning behind it.

Dietrich et al. (1981), employed water relative permeability curves for injection which were greater than those for production, explaining that as a consequence of changes in rock stresses during steam injection, micro-channels would open up and lead to increased absolute permeability. The micro-channels would then close on production as rock stresses were relieved. The first model simulations performed on the PHOP data for well IP1, first cycle, were reported by Todd, Dietrich, and Chase (TDC) in 1981. The same process representation is the basis for much of the thesis numerical simulator input data. Dilation is accounted for using similar modified relative permeability curves. Further discussion of the use of modified permeability curves is given in section 10.3.

6.2 Production Data Validation

Production data is deemed acceptable if the bitumen production per well for each cycle shows a general trend of decreasing rates with time. Production data from

Appendix C exhibit the typical delay in production of bitumen as steam near the wellbore is produced first. This can last one to three weeks. Once the steam diminishes and the chloride concentration in the water increases to 400-500 PPM, bitumen rates will quickly increase to a maximum, then fall towards zero at a decline dependant upon the volume and rate of steam injected. There are daily fluctuations in bitumen production rate probably due to the inaccuracies of measuring manifolded production for the case of more than one well producing at a time into the same production facilities. Also, the bitumen appears to flow back in slugs extending from a few hours to many days. The numerical simulator cannot handle slug flow so averaging is unavoidable.

The ***SOR*** (Table A1.1c) is normally high in the first cycle and drops to a minimum about the second or third cycle, slowly increasing thereafter. This pattern is common because initial steam injection must start heating the reservoir and overburden from 15 °C to steam temperatures, therefore larger heat losses occur. Subsequent cycles heat the reservoir and surrounding rock from about 100 to 200 °C, and since the steam zone size does not change significantly, smaller (vertical) energy losses translate to a higher rate of heat application to a greater volume of bitumen. As the reservoir is depleted, less bitumen is available for flow back to the wellbore the ***SOR*** then begins to increase. An overall ***SOR*** of 7 for this pilot is not surprising but for production to be economic the price of a barrel of oil must be above 30$ Canadian. Interestingly, at an ***SOR*** of 12, the BTU content of the injected steam equals the BTU value of the produced bitumen, a somewhat expensive method for converting natural gas to diesel.

6.3 Summary

Overall, the injection and production data can be utilized with confidence as the correlation curves reasonably matched the pilot's actual total first cycle pilot bitumen production within 1% using modified water relative permeability curves similar to those of Todd, Dietrich, and Chase (1981). The data scatter for the injection pressure versus rate plots is acceptable.

Chapter 7

Effect of Well Completion on Production

A possible relationship between well completion and produced bitumen is investigated here. In conventional oil and gas production, downhole completion programs must be designed carefully since most wells in Alberta require some form of stimulation to attain economic feasability. Perforations must be spacially arranged to prevent restriction of injectants and/or production flow. Formation sand control such as downhole screening equipment needs to be selected to minimize interference to flow. Most wells are drilled over-balanced with water-based muds, resulting in formation damage at the sandface either from swelling clays or drilling mud filter cake. Drilling damage in Alberta wells show, on average, a skin of +3, but can be as high as +30. Zero skin is a measure of no damage. About 40% of the wells drilled in Canada (approximately 120,000 out of 300,000) since the mid-1950's have been fracture-stimulated and many more have been acid-washed or squeezed in an attempt to reduce the skin to zero or ideally in the negative range (Fracmaster, 1996). A simple derived expression which measures improvement to production from stimulation is provided in Appendix F. The calculation estimates what production should be after stimulating a well, given the initial production rate and skin. Applying the rule of eight:

$$Q_{new} = \frac{8 + skin_{old}}{8 + skin_{new}} Q_{old} \tag{7.1}$$

where Q_{old} and $skin_{old}$ are the pre-stimulation rate and skin, respectively and Q_{new} and $skin_{new}$ are respectively, the post-stimulation rate and skin.

Acid stimulations tend to reduce a wellbore skin to 0 or -1. A fracture stimulation can potentially reduce the skin from -3 to -6 (Darcie's Law will not allow a skin below -

7) depending upon whether the reservoir had a high (greater than 5 md) or low (less than 1 md) effective permeability to the reservoir fluids, respectively. Fracturing an oil sands reservoir with just water would probably give a similar skin (-3 to -6). If no bitumen is produced upon initial perforation, the rule of eight says there will be no bitumen production after fracturing. This is found true in field operations. Fracturing the well with steam would different, with most or all the bitumen production occuring from the reduced viscosity of the bitumen. The equation can be modified by changing 8 to $8/\mu_{old}$ and $8/\mu_{new}$ but could only be used to back calculate a Q_{old} from the known Q_{new} since Q_{old} is too small to be measured in the field. The difference in viscosities between the hot and cold bitumen is so great that the $skin_{old}$ becomes insignificant. The equation would only apply to initial rates unless the total drainage area was heated.

The steady-state assumption of the Darcie equation is valid for conventional oil and gas reservoirs where wells are produced at a stabilized rate soon after the fracture stimulation job. The rates are usually compared at 100 days after start of production on wells that would normally be expected to produce for five to thirty years. The rule of eight was introduced here to show that fracturing a non producing formation without heat will not improve production. This is why fracture stimulation of heavy oil reservoirs is not a common occurence..

7.1 Perforations

Standard completions practice for the PHOP Pilot used twenty-three gram jet charges at 13 shots per meter (SPM) and with 60° phasing. Overbalanced perforating in which hydrostatic bottomhole pressure in the wellbore prior to perforating is greater than reservoir pressure, is more common than underbalanced perforating where hydrostatic is less than reservoir pressure. The bottomhole pressure in terms of hydrostatic head (*HH*) is:

$$HH\ (kPa) = \text{relative density to water} \times 9.81\ (m/sec^2) \times \text{perforation depth}\ (m)$$

$$= \rho_{rw} g h$$

Well tests performed for establishing permeability normally show skins of -5, indicating no perforation damage. Since the reservoir acts as if it is already fractured, perforation design in oil sands is not usually a problem.

Experience in placing steam through perforations suggests that most of the steam enters the reservoir only through the top few perforations as a consequence of water build-up from the bottom of the wellbore. Subsequent production of steam could then be through these same upper perforations. The lower perforations would have some water fracturing but the fracture would travel upwards towards zones of lower stress. Hence perforation height should be insignificant (although data from the PHOP pilot indicates a strong correlation between perforation height and bitumen production).

Alternatively, this perforation correlation can be very much related to the presence of calcite streaks and shale layering within the pay, restricting the thickness of pay actually steamed. The negative impact of these barriers to steam injection would warrant further study in the field where a well would be perforated above or below the calcite streaks as was the case for the PHOP pilot and the Wolf Lake commercial project. The best case would include a well completion which has wellbore isolation packers to facilitate steaming into the above two perforations simultaneously through tubing and the annulus. Production would be comingled.

It is shown in this study that the calcite streaks prevent steam from entering the upper reservoir, literally cutting the reservoir and production in half.

7. 2 Wire-wrapped Screens

One of the most critical aspects of a bitumen recovery operation is sand control. Since all wells must be pumped, design problems are encountered relating to the amount of sand a bottomhole positive displacement pump can handle before seizure.

Wire-wrapped screens with 0.012 - 0.025 inch gap are typically used to keep out sand. Stabilized rate of fluid production does not appear to affect sand production, but sudden changes in fluid rate does. Sudden changes in production rate can be caused by sudden changes in pump speed. Severity of sand production appears to vary with the type of reservoir. In order to determine proper screen size, various oil sands pilots were visited and the sand sizes compared. The results were somewhat unexpected.

Conventional seive analysis recognizes sufficient bridging of sand at the downhole screen face occurs if the screen width is two times the sand diameter at the ten percentile of cumulative seive analysis as measured starting from the largest grain size. Therefore a finer grained reservoir like the Grand Rapids Formation would require a screen size of 0.012 inch (see Chapter 15, Figure 15.1.1.1). Unfortunately, bitumen will not produce freely through this narrow slit between the wire wraps.. In field tests at Wolf Lake, switching to a larger screen size (0.020 inch), produced too many fines and the pumps seized. After examining pilots producing from the Clearwater, McMurray, and Grand Rapids formations, it was determined that optimum screen size was from 0.018 to 0.025 inch, irrespective of the grain size.

The Clearwater formation appears to produce the least amount of sand even though its percentage of clays is the highest. The McMurray and Grand Rapids oil sands contain less than 4% clays in which kaolinite and smectite dominate while the Clearwater Formation contains about 30% clays mostly illite (see Chapter 15, Table 15.4.2). The reasons for the low sand production rate are possibly due to cementation or deposition of cementing precipitates, mainly SiO_2 from cooling of produced water during a production cycle. The cementation can be seen by comparing x-radiography of cores taken before and after a well has been steamed (Savoie et al., 1988). The cores taken after steaming show up lighter than they normally would, indicating deposition of cementing material such as clays including a small percentage of silica. Re-dissolution of cementation during the next injection cycle is difficult as most of the pore volume near the wellbore is occupied by steam and also because the SiO_2 deposition is very smooth-surfaced, thus the surface area for dissolution has been reduced substantially. It was also noted (Leshchyshyn et al., 1991) that unsteamed McMurray Formation oil sand wireline recovered core x-rays showed surface expansion fractures in cores with over 8 wt% bitumen. The oil sand cores taken at the depth where steaming had occured did not show any of these expansion fractures. This is because the soluble gas originally in the bitumen had been removed during the steaming process. Alternately, if enough soluble gas is available for creating these surface fractures, and the viscosity of the bitumen is low enough, there is potential for cold oil production.

At the McMurray PCEJ Pilot it was observed that, with 0.025 inch wire-wrapped screens, a well would start producing sand at a bottomhole temperature of 130 °C. The pump would handle the 3-5% by volume of sand production. By the time the bottomhole temperature dropped to 110 °C, the well would sand-in at about 15% sand-cut.

For the PHOP pilot, sand production did not seriously jeopardize production, although using a pumping cut-off of 110 °C bottomhole would probably save significant expenses on pump change-overs.

Chapter 8

Shear Fracturing or Dilation

Within this chapter is a theoretical overview of the physical processes at the center of shear fracturing, a discussion of the parameters which factor into the creation of multiple shear fractures, and an explanation for reduced fracture length. The conceptual basis for this research is the idea that massive fracturing in the shallow, unconsolidated oil sands occurs regularly and has a major impact on bitumen recovery. This proposition is expanded to account for the effects these multiple shear fractures have on conventional oil and gas fracture stimulations.

8.1 Process of Shear Parting

The process of shear parting is complex. Basic geomechanics depends largely upon the straight-line portion of a standard stress/strain plot where elastic deformation is described and Young's Modulus is calculated (Figure 8.1.1). Shear fracturing may occur in the region of higher stress (with higher associated strain). Plastic deformation can occur when the core suddenly loses stress (unrecoverable) and shows an increase in strain. In the field,"shear" fractures are initiated after the first vertical "tensile" fracture at the wellbore has started to propagate and widen. Tensile fracturing creates bending stresses in two directions, like an elliptic disc standing on end. One bend is horizontal along the wall of the tensile fracture and the second is vertical since the tips of the fracture heights have no width and width is maximum near the center of the fracture. Maximum bending of the rock, considering both vertical and horizontal directions, is at the wellbore. Maximum shearing is expected here. Integration of a two-dimensional fracture model with vertical bending (PKN) and a two-dimensional fracture model with horizontal bending (GDK) or a three-dimensional simulator would show a stress regime near actual conditions ready to create multiple shear fractures.

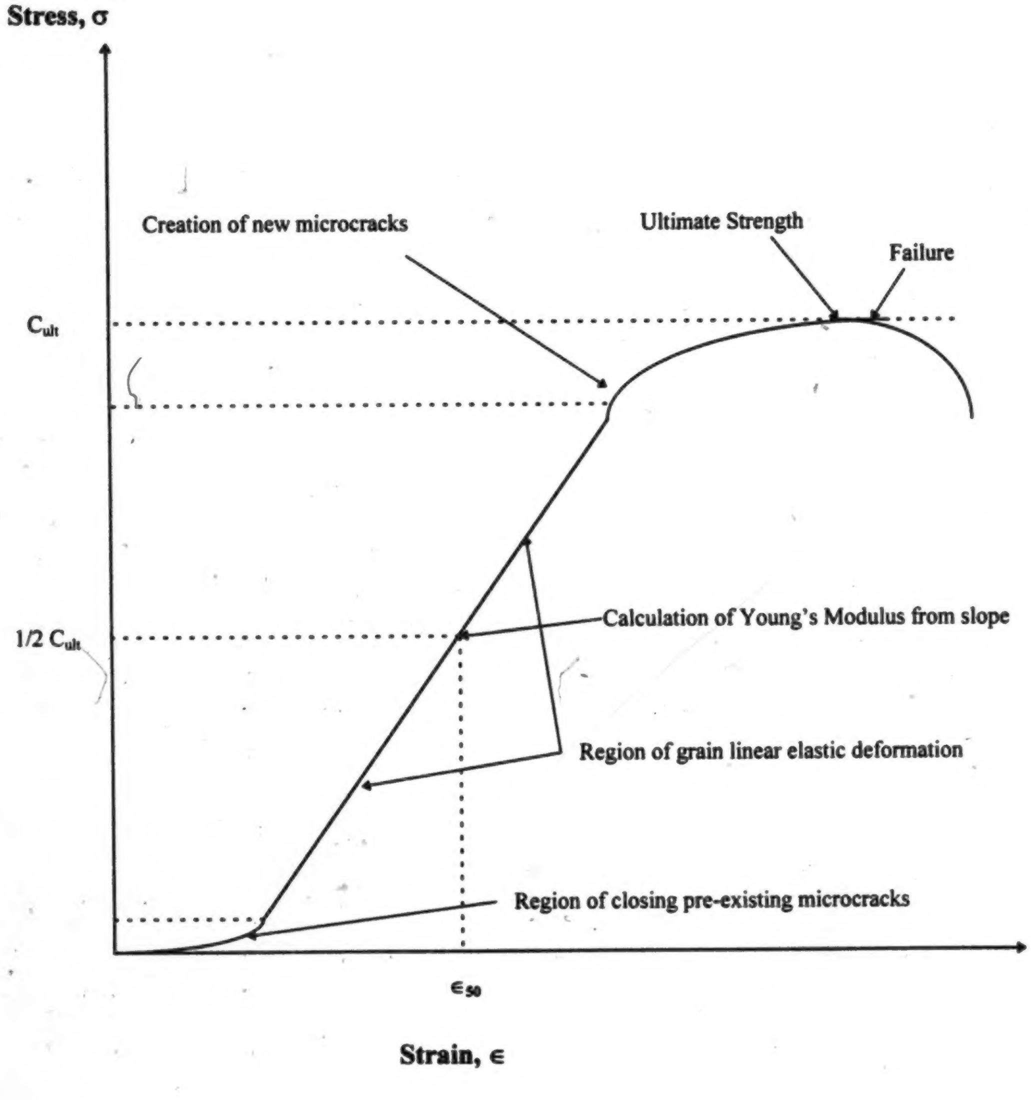

Figure 8.1.1: Stress - strain relationship for rock

Leshchyshyn et al. (1996) analyzed shear parting in various reservoirs in Alberta using well test analysis (Figure 8.1.2). The Basal Quartz Formation exhibits the most dilation. It is believed the massive shearing is due to the hardness or inflexibility of the quartz grains and at great depths, parting can be caused by failure of the Griffith cracks and not necessarily parting of the cementation material between the grains. Because the well test analysis shows very similar response between the oil sands dilation and the deeper Basal Quartz sand, it is believed the same process is creating the dilation.

There is no prevailing direction to these created shear fractures other than the general angle of cohesion being approximately 35 degrees and at which criss-crossing of the shear fractures occur (Leshchyshyn et al., 1991). From experience these fractures appear to propagate away from the wellbore where tension is at a maximum. The idea is similar to bending and breaking a pencil or tree branch where the outside edge of the bend breaks first and the cracks propagate inwards, in this case to the tensile fracture face. This phenomena is also seen in deep mine shafts and are called exploding rock "bursts".

Once the multiple shear fractures have been developed (dry), pore pressure due to fluid injection causes the shear fractures to propagate further away from the well and its tensile fracture face. The hypothesis of multiple shear fractures around the wellbore is not new and has been previously noted by Aud et al. (1994), who states that, the lower the fracturing fluid viscosity, the farther out the shear fractures will propagate. Water is considered a very low-viscosity fracturing fluid, as most conventional fracturing fluids are in the 100-1000 cp range. Steam, on the other hand, would have the least effect on shear fracture propagation since gas leak-off is about 10 times higher with steam than with water, giving less fracture width. The viscosity of steam is about 0.02 cp.

Shear fractures in oil sands are oil-wet. The fractures are initially created dry but fill up with the nearest fluid almost instantaneously. If a high saturation of bitumen is present, the freshly exposed sand grains will contact the bitumen first, becoming oil-wet. Photographs of actual core removed 10 meters from a well cyclically-steamed for 9 cycles in the McMurray oil sands show the above effect (Leshchyshyn et al., 1994). The matrix of the core shows bitumen depletion due to steaming except in close vicinity to the shear

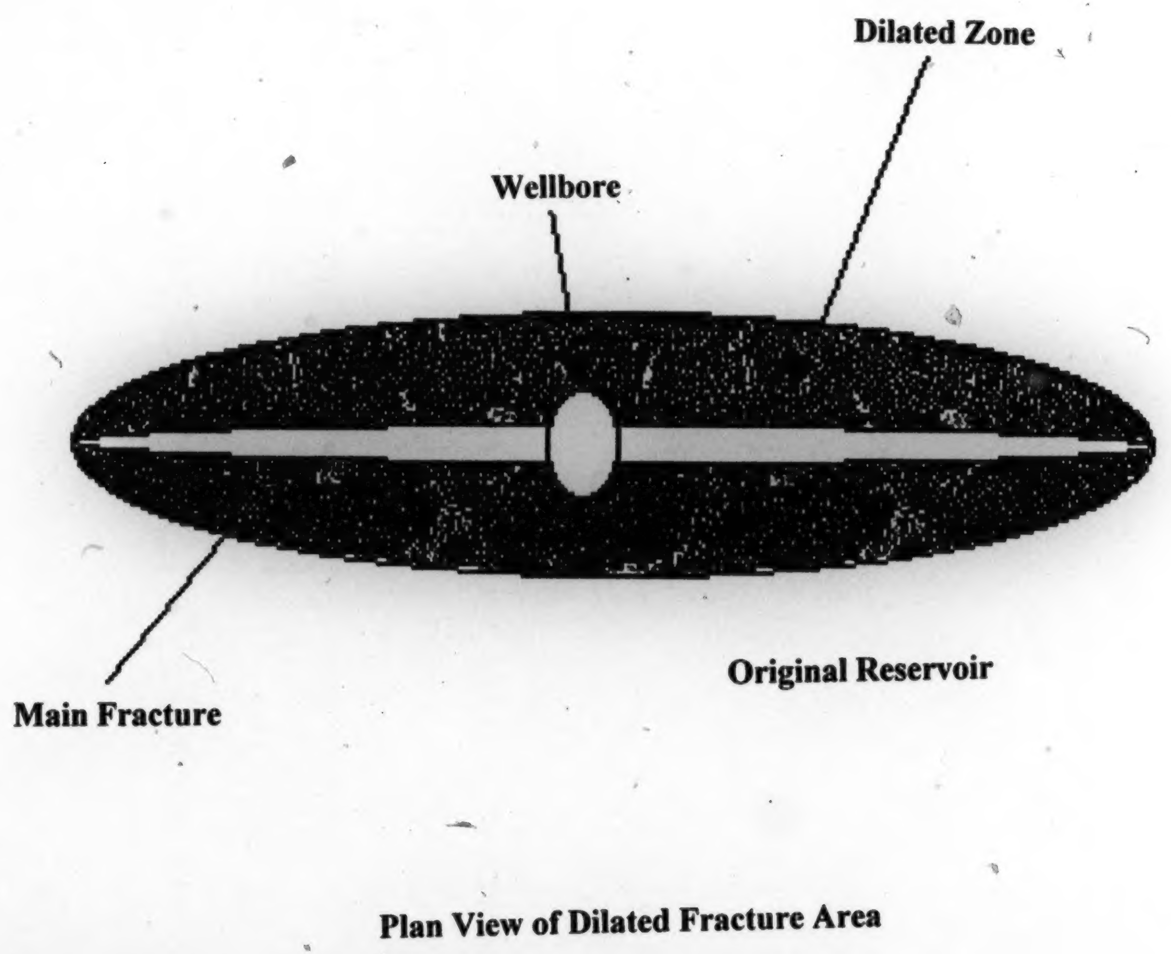
Dilated Zone
Wellbore
Main Fracture
Original Reservoir
Plan View of Dilated Fracture Area

Figure 8.1.2: Creation of a dilated zone near the wellbore

cracks, which remain high in bitumen content. Similar observations have been made on lab experiments performed on physical models at the Alberta Research Council (1975-1981) where manually-propped sand fractures (4 mm fracture diameter using 20/40 Ottawa sand), exhibited high-bitumen content if the propped sand was not first soaked in water for a minimum of one month to artificially produce a water-wet condition prior to steam injection. Even breaking apart a lump of virgin oil sand sample by hand will display the white, clean surface of the parted sand grains a fraction of a second before this surface becomes covered with bitumen. The implication is that shear fractures are new events as opposed to the widening of geologically old natural fractures which are likely extraneous cementing material and water, hence are water-wet. Griffith cracks are assumed to be present within the sand grains thereby augmenting the propagation of a new shear fracture. Dilated, multiple shear fracrures impart bulk characteristics to the reservoir matrix.

Hydraulically propagated shear fractures eventually have a direction. They may criss-cross at the wellbore or, be perpendicular to a tensile fracture and have the appearance of shattered rock. Once the fractures become filled with fluid and are forced to propagate outward as tensile fractures, their numbers decrease, as there is competition for the stresses while fracture width increases with increasing net pressure. Eventually these fewer fractures will run parallel to each other then turn directionally governed by the initial reservoir stresses, usually along the NE-to-SW fracture trend of Alberta. One would also expect net pressures (i.e., initial shut-in pressure minus minimum in-situ stress), to be high as more energy is required to open a fracture against increased localized minimum stresses. Parallel fractures rising vertically up the pay zone have been reported in the literature on McMurray oil sands (Chhina et al., 1987) and have in addition, been seen in lab fracture tests conducted on unconsolidated, triaxially-stressed, clean sand (Golder and Associates, about 1991). Following is an excerpt from the Golder associates brochure explaining oil sand dilation: "Unlike consolidated reservoir rocks, the individual sand grains in the oil sands matrix are not constrained by cementation. As injection fluid is forced rapidly into the oil sands matrix, individual sand grains slide relative to each other to accomodate the induced mechanical and/or thermal strain. Volume change significantly alters the stress field in the fracture zone and therefore controls the initiation, propagation and orientation of fractures". While this statement is shown true in the laboratory, it does not explain the fractures shown in the photographs of the post cores taken after cyclic steaming of a McMurray Formation well (Leshchyshyn et al., 1991), or the well testing response similarities of dilation in the wells at great depth (Leshchyshyn et al., 1996).

In the conventional oil and gas reservoirs of Alberta there is shear fracturing, especially in the Basal Quartz (BQ) Formation and generally throughout the Cretaceous Period Mannville Group which includes the BQ (Leshchyshyn et al., 1996). Conventional fracture stimulation treatments become difficult when the shear fractures leak-off the fracture fluid at the wellbore and not the proppant because the cracks are not wide enough. Without detection through well testing and remedial planning, the problem can cause early near-wellbore sand-off from a proppant slurry too concentrated to flow through the fractures (up to 2,000 kg dry proppant per m^3 of fracture fluid). Two remedies for reducing multiple shear fracturing are: i) use of high-viscosity fracturing fluid, or ii) initially stress-frac the formation with an explosive charge. Both methods may initiate shear fractures but they will not propagate far since pore pressure in the rock has not had a chance to increase. The rock must fail due to shear modulus rather than just tension. A third solution is to pre-inject a few tonne of 100-mesh sand to plug the multiple shear fractures, thus reducing net pressure nearer to that of a single propagating vertical fracture.

The author has recently presented a paper comparing shear fracturing of oil sands to that of other formations in Alberta (Leshchyshyn et al., 1996). The literature evaluates well test analyses of mini-fracs conducted on various conventional oil and gas wells prior to stimulation fracture treatments against data from the McMurray oil sands mini-frac tests. There is sufficient evidence to support the theory of shear fracturing even in deeper formations up to 2,000 mKB). From the fall-off of a mini-frac test, one can determine distance to the outer boundary of these shear fractures as well as the permeability inside this boundary when the fractures are open. For 20 m^3 of fluid fractured into a shearable formation, dilation boundary distances calculated by well test analysis are of the order of 5 to 10 meters and permeabilities range from 300 to 10,000 millidarcies (see Figure 8.1.3 for an example well test analysis). These values have been corroborated by numerical modeling of the mini-fracs and by thermal numerical simulation of actual cyclically steamed wells in the McMurray formation using Settari's TARFRAC/CONS model (Leshchyshyn et al., 1994) and Scientific Software's THERM program (Chan et al., 1991), respectively.

Stimulation work conducted recently has shown that multiple shear fracturing of sandstone can occur down to 2,200 m depth or 40,000 kPa fracture propagation stress. Plastic behavior appears to dominate at greater depths. A problem associated with plastic deformation is the forced "***pinch-out***" of a tensile fracture near the wellbore, as this is the zone of maximum back stress.

For other information on multiple fractures, please refer to the literature review of multiple fracturing in the paper by Leshchyshyn, 1996. The authors reviewed are: Hainey et al., 1995; Hopkins et al., 1995; Blanton et al., 1986; Mukherjee et al., 1995; Abass et al., 1992; Hallan et al., 1991; Chen et al., 1995; Warpinski et al., 1995; Wright et al., 1995; Jeffrey et al, 1995; Warpinski et al., 1993; Palmer et al., 1990; Jeffrey et al., 1987; Warpinski et al., 1991; Ely et al., 1995; Jeffrey et al., 1992; Steidl et al., 1993; Fast et al., 1992; Nolte et al., 1993; Weijers et al., 1992; Baumgartner et al., 1993; Abass et al., 1992; Brown,E. and M. Economides, unknown source; Hudson et al., 1992; Kim et al., 1991; Abou-Sayed et al., 1995; and Schuler et al., 1996.

Factors affecting multiple fracture generation are summarized in Appendix E, Table E1 while those affecting fracture length growth are compiled in Table E2. Both listings identify the set of parameters that encourage shear fracture growth in oil sands.

The two most significant parameters which promote multiple shear fractures are: i) lower injection fluid viscosity, and ii) a lower horizontal stress ratio given the observation that minimum and maximum stresses become more equalized at shallower depth of burial. Two other less important factors are: iii) resultant higher pore pressure caused by oil banking, and iv) lower wellbore confining stress due to shallower depth of burial. The

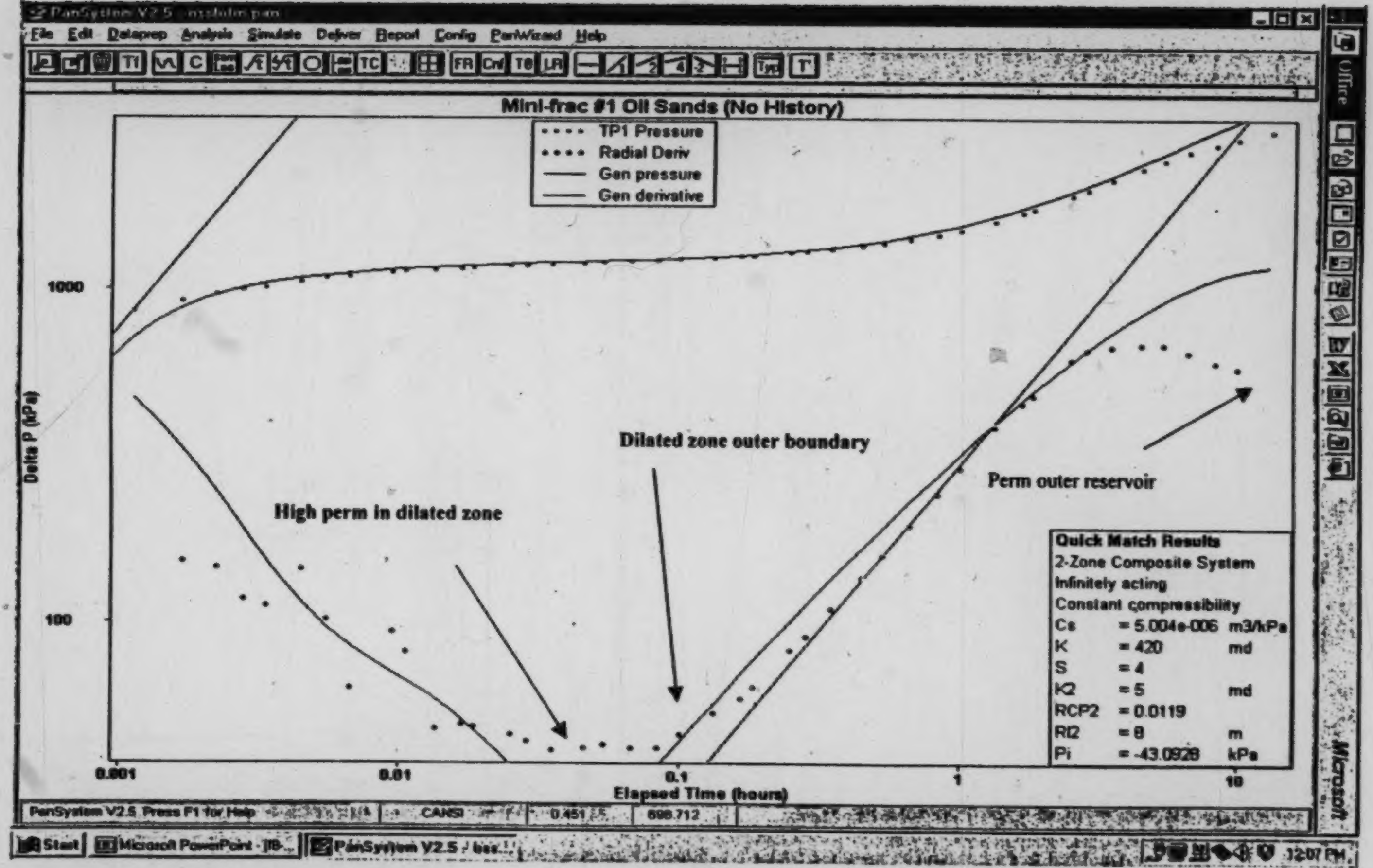

Quick Match Results
2-Zone Composite System
Infinitely acting
Constant compressibility
Cs = 5.004e-006 m3/kPa
K = 420 md
S = 4
K2 = 5 md
RCP2 = 0.0119
Rl2 = 8 m
Pi = -43.0928 kPa

Figure 8.1.3: Well test analysis of dilation in McMurray oil sands using a 2-zone composite model

The fracture propagation gradient (ISIP/depth) for most sandstone reservoirs in the world is 18 kPa/m and 19-19.5 kPa/m for shale deposits. The shallower the formation, the lower is the stress contrast between the sandstone and the shale, therefore a large amount of steam can be lost to the shale overburden. The presence of layered, energy-absorbing calcite, consisting of limestone and shale, would substantially reduce this steam loss. Unfortunately, these calcite streaks are within the pay zone and only serve to prevent steam from contacting the full net pay interval. Hence, bitumen production can be radically decreased.

The critical factors controlling fracture length propagation are: i) dilation and ii) increased permeability to water due to bitumen depletion. Also important but to a lesser degree are: i) initial higher permeability associated with higher porosity reservoirs and ii) apparent softer rock such as unconsolidated oil sands, coal, or chalk. In a softer matrix, formation creep or compaction can occur, giving a larger fracture width and shorter fracture length.

Chapter 9

Numerical Simulator

Simulation was performed using a commercial simulation product of Scientific Software-Intercomp (SSI) called THERM simulator, an implicit compositional thermal model capable of handling oil, water, and gas flows with solubility of gas-in-oil treated in the same manner as in a compositional black-oil model. Both models represent multiphase behaviour through equilibrium ratios or K- values. The user manual is: "Combustion and Steamflood Model - THERM - User's Manual," Release 2.2, October, 1984, First Printing.

9.1 Model Equations and Unknowns

The equations and boundary conditions have been given previously (Kalraise, 1987 and Demetre, 1993):

1. Combined continuity/momentum balance equations

$$\nabla \bullet \sum_{p=w,o,g} \frac{K_{vip} X_i \rho_p k k_{rp}}{\mu_p}$$

$$(\nabla p_p - \rho_p g \nabla D) = \frac{\partial}{\partial t}\left[\phi \sum_{p=o,w,g} K_{vip} X_i \rho_p S_p\right] + \tilde{q}_i \quad . \qquad (9.1.1)$$

2. Energy balance equation

$$\nabla \bullet \sum_{p=w,o,g} \frac{H_p \rho_p k k_{rp}}{\mu_p} (\nabla p_p - \rho_p g \nabla D) + \nabla \bullet (\lambda_c \nabla \theta)$$

$$= \frac{\partial}{\partial t}\left[(1-\phi) M_f \Delta\theta + \phi \sum_{p=o,w,g} S_p \rho_p E_p \right] + \tilde{q} \quad . \qquad (9.1.2)$$

3. Saturation constraint

$$\sum_{p=w,o,g} S_p = 1 \quad . \qquad (9.1.3)$$

4. Mole fraction constraint

$$\sum_{i=1}^{Nc} x_{ip} = \sum_{i=1}^{Nc} K_{vip} X_i = 1 \qquad p = w,o,g \quad . \qquad (9.1.4)$$

5. Capillary pressure equations

$$P_{cow} = P_o - P_w \qquad (9.1.5)$$

and

$$P_{cgo} = P_g - P_o \qquad (9.1.6)$$

The total number of equations is $(Nc + 2Np + 1)$ with p_o, p_w, p_g, S_w, S_o, S_g, θ, and X_i as $(Nc + 2Np + 1)$ unknowns.

Placing the capillary equation into equation (9.1.1) gives (***Nc*** + ***Np*** + 2) equations with ***po,Sw,So,Sg,*** θ**,** and ***Xi*** as (***Nc*** + ***Np*** + 2) unknowns.

Using finite-difference approximations and transmissibility terms, Equation (9.1.1) can be written as:

$$F_{i\,i,j,k}^{n+1} = \sum_{p}\left[\sum_{m} T_{p\,l}^{n+1}\left[\left(p_{p\,m}^{n+1} - p_{p\,i,j,k}^{n+1}\right) - \rho_{p\,l}^{n+1}\, g\left(z_m - z_{i,j,k}\right)\right]\right.$$

$$\left. - \frac{V_{b\,i,j,k}}{\Delta t}\left(\left[\phi K_{vip} X_i \rho_p S_p\right]_{i,j,k}^{n+1} - \left[\phi K_{vip} X_i \rho_p S_p\right]_{i,j,k}^{n}\right) - V_{b\,i,j,k}\, \widetilde{q}_{ip\,i,j,k}^{\,n+1}\right]. \quad (9.1.7)$$

Given

$$V_{b\,i,j,k}\, \widetilde{q}_{ip\,i,j,k}^{\,n+1} = q_{ip\,i,j,k}^{n+1} \qquad \text{for source/sink} \qquad (9.1.8)$$

the production term becomes

$$q_{ip\,i,j,k}^{n+1} = J'_{i,j,k}\left[\frac{k_{rp}}{\mu_p}\rho_p K_{vip} X_i\right]_{i,j,k}^{n+1}\left[p_o - p_{wf}\right]_{i,j,k}^{n+1} \quad , \qquad (9.1.9)$$

where

$$J'_{i,j,k} = \frac{2\pi k h f_h f}{\ln\left(f_g \frac{r_e}{r_w}\right) + s} \tag{9.1.10}$$

The total energy balance equation written in the finite-difference form is:

$$G^{n+1}_{i,j,k} = \sum_{p=o,w,g}\left[\sum_m T^{*\,n+1}_{p\;\;l}\left[\left(\overset{n+1}{\underset{m}{p_p}} - \overset{n+1}{\underset{m}{p_p}}\right) - \rho_{p_l} g\left(z_m - z_{i,j,k}\right)\right]\right]$$

$$- \frac{V_{b_{i,j,k}}}{\Delta t}\left(\left[\phi E_p \rho_p S_p\right]^{n+1}_{i,j,k} - \left[\phi E_p \rho_p S_p\right]^{n}_{i,j,k}\right)\Bigg]$$

$$+\sum_{m} \underset{l}{T_c}^{n+1}\left[\theta_m^{n+1} - \theta_{i,j,k}^{n+1}\right] - \frac{\underset{i,j,k}{V_b}}{\Delta t}\left(\left[(1-\phi)\rho_f H_f\right]_{i,j,k}^{n+1} - \left[(1-\phi)\rho_f H_f\right]_{i,j,k}^{n}\right)$$

$$-\underset{i,j,k}{V_b} \quad \widetilde{q}_{i,j,k} \tag{9.1.11}$$

where ***q*** contains heat loss to the overburden/underburden and heat produced/injected along with the fluids. The source/sink term is given by

$$\underset{i,j,k}{V_b} \quad \widetilde{q}_{i,j,k}\widetilde{q}_{i,j,k}^{n+1} = q_{i,j,k}^{n+1} = \underset{i,j,k}{q_{loss}^{n+1}} + \sum_{p} \underset{i,j,k}{q_p^{n+1}} \; \underset{i,j,k}{E_p^{n+1}} \tag{9.1.12}$$

where q_{loss} is heat lost to overburden/underburden for top and bottom layers.

9.2 Representation of Gas Solubility in Oil using K-Values

The model incorporates vapour-liquid phase equilibria for an oil which has been characterized as a single pseudo-component with molarity-averaged properties. An identical assumption is made to define a solution gas in the system vapour phase. Based on this system characterization, equilibrium ratios or ***k***-values are expressed as the quantity ***y/x*** where ***y*** is the mole fraction of the single pseudo-component in the gas phase and ***x*** is the mole fraction of the same pseudo-component in the liquid or oil phase.

For a system of one component only, the material balance relation is $L + V = n$, where ***n*** is the total number of moles present in both phases, ***L*** is the total moles in the liquid phase while ***V*** is the total moles in the vapour phase. Dividing both sides of the expression by ***n***, gives the phase balance $x + y = 1$ since $L/n = x$ and $V/n = y$.

K-values are entered in a table as functions of pressure and temperature.

9.3 Components and Phases

The components, designated by the label ***I*** are:

Component, ***I*** = 1 = water

Component, ***I*** = 2 = heavy (dead) oil

Component, ***I*** = 3 = gas

The Phases, ***J***, are identified as subscripts of a component, ***I***:

Phase, ***J*** = 1 = liquid water

Phase, ***J*** = 2 = oil

Phase, ***J*** = 3 = gas

The total of all the mole fractions of a component across all phases is equal to one.

Phase ⟶ **Component**	**Water**	**Oil**	**Gas**	**Σ**
H2O	✓	✗	✗	**1**
oil	✗	✓	✓	**1**
gas	✗	✓	✓	**1**

Also, within one gridblock, the sum of the mole fractions of all components in a given phase is unity, the term X_{IJ} denoting the mole fraction of component *I* in phase *J*:

$$\sum_{I=1}^{Nc} x_{IJ} = 1.0 \qquad J=1,Np \tag{9.3.1}$$

Phase, J ⟶ **Component, I**	**1 Water**	**2 Oil**	**3 Gas**
1 H2O	✓	✗	✗
2 oil	✗	✓	✓
3 gas	✗	✓	✓
Σ	**1**	**1**	**1**

The mole fraction of component *I* in phase *J* , defined by *J*'s condition of temperature and pressure is calculated as:

$$x_{IJ} = K_{vIJ} X_I \tag{9.3.2}$$

where K_{vIJ} are equilibrium is the equilibrium ratio of component ***I*** in phase ***J***, and X_I is the mole fraction of component ***I*** in ***I'***s primary or "master" phase. If phase 1 is component ***I'***s primary phase, then $K_{vII} = 1.0$. In general, when the master phase of ***I*** is ***J*** (written J_I), $KvIJ_1 = 1.0$. If component ***I*** is not "present" or soluble in phase J, then $K_{vIJ} = 0.0$.

Equilibrium ratios for master phases are initialized (in the model) as user-specified constants, ***Kv1*** to ***Kv5***. These data are the set of coefficients necessary for the analytical operation of component ***K***-Values for gas solubility situations.

The constants are as follows:

Kv1(1,1) = 1.0 = water in water

Kv1(1,2) = 0.0 = water in oil — Master Phase = Water

Kv1(1,3) = 0.0 = water in gas — (means ***J*** = 1)

Kv1(2,1) = 0.0 = oil in water

Kv1(2,2) = 1.0 = oil in oil — Master Phase = Oil

Kv1(2,3) = 0.0 = oil in gas — (means ***J*** = 2)

Kv1(3,1) = 0.0 = gas in water

Kv1(3,2) = .0198 = gas in oil — Master Phase = Gas

Kv1(3,3) = 1.0 = gas in gas — (means ***J*** = 3)

Gas in Oil Solubilities

(means ***J*** = 2)

Kv2(3,2) = -9.4525 = gas in oil

Kv3(3,2) = 2.26E-5 = gas in oil

Kv4(3,2) = -57.8 = gas in oil

Kv5(3,2) = 173.1275 = gas in oil

For $J \neq J_I$,

$$K_{vIJ} = \left[K_{V1}(I,J) + K_{V2}(I,J)/p + K_{V3}(I,J)p\right]e^{-\frac{K_{V4}(I,J)}{T - K_{V5}(I,J)}}$$

equation (9.3.3)

The equation for ***K***-value calculation is from Crookston et al (1979).

9.4 Specific Volume

Amagat's Law of Partial Volumes is used to calculate liquid phase specific volumes:

$$V_J = \sum_{I=1}^{Nc} X_{IJ} V_{IJ}, \tag{9.4.1}$$

where

V_J = specific volume of liquid phase ***J***, in m3/mole (***J*** = ***W*** or 1 for the water phase, and ***J*** = ***O*** or 2 for oil phase);

Nc = total number of components;

V_{IJ} = partial volume of component I in phase J of component I;

X_{IJ} = mole fraction of component I in phase J.

The partial volume, V_{IJ}, is calculated as

$$V_{IJ} = V^{\circ}_{IJ}[1 + C_{TI}(T-T_{ref})]\,[1 - C_I(p-p_{ref})] \tag{9.4.2}$$

where

V°_{IJ} = partial volume of component I in phase J at T_{ref}, p_{ref} of component I, (m^3/mole);

C_{TI} = coefficient of thermal expansion for component I (vol/vol-°C)

C_I = compressibility of component I (vol/vol-kPa);

T = temperature, °C;

T_{ref} = reference temperature, °C;

p = pressure, kPa;

p_{ref} = reference pressure, kPa.

9.5 Viscosities

The gas phase viscosity is

$$\mu_3 = \sum_{I=1}^{Nc} x_{I3}\mu_{I3} \tag{9.5.1}$$

where

$$\mu_{I3} = AVIS(I,3)T^{BVIS(I,3)} \qquad (9.5.2)$$

and ***AVIS*, *BVIS*** are model input keywords (Table 10.1).

The liquid phase viscosity is

$$\mu_J = \sum_{I=1}^{Nc} \mu_{IJ}^{x_{IJ}} \qquad (9.5.3)$$

The term μ_{IJ} can be evaluated from the ASTM standard form of Braden,1966:

$$\ln\left[\ln(\mu_{IJ} + \gamma\rho)\right] + a\ln T = b \qquad (9.5.4)$$

where

$\gamma \approx 0.6$ and ρ is liquid density in gm/cc

$\gamma\rho$ is replaced by 0.9999

Parameters for "***a***" and "***b***" are back-calculated from the above equation using known values of component viscosity measured at two different temperatures.

9.6 Temperature Dependency

Temperature-dependent parameters such as ***Swir (T)*, *Krwro (T)***, are translated from initial to final conditions according to the expresion:

$$X = X^{o} + \alpha(T - T_i) \qquad (9.5.1)$$

where X = value of parameter at final temperature;

X^{o} = value of parameter at initial temperature;

T = final temperature, °C;

T_i = initial temperature, °C;

α = constant for shifting temperature dependent permeabilities

Chapter 10

Simulator Input Data

Preparation of numerical model data and development of the input stream is reviewed in this chapter. An example of the simulator input file on which this thesis is based is shown in Table 10.1

10.1 Wellbore Heat Losses

Prior to conducting the model runs, heat losses down the wellbore were calculated using Intercomp's V-steam program and later substantiated by use of Dr. Farouq Ali's wellbore heat loss model (personal communication, 1991). The overburden reservoir description from the PHOP well IP1 history-matching was adopted with the assumption of 80% steam quality at the wellhead. A summary of the results, compiled in the table below represents steam flow through both the tubing and the annulus. Figure 10.1.1 presents the same results in graphical form. The optimistic bottomhole steam qualities without aquifers were employed in this study. Aquifer effects tend to reduce the heat content from surface to bottomhole by about 19% for 66 m^3/d injection rate, 15% for 110 m^3/d and 12% for 200 m^3/d. At 66 m^3/d, the operation is reduced to hot-water injection bottomhole.

BOTTOMHOLE STEAM QUALITY

Wellhead Quality (fraction)	Injection Time (days)	Injection Rate (m^3/d)	Wellhead Pressure (Mpa)	Bottomhole Quality* (no aquifer)	Bottomhole Quality* (with aquifer)
0.8	45	66.7	10	0.25	0
0.8	45	110	11.5	0.425	0.19
0.8	45	200	12	0.5	0.3

* at t = 45 days

T10-1

Table 10.1

```
TITLE PRIMROSE MODEL TO MATCH PREVIOUS SIMULATION   FILE:THERM1.IN

TITLE INJ @ 110 M3D FOR SLUG SIZE 3000
METRIC NCOL=80 JBTOT=11838 ;DEF 9000
NC 3  NAME         WATER               HOIL                SGAS
PVT
; COMPONENT        WATER               HOIL                SGAS
; ---------      ----------        -------------       ------------
MW                  18.0000         560.0000000          21.0000000
PCRIT                0.0000           0.0000000        4688.9200000
TCRIT                0.0000           0.0000000         221.1111000
COMP                 0.0000           4.9713E-04           4.9713E-04
CT                   0.0000           6.120E-04           6.120E-04
CP1                  0.0000           2.0937700           1.3500000
CP2                  0.0000           0.0000000           0.0000000
CP3                  0.0000           0.0000000           0.0000000
HVAPD                0.0000           0.0000000           0.0000000
DENST             1009.1302        1008.6000000           0.0000000
IPHASE               W                O                   G
PREF 101.35 TREF=15.56 TO=13.333 TMIN=13.333 TMAX=458 PMIN=69 PMAX=
20000
NVREAD  3
; COMPONENT        WATER               HOIL                SGAS
; ---------      ----------        -------------       ------------
;                 W      O      G      W      O      G        W     O      G
PVOL              0      0      0      0 9.9147E-4 0          0 1.035E-3 0
AVIS              0      0      0      0 1.2672E10 0    0 3.26766E-28 1.0177
5E-5
BVIS              0      0      0      0 -3.6489   0          0    9.84   1.21
66
KV1               1.0    0      0      0     1.0   0          0 1.9755E-2 1.0
KV2               0      0      0      0     0     0          0 -9.45247 0
KV3               0      0      0      0     0     0          0 2.2599E-5 0
KV4               0      0      0      0     0     0          0 -57.8016 0
KV5               0      0      0      0     0     0          0 173.1275 0
NTVIS  7
TEMPKV      13.333 100.0 200.0 300.0
PRESKV      500.0 1000.0 3000.0 6000.0 12000.0

STONE 1

SATWOT     ROCK 1  LPC  6.895  -6.895 SORMIN 0.10; W/O REL PERM ROCK
 1
;               SW                      KRW               KROW
;         --------------          -------------     --------------
            0.3000                     0.0000            1.0000
```

T10-1

```
                0.3292                  0.00060         0.90
                0.3583                  0.0011          0.79
                0.3875                  0.0017          0.685
                0.4167                  0.0022          0.59
                0.4458                  0.0050          0.49
                0.475                   0.0075          0.41
                0.5042                  0.0110          0.325
                0.5333                  0.0150          0.2450
                0.5450                  0.0180          0.2150
                0.5625                  0.027           0.168
                0.5917                  0.056           0.100
                0.6208                  0.100           0.043
                0.65                    0.16            0.0
                1.0                     1.0             0.0
SATGOT    ROCK 1 LPC 6.895  -6.895 SGR  0.05    ; G/LIQ REL PERM RO
CK 1
;               SLIQ                    KROG            KRG
;          --------------         -------------    --------------
                 0.70                   0.0000          0.20
                 0.7326                 0.016           0.136
                 0.7652                 0.040           0.088
                 0.787                  0.056           0.063
                 0.8196                 0.092           0.036
                 0.8522                 0.156           0.018
                 0.8848                 0.272           0.006
                 0.9174                 0.500           0.001
                 0.9500                 0.820           0.0000
                 1.0000                 1.0000          0.0000
SATWOT    ROCK 2  LPC  6.895  -6.895  SORMIN 0.01 ; W/O REL PERM RO
CK 2
;               SW                      KRW             KROW
;          --------------         -------------    --------------
                0.3000                  0.0000          1.0000
                0.3292                  0.00010         0.90
                0.3583                  0.0003          0.79
                0.3875                  0.0004          0.685
                0.4167                  0.0006          0.59
                0.4458                  0.0007          0.49
                0.475                   0.0011          0.41
                0.5042                  0.0018          0.325
                0.5333                  0.0032          0.2450
                0.5450                  0.0044          0.2150
                0.5625                  0.0071          0.168
                0.5917                  0.0153          0.100
                0.6208                  0.0312          0.043
                0.65                    0.07            0.0
                1.0                     1.0             0.0
```

```
SATGOT    ROCK 2 LPC   6.895  -6.895  SGR 0.05 ; G/LIQ REL PERM ROC
K 2
;            SLIQ                  KROG              KRG
;        --------------       -------------    --------------
             0.70                  0.0000            0.20
             0.7326                0.016             0.136
             0.7652                0.040             0.088
             0.787                 0.056             0.063
             0.8196                0.092             0.036
             0.8522                0.156             0.018
             0.8848                0.272             0.006
             0.9174                0.500             0.001
             0.9500                0.820             0.0000
             1.0000                1.0000            0.0000
SATWOT    ROCK 3  LPC  6.895  -6.895  SORMIN 0.01 ; W/O REL PERM RO
CK 3
;             SW                   KRW               KROW
;        --------------       -------------    --------------
            0.3000                 0.0000            1.0000
            0.3292                 0.00003           0.90
            0.3583                 0.00010           0.79
            0.3875                 0.00013           0.685
            0.4167                 0.00020           0.59
            0.4458                 0.00023           0.49
            0.475                  0.00037           0.41
            0.5042                 0.00060           0.325
            0.5333                 0.00107           0.2450
            0.5450                 0.00147           0.2150
            0.5625                 0.00237           0.168
            0.5917                 0.00510           0.100
            0.6208                 0.0104            0.043
            0.65                   0.02333           0.0
            1.0                    1.0               0.0
SATGOT    ROCK 3 LPC   6.895  -6.895  SGR 0.05 ; G/LIQ REL PERM ROC
K 3
;            SLIQ                  KROG              KRG
;        --------------       -------------    --------------
             0.70                  0.0000            0.20
             0.7326                0.016             0.136
             0.7652                0.040             0.088
             0.787                 0.056             0.063
             0.8196                0.092             0.036
             0.8522                0.156             0.018
             0.8848                0.272             0.006
             0.9174                0.500             0.001
```

```
           0.9500                 0.820            0.0000
           1.0000                 1.0000           0.0000
SATWOT     ROCK 4  LPC   6.895   -6.895   SORMIN 0.01 ; W/O REL PERM RO
CK 4
;             SW                   KRW               KROW
;        --------------       -------------     --------------
            0.0100                0.0000            1.0000
            0.10                  0.0909            0.9091
            0.20                  0.1919            0.8081
            0.30                  0.2929            0.7071
            0.35                  0.3434            0.6566
            0.40                  0.3939            0.6061
            0.45                  0.4444            0.5556
            0.50                  0.4949            0.5051
            0.55                  0.5455            0.4545
            0.60                  0.5960            0.4040
            0.65                  0.6465            0.3535
            0.70                  0.6970            0.3030
            0.80                  0.7980            0.2020
            0.90                  0.8990            0.1010
            1.0                   1.0               0.0
SATGOT     ROCK 4 LPC    6.895   -6.895   SGR 0.05 ; G/LIQ REL PERM ROC
K 4
;             SLIQ                KROG              KRG
;        --------------       -------------     --------------
             0.01                 0.0000            1.0000
             0.20                 0.1919            0.8081
             0.30                 0.2929            0.7071
             0.40                 0.3939            0.6061
             0.50                 0.4949            0.5051
             0.60                 0.5960            0.4040
             0.70                 0.6970            0.3030
             0.80                 0.7980            0.2020
             0.90                 0.8990            0.1010
             1.0000               1.0000            0.0000
;   TEMPERATURE DEPENDENCY ON RELATIVE PERMEABILITY DATA
  TEMPS
  ROCK  1  ;  FOR ROCK TYPE 1
DSWCDT     0.00054        DSWIRDT  0.00054
DSORWDT   -0.000827       DSORGDT -0.00054      DSORMDT  0.0
DKRWDT     0.0            DKRODT   0.0
CTPCW      0.0            CTPCG    0.0
;
  ROCK  2  ;  FOR ROCK TYPE 2
DSWCDT     0.00054        DSWIRDT  0.00054
DSORWDT   -0.000827       DSORGDT -0.00054      DSORMDT  0.0
DKRWDT     0.0            DKRODT   0.0
```

```
CTPCW     0.0          CTPCG    0.0
;
  ROCK  3  ;  FOR ROCK TYPE 3
DSWCDT     0.00054      DSWIRDT  0.00054
DSORWDT  -0.000827      DSORGDT -0.00054    DSORMDT  0.0
DKRWDT     0.0          DKRODT   0.0
CTPCW      0.0          CTPCG    0.0
;
  ROCK  4  ;  FOR ROCK TYPE 4
DSWCDT     0.00054      DSWIRDT  0.00054
DSORWDT  -0.000827      DSORGDT -0.00054    DSORMDT  0.0
DKRWDT     0.0          DKRODT   0.0
CTPCW      0.0          CTPCG    0.0
;
;     RESERVOIR AND OVER/UNDER BURDEN CONSTANT THERMAL DATA
KOB  190.66      CPOB  2702.76
KUB  145.88      CPUB  2655.81
KRADX  0.0  KRADY 0.0  KRADZ 0.0
DCPRDT 0.0  DKDSG 0.0
;    GRID DEFINITION AND SOLUTION METHOD
RTZ    ; RADIAL  GRID SYSTEM
NR 8  NTHET 1  NZ 1
FMULT 1.0    ; SYSTEM PERFORMANCE MULTIPLIER IS UNITY
5PT          ; 5-POINT DIFFERENCING SCHEME SELECTED
SOLUTION=ITER  ; ITERATIVE SOLUTION TECHNIQUE WILL BE USED
RW=110
R  RVAR 0.924 2.1303 4.9117 11.3245 26.1096 60.1980 138.792 320.0
DTHET  CON  360.0 ; NTHET=1
DZ ZVAR 9.5
; GRID BLOCK PROPERTIES
;
PHI VALUE       8*0.35
   MOD 1 1 1 1 1 1=1.0
CR  CON  1.42E-02  ; /MPA
KR  CON 1300
KTHET EQUALS  KR*1.0
KZ  CON 0.0
CPR CON  2347.3 ; HEAT CAPACITY ROCK
KT  CON  163.865 ; THERMAL CONDUCTIVITY KJ/DAY-M-DEGC
RTYPE CON 1
   MOD  1 1 1 1 1 1=4
HTOP  CON  495.0 ; TOP OF RESERVOIR
EQUIL  ; EQUILIBRATION DATA FOLLOWS
        BOUND      2    8    1   1    1    1 ; I-I,J-J,K-K
        PINIT      2503.35
        TINIT      13.333
        SWATER     0.50
        SOIL       0.50
        SGAS      0.0
        NGAS      3
        X         1.0000    0.8807       1.0
EQUIL
        BOUND     1    1    1   1    1    1 ; I-I,J-J,K-K
        PINIT     2503.35
        TINIT     13.333
        SWATER    1.00
        SOIL      0.00
        SGAS      0.0
        NGAS      3
        X         1.0000    0.8807       0.0
;       OUTPUT=OFF  PRINT=RZ
; ==================================================================
==========
RUN

WELL 1  I 1 J 1
        INJ   1
        PERF  1  1  1
        KHL   1  300    ; HIGH
        BHP   1  14000.0
        KBHP  1  1
        WMULT 1  1
        PINJ  1  9200.0
        TINJ  1   304.89
        QUAL  1      .20
        IRATE 1   66.7    0.0   0.0
 ;      WELLZERO 1 OFF

WELL 2  I 1 J 1
        PROD    2
        PERF    2  1  1
        KHL     2  100  ;  HIGH
        BHP     2  420.
        KBHP    2  1
        WMULT   2  1
        PRATE   2  0.0
;       PRUNITS 2  STBLIQ
;       QOLIM   2  0.5
;       TEMPLIM 2  50.
;       STMMAX  2  0.0
;       GASMAX  2  0.0
;       WELLZERO 2 OFF

TFREQ=1  WFREQ=5
CPACSUM=OFF DENSUM=ON MFSUM=OFF RSUM=OFF SUMFILE=OFF VISSUM=ON
WSUM=ALL H2OSUM=OFF
```

```
   DSITN=0.2             ;   FRACTION
   DPITN=500.0           ;   KPA
   DTITN=25              ;   DEG. C
   DXITN=0.15            ;   FRACTION
   DTMAX = 10.0          ;         90
   DTMIN = 0.0001        ;         0.0001
   DSMAX =  0.4          ;         .2
   DPMAX = 1500.0        ;         1000
   DTPMAX= 80.0          ;         80
   DXMAX=2.00
;
;  DPITN = 400           ;         400
;  TOLS  = 0.01          ;         0.01
;  TOLP  = 20            ;         20
;  TOLR  = 0.01          ;         0.01
;  ITNPC = 1             ;         0  OUTPUT DEBUG
;  TOLPI = 0.007         ;         0.007

; ==================================================================
=====
;
; ==================================================================
=====
RSTWR=-1 ; NOREWIND
MINITN=3   MAXITN=15  ITNPC 3
TFREQ=1   WFREQ=5  AFREQ=5  MFSUM=ON  CATWR=3
     DTAUTO=1.0 ;DTMAX=20.0 DTMIN=0.25
TIME=45     ;  END OF 45 DAYS INJECTION
        PINJ  1  9200.
        TINJ  1   304.89
        QUAL  1      0.2
        IRATE 1   0.0     0.0   0.0

        PRATE   2  0.0
OVER    RTYPE 2 8 1 1 1 1 = 2
TIME=55     ;  END OF 10 DAYS SOAK
        PINJ  1  9200.
        TINJ  1   304.89
        QUAL  1      0.2
        IRATE 1   0.0     0.0   0.0

        PRATE   2  40.0
RSTWR=0
TIME=115  ; END OF 60 DAYS PRODUCTION

STOP
ENDJOB
□
```

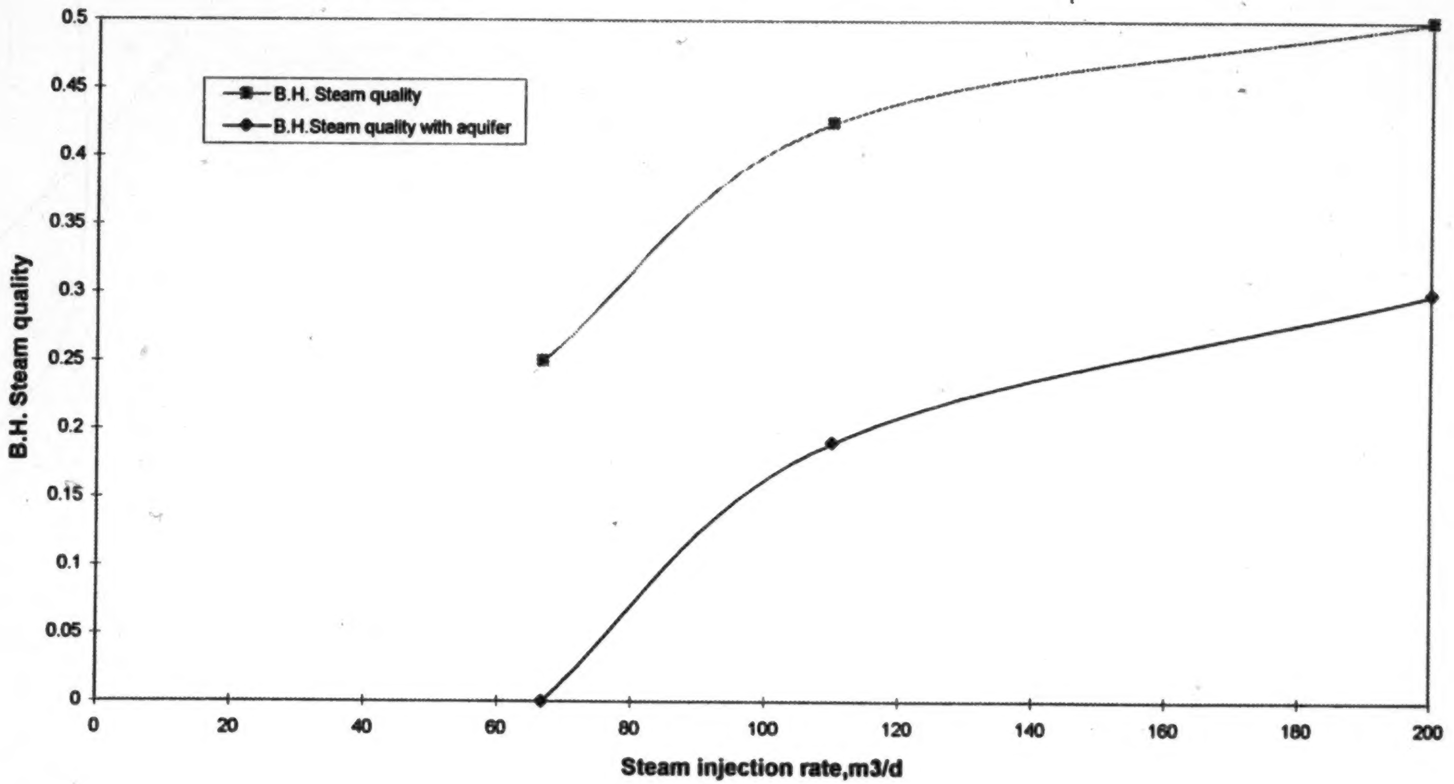

Figure 10.1.1: Estimated bottomhole steam quality assuming 80% wellhead quality Vs steam injection rate

10.2 Reservoir Description and Well Completion

Original reservoir descriptions drawn up for PHOP wells are presented here. Location depths range from 490 to 529 mKB, the average net pay consisting of 20 m of rich oil sand and 7 m of 20% shaley oil sand. A typical or weighted-average well description was generated from these wells and was essential to creating a single- layer model upon which the correlation curves were developed. Reservoir descriptions for each pilot well including the averaged characterization of the composite well are given in Tables 10.2.1 through 10.2.9.

The calcite streaks (denoted as ***SH***) have a critical bearing on recoverable reserves since they divide the pay into two almost equal non-communicating zones of interest. Perforating either the upper or lower reservoir will yield only bitumen production from the perforated half of the pay. The phrase "calcite streak" is used by the oil industry to identify a thin zone of a calareous/shale mixture capable of reducing or preventing fracture height growth and not necessarily the calcite mineral.

Most of the wells were actually perforated in the lower zone at the start, though IP1 is the exception where both halves were opened to the wellbore. It was believed that steam rises so eventually the upper oil sands will produce into the lower perforations. This theory was proved from laboratory tests using vertical and horizontal wells. However, that research stopped short of performing cyclic steam tests with impermeable boundaries halfway through the pay as it was incorrectly reasoned that this procedure merely reduced the size of the experiment by one-half. Heat transfer by conduction to the upper zone was not tested since heat conduction alone is far too slow for economic production, although future projects might take advantage of this heat loss. The Husky Frog Lake project and the take-over of the Wolf Lake project by Amoco are two cases in point.

Table 10.2.1

PHOP RESERVOIR DESCRIPTION, WELL IP-1

Depth mKB	Thickness m	Sw %	So %	kh md	kv md	Porosity	Lithology
490.00							
	1.95	99	1	0.5	0.2	0.16	SH
491.95							
	6.75	31	69	1300	600	0.33	OS
498.70							
	4.83	30	70	1300	600	0.33	OS
503.53							
	1.22	99	1	0.5	0.2	0.16	SH
504.75							
	5.70	35	65	1300	600	0.33	OS
510.45							
	1.00	99	1	0.5	0.2	0.16	SH
511.45							
	3.05	44	56	1300	600	0.33	OS
514.50							
	3.70	48	52	1300	600	0.33	OS
518.30							
	10.80	99	1	0.5	0.2	0.16	SH
529.00							

OS = Unconsolidated Oil sand
SH = Shale-like, indurated, impermeable zone

Perforations, mKB: 493.5 - 495.3
496.5 - 499.0
501.4 - 503.8
505.0 - 508.0
509.0 - 510.0

Table 10.2.2

PHOP RESERVOIR DESCRIPTION, WELL IP-2

Depth mKB	Thickness m	Sw %	So %	Kh md	Kv md	Porosity	Lithology
490.00							
	4.50	99	1	0.5	0.2	0.16	SH
494.50							
	8.00	31	69	1300	600	0.33	OS
502.50							
	4.50	31	69	1300	600	0.33	OS
507.00							
	0.75	99	1	0.5	0.2	0.16	SH
507.75							
	4.75	36	64	1300	600	0.33	OS
512.50							
	4.20	39	61	1300	600	0.32	OS
516.70							
	1.80	49	51	1000	400	0.31	OS
518.50							
	1.50	61	39	500	15	0.2	OS
520.00							
	2.00	46	54	1300	500	0.31	OS
522.00							
	7.00	99	1	0.5	0.2	0.16	SH
529.00							

OS = Unconsolidated Oil sand
SH = Shale-like, Indurated, Impermeable zone

Perforations, mKB: 512 - 518.1

Table 10.2.3

PHOP RESERVOIR DESCRIPTION, WELL IP-3

Depth mKB	Thickness m	Sw %	So %	Kh md	Kv md	Porosity	Lithology
490.00							
	4.60	99	1	0.5	0.2	0.16	SH
494.60							
	6.40	32	68	1300	600	0.33	OS
501.00							
	0.50	99	1	0.5	0.2	0.16	SH
501.50							
	4.00	34	66	1300	600	0.33	OS
505.50							
	1.00	99	1	0.5	0.2	0.16	SH
506.50							
	3.70	34	64	1300	600	0.33	OS
510.20							
	0.30	99	1	0.5	0.2	0.16	SH
510.50							
	5.70	42	58	1300	600	0.33	OS
516.20							
	5.90	45	55	1300	600	0.33	OS
522.10							
	6.90	99	1	0.5	0.2	0.16	SH
529.00							

OS = Unconsolidated Oil sand
SH = Shale-like, indurated, impermeable zone

Perforations, mKB: 509.1 - 516.1

Table 10.2.4

PHOP RESERVOIR DESCRIPTION, WELL IP-4

Depth mKB	Thickness m	Sw %	So %	Kh md	Kv md	Porosity	Lithology
490.00							
	4.00	99	1	0.5	0.2	0.16	SH
494.00							
	8.60	31	69	1300	600	0.33	OS
502.60							
	1.15	99	1	0.5	0.2	0.16	SH
503.75							
	3.75	35	65	1300	600	0.33	OS
507.50							
	1.00	99	1	0.5	0.2	0.16	SH
508.50							
	15.00	46	54	1300	600	0.33	OS
523.50							
	5.50	99	1	0.5	0.2	0.16	SH
529.00							

OS = Unconsolidated Oil sand
SH = Shale-like, indurated, impermeable zone

Perforations, mKB:	505.5 - 507.5
	504.5 - 513.5

Table 10.2.5

PHOP RESERVOIR DESCRIPTION, WELL IP-5

Depth mKB	Thickness m	Sw %	So %	Kh md	Kv md	Porosity	Lithology
490.00							
	1.84	99	1	0.5	0.2	0.16	SH
491.84							
	1.10	39	61	1300	600	0.33	OS
492.94							
	6.10	30	70	1300	600	0.33	OS
499.04							
	0.40	99	1	0.5	0.2	0.16	SH
499.44							
	4.10	32	68	1300	600	0.33	OS
503.54							
	0.50	99	1	0.5	0.2	0.16	SH
504.04							
	4.40	32	68	1300	600	0.33	OS
508.44							
	3.75	37	63	1300	600	0.33	OS
512.19							
	3.45	41	59	1300	600	0.33	OS
515.64							
	8.30	47	53	1300	15	0.33	OS
523.94							
	5.00	47	53	1300	15	0.33	OS
528.94							

OS = Unconsolidated Oil sand
SH = Shale-like, indurated, impermeable zone

Perforations, mKB: 505.9 - 513.9

Table 10.2.6

PHOP RESERVOIR DESCRIPTION, WELL IP-6

Depth mKB	Thickness m	Sw %	So %	Kh md	Kv md	Porosity	Lithology
490.00							
	0.50	99	1	0.5	0.2	0.16	SH
490.50							
	3.00	40	60	1300	600	0.33	OS
493.50							
	3.50	35	65	1300	600	0.33	OS
497.00							
	5.30	35	65	1300	600	0.33	OS
502.80							
	1.90	99	1	0.5	0.2	0.16	SH
504.70							
	9.50	45	55	1300	600	0.33	OS
514.20							
	14.80	99	1	0.5	0.2	0.16	SH
529.00							

OS = Unconsolidated Oil sand
SH = Shale-like, indurated, impermeable zone

Perforations, mKB:	499.5 - 502.5
Plug, mKB:	504.0
Perforations, mKB:	505.5 - 514.25

Table 10.2.7

PHOP RESERVOIR DESCRIPTION, WELL IP-7

Depth mKB	Thickness m	Sw %	So %	Kh md	Kv md	Porosity	Lithology
490.00							
	3.60	99	1	0.5	0.2	0.16	SH
493.60							
	5.50	33	67	1300	600	0.33	OS
499.10							
	1.70	99	1	0.5	0.2	0.16	SH
500.80							
	4.30	29	71	1300	600	0.33	OS
505.10							
	0.50	99	1	0.5	0.2	0.16	SH
505.60							
	10.50	35	65	1300	600	0.33	OS
516.10							
	1.00	99	1	0.5	0.2	0.16	SH
517.10							
	2.00	39	61	1300	600	0.33	OS
519.10							
	5.00	45	55	1050	15	0.32	OS
524.10							
	4.90	99	1	0.5	0.2	0.16	SH
529.00							

OS = Unconsolidated Oil sand
SH = Shale-like, indurated, impermeable zone

Perforations, mKB: 513.1 - 523.1

Table 10.2.8

PHOP RESERVOIR DESCRIPTION, WELL IP-8

Depth mKB	Thickness m	Sw %	So %	Kh md	Kv md	Porosity	Lithology
490.00							
	5.70	99	1	0.5	0.2	0.16	SH
495.70							
	5.40	35	65	1300	600	0.33	OS
501.10							
	1.00	99	1	0.5	0.2	0.16	SH
502.10							
	7.40	35	65	1300	600	0.33	OS
509.50							
	6.75	39	61	1300	600	0.33	OS
516.25							
	0.50	99	1	0.5	0.2	0.16	SH
516.75							
	2.15	41	59	1300	600	0.33	OS
518.90							
	0.50	99	1	0.5	0.2	0.16	SH
519.40							
	3.70	46	54	1050	15	0.32	OS
523.10							
	3.00	51	49	1050	15	0.32	OS
526.10							
	2.90	99	1	0.5	0.2	0.16	SH
529.00							

OS = Unconsolidated Oil sand
SH = Shale-like, indurated, impermeable zone

Perforations, mKB: 512.8 - 523.1

Table 10.2.9

PHOP RESERVOIR DESCRIPTION, GENERAL WELL

Depth mKB	Thickness m	Sw %	So %	Kh md	Kv md	Porosity	Lithology
490.00							
	5.00	99	1	0.5	0.2	0.16	SH-67%
		37	63	1300	600	0.33	OS-33%
495.00							
	8.00	32	68	1300	600	0.33	OS
503.00							
	1.00	99	1	0.5	0.2	0.16	SH
504.00							
	7.00	36	64	1300	600	0.33	OS
511.00							
	5.00	41	59	1300	600	0.33	OS
515.00							
	7.00	46	54	1200	340	0.33	OS-80%
		99	1	0.5	0.2	0.16	SH-20%
523.00							
	6.00	48	52	1200	15	0.33	OS-20%
		99	1	0.5	0.2	0.16	SH-80%
529.00							

OS = Unconsolidated Oil sand
SH = Shale-like, indurated, impermeable zone

Perforations, mKB:

The oil sands can be separated into two general categories, rich and lean. The rich oil sand has a porosity of 33% and horizontal and vertical permeabilities of 1,300 md and 600 md, respectively. A value of about 0.45 is found for the permeability ratio, ***kv/kh***. These values were taken from special core analysis in which brine was the testing fluid. Water Saturation is about 30-50%.

The lean oil sand has lower porosities of about 20-30%, horizontal and vertical permeabilities of 1050 md and 15 md respectively, and water saturation of about 45-60%. Thus, the permeability ratio, ***Kv/Kh***, is near 0.015. Modeling has shown that initial water saturations greater than 45% will not economically produce bitumen by cyclic steaming using today's technology, so the lean oil sand has essentially no recoverable reserves. However, these layers are important for the lateral connective transport of heat away from the wellbore, especially in reservoirs where water saturations are too low to allow significant matrix steam injection. Delivery of steam to the reservoir would require some form of fracture stimulation. As illustration, the PCEJ project where initial water saturation is 5-10%, only 10 m^3/d of steam could be delivered below fracture pressure to the reservoir. An ideal water saturation and thickness for a bottom-water layer would be around 45% and 4 m, respectively, to effectively heat the upper rich oil sands above without extensive heat loss or pressure drop. An underlying lean oil sand layer at Peace River has contributed to Shell Oil's commercial production of the rich oil sand above using a steamflood-cyclic steaming process.

The wells were cemented with 190.5 mm (7 1/2 inch) casing and perforated by wireline with 23-gram charges at 13 shots per meter (SPM) with 90° phasing, sufficient to allow unobstructed fluid flow in either direction at the sandface. Well tests performed on virgin wells in the rich oil sands (Leshchyshyn et al., 1990), indicate an overall skin of -5, an enhanced flow condition equivalent to that of a well with a very efficient propped fracture. The reason for such an improvement is that perforating creates a large, effective wellbore radius across the cement and into the oil sand beyond skin caused by drilling mud cake remaining prior to cementing in the production casing. The perforations are assumed to be clean as the oil sand is composed of 65-80% fine-grained quartz (as opposed to very-fine-grained sand and silt) and less pulverization of the rock is expected as a result of the blast. This compares with conventional oil and gas drilling and completions, which normally sees initial average skin of +3 upon well testing. A possible explanation for this result is that oil moves during conventional oil drilling (live oil viscosity about 0.85 cp), causing mud filter cake build-up, but the same is not true in oil sands drilling (here, live oil viscosity is about 80,000 cp). For interest's sake, acidizing a conventional oil well will reduce the skin to only 0 to -2.

10.3 Relative Permeability Curves

Various sets of water-oil permeability curves designed for the PHOP pilot are described here, while only one is selected for modelling both the injection and production for cycle one.

Water-oil and gas-oil permeability curves are presented in Table 10.1. The tabulated data is plotted in Figures 10.3.1 to10.3.4. This set of plots are not direct results of core analysis but instead are "***calibrated permeability curves***" generated over a few years of actual field production experiences, initially by Gulf, then by Intercomp as consultants for Petro-Canada. These curves may include reservoir simulation characterizations not considered elsewhere in the thermal numerical model such as shear fracturing and/or fingering. Unfortunately, the only way lab-generated permeability curves are directly applicable is to design a numerical model which takes into account all of the properties and mechanisms of rock. Such a model would require the addition of many process variables including tortuosity, friction, wettability, linear and bilinear flow, and compaction.

The irreducible water saturation (***SWIR***) is an empirical estimation though it may also be calculated from capillary pressure curves corrected to model conditions representing actual field data, then further adjusted for a differential pressure of 7 kPa (1 psi) capillary pressure per model layer.

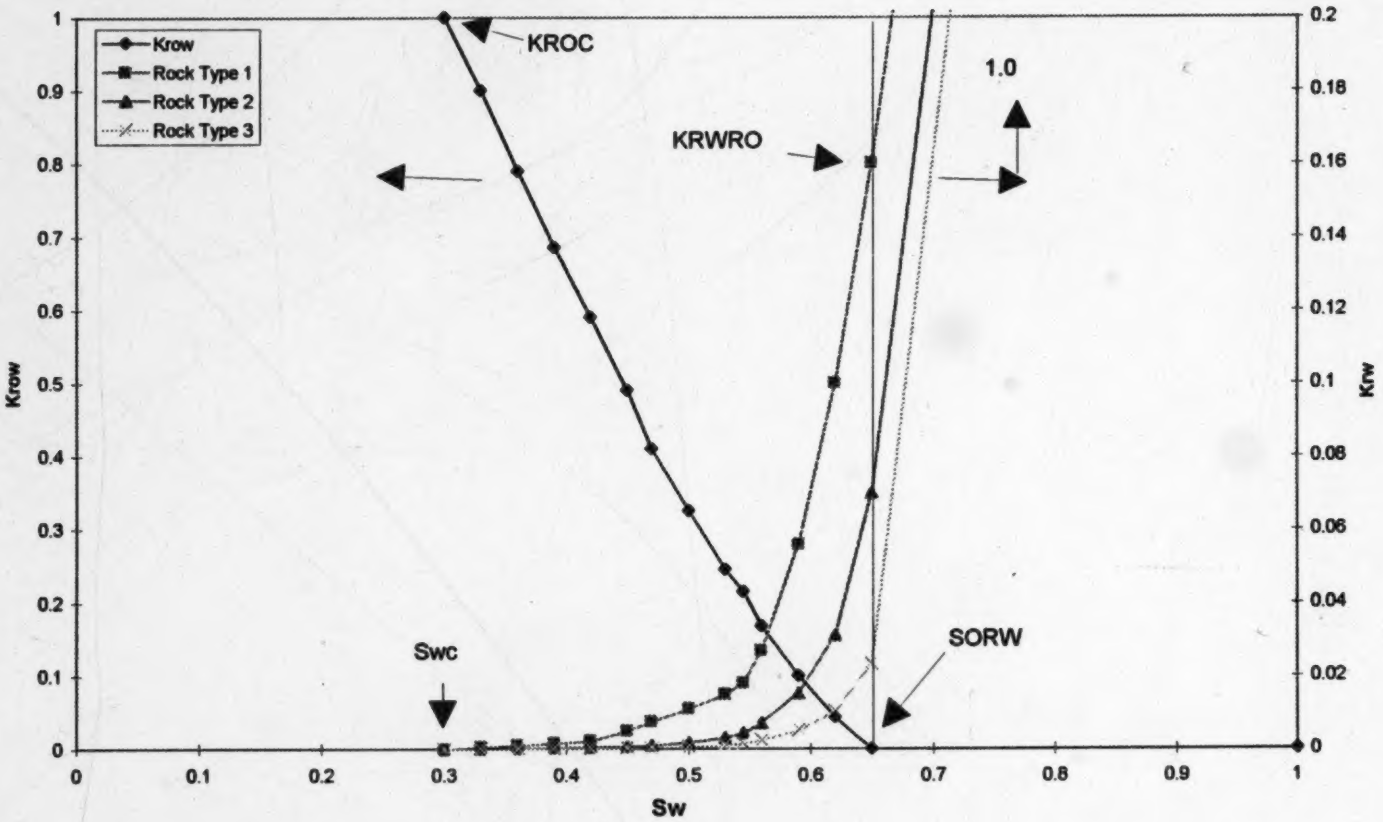

Figure 10.3.1: Water - Oil Rock Types 1 - 3, PHOP relative permeability data

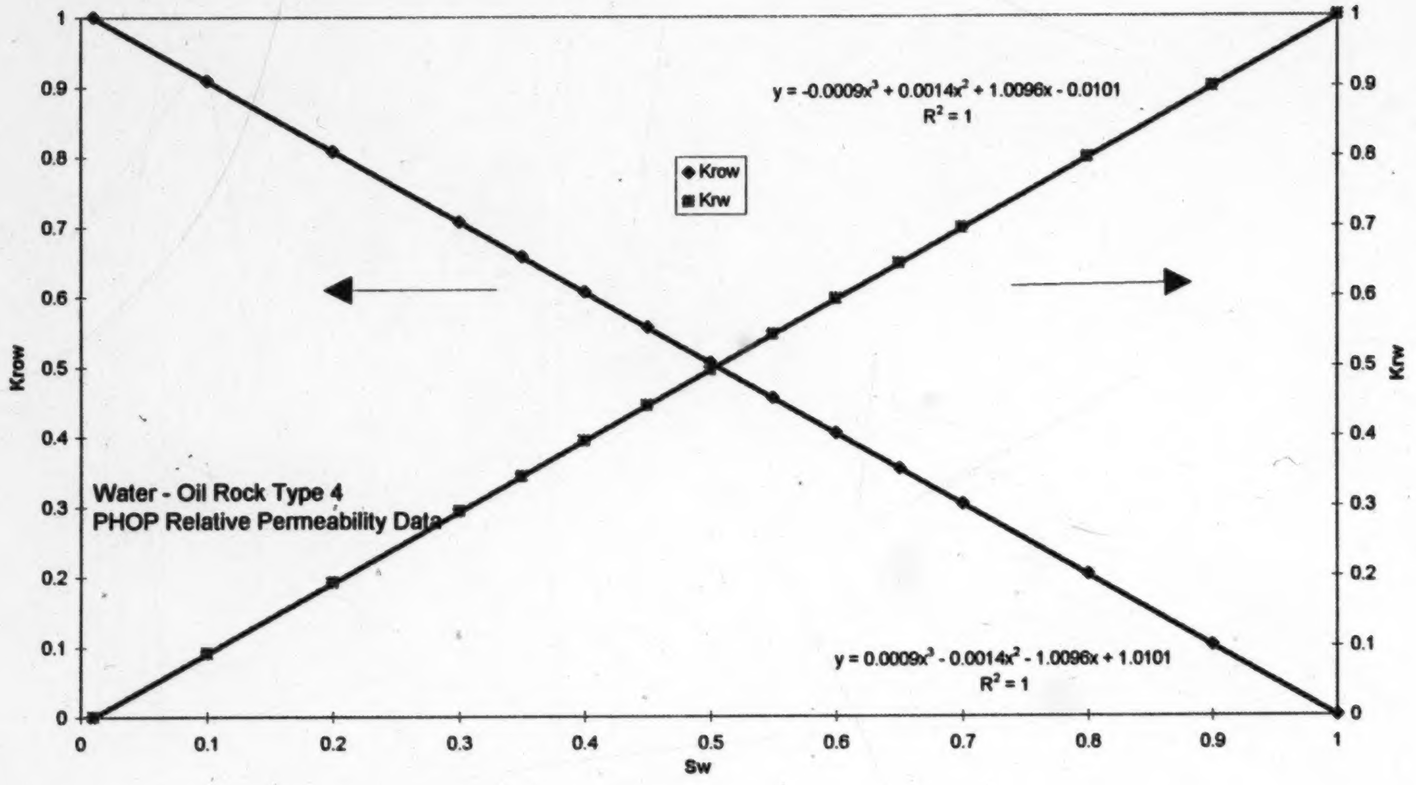

Figure10.3.2: Water - Oil Rock Type 4, PHOP relative permeability data

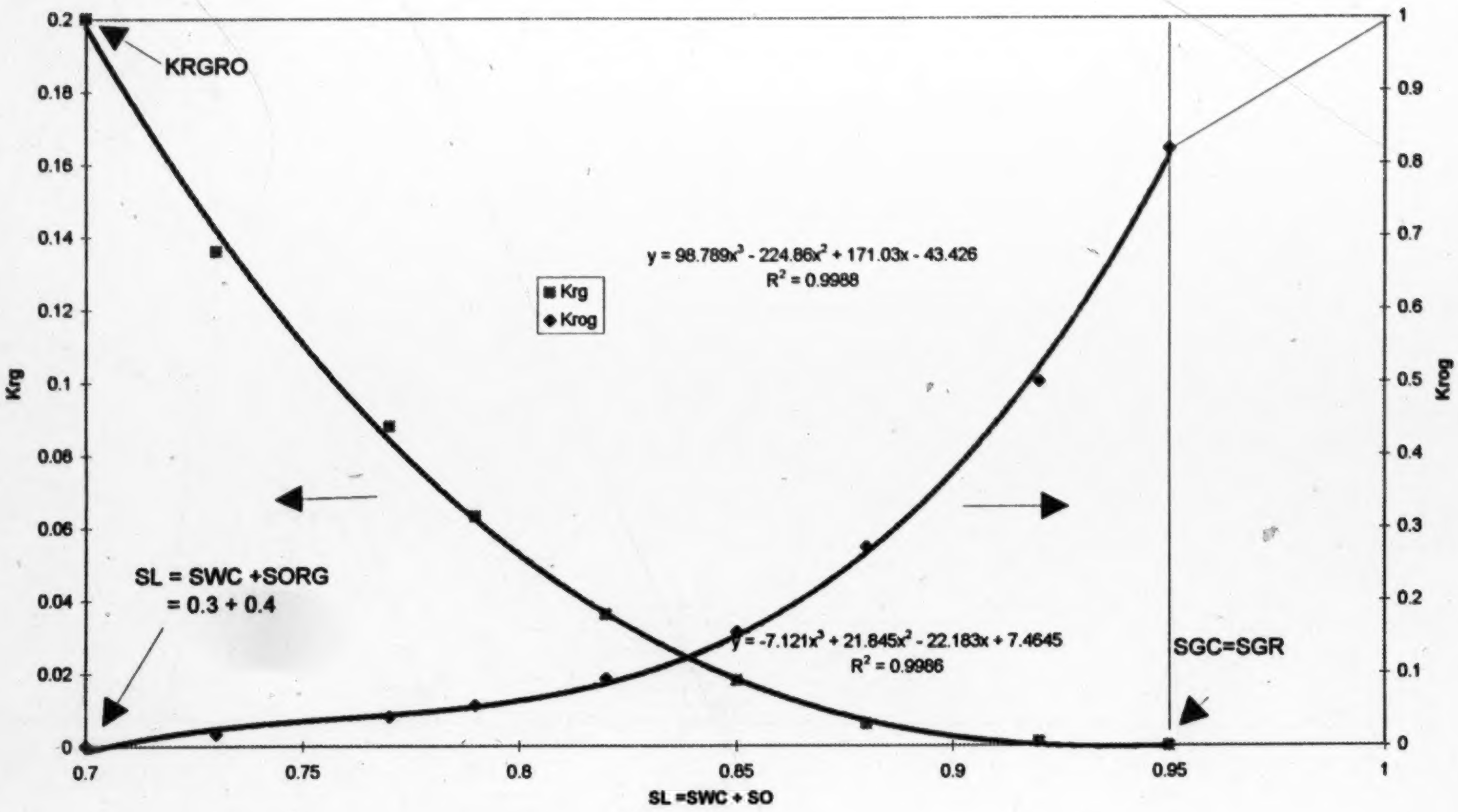

Figure 10.3.3: Gas-Oil Rock Types 1 - 3, PHOP relative permeability Data

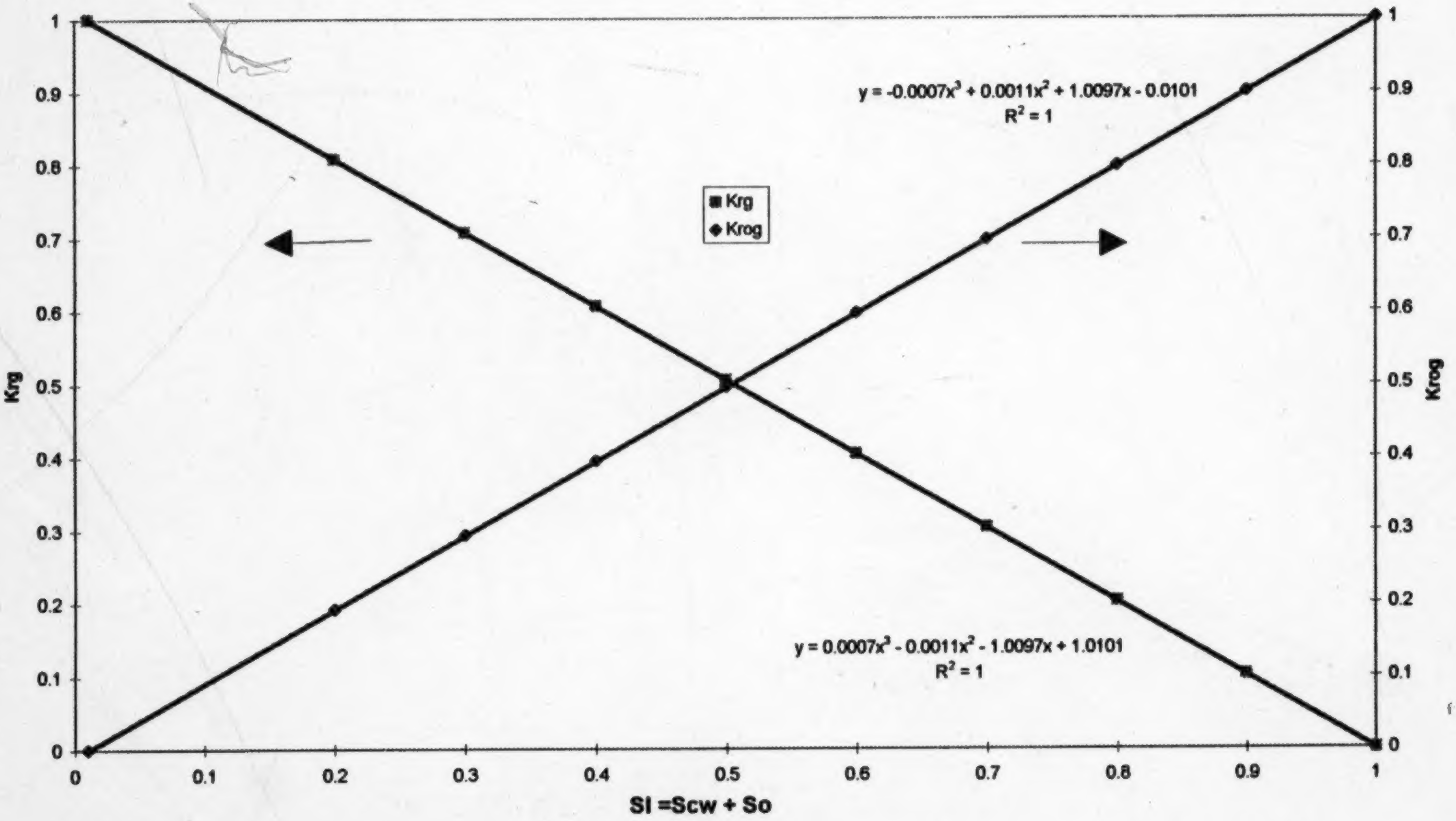

Figure 10.3.4: Gas - Oil Rock Type 4, PHOP relative permeability data

Initial use of the model required Rock Type 1 for cycle 1 steam injection and production. This formation description alone was taken from the model to generate the production correlation curves.

Second cycle injection normally was initialized to Rock Type 2 or 3 for injection and Rock Type 1 for production. Field data show higher injection pressures are evident during cycles subsequent to cycle 1 and these pressures slowly fall to cycle one injection pressures in later cycles. The reason for the higher injection pressures is clarified by the theory presented in Chapter 6 section 6.1.2, which connects the effects of imbibition and drainage on sandstone containing clays, especially kaolinite. Briefly, kaolinite bridging and clay clumping are responsible for these pressure profiles.

Rock Type 4 can be used as a "well cell", an invention of the author, in the first grid blocks containing the wellbore where $I = 1, J = 1, K = 1,n$. The purpose of this construct is to simulate an open annulus with perforations only in the required layers, or portions thereof, using a concurrent modification to the ***TX***, ***TY***, and ***TZ*** transmissibilities. The ***KHL*** calculations for wellbore flow are now only tubing flow. The well-cell method was originally designed to work within the framework of the simulator's direct formulation option instead of it's implicit form. This technique provides a capability for handling of cross-flow instabilities within the wellbore itself and has the added benefits of model stability and more accurate output. The well-cell dictates that reservoir flow begins at grid block $I = 2$, $J = 2$. This method can also be applied easily to horizontal well configurations.

10.4 Viscosity Calculations with Temperature

The general equation matching the straight lines on the ASTM viscosity versus temperature graphs is given by:

$$\mu = EXP(A \cdot T^{B}) \tag{10.4.1}$$

where $B = \ln(\ln\mu_1/\ln\mu_2)/\ln(T_1/T_2)$

and $\ln(A) = \ln(\ln \mu_1) - B \ln(T_1)$

μ_1 and μ_2 = viscosities (mPa.s) of bitumen measured at temperatures T_1 and T_2 respectively.

Chapter 11

Development of the Semi-Analytical/Correlative Model

11.1 Summary of Correlation Curve Development

Correlation curves for oil production were developed after numerical simulation matching of first-cycle injection and production for three of the eight PHOP pilot wells. Reservoir characteristics and conditions of the eight individual wells were translated to a single well description representing the well group's weighted-average, using the PVT properties from these matches. The transformation scheme consolidated about ten individual layers to a generic one characterizing the whole reservoir. Sensitivities to production were numerically investigated by varying water saturation, steam injection rate, and injection volume in a simple ten-meter thick pay zone corresponding to one-half of a 20-m thick reservoir separated by an impermeable calcite streak. Production data from these sensitivity studies were then converted to an equivalent calendar day oil rate (CDOR) per meter of perforation (or per 10 meters of perforated net pay), and plotted against original water saturation, which is defined as irreducible water saturation plus mobile water. The water saturation scale was shifted horizontally such that the irreducible water saturation crossed the y-axis, leaving only mobile water saturations positioned on the graph. This approach is used to investigate whether or not oil production is a very strong function of mobile water saturation. The developed correlation plot in Chapter 12, Figure 12.3.3.1 is intended to show the effects of changing water saturations. It is interesting to note that a mobile water saturation (S_w less S_{wir}) greater than 25% will result in very little oil production unless injection rates exceed 200 m^3/d. If irreducible water saturation is 30%, as for this pilot (PHOP), a water saturation of 55% would be considered an upper limit for any reasonable oil production, giving a maximum mobile water saturation of 25%. In the McMurray oil sands where the irreducible water saturation is 15%, the expected upper water saturation limit is 40%. The relative permeability curves used in the model were kept constant.

Correspondingly, the y-axis signifies that oil production is a function of meters of perforation and net pay. Perforation heights were used in place of net pay because there seems to exist a stronger correlation with perforation height with the addition of up to two meters of net pay above and below the perforations, than to just net pay. Net pay above or below the 2-meter limit seems not to affect production. This hypothesis is unproven. If the dependency of production on the 2-meter bounds is in fact real, then some other phenomenon not considered here such as: i) injected steam travels only goes through the uppermost perforations because of gravity segregation; ii) only the top half of the perforations flow on production; and/or iii) vertical fractures climb at 45° resulting in only about one half of the net pay being contacted.

The curve shifting technique also provides a visual analysis of oil production as a function of steam injection rate and slug size. It shows the higher the steam injection rate the more oil will be produced, as long as the fracture does not extend beyond the formation. The effect of steam volume, or slug size, is less apparent. Sensitivity runs indicated that there is an optimum steam-oil ratio (***SOR***) for a given slug size, since the distance heated oil must travel during a production cycle governs how much oil will actually reach the wellbore. For the Primrose pilot used in this study, the optimum slug size is about 5,000 m^3 cold water equivalent (***CWE***). The correlation curves handle slug size on the y-axis by way of "***operating days***". An operating day is by definition, when there are no shut-in periods, "days on injection plus production", the exact equivalent to a calendar day oil rate (***CDOR***). Of interest, the curves show the same amount of oil will be produced by a 3,000 m^3 slug injected at 200 m^3/d as would be produced by a 5,000 m^3 slug injected at 66 m^3/d, but note, for the same number of operating days. Operational efficiency is deemed to be a function of useable heat injected and distance the bitumen can travel towards the well before pressure and temperature drops make it too viscous.

Bottomhole steam quality adjustments for the numerical model runs were made to compensate for wellbore heat losses as a function of rate.

Certain questions were raised about the numerical model itself. Would lack of gravity in a one-layer model affect results, given the inevitable nature of steam override?

Sensitivity runs showed no impact for first-cycle production. The next question was, since only three wells were matched for first-cycle production, would the correlations work for the other five pilot wells plus the three single-well tests of the first cycle, even without considering multiple cycles? Whether the correlation curves could be validated by the first cycle was no guarantee that they would work for multiple cycles since first-cycle production could be accurately predicted by simple Marx-Langenheim or Mandl-Volek calculations. Neither of these calculations can be extended successfully to multiple cycles, as most thermal recovery engineers have discovered (personal communication Dr. Farouq Ali, 1992). Appendix G outlines the above calculation of steam volumes by Mandl-Volek. Figures 11.1.1 and 11.1.2 contain the irreducible bitumen saturations as measured from steamed field cores. The tests were repeated on the same core at increasing hot water and steam temperatures until neither steam nor hot water produced extra bitumen. Note that hot water and steam have the same effect after 250 °C. Using the above figures for a Wabiskaw Formation PHOP well will give an oil recovery of approximately 16% if the final production temperature is 150 °C. Appying this recovery to the heated oil zone as calculated by Mandl-Volek, will give a reasonable bitumen production value for first cycle production. For example, for Well IP5 first cycle, 16% of bitumen in a steam volume of 14,413 m^3 or a radius of 24 m and thermal pay height 8 m at initial oil saturation of 65%, gives a calculated bitumen production of 500 m^3. The actual first cycle bitumen production was 771 m^3.

Perhaps the most elusive question is whether or not numerical models in general can even predict field production. In later sections of this work, examples are given on the failed Wolf Lake project, which serve precisely as a very important lesson on the consequences of favoring numerical modeling over thorough formation evaluation (which considers reservoir properties and fracture phenomena as the controlling factors in actual production).

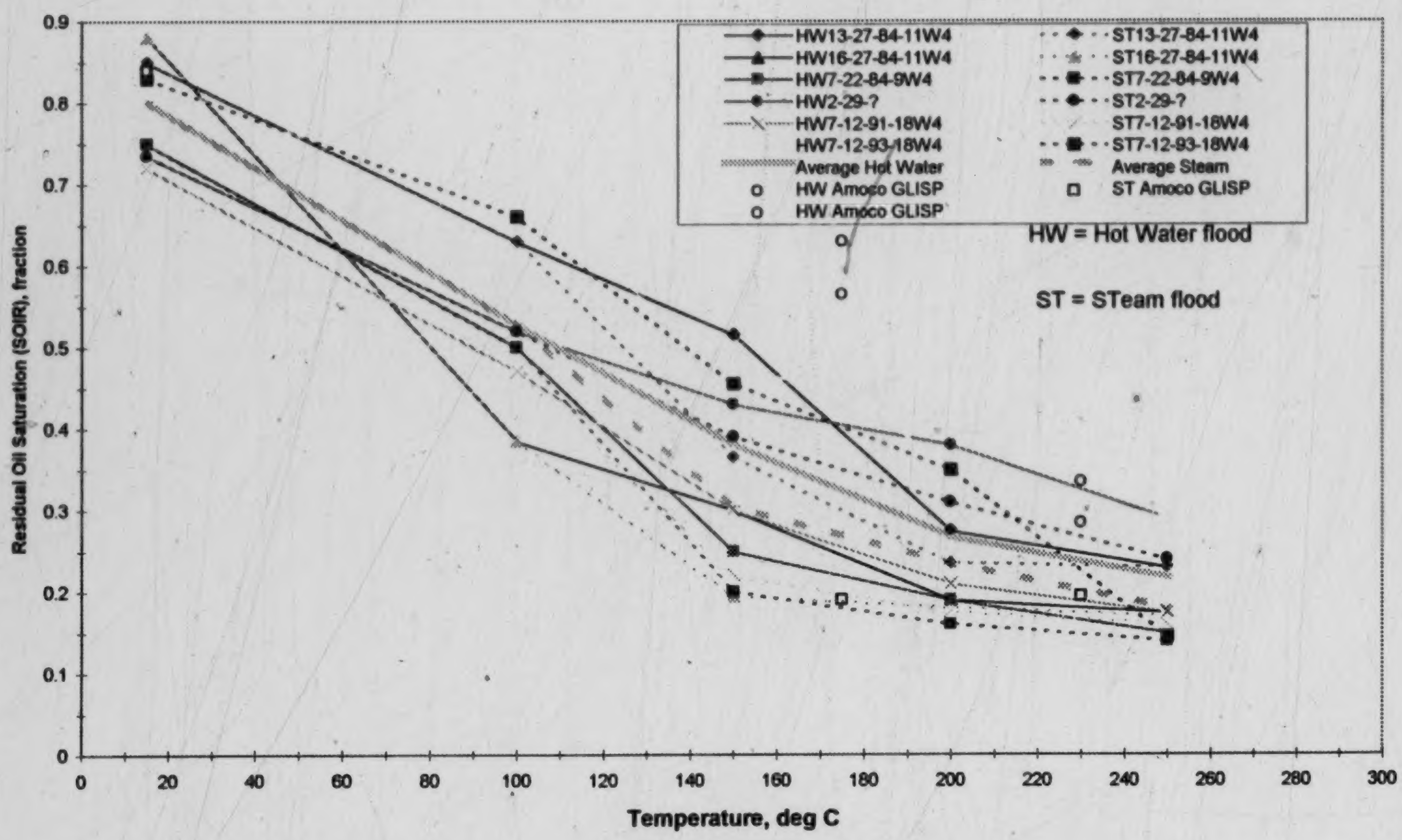

Figure 11.1.1: PCEJ McMurray oil sands residual oil saturation vs temperature for hotwater/steamflood

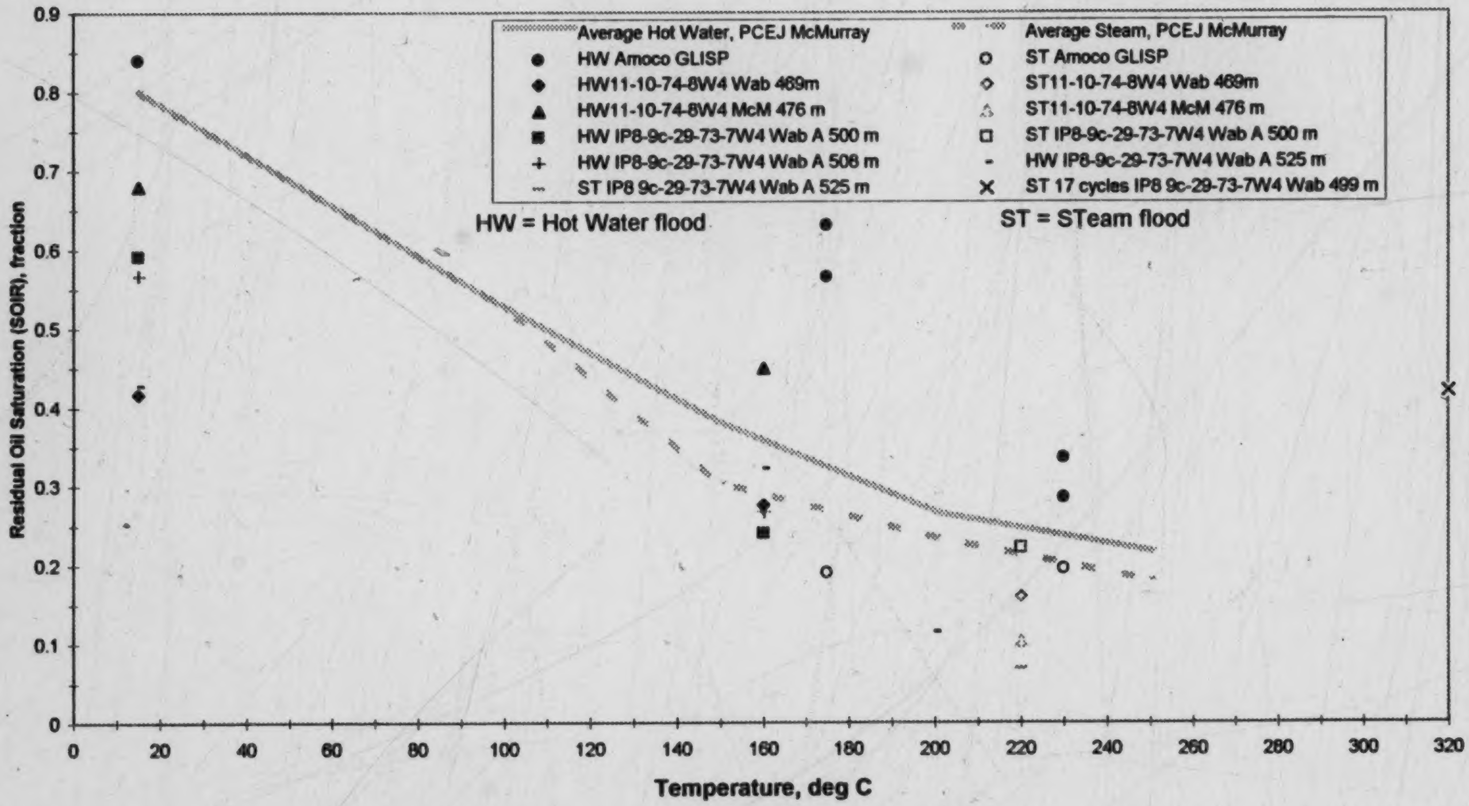

Figure 11.1.2: PHOP Wabiskaw & McMurray vs PCEJ & GLISP oil sands residual oil saturation with temperature for hotwater/steamflood

11.2 Introduction to Correlation Curve Model Development

Designing the correlation curves is predicated on core and well test analyses. Previous studies (Leshchyshyn et al, 1990-94) of a hydraulically-fractured well in the McMurray oil sands formation of north-eastern Alberta, showed that shear fracturing of the oil sands, which causes the rock around the fracture to physically shatter, produces a close-to-radial distribution of heat around the wellbore. This "***dilation***" phenomenon plays a critical role in explaining bitumen production during cyclic steaming of oil sands.

Core analysis was performed on actual cores taken from three observation wells, after 8 cycles of steam injection and production. Photographs taken of the shear fractures in these cores confirmed an expected parting or friction angle of 35°. The same fracture geometry was identified by Dr. Don Scott in 1991, for samples submitted by the author to the University of Alberta.

Shear parting or "***fingering***" has also been reported by Todd, Dietrich, and Chase (TDC,1980) or Dietrich (1981), Kry (1990), Gronseth (1990), and Boone (1991) on the Clearwater Formation at Cold Lake, Alberta. As well, shear parting has been observed throughout northern Alberta in the conventional reservoirs of the Mannville Group (Leshchyshyn et al., 1996). These sandstone formations are high in quartz content, which have either sufficient natural fractures or Griffith cracks to initiate fracturing at stresses lower than the measured minimum horizontal stresses. For example, the McMurray oil sands at Hangingstone, near the town of Fort McMurray indicated an initial-shut-in-pressure (***ISIP***) of 5,200 kPa, but by pressuring up the formation below ***ISIP*** during a constant rate test, it appeared that parting started to occur around 4,500 kPa. This pressure relation was substantiated by identification of the shear fractures using a standard well test analysis package, beginning at a minimum stress of 4,200 kPa. From the conclusion that shear parting of oil sands is not only a feasible outcome, but a likely one at that, it is reasonable to hypothesize that at least the first cycle of steam injection usually develops a steam zone that is somewhat radial, at reasonable steam slug sizes, due to the presence of the shear fractures. Dilation accounts for the apparent success of the Marx-Langenheim equation in matching first cycle cyclic steam production for a substantial range of projects.

Based on this conceptual "***dilation***" effect, a numerical thermal simulator originally used in the Cartesian mode for history-matching and predicting bitumen production during cyclic steaming could be operated in the radial mode with either a fracture in place, or with permeability curves modified to incorporate "***fingering***" (as first introduced by TDC, Dietrich, 1981). In this study, the "***fingering***" approach alone was satisfactory, rather than placing a tensile fracture with adjacent shear fractures in the form of pseudo relative permeabilities as a function of pressure. Tamim (1996) treated similar assumptions in his production predictions with reasonable success.

Knowledge and experience gained recently by the author from designing, performing, and analyzing fracture treatments in reservoirs throughout western Canada confirm that multiple shear fracturing is a frequent event, and that well test analysis is an indispensable tool for helping to identify such fractures.

In summary, the composite investigation lends itself to a fully-unified empirical procedure employing numerical simulation as a heat-balance tool. It is believed that in modeling the generation of shear fractures, i) in comparison of the techniques of using permeability enhancement coupled to increasing pressure in the grid blocks surrounding a fracture, with ii) permeability curves established in the lab, unmodified, would yield comparable production results.

11.3 Reservoir Characterization

By far, the most critical element in any recovery and performance study is reservoir description. Formation evaluation is not quite as important for gas reservoirs since all that is required is: reservoir pressure and temperature, net pay, porosity, density, water saturation, permeability to gas, wellbore skin damage, and well spacing to accurately predict the typical 30-year life of gas pool. Extended conventional oil pools where several more reservoir parameters are essential to proper characterization: formation volume factor, oil density and viscosity, bubble-point or total average compressibility, and relative permeability to oil.

Oil sands reservoir performance analysis, on the other hand, demands considerably more data, with which to adequately describe thermal processes, namely, injection of heat, three-phase flow in the reservoir, and temperature-dependent fluid properties. When heat is injected into a formation, the ability to estimate the magnitude and spatial distribution of heat delivered to the reservoir is tantamount. Connective heat transfer is recognized as being material to the analysis, but the problem is in knowing where convection occurs. For example, if a well is completed in the lowest 5 meters of a 20-m thick reservoir and there is a 2-meter thick calcite streak which has areal extent across the center of the reservoir, the chances of steam fracturing into the upper 10 meters is slim. Therefore, production is only from 10 meters of pay as opposed to 20 meters of pay, corresponding to one-half the recoverable bitumen reserves. The failure to understand lithology as a controlling factor in recovery is partly responsible for the ill-fated Wolf Lake project. Had proper procedures been followed for running temperature logs, the discovery of these impermeable barriers might have corrected future injection strategies, well completions, or procedures for drilling well pads.

11.3.1 Definitions of Thermal Pay, Net Pay, and Gross Pay

The following terminology describes the oil sands formation in much the same way as the standard definitions used to estimate the various categories of conventional reserves: original-oil-in-place (***OOIP***), proven, unproven, probable etc.

Gross pay is the true, contiguous formation interval. It includes all oil bearing sands plus any calcite streaks or shale layers or other non-productive zones. ***Net pay*** is the thickness of oil sand pay above a minimum wt% bitumen cut-off, or gross pay subtracting out the shales, calcites or any other non-productive layer. ***Thermal pay*** is the reservoir interval that heat will potentially contact and from which bitumen will be produced. If oil sands net pay intervals are separated by more than 3 meters of shale, or one meter of calcite, only the interval which is completed will produce since there is no communication to the interval which is not completed. In this study only the thermal pay is considered, since the remainder of the reservoir interval does not contribute to bitumen production.

11.3.2 Fracturing Through Shale

Experience obtained from actual conventional fracture treatments has revealed some differences between theoretical prediction and actual observation. For example, theoretical models (such as the Meyer Mfrac model) predict that a vertical fracture may and will propagate vertically through a shale 6 meters in thickness if the leak-off of fracture fluid in the sandstone reservoir is low, less than 0.001 ft/√min. However, in reality, the fracture is usually contained. While the divergence between theory prediction, such as stress-log analysis, and actual fracture height through shales is not precisely known, this can be remedied in the fracture model by doubling the stresses in the shale layers. From a geomechanical point of view, the adjustment takes into account the physical flexing of shales upon their absorption of vertical fracture tip energy.

It is important to point out that theoretical models quite often do not comprehensively incorporate all of these sometimes complex variables in their formulation and in the solution they derive. An example is the fracture-resistant Poker Chip Formation shale in central Alberta (Petro-Canada, 1995). It is believed that the fracture resistance arises from the properties of the shale itself. Structurally, shale is layered. The laminated structure tends to flex easily, much akin to stacked layers of elastic or rubber. Consequently, when an upper or lower edge of a propagating fracture contacts this shale from below or above, the energy from the fracture is readily absorbed and distributed throughout shale. Slippage occurs between the formation and the shale and also within the shale layer itself. The rock above or below the shale on the other side of the propagating fracture will bend only slightly, but over a larger area.

A typical sandstone rock in Alberta has a Poisson's ratio of about 0.23 - 0.25. Shales, on the other hand, can have a Poisson's ratio of 0.28 - 0.40, a higher number signifying more conversion of the vertical stresses, from the weight of overburden, acting on the shale to produce horizontal strains, comparing to horizontal stresses seen in sandstone. If minimum horizontal stresses are increased, then the stress required to create a vertical fracture is increased in direct proportion to the increase in the horizontal stress. This phenomenon also holds true for naturally-fractured coal, which does not hydraulically fracture through as easily because overburden vertical stresses have been converted to higher horizontal stresses. Again, the degree of conversion is reflected by a Poisson's ratio for coal of 0.38-0.50. If a formation was made of a sponge filled with water only, the vertical stresses would equal the horizontal stresses and Poisson's ratio would be at the maximum value of 0.50. No vertical fracture would ever propagate across the water barrier, although, if pressures were high enough, the whole overburden would lift vertically as if a horizontal fracture were being created.

11.3.3 Fracturing Through Calcite Streaks, and other Lithologies

Much effort has been directed towards the subject of formation stress analysis since a factor in determining thermal pay for the correlation curves on which this thesis is based, is a calcite streak about one meter in thickness, or greater. A calcite streak, a mixture of calcium carbonate and shale (not the mineral calcite), behaves somewhat like the latter, having a flexibility imparted by similar mechanical characteristics. Like shale, the calcite streak under investigation, is believed to physically prevent steam or water fractures from propagating through. Also, it is known that gas (or steam) cannot create as much fracture height as water since the leak-off to gas across the fracture face is about ten times greater, leading to a reduction in the fracture width, hence fracture height. Thus, the chance of the steam fracture propagating through the calcite is reduced. The objective here is to clearly demonstrate, with the aid of the correlative model, that the calcite streaks at the PHOP site controlled and minimized production insofar as making the applied cyclic steam process uneconomic.

When designing conventional fracture stimulations for wells in Alberta, the following average fracture gradient stresses (with net pressure corrections) are used to determine minimum stresses up to 2,200 m depth. Below 2,200 m or 40,000 kPa stress, the rock displays more plastic deformation than elastic behavior. It appears that rock begins to flow and fractures can close in on themselves. In Carbonate reservoirs, a small pre-conditioning acid fracture treatment reduces the "choking" effect, and allows greater volumes of proppant to be placed. No lab tests are available to substantiate the above hypothesis.

This example shows estimated ISIP horizontal stresses (σ_3) at a depth of 500 m using the standard conventional frac gradients:

Lithology	FracGradient	Propagation Stress
Sandstone	18 kPa/m	= 9,000 kPa
Shale	19 kPa/m	= 9,500 kPa
Calcite/limestone	20 kPa/m	= 10,000 kPa
Dolomite	21 kPa/m	= 10,500 kPa
Coal	22 kPa/m	= 11,000 kPa
Weight of Overburden	21.6 kPa/m	= 10,800 kPa

The values given include net pressure, which is the pressure above the closure stress, or the minimum stress, required to keep the fracture propagating. Net pressure must therefore be subtracted from ISIP:

Minimum stress, Sandstone: 15 kPa/m@500m = 7,500 kPa,

or, using the table above, = 18 kPa/m@500m - 1,500 kPa net pressure.

Where porosity of other lithologies, aside from sandstone, falls below 5%, the net pressure is less than 1,000 kPa. Then the ***ISIP*** is essentially the minimum horizontal stress, σ_3.

From the above table, it can be concluded that a 2 kPa/m stress gradient exists between sandstone and calcite, or at 500 m depth, there is a difference of 1,000 kPa between minimum stresses (or more likely 1000 + 1500 net pressure = 2500 kPa). A bottomhole steam injection pressure of 12,000 kPa is presumably the sum of 9,000 kPa fracture propagation pressure plus a 3,000 kPa pressure drop through the perforations. As most steam is injected through the uppermost perforation, higher rates and steam quality may open more perforations. The 9,000 kPa propagation pressure has the components of 7500 kPa minimum stress and 1,500 kPa net pressure as estimated above. Apparently a fracture may turn from vertical to horizontal before fracturing through calcite, dolomite or coal and form a T-frac at greater than 1.1 times the weight of overburden or 11,900 kPa. A T-frac is created when an initial vertical fracture is in communication with a top horizontal fracture located just below the shale, calcite, dolomite or coal. It is also possible the horizontal fracture may be more directional than radial since, while the pore pressure has exceeded the maximum stress, or weight of overburden, there may be sufficient tectonic stresses to cause a horizontal fracture to grow in the same direction as the vertical fracture. Shallower horizontal fractures, at 200 m depth or less, may be less directional and more radial than at greater depths due to a smaller differential stress between the two minimum stresses, and the one maximum stress, σ_3, σ_2, and σ_1, respectively. It is then possible for a horizontal fracture to exist below 1.4 times the weight of overburden following almost any path or direction, perhaps dictated by the lateral direction of a sandbar on a deltaic river channel.

Another possibility for higher injection pressures is the increase in near-wellbore stress caused by the expansion of heated rock. The obvious proof is that injection of cold water into an oil sands reservoir is at a lower pressure than steam injection.

Maximum PHOP injection pressures were at about 9,000-10,000 kPa at the sandface. Assuming restricted fracture height growth, the net pay above these higher stressed layers of calcite is eliminated.

11.3.4 Effect of Fracture Height Growth and Perforation Height on Bitumen Production

The correlative model assumes no fracturing through calcite streaks greater than one meter in thickness. As described in section 11.3.3, the fracture-resistant calcite layer is a parameter which limits fracture height. It is required in the development of the correlation curves. A further reduction in net pay to account for perforation thickness made the correlation curves viable for the PHOP pilot. The proposed technique recognizes that perforation height also controls bitumen production, and that only an incremental 2 meters of pay above and below the perforations contribute to production. This phenomenon is difficult to explain. Although a 2-meter limit below the perforations may actually exist and heat from the assumed bottom hot water can travel downwards, there is insufficient energy to force the bitumen up through the less dense water phase against the forces of gravity. The case for the upper 2-meter limit is as yet, unexplainable, but is possibly a function of formation layering or thin calcite streaks not identified by the logs. These limits do not seem to exist in the early phases of commercial production at Esso Cold lake where the oil sand is much cleaner. More recent stages of recovery should be similar to the reservoir behavior at Wolf Lake due to an anticipated increase in reservoir heterogeneity.

11.3.5 Measuring the Restricted Height Growth

Consider a reservoir having a gross pay of 50 meters, a net pay of 30 meters, and a thermal pay of only 15 meters. Project economics for such a reservoir are evaluated on the basis of 15 meters of thermal pay. Proper temperature logging technique or placement of cemented thermocouples is required to determine, within one meter, the distribution of heat in individual wells.

"***In***" and "***out***" logging passes using a conventional temperature logging tool connected to a wireline, will not suffice given that the heat transfer to the temperature measuring device, or RTD (Resistance Type Device), is a function of time especially if the tool travels through viscous bitumen. To overcome operational difficulties in thermal recovery, a specialized temperature logging tool and procedure for obtaining accurate temperature profiles in a well has been developed (Leshchyshyn and Seyer et al., 1989). The basic design of the tool is a frontal RTD protected by a small cage as opposed to the usual mid-length location. This configuration allows the logging engineer to perform frequent "***stationary stops***" with the tool at various depths since the temperature stabilizes quickly, thus allowing for multiple recordings of stabilized temperatures. Conventional temperature tools normally require up to thirty minutes to stabilize (a consequence of poor heat transfer design), whereas the new tool would stabilize in just one or two minutes, a benefit to multiple stationary stops of reasonable duration, usually less than three minutes. Stabilized temperature is defined as the temperature of the RTD when it does not change more than one degree Fahrenheit over a two-minute period.

Unfortunately, this tool was not developed until after the PHOP operations had ceased, therefore, no quality temperature logging data is available for this pilot.

11.3.6 Effect of Initial Water Saturation on Bitumen Production

Another important set of reservoir parameters affecting bitumen production is ***irreducible*** and ***original or connate*** water saturations. The difference between the two is ***mobile*** water. Since mobile water saturation is a critical factor in convection, accurate values for both irreducible and original saturations are desirable. From the correlation curves it can be seen that a mobile water saturation of about 10% maximizes oil production while a doubling to 20% can reduce bitumen production by as much as 50%. Various parameters associated with reservoir water saturation and the influence each has on the model formulation are covered in the remainder of the chapter.

Irreducible water

For oil sands, selection of a value for irreducible water saturation (***S_{WIR}***) may not be as simple as reading the vertical slope from a capillary-pressure plot. There are two possible sources for inaccuracy of such values. Capillary tests are performed in the lab and for the test results to be of use, information must be converted to field conditions. Second, an input data stream acceptable to a numerical model may include a standard capillary pressure drop of 6.9 kPa (1 psi) per 4 meters of pay or so. As such, the ***S_{WIR}*** must reflect the capillary pressure of each layer included in the model. A previous study examined these two problems (Chew and Leshchyshyn et al., 1985). As a matter of convenience, the J-function capillary curves for the Clearwater and McMurray formations at the PHOP site are taken from the study. For the Clearwater Formation an irreducible water saturation of 30% is used, while for the McMurray Formation a value of 15% is assigned. In the transition zone between the Clearwater and McMurray formations the value taken is 20%. Overall, data for irreducible water saturation determined from the lab capillary curves are found to be too low which warrants shifting (the set of) lab capillary curves to the right. Without reasonable correlation between the lab, the thermal model, and actual field production data, forecasts of bitumen recovery or planned commercial projects may well be in error. This is particularly true for oil sands projects, where profit margins are already low.

Original water

For a conventional light oil or gas reservoir, the reported water saturation calculated is usually the irreducible water saturation. This approach is not necessarily relevant for oil sand reservoirs, and could easily lead to inappropriate use of simulation tools. In oil sand or heavy oil reservoirs it is common to have a "***water sand***" with only 4 weight percent (***wt%***) bitumen and 33% porosity, or 75% water saturation. The permeability to water in "***water sand***" is typically 3,000 md. These water sand layers may be located above, below, or intermixed in the productive oil sand pay zone.

For example, a thermal recovery study (Towson and Boberg et al., 1990) determined that the poor bitumen production of a cyclically-steamed well, located at the PCEJ Stoney Mountain Electric Preheat Project near Fort McMurray, was due to a water sand of one-meter thickness which was capable of drawing all the injected steam (80 m^3/d) into it. The subject water sand interval showed up only as "***lost core***" from core analysis but was detectable from dual induction log analysis. Bitumen was moved upwards and downwards by steam at the horizontal boundaries of this water sand layer but not laterally, resulting in very poor bitumen recovery. A higher steam injection rate, 150 m^3/d, would probably have stimulated the well's production through increased fracturing of recoverable oil sand. Water sand layers at the PHOP location, were incorporated into the numerical simulations (see PHOP well IP1, Table 10.2.1). A weighted averaging technique could not be implemented in this case, as the heat would be spread too much vertically rather than being localized to one small layer. The correlation curves would not work for the water sand lense scenario, unless it were known exactly where the heat destined for, and thermal pay was reduced to the water sand thickness with a corresponding mobile water saturation for that layer only. For the same reasons, numerical simulations without the water sand layer were unsatisfactory.

Estimating Original Water Saturations

Original water saturations can be estimated from either log analysis or core analysis. As a cautionary note, data obtained from a single analysis procedure is often biased. The preferred method is to correlate both analyses, hopefully with the means of internal validation. It is wise not to directly use the saturations given by standard core analysis that are reported by the various commercial labs, as the porosities entered into the calculations of such reports are normally at least 2% higher (i.e. if the reported core porosity is 35%, the actual field porosity is most likely 33%). Appendix D provides actual field data showing this discrepancy. It is easily seen that a core containing 12 wt% bitumen with a porosity error of 2% (as above) will give a calculated error in water saturation of 4.2%. Changes of 3% water saturation in a numerical model can make substantial differences in bitumen production.

A simple formula normally used for estimating water saturation from cores is:

$$S_w = 1 - S_o \qquad \text{where } S_o = (\text{wt\% Bitumen} \times 2.05\ \text{gm/cc}) / \text{porosity in \%}$$

This equation can be made more accurate if the core porosity is determined after applying at least four cycles of double the overburden pressure to the core or, by using log density-porosity. The overburden pressure is doubled to compensate for the extra overburden applied to the reservoir during the previous ice ages. An additional correction to the formula is to use the oil sand density values in the table below at each porosity instead of using the above given density constant of 2.05 gm/cc, which is skewed towards being most accurate for rich, high porosity oil sand.

Oil Sand Density as a Function of Porosity

Porosity, Ø % **(%)**	**Oil Sand Density, ρ_o** **(gm/cc)**
24	2.254
26	2.221
28	2.188
30	2.155
32	2.122
33	2.1055
34	2.089
36	2.056

Water saturation can be approximated from the correlation of logs to cores using R_t, then plotting the measured formation resistivity from an induction logging tool, against wt% bitumen or grain wt% bitumen from cores. Wt% bitumen from cores can be used directly if there is no water invasion during coring, that is, the porosity has not increased by 2% or more. The definition for ***weight% bitumen*** is the weight of bitumen divided by the weight of bitumen plus water plus sand. By contrast, the definition for ***grain weight% bitumen*** is the weight of bitumen divided by the weight of sand. In situations where filtrate water has encroached into the formation through drilling mud invasion, grain weight% is appropriate since no water is considered in its computation.

Also, while constructing the R_t versus ***wt% bitumen*** curve for a given reservoir, one must keep in mind the limitations of logging tools. A shallow or spherical induction log, for instance, will see only about 0.15 m (6 inches) into the formation, an exceedingly small distance often drastically altered by invading drilling mud or hole sloughing. A medium induction log has a wider scan of about 0.5 m (18 inches) into the formation which can also be affected by drilling mud invasion or caving, but to a lesser degree. A deep induction log reads about 2 meters (80 inches) distance where the formation is usually outside the damage zone. If thin bedding effects (layers 3 m or less) are added to the signal it becomes apparent that the measured resistivity must be carefully chosen to ensure that it actually represents the true grain weight % bitumen arrived at through core analysis. A final precaution to be heeded in the correlation of logs and cores is the difficulty caused by a core being off-depth.

The following guidelines can help establish the merits of correlating log and core analysis and in particular, draw attention to pitfalls when proceeding to do so:

1. Use only ***grain weight% bitumen*** from cores unless it has been determined that no water invasion has occurred during coring.

2. Do not perform regression analysis from a R_t ***versus wt% bitumen*** plot when the data set includes many intervals, across many wells, and the bedding effect is prevalent. The resulting plot is a "shot-gun" chart and a best-fit approach will be in error due to inherent inaccuracies of R_t measurements. To compensate for the bedding effects, it is advisable

to use only four or five selective wells to obtain a more realistic plot. This can be done by choosing only wells that have at least 4 meters of homogeneous pay, and using these resistivities for the plot. Select a variety of wells which have different wt% bitumen so that a complete graph can be constructed. Ideally, the range of wt% bitumen should be from at least 4 wt% (water sand at about 75% Sw) to 16 wt% (oil sand at about 5% Sw). An equation can then be calibrated especially to the "bottom end" (or lower wt%) of the curve from a resistivity versus wt % bitumen plot. The "top end" of the curve is less critical because, at the lower end, in most oil sands reservoirs, the bedding has become either 8 wt% bitumen or straight shale, there are no intermediate levels such as 6 wt%, the figure most often used by geologists as the cut-off in reserves analyses. Most likely the 6 wt% is a thin layer of 8 wt% with layers of shale in-between.

The procedure for lab analysis of cores is very important. It has been experienced, in the McMurray oil sands, that if one inch horizontal plug cores are selected, ignoring the thin shale layers, versus taking six inch slab samples, the above statement is easily proven. Flow of steam and bitumen through the layered scenario is much different than flow through an averaged 6 wt% thicker layer which has a higher water saturation. Furthermore, a significant amount of bitumen reserves (up to 50%) can be added mistakenly if a general rule for delineation has not been established.

3. It must be emphasized that porosity also varies with wt % bitumen so the developed equation for determining water saturation should justifiably include porosity. The larger the pore size, or increased porosity, the lower is the ireducible water saturation, hence the oil saturation is higher.This equation must work equally well for water sand or bitumen-rich sand.

A sample R_t versus ***wt% bitumen*** plot determined by the author for the McMurray oil sands at PCEJ is shown in Figure 11.3.6.1. The equation formulated for this plot is simply Archie's equation using appropriate values for parameters m and n. These are empirical constants tied to the electrical properties of the cores.

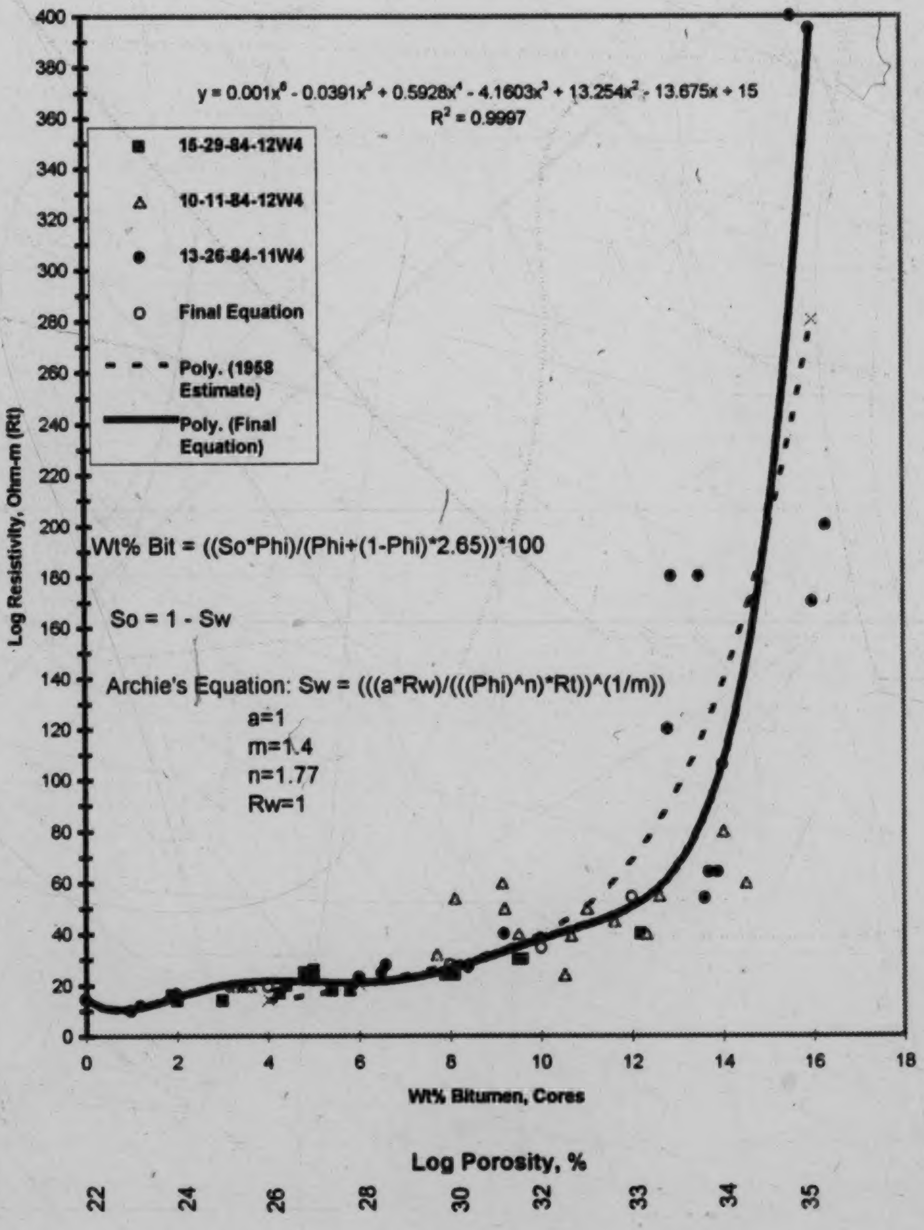

Figure 11.3.6.1: PCEJ cut-off curve, McMurray oil sands

The Archie equation is:

$$S_w = \left(aR_w \Big/ \phi^m R_t \right)^{1/n} \tag{11.3.6.1}$$

knowing that $S_o = 1 - S_w$,

the ***wt% bitumen*** can be found from

$$wt\%\ Bitumen = ((S_o \cdot \varnothing)/((\varnothing + (1-\varnothing) \cdot 2.65))) \times 100. \tag{11.3.6.2}$$

The denominator of the wt % equation equals the density of oil sand where both the density of bitumen and water are assumed to be 1,000 kg/m^3, and the density of the sand is 2.65 gm/cc or mostly quartz.

The following table for wt% bitumen has been generated from the Archie equation using $a = 1$, $R_w = 1$ ohm-m, $m = 1.4$, and $n = 1.77$.

Calculation of Weight Percent Bitumen Based on Logs for the PCEJ McMurray Oil Sands

Porosity, $\varnothing$ from Log (fraction)	Resistivity, R_t from Log (ohm-m)	Calculated water Saturation, S_w (fraction)	Calculated Oil Saturation, S_o (fraction)	Calculated Wt% Bitumen (%)
0.22	14.58	1.00	0.00	0
0.24	16.72	0.81	0.19	2
0.26	19.5	0.66	0.34	4
0.28	23.1	0.53	0.47	6
0.30	27.9	0.43	0.57	8
0.32	34.5	0.34	0.66	10
0.33	54.3	0.23	0.77	12
0.34	106	0.14	0.86	14
0.35	395	0.05	0.95	16
0.35*	10	0.73	0.27	4.6

*The last entry in the table shows a typical analysis for water sand.

Log porosities are normally the density porosities read from density logs. Effective porosities ($\varnothing_e$) can be calculated by correcting for shale from the gamma ray log. Here,

$$\varnothing_e = \varnothing_T - V_f \cdot \varnothing_{SH} \qquad (11.3.6.3)$$

where $\varnothing_T = (\varnothing_D + \varnothing_N)/2$

and

$\varnothing_T$ = total log porosity, fraction

$\varnothing_D$ = density porosity, fraction

$\varnothing_N$ = neutron porosity, fraction

V_f = volume fines fraction, fraction

$\varnothing_{SH}$ = indicated shale porosity at GR_{max}

GR_{max} = API log value at 100% shale content

Also, $V_f = 0.83(RGRD)^2 + 0.17(RGRD)$, where

$RGRD$ = average gamma ray deflection for zone of interest divided by maximum gamma ray deflection for the McMurray formation

$= (GR_{avg}-GR_{min})/(GR_{max}-GR_{min})$, where

GR_{avg} = API log value for zone of interest

GR_{min} = API log value at 0 % shale content.

Figure 11.3.6.2 is a plot of wt% bitumen versus porosity or bulk volume water ***(BVW)***. The ***BVW*** in percent is simply ***($\varnothing$ x S_w x 100)***, when the values of $\varnothing$ and S_w are stated as fractions. In oil sands, the general trend is porosity increases and ***BVW*** decreases as ***wt% bitumen*** increases. For conventional reservoirs, a ***BVW*** greater than 6.5% will produce substantial formation water with the oil. The same is true for an oil sands reservoir with any pay containing less than 12 ***wt% bitumen***.

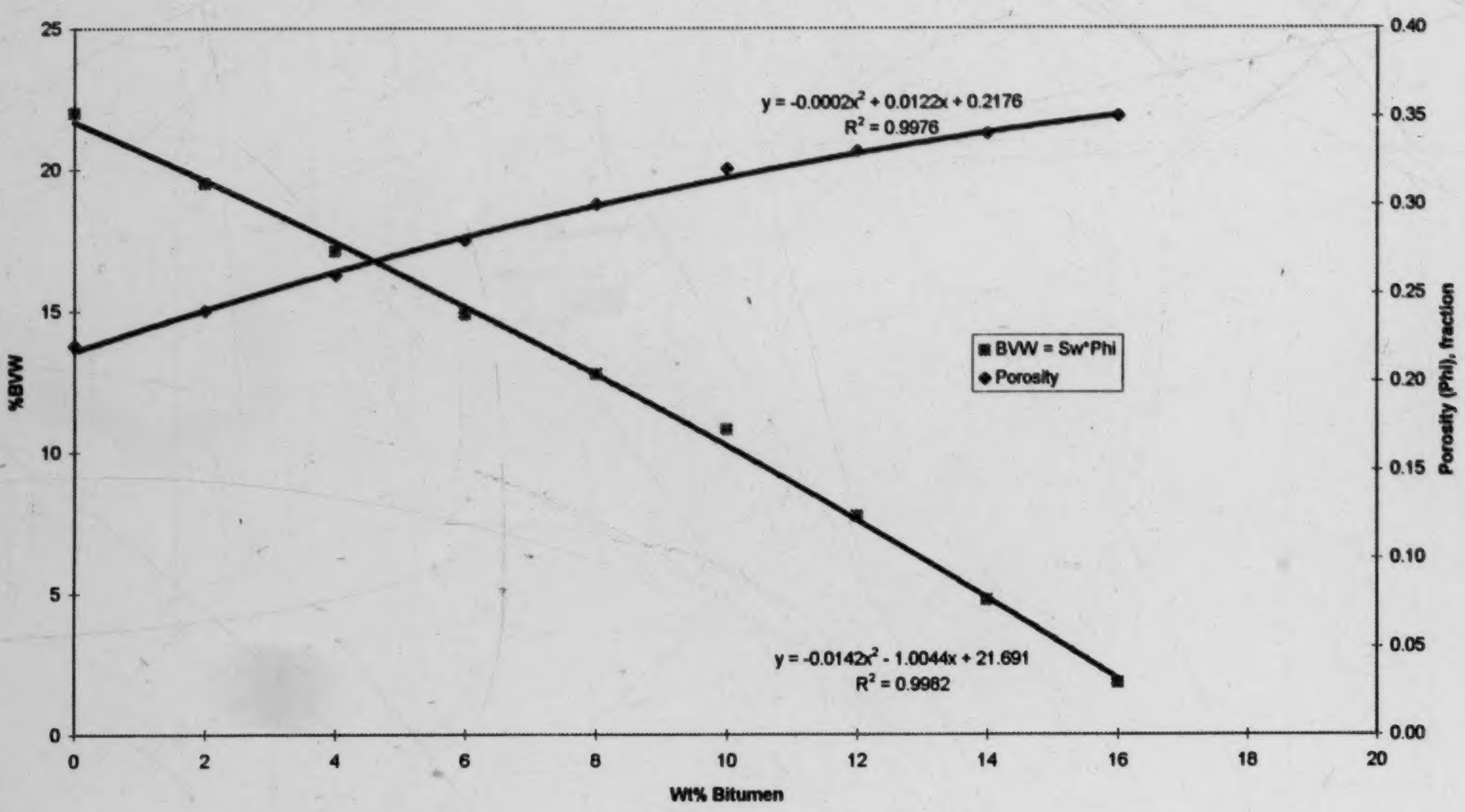

Figure 11.3.6.2: Bulk Volume Water (BVW) and porosity vs wt% bitumen for PCEJ

Chapter 12

Running the Numerical Simulator to Generate the Correlation Curves

A step-wise procedure for building the final set of correlation curves is outlined and discussed in this chapter.

The initial stage of the development involved discretization of the reservoir using an appropriate geometry and selection of the proper grid size. This spatial framework was initialized in the numerical simulator chosen to generate the PHOP bitumen production correlation curves. A decision had to be made between a representation using a single-layer model (1-D radial coordinate) or a multi-layered model (2-D radial coordinate). The number and spacing of lateral grid rings were investigated to determine the effects of oil banking or "lost oil". Steam injection rates and slug sizes were varied, along with steam quality, to ascertain the effects of the grid spacing on bitumen production.

Table 10.1 is an example of a simulation input data file containing the actual grid size parameters declared in the correlation curve numerical modeling. The simulators keywords are for "***RTZ***" radial grid system, "***NR***" for number of rings, "***R***" for radius of rings, and "***RVAR***" meaning actual radii.

12.1 Varying Number of Layers and Lateral Ring Size

Model sensitivity studies were conducted to determine whether a single-layer 1-D radial coordinate system or a multi-layered 2-D radial coordinate system would be sufficient to generate the production correlation curves desired for first-cycle history matching at the PHOP pilot.

A total of 12 runs were first performed (Table 12.1.1, runs 1A to 12A), using only a single layer, 8 rings, and initial $S_w = 0.5$. Steam injection rates, slug sizes, and bottomhole steam quality were varied to measure change in production.

Table 12.1.1

Operating Conditions-Single Layer Model: Optimization of Injection Rates and Slug Size
Initial Water Saturation, Swi = 0.5

Run No.	Injection Rate m3/d	Time Injection days	Slug Size m3	Bottomhole Steam Quality	Bottomhole Inj Pressure MPa	Res Press End Inj MPa	Heat Injected $x10^{10}$KJ	Production Fluid Rate m3/d	No. of Producing days	Water Production m3	Oil Production m3	Steam Oil Ratio
1A	66.7	45	3000	0.2	9.2	6.15	0.4876	40	60	673	21	143
2A	66.7	75	5000	0.2	9.2	5.41	0.8131	40	60	704	232	21.6
3A	66.7	105	7000	0.2	9.2	5.25	1.138	40	60	847	244	28.7
4A	110	27	3000	0.425	11.6	8.22	0.602	40	60	707	25	120
5A	110	45.5	5000	0.425	11.6	6.33	1.012	40	60	812	344	14.5
6A	110	63.6	7000	0.425	11.6	6.65	1.412	40	60	959	249	28.1
7A	200	15	3000	0.5	12	10.95	0.642	40	60	733	133	22.6
8A	200	25	5000	0.5	12	8.29	1.067	40	60	947	410	12.2
9A	200	35	7000	0.5	12	8.86	1.492	40	60	1182	275	25.5
10A	110	27	3000	0.2	9.2	7.39	0.4845	40	60	770	34	88.2
11A	110	45.5	5000	0.2	9.2	6.7	0.8158	40	60	808	291	17.2
12A	110	63.6	7000	0.2	9.2	6.4	1.139	40	60	969	286	24.5

The number of layers was then set at 5 or 10 and the thickness of each layer adjusted to give a total reservoir thickness of 9.5 meters. Modifying height in this way allowed a comparison to be made of the effects of steam override plus gravity drainage.

Radial cells numbered either 8 (geometric) or 15 (a combination of geometric plus equal volume spacing) outward a total distance of 320 meters (Figure 12.1.1). The variation in cell count modeled the effect of "lost oil" due to hot oil from one grid moving into the cold zone of the next outer grid, thus creating a non-producible "cold oil" bank ahead of the steam. The smaller, equal volume grids would move less oil from the hot grid out to the cooler adjacent one due to their smaller volume and display a more realistic oil-banking effect. Geometric selections provide equal spacing on a semi-log plot and therefore equal horizontal transmissibilities, which helps the model to run smoothly and more accurately. The other alternative for grid size, the system of equal volume (smaller grid blocks, also shown in Figure 12.1.1), gives a sharper steam front and can provide more accurate bitumen production forecast for the steam slug size injected. More grid blocks are required for this method, especially when multiple cycles are modeled, since the steam front moves out slowly after the first cycle injection and the equal volumes grid boundaries must move slowly with the steam front. If the steam front grid block is too large, the steam front will appear stationary, the only indication being an increase in temperature

Production values were compared at three different steam injection rates of 66.7 m^3/d, 110 m^3/d, or 200 m^3/d, and at three different slug sizes of 3,000 m^3, 5,000 m^3, or 7,000 m^3. Production time was normally 60 days but was extended in some runs to 90 or 120 days. Steam quality was adjusted to account for wellbore heat losses and three sensitivity runs were made to observe the effects of these adjustments. Results are presented in Tables 12.1.1 and 12.1.2. The six benchmark model runs are summarized in Figures 12.1.1.1a to 12.1.1.3b. Daily oil and water production are plotted for the single-layer, 8-ring case base cases.

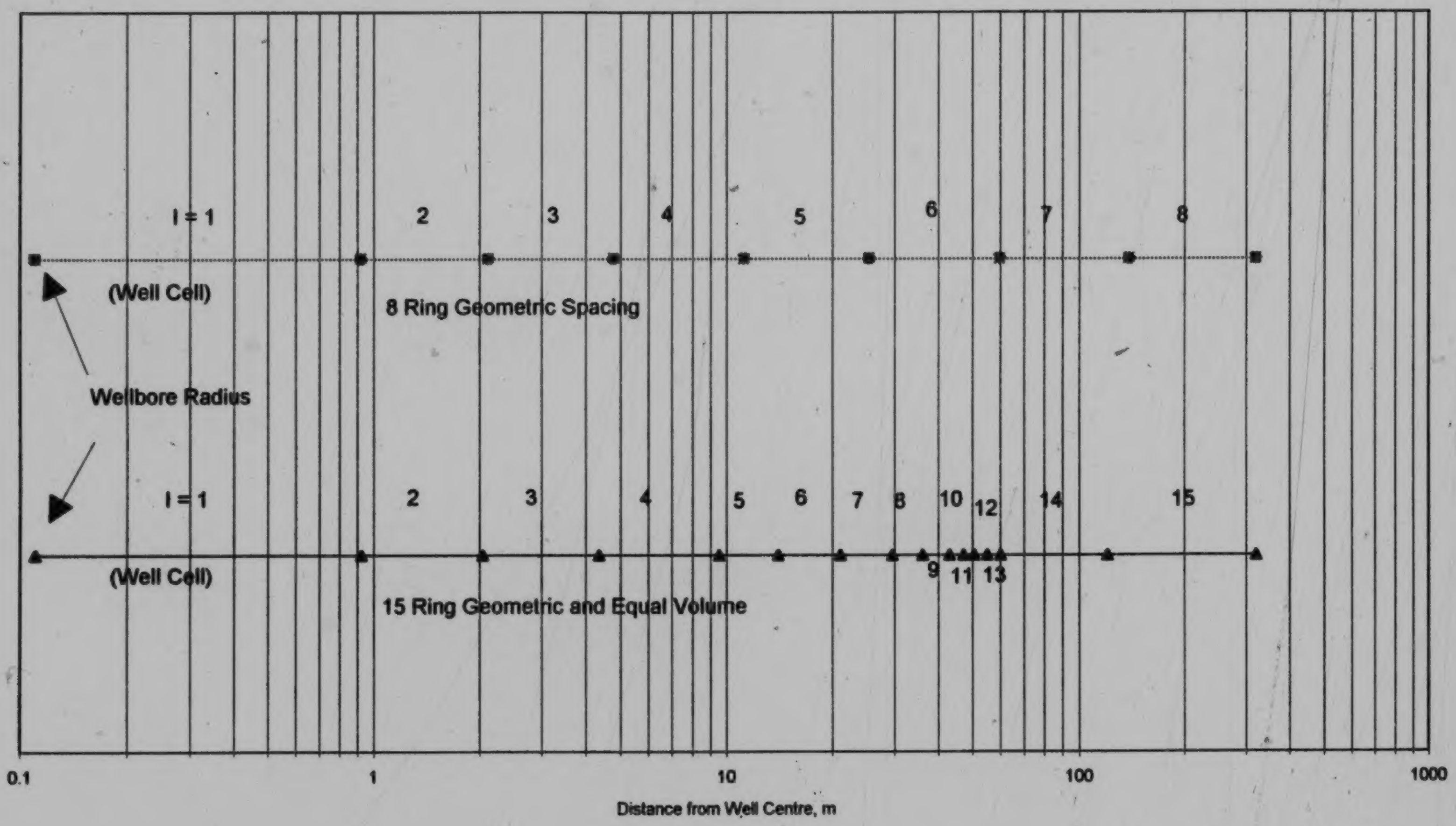

Figure 12.1.1: Spacing for 8 and 15 ring grids, radial model

Table 12.1.2

Operating Conditions-Single Layer Model: Optimization of Injection Rates and Slug Size
Initial Water Saturation, Swi = 0.5

Run No.	No. Layers	No. Radial Cells	Injection Rate m3/d	Time Injection days	Slug Size m3	Bottomhole Steam Quality	Bottomhole Inj Pressure MPa	Res Press End Inj MPa	Heat Injected $x10^{10}$KJ	Production Fluid Rate m3/d	No. of Producing days	Water Production m3	Bitumen Production m3	Gas Production Nm3	Steam Oil Ratio
1A	1	8	66.7	45	3000	0.2	9.2	6.2	0.4876	40	60	673	21	1801	143
1B	10	8	66.7	45	3000	0.2	9.2	5.7		40	60	707	85	2631	35
2A	1	8	66.7	75	5000	0.2	9.2	5.4	0.8131	40	60	704	232	6913	22
2B	10	8	66.7	75	5000	0.2	9.2	5.0		40	60	874	288	8985	17
2C	5	8	66.7	75	5000	0.2	9.2	5.0		40	60	868	282	8824	18
3A	1	8	66.7	105	7000	0.2	9.2	5.3	1.138	40	60	847	244	9203	29
4A	1	8	110	27	3000	0.425	11.6	8.2	0.602	40	60:120	707:1147	25:94	1200:3500	120:32
4B	10	8	110	27	3000	0.425	11.6	6.0		40	60	891	264	7479	11
4C	5	8	110	27	3000	0.425	11.6	6.3		40	60	1474	300	8343	10
4D	5	15	110	27	3000	0.425	11.6	7.9		40	120	1253	197	6727	15
5A	1	8	110	45.5	5000	0.425	11.6	6.3	1.012	40	60	812	344	9541	15
5B	10	8	110	45.5	5000	0.425	11.6	6.1		40	60	1089	288	9706	17
5C	5	8	110	45.5	5000	0.425	11.6	6.1		40	60	1070	295	9531	17
5D	5	15	110	45.5	5000	0.425	11.6	8.5		40	120	1346	313	10240	11
6A	1	8	110	63.6	7000	0.425	11.6	6.7	1.412	40	60	959	249	9047	28
6B	10	8	110	63.6	7000	0.425	11.6	6.5		40	60	1125	242	9825	29
6D	5	15	110	63.6	7000	0.425	11.6	10.1		40	180:210	1767:2000	191:224	14290:1429(	37:31
7A	1	8	200	15	3000	0.5	12	11.0	0.642	40	60:90	733:980	133:192	1679:4070	23:16
7B	10	8	200	15	3000	0.5	12	7.7		40	60	1102	280	8387	11
8A	1	8	200	25	5000	0.5	12	8.3	1.067	40	60	947	410	9847	12
8B	10	8	200	25	5000	0.5	12	8.0		40	60	1273	310	9681	11
9A	1	8	200	35	7000	0.5	12	8.9	1.492	40	60	1182	275	8765	26
9B	10	8	200	35	7000	0.5	12	8.6		40	60	1325	218	9731	35

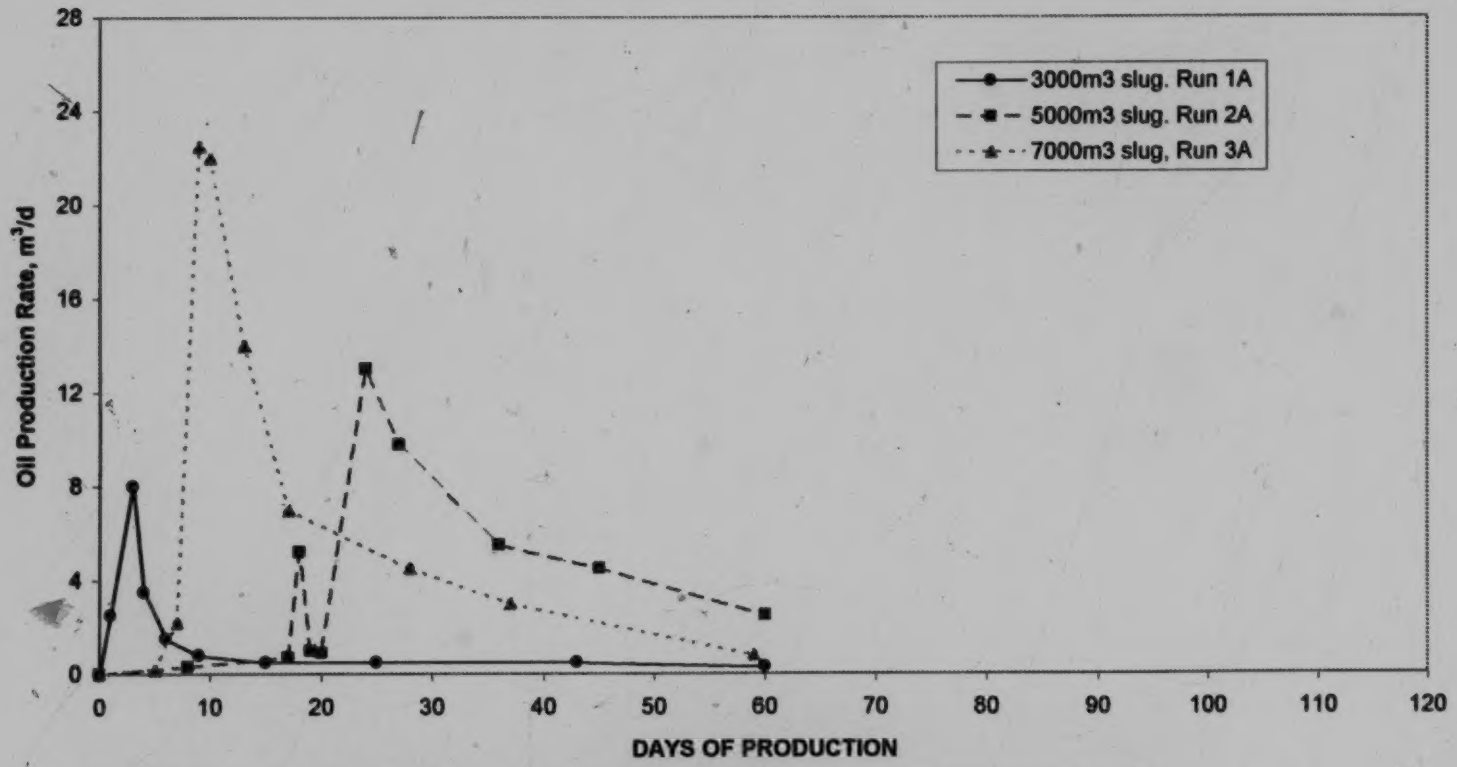

Figure 12.1.1.1a: RUN NO.'s 1A, 2A, and 3A oil production for Sw = 0.50, injection rate = 66.7 m^3/d, slug sizes = 3000, 5000, and 7000 m^3, 0.2 BHQ

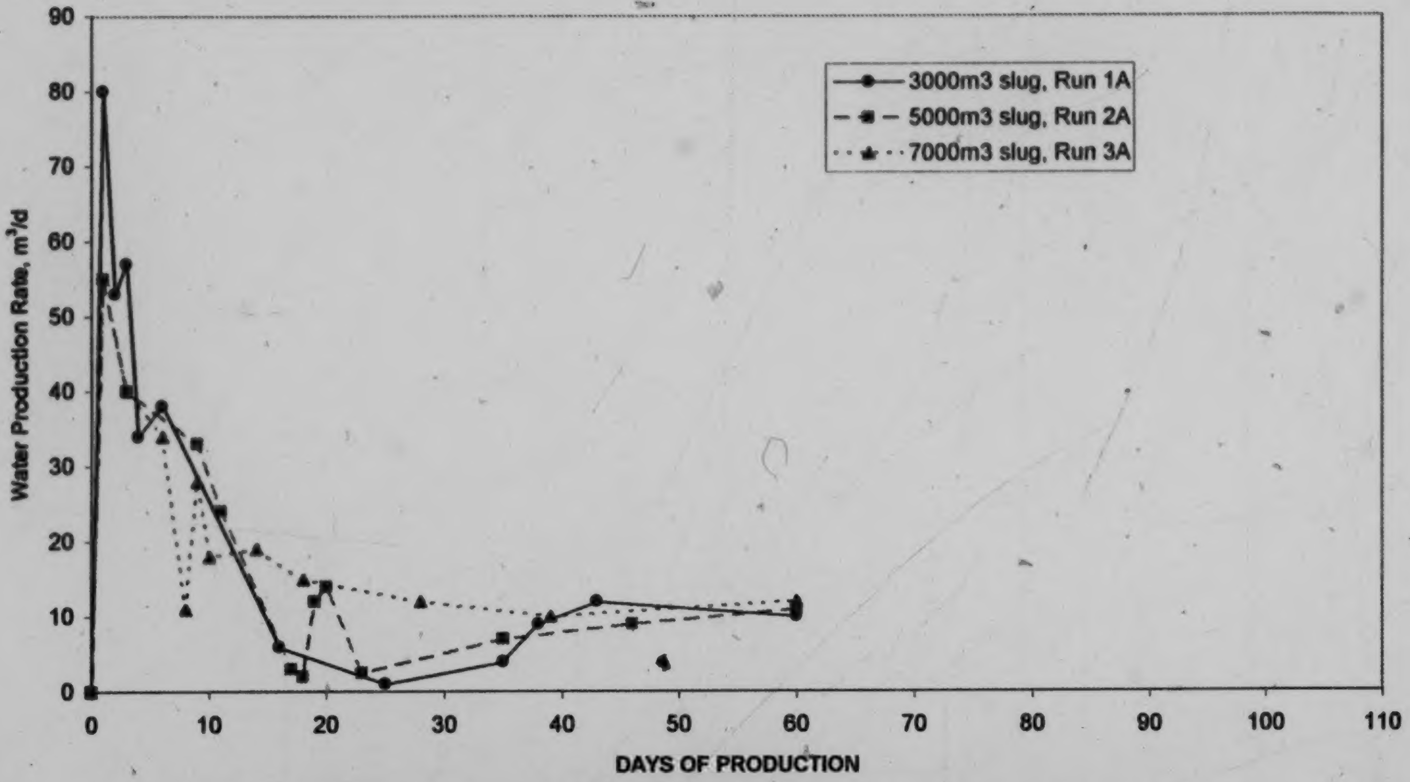

Figure 12.1.1.1b: RUN NO.'s 1A, 2A, and 3A water production for Sw = 0.50, injection rate = 66.7 m^3/d, slug sizes = 3000, 5000, and 7000 m^3, 0.2 BHQ

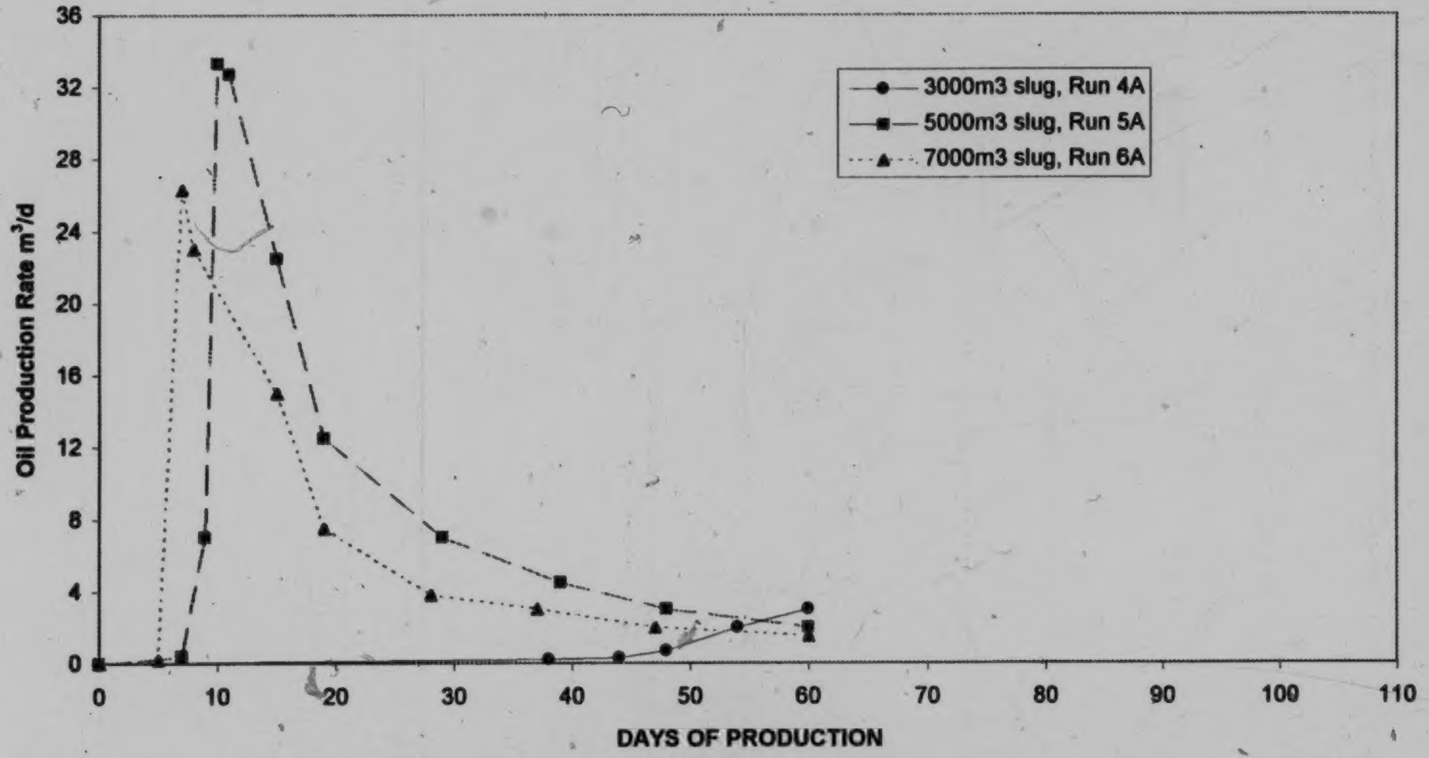

Figure 12.1.1.2a: RUN NO.'s 4A, 5A, and 6A oil production for $Sw = 0.50$, injection rate = 110.0 m^3/d, slug sizes = 3000, 5000, and 7000 m^3, 0.425 BHQ

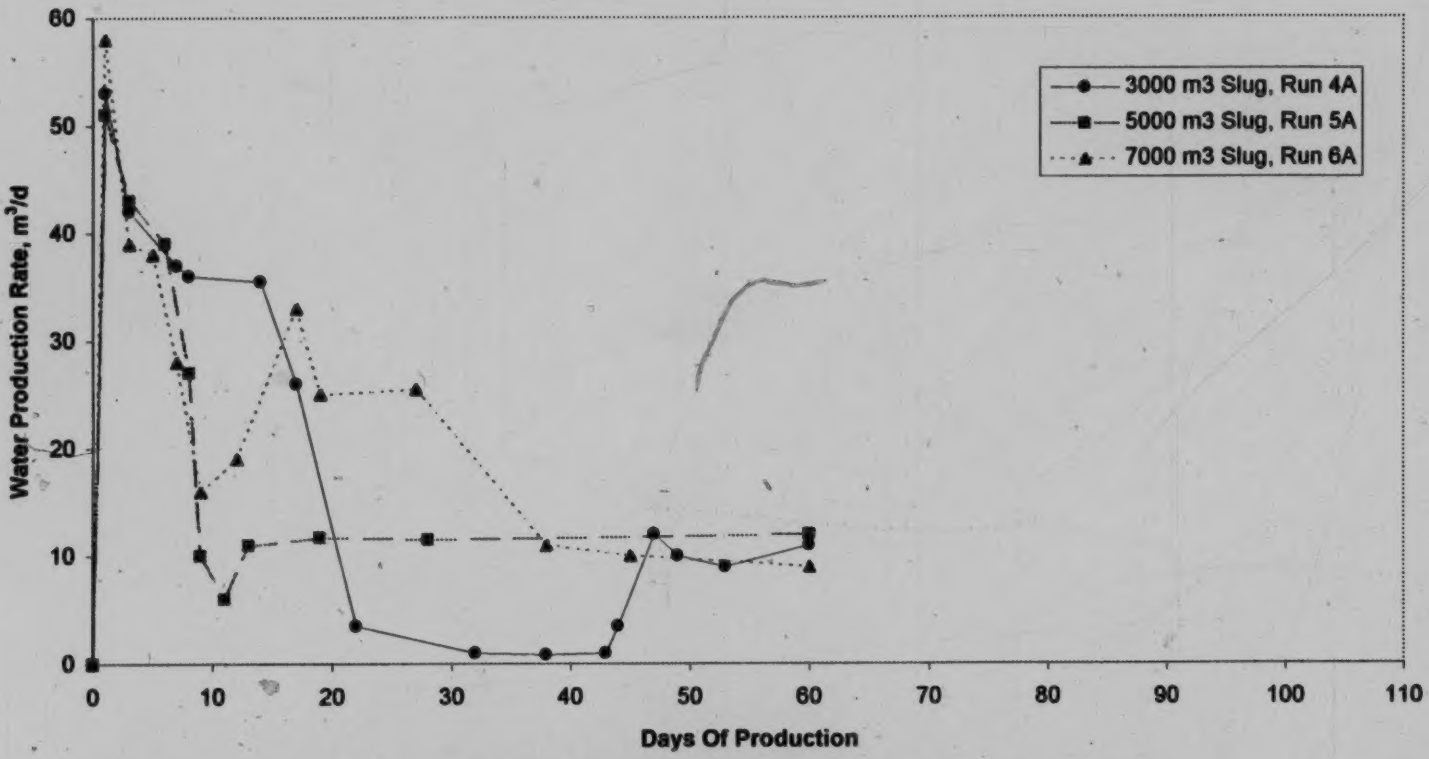

Figure 12.1.1.2b: RUN NO.'s 4A, 5A, and 6A water production for Sw = 0.50, injection rate = 110.0 m^3/d, slug sizes = 3000, 5000, and 7000 m$^{3.}$ 0.425 BHQ

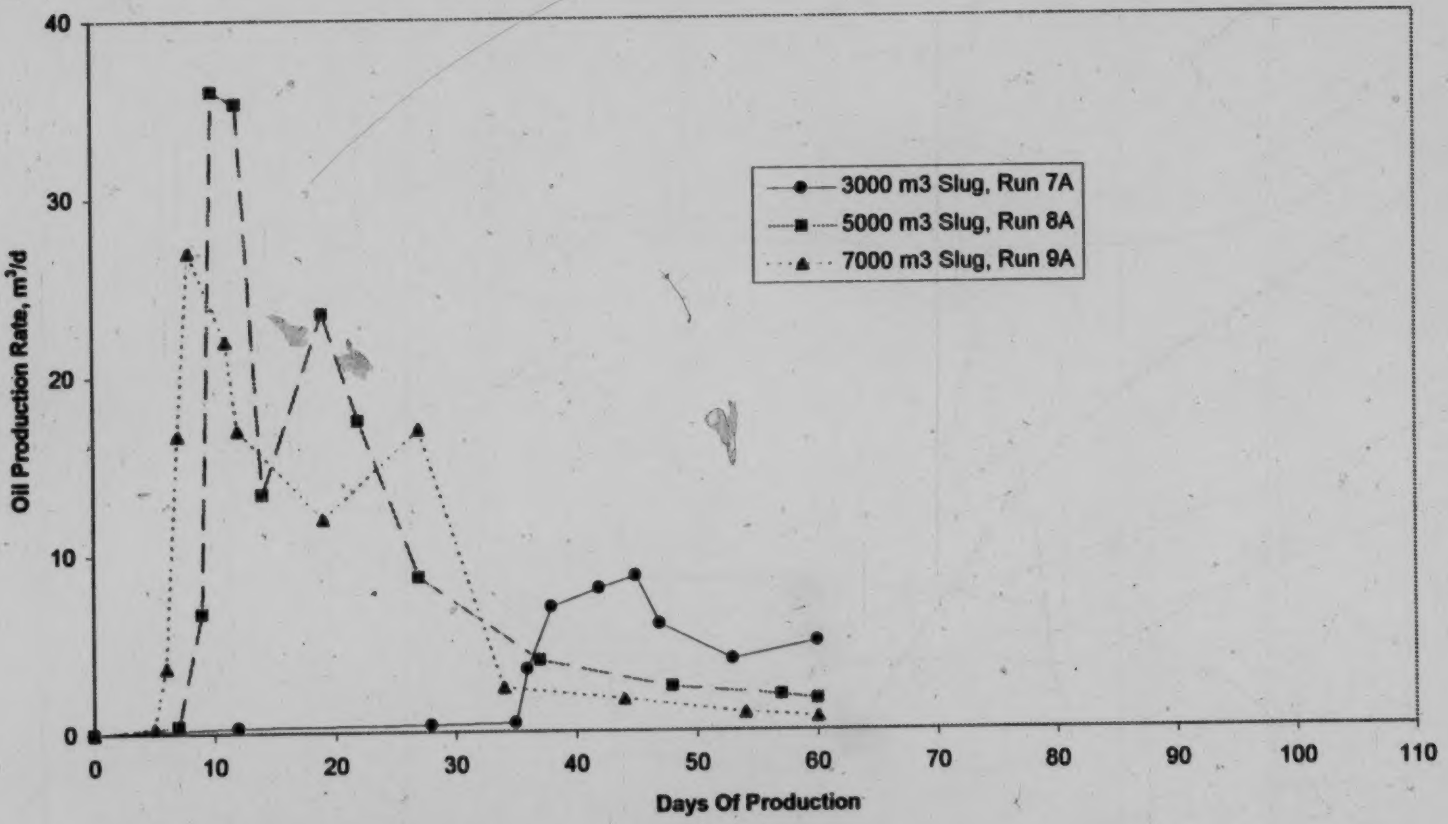

Figure 12.1.1.3a: RUN NO.'s 7A, 8A, and 9A oil Production for Sw = 0.50, injection rate = 200.0 m^3/d, slug sizes = 3000, 5000, and 7000 m^3, 0.5 BHQ

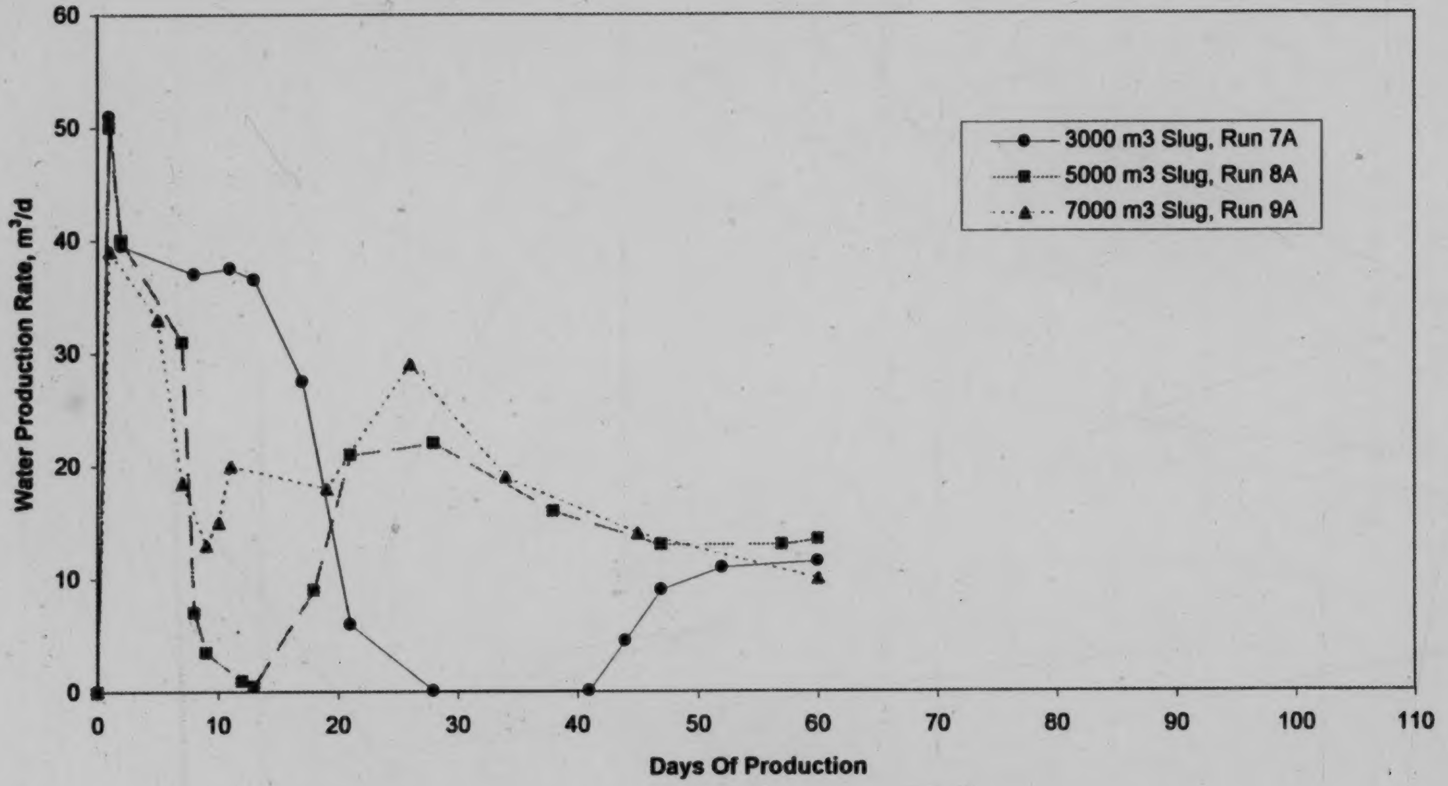

Figure 12.1.1.3b: RUN NO.'s 7A, 8A, and 9A water production for $S_w = 0.50$, injection rate = 200.0 m^3/d, slug sizes = 3000, 5000, and 7000 m^3, 0.5 BHQ

12.1.1 Interpretation of the Sensitivity Runs

A straightforward conclusion drawn from the generated data is the constancy in the volume of bitumen production using either 10 layers or 5 layers. Making a choice between one layer and five layers, or an 8 and 15-ring spacing for the correlation curve runs are more difficult as the degree of oil banking changes the bitumen production significantly.

Final grid sizing for the correlation curve generation was initialized to ***single-layer*** (1-D) with ***8-ring geometric*** radial spacing. It is believed that the finer grid selection using multiple-layering and equal volumes could affect the resulting bitumen production in either a positive or negative direction depending on rate and volume of steam injected. This view is reasonable given that grid block dimensions are fixed but for any particular run, the final position of the steam front could be located before, within, or past the fine grid system. The simpler grid selection has provided valid data for the correlation curves in light of the fact that first cycle production for eight PHOP pilot wells was matched within 1% error. The next section details supporting arguments for the above constructs and decision-making.

12.2 Detailed Analysis of Production Data from the Simulation Model

An analysis of the simulation results is expanded here as illustration of the complexity of numerical modeling heat, fluid, and gas flow regimes simultaneously.

A comprehensive investigation of all the data is best done by cataloging the production runs by slug size.

12.2.1 Slug Size of 3,000 m^3

For a 3,000 m^3 slug size, the use of multiple-layers for delineating a homogeneous formation leads to the production of some additional oil, water and gas.

a) Rate at 66.7 m^3/d

At an injection rate of 66.7 m^3/d (Figures 12.2.1.1a and 12.2.1.1b), the oil production is delayed in the 10-layer model. After 25 days steam cycle injection, oil production begins, compared to the single-layer model where oil is produced a few days after the end of steaming. A five-layer model instead of a ten-layer one would have sufficed for this research since results show very little difference between the two geometries (see Table 12.1.1). For ten layers, due to steam override, the steam front advances further out into some parts of the reservoir as a stacked series of fronts somewhat analogous to a channeling effect. Variation in the way heat travels in the individual layers is pronounced causing fronts to be further out in the upper layers. Steam override worsens bypassing of oil near the producing well. The ten-layer model predicts production, a mixture of formation gas and injected steam ("gas"), at a slower rate than in the case of a single-layer model. The overall result is a delay in oil production with somewhat more oil produced during the defined cycle time. The cumulative oil production is quite low. Both runs verify the low oil production characteristics observed in the field for well IP6 (see runs 1A and 1B, Table 12.1.2).

b) Rate of 110 m^3/d

At an injection rate of 110 m^3/d (Figures 12.2.1.2a and 12.2.1.2b) and a slug size of 3,000 m^3, oil production for the ten-layer case occurs somewhat earlier than in the single-layer case. In the ten-layer model, the "gas" is produced much sooner with six times more gas produced volume. As a result, oil is also produced sooner in the ten-layer model, and as in Figure 12.1.1.1a, which shows more oil is recovered because of the increased channeling effect during injection.

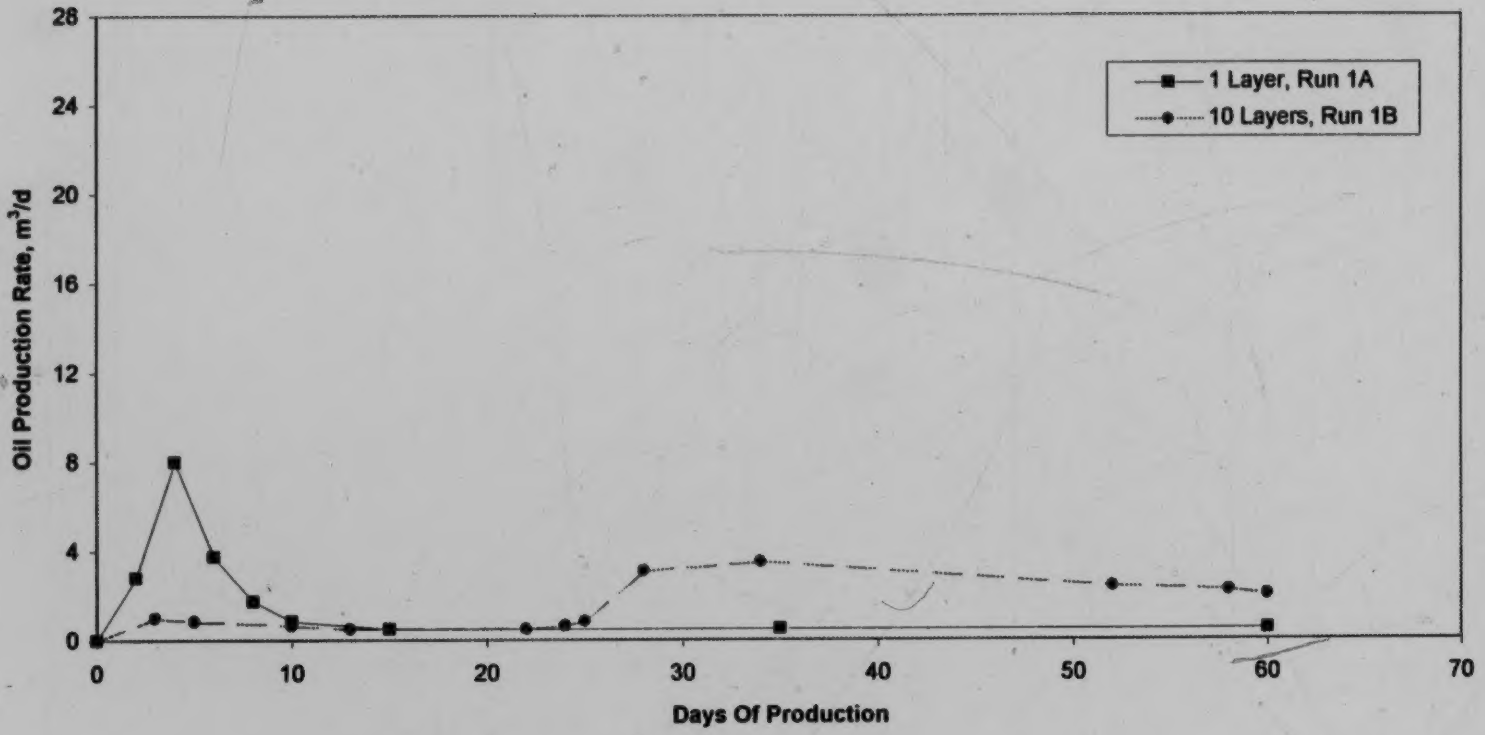

Figure 12.2.1.1a: RUN NO.'s 1A, and 1B Oil production for Sw = 0.50, injection rate = 66.7 m^3/d, slug size = 3000 m^3, 1 and 10 layers

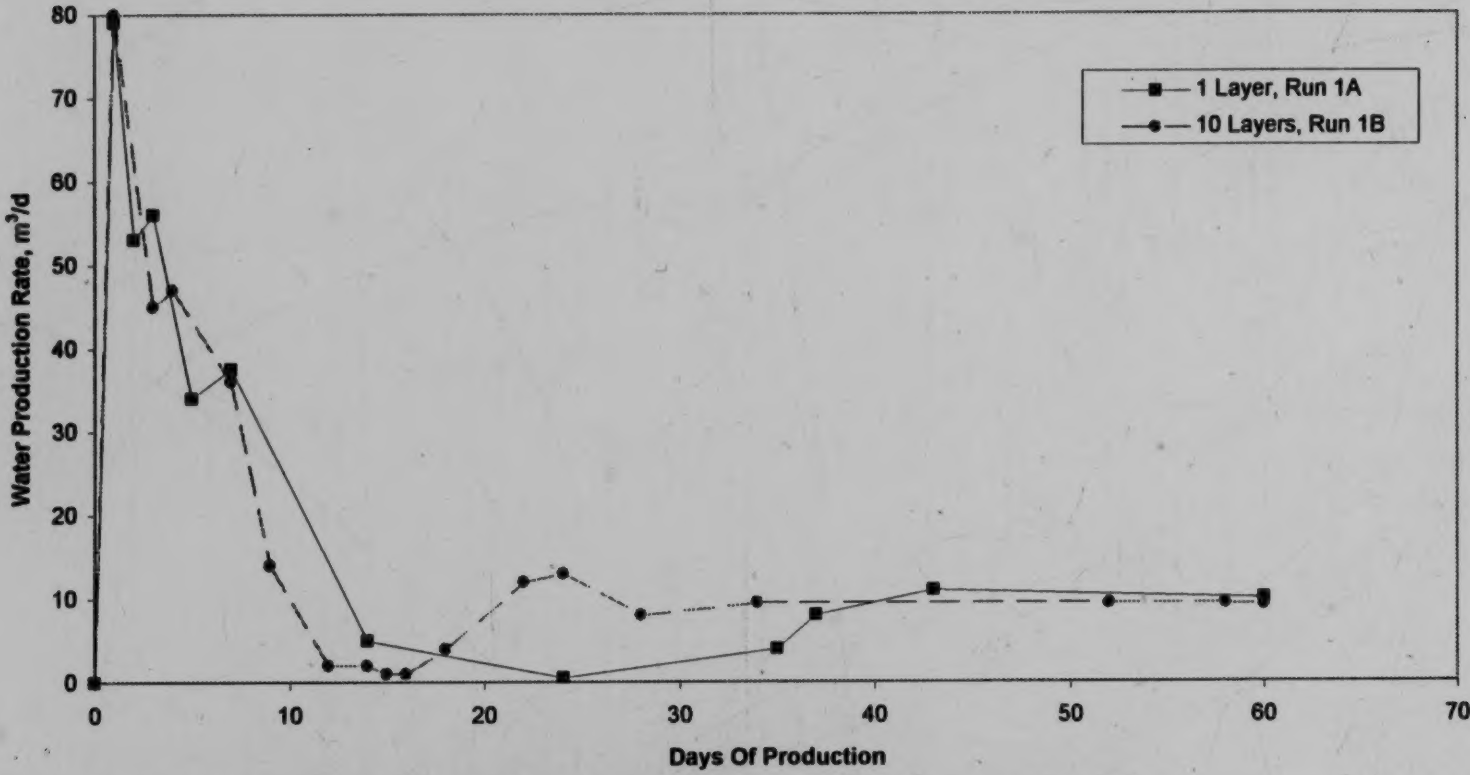

Figure 12.2.1.1b: RUN NO.'s 1A, and 1B water production for Sw = 0.50, injection rate = 66.7 m^3/d, slug size = 3000 m^3, 1 and 10 layers

Table 12.2.1

Operating Conditions-Single Layer Model: Optimization of Injection Rates and Slug Size
Initial Water Saturation, Swi = 0.5

Run No.	No. Layers	No. Radial Cells	Injection Rate m3/d	Time Injection days	Slug Size m3	Bottomhole Steam Quality	Bottomhole Inj Pressure MPa	Res Press End Inj MPa	Heat Injected x10^{10}KJ	Production Fluid Rate m3/d	No. of Producing days	Water Production m3	Bitumen Production m3	Gas Production Nm3	Steam Oil Ratio
1A	1	8	66.7	45	3000	0.2	9.2	6.2	0.4876	40	60	673	21	1801	143
1B	10	8	66.7	45	3000	0.2	9.2	5.7		40	60	707	85	2631	35
2A	1	8	66.7	75	5000	0.2	9.2	5.4	0.8131	40	60	704	232	6913	22
2B	10	8	66.7	75	5000	0.2	9.2	5.0		40	60	874	288	8985	17
2C	5	8	66.7	75	5000	0.2	9.2	5.0		40	60	868	282	8824	18
3A	1	8	66.7	105	7000	0.2	9.2	5.3	1.138	40	60	847	244	9203	29
4A	1	8	110	27	3000	0.425	11.6	8.2	0.602	40	60:120	707:1147	25:94	1200:3500	120:32
4B	10	8	110	27	3000	0.425	11.6	6.0		40	60	891	264	7479	11
4C	5	8	110	27	3000	0.425	11.6	6.3		40	60	1474	300	8343	10
4D	5	15	110	27	3000	0.425	11.6	7.9		40	120	1253	197	6727	15
5A	1	8	110	45.5	5000	0.425	11.6	6.3	1.012	40	60	812	344	9541	15
5B	10	8	110	45.5	5000	0.425	11.6	6.1		40	60	1089	288	9706	17
5C	5	8	110	45.5	5000	0.425	11.6	6.1		40	60	1070	295	9531	17
5D	5	15	110	45.5	5000	0.425	11.6	8.5		40	120	1346	313	10240	11
6A	1	8	110	63.6	7000	0.425	11.6	6.7	1.412	40	60	959	249	9047	28
6B	10	8	110	63.6	7000	0.425	11.6	6.5		40	60	1125	242	9825	29
6D	5	15	110	63.6	7000	0.425	11.6	10.1		40	180:210	1767:2000	191:224	14290:1429	37:31
7A	1	8	200	15	3000	0.5	12	11.0	0.642	40	60:90	733:980	133:192	1679:4070	23:16
7B	10	8	200	15	3000	0.5	12	7.7		40	60	1102	280	8387	11
8A	1	8	200	25	5000	0.5	12	8.3	1.067	40	60	947	410	9847	12
8B	10	8	200	25	5000	0.5	12	8.0		40	60	1273	310	9681	11
9A	1	8	200	35	7000	0.5	12	8.9	1.492	40	60	1182	275	8765	26
9B	10	8	200	35	7000	0.5	12	8.6		40	60	1325	218	9731	35

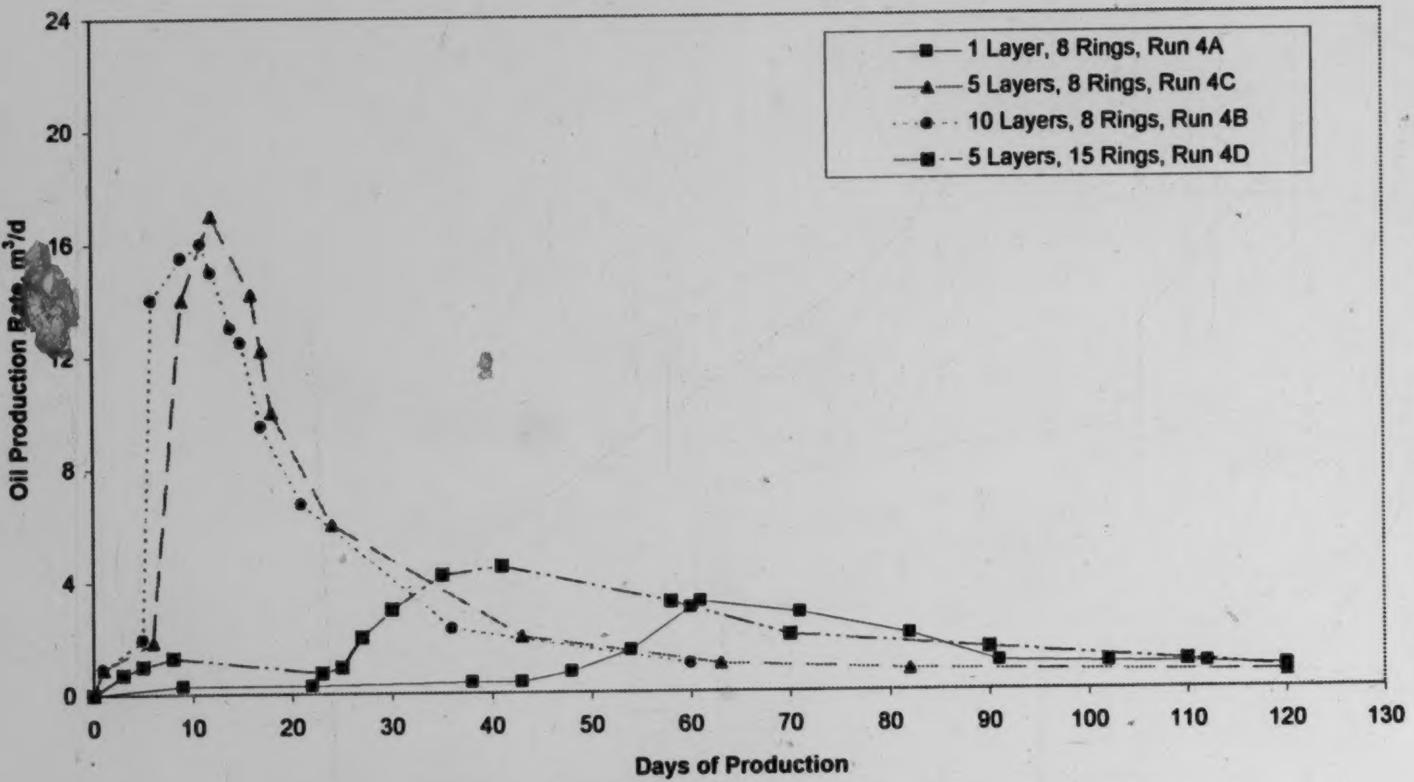

Figure 12.2.1.2a: RUN NO.'s 4A, 4B, 4C and 4D oil production for Sw = 0.50, injection rate = 110 m^3/d, slug size = 3000 m^3, 1, 5, and 10 layers

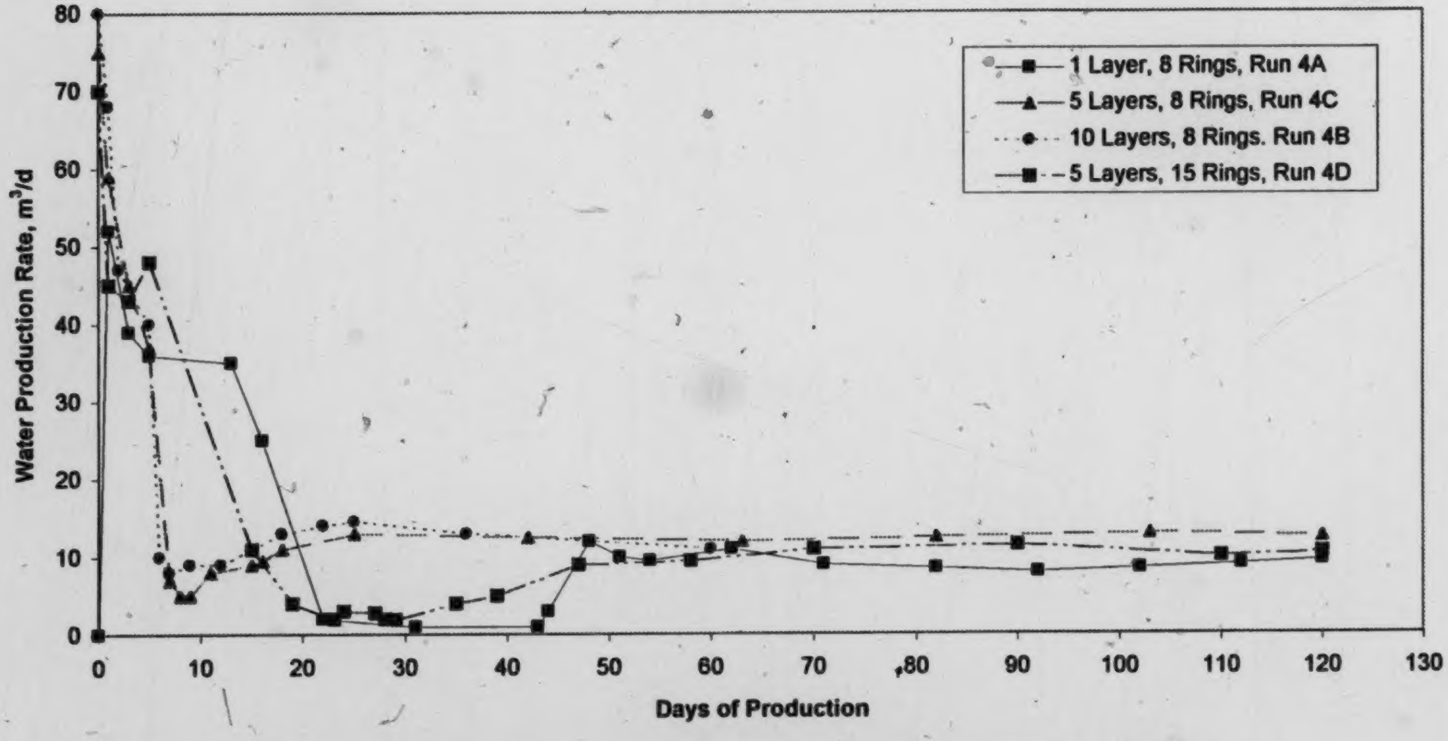

Figure 12.2.1.2b: RUN NO.'s 4A, 4B, 4C and 4D water production for Sw = 0.50, injection rate = 110 m^3/d, slug size = 3000 m^3, 1, 5, and 10 layers

Comparing rate performance at 66.7 m^3/d and 110 m^3/d, significantly more oil was produced at a 110m^3/d injection rate. The pressure and temperature are also higher near the wellbore for 110m^3/d, and this tends to increase mobility and flow during production. Because of high rates, approximately 23% more heat entered into the formation than at lower rates for the same slug size. This resulted in a 19% increase in oil production (21-25 m^3) in the single-layer model and a 210% increase (85-264 m^3) in the ten-layer model. These values are for 60 days production only and would change if the production cycle was extended.

c) Rate of 200 m^3/d

An injection rate of 200 m^3/d (all the rates examined here are at 3,000 m^3 slug size) shows a trend similar to the 110 m^3/d case. Note that 7% more heat is injected at 200 m^3/d than at 110 m^3/d, referring to Figures 12.2.1.3a and 12.2.1.3b, and Table 12.1.1., with a 432% increase in bitumen production (25-133 m^3). At 60 days production, 110% more oil was produced with ten layers than with a single-layer. Again, "gas" production was higher for the ten layer model.

d) General Comments on Layering

Whether a single-layer model or a five or ten-layer model is employed, the trends in production performance are similar. However, if accurate predictions are required, at least a five-layer model is recommended to account for both steam override and gravity drainage. The ten layer configuration will not improve accuracy over the five-layer option.

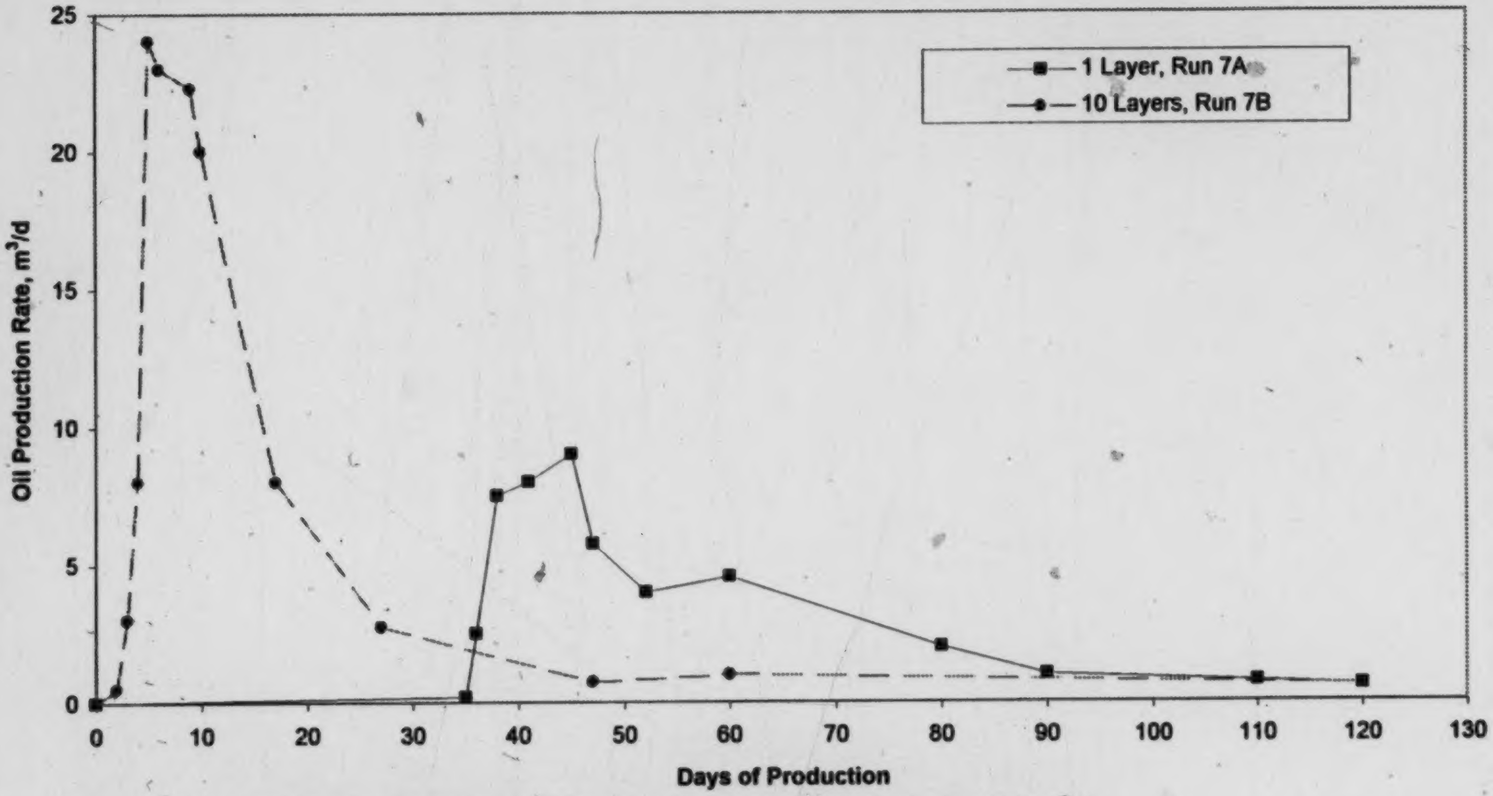

Figure 12.2.1.3a: RUN NO.'s 7A and 7B oil production for Sw = 0.50, injection rate = 200 m^3/d, slug size = 3000 m^3, 1 and 10 layers

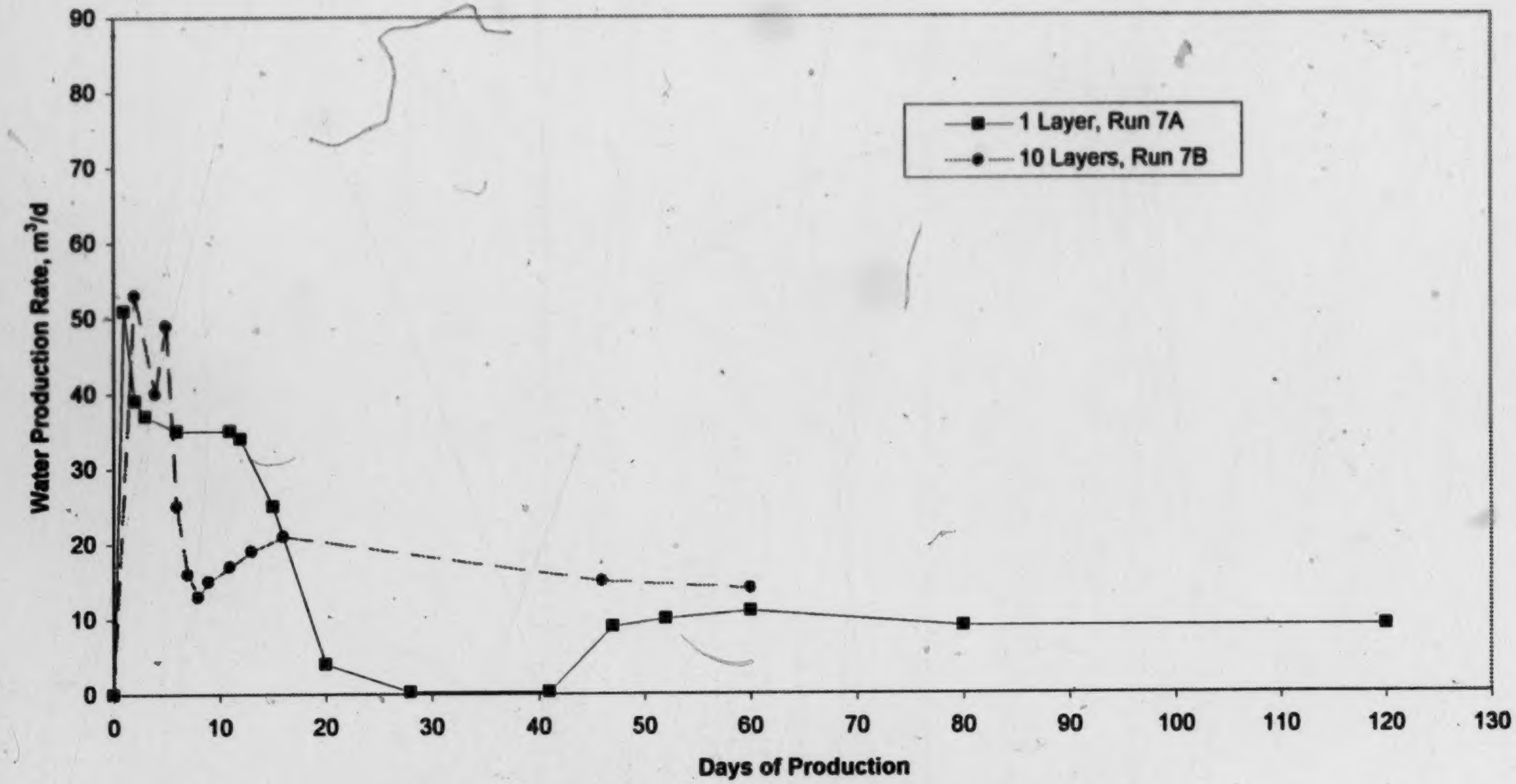

Figure 12.2.1.3b: RUN NO.'s 7A and 7B Water production for Sw = 0.50, injection rate = 200 m^3/d, slug size = 3000 m^3, 1 and 10 layers

12.2.2 Slug Size 5000 m^3

For a 5,000 m^3 slug size, the case for an increased number of formation layers tends to produce more oil at a 66.7 m^3/d injection rate (Table 12.1.1 and Figures 12.2.2.1a and 12.2.2.1b). This observation is similar to the 3,000 m^3 slug size. But for a 5,000 m^3 slug, injected at either 110 m^3/d (Figures 12.2.2.2a and 12.2.2.2b) or at 200 m^3/d (Figures 12.2.2.3a and 12.2.2.3b), the finer formation layering reduces the amount of oil produced. An explanation for these interdependencies is given in the next paragraph.

For all the injection rates, the oil is produced earlier in time using ten layers than when a single-layer is modeled. A 5,000 m^3 slug injected at 66.7 m^3/d has an effect on the reservoir similar to a 3,000 m^3 slug at 110 m^3/d, as long as the operating days are the same. The steam front of a ten-layer model does not advance as far out into the reservoir as does a front in the single-layer model, consequently, more oil is left behind in the vicinity of the production well as "lost oil".

A 5,000m^3 slug at 110 m^3/d behaves differently from a 3,000 m^3 slug as the ten-layer model yields less oil than the single-layer model. This can be accounted for by steam override, whereby large amounts of steam and gas migrate to the upper model layers during injection. More steam will be produced as a gas because of override, resulting in a higher cumulative water production. The effect is less at a 3,000 m^3 slug size. For this trial, there is a 25% increase in water production over a single-layer simulation. Steam override has a maximum effect at a 5,000 m^3 slug contributing to a 35% increase in water production over a single-layer. The same 35% increment is observed in the case of a 7,000 m^3 slug size. Energy lost to steam override translates to a loss in oil production, since the steam produced, as cold-water equivalent, is from the region of residual oil saturation where heat is considered wasted.

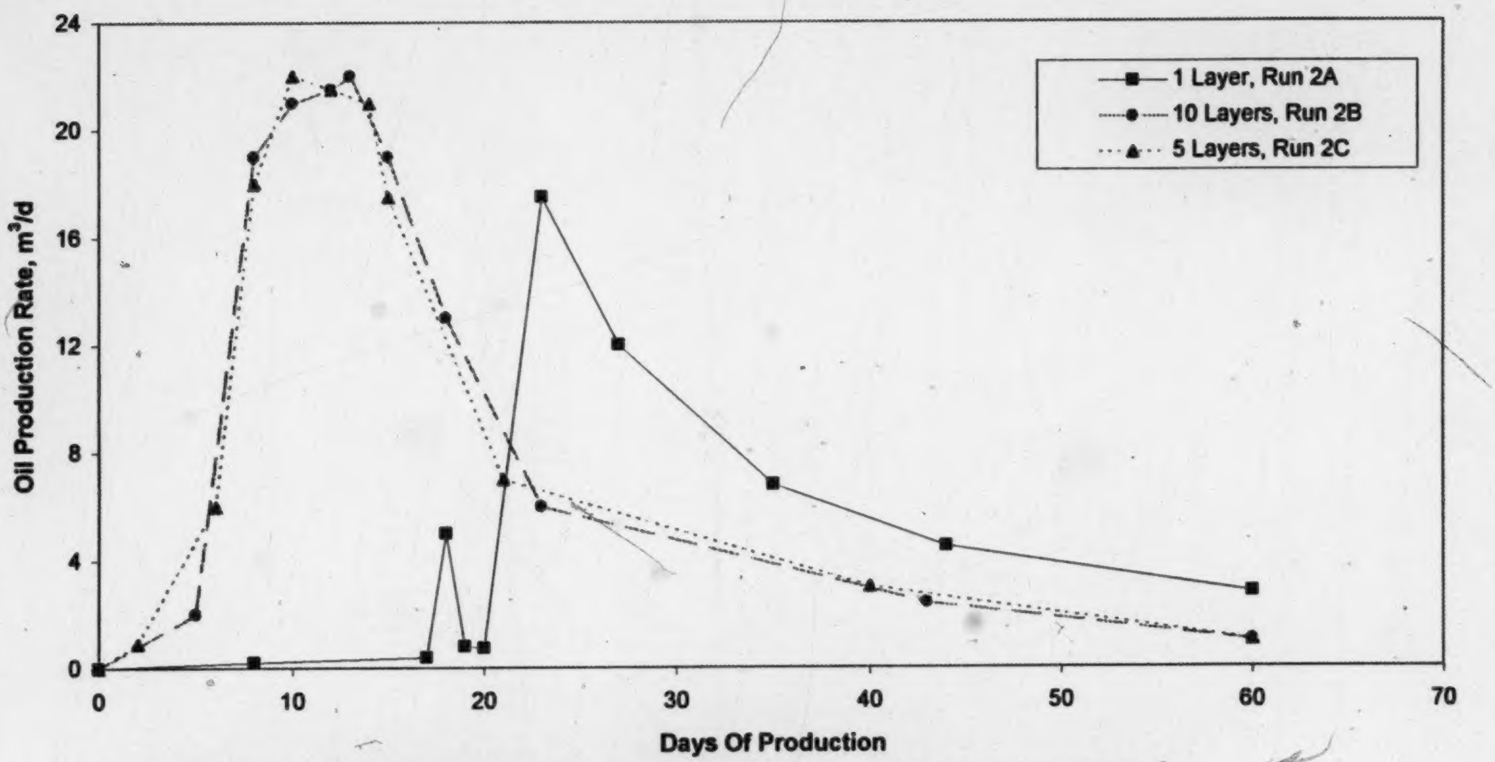

Figure 12.2.2.1a: RUN NO.'s 2A, 2B, and 2C oil production for Sw = 0.50, injection rate = 66.7 m^3/d, slug size = 5000 m^3, 1, 5, and 10 layers

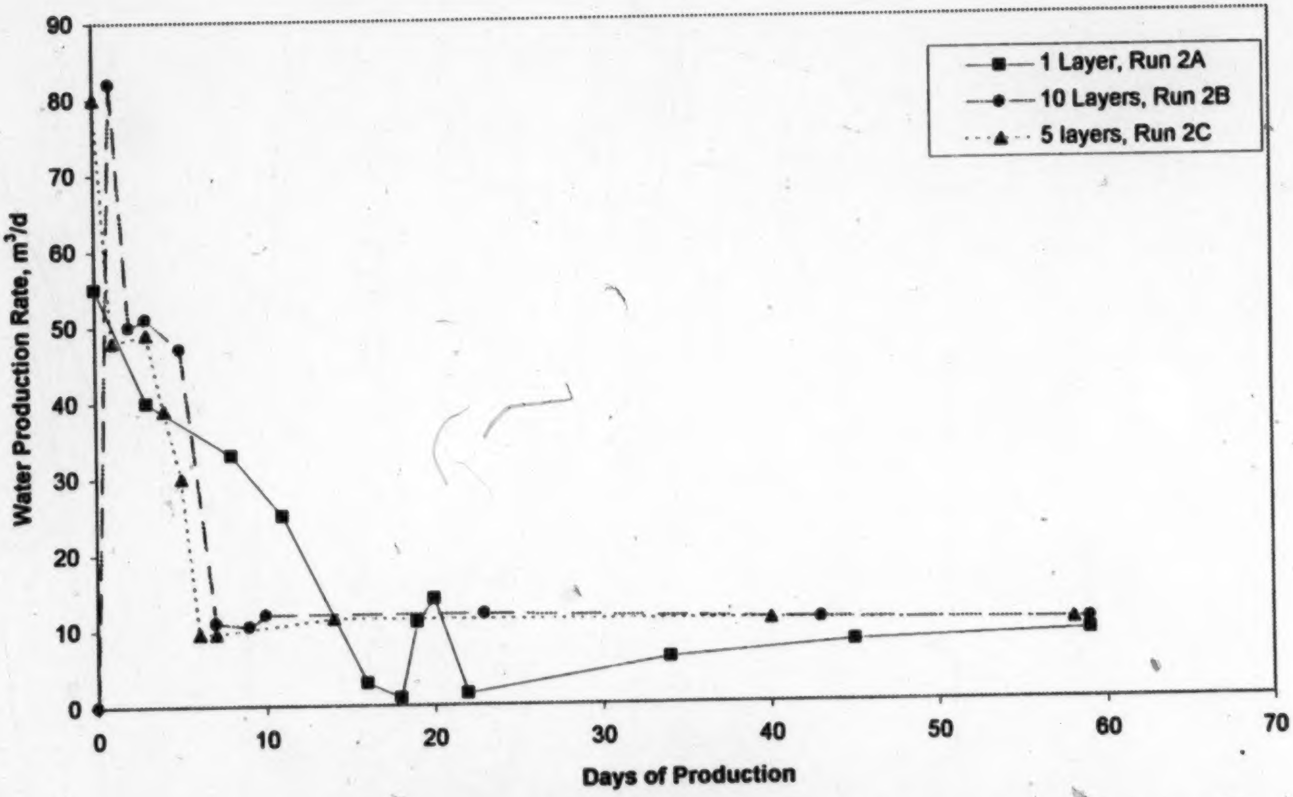

Figure 12.2.2.1b: RUN NO.'s 2A, 2B, and 2C water production for Sw = 0.50, injection rate = 66.7 m^3/d, slug size = 5000 m^3, 1, 5, and 10 layers

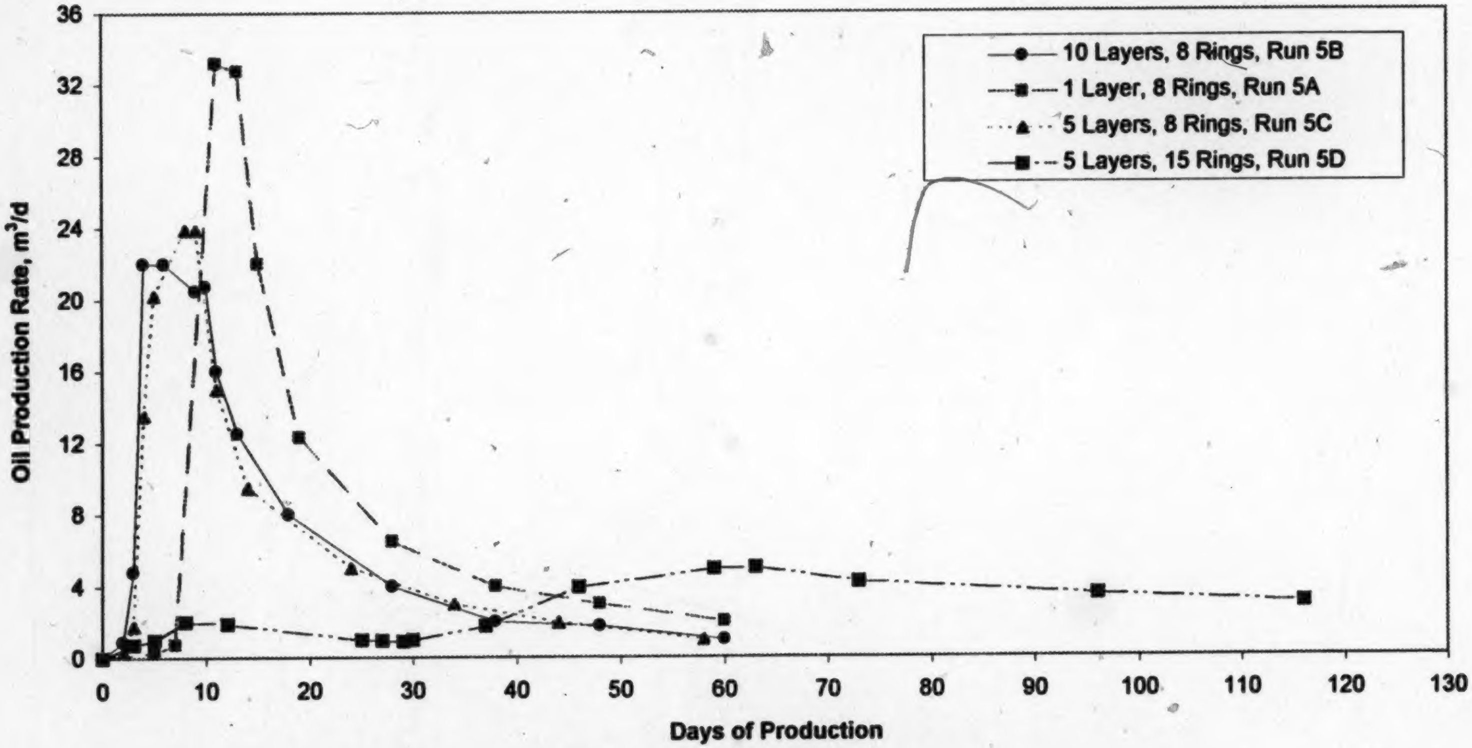

Figure 12.2.2.2a: RUN NO.'s 5A, 5B, 5C, and 5D oil production for Sw = 0.50, injection rate = 110 m^3/d, slug size = 5000 m^3, 1, 5, and 10 layers

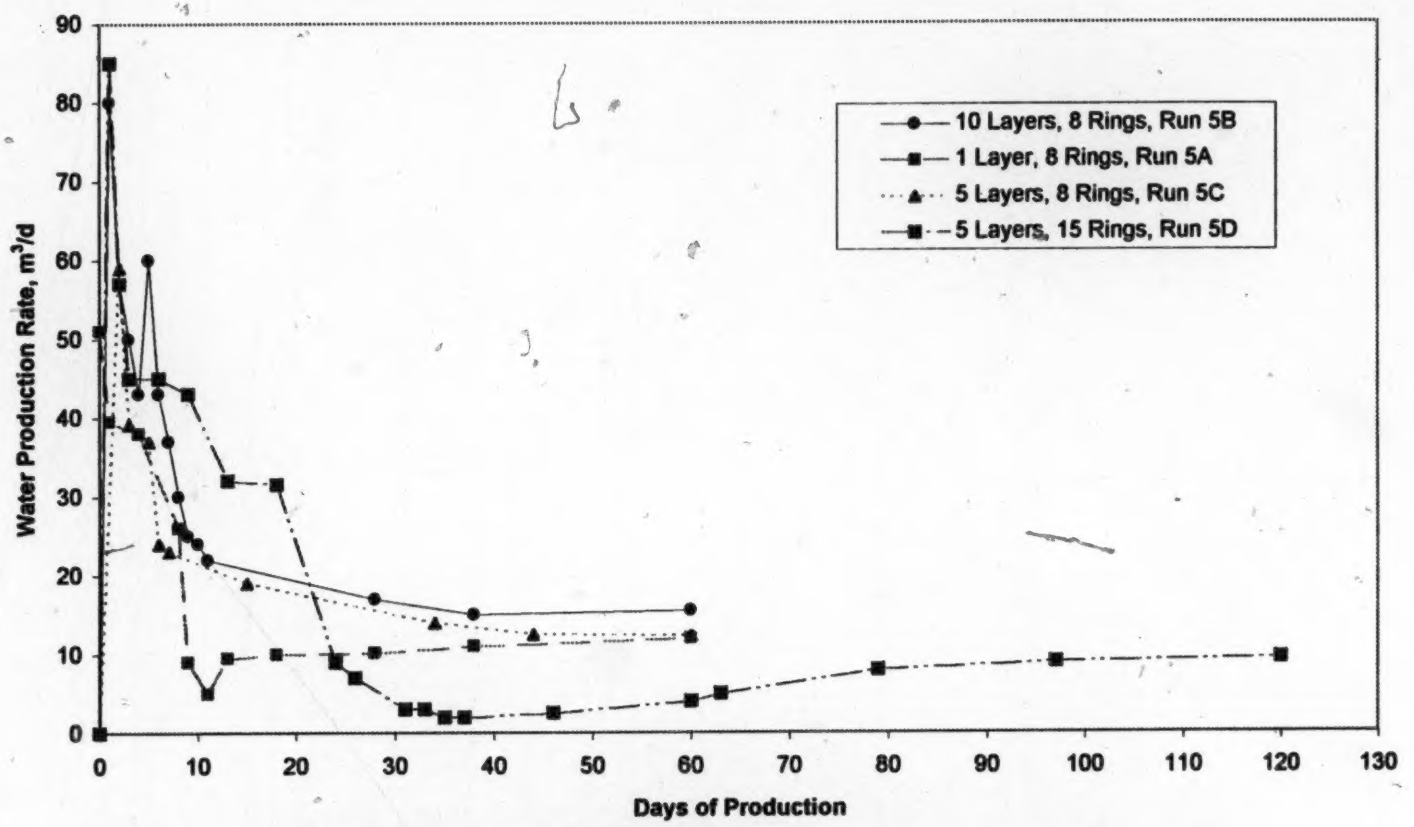

Figure 12.2.2.2b: RUN NO.'s 5A, 5B, 5C, and 5D water production for Sw = 0.50, injection rate = 110 m^3/d, slug size = 5000 m^3, 1, 5, and 10 layers

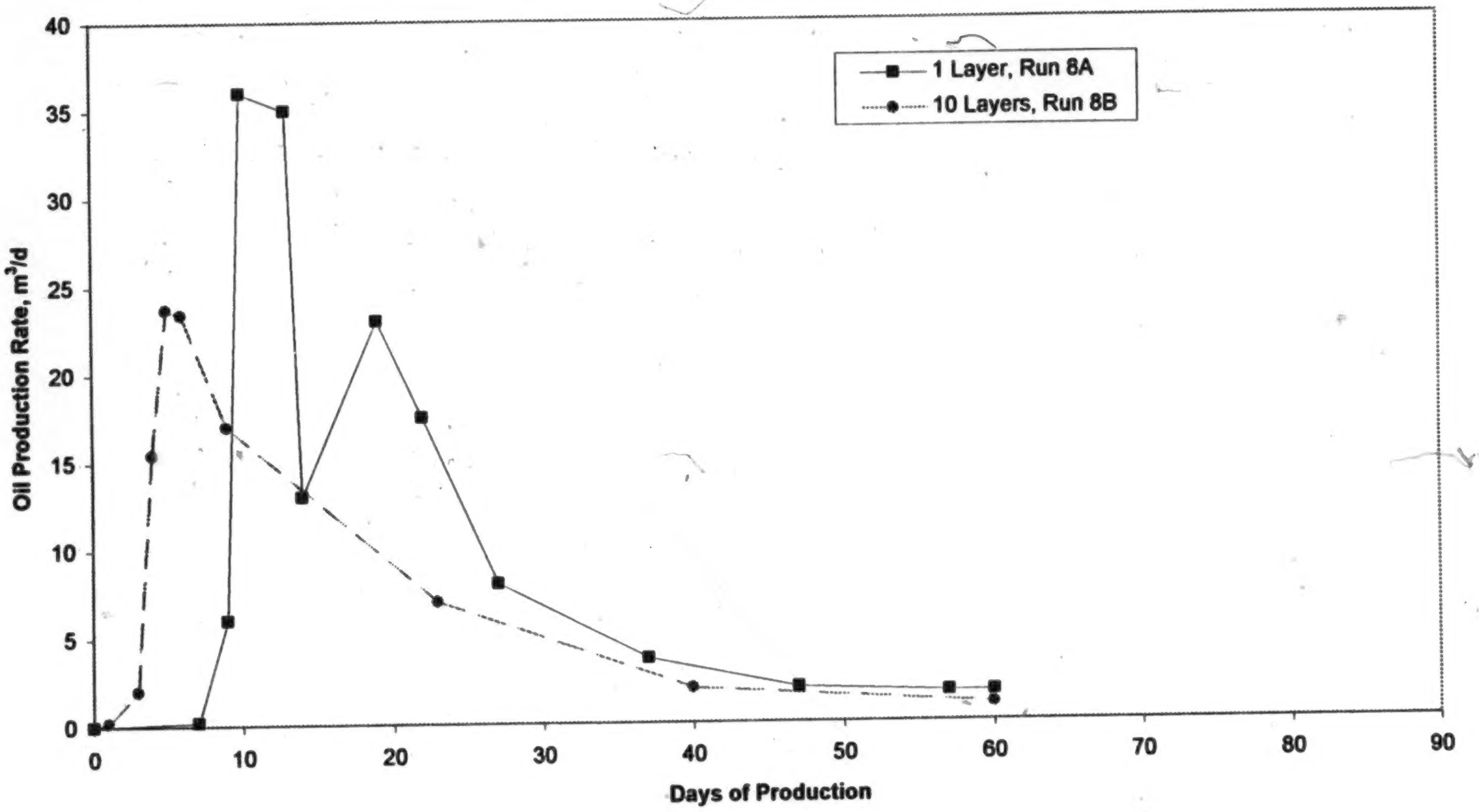

Figure 12.2.2.3a: RUN NO.'s 8A and 8B Oil production for Sw = 0.50, injection rate = 200 m^3/d, slug size = 5000 m^3, 1 and 10 layers

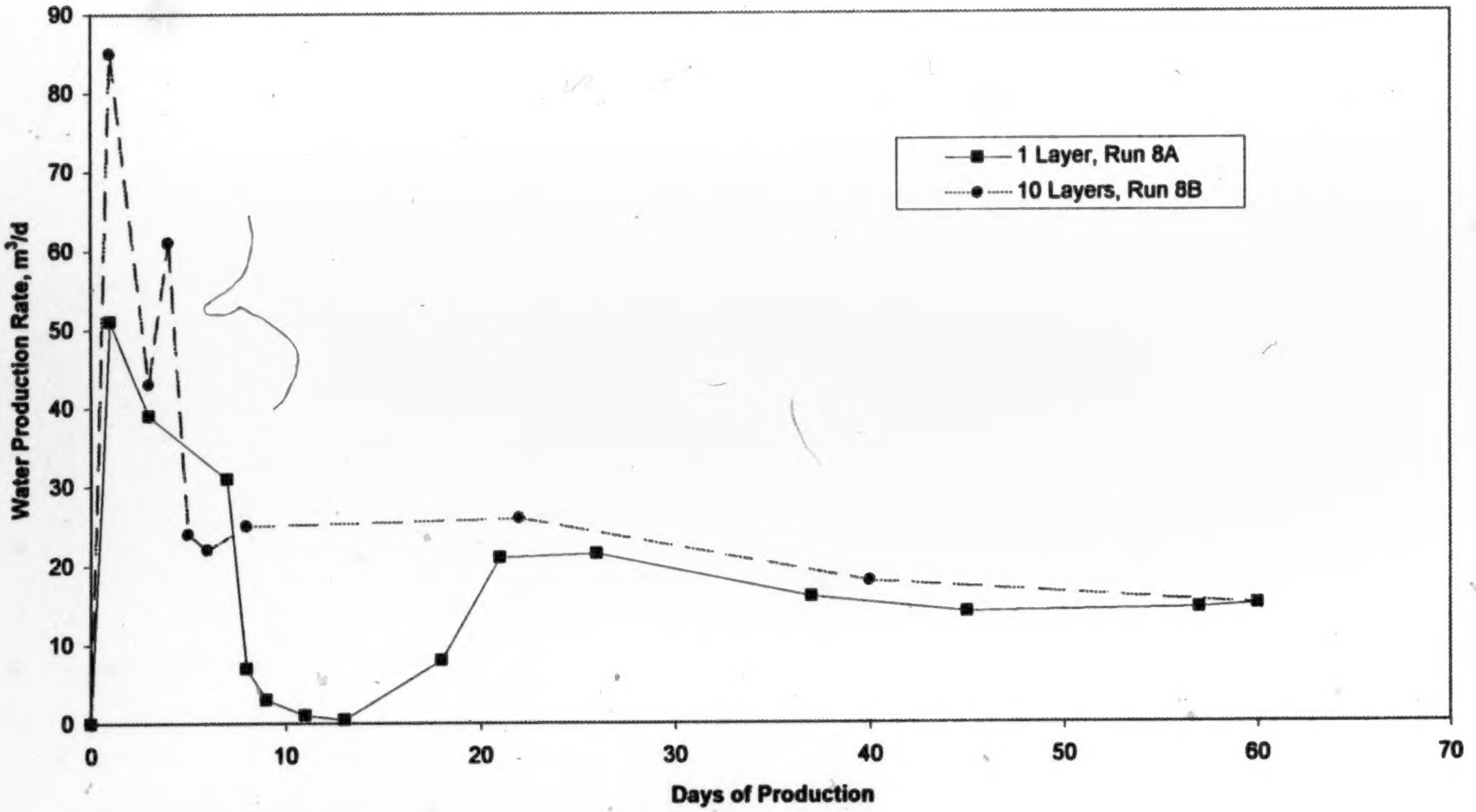

Figure 12.2.2.3b: RUN NO.'s 8A and 8B water production for Sw = 0.50, injection rate = 200 m^3/d, slug size = 5000 m^3, 1 and 10 layers

12.2.3 Slug Size of 7,000 m^3

For a 7,000 m^3 slug size, the trends are the same as for the 5,000 m^3 slug size. See Figures 12.2.3.1a to 12.2.3.2b.

12.2.4 Comparing 3,000 m^3, 5,000 m^3, and 7,000 m^3 Slug Sizes

Limited information is available here, as the problem appears to be more complex than what is reflected in the model results. Part of this may be the selection of grid size, which is sensitive to the injection rate and slug size. The next section addresses this concern.

12.2.5 Effect of Radial Grid Size on 3,000 m^3, 5,000 m^3, and 7,000 m^3 Slug Sizes

By maintaining a constant rate, the effect of radial grid size on oil production was tested (see Table 12.1.1). The initial grid pattern used for the radial modeling contained 8 concentric rings (Figure 12.1.1) whose radii follow a geometric progression. Another grid pattern tested was a 15-ring arrangement which combines equal volume spacing with the previous 8-ring geometric grid spacing. Five layers were selected instead of ten because it was observed that a five-layer model is satisfactory for all practical purposes (Runs 4D, 5D, and 6D, with Figures 12.2.5.2a and 12.2.5.2b). Final injection pressures for the 15 rings were about 2 MPa higher than for the 8-ring simulations (Figure 12.2.5.1). The pressure difference increased as slug size became larger. This pattern suggests the heated zone has stopped expanding due to cold oil banking in the smaller, equal-volume grids, and the hot zone is pressuring up. Because of oil banking problems, 15 rings could not be used for developing the correlation curves. Fracturing in a field situation allows a bank to form along the length of a fracture, but perpendicular to the fracture face. The 8-ring geometric spacing can model this process, although in all directions, which is acceptable when dilation is considered, and fracture lengths are short. This implies that only a fully-coupled fracture model, which includes dilation effects, can employ small Cartesian grids. However, the persistent oil banking problem forces grid blocks to be square.

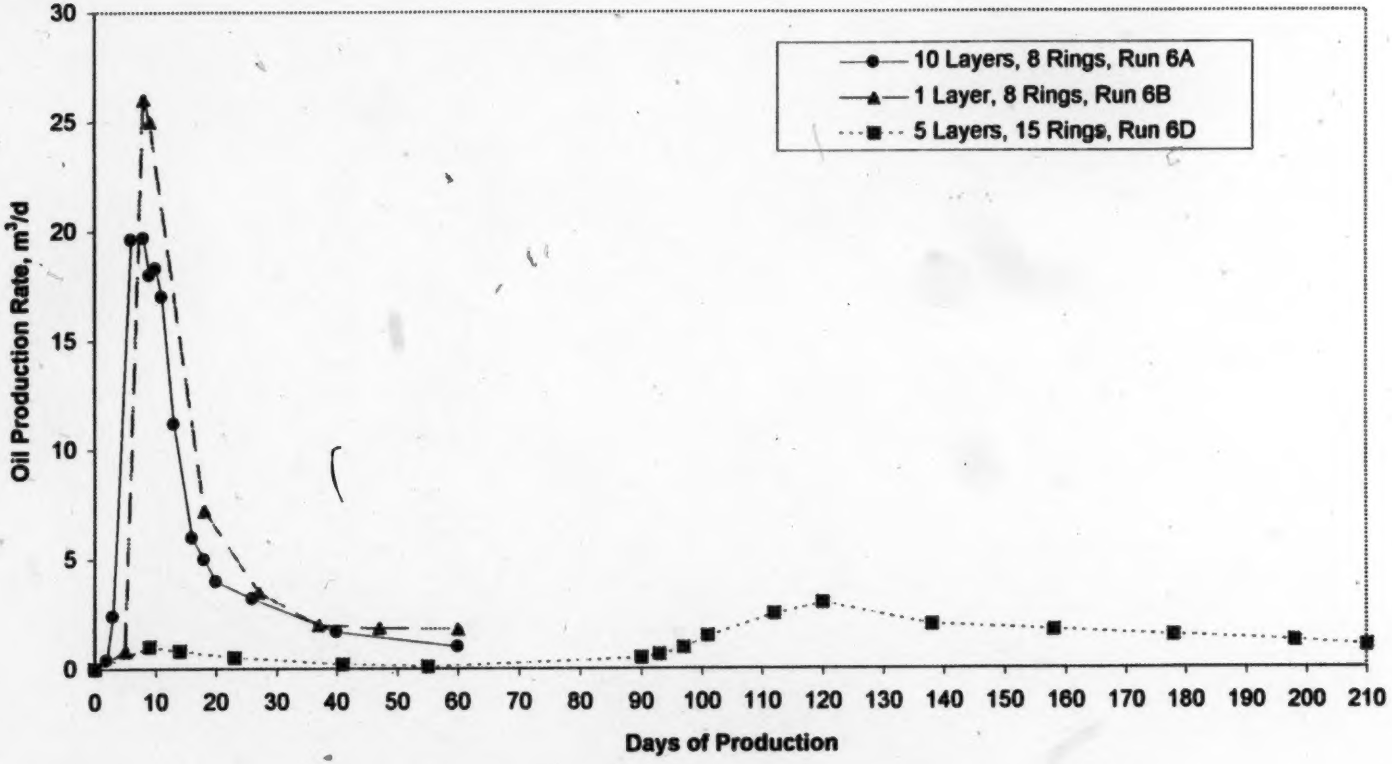

Figure 12.2.3.1a: RUN NO.'s 6A, 6B, and 6D Oil production for Sw = 0.50, injection rate = 110 m^3/d, slug size = 7000 m^3, 1, 5 and 10 layers

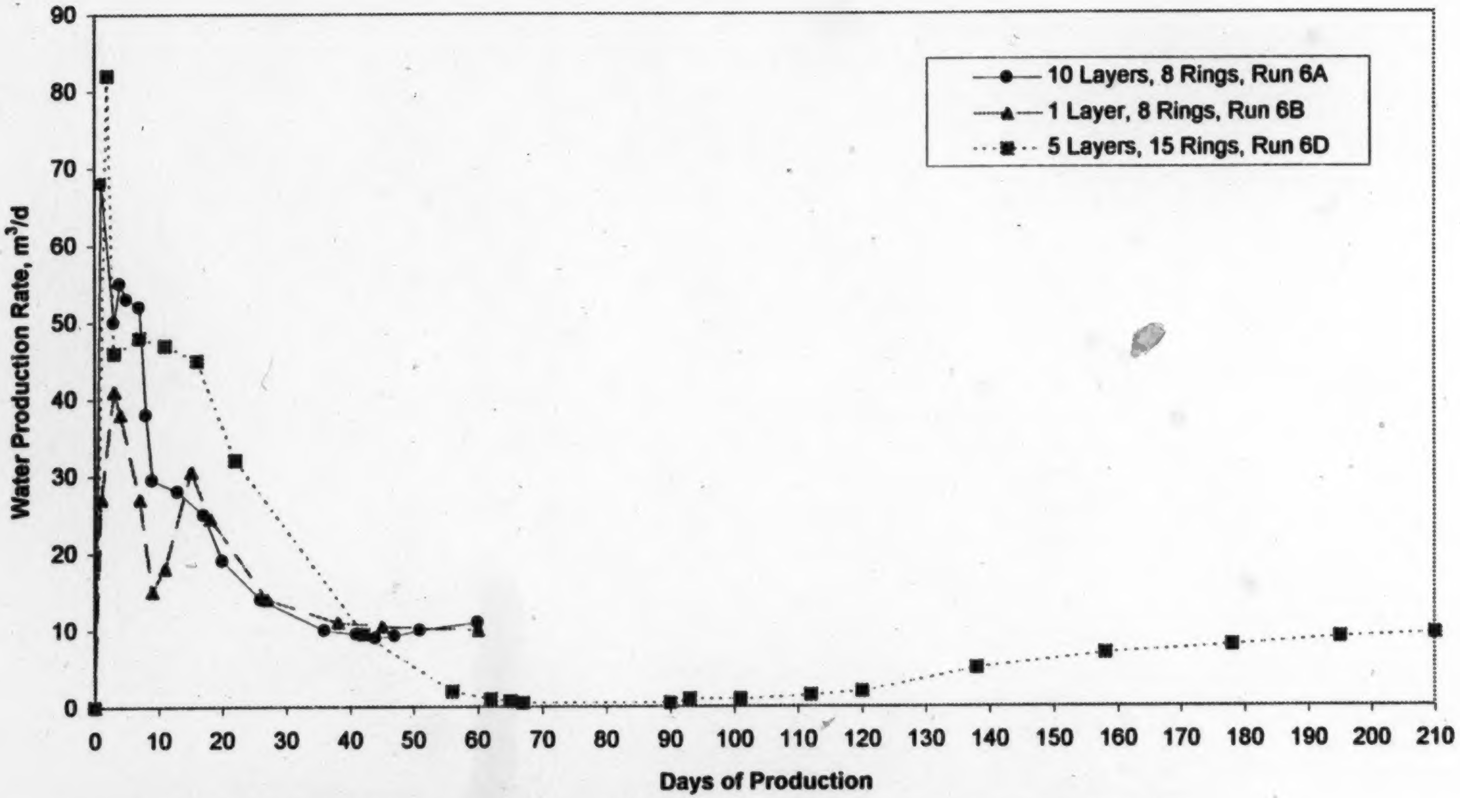

Figure 12.2.3.1b: RUN NO.'s 6A, 6B, and 6D water production for Sw = 0.50, injection rate = 110 m^3/d, slug size = 7000 m^3, 1, 5 and 10 layers

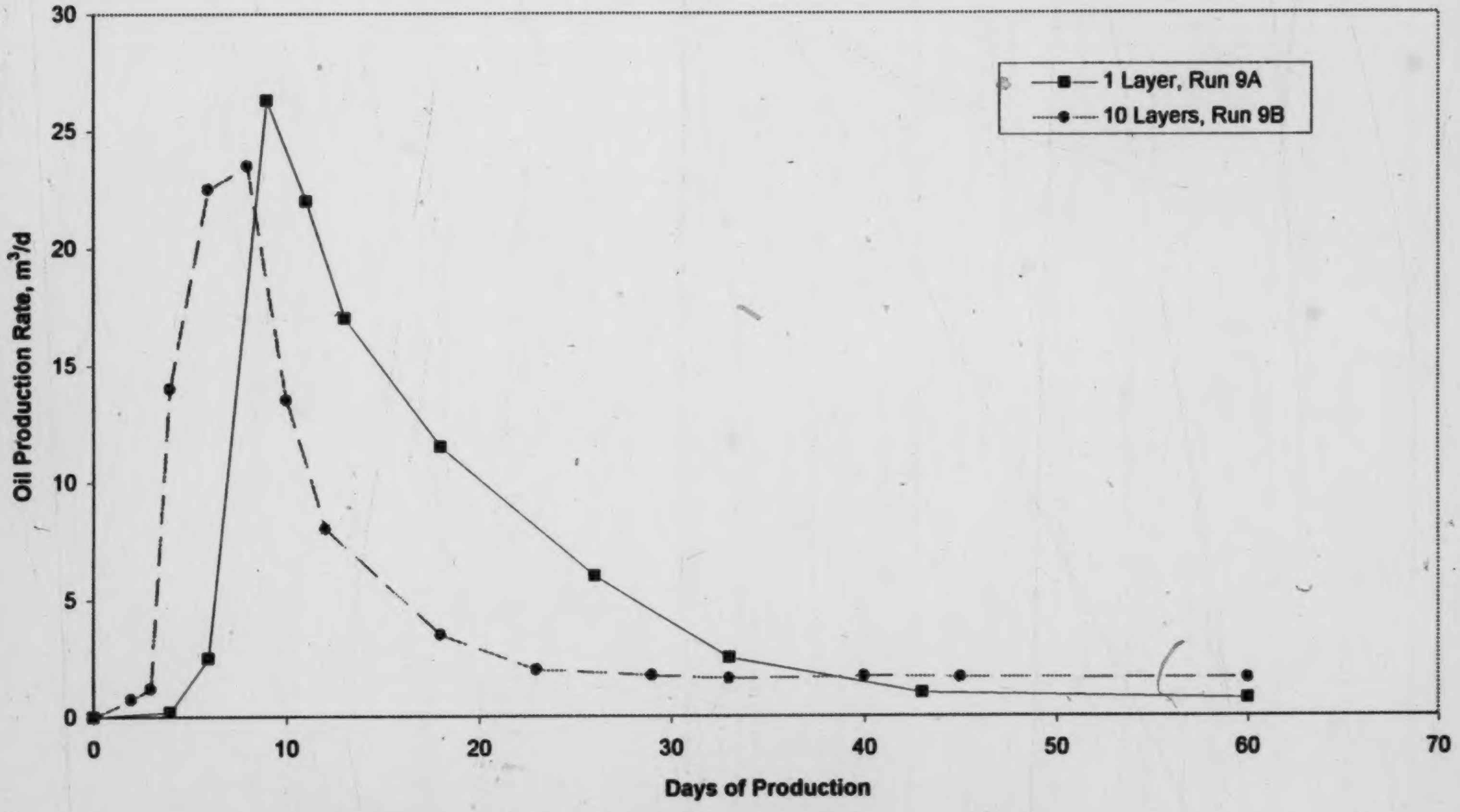

Figure 12.2.3.2a: RUN NO.'s 9A and 9B oil production for Sw = 0.50, injection rate = 200 m^3/d, slug size = 7000 m^3, 1 and 10 layers

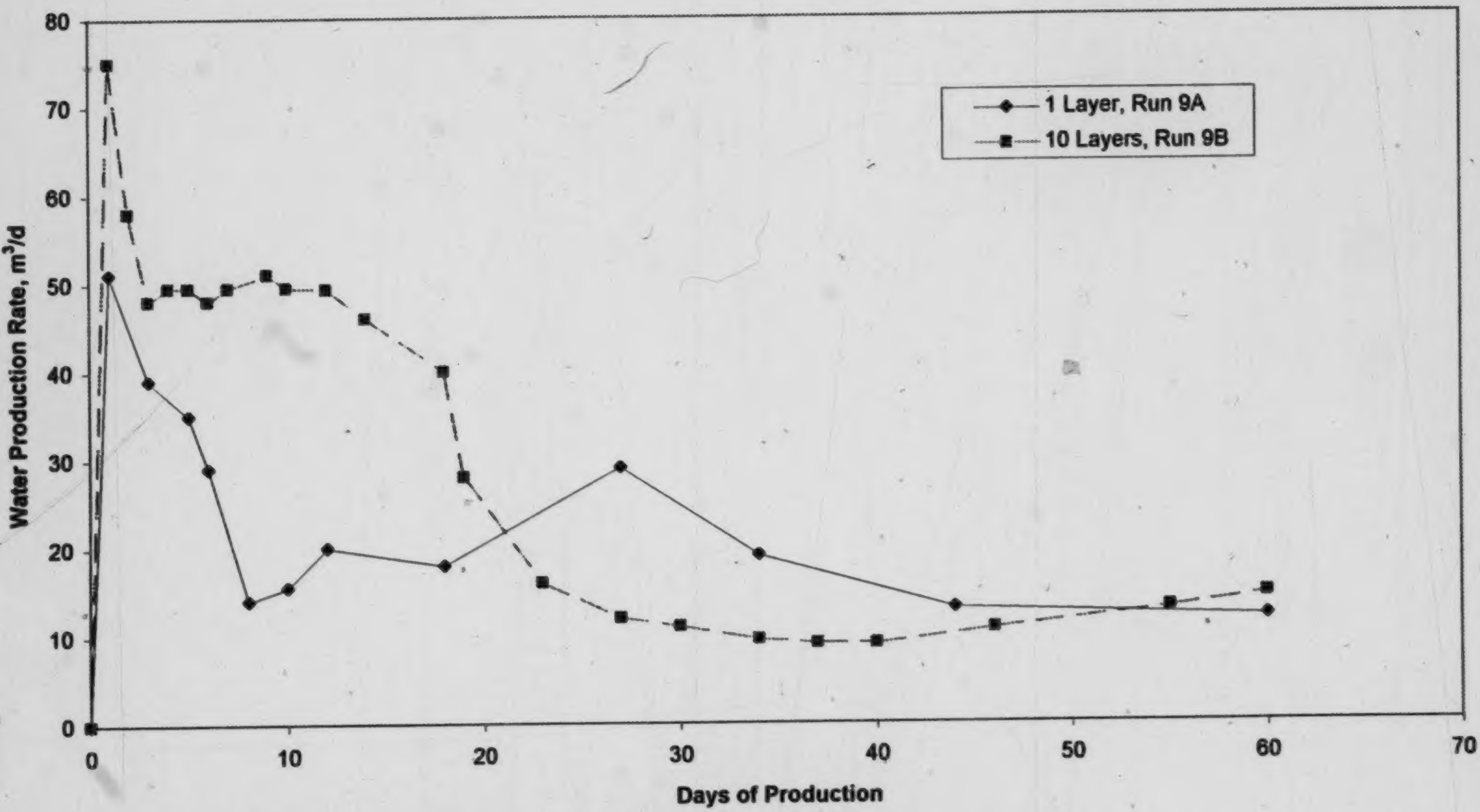

Figure 12.2.3.2b: RUN NO.'s 9A and 9B water production for Sw = 0.50, injection rate = 200 m^3/d, slug size = 7000 m^3, 1 and 10 layers

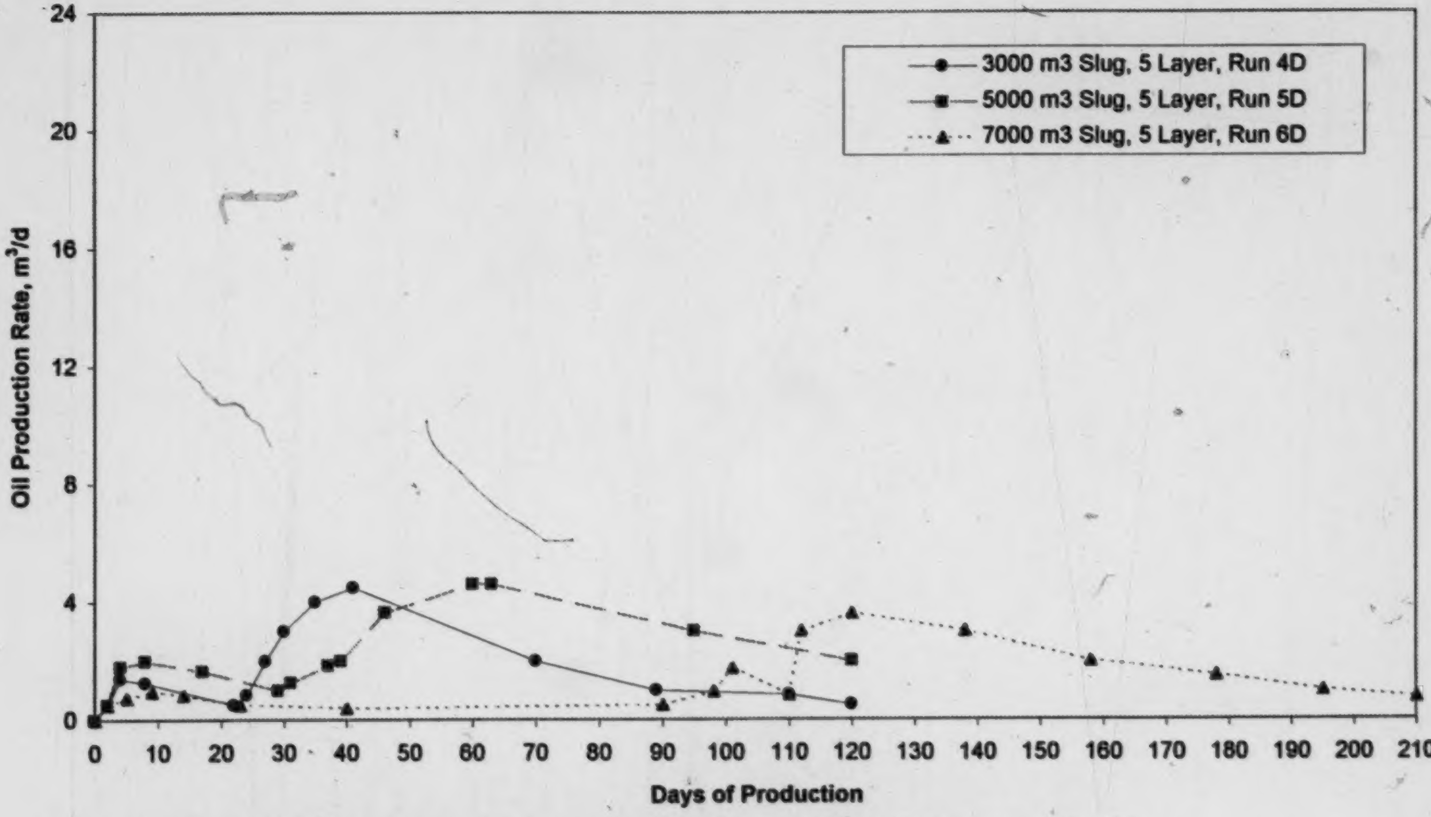

Figure 12.2.5.2a; RUN NO.'s 4D,5D, and 6D oil production for Sw = 0.50, injection rate = 110 m^3/d, slug size = 3000, 5000, and 7000 m^3, 5 layers, 15 rings

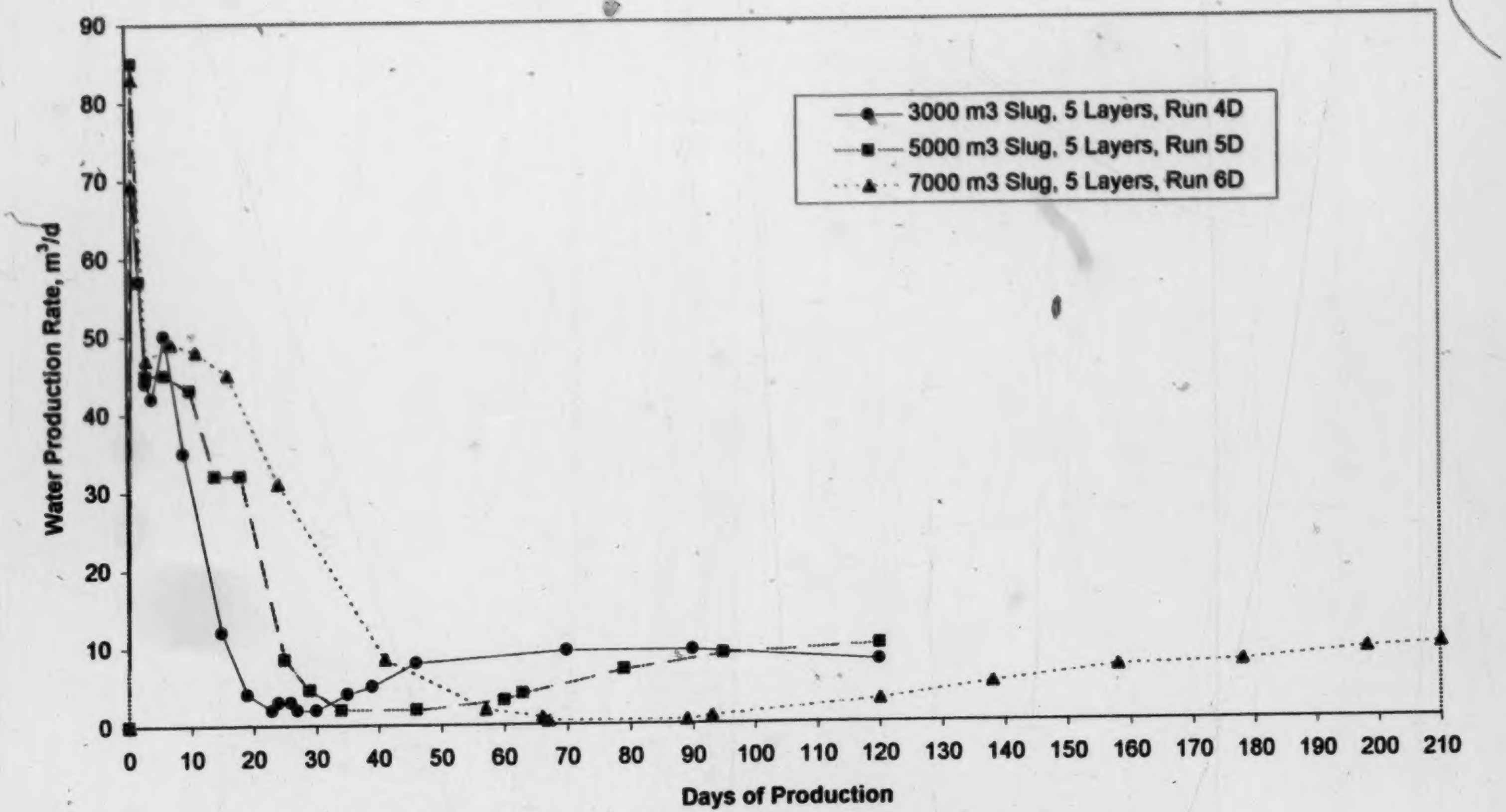

Figure 12.2.5.2b: RUN NO.'s 4D,5D, and 6D water production for Sw = 0.50, injection rate = 110 m^3/d, slug size = 3000, 5000, and 7000 m^3, 5 layers, 15 rings

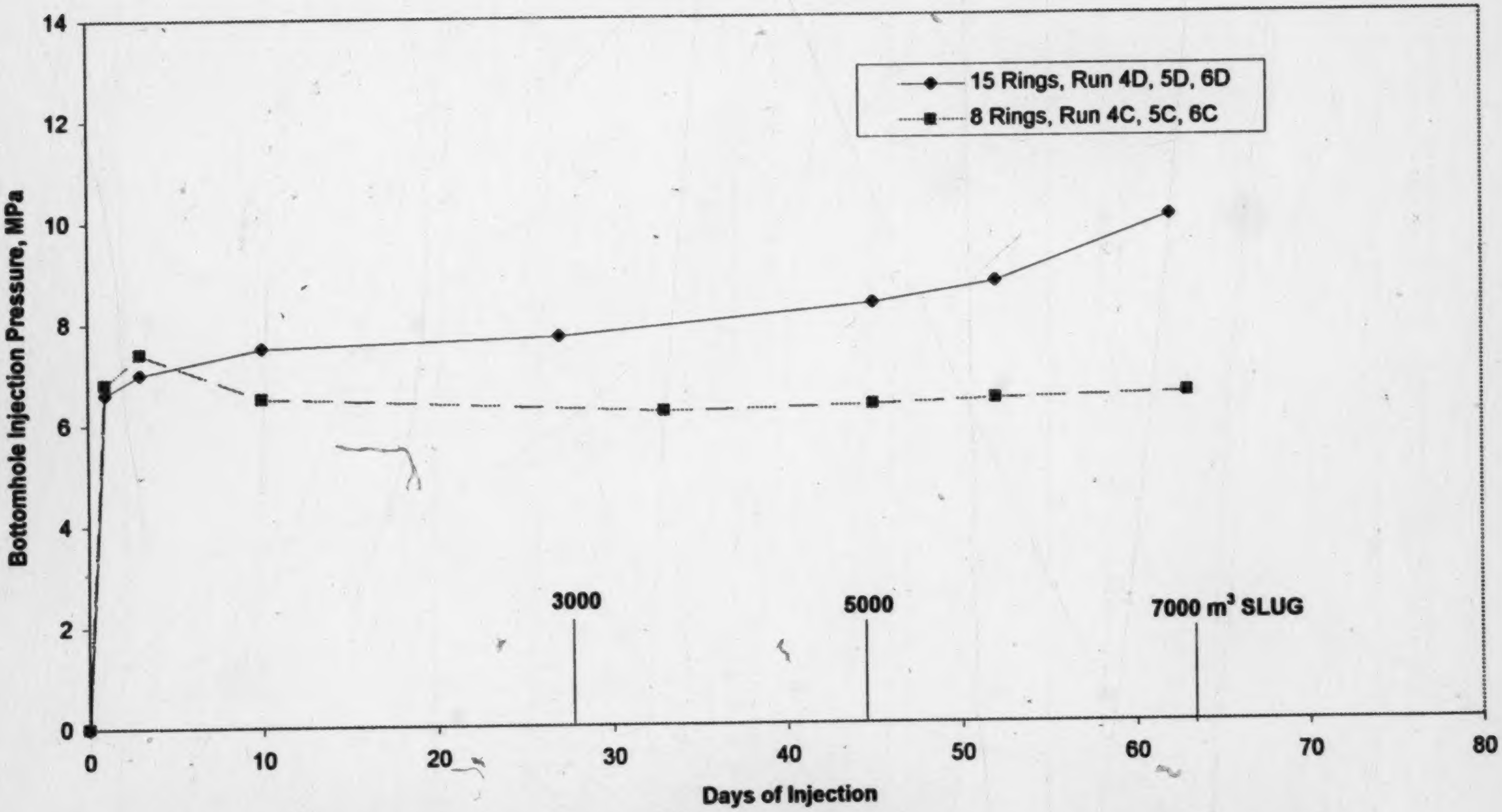

Figure 12.2.5.1: RUN NO.'s 4D,4D,5C,5D,6C, and 6D bottomhole injection pressure for Sw = 0.50, injection rate = 110 m^3/d, slug size = 3000, 5000, and 7000 m^3, 8 and 15 rings, 5 layers

Changing the grid size (geometric spacing plus equal-volume) appears to have made the model more sensitive to "cold oil banking". A pressure transient moves oil into zones of colder temperatures. This part of the oil bank is not produced. A good approximation for this "lost oil" is to calculate the amount of oil that has migrated into the colder zones by assuming 16% is ultimately recovered. A recovery factor of 16% is based on predicted recovery from a single well modeled over a nine-year producing life or by using Figure 11.1.2 and assuming the oil saturation will decrease from 60% to 30% during steam injection (as a steamflood) but will resaturate to 50% as the production temperature reduces from 320 °C to 100 °C (as a cylic drawdown). The cold oil banking was not considered for the geometric progression grids because the permeability curves were designed to compensate for lost oil. The grids are much smaller for the 15-ring case runs, and therefore have much higher transmissibilities. Also, pressures and oil saturations are higher. Calculating the actual volume corresponding to the cold oil bank, reveals that an eight-ring grid system simulates the most lost oil. in summary, a 15-ring case run may produce more oil than an 8-ring trial with the same injection rate and slug size (see Figure 12.2.5.3, lost oil).

Lost oil was estimated by calculating the extra heat in the subsequent gridblock past the steam front as a volume at steam temperatures, then taking 16% of the heated oil in that volume.

a) Slug Size of 3,000 m^3

For a slug size of 3,000 m^3, it appears that a finer definition of the areal extent of the reservoir leads to less oil production (Runs 4C and 4D, Table 12.1.1). In the eight-ring case run, the temperature front at the end of the first injection cycle has advanced to a radius of 26.0 m while in the fifteen-ring trial, the temperature front moves outward to a radius of 21.0 m. Due to decrease in the heated volume, a smaller cold oil bank forms and more oil remains in the reservoir. Overall, there is less oil, water, and "gas" produced in a fifteen-ring grid than in the eight-ring system.

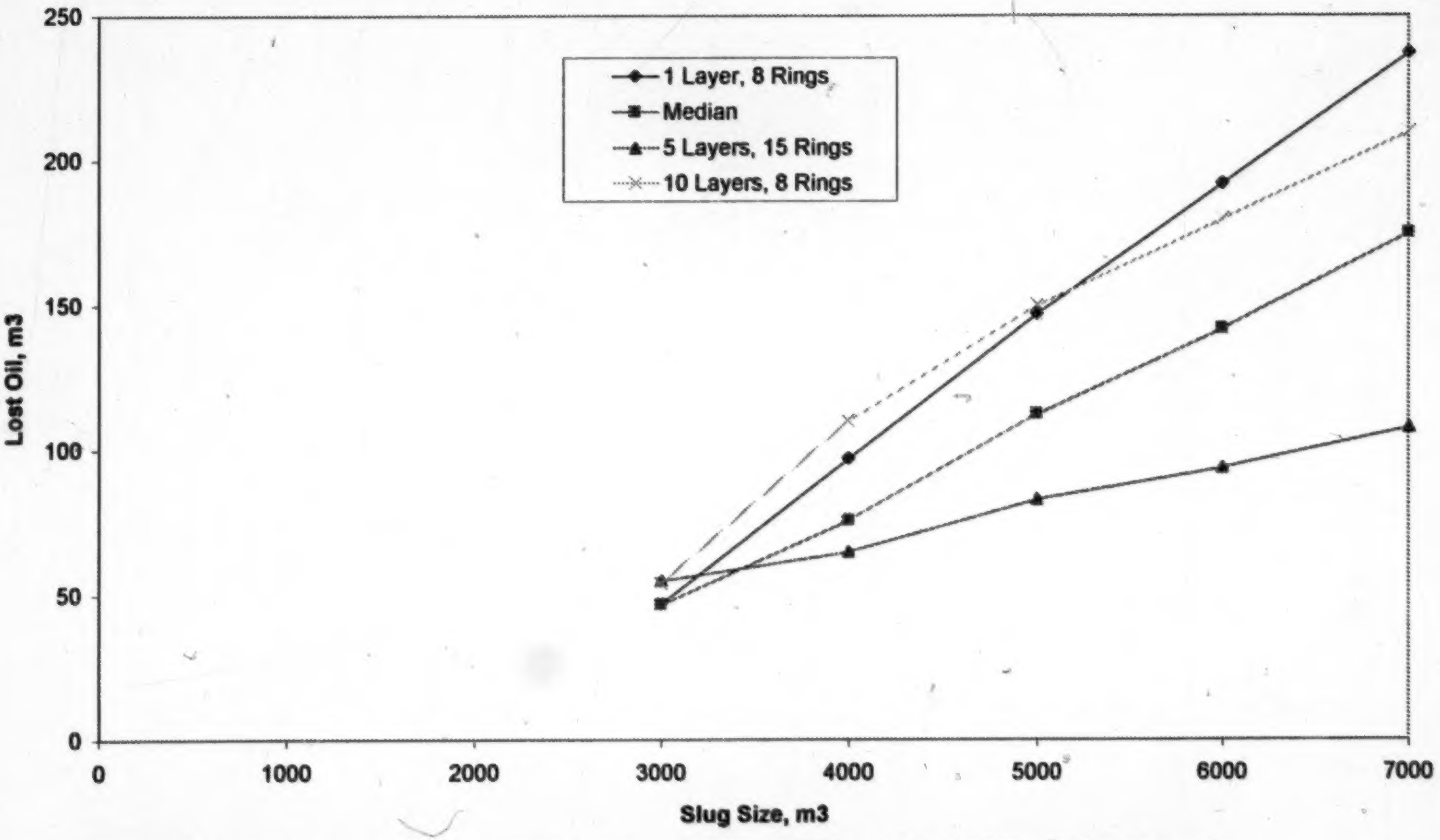

Figure 12.2.5.3: Effect on lost oil by varying layer number and grid size using 110-200 m^3/d injection rates

b) Slug Size of 5,000 m^3

The sensitivity runs for cases 5C and 5D are given in Table 12.1.1. The heat front has moved out a total of 30 meters into the next ring (i.e., the outer radius of ring 7 compared to a total of 21 m^3, the outer boundary of ring 6 for the 3,000 m^3 slug), in the 15-ring case run. Refer to the ring spacing shown in Figure 12.1.1.

For the 8-ring trial, heat is limited to the fifth ring having a 26-m outer radius. The heat front has advanced into the same ring as for the 3,000 m^3 slug size. More water, oil, and "gas" is produced in the 15-ring case (see Figure 12.2.5.2a). In other words, the cold oil bank which developed in the seventh ring of the 15-ring model (i.e., ring with 30-m outer radius), is now being produced. The effect of oil banking is reduced.

c) Slug Size of 7,000 m^3

The 7,000 m^3 slug size test for the 15-ring system should have produced more oil than for the 8-ring system but the opposite occurred (Runs 6B and 6D, Table 12.1.1). The reverse trend is likely due to the oil front moving so far away from the well that it was impossible to produce it within a reasonable time (see Figure 12.2.5.2a). Again, there is less "cold oil banking" than in the 8-ring system. Despite the availability of extra oil production, it was too distant from the well to be recovered within 200 operational days.

12.2.6 Conclusions on Layering and Ring Size

1. In general, whether one uses more formation layers or more radial grids to define the physical problem, the trend of slug sizes and injection rates are quite similar to that given by the single-layer model runs. This generalization applies to cumulative production numbers only. But for specific engineering purposes, where daily production rates for history matching are required, one should use a five-layer model to more accurately show the timing of peak production rates and not just final cumulatives.

2. When using geometric progression as the basis for ring geometry in a radial model, having more vertical layers increases oil production for low injection rates or small slug sizes given that steam override leaves more oil near the wellbore, above and below the steam chest. For higher injection rates and corresponding higher pressures, and larger slug sizes, less oil is produced. Despite further advancement of the heat front, there exists a larger volume near-wellbore at residual oil saturation. In order for oil production to commence, this residual oil saturation zone must be resaturated with the oil initially pushed away from the wellbore. This delays the time of initial oil production into the wellbore.

3. Converting from a system of geometric progression to one of equal volume requires an increase in the number of radial grids. The additional grids do not necessarily improve recovery, due to a delay in initial oil production. Extra grid blocks are necessary for multi-cycle steam stimulation, assuming the effect of cold oil banking will become more significant after the first few cycles (larger outer grid blocks will be slowly heated with time). The model's permeability curves are not intended to control oil banking. Switching to a finer radial grid system or a coordinate square grid system may allow for use of lab generated permeability curves but dilation and compaction features would also have to be applied.

12.3 Building the Correlation Curves

Table 12.1.1 contains a summary of all the numerical simulator runs performed with an initial S_w of 0.5. The cases labeled 1A, 2A, 5A, and 8A, cover injection rates of 66.7, 110, and 200 m^3/d, at slug sizes of 3,000 or 5,000 m^3. These model runs supply data points for the correlation curves at a fixed water saturation value on the x-axis.

12.3.1 Varying Initial Water Saturation

Further values were required below an initial water saturation (S_{wi}) of 0.5 to generate the curves. An additional six cases were tested for equal to S_{wi} of 0.35, 0.40, and 0.45 at the three different injection rates, mainly at the 5,000 m^3 slug size (see Table 12.3.1.1). Two runs were performed at the 3,000 m^3 slug size. The 7,000 m^3 slug size was not further analyzed because the reservoir would over-pressurize at the lower initial water saturations and the run would have to be terminated. The injection pressure profiles for the various initial water saturations are shown in Figure 12.3.1.1 Excessive pressures in the numerical model become noticeable as Swi approaches 0.40. Production results for the various case runs are plotted in Figures 12.3.1.2 to 12.3.1.4.

12.3.2 Determining Optimum Slug Size for the Correlation Curves

An optimum rate and slug size for a single-well cyclic steam injection program are normally determined through graphical means (Figures 12.3.2.1 to 12.3.2.3). Plots were created for cumulative steam-to-oil ratios (SOR) and cumulative oil production versus slug size for injection rates of 66.7, 110, and 200 m^3/d, respectively. For all three rates, the optimum slug size is in the order of 5,000 m^3. This finding partly explains why data points selected for the correlation curves incorporate many of the data points representing the 5,000 m^3 slug size. Well performance is summarized in Figure 12.3.2.4, which verifies that a change in layer or ring complement does not render a new optimum slug size. Heat injected versus slug size is also plotted on this graph, showing that oil produced is not a direct function of heat injected. Figure 12.3.2.5 is a transformation of Figure 12.3.2.4 plotted with the amount of heat injected on the secondary y-axis.

12.3.3 Plotting the Correlation Curves

Drawing on the one-layer oil production data at various water saturations and a 5,000 m^3 slug size, a set of correlation curves were developed for initial water saturation, or mobile water saturation, versus oil production (Figure 12.3.3.1). The y-axis is denoted "Oil Production Capability Index" (OPCI) and the units are m^3 oil per operating day per meter of perforation.

Table 12.3.1.1

Operating Conditions-Single Layer Model: Varying Initial Water Saturation
Sensitivities for Runs 5A,7A, and 1A

Run No.	Sw	Injection Rate m3/d	Time Injection days	Slug Size m3	Bottomhole Steam Quality	Bottomhole Inj Pressure MPa	Res Press End Inj MPa	Production Fluid Rate m3/d	No. of Producing days	Water Production m3	Oil Production m3	Steam Oil Ratio
13	0.50	110	45.5	5000	0.425	11.6	6.33	40	60	812	344	14.5
14	0.45	110	45.5	5000	0.425	11.6	8.02	40	60	768	400	12.7
15	0.40	110	45.5	5000	0.425	11.6	11.21	40	60	869	529	9.7
16	0.35	110 *(70)	45.5	5000 *(3200)	0.425	11.6	14	40	60	668	257	12.5
17	0.50	200	25	5000	0.5	12	8.29	40	60	947	410	12.2
18	0.45	200	25	5000	0.5	12	10.4	40	60	943	480	10.4
19	0.40	200 *(120)	25	5000 *(3000)	0.5	12	14	40	60	679	207	14.6
20	0.50	66.7	45	3000	0.2	9.2	6.15	40	60	673	21	143
21	0.45	66.7	45	3000	0.2	9.2	8.37	40	60	615	50	60

* The reservoir could not take the indicated rate at a limiting bottomhole pressure of 14 MPa, so these are maximum rates and slug sizes for the time of injection.

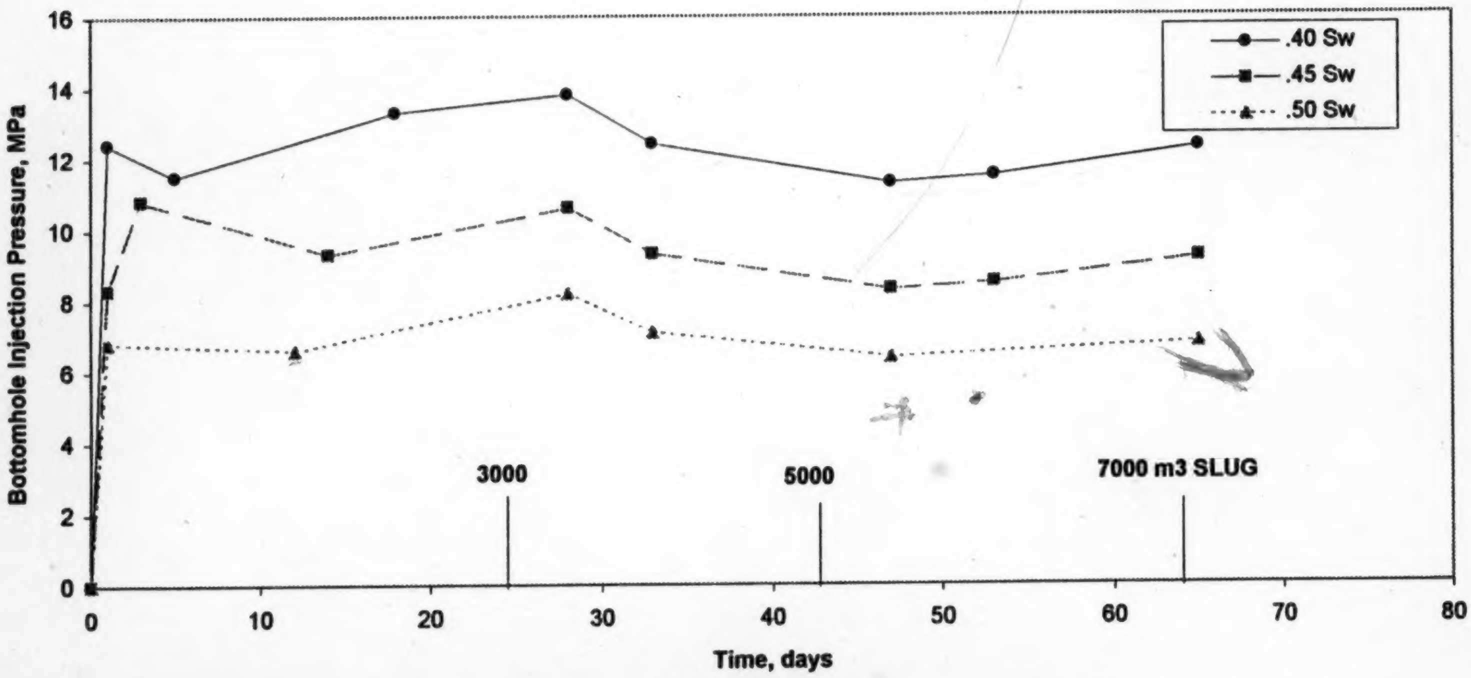

Figure 12.3.1.1: RUN NO.'s 13,14, and 15 Bottomhole injection pressure for Sw = 0.40,0.45, and 0.50, injection rate = 110.0 m^3/d, slug sizes = 3000, 5000, and 7000 m^3

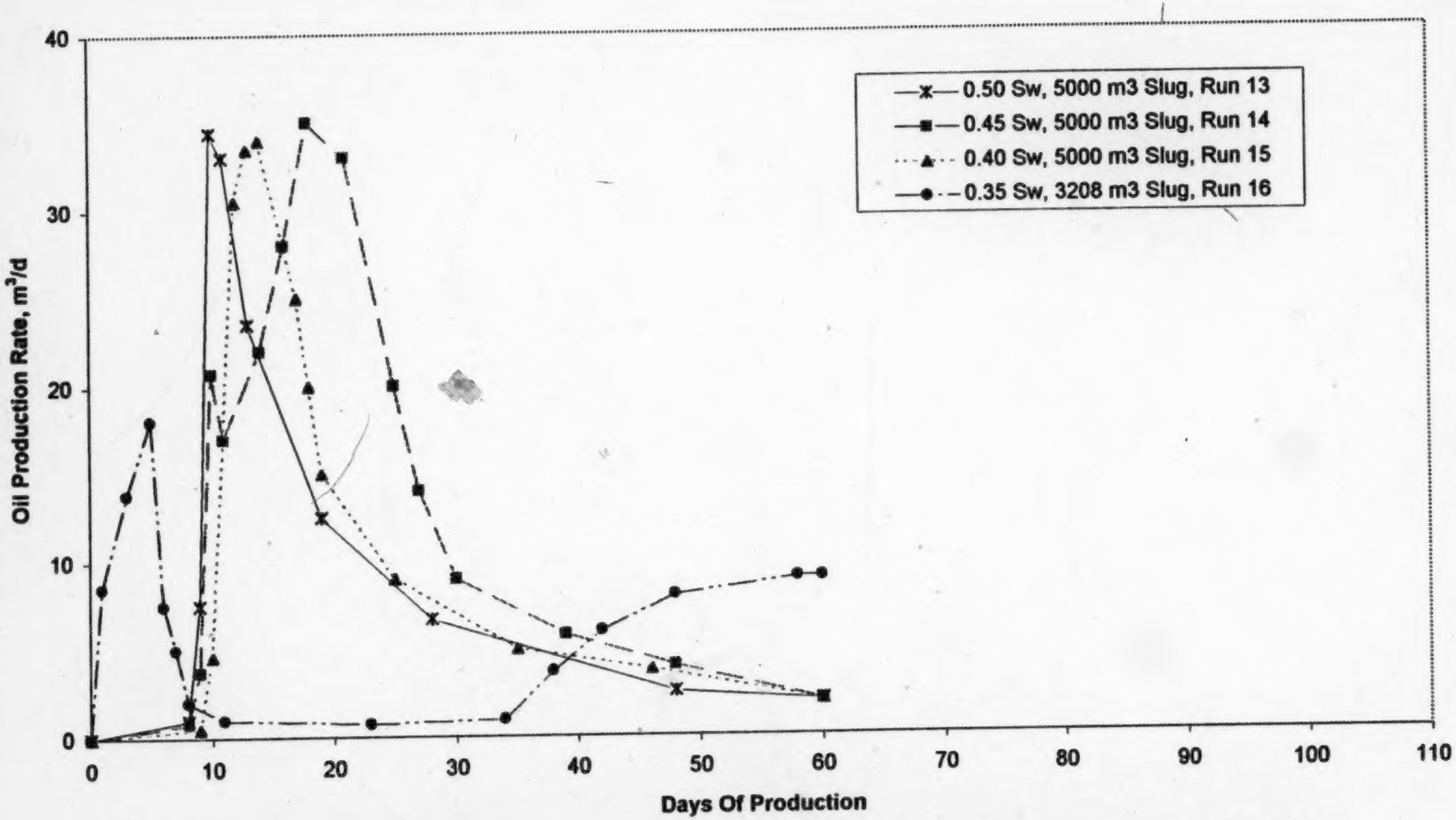

Figure 12.3.1.2: RUN NO.'s 13,14, 15, and 16 oil production for Sw = 0.35,0.40,0.45, and 0.50, injection rate = 110.0 m^3/d, slug sizes = 3000 or 5000 m^3

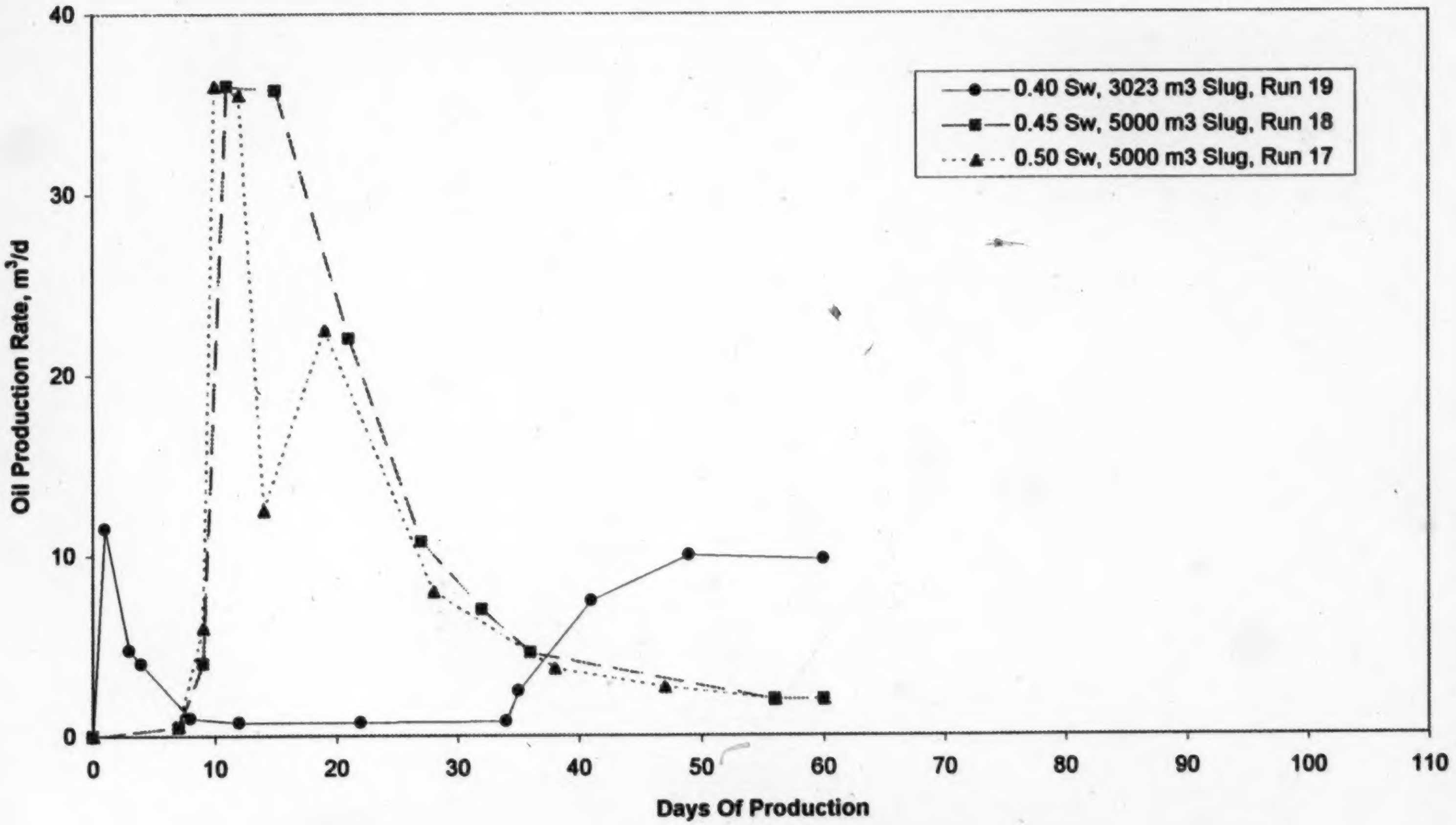

Figure 12.3.1.3: RUN NO.'s 17,18, and 19 oil production for Sw = 0.40,0.45, and 0.50, injection rate = 200.0 m^3/d, slug sizes = 3000 or 5000 m^3

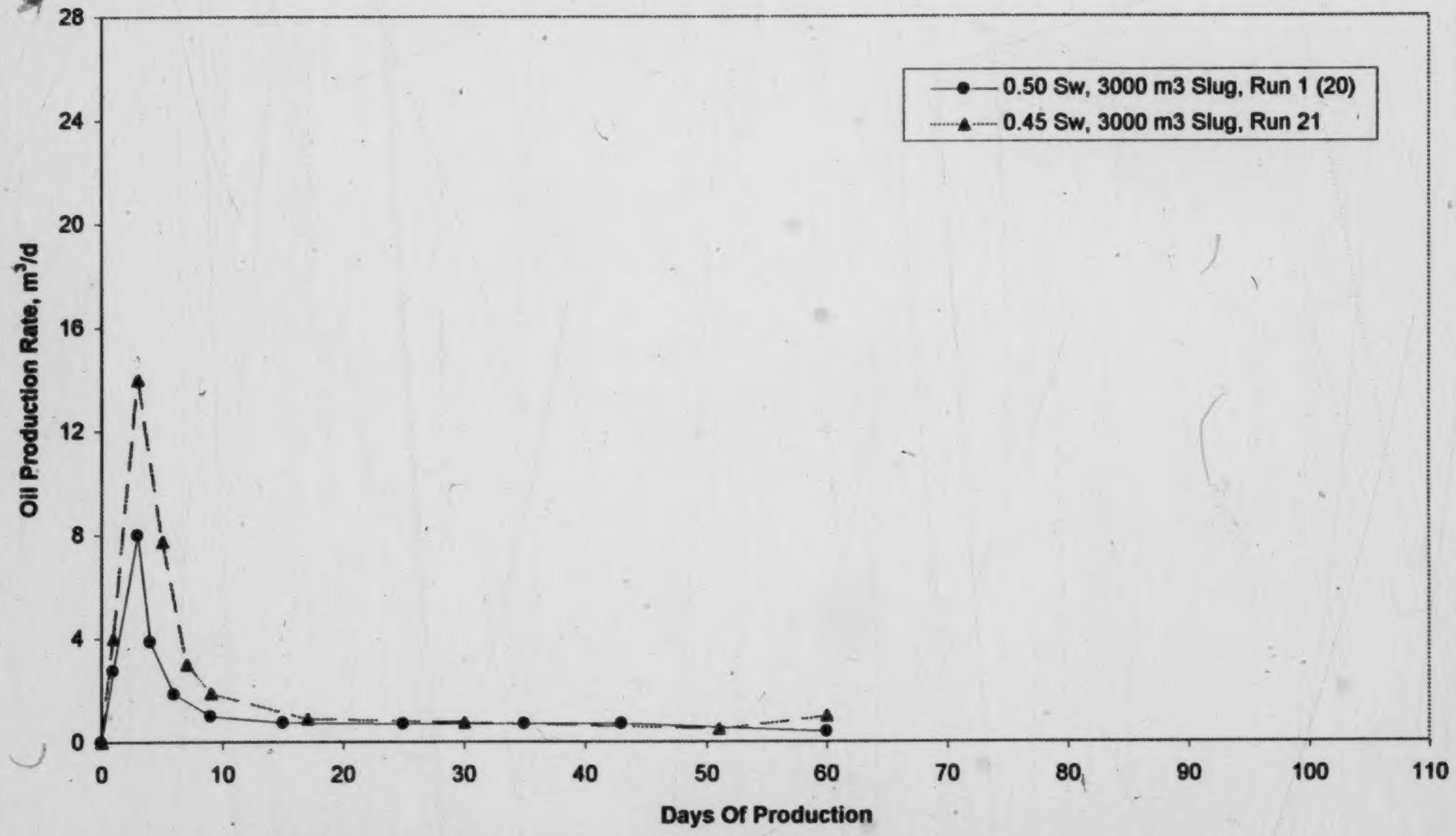

Figure 12.3.1.4: RUN NO.'s 1A (20), and 21 oil production for Sw = 0.45, and 0.50, injection rate = 66.7 m^3/d, slug size = 3000 m^3

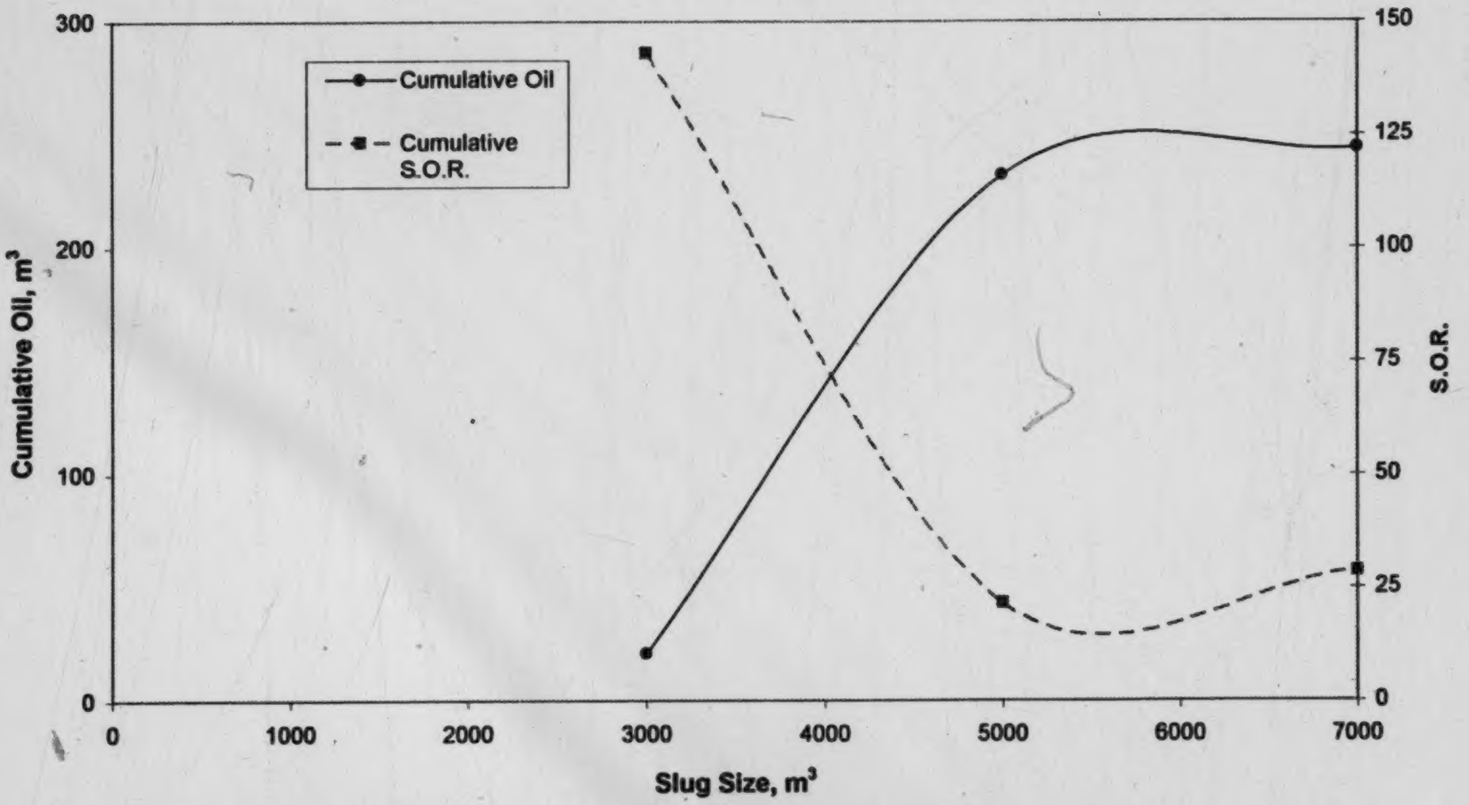

Figure 12.3.2.1: RUN NO.'s 1A,2A, and 3A, optimization of well performance at 60 days production, Sw = 0.50, injection rate = 66.7 m^3/d, slug sizes = 3000, 5000, and 7000 m^3

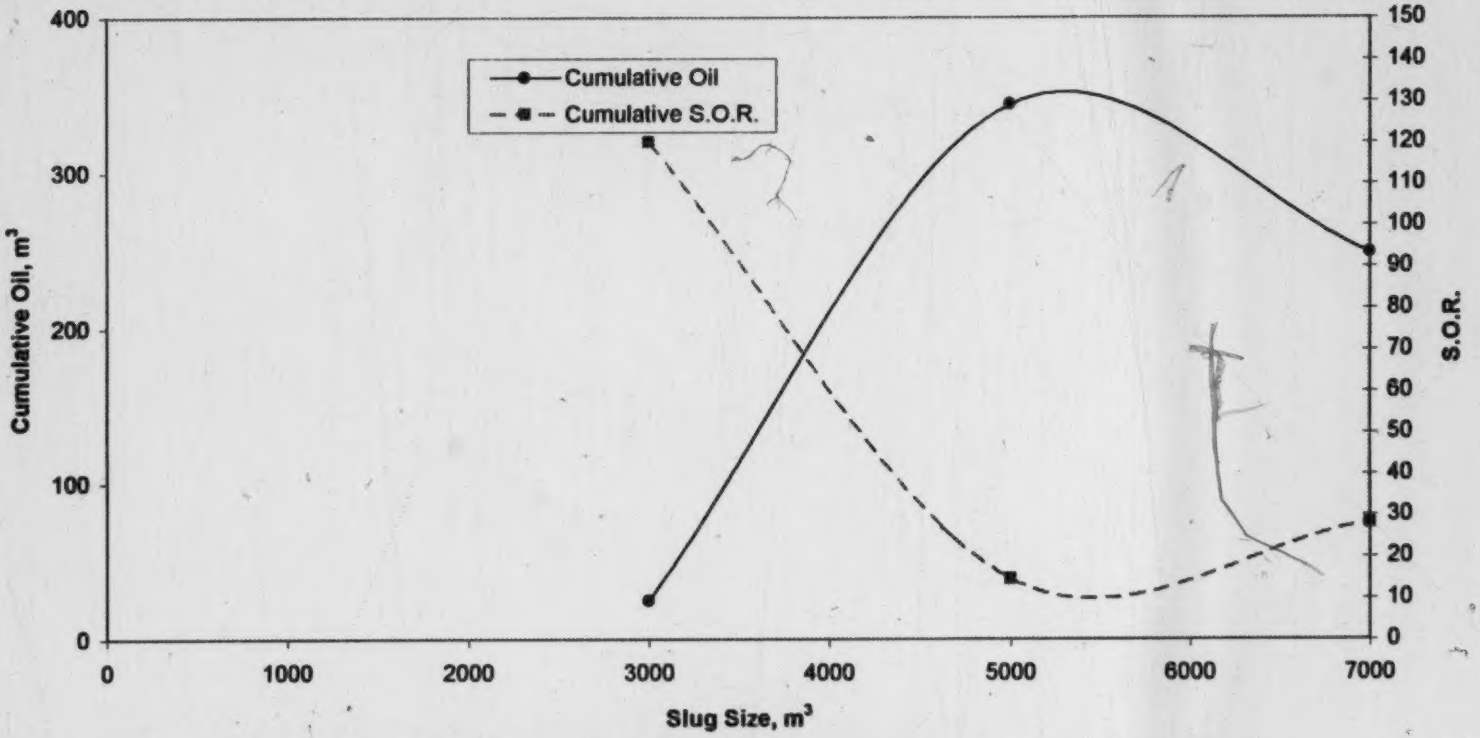

Figure 12.3.2.2: RUN NO.'s 4A,5A, and 6A, optimization of well performance at 60 days production, Sw = 0.50, injection rate = 110 m^3/d, slug sizes = 3000, 5000, and 7000 m^3

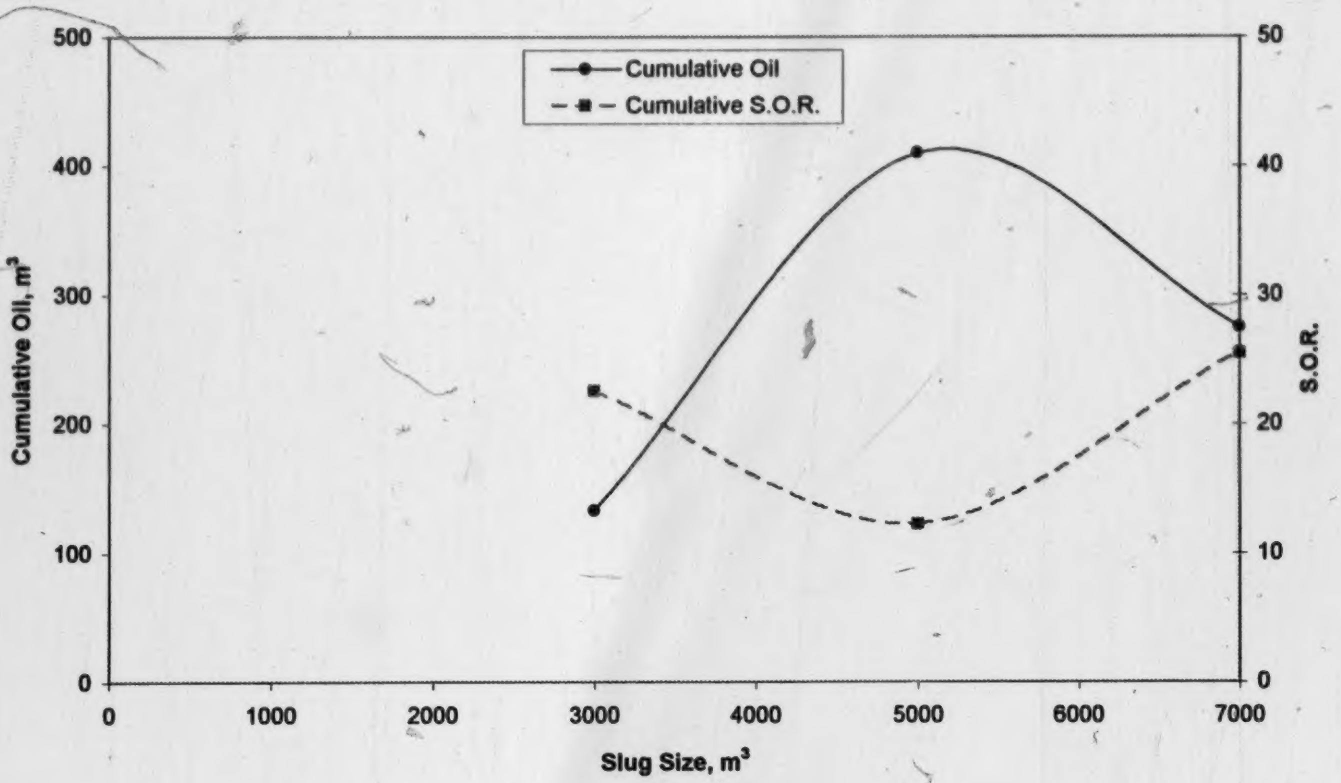

Figure 12.3.2.3: RUN NO.'s 7A,8A, and 9A, optimization of well performance at 60 days production, Sw = 0.50, injection rate = 200 m^3/d, slug sizes = 3000, 5000, and 7000 m^3

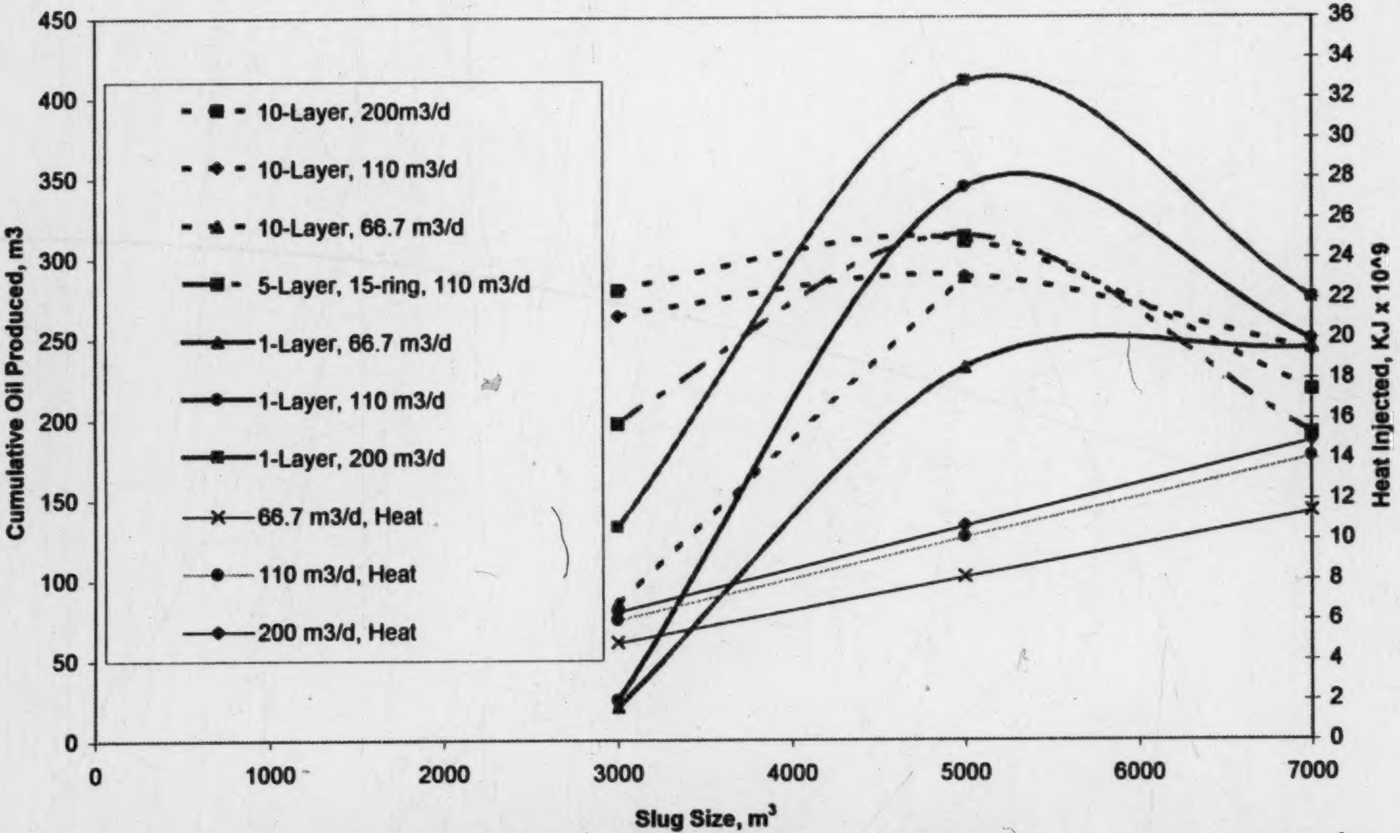

Figure 12.3.2.4: RUN NO.'s 1A to 9B Summary of well performance, Sw = 0.50, injection rate = 66.7, 110, and 200 m^3/d, slug size = 3000, 5000, and 7000 m^3, 8 and 15 rings, 1,5, and 10 layers

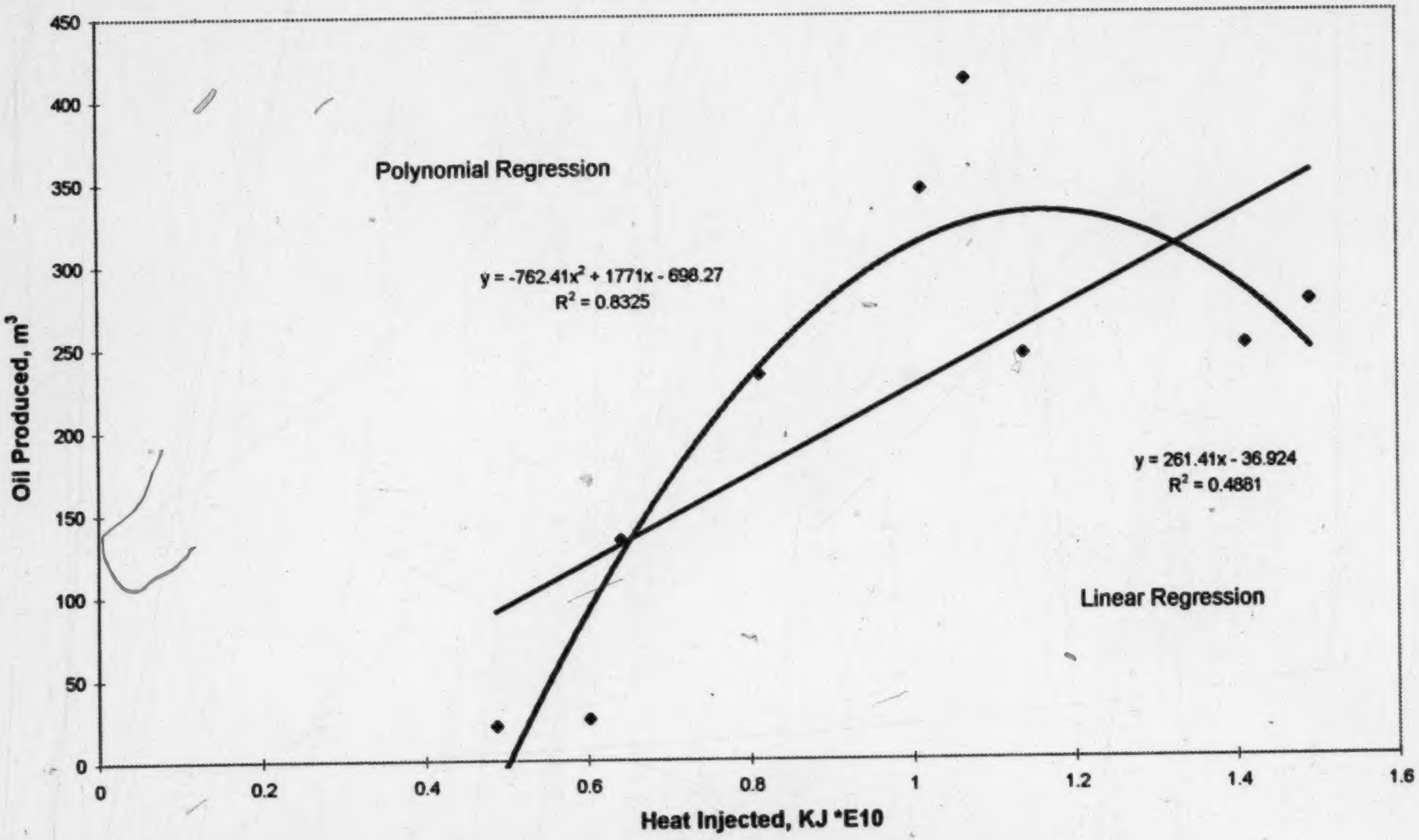

Figure 12.3.2.5: RUN NO.s 1A to 9A heat injected vs oil produced, Sw = 0.5, injection rate = 66.7, 110, and 200 m3/d, slug size = 3000, 5000, 7000 m3, 1 layer, 8 rings

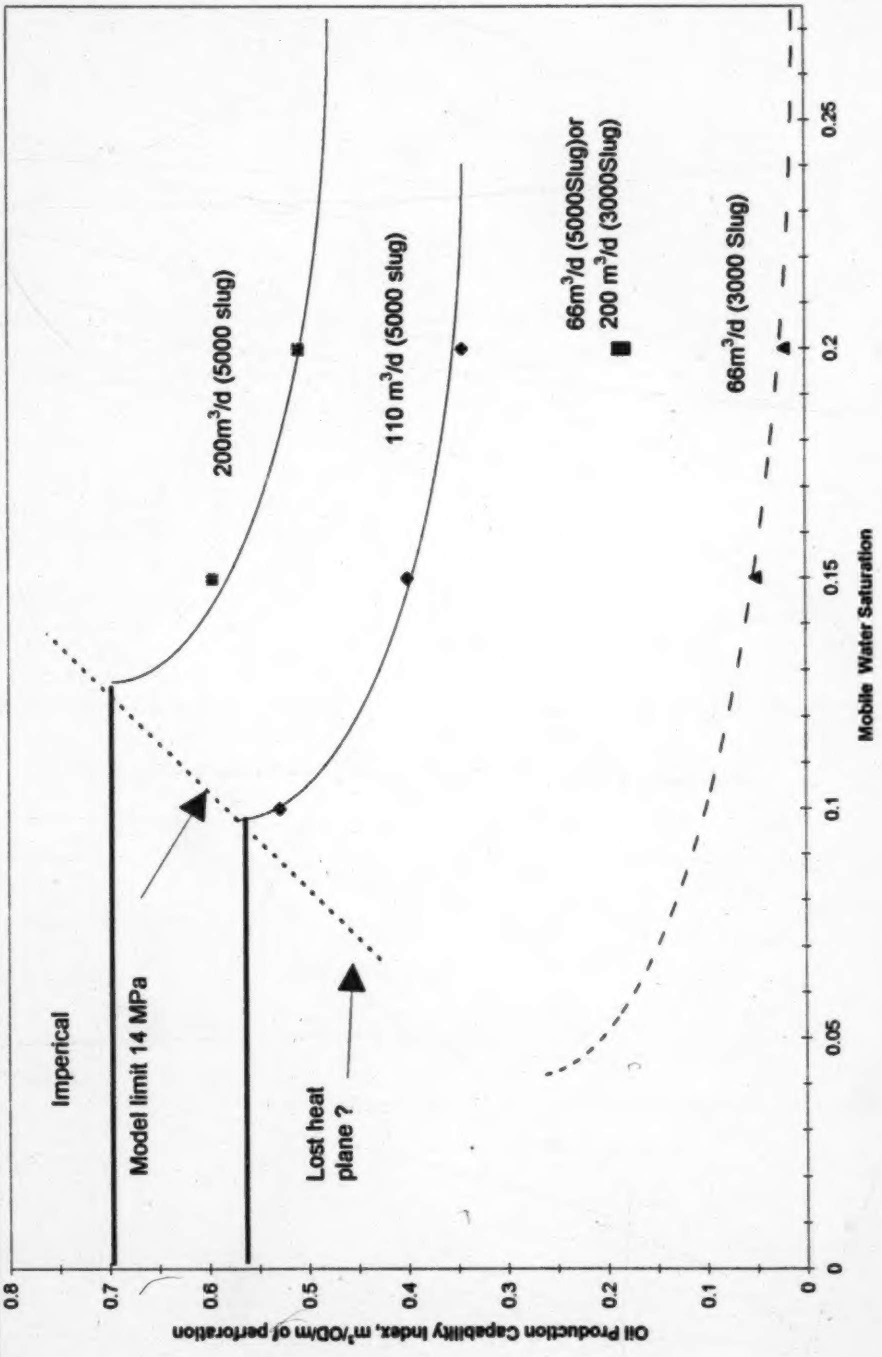

Figure 12.3.3.1: Correlation curves for PHOP 1st cycle steam stimulation

Total operating days includes injection plus producing days, omitting shut-in days. The index is normalized by operating days to account for slug sizes other than 5,000 m^3/d.

The full 9.5 meters of the pay zone were perforated in the single-layer numerical model. The perforation interval was chosen for proper estimation of bitumen production per meter of thermal net pay.

The origin of the x-axis is either 0.0 mobile water saturation, or the S_{wir} of the reservoir under investigation (Figure 12.3.3.2). For the Wabiskaw Formation, S_{wir} is 0.30; for the McMurray formation, S_{wir} equals 0.15; and for the Wabiskaw-McMurray transition zone, S_{wir} is 0.20.

End-points were extrapolated in both directions using a French Curve. The fact that oil production is an exponential function of the mobile water saturation of an oil sands reservoir is not surprising as a higher initial oil saturation should logically produce more oil if the residual oil saturation remains constant or is lowered. At high mobile water saturations, the change in oil production with a small change in mobile water saturation would be small. Once the plot is completed, generalizations can be made from the curves concerning performance production of an oil sands reservoir.

The curves show that a reservoir with a mobile water saturation between 10 and 12% produces the maximum amount of oil. For mobile water saturations greater than 20% there is up to 50% less oil. At a 110 m^3/d injection rate into a formation having mobile water saturations less than 10%, extra oil is not produced when rate is increased, signifying a maximum (plateau) has been reached. The same is true for a rate of 200 m^3/d, although the maximum OPCI is higher, which will ultimately yield a higher cumulative production. The numerical model could not be used to predict production outside the range of the curves because of over-pressurization.

According to the correlation curves, a higher injection rate simply produces more oil. There appears to be an upper limit to the injection rates and a lower limit to the mobile water saturation at the top left corner of the plot. The term assigned to this region is "fracture plane". The best explanation for the flattening of the curves is that, with

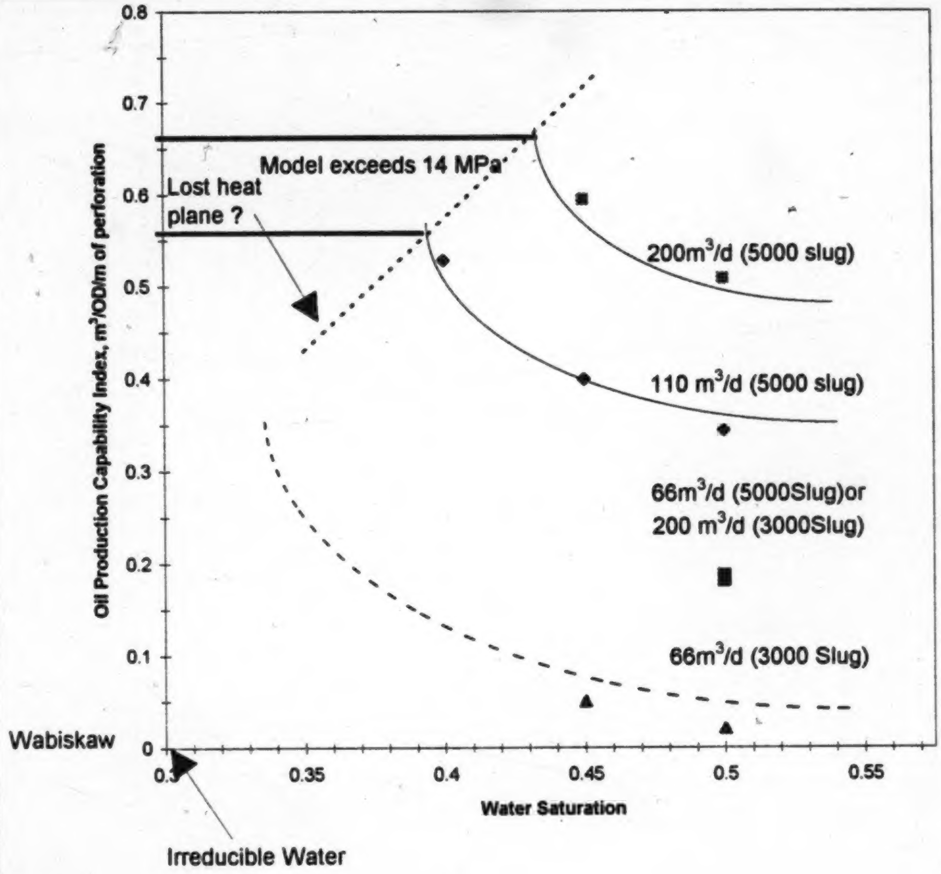

Mobile Water	0.0	0.1	0.2
Wabiskaw-McMurray Well (11-10)	0.2	0.3	0.4
McMurray Well (10-34)	0.15	0.25	0.35

Figure 12.3.3.2: Correlation curves for PHOP 1st cycle steam stimulation

increased injection rates, significant fracturing has occurred outside the reservoir or at some distance from the wellbore and a fraction of the injected heat is lost, either temporarily or permanently. This fracture plane could not be moved upwards, since, along the plane, the correlation curves become nearly vertical. Logically, there must be a maximum. For projects near Fort McMurray, one could move the fracture plane downwards for the McMurray Formation, which, could correspond to more lost steam (see section 15.2.3) where it is shown a history match can be made if it is assumed half of the injected steam rate has been lost outside the productive reservoir). This plane could move upwards at the Esso Cold Lake Clearwater projects where net pay is much thicker and cleaner, with less fracture height growth, or steam loss, outside the oil sands formation. It is important to remember that the maximum for these curves has been drawn arbitrarily but the critical point or maximum value for the fracture plane has been proven by field data.

It should also be noted that the same OPCI is observed for both a 200 m^3/d-3,000 m^3 slug size and a 66.7 m^3/d-5,000 m^3 slug size. This does not mean that the same amount of oil is produced as the total operating days are different. Furthermore, injecting a 3,000 m^3 slug size into the Wabiskaw Formation at 66.7 m^3/d yields negligible oil. The latter is actually a history match of the first cycle of PHOP well IP6 where only 45 m^3 bitumen was produced. The correlation curves predicted 33 m^3 bitumen for the same number of operating days.

Various scenarios for constructing the correlation curves were investigated and tried, such as considering oil production versus heat injected, but history matchs could not be consistently made, probably because optimum steam slug sizes were not always injected (see Figures 12.3.2.1 to 12.3.2.4). Using producing days only to predict oil production did not work because differences in injected slug size volumes were not accounted for. For the correlation curves to account for various rates and slug sizes without using total operating days, different sets of curves for each slug size would have to be constructed, making the analysis more complex. It is not fully understood why using operating days instead of producing days gives better results.

The prediction for the first month of production is considered inaccurate but can be improved if only production days are used here instead of operating days.

Chapter 13

First-Cycle Prediction of Bitumen Production

With the correlation curves generated in the previous chapter in hand, a methodology for history-matching or predicting first-cycle bitumen production at the PHOP pilot from these curves can now be developed as the next step in the correlation procedure. An example calculation for well IP2 is presented here. The remainder of the IP wells are then history-matched. Comments are made on selection of the net pay factor for the various IP wells. The predicted bitumen results and actual produced bitumen are tabulated while an interpretation is also provided concerning the significance of predicted bitumen production compared against actual production and/or the well injection history as the number of producing days may fall short of the expected producing time. An excellent history match of bitumen production was obtained, in particular, the aggregate of all the recovery from the IP wells as a group. Three other PHOP wells were also history-matched: 11-10, 10-34 and 11-21. These wells were completed in the Wabiskaw Formation, the transition zone between the Wabiskaw and McMurray, and the McMurray formations, respectively. The axis for water saturation (S_w) on the correlation curves had to be shifted to accommodate reservoirs having different character.

13.1 Step-by-Step Method for Estimating First Cycle Bitumen Production

To attain a history-match or prediction of first-cycle production the following step-wise procedure has been developed:

1. From each individual well description, obtain the perforation interval, m_{perf} (usually about 10 meters), and decide whether (a) there is oil sand above and below the perforations (to a maximum of 2 meters above and below); and (b) there are significant calcite or shale streaks within the production interval. The thickness of these impermeable indurations should be subtracted from the

perforation height to obtain a thermal net pay. A net pay factor between 1.0 and 1.4 is then determined from Figure 13.1.1 (to a maximum of 2 meters of oil sand above and 2 meters below the perforations). If there are two sets of perforations separated by five meters of shale or by a calcite streak, the reservoir layer with the lowest S_w would not be considered for this calculation as the steam would only enter the layer of highest S_w where fracturing is feasible (e.g. see IP1 reservoir description, Table 10.2.1). When the formation contains a calcite streak greater than 1 meter thickness, the steam will not fracture through this layer.

2. Obtain the average initial connate water saturation (S_{wc}) and irreducible water saturation (S_{wir}) for the interval under investigation, from log ***and*** core analyses including special core analysis, such as capillary pressure curves. The difference between S_{wc} and S_{wir} is the mobile water saturation, or mobility to steam injection.

3. Obtain an average steam injection rate CWE (Cold Water Equivalent) per day. This measurement is normally taken from orifice flow readings corrected to boiler feed pump volumes and feed tank gauges. Generally, for most reservoirs, a target rate is 150 -175 m^3/d. A rate less than 120 m^3/d fails to heat the reservoir sufficiently while a rate exceeding 175 m^3/d causes severe fracturing through which steam can escape from the formation. Steam lost to a thief zone may be invisible until possibly the third or fourth production cycle, its return signaled by a sudden decrease in the chloride content of the produced water, if at all.

4. Obtain a steam injection slug size CWE for the first cycle of injection. A typical range is 5,000 to 10,000 m^3. When not enough steam is injected, the

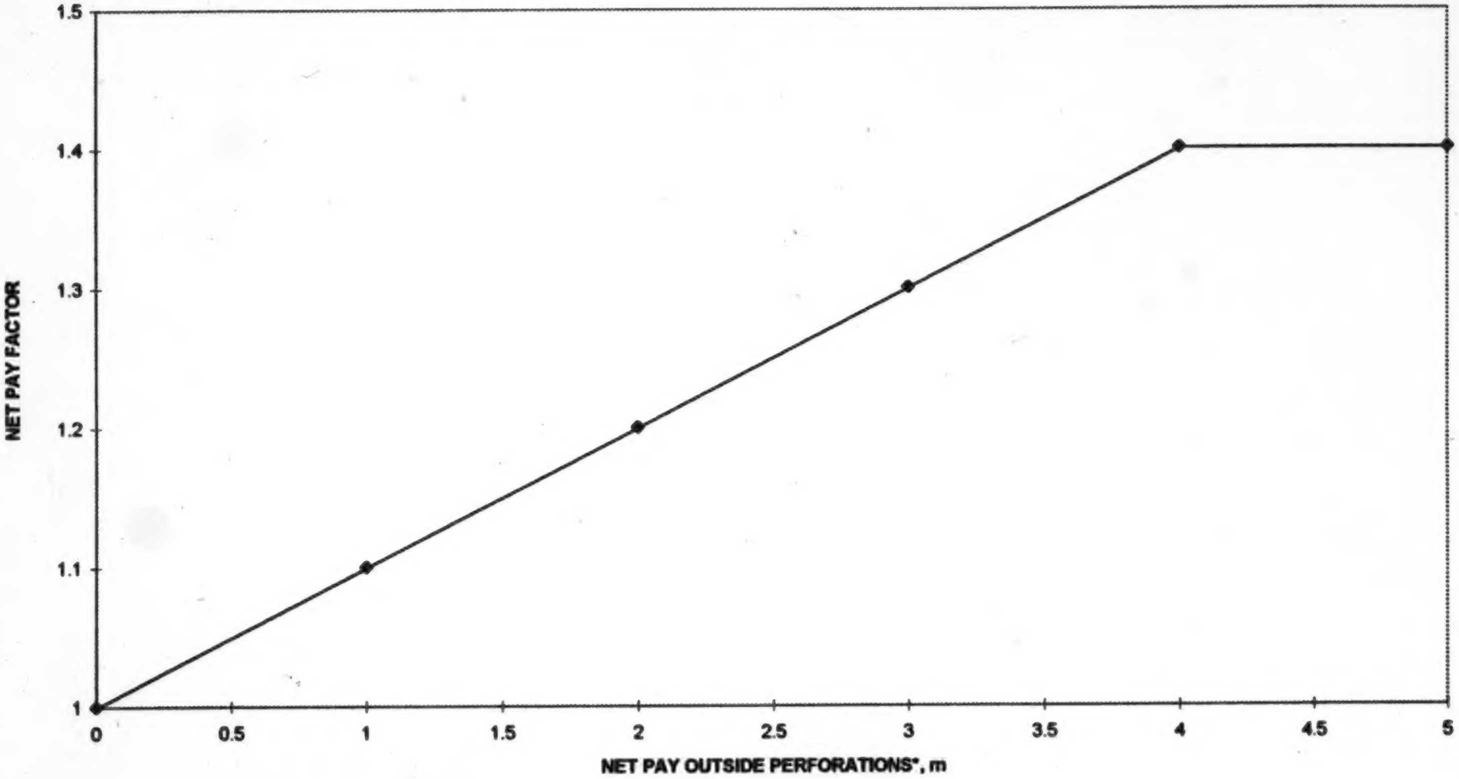

* overburden + underburden to maximum of 4m

Figure 13.1.1: Net pay factor to account for production of bitumen above and below perforations

well cools off too quickly and production drops. If too much steam is injected, the heat is placed too far from the well for the bitumen to flow back in a reasonable amount of time.

5. From the correlation curves (Figure 12.3.2.1), determine the Oil Production Capability Index, ***OPCI***. All values for the PHOP pilot fall between 0 and 0.8 $m^3/OD/m_{perf}$.

6. Compute "total operating days" as days of injection plus days of production. Note that shut-in days and/or down-time are excluded from the calculation. If producing days are not available, assume the production time is four times the number of injection days. Coincidentally, this approximation is also a rule-of thumb in well test analysis. For example, 1 month of steam injection would require about (4 x 1 month) = 4 months of production, giving about 150 (30 + 4 x 30) total operating days ***(OD)***.

7. Calculate cumulative oil production by multiplying effective thermal pay by total operating days and by oil production capability index, where ***thermal net pay*** equals m_{perf} x ***net pay factor***. That is, ***TOIL = tpay x OD x OPCI***

13.2 Example Calculation for PHOP Well IP2

PHOP Well IP2 1st cycle performance is used as an example below:

1. From the reservoir description for IP2 (Table 10.2.2), the perforation interval is 512-518 mKB or 6 meters of perforation height. The variable m_{perf} is assigned a value of 6. There are 4 meters of oil sand above and below the

perforations giving a ***Net Pay Factor*** of 1.4 (Figure 13.1.1). No shale streaks are found within this interval.

2. The average S_{wi} within the production zone is calculated as:

((Height of Perforation interval 1 x Swi for this interval +
Height of perforation interval 2 x Swi for this interval))/
(Height of Perf. Interval 1 + Height of Perf Interval 2)
= [(4 meters between 512.5-516.5 mKB)(0.39) +
(2 meters between 516.5-518.5 mKB)(0.49)/ (4+2)
= 0.42, the weighted average.

3. From Table A1.1a, the average field steam injection rate = 180 m^3/d (CWE).

4. From Table A1.1a, the steam injection slug size = 4,900 m^3 steam (CWE).

5. Determine the "Oil Production Capability Index" (OPCI) from the correlation graph (Figure 12.3.3.2):
   i) Draw a new curve at 180 m^3/d (by linear interpolation).
   ii) Select the x-axis scale corresponding to the formation of interest. The Wabiskaw Formation axis is chosen here.
   iii) Find the intersection of S_{wi} = 0.42 on this new curve.
   iv) Read "Oil Production Capability Index",***(OPCI)*** = 0.65, $m^3/OD/m_{perf}$, the y-coordinate of the intersection point.

6. Now from Table A1.1a, operational days = 28 days of injection plus 30 days of production , for a total of 58 days. Therefore, ***OD*** is set to 58.

7. Calculate cumulative oil production for this time period using the formula given in Step 7 of Section 13.1:

   TOIL = tpay x OD x OPCI

   = (6 m x 1.4 net pay factor) x 0.65 m^3/OD/m x 58 operating days = **317 m^3** bitumen

This predicted volume is in good agreement with actual field production value of **304** m^3 of bitumen.

13.3 Calculation of Bitumen Production for the Remainder of the PHOP IP Wells

The same criteria outlined in Section 13.2 have been applied to other PHOP wells. The results are presented in Table 13.3.1. The rationale for determining net pay for the individual IP wells is briefly outlined below:

IP1 The upper perfs were not included since the initial S_w was too low in this interval thus allowing the steam to preferentially travel through the bottom perforations. There is a calcite streak between the upper and lower perforations. The initial S_w at the deeper perforations was low (0.35) so the horizontal extension (to the left) of the correlation curve was used.

IP2 As described by the example in Section 13.2.

IP3 Similar to IP2, Net Pay Factor = 1.4.

Table 13.3.1

1st Cycle Primrose Pilot: Prediction of Produced Oil vs Actual (Wabiskaw Formation, SWIR=0.30)

Well No.	Perfs mKB	Perf Height m	Perf Pay Factor	Ave. Sw	Steam Inj. Rate CWE m^3/d	Steam Slug Size CWE m^3	Operational days			Production Capability Index m^3/OD/m$_{perf}$	Calculated Oil Production m^3	Actual Oil Production m^3	Comment or %error
							Injection	Production	Total				
IP-1 upper perfs not incl.	505-508 509-510	4	1.4	0.35	155.6	4200	27	19	46	0.64	165 *see below for calcs.	193	14.6
IP-2	513-519	6	1.4	0.42	180.8	4882	27	30	57	0.65	311	304	-2.4
IP-3	510-517	7	1.4	0.41	202.9	4869	24	36	60	0.7	412	330	-24.7
											903	932	3.1
IP-4	507-509 511-515	6	1.4	0.4	173.7	5036	29	61	90	0.65 communication between wells	491	602	18.4
IP-5	507-515	8	1.4	0.36	172.0	7054	41	61	102	0.65	743	771	3.7
IP-6** shale bounded	507-515	8	1.1	0.45	70.0	3219	46	29	75	0.05	33	45	26.7
IP-7 1 m o.s. below perfs	514-524 1 m shale	9	1.3	0.4	182.4	5838	32	32	64	0.67	502	419	-19.7
IP-8	514-524 1.5 m shale	8.5	1.4	0.435	161.8	5339	33	41	74	0.54	476	435	-9.3
										Total =	3132	3099	-1.1

*IP-1 predicted oil = 4x1.4x46x0.64=165 m3

** use lower curve

IP4 Similar to IP 2, Net Pay Factor = 1.4.

IP5 Similar to IP 2, Net Pay Factor = 1.4.

IP6 Shale-bounded, Net Pay Factor = 1.1; only 1 m oil sand above perfs.

Because of the low injection rate and slug size, the lower curve had to be used.

IP7 Within the perforation zone, there is one meter of shale, so only 9 meters are considered thermal pay.

2 m oil sand above perfs + 1 m oil sand below perfs, Net Pay Factor = 1.3.

IP8 Within the perforation zone, there is 1.5 m shale, so only 8.5 meters are considered thermal pay:

Net Pay Factor = 1.4.

13.4 Related Comments on Bitumen Production for the PHOP IP Wells

The predicted results closely match the field data to the point of showing satisfactory trends. Related commentary follows:

IP1 A small amount of bitumen may have been produced from the upper perfs in the order of 30 m^3.

Temperature logs indicate that some steam went below the perforations.

IP2 Excellent match.

IP3, IP4 IP3 was on injection at the same time IP4 was producing. Field data indicated pressure communication between IP3 and IP4. One would anticipate IP4 to produce more oil than normally expected and IP3 to produce less. The correlation curves assume no interwell communication , so the calculated recovery for IP3 is high while that for IP4 is low. However, combined bitumen production of IP3 plus IP4 are in excellent agreement with field data.

IP5 Excellent match despite the slug size being larger than that used to generate the correlation curves. The prediction was extrapolated by the increasing the number of operating days.

IP6 Excellent match, bearing in mind that the history match was for this well, the framework for generating the correlative model.

IP7 The correlation curve predicted slightly higher than what was produced in the field. This may be due to the fact that IP7 experienced fluid communication with IP1 during IP7 injection and some steam was lost. Loss of steam is estimated to be in the range of 1,000 - 2,000 m^3 of steam (***CWE***).

IP8 Excellent match.

If aggregate bitumen production for the eight-well pilot is considered, then the overall match has an eight-fold excellence, given the predicted cumulative production of 2,961 m^3 versus the actual field total of 2,906 m^3. With only a 1.9% margin of error, the correlation technique is more accurate than numerical models can history match.

13.5 Calculation of Bitumen Production for PHOP Single Well Tests

For the purpose of validating the generality of the correlation curves in the three single-well tests (SWT), the production performance of 11-10, 10-34, and 11-21 completed in the Wabiskaw, Wabiskaw-McMurray, and McMurray formations, respectively, is investigated. The results are shown in Table 13.5.1. For these three wells, the correlation curves were shifted by the amount of change in irreducible water saturation before being used to predict production.

Table 13.5.1

Ist Cycle MITS (Single Well Tests):Prediction of Produced Oil vs Actual

Well No.	Perfs mKB			Ave. Sw	Inj. Rate m^3/d	Slug Size m^3	Operational days			Production Capability Index m^3/OD/m$_{perf}$	Calculated Oil Production m^3	Actual Oil Production m^3	Comment or %error
							Injection	Production	Total				
*11-10 Clearwater-McMurray	478-482	4	1.4	0.31 Swc = 0.20	218.4	10046	46	110	156	0.7	612	636	3.8
*10-34 shale below McMurray	504-510	6	1.2	0.34 Swc = 0.15	147.0	5144	35	159	194	0.425	594	602	1.4
*11-21 McMurray	543-553	10	1.4	0.25 Swc = 0.15	150.9	6488	43	90	133	0.59	1099	892	-23.2
										Total	2304	2130	-8.2

Well 11-10

The slug size is twice that from which the correlation curves were designed and the production cycle is rather long. Nevertheless, the predicted value of cumulative oil is quite close to the field number (651 m^3 versus 636 m^3 bitumen). The point where the water saturation falls on the curve indicates that the perforated zone could not accept the injection rate and some steam was lost elsewhere.

Well 10-34

Well 11-10 is considered to be completed in the transition zone between the Wabiskaw and McMurray. S_{wir} of 0.20 was therefore used. Well 10-34 is completed in the McMurray Formation and 0.15 was selected for S_{wir}, the same value used for the PCEJ wells. In spite of a long production cycle of 160 days, an excellent match has been achieved 597 m^3 versus 602 m^3 bitumen). The computed data also show that the injection pressure for 10-34 should be low as compared to that of 11-10 or the PHOP Wabiskaw Formation wells.

Well 11-21

Well 11-21 is completed in the McMurray Formation. Again S_{wir} is 0.15. The perforation interval is larger resulting in a prediction of incremental bitumen production though the total amount is still close (1,100 m^3 versus 892 m^3 of actual production).

In summary, the correlation curves developed in this thesis satisfactorily history-matched the eight PHOP pilot wells plus the three PHOP SWT wells for first-cycle production. The process of bitumen production for any new wells drilled near the Primrose Pilot will be fairly accurate as long as there is no between-well interference. The consolidated production from all project wells may match actual production. If steam injection rates are too high and steam is lost elsewhere, production from the lost steam may not show up until later cycles.

Not shown here are the many other attempts at trying to predict bitumen production. Using net pay instead of perforation height over-predicted production; using only perforation height under-predicted production. Having injected heat on the x-axis instead of mobile water saturation was not consistant. Using only producing days in the calculations did not work because there was no accounting for slug size. Using only water saturation instead of mobile water saturation did not account for varying lithologies. Only a specific combination of variables with the proper set of correlation curves would supply consistent predictions. The underlying suggestion is that at least the Wabiskaw Formation oil sand at the PHOP site is multilayered with shale and calcite streaks controlling affected net pay hence production.

Because the first cycle of bitumen production for the PHOP pilot was successfully history-matched, the application of the correlation curves was extended to history-match the remaining cycles of the project and also other oil sands pilots in Alberta completed in the same or analogous reservoirs. The expanded studies and their results are reviewed in the next sections.

Chapter 14

Multi-cycle History-match and Prediction for the PHOP IP Wells and SWT's

The first-cycle prediction of oil production based on the proposed correlation curves was shown to be satisfactory. As a demonstration of their range of applicability, a next step is to predict production from multiple cycles. The original set of curves will be used with either logical or empirical modification. Two methods will be presented here, each of which reasonably predicts oil production for up to seven cycles.

14.1 Method 1 for Estimating Multi-cycle Bitumen Production.

The first technique is simpler, has an empirical foundation, and is preferred over the alternate method. Each successive cycle is treated identically as the first cycle. For at least a few cycles, the reservoir's initial oil saturation is used, as an assumption is made that the injected steam for each successive cycle will heat up and produce a volume of oil at least equivalent to the oil that would be produced from a first cycle using the rate and slug size of the cycle being analyzed. This suggests the depletion from the previous cycle(s) is balanced by the oil resaturation in the reservoir plus heat left after previous production is complete. This replaces the task of increasing the "Net Pay Factor" and reservoir "water saturation" for each successive cycle calculation. After more than four cycles, or a specific cumulative steam injection, it will be necessary to account for heated oil at a greater distance from the well and higher water saturation near the wellbore. The total net pay has already been heated near the well, so injected steam will move progressively into the formation. Also, heat losses to the overburden and underburden will increase as the swept area becomes larger. This behavior can be appropriately represented by an efficiency multiplication factor (EMF) less than one and approaching zero as the cycle numbers increase. The EMF can be drawn as a horizontal straight line for the first few cycles on an EMF versus cycle number Cartesian plot (Please see next chapter 15, Figure 15.2.3.1a). Latter cycles are marked by a straight line but with negative slope.

14.2 Method 2 for Estimating Multi-cycle Bitumen Production

The second procedure has a logical basis and takes into account the cumulative operating days (actual injection plus producing days) including those from previous cycles. The original water saturation is used at all times and the injection rate is calculated by computing a weighted-average for all cycles considered. Oil from a latter cycle is calculated by subtracting the cumulative oil production from previously predicted cycles. This method is equivalent to a material balance performed on cumulative steam injection versus cumulative bitumen produced. If bitumen is not produced in a previous cycle due to a restriction on the number of producing days, this oil will be produced in a later cycle. One advantage for injecting steam is that even if the steam zone collapses from a fall in temperature after loss of latent heat, by reducing the production pressure, steam will again be recovered in the form of a gas drive towards the wellbore. One keeps track of this event by monitoring produced water chloride content, which is normally increasing with time, but which take a severe drop as new steam is produced.

As discussed in a later section, Tables 14.6.1a to 14.6.6a compare the results of the two prediction techniques to a maximum of seven cycles. Note that IP1 was the only well to produce up to seven cycles of steam injection.

14.3 Summary of Prediction Method for First-Cycle Bitumen Production

Below is a summary for calculating the first-cycle of bitumen production. Here the two methods are identical as there are no cumulative values.

Using the Oil Production Capability Index (***OPCI***) identified by average injection rate and average S_w at the perforations, on the correlation curves:

Oil Produced (m^3) = ***OPCI*** ($m^3/OD/m_{perf}$) x perf height (m) x Net Pay Factor (NPF, 1 to 1.4) x operating days (down time is excluded).

Table 14.6.1a

2nd Cycle PHOP: Prediction of Produced Oil, Wells IP1- IP5

$\boxed{999}$ = method 2 calculations=sum of previous cycles

Well No.	Perfs mKb	Perf Height m	Perf Height Factor	Ave. Sw at Perfs	Injection Rate m³/d	Slug Size m³	Operational Days Inj	 Prod	 Prod/Inj d/d	 Total	Production Capability Index m3/OD/mPerf	Efficiency Multiplication Factor	Calc. Oil m³	Field Oil m³	Comment or %error
IP1	494-495	6	1.4	0.35	86.0	3010	35	27	0.77	62	0.5	0.95	247	482	48.7
2m upper	497-499	6	1.4		116.3	7210	62	46	0.74	108	0.64	0.84	323		33.0
perfs incl	502-504														gas drive?
N2 frac	2m of above														or cum?
	505-508														
	509-510														
IP2	513-519	6	1.4	0.42	59.2	5390	91	155	1.70	246	0.3	0.95	589	417	-41.2
		6	1.4		87.1	10272	118	185	1.57	303	0.45	0.84	651		-56.1
IP3A	510-517	7	1.4	0.41	79.9	5750	72	95	1.32	167	0.36	0.95	560	556	-0.7
		7	1.4		110.6	10619	96	131	1.36	227	0.46	0.84	448		19.4
IP3B		7	1.4		85.2	1022	12	57	4.75	69	0.36	0.95	231	237	2.4
		7	1.4		107.8	11641	108	188	1.74	296	0.49	0.84	334		-41.1
IP4A	507-509	6	1.4	0.4	81.9	5900	72	95	1.32	167	0.38	0.95	506	460	-10.1
	511-515	6	1.4		108.3	10936	101	156	1.54	257	0.6	0.84	597		-29.7
IP4B		6	1.4		92.8	1113	12	53	4.42	65	0.42	0.95	218	225	3.2
		6	1.4		106.6	12049	113	209	1.85	322	0.59	0.84	252		-12.2
IP5	507-515	8	1.4	0.36	102.5	5124	50	133	2.66	183	0.55	0.95	1071	857	-25.0
		8	1.4		133.8	12178	91	194	2.13	285	0.62	0.84	920		-7.3

Table 14.6.1a (cont...)

2nd Cycle PHOP: Prediction of Produced Oil, Wells IP6 - IP8

$\boxed{999}$ = method 2 calculations=sum of previous cycles

Well No.	Perfs	Perf Height	Perf Height Factor	Ave. Sw at Perfs	Injection Rate	Slug Size	Operational Days				Production Capability Index	Efficiency Multiplication Factor	Calc. Oil	Field Oil	Comment or %error
	mKb	m			m^3/d	m^3	Inj	Prod	Prod/Inj d/d	Total	m3/OD/mPerf		m^3	m^3	
IP6,new	496-499	3	1.3	0.35	92.0	4600	50	59	1.18	109	0.53	0.95	214	180	-18.9
upper perfs															
lower close	shale														
IP7	514-524	9	1.3	0.4	86.0	4384	51	183	3.59	234	0.52	0.95	1352	1413	4.3
1mO.S.		9	1.3		$\boxed{123.2}$	$\boxed{10222}$	$\boxed{83}$	$\boxed{215}$	$\boxed{2.59}$	$\boxed{298}$	$\boxed{0.63}$	$\boxed{0.84}$	$\boxed{1343}$		4.9
below	1m shale														
perfs															
IP8	514-524	8.5	1.4	0.435	104.7	4920	47	164	3.49	211	0.42	0.95	1002	1179	15.0
		8.5	1.4		$\boxed{128.2}$	$\boxed{10259}$	$\boxed{80}$	$\boxed{205}$	$\boxed{2.56}$	$\boxed{285}$	$\boxed{0.5}$	$\boxed{0.84}$	$\boxed{949}$		19.5
	1.5m shale														
												Total	5991	6006	0.3
													$\boxed{6031}$		-0.4

Table 14.6.1b

2nd Cycle Single Well Tests: Prediction of Produced Oil vs Actual

999 = method 2 calculations=sum of previous cycles

Well No.	Perfs mKb	Perf Height m	Perf Height Factor	Ave. Sv at Perfs	Injection Rate m³/d	Slug Size m³	Operational Days				Production Capability Index m3/OD/mPerf	Efficiency Multiplication Factor	Calc. Oil m³	Field Oil m³	Comment or %error
							Inj	Prod	Prod/Inj Days/Days	Total					
Single Well Tests															
11-10	478-482	4	1.4	0.31	156.85	3341	21	71.6	3.36	92.9	0.54	1	281	310	9.4
Transition	Swir=.2	4	1.4		198.92	13387	67	182	2.70	248.9	0.68	1	336		-8.5
10-34	504-510	6	1.2	0.34	147.21	7066	48	143	2.98	191	0.51	1	701	2480	71.7
shale belov	Swir=.15	6	1.2		147.11	12210	83	302	3.64	385	0.48	1	737		70.3
McMurray															primary prod ?
11-21	543-553	10	1.4	0.25	146.72	10124	69	158	2.29	227	0.59	1	1875	2212	15.2
McMurray	Swir=.15	10	1.4		148.32	16612	112	248	2.21	360	0.59	1	1875		15.2
												Total	2857	5002	42.9
													2948		41.1

Table 14.6.2a

3rd Cycle PHOP: Prediction of Produced Oil, Wells IP1 - IP8 excl. IP6

999 = method 2 calculations = sum of previous cycles

Well No.	Perfs mKb	Perf Height m	Perf Height Factor	Ave. Sw at Perfs	Injection Rate m³/d	Slug Size m³	Operational Days Inj	 Prod	 Prod/Inj Days/Days	 Total	Production Capability Index m3/OD/mPerf	Efficiency Multiplication Factor	Calc. Oil m³	Field Oil m³	Comment or %error
IP1	494-495	6	1.4	0.35	191	4959	26	62	2.38	88	0.7	0.92	438	475	7.8
2m upper	497-499	6	1.4		138	12169	88	108	1.23	196	0.64	0.92	404		14.9
perfs incl	502-504														
	only 2m of above														
	505-508	509-510													
IP2	513-519	6	1.4	0.42	124	4722	38	141	3.71	179	0.5	0.92	636	962	33.9
		6	1.4		96	14994	156	326	2.09	482	0.46	0.92	614		36.1
IP3	510-517	7	1.4	0.41	129	6714	52	212	4.08	264	0.56	0.92	1226	1021	-20.1
	496-502*	7	1.4		115	18355	160	400	2.50	560	0.5	0.92	1129		-10.5
	503-506*														
IP4	507-509	6	1.4	0.4	144	7611	53	212	4.00	265	0.64	0.92	1206	889	-35.6
	511-515	6	1.4		118	19660	166	421	2.54	587	0.61	0.92	1205		-35.6
	496-502*	503-506*													
IP5	507-515	8	1.4	0.36	134	5239	39	197	5.05	236	0.63	0.92	1409	1432	1.6
	497-499*	8	1.4		134	17417	130	391	3.01	521	0.63	0.92	1449		-1.2
	502-504*														
IP7	514-524	9	1.3	0.4	70	2645	38	142	3.74	180	0.35	0.92	624	610	-2.3
1mO.S.		9	1.3		106	12867	121	357	2.95	478	0.6	0.92	995		-63.1
below perf	1m shale														
IP8	514-524	8.5	1.4	0.435	162	5008	31	110	3.55	141	0.58	0.92	824	975	15.5
	1.5m shale	8.5	1.4		138	15267	111	315	2.84	426	0.51	0.92	764		21.7
												Total	6363	6364	0.0
													6560		-3.1

* New perfs not considered this cycle

Table 14.6.2b

3rd Cycle Single Well Tests: Prediction of Produced Oil

999 = method 2 calculations = sum of previous cycles

Well No.	Perfs	Perf Height	Perf Height Factor	Ave. Sw 'at Perfs	Injection Rate	Slug Size	Operational Days				Production Capability Index	Efficiency Multiplication Factor	Calc. Oil	Field Oil	Comment or %error
							Inj	Prod	Prod/Inj Days/Days	Total					
	mKb	m			m³/d	m³					m3/OD/mPerf		m³	m³	
11-10	478-482	4	1.4	0.31	149	1046	7	19	2.71	26	0.52	1	76	17	-345.4
Transition	Swir=.2	4	1.4		194	14433	74	201	2.70	275	0.65	1	53		-210.7
10-34	504-510	6	1.2	0.34	213	10224	48	234	4.88	282	0.53	1	1076	3374	68.1
shale below		6	1.2		171	22434	131	536	4.09	667	0.45	1	831	primary	75.4
McMurray	Swir=.15													prod ?	
												Total	1152	3391	66.0
													883		74.0

Table 14.6.3a

4th Cycle PHOP: Prediction of Produced Oil, Wells IP1 - IP8 excl. IP6

$\boxed{999}$ = method 2 calculations = sum of previous cycles

Well No.	Perfs	Perf Height	Perf Height Factor	Ave. Sw at Perfs	Injection Rate	Slug Size	Operational Days				Production Capability Index	Efficiency Multiplication Factor	Calc. Oil	Field Oil	Comment
							Inj	Prod	Prod/Inj Days/Days	Total					or %error
	mKb	m			m³/d	m³					m3/OD/mPerf		m³	m³	
IP1	494-495	6	1.4	0.35	82.2	4194	51	183	3.59	234	0.7	0.875	1053	925	-13.9
2m upper	497-499	6	1.4		117.7	16363	139	291	2.09	430	0.64	0.905	1001		-8.3
perfs incl	502-504														
	only 2m of above														
	505-508, 509-510														
IP2	513-519	6	1.4	0.42	139.6	5305	38	191	5.03	229	0.5	0.875	736	1209	39.1
		6	1.4		104.6	20299	194	517	2.66	711	0.46	0.905	674		44.3
IP3	510-517	7	1.4	0.41	113.5	6585	58	178	3.07	236	0.56	0.875	992	838	-18.3
	496-502*	7	1.4		114.4	24940	218	578	2.65	796	0.5	0.905	872		-4.1
	503-506*														
IP4	507-509	6	1.4	0.4	115.4	6692	58	161	2.78	219	0.64	0.875	901	773	-16.6
	511-515	6	1.4		117.6	26352	224	582	2.60	806	0.61	0.905	837		-8.2
	496-502*														
	503-506*														
IP5	507-515	8	1.4	0.36	181.0	6154	34	180	5.29	214	0.63	0.875	1156	1023	-13.0
	497-499*	8	1.4		143.7	23571	164	571	3.48	735	0.63	0.905	1136		-11.1
	502-504*														
IP7	514-524	9	1.3	0.4	97.3	3697	38	188	4.95	226	0.35	0.875	709	977	27.5
1mO.S.		9	1.3		104.2	16564	159	545	3.43	704	0.6	0.905	1208		-23.6
below perfs	1m shale														
IP8	514-524	8.5	1.4	0.435	175.0	5949	34	228	6.71	262	0.58	0.875	1384	1171	-18.2
	1.5m shale	8.5	1.4		146.3	21216	145	543	3.74	688	0.51	0.905	1232		-5.2
												Total	6932	6916	-0.2
													6959		-0.6

* New perfs not considered this cycle

Table 14.6.3b

4th Cycle Single Well Tests: Prediction of Produced Oil, Wells IP1 - IP8 excl. IP6

999 = method 2 calculations = sum of previous cycles

Well No.	Perfs	Perf Height	Perf Height Factor	Ave. Sw at Perfs	Injection Rate	Slug Size	Operational Days				Production Capability Index	Efficiency Multiplication Factor	Calc. Oil	Field Oil	Comment or %error
							Inj	Prod	Prod/Inj Days/Days	Total					
	mKb	m			m^3/d	m^3					m3/OD/mPerf		m^3	m^3	
11-10	478-482	4	1.4	0.31	134.4	4031	30	66	2.20	96	0.52	1	280	370	24.4
Transition	Swir=.2	4	1.4		177.0	18464	104	266.6	2.56	371	0.65	1	349		5.6
10-34	504-510	6	1.2	0.34	211.9	11017	52	255	4.90	307	0.53	1	1172	2860	59.0
shale below		6	1.2		182.8	33451	183	791	4.32	974	0.45	1	995	primary	65.2
McMurray	Swir=.15													prod ?	
												Total	1451	3230	55.1
													1344		58.4

Table 14.6.4a

5th Cycle PHOP: Prediction of Produced Oil, Wells IP1,IP2,IP7, & IP8

☐ = method 2 calculations = sum of previous cycles

Well No.	Perfs	Perf Height	Perf Height Factor	Ave. Sw at Perfs	Injection Rate	Slug Size	Operational Days				Production Capability Index	Efficiency Multiplication Factor	Calc. Oil	Field Oil	Comment or %error
	mKb	m			m³/d	m³	Inj	Prod	Prod/Inj Days/Days	Total	m3/OD/mPerf		m³	m³	
IP1	494-495	6	1.4	0.35	115.3684	4384	38	138	3.63	176	0.7	0.83	713	796	10.4
2m upper	497-499	6	1.4		117.2147	20747	177	429	2.42	606	0.64	0.88	630		20.9
perfs incl	502-504														
	only 2m of above														
	505-508														
	509-510														
IP2	513-519	6	1.4	0.42	113.0862	6559	58	177	3.05	235	0.5	0.83	680	1105	38.5
		6	1.4		106.5794	26858	252	694	2.75	946	0.46	0.88	581		47.5
IP7	514-524	9	1.3	0.4	114.1379	6620	58	178	3.07	236	0.35	0.83	666	591	-12.7
1mO.S.		9	1.3		106.8387	23184	217	723	3.33	940	0.6	0.88	1062		-79.8
below	1m shale														
perfs															
IP8	514-524	8.5	1.4	0.435	174.5641	6808	39	235	6.03	274	0.58	0.83	1303	1468	11.3
		8.5	1.4		152.3043	28024	184	778	4.23	962	0.51	0.88	1101		25.0
	1.5m shale														
												Total	3361	3389	0.8
													3374		0.4

* New perfs not considered this cycle

Table 14.6.5a

6th Cycle PHOP: Prediction of Produced Oil, Well IP1

☐ = method 2 calculations = sum of previous cycles

Well No.	Perfs	Perf Height	Perf Height Factor	Ave. Sw at Perfs	Injection Rate	Slug Size	Operational Days				Production Capability Index	Efficiency Multiplication Factor	Calc. Oil	Field Oil	Comment or %error
							Inj	Prod	Prod/Inj Days/Days	Total					
	mKb	m			m³/d	m³					m3/OD/mPerf		m³	m³	
IP1	494-495	6	1.4	0.35	157.3	5976	38	191	5.03	229	0.7	0.87	1019	1027	0.8
2m upper	497-499	6	1.4		124.3	26723	215	620	2.88	835	0.64	0.89	1033		-0.6
perfs incl	502-504														
	only 2m of above														
	505-508														
	509-510														

Table 14.6.6a

7th Cycle PHOP: Prediction of Produced Oil, Well IP1

☐ = method 2 calculations = sum of previous cycles

Well No.	Perfs	Perf Height	Perf Height Factor	Ave. Sw at Perfs	Injection Rate	Slug Size	Operational Days				Production Capability Index	Efficiency Multiplicatio Factor	Calc. Oil	Field Oil	Comment or %error
	mKb	m			m³/d	m³	Inj	Prod	Prod/Inj Days/Days	Total	m3/OD/mPerf		m³	m³	
IP1	494-495	6	1.4	0.35	117.6	6822	58	177	3.05	235	0.7	0.72	716	713	-0.5
2m upper	497-499	6	1.4		122.9	33545	273	797	2.92	1070	0.64	0.855	649		8.9
perfs incl	502-504														
	only 2m of above														
	505-506														
	509-510														

14.4 Calculation of Multiple Cycles of PHOP Bitumen Production using Method 1

Assume cycle 2 or cycle 3, etc., is producing as if it were the first cycle, but use the OPCI as calculated from the steam injection rate for each separate cycle. Maintain the value of S_w at initial conditions, so the only required shift on the correlation curve is adjustment for steam injection rate of each individual cycle. Rather than compensate for an increase in S_w with an increase in cycle number, the Efficiency Multiplication Factor or EMF, having a starting value of 1.0 and decreasing towards zero as cycle number increases, is used. An attempt is made to assign the same EMF value to each cycle and all wells although the value should in some way be connected with cumulative steam injection and bitumen production.

14.4.1 Example Prediction of Second-cycle IP5 Bitumen Production using Method 1

An example calculation is provided here for the second cycle of well IP5. Performing the same calculation as for first-cycle of IP5 and applying the EMF:

Oil produced (m^3) = OPCI x m_{perf} x NPF x OD x EMF

= 0.55 m^3/OD/m_{perf} x 8 m x 1.4 x 183 OD x 0.95

= 1071 m^3

Actual oil = 857 m^3, an error of 25%.

The error is measured as ((predicted oil - actual oil)/ actual oil) x 100.

For thermal numerical modeling, an error of ± 20% is considered reasonable. The error calculated for IP5 production is slightly higher for this particular cycle due to the fact the author is assigning the same EMF for all the pilot wells as a simple generalization. The combined error across eight wells for the second cycle since the EMF was selected to minimize the consolidated deviation.

14.5 Calculation of Multiple Cycles of PHOP Bitumen Production using Method 2.

Assume cycle 2 or cycle 3, etc., is producing as if it were the "running total" of injection days plus production days including first cycle, but use the ***OPCI*** as calculated from the average steam injection rate (CWE) and cumulative slug size of the combined cycles. Keep the S_w at initial conditions, so the only shift on the correlation curve is for the average steam injection rate of the cumulative cycles. As for Method 1, rather than compensating for an increase in S_w with increase in cycle number, apply the Efficiency Multiplication Factor. The EMF, again has a starting value at 1.0 and approaches zero with an increase in cycle number.

14.5.1 Example Prediction of Second-cycle IP5 Bitumen Production using Method 2

An example calculation is provided here for the second cycle of well IP5. From the new averaged steam injection rate and cumulative operating days, a new OPCI is obtained and an overall adjustment is made through the EMF:

$$\begin{aligned} \text{Oil produced } (m^3) &= \text{OPCI x mperf x NPF x OD x EMF} \\ &= 0.62 \text{ m}^3/\text{OD}/\text{m}_{\text{perf}} \text{ x } 8 \text{ m x } 1.4 \text{ x } 285 \text{ OD x } 0.84 \\ &= 920 \text{ m}^3 \end{aligned}$$

Actual oil = 857 m^3, an error of 7.4%.

As before, the error is measured as ((920-857)/857) x 100.

The same EMF is used for all the pilot wells in order to generalize. The combined error across eight wells for the second cycle is 0.5%. Such a small margin is negligible.

Well IP5 produced a total of 4,081 m^3 oil over 4 cycles. Method 1 predicted 4,379 m^3 where Method 2 estimated 4,248 m^3, an error of 7.3 and 4.1% respectively, well within the comparable error associated with any history-match done using a numerical model.

14.6 Summary of Multiple Cycles of PHOP Bitumen Production and Associated Errors

Predicted bitumen production from the PHOP injection-production wells for each cycle beginning with cycle 2, is compiled in Tables 14.6.1a to 14.6.6a. Similar predictions made for the PHOP SWT's are shown in Tables 14.6.1b, 14.6.2b, and 14.6.3b. All of the referenced tables, including those for cycle one (Table 13.3.1 for IP1-IP8 and Table 13.5.1 for the SWT's), comprise one Microsoft EXCEL spreadsheet with a built-in function for easily re-calculating data for the studied PHOP wells or, any new wells requiring a prediction by either Method 1 or Method 2.

The majority of multi-cycle bitumen production history-matches for these pilot wells have less than a 20% error in total production, except for IP-2 which is low by 30% and IP-7 for which Method 2 is high by 25% (Table 14.6.7). A possible explanation is communication between IP2 and IP7 for cycles 3, 4, and 5 as they are adjacent to each other and along the fracture trend, similar to the interference between IP3 and IP4 in the first cycle. Summing oil production from the three cycles of IP2 and IP7 wells using Method 2 and comparing with actual production, yields an error of only 6.8%.

Overall, both Method 1 and 2 have an aggregate error for the PHOP pilot of approximately 3%, with Method 2 being only marginally better. The sum of the two SWT's, 11-10 and 11-21 had a slightly larger error of about 5%. Well 10-34 deviated over 60% due to the well's recovery largely by primary production.

Any attempt by numerical simulation to history-match the total pilot by only changing the reservoir description for each well, would never match production so closely. At the very least, the permeability curves would have to be modified for later cycles, which some numerical models cannot handle. The whole process of history-matching would be very time consuming, which is why it has never been attempted for

Table 14.6.7

Summary of Predicted Oil Production using both Methods and Associated Error (by Well)

☐ = method 2 calculations = sum of previous cycles

Well	Cycle 1 m^3	Cycle 2 m^3	Cycle 3 m^3	Cycle 4 m^3	Cycle 5 m^3	Cycle 6 m^3	Cycle 7 m^3	Cum Oil m^3	Actual Oil m^3	Cum Error, %
IP1	165	247	438	1053	713	1019	716	4352	4611	5.6
		323	404	1001	630	1033	649	4205		8.8
IP2	311	589	636	736	680			2953	4203	29.7
		651	614	674	581			2831		32.7
IP3	412	791	1226	992				3420	2982	-14.7
		782	1129	872				3195		-7.1
IP4	491	724	1206	901				3323	2948	-12.7
		849	1205	837				3383		-14.7
IP5	743	1071	1409	1156				4379	4081	-7.3
		920	1449	1136				4248		-4.1
IP6	33	214						247	245	-0.8
IP7	502	1352	624	709	666			3852	4008	3.9
		1343	995	1208	1062			5110		-27.5
IP8	476	1002	824	1384	1303			4988	5227	4.6
		949	764	1232	1101			4521		13.5
							total	27515	28305	2.8
								27492		2.9
10-11	612	281	76	280				1248	1332	6.3
		336	53	349				1350		-1.4
10-34	594	701	1076	1172				3543	9312	62.0
		737	831	995				3156		66.1
11-21	1099	1875						2974	3104	4.2
		1875						2974		4.2
							total	7764	13748	43.5
								7479		45.6

this problem, and most other multi-well/multi-cycle pilots. Indeed, it is far easier to model an average well.

14.7 The Utility of Predictions After Successful History-matching

There are always concerns regarding the benefits of numerical modeling to predict production after successful history matches have been made. Following is a general rule-of-thumb when evaluating thermal numerical simulation as an investigative tool for reservoir performance:

1. Predictions of multiple cycles after history-matching only one cycle of steam injection are of no use as the first-cycle can be history-matched a substantial number of ways.
2. Predictions of multiple cycles after history-matching only the first two cycles are slightly better, posing a somewhat higher level of difficulty, but can still be history-matched a number of ways.

3. Predictions of multiple cycles after history-matching three steam injection cycles are more reliable and at best can result in accuracies of ± 20% actual oil production, provided there is no interwell communication. A modified "Hall" plot (Hall initially designed this technique for observing reative permeability changes during water flooding) is now used to approximate steam zone volumes. Combined with the above is a new "Fracture Growth" plot, developed to correlate fracture length with injection time, and to estimate actual steam zone volumes. Steam breakthrough is identified as an instantaneous change in slope whereas steam flood interference would be read as gentle changes in slope of the afore mentioned plots (Leshchyshyn et al, 1991).

The development scheme for the correlation curves appears to be a function of first-cycle history-matching alone but is actually based on a first-cycle history-match applying a numerical model which already has been calibrated against at least three cycles of steaming for wells IP1 and IP7. Therefore first-cycle history-matching of first cycle of other wells in the pilot, using the calibrated simulator, was as easy as changing the reservoir description for that particular well and injecting steam at the required rate and volume. The exception was wells IP3 and IP4 where inter-well communication had occured.

As a warning, numerical modelers often input actual daily fluid volumes produced, essentially copying field reports. One can certainly understand why total fluid volumes exactly match for a given cycle. By comparison, for true numerical model history-matching, maximum allowable total volume of daily producible fluids is used for this model. Such volumes are controlled by the well choke when the well is flowing, or by pump stroke capacity. Predictions obtained from this style of history-matching can be employed with greater confidence and calibration of the model is well-grounded. Unfortunately, the predictions based on the correlation curves also require an estimate of the number of days of production for a given cycle, similar to numerical model history matching and prediction, as the numerical model will not stop itself at the proper end of production, when compared to actual cycle end.

Chapter 15

Multiple-cycles of Other Oil Sands Reservoirs in Alberta

Because the multi-cycle bitumen production history-matching of the PHOP pilot wells was successful, the same history-matching strategy was tested on other pilots and reservoirs in Alberta. This similar approach for the new areas of interest provided reasonable results. The field operations investigated were the BP/ Petro-Canada Wolf Lake-Clearwater oil sands at Wolf Lake, the Imperial/Esso-Clearwater oil sands at Cold Lake, and the PCEJ-McMurray oil sands at Fort McMurray. The research was followed up with a comparative study of these projects and respective production trends, to the modeled reservoir performance at the PHOP pilot.

15.1 Descriptions for Various Oil Sands Reservoirs

Formation descriptions for the Imperial-Clearwater oil sands at Cold Lake, the BP/Petro-Canada-Clearwater oil sands at Wolf Lake, and the PCEJ McMurray oil sands at Fort McMurray are presented in Tables 15.1.1.1 to 15.1.3.1. Each reservoir description represents an average well completed in that formation.

15.1.1 Comparison of Average Reservoir Properties

Table 15.1.1.1 compares average reservoir properties for the various reservoirs. Depth of burial, reservoir temperatures, porosities, bitumen saturations, and reservoir pressures are similar. The Imperial project has twice to three times the net pay thickness of the other reservoirs under consideration, and this appears to have the most impact on production capability.

TABLE 15.1.1.1

Comparison of Average Reservoir Properties

Parameter	ESSO	BP	Petro-Canada	
	Cold Lake	Wolf Lake	Primrose	Primrose
Formation	Clearwater	Clearwater	Wabiskaw (Clearwater)	McMurray
Overburden, m	412 - 484	440-450	470-490	500
Gross Pay Thickness, m	48	35	29	53
Net Pay Thickness, m (> wt%)	46 (6%)	23 (8%)	15 (6%)	15 (6%)
Net/Gross Ratio	0.96	0.65	0.52	0.28
Porosity	0.31	0.31	0.31	0.31
Bitumen Saturation	0.65	0.65	0.65	0.7
Bitumen Weight%	10	10	10	10.9
Reservoir Temperature, deg C	12.7	16	14	14
Reservoir Pressure, kPa	3100	2800	2500	
Reserve Density, m3/m2	9.27	4.63	3.02	3.26

TABLE 15.1.1.2

Comparison of Average Mineral Constituents for Various Reservoirs

Parameter	ESSO Cold Lake	BP Wolf Lake	Petro-Canada Primrose	Primrose
Formation	Clearwater	Clearwater	Wabiskaw (clearwater)	McMurray
Grain Fraction:				
% of Rock	80-95			
Quartz	21		27	95.9
Feldspar	30		10	1.7
Chert	15			
Unclassed Rock Fragments	6		47	
Volcanic Rock Fragments	28			
Mica			15	
Glauconite			1	
Total	100		100	
Fines (<0.045 mm) Fraction:				
% of Rock	5-20			
Silt (<0.063 mm)	45			
Clay	55		0	
Quartz	20		60.7	
Feldspar	12		31.1	
Siderite	7			
Carbonate	3			0.4
Other	3		0.7	
Clay	55		7.5	
Total	100		100	
Clays:				
Montmorillonite (smectite)	17		19	0.8
Mixed Layer	13			
Illite	40		8	0.4
Kaolinite	20		73	0.7
Chlorite	10			
Total	100		100	100

Table 15.1.1.3

Reservoir Model of Wolf Lake Project Average Well (Well 4G)

Layer No.	Depth mKB	Thickness m	Porosity	So	Kx md	Ky md	Kz md
	443.5						
1		4.77	0.31	58	1050	1050	500
	448.27						
2		5.1	0.21	38	100	100	10
	453.37						
3		3.91	0.28	65	850	850	400
	457.28						
4		0.72	0.1	1	0.5	0.5	0.3
	458						
5		3.9	0.3	50	850	850	400
	461.9						
6		3.44	0.31	70	1050	1050	500
	465.34						
7		0.56	0.1	1	0.5	0.5	0.3
	465.9						
8		2.88	0.32	70	1050	1050	500
	468.78						
9		0.62	0.1	1	0.5	0.5	0.3
	469.4						
10		7.12	0.3	50	850	850	400
	476.2						
	Total	33.02					

Perforation: all layers

TABLE 15.1.2.1

Comparison of Average Bitumen Properties

Parameter		ESSO	BP	Petro-Canada	
		Cold Lake	Wolf Lake	Primrose	Primrose
Formation		Clearwater	Clearwater	Wabiskaw	McMurray
Density, kg/m3		1004	993	1000	1020
API		9.3		9-10	6.5-9.5
Viscosity, mPaS					
	Temp, degC				
	13	1.00E+05		1000000*	
	38		9100	16000	3.5-9.6E5
	60		886	3000	16000
	90			300	550-960
	100	160	111		
Sulfur, wt%		4.68	4.3	4.5	4.9

* Dead Oil Atmospheric Pressure
1 mPaS = 1 cp

Table 15.2.1.1

Wolf Lake Comparison of Type Curve and Simulated Production, PCI Simulation similar to OP. Strategy as in Case (7) of BP Study No. 640

Swi=0.26 Swavg=0.48 h=33m rate=250 m3/d perfs=11m

								Total		model		model	
Cycle	Production Capability Index m3/OD/mperf	Perfs m*	Perf factor	Injection Days	Steam Inj Volume M3 CWE	Producing Days	Prod/Inj Days/Days	Operating Days	Multicycle factor	Water Productior m3	Type curve prediction m3	Simulation prediction m3	difference m3
1	0.65	11	1.4	40	10000	183	4.575	223	1	3367	2232	2180	-52
2	0.65	11	1.4	44	11000	203	4.6136364	247	1	4811	2472	2611	139
3	0.65	11	1.4	48	12000	235	4.8958333	283	1	6642	2833	2888	55
4	0.65	11	1.4	50	12500	261	5.22	311	0.91	8760	2833	2771	-62
5	0.65	11	1.4	52	13000	291	5.5961538	343	0.72	11010	2472	2410	-62
6	0.65	11	1.4	54	13500	323	5.9814815	377	0.57	13040	2151	2110	-41
7	0.65	11	1.4	56	14000	359	6.4107143	415	0.47	14870	1952	1910	-42
8	0.65	11	1.4	58	14500	399	6.8793103	457	0.39	16540	1784	1740	-44
9	0.65	11	1.4	59	14750	431	7.3050847	490	0.35	17730	1717	1580	-137
10	0.65	11	1.4	59	14750	460	7.7966102	519	0.28	18530	1455	1430	-25
			Total	520	130000	3145	6.0480769	3665		115300	21901	21630	-271

* a perf height of 11 m was required to match 1st cycle production using the correlation curves. Actual perf height is unknown.

TABLE 15.1.3.1

Fracture Parameters Compared between Athabasca (McMurray) and Cold Lake (Clearwater and Lower Grand Rapids)

Parameters	13-27-84-11W4 McMurray	16-27-84-11W4 McMurray	Typical McMurray	Wolf Lake Clearwater (C-Unit)	Wolf Lake L.G. Rapids (B-Unit)
Slug size, s (m3)	8982	6971	7500	8000	9020
Injection rate, I (m3/d)	209	170	170	220	173
Injection time, tI (min)	43	41	44	36	52
Fracture height, h_f (m)	44(24)*	34**(25)$^{+}$	18***	33 (26)$^{+}$	42^{+++}(31)$^{++}$(16)$^{+}$
Initial reservoir pressure, P_R (kPa)	2200	2000	2200	2700	2650
Injection pressure, P_i (kPa)	6600	7200	6200	9000	8200
Average injection Pressure along the fracture, $\underline{P_i}$	5900	6200	5700	7300	6750
Delta P = ($\underline{P_i}$ -P_R) (kPa)	3700	4200	3500	4600	4100
Injection Temperature, T_i (deg C)	292	280	275	302	297
Wellhead injection quality, X_i	0.71	0.78	0.75	0.75	0.54
Porosity, Phi	0.33	0.33	0.33	0.28	0.35
Initial oil saturation, S_{oi}	0.81	0.81	0.8	0.55	0.77
Effective Porosity, $Phi_e = Phi(1-S_{oi})$	0.063	0.063	0.066	0.126	0.081
Effective Compressibility, c_e (kPa^{-1})	1.00E-06	1.00E-06	1.00E-06	1.00E-06	1.00E-06
Effective Permeability, k_e (m^2)	1.30E-15	1.00E-15	1.30E-15	4.00E-15	2.50E-15
Effective Viscosity, u_e (cp)	0.093	0.096	0.1	0.09	0.093
Fracture pressure, P_f (kPa)	5200	5200	5200	5600(?)	5300
Fluid loss coefficient, C ($m/d^{1/2}$)	0.0182	0.0178	0.0166	0.0571	0.0317
Fracture half length, L_{fp} (m)	272 (499)*	286**(389)$^{+}$	600	111 (140)$^{+}$	133^{+++}(179)$^{++}$(348)$^{+}$

* Refers to the lower zone only.

** Gross pay zone, assuming fracture migrates through the thin shales to the over/underburden.

*** This number may increase to about 30 - 40 m if there are thin shales separating thin pay zones.

+ If just the main pay zone is fractured.A31

1 mD = 1E-15 m^2

Table 15.1.1.2 summarizes XRD clay analyses for various formations. The Wabiskaw and Clearwater formations are alike in rock descriptions with only 20-30% quartz, the rest being feldspar, chert, and volcanic rock fragments. By comparison, the McMurray Formation is 95% quartz with only about 4% clays, to the Clearwater's 5-20%. Most of the clays in the Clearwater Formation are non-swelling kaolinite and illite. About 20% of the clays are swelling (smectite) but do not appear to cause any serious production problems. Sieve analysis (Figure 15.1.1.1) indicates the McMurray oil sands to be the largest grained, followed by Primrose-Wabiskaw. The next smallest grain size is the Lindberg-Grand Rapids, followed by the Cold Lake-Clearwater. The smallest grain size is found in the Cold Lake-Grand Rapids, proving the formation is the most difficult to produce as bitumen recovery is not without significant sand production. Here, bitumen laden with sand causes the bottomhole positive displacement pumps to seize.

A field study of various oil sands pilots was coducted to determine optimum screen size as a countermeasure to excessive sand production (Leshchyshyn, 1990). The main conclusion was that sand size did not control optimum downhole screen size actually used, which was 0.018 to 0.025 inches. In retrospect, the Cold Lake-Grand Rapids formation may qualify as a good candidate for "cold production-compaction drive" where sand production is encouraged while producing bitumen, through installation of appropriate pumping equipment (i.e., progressive-cavity screw pumps). Such an operation would see initial sand production cuts as high as 80 percent and later decreasing to 15%.

In Table 15.1.1.3 is the average well reservoir description used for the Wolf Lake simulations.

15.1.2 Comparison of Average Bitumen Properties

Table 15.1.2.1 is a comparison of average bitumen properties for the various reservoirs. API gravities and sulfur contents are similar but the Clearwater bitumens at Wolf Lake and Cold Lake are less viscous than the Wabiskaw or McMurray. Effective viscosities at steam temperatures are very similar at about 0.1 cp, as can be seen in Table 15.1.3.1. A comparison of viscosities between the various reservoirs is also presented in

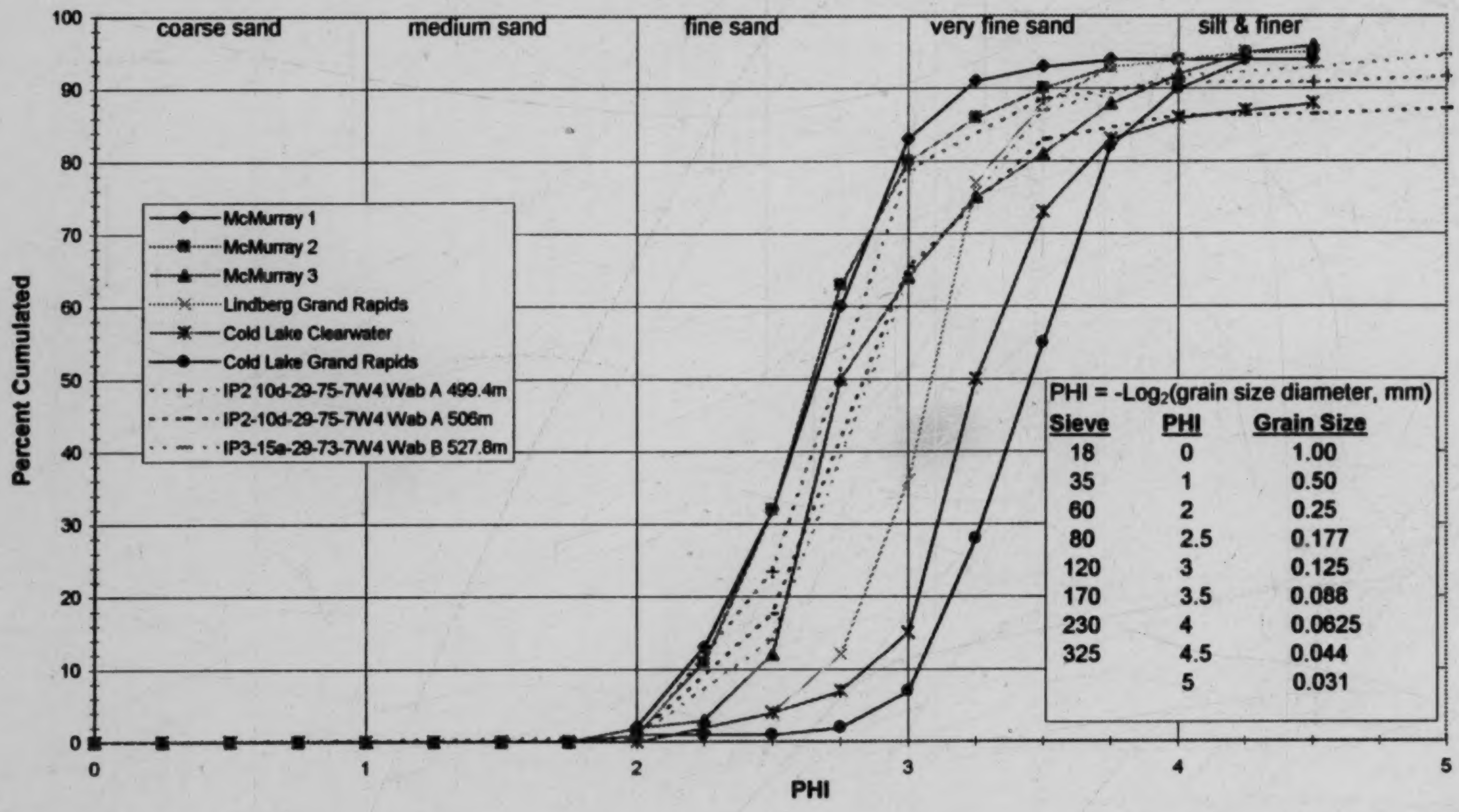

Figure 15.1.1.1: Comparison of sieve analysis from cores of various oil sands formations

15.1.3.1. A comparison of viscosities between the various reservoirs is also presented in Table 15.1.2.1 and Figure 15.1.2.1. These are dead oil viscosities, and since the GOR's are close in all the reservoirs at about 5-10 Nm^3/m^3, the order of least-to-most viscous is still correct. At reservoir temperature, the dead-oil viscosity for the McMurray oil sands at Fort McMurray is about 1,000,000 cp meaning bitumen will not flow freely into a newly-completed vertical well. However, the Primrose operation appears to produce McMurray bitumen through significant primary production, the true mechanism still unknown. Recovery is possibly due to more extensive dilation/compaction. It would have been possible to shift the correlation curves upwards to compensate for production increases due to reduced initial bitumen viscosities, but for the reservoirs studied, no significant effects due to viscosity variation were discernible.

15.1.3 Comparison of Steam Injection and Fracture Properties

Table 15.1.3.1 is a compilation of the steam injection and fracture properties of the various reservoirs. Injection temperatures range from 275-300°C at pressures ranging from 6,200-9,000 kPa. Initial oil saturations are 80% for the McMurray Formation as compared to 55-65% for the Clearwater. The Grand Rapids Formation oil saturation is closer to the McMurray at 75%. Created hydraulic fracture lengths (without considering dilation) in the McMurray are longer due to less leak-off from the fracture face. The equation for estimating half-fracture lengths , L_f, a simplification of the Carter equation, can be applied as follows:

For any fracture propagated at constant height, the calculated fracture length is:

$$L_f = ci\sqrt{t} \qquad (15.1.3.1)$$

Where L_f = half fracture length, m

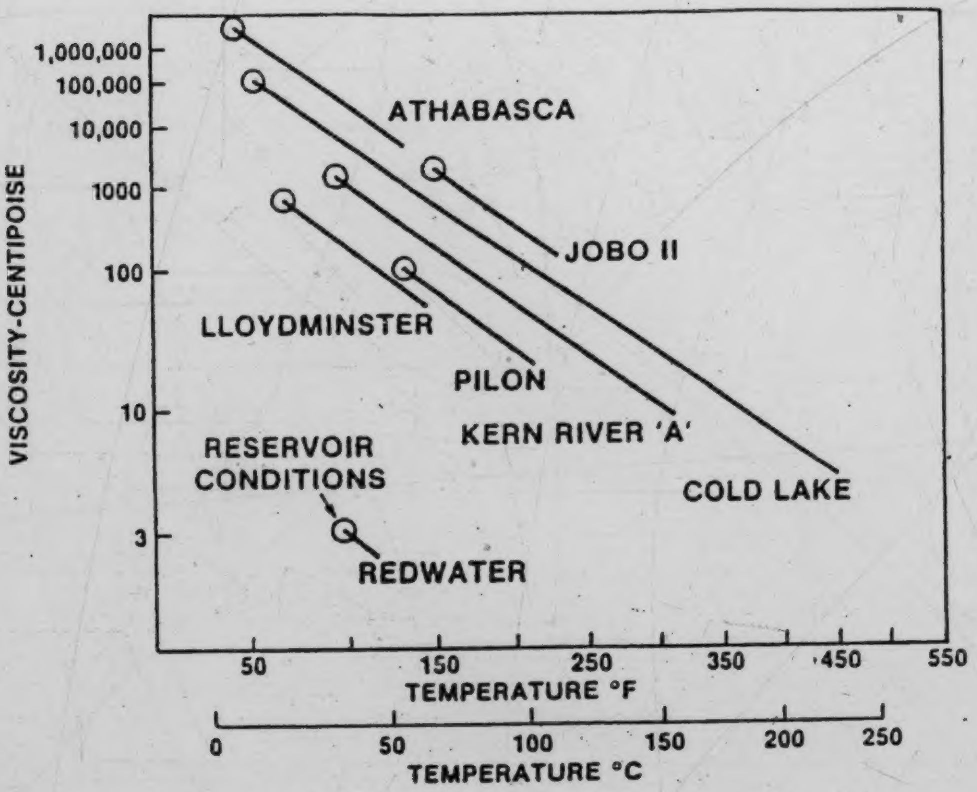

Figure 15.1.2.1: Viscosity of heavy crudes as a function of temperature (ref. Buckles, 1979)

i = steam injection rate (CWE), m^3/d

t = steam injection time, days

and c = a constant that is a composite of fracture height, leak-off coefficient, and injection pressure.

For the McMurray formation,

$$L_f = 0.285 i \sqrt{t} \qquad (15.1.3.2)$$

And for the Clearwater formation,

$$L_f = 0.19 i \sqrt{t} \qquad (15.1.3.3)$$

The constants 0.285 and 0.19 were back calculated from a single numerical model run, each in the McMurray and Clearwater formations, respectively. The constant values imply that fracture lengths in the McMurray formation are 50% longer than in the Clearwater formation. In Figure 15.1.3.2, the estimated fracture length is plotted against steam volume (CWE) injected at various rates (taken from Leshchyshyn et al, 1991). The Clearwater Formation fracture lengths shown here very closely match the values derived in a BP/Wolf Lake numerical simulation study, for each varied steam rate and slug size.

This simple equation was originally designed to accurately calculate fixed fracture lengths required by the thermal numerical simulator for matching actual steam injection pressures at the end of a steam injection cycle. These fracture lengths assume a single vertical fracture without dilation. Dilation can be introduced by the multiplication of another constant (c_2) less than one. For the McMurray Formation, one c2 value was

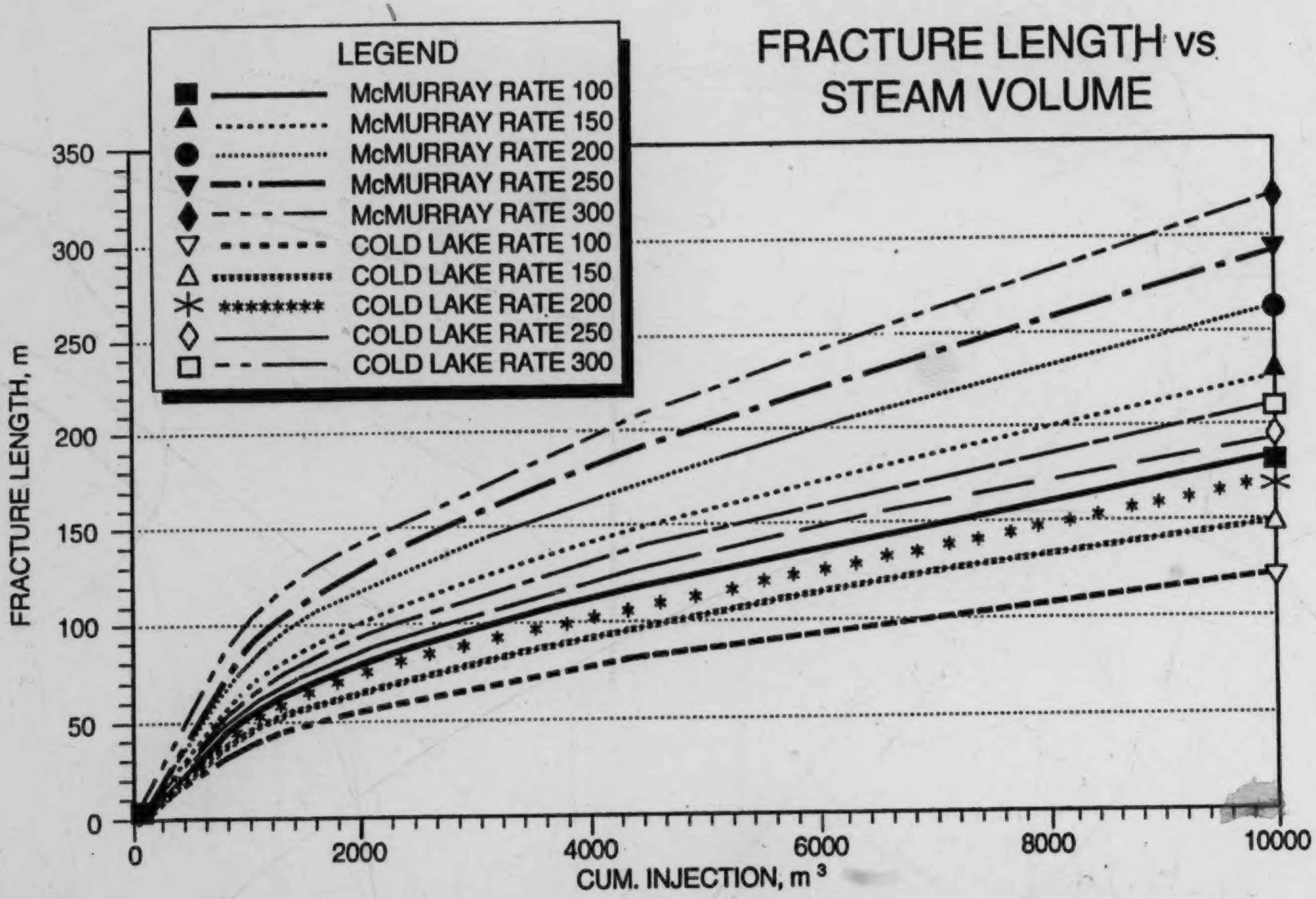

Figure 15.1.3.2: Comparison of fracture lengths versus cumulative steam injected at various injection rates in the Cold Lake-Clearwater and Fort McMurray-McMurray oil sands formations (Leshchyshyn, 1991)

estimated at about 0.25- 0.40 for a 20 m^3 water minfrac where dilated fracture lengths were 5-8 metres instead of an expected 20 metres (Leshchyshyn, 1994).

15.2 History-Matching Other Reservoirs using the PHOP Production Correlation Curves

Repeating the correlative procedure designed for the PHOP study, history-matching was performed with reasonable success on the Wolf Lake-Clearwater, the Imperial-Clearwater, and the Fort McMurray-McMurray formations. These matches were based on either the individual company numerical simulation forecasts, or a reservoir characterization of a typical project well and not actual production. An average well reservoir description assumed for the Wolf Lake-Clearwater numerical modeling is given in Table 15.1.1.3. A combined production history-match/ forecast for PHOP well IP8 undergoing 13 cycles, the first 5 of which are history, is summarized in Table 15.2.1.

15.2.1 History-matching of the Wolf Lake-Clearwater Average Well Simulation

The PHOP correlation curves established a history-match for a Wolf Lake-Clearwater average well simulation initially conducted by BP using Computer Modeling Group's (CMG) simulation software, "STARS". The S_{wir} was initialized to 0.26 and the S_{wavg} to 0.48. The assumed perforation height was 11 m although the actual height is unknown. Contained in Table 15.1.1.3 is the average well reservoir description. Tables 15.2.1.1 and 15.2.1.2 outline simulated production from a steam injection rate of 250 m^3/d and 160 m^3/d, respectively.

The oil production capability index was 0.65 and 0.43 $m^3/OD/m_{perf}$, respectively, for the two injection rates. In the case of the 250 m^3/d steam injection, the injection time was increased with cycle number from 40 days to 59 days . For the 160 m^3/d rate, the number of injection days was held constant at 30 for each cycle. Total bitumen production for the well average at 250 m^3/d was 21,500 m^3 and at 160 m^3/d was 9,500 m^3.

Table 15.2.1

PHOP Well IP8 Comparison of Type Curve and Simulated Production

inj rate=200m3/d 1st cycle,250m3/d rest(8000,10000 slug rest)

Cycle	Production Capability Index m3/OD/mperf	Perfs m	Perf factor	Steam Size m3	Injection Days	Production Days	Prod/Inj Days/Days	Operating Days	Multicycle factor	Type curve prediction m3	Simulation prediction m3	difference m3	actual production
1	0.57	8.5	1.4	8000	40	109	2.73	149	1	1011	733	-278	435
				8000	40	109	2.73						
2	0.58	8.5	1.4	10000	40	145	3.63	185	1	1277	1290	13	1178
				18000	80	254	3.18						
3	0.6	8.5	1.4	10000	40	141	3.53	181	1	1292	1605	313	975
				28000	120	395	3.29						
4	0.61	8.5	1.4	10000	40	144	3.60	184	1	1336	1576	240	1171
				38000	160	539	3.37						
5	0.62	8.5	1.4	10000	40	177	4.43	217	1	1601	1791	190	1468
				48000	200	716	3.58						
6	0.63	8.5	1.4	10000	40	210	5.25	250	0.93	1743	1787	44	
				58000	240	926	3.86						
7	0.66	8.5	1.4	10000	40	225	5.63	265	0.85	1769	1678	-91	
				68000	280	1151	4.11						
8	0.67	8.5	1.4	10000	40	243	6.08	283	0.78	1760	1720	-40	
				78000	320	1394	4.36						
9	0.67	8.5	1.4	10000	40	260	6.50	300	0.7	1674	1700	26	
				88000	360	1654	4.59						
10	0.67	8.5	1.4	10000	40	275	6.88	315	0.62	1557	1580	23	
				98000	400	1929	4.82						
11	0.67	8.5	1.4	10000	40	290	7.25	330	0.55	1447	1450	3	
				108000	440	2219	5.04						
12	0.67	8.5	1.4	10000	40	305	7.63	345	0.47	1293			
				118000	480	2524	5.26						
13	0.67	8.5	1.4	10000	40	320	8.00	360	0.4	1148			
				128000	520	2844	5.47						

Table 15.2.1.1

Wolf Lake Comparison of Type Curve and Simulated Production, PCI Simulation similar to OP. Strategy as in Case (7) of BP Study No. 640

Swi=0.26	Swavg=0.48	h=33m	rate=250 m3/d		perfs=11m					model		model	
Cycle	Production Capability Index m3/OD/mperf	Perfs m*	Perf factor	Injection Days	Steam Inj Volume M3 CWE	Producing Days	Prod/Inj Days/Days	Total Operating Days	Multicycle factor	Water Productior m3	Type curve prediction m3	Simulation prediction m3	difference m3
1	0.65	11	1.4	40	10000	183	4.575	223	1	3367	2232	2180	-52
2	0.65	11	1.4	44	11000	203	4.6136364	247	1	4811	2472	2611	139
3	0.65	11	1.4	48	12000	235	4.8958333	283	1	6642	2833	2888	55
4	0.65	11	1.4	50	12500	261	5.22	311	0.91	8760	2833	2771	-62
5	0.65	11	1.4	52	13000	291	5.5961538	343	0.72	11010	2472	2410	-62
6	0.65	11	1.4	54	13500	323	5.9814815	377	0.57	13040	2151	2110	-41
7	0.65	11	1.4	56	14000	359	6.4107143	415	0.47	14870	1952	1910	-42
8	0.65	11	1.4	58	14500	399	6.8793103	457	0.39	16540	1784	1740	-44
9	0.65	11	1.4	59	14750	431	7.3050847	490	0.35	17730	1717	1580	-137
10	0.65	11	1.4	59	14750	460	7.7966102	519	0.28	18530	1455	1430	-25
			Total	520	130000	3145	6.0480769	3665		115300	21901	21630	-271

* a perf height of 11 m was required to match 1st cycle production using the correlation curves. Actual perf height is unknown.

Table 15.2.1.2

Wolf Lake Comparison of Type Curve and Simulated Production, PCI Simulation similar to OP. Strategy as in Case (7) of BP Study No. 640
Wolf Lake Average Well (4G)

Swi=0.26 Swavg=0.48 h=33m rate=160 m3/d** perfs=11m

Cycle	Production Capability Index m3/OD/mperf	Perfs m*	Perf factor	Injection Days	Steam Inj Volume M3 CWE	Producing Days	Prod/Inj d/d	Total Operating Days	Multicycle factor	model Water Productior m3	Type curve prediction m3	model Simulation prediction m3	difference m3
1	0.43	11	1.4	30	4770	102	3.40	132	1	1530	874	960	86
				30	4770	102	3.40						
2	0.43	11	1.4	30	4770	118	3.93	148	1	2397	980	1135	155
				60	9540	220	3.67						
3	0.43	11	1.4	30	4770	139	4.63	169	1	3150	1119	1281	162
				90	14310	359	3.99						
4	0.43	11	1.4	30	4770	162	5.40	192	0.91	4183	1157	1169	12
				120	19080	521	4.34						
5	0.43	11	1.4	30	4770	187	6.23	217	0.72	5120	1035	1084	49
				150	23850	708	4.72						
6	0.43	11	1.4	30	4770	212	7.07	242	0.57	6010	913	950	37
				180	28620	920	5.11						
7	0.43	11	1.4	30	4770	240	8.00	270	0.47	7048	840	842	2
				210	33390	1160	5.52						
8	0.43	11	1.4	30	4770	268	8.93	298	0.39	7520	770	746	-24
				240	38160	1428	5.95						
9	0.43	11	1.4	30	4770	296	9.87	326	0.35	8100	756	680	-76
				270	42930	1724	6.39						
10	0.43	11	1.4	30	4770	326	10.87	356	0.28	8600	660	634	-26
			Total	300	47700	2050	6.83						
								2350		53658	9104	9481	377

* a perf height of 11 m was required to match 1st cycle production using the correlation curves. Actual perf height is unknown.

** only capability was changed due to rate reduced from 250 m3/d to 160 m3/d and slug size kept at 4770 m3

The same multi-cycle efficiency multiplication factor (EMF) was assigned to both cases and gave a less than 5% error in total bitumen production error. It can be inferred that for the total life of a well, the EMF is essentially independent of cumulative steam injection but has a direct relationship to cycle number, the underlying reasons as yet unknown. This loose correlation facilitates the predictive process for other steam rates and slug sizes. Since one would only have to know the ratio of producing days to injection days to obtain results similar to numerical modeling.

The ratio of producing days over injection days for the 160 m^3/d rate case (shown later in Figures 15.2.3.2a and 15.2.3b), starts at about 4 days/days and increases towards 8 days/days with an increase in cycle number. By comparison, the imperial-Cold Lake project has a production/injection ratio starting at about 2.5 days/days, rising rapidly to 8 days/days by cycle 3 and then slowly increasing to 9.5 by cycle 8.

With respect to the correlation curve calculations, the difference in oil production between the two rates was due to the ratio of different oil production capability indices (0.65/0.43 = 1.51), and the total operating days (3,665/2,350 = 1.56). The product of the two ratios gives an increase in production of 2.35 for the 250 m^3/d rate versus the 160 m^3/d rate.

15.2.2 History Matching of an ESSO Cold Lake-Clearwater Average Well Simulation

The Imperial-Cold Lake-Clearwater forecast (Table 15.2.2.1) could be matched only when perforation heights were multiplied by a factor of about 2. Herein lies proof that actual perforation height fails to produce the desired results in every reservoir prediction and that a problem can be solved by electing the "effective net thermal pay" instead, taking into account any impermeable streaks which may arrest hydraulically-induced fracture height propagation. A height of 46 m of net pay was available and a perforation height of 17 m was used. With the net pay factor at 1.4 this gave an equivalent net pay of 24 m which likely represents the net pay actually entered into the numerical model

Table 15.2.2.1

ESSO Cold Lake Comparison of Type Curve and Simulated Production, ERCB Application March Phase III & IV, 1984

Swi=0.26 Swavg=0.3 h=46m rate=225m3/d

Cycle	OPCI m3/OD/mper	Perfs m*	Perf factor	Injection Days	Steam Inj Volume M3 CWE	Producing Days	Prod/Inj Days/Days	Operating Days	Multicycle factor	model Water Production m3	Type curve prediction m3	model Simulation prediction m3	difference m3
1	0.75	17	1.4	49	11000	120	2.45	169	1	4800	3017	3000	-17
2	0.75	17	1.4	31	7000	168	5.42	199	0.9	4500	3197	3200	3
				80	18000	288	3.60	368					
3	0.75	17	1.4	36	8000	286	7.94	322	0.7	6800	4023	4000	-23
				116	26000	574	4.95	690					
4	0.75	17	1.4	38	8500	318	8.37	356	0.55	8000	3495	3500	5
				154	34500	892	5.79	1046					
5	0.75	17	1.4	40	9000	344	8.60	384	0.45	9000	3084	3100	16
				194	43500	1236	6.37	1430					
6	0.75	17	1.4	42	9500	363	8.64	405	0.4	10200	2892	2900	8
				236	53000	1599	6.78	1835					
7	0.75	17	1.4	44	10000	386	8.77	430	0.35	10800	2686	2700	14
				280	63000	1985	7.09	2265					
8	0.75	17	1.4	47	10500	433	9.21	480	0.3	11700	2570	2600	30
				327	73500	2418	7.39	2745					
			Total	327	73500	2418	7.39	2745		65800	24965	25000	35

* a perf height of 17 m was required to match 1st cycle production using the correlation curves. Actual perf height is unknown.

through the reservoir description. S_{wir} was 0.26 and S_{wavg} was 0.30 while the steam injection rate was 225 m^3/d.

The multi-cycle efficiency multiplication factor (EMF) for the Cold Lake-Clearwater average well showed a similar range from 1 to 0.3 with increasing cycle number but decreased sooner as compared to the Wolf Lake-Clearwater factor. If the numerical models used to generate this data are correct, then the field bitumen has also been history-matched. The Wolf Lake production, though, has been about one-half of forecast.

15.2.3 Comparison of History-matching of the Various Reservoirs

Comparing the PCEJ-McMurray prediction (Table 15.2.3.1) to actual field performance using the same procedure as the PHOP-McMurray history-matching (Table 15.2.3.2), reveals an inability of the correlation curves or the numerical simulation to reasonably predict reservoir production prior to actually drilling and steaming a well in a new area. Table 15.2.3.1 indicates the forecasts were high by a factor of 3. Extensive investigation has shown that, at the PCEJ project, bitumen production was significantly lower than expected since steam was either lost to the overburden (30-50% of the steam slug), or the useful fracture length was substantially exceeded by up to hundreds of meters of ineffective fracturing and the heated oil was too far away from the well to be produced. If one-half the steam injection rate is used, assuming one-half of the steam is lost, Table 15.2.3.1 shows a good history match is obtained for all three cycles.

As mentioned above, it is believed the actual bitumen recovery from the Wolf Lake-Clearwater project was about one-half the simulated prediction (the forecast only was history matched) due to the unfractured, impermeable calcite streaks situated in the middle of the reservoir just above the perforations. Steam would not necessarily be lost though it could initiate long, directional, horizontal fractures below these streaks, thereby increasing pressure in wells up to some 600 meters distance. Had the Wolf Lake project been fully developed by the application of steam across mega-rows, with the wells being dually-completed above and below the calcite streaks, the project may have succeeded. Perhaps the technology for dual completion was not available at that time (i.e., snubbed

Table 15.2.3.1

PCEJ Well 13-27-84-11W4 Comparison of Correlation Curve and Simulated Production

net pay = 16m So=0.81

inj rate=210 m^3/d 1st cycle, 220 m^3/d rest (9240 m^3 1st cycle,10000 m^3 slug rest)

Cycle	Production Capability Index m^3/OD/mperf	Perfs m	Perf factor	Injection Days	Production Days	Total Operating Days	Efficiency Multicycle factor	Correlation Oil prediction m^3	Simulation prediction m^3	difference m^3	actual inj rate m^3/d	actual production m^3
1	0.72	12	1.4	44	181	225	1	2722	2570	-152		
1/2actual*	0.7	12	1.4	49.6	181	230.6	0.355	963			206	962
2	0.72	12	1.4	45	247	292	1	3532	4030	498		
1/2actual	0.65	12	1.4	46	159	205	0.42	940			176	939
3	0.72	12	1.4	45	276	321	1	3883	4100	217		
1/2actual	0.64	12	1.4	28	236	264	0.295	837			142	841
4	0.72	12	1.4	45	301	346	0.84	3516				
1/2actual	0.7	12	1.4	30.5	193	223.5	0.17	447			197	445
5	0.72	12	1.4	45	331	376	0.77	3502				
6	0.72	12	1.4	45	363	408	0.7	3455				
7	0.72	12	1.4	45	400	445	0.59	3176				
8	0.72	12	1.4	45	440	485	0.52	3051				
9	0.72	12	1.4	45	470	515	0.45	2803				
10	0.72	12	1.4	45	500	545	0.38	2505				
			Total	603.1	4278	4881.1		35330.53				

* efficiency multicycle factor changed to match actual production to take into account steam lost to overburden

Table 15.2.3.2

PHOP Well McMurray Comparison of Correlation Curve and Simulated Production,PCI August 1983 perfs=14m x 1.4perf factor

Swir=0.15 Sw=0.22 perf = 14m

			Operational days						Numerical model	Correlation Curve	Numerical model		Well 10-34
Cycle	Inj Rate m3/d	Slug size m3	Inj	Prod	Prod/Inj d/d	Total	Production Capability Index m3/OD/mperf	Multicycle factor	Water Production m3	Predicted Bit. production m3	Bitumen production m3	difference m3	Bitumen actual m3
1	200	8000	40	140	3.50	180	0.70	1.00	5000.00	2470	1400	-1070	602
		8000	40	140	3.50								
2	250	10000	40	140	3.50	180	0.75	1.00	5000.00	2646	2500	-146	2479
		18000	80	280	3.50								
3	250	10000	40	140	3.50	180	0.75	1.00	5000.00	2646	2500	-146	
		28000	120	420	3.50								
4	250	10000	40	155	3.88	195	0.75	0.84	6000.00	2408	2400	-8	
		38000	160	575	3.59								
5	250	10000	40	165	4.13	205	0.75	0.77	6930.00	2320	2310	-10	
		48000	200	740	3.70								
6	250	10000	40	175	4.38	215	0.75	0.70	7700.00	2212	2200	-12	
		58000	240	915	3.81								
7	250	10000	40	195	4.88	235	0.75	0.59	8160.00	2038	2040	2	
		68000	280	1110	3.96								
8	250	10000	40	220	5.50	260	0.75	0.52	8955.00	1987	1990	3	
		78000	320	1330	4.16								
9	250	10000	40	245	6.13	285	0.75	0.45	9400.00	1885	1880	-5	
		88000	360	1575	4.38								
10	250	10000	40	280	7.00	320	0.75	0.38	9487.00	1788	1790	2	
		98000	400	1855	4.64								
11	250	10000	40	300	7.50	340	0.75	0.31	9610	1549	1550	1	
		108000	440	2155	4.90								

endless-tubing). Research and development of specialized well equipment might have advanced very quickly if the operator recognized remedial work would save the project.

Multi-cycle efficiency multiplication factors (EMF) declared in the multi-reservoir bitumen production matches exhibit a characteristic negative slope for each reservoir studied (Figures 15.2.3.1a and 15.2.3.1b). Actual EMF factors for PHOP-Wabiskaw actual, imperial-Clearwater, and Wolf Lake C-Unit follow the same general trend in terms of cycle number or cumulative steam injected. The EMF is only 1.0 for up to 20,000 m^3 of cumulative steam injection, then falls off to 0.3 with 45,000-75,000 m^3 of steam injected. The PHOP-McMurray and PHOP IP8 well EMF's remain near 1.0 longer, to 35,000 m^3 and 55,000 m^3 steam injection, respectively. This seems unrealistic and one may have to question the validity of the two simulations. Also, observing trends by cycle number alone can be misleading as slug size volume for each cycle is not consistent between wells or reservoirs.

Ratios of production days to injection days were compared for the various reservoirs considered (Tables 15.2.1,15.2.1.1, 15.2.1.2, 15.2.2.1 and Figures 15.2.3.2a to 15.2.3.2c). The Cold Lake-Clearwater and Wolf Lake-Clearwater reservoirs have the highest ratio (as high as 9.2 on an individual cycle basis and 7.4 on a ***cumulative production days/ cumulative injection days*** basis). The production/injection ratio measures the ease of production after steaming, the larger the numbers the easier it is to produce the reservoir. A general rule-of-thumb for conventional well-testing is to monitor bottomhole pressure build-up time to at least four-to-ten times longer than the draw-down used to create the build-up. This allows the transient build-up pressure the time to reach the outer boundaries seen by the drawdown. Therefore, it is not surprising that on a cumulative basis, the bitumen production time is within reason of 4-to-10 times (usually 4 times) the steam injection time. The actual PHOP cumulative production/injection ratio for IP8 after five cycles is 4.23. The purpose of investigating the production/injection ratio is to find an empirical method to derive a ratio for reservoirs lacking data to make production day estimations substantially more accurate. A numerical model at later time in a production cycle, will continue to produce bitumen unless cut-off criteria are specified. In reservoirs

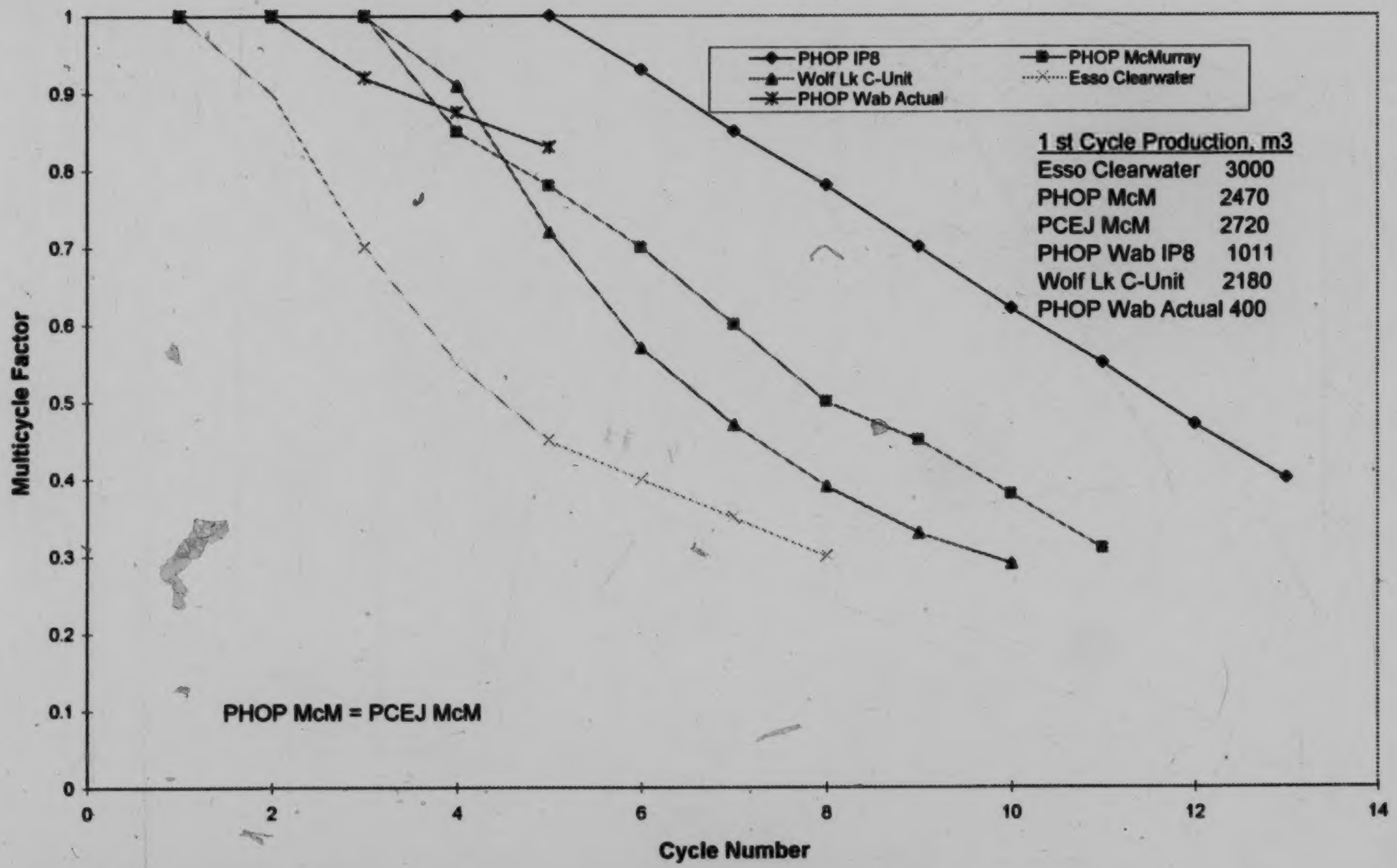

Figure 15.2.3.1a: Multicycle efficiency factors for various reservoirs versus cycle number

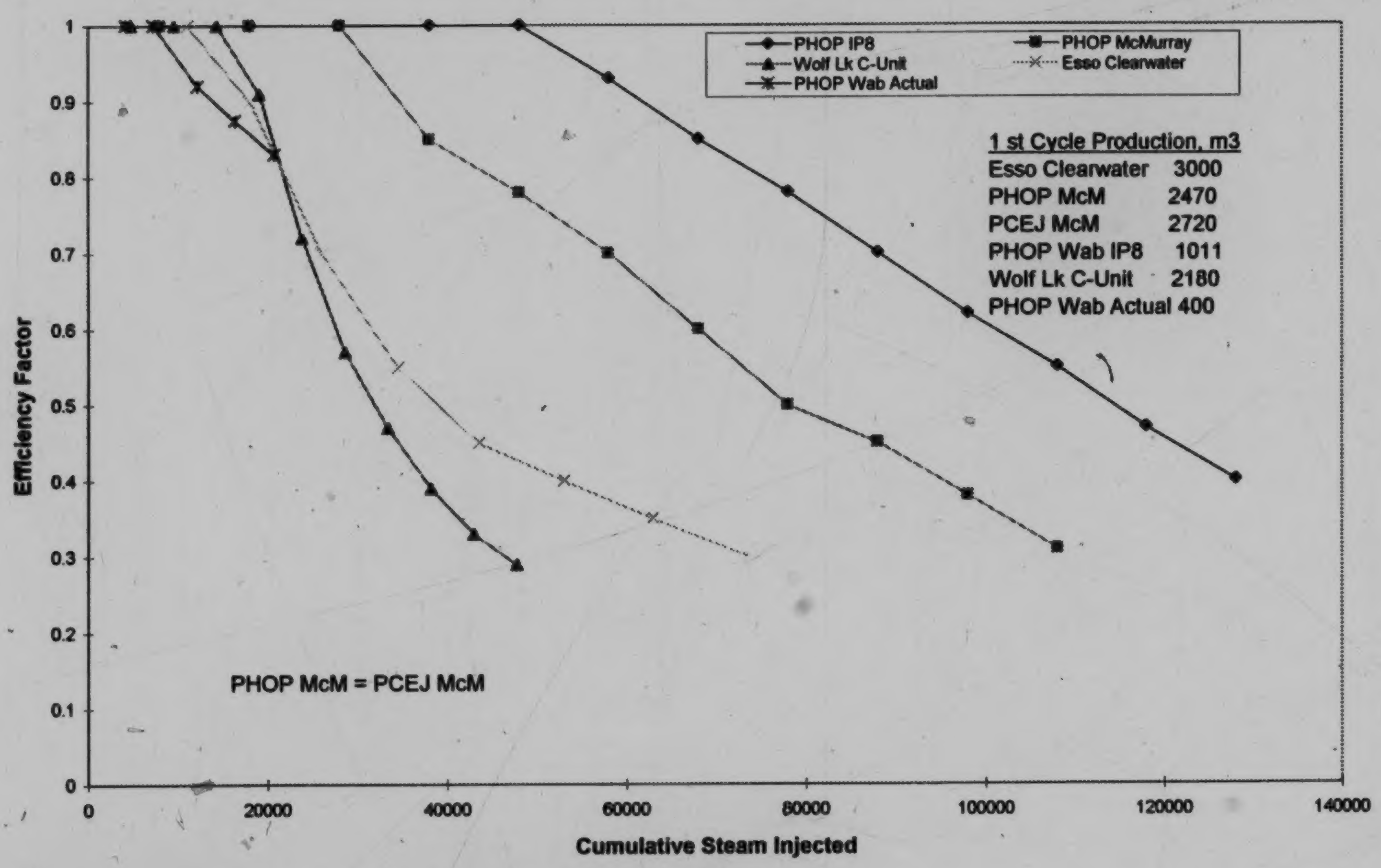

Figure 15.2.3.1b: Efficiency Factors for correlation curve calculations for various

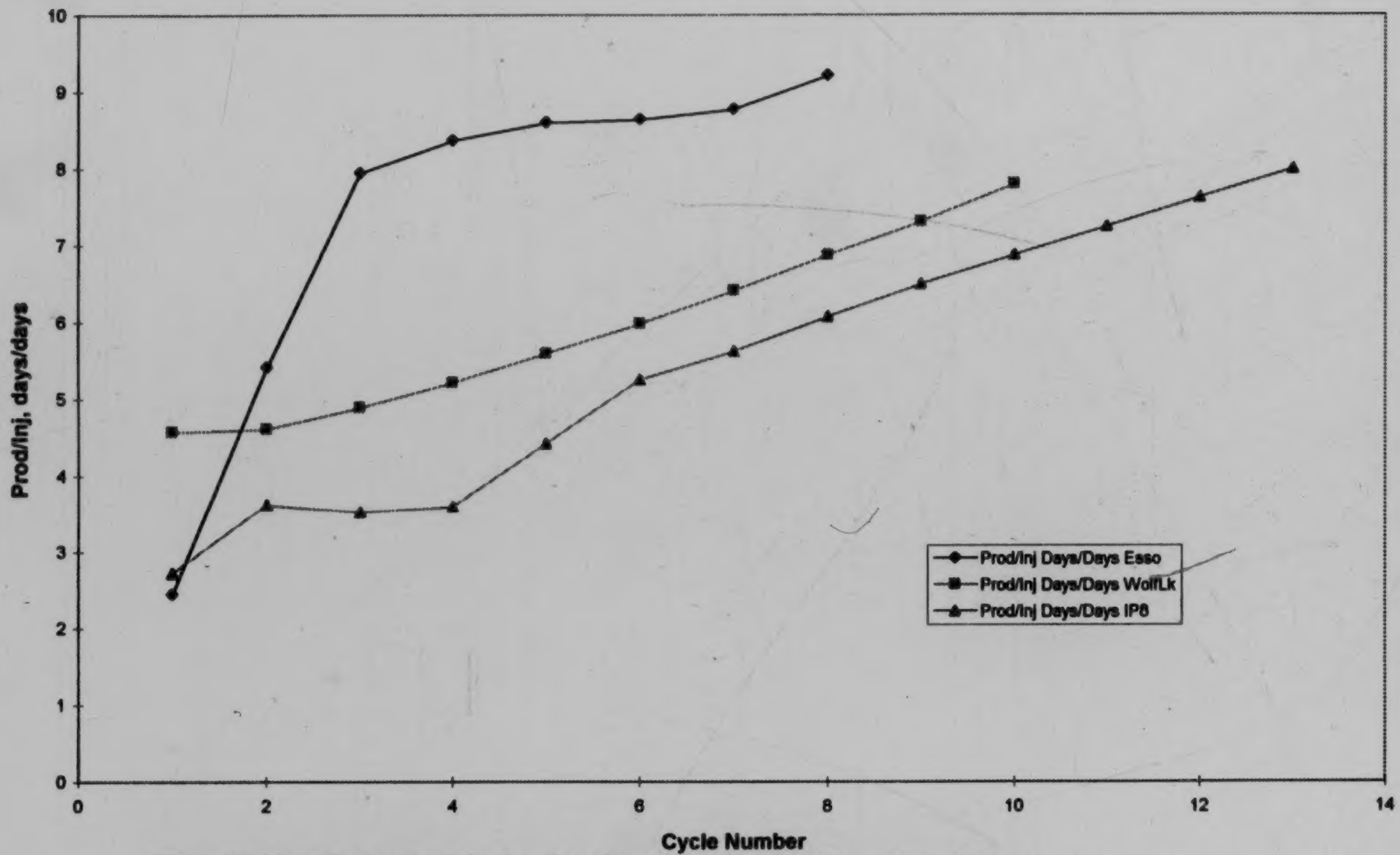

Figure 15.2.3.2a: Production/injection days for various reservoirs Vs cycle number

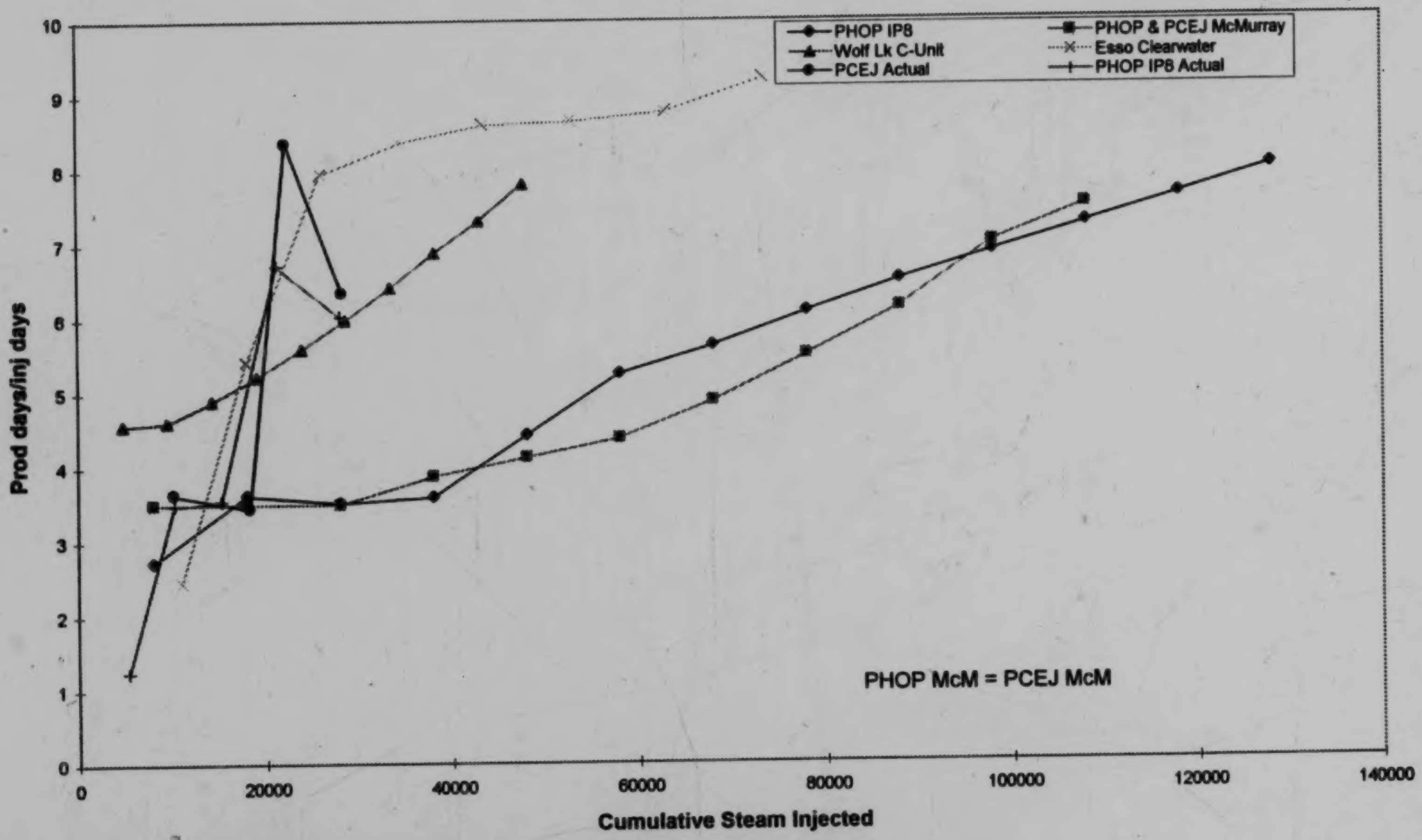

Figure 15.2.3.2b: Production/injection days for various reservoirs Vs cumulative steam injected

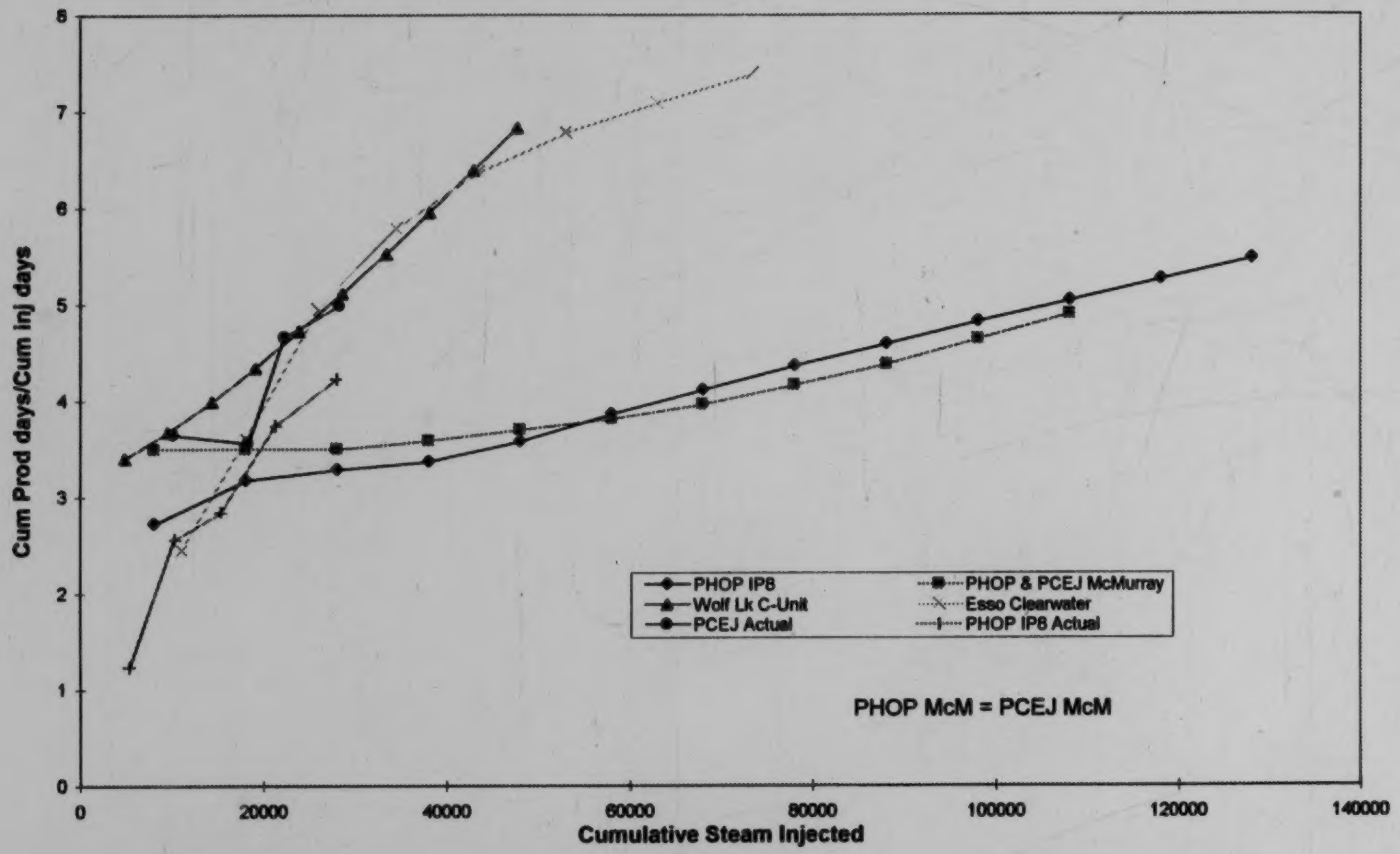

Figure 15.2.3.2c: Cumulative production/injection days for various reservoirs Vs cumulative steam injected

with a significant amount of compaction, as Imperial claims is occurring in their Clearwater project, it may be possible to double the rule-of-thumb ratio to 8. The adjustment is warranted since the pressure transient can be transferred geomechanically via dilation and thermally via expansion to the rock and spreads over a larger drawdown distance from the wellbore, corresponding to a longer build-up time.

A comparative evaluation of PHOP-Wabiskaw well IP8, PHOP-Wabiskaw (actual), PHOP-McMurray, Wolf Lake-Clearwater (C-Unit), and Imperial-Clearwater bitumen production per cycle versus cycle number (Figure 15.2.3.4a), clearly identifies Cold Lake-Clearwater as a superior reservoir with both the Wolf Lake-Clearwater and PHOP-McMurray formations in second place. The PHOP IP8 forecast is at least two times less than Cold Lake-Clearwater, and the PHOP-Wabiskaw actual produced about three times less than Cold Lake-Clearwater. Bitumen production per cycle versus cumulative steam injection (Figure 15.2.3.4b) shows Cold Lake-Clearwater averaging about 3,000 m^3 bitumen/cycle for a cumulative steam injection of 75,000 m^3 (CWE), while Wolf Lake-Clearwater seems to drop off more rapidly to an average of about 2,000 m^3 bitumen/cycle for a cumulative steam injection of 50,000 m^3 (CWE). The PHOP-McMurray reservoir also averaged about 2,000 m^3 bitumen /cycle while cumulative steam injection reached 115,000 m^3 (CWE). The PHOP-Wabiskaw IP8 averaged about 1,500 m^3 bitumen/cycle with cumulative steam to 130,000 m^3 (CWE). The PHOP-Wabiskaw actual data looked poor at 1,000 m^3 bitumen/cycle and the actual cumulative steam was no more than 22,000 m^3 (CWE).

Comparing the above reservoirs for cumulative bitumen produced versus cumulative steam injected (Figure 15.2.3.4c), places Wolf Lake-Clearwater forecast ahead of Cold-Lake-Clearwater due to more efficient early-cycle production, possibly because of a more optimized smaller first-cycle steam slug size. The PHOP-Wabiskaw (actual) cumulative production exceeds the PHOP-Wabiskaw IP8 forecast. This is opposite to the trends on previous graphs, where PHOP-Wabiskaw (actual) was worse than the PHOP-Wabiskaw IP8 forecast. Depending on the manner in which way the data is plotted, one simulation or reservoir can look better than the other. It is always better to make multiple plots for

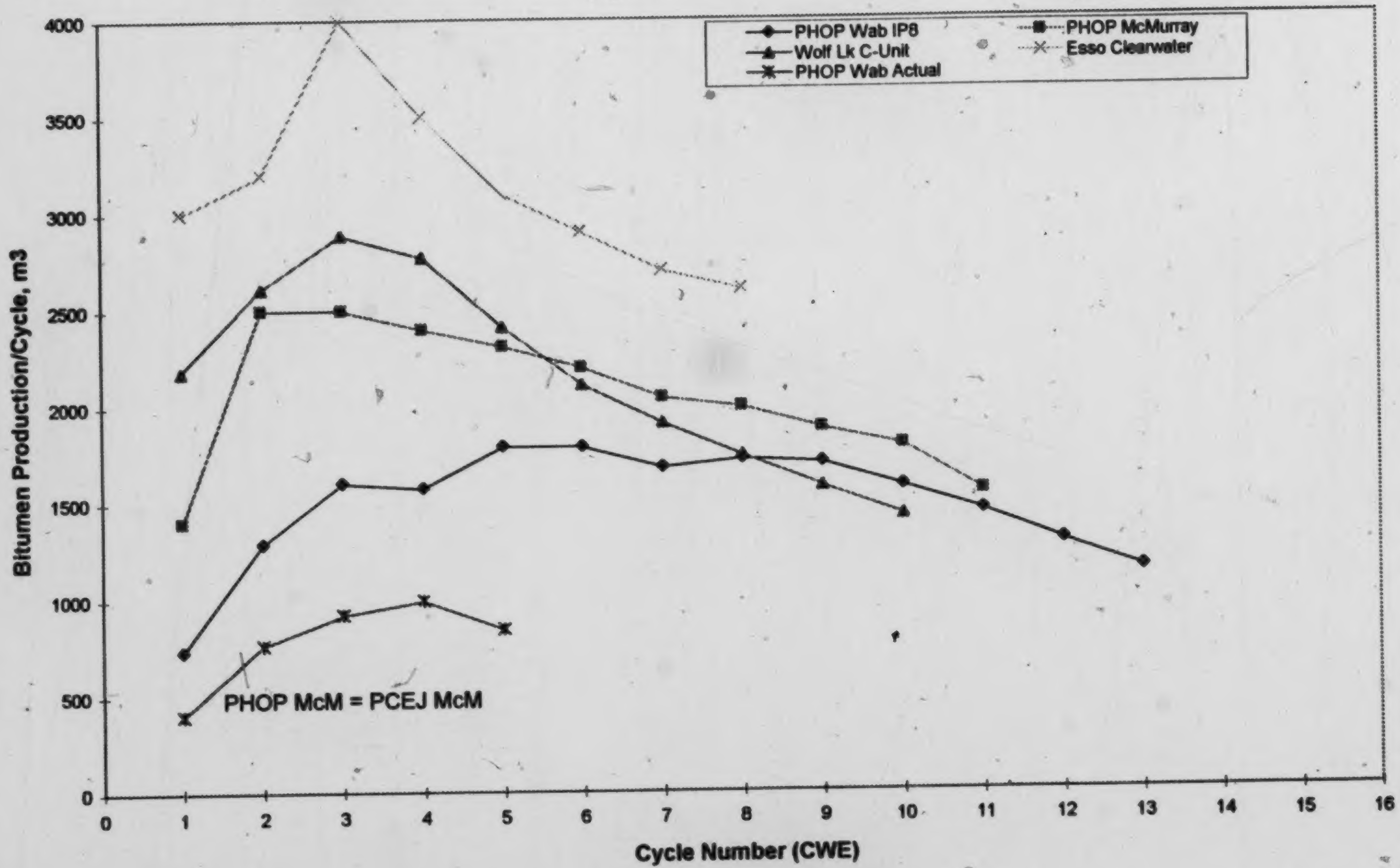

Figure 15.2.3.4a: Bitumen production/cycle for various reservoirs versus cycle number

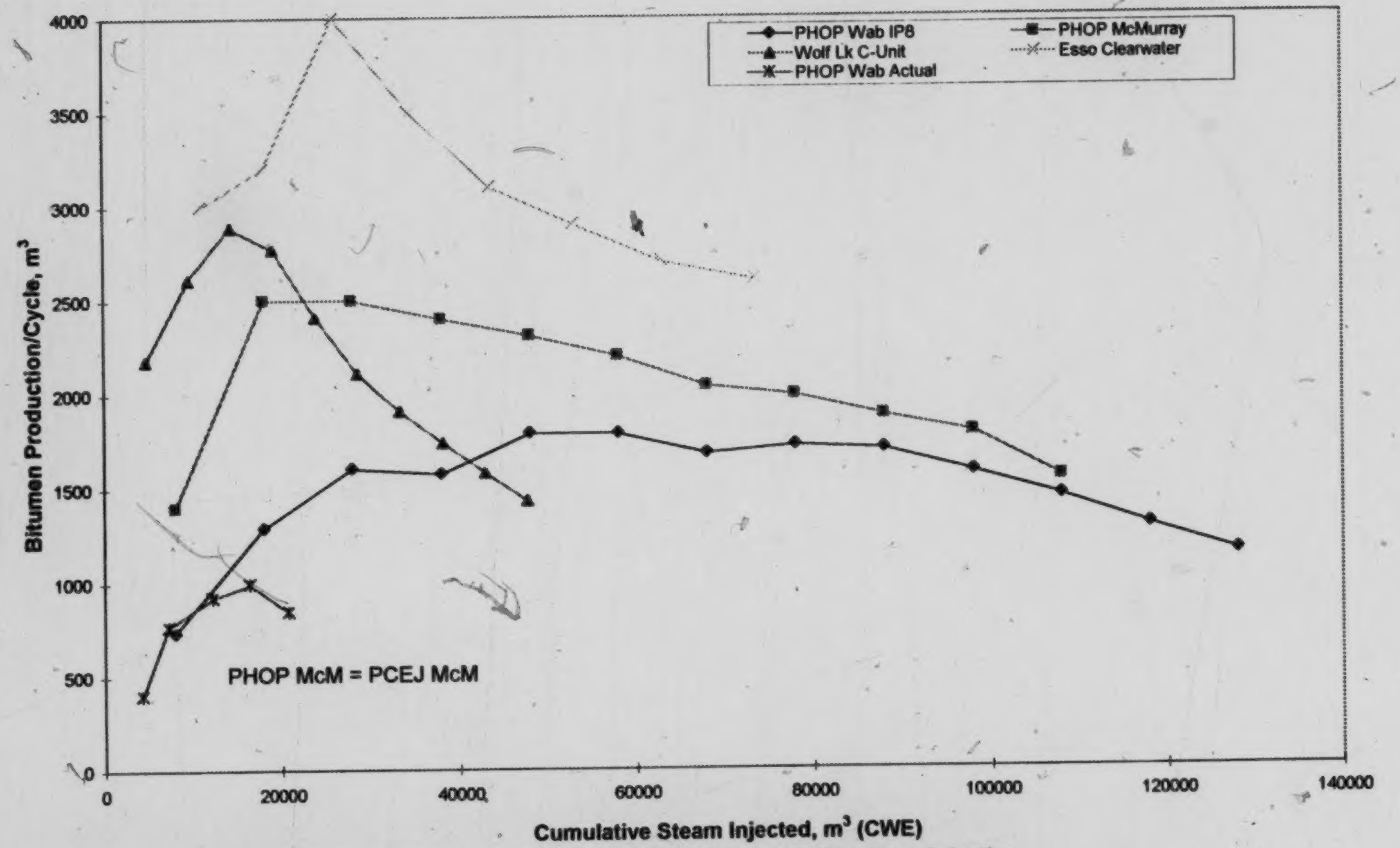

Figure 15.2.3.4b: Bitumen production/cycle for various reservoirs Vs cumulative steam injection

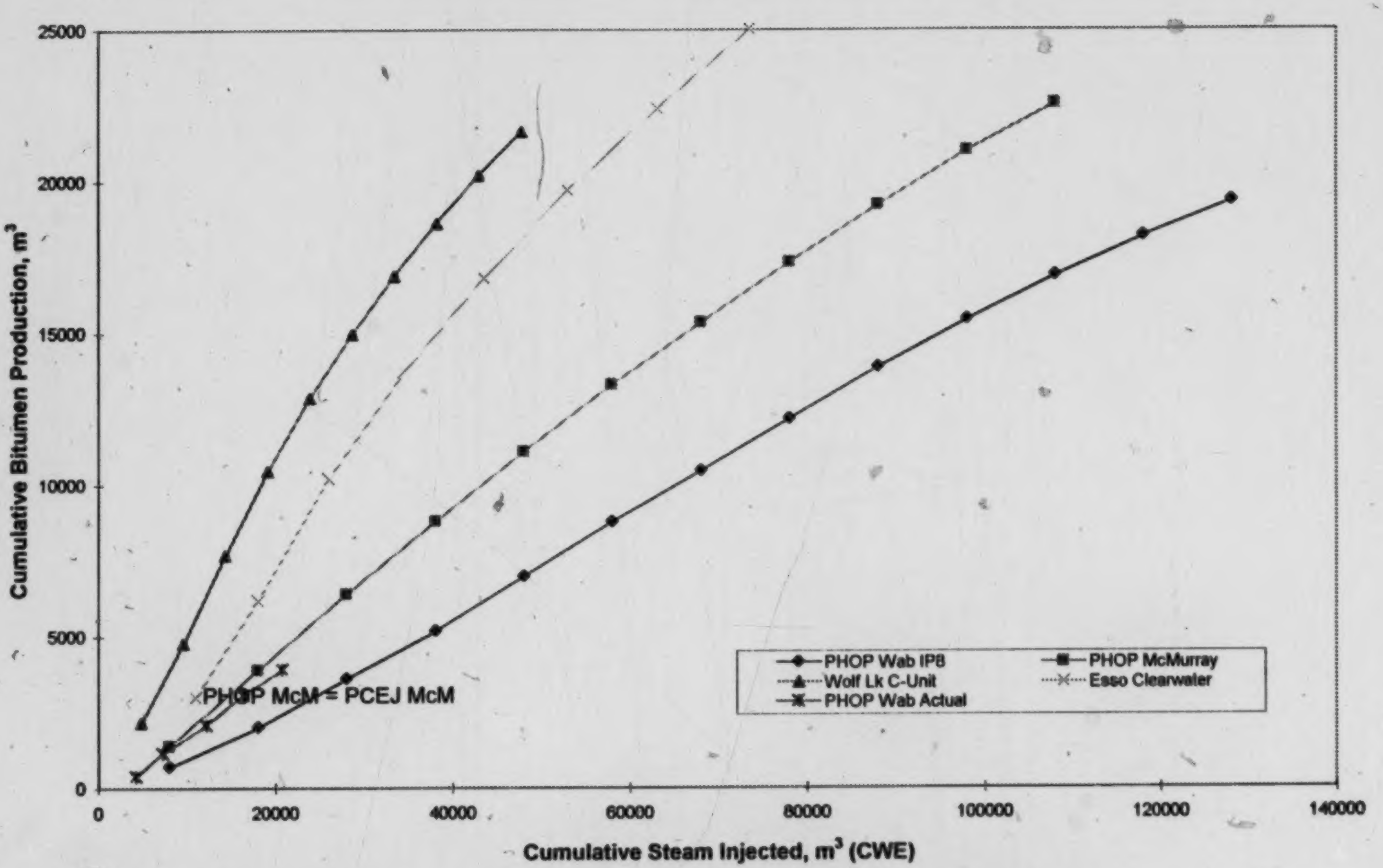

Figure 16.2.3.4c: Cumulative bitumen production for various reservoirs Vs cumulative steam injected

different perspectives of the same variables. The highest final cumulative bitumen production is still achieved by the Cold Lake-Clearwater formation. Wolf Lake-Clearwater final cumulative bitumen is reached with about 2.5 times less steam injection than that delivered to the PHOP-McMurray reservoir.

In view of the demonstrated merit of the simulations, the overall ranking of the reservoirs would place Cold-Lake-Clearwater number one, Wolf Lake-Clearwater at number two, PHOP-McMurray at number three, and PHOP-Wabiskaw last. This relative performance suggests the order in which these reservoirs should be commercially exploited. Thus far, the above ordering has been followed. Actual Wolf Lake production (not shown here), about one-half that forecasted, would have performed much better had the wells been dually completed and steamed together. Alternatively, two wells drilled at each location with completions at different depths to target above and below the calcite streaks would have improved recovery. The paired wells could be steamed separately in the beginning but then concurrently if inter-well communication is detected. Finally, the completed wells would have to be drilled and completed at less cost than the wells already in place as an economic imperative. Both the modified Hall and fracture growth plots for real-time injection analysis would be very useful here.

Chapter 16

Discussion

The objectives of the thesis have been met through the design, development, application, testing, and documentation of an integrated numerical-empirical correlation method for predicting bitumen production at the PHOP Pilot and SWT's, including comparative studies of other oil sands reservoirs.

The importance of reservoir characterization is essential to a comprehensive understanding of the effect steam injection has on various oil sands reservoirs. Correct interpretation of both aspects of the problem was a prerequisite to constructing a universal set of correlation curves. Field records were adequate for proper analysis and importantly, had observed trends from which key variables such as pressure and rate could be readily correlated. Also, a combination of actual data and numerical simulator results was a composite basis for a general consensus redarding numerical model accuracy for history-matching and predictions.

The main controlling factor in numerical simulation of bitumen recovery is the initial amount of mobile water in the oil sands. Model tests which identified limiting conditions showed that too little mobile water saturation caused fracturing out of zone or too far away from the wellbore, while too much mobile water saturation reduced bitumen production significantly.

Appropriate choices for permeability curves provided a means of modeling processes associated with dilation and/or compaction. This technique appeared to sufficiently represent the bulk geomechanical behavior of oil sands near the wellbore. Explicit placement of the fracture in the numerical model was not required. Rather, a set of permeability curves, when assigned to a simplified, fully-perforated, single-layer, radial numerical model, was able to successfully history-match the first-cycle of PHOP Pilot performance. This infers that steam-overide/gravity drainage has little impact on the early cycles of bitumen production. Dilation, on the other hand, is a major influence on production.

Various modeled reservoir geometries using multiple layering (up to ten intervals) and grid spacing (geometric versus equal volume) produced overly complex simulations and too many differences in bitumen production as a function of steam-injection slug sizes and rates. The problem was then reduced to merely a game of tracking varying amounts of "lost oil" from attempting to control the shape and movement of the steam front.

Numerical simulations used to generate the correlation curves were specific to the Wabiskaw Formation at the PHOP site, yet through a comparative adjustment of mobile water saturation, the correlative method was expanded to the transition zone between the Wabiskaw and McMurray formations and to the McMurray Formation itself. An unanticipated primary production from one of the McMurray wells was also noted.

At the PCEJ project, wells in the McMurray formation produced less oil than predicted, a reasonable explanation being that 30-40% of the injected steam was lost to the overburden. The correlation curves were intially designed for first cycle bitumen production only. Calculations were extended to multiple cycle history-matches by assuming the next few cycles were analagous to the first-cycle of production, and by virtue of the same depletion mechanisms at work in the reservoir, subsequent cycles used a linear-based efficiency multiplication factor (EMF) to model production decline. Various oil sands reservoirs had different starting points for EMF as well as variable slopes, both parameters anchored by the cumulative steam injected at the time step of interest. The curves were also adapted for analysis of the Clearwater Formation at Cold Lake and Wolf Lake. For future work, by shifting the correlation curves up or down, they could be applied with ease to international reservoirs, after a simple conversion from SI to Imperial oilfield units, if need be.

On the basis of history-matching, bitumen production appears to be strongly controlled by either the perforation height, the presence of calcite streaks, or the thermal net pay. Bitumen recovery is governed by the cumulative thickness of the shale streaks within the pay and the height of productive pay limited to no more than two meters of oil sand above and/or below the perforations. With respect to Cold Lake-Clearwater production, the PHOP and Wolf Lake projects apparently produced much less bitumen because net pay was reduced by fracture resistant calcite streaks and shales. Future work center on the technology transfer needed to design innovative dual well completions for targeting the oil sand thermal pay above and below the calcite streaks simultaneously, thereby optimizing production. The Wolf Lake project could possibly have been spared from closing had the joint venture partners uncovered potential reservoir problems during the evaluation stage.

The correlation curves could match either the numerical model results or actual production depending upon the choice of thermal net pay or the total producing days as the matching criteria. Once an actual EMF depletion slope was derived using the correlation curves, the predictions for the remaining productive life of the well would have better accuracy than from application of the numerical model. This is due to the fact that the simulation program is restricted to a window of calculations and material balances, while the EMF values can be modified to fit virtually any actual formation trend, understood or not.

Investigation of a sufficiently large number of reservoirs using the correlation curves or similar techniques will both validate the theoretical framework of these methods and formulate with confidence, universal and specific rules for reservoir performance calculations. Ideally, the scope of study will allow these same principles or some modification therof to be rigorously applied to lighter heavy oils, or even SAGD. Having analyzed hundreds of wells throughout Canada and the world, the drawn conclusion is that well performance must be viewed in terms of variable formation factors, and problems must be solved individually to optimize production.

Chapter 17

Conclusions

The conclusions below are not ranked according to usual economic imperative, but rather are arranged in the order as drawn from this thesis:

1. Taking a unified approach, a set of **correlation curves** have been constructed using numerical simulation and empirical methods to match actual **first-cycle** bitumen production for the Primrose Heavy Oil Pilot (PHOP) IP Wells and Single Well Tests. The development and application of a simple, single-layer, 8-ring radial numerical model reduced the problematic complexities associated with simulating bitumen recovery under various steam injection rates and slug sizes. Adding relative permeability curves for "fingering" to the model sufficiently accounts for dilation and other geomechanical processes occuring in the formation during injection.

2. The **correlation curves** have proven capability for history-matching **multiple cycles** of bitumen production at the PHOP Pilot and Single Well Tests. A convergence variable, the declining efficiency multiplication factor (EMF), improves the matching process after the second or third cycle of bitumen production from most of the wells.

   Calculating individual multiple cycles as if they were assumed to all be first cycles (Method 1), gave similar bitumen production predictions when compared to integrating the cycles of steam injected into a well and averaging injection rates with subsequent cycles (Method 2).

3. It was demonstrated by example, that the correlation curves can similarly history-match the numerical simulation of several other oil sands reservoirs in northern Alberta.

Once the correlative model has been calibrated from earlier cycle history-matching, the curves can predict oil production during subsequent cycles. Also, new wells can be predicted from cycle one onwards.

4. All oil sands reservoirs followed similar depletion trend slopes (EMF), but were shifted by the amount of cumulative steam injection required to optimize bitumen recovery under cyclic steam stimulation (CSS).

5. It was determined that calcite streaks of one-meter thickness or greater can prevent steam from fracturing upwards to contact more thermal net pay. These impermeable layers are continous throughout the center of the thermal net pay over the PHOP Pilot area. The Wolf Lake Project may have suffered the same consequences, resulting in only one-half of expected bitumen recovery. By the same principle, the Imperial Cold Lake-Clearwater formation has the highest-ranked productive performance because the reservoir rock is without these calcite streaks. The best history-match of Cold Lake bitumen was attained by assuming all of the thermal net pay was in contact with injected steam.

6. Selection of actual net pay using appropriate log cut-offs and core analyses can yield more realistic values for thermal net pay and reserves. At the Wolf Lake Project, thermal reserves were over-estimated as a cosequence of poor formation evaluation..

7. There is a direct relationship between perforation height and bitumen production. But, instead, a correlation may simply exist between the actual contacted thermal net pay and bitumen production, taking into account any calcite and streaks limiting steamed height growth above and below the perforations.

REFERENCES

Abass, H.H., S. Hedayati and D.L. Meadows: " Nonplanar Fracture Propagation From a Horizontal Wellbore: Experimental Study," SPE 24823, presented at the SPE Annual Technical Conference and Exhibition held in Washington, D.C., October 4-7, 1992.

Abou-Sayed, I.S., S. Schueler, E. Ehrl and W. Hendricks: "Multiple Hydraulic Fracture Stimulation in a Deep Horizontal Tight Gas Well," SPE 30532, presented at the SPE Annual Technical Conference & Exhibition held in Dallas, U.S.A., October 22-25, 1995.

Agar, J.G., N.R. Morgenstern and J.D. Scott: "Shear Strength and Stress-Strain Behaviour of Athabasca Oil Sand at Elevated Temperatures and Pressures," Canadian Geotechnical Journal, Vol. 24, 1987, pp1 – 10.

Arthur, John E., Donald A. Best, Kamal N. Jha and Frank M. Mourits: "An Analytical Composite Model for Cyclic Steam Stimulation in Elliptical Flow Geometry," Heavy Crude and Tarsands –Hydrocarbons for the 21st Century, Canadian Heavy Oil Association, 1988?, pp169 – 189.

Aud, W.W., T.B. Wright, C.L. Cipolla, J.D. Harkrider, and J.T. Hansen: "The Effect of Viscosity on Near-Wellbore Tortuosity and Premature Screen-outs", SPE 28492, Technical Conference, New Orleans, September, 1994.

Baumgartner, W.E., J. Shlyapobersky, A. Sayed and R.C. Jacquier: "Fracture Stimulation of a Horizontal Well in a Deep, Tight Gas Reservoir: A Case History from Offshore The Netherlands," SPE 26795, presented at the Offshore European Conference held in Aberdeen, September 7-10, 1993.

Beadall, Kris: Reports Covering Fence Diagram, Stratigraphy, Reservoir descriptions, Petro-Canada PHOP Project, 1980-83.

Beattie, C.I., T.C. Boberg and G.S. McNab: "Reservoir Simulation of Cyclic Steam Stimulation in the Cold Lake Oil Sands," SPE Reservoir Engineering, May, 1991, pp200 – 206.

Ben-Naceur, K. and P. Stephenson: "Models of Heat Transfer in Hydraulic Fracturing," SPE/DOE paper number 13865, May, 1985, pp163 – 169.

Bennion, D.B., Gurk Sarioglu, M.S. Chan, Toshiyuki Hirata, Dave Courtinage and John Wansleeben: "Steady-State Bitumen-Water Relative Permeability Measurements at Elevated Temperatures in Unconsolidated Porous Media," SPE 25803, International Thermal Operations Symposium, Bakerfield, February, 1993, pp255 - 267.

Bidner, M. Susana, Horaclo M. Kostiria and Victoria C. Vampa: "Analysis of the Transient Production of a Thermally Stimulated Well," SPE Reservoir Engineering, November, 1990, pp539 - 543.

Biot, M.A., L. Masse and W.L. Medlin: "Temperature Analysis in Hydraulic Fracturing," Journal of Petroleum Technology, November, 1987, pp1389 – 1397.

Bitter,B and T.Leshchyshyn: "Identification of Interwell Communication in Cyclic Steam Projects," presented at Canadian Heavy Oil Association Symposium, 1989.

Blanton, T.L.: " Propagation of hydraulically and Dynamically Induced Fractures in Naturally Fractured Reservoirs," SPE 15261, presented at the 1986 Unconventional Gas Technology Symposium, Louisville, KY, May 18-21, 1986.

Boberg, T.C. and R.B. Lantz: "Calculation of the Production Rate of a Thermally Stimulated Stimulated Well," J. Pet. Tech., December, 1996, pp1613 - 1623.

Boone, T.J., P.R.Kry, S. Bharatha and J.M. Gronseth: "Poroelastic Effects Related to Stress Determination by Micro-frac Tests in Permeable Rock," Rock Mechanics as a Multidisciplinary Science, Roegiers (ed.), 1991, Balkema, Rotterdam, ISBN 90 6191 194X, pp25 – 35.

Boone, T.J. and S.Bharatha: "Temperature Distributions Along Propagating Leakoff-Dominated Hot Water or Steam-Induced Fractures," SPE paper number 25791, Bakersfield, February, 1993, pp155 – 163.

Braden, W. B.: "A Viscosity-Temperature Correlation at Atmospheric Pressure for Gas-Free Oils," J. Pet. Tech., Nov,1966,pp1487 - 1490.

Brown, E. and M. Economides: "Solutions to Special Problems Pertaining to Fracturing Horizontal wells," Source Unknown.

Buckles, R.S.: "Steam Stimulation Heavy Oil Recovery at Cold Lake, Alberta," SPE paper number 7994, April, 1979.

Butler,R.M. and D.J. Stephens: "The Gravity Drainage of Steam-Heated Heavy Oil to Parallel Horizontal Wells," Journal of Canadian Petroleum Technology, April-June, 1981, pp90 – 96.

Butler, R.M., G.S. McNab and H.Y. Lo: "Theoretical Studies on the Gravity Drainage of Heavy Oil During In-Situ Steam Heating," The Canadian Journal of Chemical Engineering, Vol. 59, August 1981, pp455 – 460.

Butler, R.M.: "A New Approach to the Modelling of Steam-Assisted Gravity Drainage," Journal of Canadian Petroleum Technology, May-June, 1985, pp42 – 51.

CANMET/PCEJ/Munoz, V.A, W.W. Lam and R.J. Mikula: Report "Microscopic Evaluation of Steam Flooded Oil Sand Core Samples," Report prepared by CANMET for PCEJ, 1990.

Chan, M.Y., T. Hirata, and D.E.Towson: "Numerical Modeling of Cyclic Steam Stimulation Process Incorporating Temperature, Pressure, and Dynamic Fracture Properties," presented at the 6th Unitar Conference on Heavy Crude and Tarsands, Caracus, Venezuala, August 4-9, 1991.

Chan, M.Y.S., J. Fong and T. Leshchyshyn: "Effects of Well Placement and Critical Operating Conditions on the Performance of Dual Well SAGD Well Pair in Heavy Oil Reservoir," SPE paper number 39082, September, 1997.

Chen, Z. and M.J. Economides: "Fracturing Pressures and Near-well Fracture Geometry of Arbitrary Oriented and Horizontal Wells," SPE 30531, presented at the SPE Annual Technical Conference & Exhibition held in Dallas, U.S.A., October 22-25, 1995.

Chew, L. and T. Leshchyshyn: "Generalized Capillary Pressure – Water Saturation; Relationship for Heavy Oil Reservoirs in Alberta, CIM, 1985.

Chhina, H.S., R.W. Luhning, R.A. Bilak and D.A. Best: "A Horizontal Fracture Test in the Athabasca Oil Sands," CIM paper no. 87-38-56, Calgary, June, 1987, pp931 - 966.

Closmann, P.J.: "A Simplified Gravity Drainage Oil Production Model for Mature Steamdrives," SPE paper number 25790, Bakersfield, February, 1993.

De Haan, H.J. and L. Schenk: "Performance Analysis of a Major Steam Drive Project in the Tia Juana Field, Western Venezuela," SPE, January, 1969.

Demetre, George Paul, "Contigous Hyperhybrid Grids in Steam Injection Simulation," PhD. Thesis, Petroleum Engineering, University of Alberta, Edmonton, 1993.

Denbina, E.S., T.C. Boberg and M.B. Rotter: "Evaluation of Key Reservoir Drive Mechanisms in the Early Cycles of Steam Stimulation at Cold Lake," SPE Reservoir Engineering, May, 1991, pp207 – 211.

De Swaan O., Abraham: "Improved Numerical Model of Steam-Soak Process," The Oil and Gas Journal, January, 1972, pp58 – 62.

Dietrich, James K. and Paul L. Bondor: "Three-Phase Oil Relative Permeability Models," SPE paper number 6044, presented at the 51st Annual Fall Technical Conference, October 3 – 6, 1976.

Dietrich, J.K.: "Relative Permeability During Cyclic Steam Stimulation of Heavy-Oil reservoirs," Journal of Petroleum Technology, October, 1981, pp1987 –1989.

Dietrich, J.K.: "Cyclic Steaming of Tar Sands Through Hydraulically Induced Fractures," SPE Reservoir Engineering, May, 1986, pp217 – 228.

Duerksen, John H., Glenn W. Cruikshank, and Mel L. Wasserman: "Performance and Simulation of a Cold Lake Tar Sand Steam-Injection Pilot," JPT,October, 1984, pp1781 - 1790.

Dykstra, Herman: "The Prediction of Oil Recovery by Gravity Drainage," Journal of Petroleum Technology, May, 1978, pp818 – 830.

Ely, J.W., T.D. Brown and S.D. Reed: "Success Achieved in Lenticular Reservoirs Through Enhanced Viscosity, Increased Sand Volume, and Minimization of Echelon Fractures," SPE 30479, presented at the SPE Annual Technical Conference & Exhibition held in Dallas, U.S.A., October 22-25, 1995.

ERCB Application Wolf Lake II, Aostra File #, 012748, 1985, pp36 –39.

Ershagi, Iraj, M.S. Al-Adawiya and V.D. Kagawan: "A Graphical Method for Estimation of Production Response from Cyclic Steam Stimulation Using Past Performance Data," SPE paper 11954, San Francisco, 1983.

Farouq Ali, S.M. and W.S. Tortike: "Realistic Simulation of Formation Fracturing During Steam Injection Operations and Performance Prediction," AOSTRA Contract 477, June, 1987.

Farouq Ali, S.M.: Personal conversation, August, 1993.

Farouq Ali, S.M.: "CSS – Canada's Super Strategy for Oil Sands," JCPT Distinguished Authors Series, The Journal of Canadian Petroleum Technology, November,1994, Volume 33, No. 9, pp16 – 19.

Fast, R.E., A.S. Murer and R.S. Timmer: "Description and Analysis of Cored Hydraulic Fractures, Lost Hills Field, Kern County, California," SPE 24853, presented at the SPE Annual Technical Conference & Exhibition held in Washington, D.C., October 4-7, 1992.

Fialka, B.N., R.K. McClanahan, G.A. Robb and F.J. Longstaffe: "The Evaluation of Cyclic Steam Stimulation in an Oil Sand Reservoir using Post-Steam Core Analysis," Paper no. CIM/SPE 90 - 108, Calgary, June, 1990, pp108-1 - 108-17.

Fracmaster Fracture Course notes, "Practical Aplications of Hydraulic Fracturing", data searched from Accumap®™, August, 1996.

Gajdica, R.J., W.E. Brigham and K. Aziz: "A Semianalytical Thermal Model for Linear Steamdrive," SPE/DOE paper number 20198, April, 1990, pp259 – 274.

Gallant, R.J., S.D. Stark and M.D. Taylor: "Steaming and Operating Strategies at a Midlife CSS Operation," SPE paper number 25794, February, 1993, pp183 – 194.

Golder Associates brochure: "Large Scale Laboratory Simulation of hydraulic Fracture Propagation in Oil Sands", 1991.

Gomaa, Ezzat E.: " Correlations for Predicting Oil Recovery by Steamflood," Journal of Petroleum Technology, February, 1980, pp325 – 332.

Grabowski,Janusz W., Paul K. Vinsome, Ran C. Lin, Alda Behie and Barry Rubin: "A Fully Implicit General Purpose Finite-Difference Thermal Model for In Situ Combustion and Steam," SPE paper number 8396, 1979.

Grant, Malcolm A. and Michael L. Sorey: "The Compressibility and Hydraulic Diffusivity of a Water-Steam Flow," Water Resources Research, Vol. 15, NO. 3, June, 1979, pp684 –686.

Haan, H.J. and J. Van Lookeren: "Early Results of the First Large-Scale Steam Soak Project in Tia Juana Field, Western Venezuela," J. Pet. Tech., January, 1969, pp101- 110.

Hainey, B.W., X. Weng, and R.F. Stoitsits: "Mitigation of Multiple Fractures from Deviated Wellbores," SPE 30482, presented at the SPE Annual Technical Conference & Exhibition held in Dallas, U.S.A., October 22-25, 1995.

Hallam, S.D. and N.C. Last: "Geometry of Hydraulic Fractures From Modestly Deviated Wellbores," JPT, June, 1991, p742.

Hearn, C.L.: "Effect of Latent Heat Content of Injected Steam in a Steam Drive," Journal of Petroleum Technology, April, 1969, pp374 – 375.

Hopkins, C.W., J.H. Frantz Jr., D.G. Hill and F. Zamora: "Estimating Fracture Geometry in the Naturally Fractured Antrim Shale," SPE 30483, presented at the SPE Annual Technical Conference & Exhibition held in Dallas, U.S.A., October 22-25, 1995.

Howard, G.C. and C.R. Fast: "Optimum Fluid Characteristics for Fracture Extension, Drilling and Production Practices," API (1957), p.261.

Hudson, P.J. and R. P. Matson: "Hydraulic Fracturing in Horizontal Wellbores," SPE 23950, presented at the 1992 SPE Permian Basin Oil and Gas Recovery Conference held in Midland, Texas, U.S.A. March 18-20, 1992.

Ito,Yoshiaki: "The Introduction of the Microchanneling Phenomenon to Cyclic Steam Stimulation and its Application to the Numerical Simulator (Sand Deformation Concept)," Society of Petroleum Engineers Journal, August, 1984, pp417 – 430.

Jeffery, R.G., L. Vandamme and J.C. Roegiers: "Mechanical Interactions in Branched or Subparallel Hydraulic Fractures," SPE 16422, presented at the 1987 SPE/DOE Symposium on Low Permeability Reservoirs held in Denver, May 18-19, 1987.

Jeffrey, R.G. Jr., R.P. Brynes, P.J. Lynch and D.J. Ling: "An Analysis of Hydraulic Fracture and Mineback Data for a Treatment in the German Creek Coal Seam," SPE 24362, presented at the SPE Rocky Mountain Regional Meeting held in Casper, Wyoming, May 18-21, 1992.

Jeffrey, R.G., A. Settari and N.P. Smith: "A Comparison of Hydraulic Fracture Field Experiments, Including Mineback Geometry Data, with Numerical Fracture Model Simulations," SPE 30508, presented at the SPE Annual Technical Conference & Exhibition held in Dallas, U.S.A., October 22-25, 1995.

Kasraie, Mahnaz: "Simulation of Modified Steam Injection Processes Applied to Bottom Water Reservoirs," PhD. Thesis, Petroleum Engineering, University of Alberta, Edmonton, 1987.

Kim, C.M. and H.H. Abass: "hydraulic Fracture Initiation from Horizontal Wellbores: Laboratory Experiments," Rock Mechanics as a Multidisciplinary Science, Rogier (ed.) Balkema, Rotterdam, 1991, p231.

Kry, R.: Personal Communication, approximately January, 1987.

Kry, R. and Leshchyshyn,T.H.: "Fracture Orientation Observations from an Athabasca Oil Sands Cyclic Steam Stimulation Project", presented at CIM Conference, 1992.

Karampudi, R.S.: "Evaluation of Cyclic Steam Performance and Mechanisms in Mobile Heavy Oil Reservoir at Elk Point Thermal Pilot," CIM 93-48, Annual Technical Conference, Calgary, May, 1993.

Kumar, D., H.N. Patel and E.S. Denbina: "Use of a Gravity Override Model of Steam Flooding at Cold Lake," Canadian Heavy Oil Association Reservoir Handbook, CIM 1986.

Kumar, Mridul and K.C. Hong: "Effects of Wellbore Steam Segregation on Steamflood Performance," SPE Reservoir Engineering, February, 1992, pp52 – 58.

Leshchyshyn, T.H., K. Beadall, and M. Saltuklaroglu: "Results for Steam Front Calculations for IP4 and IP5 using Mandl-Volek Calculations," Internal memorandum, Petro-Canada, July, 1983.

Leshchyshyn,T.H. and Walter Seyer: "In Situ Oil Sands Temperature Logging," presented at Canadian Heavy Oil Association Symposium, 1989.

Leshchyshyn,T.H. and Walter Seyer: "Three Field Techniques to Estimate the Effective Permeability and Fracture Properties in the Athabasca Oil Sands," presented at CIM/SPE Conference, 1990.

Leshchyshyn,T.H., Walter Seyer, and Ian Langdon: "Hall Plot and Fracture Growth Analysis as Applied to the PCEJ Cyclic Steam Process in the McMurray Oil Sands," presented at the Canadian Heavy Oil Association Symposium, 1991.

Leshchyshyn,T.H. and Wayne Kennedy: "Post Core Analysis to Determine the Steam Flow Path in the McMurray Oilsands," presented at CIM Conference, 1991,published in JCPT, September 1994.

Leshchyshyn,T.H., S.M. Farouq Ali, A. Settari and M.Y. Chan: "Estimation of Dilation from Fall-off Data in a Hydraulically Fractured McMurray Oil Sands Well,"presented at CIM/AOSTRA Conference, Calgary, Alberta, June, 1994.

Leshchyshyn,T.H., S.M. Farouq Ali, and Mark Chan: "A Practical Method for Improving the Accuracy of Well Test Analysis," presented at CIM/AOSTRA Conference, Banff, Alberta, May, 1995,and JCPT, January, 1999.

Leshchyshyn,T.H., S.M. Farouq Ali and A. Settari: "Mini-frac Analysis of Shear Parting in Alberta Reservoirs and its Impact Towards On-site Fracture Design," presented at CIM Conference, Calgary, Alberta, 1996.

Leshchyshyn,T.H., P. Meier, G. Simpson and K. Welsh: "Comparison of Fracturing a Vertical, Deviated, and Horizontal Gas well in the Glauconite Formation of Central Alberta," presented at SPE Conference, Calgary, Alberta, 1997.

Leshchyshyn,T.H.: "Analytical Technique for Estimating Cold Lake Cyclic Steam Performance Including Application to Other Oil Sands and Heavy Oil Reserves," student paper presented at CIM Conference, Calgary, Alberta, 1998.

Leshchyshyn, T.H. and Alex Reed: "Well Testing & Tiltmeter Monitoring of Slurry Fracture Injection: 400 Tonne Waste Sand/day into 1000 md Reservoirs," presented to Special Interest Group, Well Testing Chapter of CIM, February, 1999, no hand-out, powerpoint slides available upon request.

Leshchyshyn, T.H., Archie Poleschuk, Keith Hemke, Malcolm A. Lamb: "Technical & Economic Rationalization of Oil Re-fracture Programs on Wells Previously Stimulated with Water-based Fracture Fluids," CIM 99-60, 50th Annual Technical Meeting, Calgary Alberta,June,1999.

Mandel, G. and C.W. Volek: "Heat and Mass Transport in Steam-Drive Processes," J. Pet. Tech., March, 1969, pp59 - 79.

Mar, A. and T. Leshchyshyn: "Interfacial Phenomena During In Situ Recovery of Bitumen Using Steam," presented at AOSTRA Conference, 1980.

Marx, J.W. and R.H. Langenheim: "Reservoir Heating by Hot Fluid Injection," Trans. AIME, 1959, p216, pp312-315.

Matthews, C.S. and H.C. Lefkovits: "Gravity Drainage Performance of Depletion-Type Reservoirs in the Stripper Stage," Journal of Petroleum Technology, Vol. 207, 1956, pp265 – 272.

McGee, B.C.W., J.E. Arthur and D.A. Best: "Analytical Analysis of Cyclic Steam Stimulation Through Vertical Fractures," Petroleum Society of CIM, Paper number 87-38-41, June, 1987, pp655 – 670.

Mehrotra, Anil K. and William Y. Svrcek: "Correlations for Properties of Bitumen Saturated with CO2, CH4, and N2, and Experiments with Combustion Gas Mixtures," Journal of Canadian Petroleum Technology, November-December, 1982, pp95 – 104.

Mehrotra, Anil K. and William Y. Svrcek: "Correlation and Prediction of Gas Solubility in Cold Lake Bitumen," Canadian Journal of Chemical Engineering, Volume 66, August, 1988, pp666 – 669.

Meldau, Robert F., Robert G. Shipley, Keith H. Coats: "Cyclic Gas/Steam Stimulation of Heavy-Oil Wells," Journal of Petroleum Techno;ogy, October, 1981, pp1990 – 1998.

Meyer, B.R.: "Heat Transfer in Hydraulic Fracturing," SPE paper number 17041, October,1987, pp133 – 151.

Miller, M.A. and W.K. Leung: "A Simple Gravity Overide Model of Steamdrive," SPE paper number 14241, September, 1985.

Miller, Karl A.: "Heavy Oil and Bitumen – Not Glamorous, but Often Profitable," Journal of Canadian Petroleum Technology, Distinguished Authors Series, April 1994, Volume 33, No.4, pp13 – 15.

Mossop, G.D., J.W. Kramers, P.D. Flach and B.A. Rottenfusser, "The Future of Heavy Crude and Tar Sands," McGraw Hill Inc., 1981, ch. 25.

Mukherjee, Hemanta and Michael J. Economides: "A Parametric Comparison of Horizontal and Vertical Well Performance," SPE paper number 18303, October, 1988, pp411 – 419.

Mukherjee, H, B. Poe, H. Heidt and R.D. Baree: " Effect of Pressure Depletion on Fracture Geometry Evolution and Production Performance," SPE 30481, presented at the SPE Annual Technical Conference and Exhibition held in Dallas, U.S.A., October 22-25, 1995.

Nakornthap, K. and Ronald D. Evans: "Temperature-Dependent Relative Permeability and its Effect on Oil Displacement by Thermal Methods," SPE Reservoir Engineering, May, 1986, pp230 – 242.

Narayan, S.P., Z. Yang and S.S. Rahman: "Propant Free-Shear Dilation: An Emerging Technology for Exploiting Tight to Ultra-tight Gas Resources," SPE paper no. 49251, New Orleans, September, 1998.

Nolte, K.G.: "Discussion of Examination of a Cored hydraulic Fracture in a Deep Gas Well," SPE Production and Facilities, August, 1993, p159.

Nzekwu,Ben I., Richard J. Hallam and G.J.J. Williams: "Interpretation of Temperature Observations From a Cyclic-Steam/In-Situ-Combustion Project," SPE Reservoir Engineering, May, 1990.

Palmer, I.D. and R.W. Veatch: "Abnormally High Fracturing Pressures in Step-rate Tests," SPEPE, August, 1990, p315, Trans., AIME p289.

Pang, H.W.: "Hysteresis Effect on Heavy Oil Recoveries During a Single Well Cyclic Steam Process," Unsolicited, April, 1982, SPE paper number 10945.

Patel, H.N., J.H. Masliyah and J. Mathews: "One-Dimensional Numerical Model for Cyclic Steam Injection in an Oil Reservoir," Oil Sands, 1977, pp411 – 418.

PCEJ internal reports, Petro-Canada, 1988-1991.

Pethrick, W.D., E.S. Sennhauser and T.G. Harding: "Numerical Modelling of Cyclic Steam Stimulation in Cold Lake Oil Sands," Journal of Canadian Petroleum Technology, November-December, 1988, Volume 27, No. 6, pp89 – 97.

Petro-Canada, discussions with Petro-Canada personnel, 1995.

Prats, Michael: "A Current Appraisal of Thermal Recovery," Journal of Petroleum Technology, August, 1978, pp1129 – 1136.

Reis, J.C.: "Studies of Fractures Induced During Cyclic Steam Injection," SPE number 20033, Ventura California, April, 1990, pp187 – 196.

Rubin, M.B.: "On Fluid Leak-Off During Propagation of a Vertical Hydraulic Fracture," U.S.M.S., Paper no. 10556, August, 1981.

Savoie, C.L.: "Practical Applications of X-radiography Techniques in Tarsands: Paper No. 70, 4th UNITAR/UNDP Conference on Heavy Crude and Tarsands, Edmonton, Alberta, August, 1988.

Schmidt,T. and T. Leshchyshyn: "Diffussion of CO_2 into Bitumen," CIM, 1982.

Schuler, Siegfried and Rene Santos: "Fraced Horizontal Well Shows Potential of Deep Tight Gas," Oil & Gas Journal, January 8, 1996, pp46-53.

Scott, J.D.: Work performed by the University of Alberta on PCEJ McMurray Formation oil sands cores, 1989.

Scott, J.D., D. Adhikary and S.A. Proskin: "Volume and Permeability Changes Associated with Steam Stimulation in an Oil Sands Reservoir," Preprint Paper number CIM/AOSTRA 91-63, 1991.

Scott, J.D., personal communication, 1991.

Seba, R.D. and G.E. Perry: "A mathematical Model of Repeated Steam Soaks of Thick Gravity Drainage Reservoirs," J. Pet. Tech., January, 1969, pp87 - 94.

Settari, A. and J.M. Raisbeck: "Fracture Mechanics Analysis in In-Situ Oil Sands Recovery," Journal of Canadian Petroleum Technology, April-June, 1979, pp86 – 94.

Settari, A. and J.M. Raisbeck: "Analysis and Numerical Modeling of Hydraulic Fracturing During Cyclic Steam Stimulation in Oil Sands," Journal of Petroleum Technology, November, 1981, pp2201 – 2212.

Settari, A.: "Physics and Modeling of Thermal Flow and Soil Mechanics in Unconsolidated Porous Media," SPE paper number 18420, February, 1989, pp155 – 168.

Shepherd, D.W.: "Predicting Bitumen Recovery From Steam Stimulation," World Oil, September, 1979, pp68 – 72.

Sinclair, A. Richard: "Heat Transfer Effects in Deep Well Fracturing," Journal of Petroleum Technology, December, 1971, pp1484 – 1492.

Smith-Magowan, David, Arne Skauge and Loren G. Hepler: "Specific Heats of Athabasca Oil Sands and Components," Journal of Canadian Petroleum Technology, May-June, 1982, pp28 – 32.

Soliman, M.Y.: "Interpretation of Pressure Behavior of Fractured, Deviated and Horizontal Wells," SPE paper number 21062,October, 1990.

Souza, Antonio Luiz S., Oswaldo A. Pedrosa Jr. and Dan Marchesin: "A New Approach for Calculating Formation Heat Losses," II Simposio Internacional Sobre Recuperacion Mejorada De Crudc, Maracaibo, Venezuala, February, 1987, SRM – 247, pp115 – 128.

Steidl, P.F.: "Evaluation of Induced Fractures Intercepted by Mining," 9377, Proceedings of the 1993 International Coalbed Methane Symposium, Birmingham, Alabama, May 17-21, 1993.

Svrcek, William Y. and Anil K. Mehrotra: "Gas Solubility, Viscosity, and Density Measurements for Athabasca Bitumen," Journal of Canadian Petroleum Technology, July-August, !982, pp31 – 38.

Svrcek, William Y. and Anil K. Mehrotra: "One Parameter Correlation for Bitumen Viscosity," Chem Eng Res Des, Vol. 66, July, 1988, pp323 – 326.

Tamim thesis, University of Alberta, 1996.

Todd, Dietrich, and Chase: Internal Petro-Canada report on First Cycle IP1 Steam Injection, 1980.

Tortike, W.S. and S.M. Farouq Ali: "Saturated-Steam-Property Functional Correlations for Fully Implicit Thermal Reservoir Simulation, SPE Reservoir Engineering, November 1989, pp471 - 473.

Tortike, W.S. and S.M. Farouq Ali: "Prediction of Oil Sand Failure due to Steam-Induced Stresses," Journal of Canadian Petroleum Technology, January-February, 1991, pp87 – 96.

Towson, D.E. and T.C.Boberg: "Gravity Drainage in Thermally Stimulated Wells," Journal of Canadian Petroleum Technology, October-December, 1967, pp130 – 135.

Towson,D.E.: "Canada's Heavy Oil Industry: A Technology Revolution," SPE 37972, International Thermal Operations and Heavy Oil Symposium, Bakersfield, February, 1997,pp513 - 523.

Van Der Ploeg, R.R., Don Kirkham and C.W. Boast: "Steady State Well Flow Theory for a Confined Elliptical Aquifer," Water Resources Research, Vol. 7, No. 4, August, 1971, pp942 – 954.

Van Wunnik, John N.M. and Krijn Wit: "Improvement of Gravity Drainage by Steam Injection into a Fractured Reservoir: An analytical Evaluation," SPE Reservoir Engineering, February, 1992, pp59 – 65.

Vinsome, P.K.W. and J. Westerveld: " A Simple Method for Predicting Cap and Base Rock Heat Losses in Thermal Reservoir Simulators," Journal of Canadian Petroleum Technology, July-September,1980, pp87 –90.

Vittoratos,E.: "Flow Regimes During Cyclic Steam Stimulation at Cold Lake," CIM/SPE 90-107, Joint International Technical Meeting of SPE and CIM,Calgary, June, 1990,pp107-1 - 107-13.

Vogel, Jack V.: "Gravity Drainage Vital for Understanding Steam Floods," Oil & Gas Journal, Nov., 1992, pp42 – 47.

Walsh Jr.,John W., H.J. Ramey Jr. and W.E. Brigham: "Thermal Injection Falloff Testing," SPE number 10227, October, 1981.

Warpinski, Norman R.: "Hydraulic Fracturing in Tight, Fissured Media," JPT, February, 1991, p146.

Warpinski, Norman R., J.C Lorenz, P.T. Branagan, F.R. Myal, and B.L. Gall: "Examination of a Cored Hydraulic Fracture in a Deep Gas Well," SPE Production and Facilities, August, 1993, p 150.

Warpinski, N.R., B.P. Engler, C.J. Young, R. Peterson and P.T. Branagan: "Microseismic Mapping of Hydraulic Fractures Using Multi-level Wireline Receivers," SPE 30507, presented at the SPE Annual Technical Conference & Exhibition held in Dallas, U.S.A., October 22-25, 1995.

Weijers, L., C.J. dePater, K.A. Owens and H.H. Kogsboll: "Geometry of Hydraulic Fractures Induced From Horizontal Wellbores," SPE 25049, presented at the European Petroleum Conference held in Cannes, France, November 16-18, 1992.

Wheeler, J.A.: "Analytical Calculations for Heat Transfer from Fractures," SPE paper number 2494, 1969.

Whitsitt, N.F. and G.R. Dysart: "The Effect of Temperature on Stimulation Design," Journal of Petroleum Technology, April, 1970, pp493 – 502.

Williamson,A.S., L.P. Dake and [illegible] Chappelear: "A Steam-Soak Model for an Isothermal Reservoir Simulator," SPE paper number 5739, 1975?.

Wright, C.A. and R.A. Conant: "Hydraulic Fracture Reorientation in Primary and Secondary Recovery from Low-permeability Reservoirs," SPE 30484, presented at the SPE Annual Technical Conference & Exhibition held in Dallas, U.S.A., October 22-25, 1995.

APPENDIX A

PHOP Pilot and Single Well Tests

Summary of Injection and Production Data

Table A1.1c
Summary of Injection and Production Data, WOR,PDOR,CDOR, and SOR by Well for PHOP Pilot

Well	Cycle	Cum Steam m3	Injection Days	Cum oil Production m3	Cum water Production m3	Producing Days	Total Days	WOR** m3/m3	PDOR** m3/d	CDOR** m3/d	SOR**
IP-1	1*	4200	27	193	280	19	46	1.45	10.16	4.20	21.76
	2*	3010	35	482	277	27	62	0.57	17.85	7.77	6.24
	3	4959	26	475	2816	62	88	5.93	7.66	5.40	10.44
	4	4194	51	925	6777	183	234	7.33	5.05	3.95	4.53
	5	4384	38	796	3485	138	176	4.38	5.77	4.52	5.51
	6	5976	38	1027	4024	191	229	3.92	5.38	4.48	5.82
	7	6822	58	713	2054	177	235	2.88	4.03	3.03	9.57
	Subtotal	**33545**	**273**	**4611**	**19713**	**797**	**1070**	**4.28**	**5.79**	**4.31**	**7.27**
IP-2	1	4882	27	304	939	30	57	3.09	10.13	5.33	16.06
	2	5390	91	623	1087	155	246	1.74	4.02	2.53	8.65
	3	4722	38	962	2493	141	179	2.59	6.82	5.37	4.91
	4	5305	38	1209	2671	191	229	2.21	6.33	5.28	4.39
	5	6559	58	1105	3441	177	235	3.11	6.24	4.70	5.94
	Subtotal	**26858**	**252**	**4203**	**10631**	**694**	**946**	**2.53**	**6.06**	**4.44**	**6.39**
IP-3	1	4869	24	330	546	36	60	1.65	9.17	5.50	14.75
	2A	5750	72	556	1658	95	167	2.98	5.85	3.33	10.34
	2B	1022	12	237	994	57	69	4.19	4.16	3.43	4.31
	3	6714	52	1021	3085	212	264	3.02	4.82	3.87	6.58
	4	6585	58	838	1364	178	236	1.63	4.71	3.55	7.86
	Subtotal	**24940**	**218**	**2982**	**7647**	**578**	**796**	**2.56**	**5.16**	**3.75**	**8.36**
IP-4	1	5036	29	602	1990	61	90	3.31	9.87	6.69	8.37
	2A	5900	72	461	885	95	167	1.92	4.85	2.76	12.80
	2B	1113	12	223	424	53	65	1.90	4.21	3.43	4.99
	3	7611	53	889	3177	212	265	3.57	4.19	3.35	8.56
	4	6692	58	773	1513	161	219	1.96	4.80	3.53	8.66
	Subtotal	**26352**	**224**	**2948**	**7989**	**582**	**806**	**2.71**	**5.07**	**3.66**	**8.94**
IP-5	1	7054	41	770	8118	61	102	10.54	12.62	7.55	9.16
	2	5124	50	856	2623	133	183	3.06	6.44	4.68	5.99
	3	5239	39	1432	3440	197	236	2.40	7.27	6.07	3.66
	4	6154	34	1023	1845	180	214	1.80	5.68	4.78	6.02
	Subtotal	**23571**	**164**	**4081**	**16026**	**571**	**735**	**3.93**	**7.15**	**5.55**	**5.78**
IP-6	1	3219	46	45	431	29	75	9.58	1.55	0.60	71.53
	2	4600	50	200	1141	59	109	5.71	3.39	1.83	23.00
	Subtotal	**7819**	**96**	**245**	**1572**	**88**	**184**	**6.42**	**2.78**	**1.33**	**31.91**
IP-7	1	5838	32	419	465	32	64	1.11	13.09	6.55	13.93
	2	4384	51	1411	1702	183	234	1.21	7.71	6.03	3.11
	3	2645	38	610	1002	142	180	1.64	4.30	3.39	4.34
	4	3697	38	977	1718	188	226	1.76	5.20	4.32	3.78
	5	6620	58	591	5067	178	236	8.57	3.32	2.50	11.20
	Subtotal	**23184**	**217**	**4008**	**9954**	**723**	**940**	**2.48**	**5.54**	**4.26**	**5.78**
IP-8	1	5339	33	435	1132	41	74	2.60	10.61	5.88	12.27
	2	4920	47	1178	685	164	211	0.58	7.18	5.58	4.18
	3	5008	31	975	1480	110	141	1.52	8.86	6.91	5.14
	4	5949	34	1171	6318	228	262	5.40	5.14	4.47	5.08
	5	6808	39	1468	2758	235	274	1.88	6.25	5.36	4.64
	Subtotal	**28024**	**184**	**5227**	**12373**	**778**	**962**	**2.37**	**6.72**	**5.43**	**5.36**
	Total	**194293**	**1628**	**28305**	**85905**	**4811**	**6439**	**3.03**	**5.88**	**4.40**	**6.86**

* IP-1 1st & 2nd cycles were performed as single well tests prior to the pilot construction

** WOR = water/oil ratio, PDOR = producing day oil rate, CDOR = calendar day oil rate, SOR = steam/oil ratio

Table A1.1a
Summary of Injection and Production Data by Well for PHOP Pilot

Well	Cycle	Cum Steam m3	Average Rate m3/d	Average Quality %	Average Pressure kPa	Injection Days	Cum oil Production m3	Cum water Production m3	Producing Days	Total Days
IP-1	1	4200	155		10200	27	193	280	19	46
	2	3010	88			35	482	277	27	62
	3*	4959	190	80	11224	26	475	2816	62	88
	4	4194	82	77	11335	51	925	6777	183	234
	5	4384	115	79	11030	38	796	3485	138	176
	6	5976	157	75	11504	38	1027	4024	191	229
	7	6822	118	75	11857	58	713	2054	177	235
	Subtotal	**33545**				**273**	**4611**	**19713**	**797**	**1070**
IP-2	1	4882	181	68	10186	27	304	939	30	57
	2	5390	59	79	6574	91	623	1087	155	246
	3	4722	124	79	11093	38	962	2493	141	179
	4	5305	140	75	11127	38	1209	2671	191	229
	5	6559	113	75	11110	58	1105	3441	177	235
	Subtotal	**26858**				**252**	**4203**	**10631**	**694**	**946**
IP-3	1	4869	203	81	10658	24	330	546	36	60
	2A	5750	80	74	11322	72	556	1658	95	167
	2B	1022	85			12	237	994	57	69
	3	6714	129	77	12872	52	1021	3085	212	264
	4	6585	114	75	11756	58	838	1364	178	236
	Subtotal	**24940**				**218**	**2982**	**7647**	**578**	**796**
IP-4	1	5036	174	79	10115	29	602	1990	61	90
	2A	5900	82	74	11428	72	461	885	95	167
	2B	1113	92			12	223	424	53	65
	3	7611	144	76	11842	53	889	3177	212	265
	4	6692	115	75	11682	58	773	1513	161	219
	Subtotal	**26352**				**224**	**2948**	**7989**	**582**	**806**
IP-5	1	7054	172	78	10478	41	770	8118	61	102
	2	5124	103	79	10881	50	856	2623	133	183
	3	5239	134	64	11010	39	1432	3440	197	236
	4	6154	181	77	12444	34	1023	1845	180	214
	Subtotal	**23571**				**164**	**4081**	**16026**	**571**	**735**
IP-6	1	3219	70	80	9268	46	45	431	29	75
	2	4600	92	69	12257	50	200	1141	59	109
	Subtotal	**7819**				**96**	**245**	**1572**	**88**	**184**
IP-7	1	5838	182	81	10922	32	419	465	32	64
	2	4384	86	79	11796	51	1411	1702	183	234
	3	2645	50	79	11596	38	610	1002	142	180
	4	3697	97	75	12677	38	977	1718	188	226
	5	6620	114	75	10423	58	591	5067	178	236
	Subtotal	**23184**				**217**	**4008**	**9954**	**723**	**940**
IP-8	1	5339	162	75	11151	33	435	1132	41	74
	2	4920	105	79	11400	47	1178	685	164	211
	3	5008	162	63	11508	31	975	1480	110	141
	4	5949	175	80	11838**	34	1171	6318	228	262
	5	6808	175	70	11780	39	1468	2758	235	274
	Subtotal	**28024**				**184**	**5227**	**12373**	**778**	**962**
	Total	**194293**				**1628**	**28305**	**85905**	**4811**	**6439**

* IP-1 1st & 2nd cycles were performed as single well tests prior to the pilot construction

** Tubing pressure as casing pressure guage malfunctioned

Table A1.1b

Summary of Injection and Production Data and Depletion Index by Well for PHOP Pilot

Well	Cycle	Cycle Steam m3	Cum Steam m3	Cycle oil Production m3	Cum oil Production m3	Cycle water Production m3	Cum water Production m3	Cycle Depletion Index m3/m3	Cum Depletion Index m3/m3	Cum fluid Left in Reservoir m3
IP-1	1*	4200	4200	193	193	280	280	0.11	0.11	3727
	2*	3010	7210	482	675	277	557	0.25	0.17	5978
	3	4959	12169	475	1150	2816	3373	0.66	0.37	7646
	4	4194	16363	925	2075	6777	10150	1.84	0.75	4138
	5	4384	20747	796	2871	3485	13635	0.98	0.80	4241
	6	5976	26723	1027	3898	4024	17659	0.85	0.81	5166
	7	6822	33545	713	4611	2054	19713	0.41	0.73	9221
	Subtotal	**33545**		**4611**		**19713**		**0.73**		
IP-2	1	4882	4882	304	304	939	939	0.25	0.25	3639
	2	5390	10272	623	927	1087	2026	0.32	0.29	7319
	3	4722	14994	962	1889	2493	4519	0.73	0.43	8586
	4	5305	20299	1209	3098	2671	7190	0.73	0.51	10011
	5	6559	26858	1105	4203	3441	10631	0.69	0.55	12024
	Subtotal	**26858**		**4203**		**10631**		**0.55**		
IP-3	1	4869	4869	330	330	546	546	0.18	0.18	3993
	2A	5750	10619	556	886	1658	2204	0.39	0.29	7529
	2B	1022	11641	237	1123	994	3198	1.20	0.37	7320
	3	6714	18355	1021	2144	3085	6283	0.61	0.46	9928
	4	6585	24940	838	2982	1364	7647	0.33	0.43	14311
	Subtotal	**24940**		**2982**		**7647**		**0.43**		
IP-4	1	5036	5036	602	602	1990	1990	0.51	0.51	2444
	2A	5900	10936	461	1063	885	2875	0.23	0.36	6998
	2B	1113	12049	223	1286	424	3299	0.58	0.38	7464
	3	7611	19660	889	2175	3177	6476	0.53	0.44	11009
	4	6692	26352	773	2948	1513	7989	0.34	0.42	15415
	Subtotal	**26352**		**2948**		**7989**		**0.42**		
IP-5	1	7054	7054	770	770	8118	8118	1.26	1.26	-1834
	2	5124	12178	856	1626	2623	10741	0.68	1.02	-189
	3	5239	17417	1432	3058	3440	14181	0.93	0.99	178
	4	6154	23571	1023	4081	1845	16026	0.47	0.85	3464
	Subtotal	**23571**		**4081**		**16026**		**0.85**		
IP-6	1	3219	3219	45	45	431	431	0.15	0.15	2743
	2	4600	7819	200	245	1141	1572	0.29	0.23	6002
	Subtotal	**7819**		**245**		**1572**		**0.23**		
IP-7	1	5838	5838	419	419	465	465	0.15	0.15	4954
	2	4384	10222	1411	1830	1702	2167	0.71	0.39	6225
	3	2645	12867	610	2440	1002	3169	0.61	0.44	7258
	4	3697	16564	977	3417	1718	4887	0.73	0.50	8260
	5	6620	23184	591	4008	5067	9954	0.85	0.60	9222
	Subtotal	**23184**		**4008**		**9954**		**0.60**		
IP-8	1	5339	5339	435	435	1132	1132	0.29	0.29	3772
	2	4920	10259	1178	1613	685	1817	0.38	0.33	6829
	3	5008	15267	975	2588	1480	3297	0.49	0.39	9382
	4	5949	21216	1171	3759	6318	9615	1.26	0.63	7842
	5	6808	28024	1468	5227	2758	12373	0.62	0.63	10424
	Subtotal	**28024**		**5227**		**12373**		**0.63**		
	Total	**194293**		**28305**		**85905**		**0.59**		**80083**

* IP-1 1st & 2nd cycles were performed as single well tests prior to the pilot construction

Table A1.2

Summary of 11-10 Injection-Production Data as of February 28, 1985

Cumulative:	First Cycle	Second Cycle	Third Cycle	Fourth Cycle	Total
Oil Produced, m3	635	310	16.9	370.2	1332.1
Water Produced, m3	3057.8	2394.1	744.1	2717.8	8913.8
Injection Days	46	21.3	6.55	29.7	103.55
Slug Size, m3	10046	3341	1045.9	4031	18463.9
Average Rate, m3/d	221.8	128.5	130.7	135.2	
Average Pressure, kPa	8851	7623.6	7572.8	8146.7	
Average Quality	79.1	60.8	75.5	73.4	
Producing Days	109.9	71.8	19.25	66.34	267.29
Producing Day, m3/d	3.8	4.3	0.81	5.4	
Calendar Day, m3/d	3.6	3.1	0.6	3.6	
Water Rate, m3/d	27.8	33.3	38.6	41.2	
Steam/Oil Ratio	15.8	10.8	61.6	10.9	
Water/Oil Ratio	4.8	7.7	43.8	7.3	
Calendar Days	179	99	29	102	409
Downtime, %	12.9	5.96	11.03	5.69	

Table A1.3

Summary of 10-34 Injection-Production Data as of February 28, 1985

Cumulative:	First Cycle	Second Cycle	Third Cycle	Fourth Cycle	Total
Oil Produced, m3	599.9	2478.2	3373.5	2860.4	9312
Water Produced, m3	4679.5	5449.5	12568	14208.5	36905.5
Injection Days	35	48	48	52	183
Slug Size, m3	5143.5	7066	10223.5	11017.2	33450.2
Average Rate, m3/d	147	147	213	212	
Average Pressure, kPa	2476	2384	2993	3117	
Average Quality	51.8	53.8	75	75.8	
Producing Days	159	143	234	255	791
Producing Day, m3/d	3.8	17.3	14.4	11.2	
Calendar Day, m3/d	2.4	12.8	11.9	9.3	
Water Rate, m3/d	29.4	38.1	53.7	55.7	
Steam/Oil Ratio	8.6	2.9	3	3.9	
Water/Oil Ratio	7.8	2.2	3.7	5	
Calendar Days	248	194	283	309	1034
Downtime, %	20.1	1.5	0.35	0.65	

Table A1.4

Summary of 11-21 Injection-Production Data as of December 31, 1984

Cumulative:	First Cycle	Second Cycle	Total
Oil Produced, m3	891.8	2211.9	3103.7
Water Produced, m3	939.7	4139.9	5079.6
Injection Days	43	69	112
Slug Size, m3	6487.8	.10124.4	16612.2
Average Rate, m3/d	150.9	146.7	
Average Pressure, kPa	8249	9241	
Average Quality	69.83	76.9	
Producing Days	89.6	157.8	247.4
Producing Day, m3/d	9.95	14	
Calendar Day, m3/d	6.28	9.33	
Water Rate, m3/d	10.32	26.23	
Steam/Oil Ratio	7.3	4.57	
Water/Oil Ratio	1.05	1.87	
Calendar Days	142	237	379
Downtime, %	4.5	2.6	

APPENDIX B

PHOP Pilot, Wells IP2 and IP8
and
Single Well Test 10-34
Daily Injection Data

Note: In this appendix, The Table Heading denotes the injection data for the individual well, for different cycles, as follows in the example:

Table BIP2IC1 for the PHOP Wells means:

Appendix "B", Well "IP2", "I"= injection, "C1" Cycle number 1

Table BW1034IC1 for the Single Well Tests means:

Appendix "B", "W"Well "10-34", "I"= injection, "C1" Cycle number 1

Table BIP2IC1

Primrose Cycle 1;   IP2 Injection Data

Date d-mmm-yy	Days	Hours on Injection	Inj Rate m^3/d	Inj pressure kPa	Temperature Degree C	Quality Percent
3-Mar-82	1.0	23	220.4	7920		33
4-Mar-82	1.9	23.7	224.6	8358	304.4	38
5-Mar-82	2.9	23	193.6	9808	302.2	61
6-Mar-82	3.6	17.8	138.7	9540	279.4	67.6
7-Mar-82	4.6	24	181.2	9633	303	80
8-Mar-82	5.5	20.3	202.8	9917	314.6	78.7
9-Mar-82	6.5	24	217.9	10816	312.5	74
10-Mar-82	7.5	24	216.6	10516	311.6	78.4
11-Mar-82	8.5	24	241.1	11516	318	71
12-Mar-82	9.2	16	154.7	10500	309.8	54.6
13-Mar-82	10.0	21	190.8	8500	303.1	58
14-Mar-82	10.9	21	144	9760	313.3	70.5
15-Mar-82	11.9	24	133.4	9680	300	74.6
16-Mar-82	12.9	24	132	9900	289	69.2
17-Mar-82	13.9	24	126.2	10100	320	74.3
18-Mar-82	14.9	24	190.8	10500	325	69.1
19-Mar-82	15.9	24	191.1			64.8
20-Mar-82	16.9	24	191.5	11000	320	67.1
21-Mar-82	17.9	24	153.2	9600	320	54.5
22-Mar-82	18.9	24	137.4	10000	320	52
23-Mar-82	19.9	24	172.5	10633	285	62.9
24-Mar-82	20.9	24	170.2	10900		83
25-Mar-82	21.8	20.5	181.70	10966	289	83.00
26-Mar-82	22.8	24	197.70	11166	292	83.30
27-Mar-82	23.8	24	213.10	11166	295	81.00
28-Mar-82	24.8	24	190.40	11183	280	79.00
29-Mar-82	25.8	24	155.10	10933	285	80.00

Table BIP2IC2

Primrose Cycle 2; IP2 Injection Data

Date d-mmm-yy	Days	Hours on Injection	Inj Rate m^3/d	Inj pressure kPa	Temperature Degree C	Quality Percent
3-Jul-82	0.5	12	20.4	2800	110	78.6
4-Jul-82	1.5	24	28.77	2600	200	80
5-Jul-82	2.5	24	29.85	2800	220	78
6-Jul-82	3.5	24	38.16	2900	210	89.7
7-Jul-82	4.5	24	36.65	2900	214	80
8-Jul-82	5.5	24	51.13	2800	205	80.1
9-Jul-82	6.5	24	51.1	2370	320	79
10-Jul-82	7.5	24	51	2205	318	79.8
11-Jul-82	8.5	24	42.9	850	320	79
12-Jul-82	9.5	24	61.8	700	320	79.8
13-Jul-82	10.5	24	14.2	600	320	80
14-Jul-82	11.5	24	22.37	950	320	80
15-Jul-82	12.5	24	13.58	1090	320	79
16-Jul-82	13.5	24	13.48	350	320	81
17-Jul-82	14.5	24	7.67	345	320	82
18-Jul-82	15.5	24	9.73	300	320	81.5
19-Jul-82	15.6	1.25	0.98	300	320	81
20-Jul-82	15.6	0				
21-Jul-82	15.6	0				
22-Jul-82	15.6	0				
23-Jul-82	15.6	0				
24-Jul-82	15.6	0				
25-Jul-82	15.6	0				
26-Jul-82	16.6	24	35	700	145	80.2
27-Jul-82	17.6	24	19	1000	155	79.3
28-Jul-82	18.6	24	18	300	120	79
29-Jul-82	19.6	24	20			76
30-Jul-82	20.6	24	6.00			78.00
31-Jul-82	21.6	24	8.00	350	150	79.00
1-Aug-82	22.6	24	8.00	500	130	81.00
2-Aug-82	23.6	24	5.00	400	130	78.00
3-Aug-82	24.6	24	10.80	385	121	78.20
4-Aug-82	25.6	24	7.33	382	121	77.8
5-Aug-82	26.6	24	17.9	360	127	78.3
6-Aug-82	27.6	24	26.1	284	120	77.8
7-Aug-82	28.2	15	18.8	258	118	80
8-Aug-82	29.2	24	29.62	235	117	81.3
9-Aug-82	30.2	24	30.08	246	115	79.6
10-Aug-82	31.2	24	5	200	103	80
11-Aug-82	32.2	24	15	800	155	79
12-Aug-82	33.2	24	20	800	165	80
13-Aug-82	34.2	24	0.25	700	160	79
14-Aug-82	35.2	24	10	600	160	84

Table BIP2IC2

Primrose Cycle 2; IP2 Injection Data

Date d-mmm-yy	Days	Hours on Injection	Inj Rate m^3/d	Inj pressure kPa	Temperature Degree C	Quality Percent
15-Aug-82	36.2	24	25	4500	255	79.5
16-Aug-82	37.2	24	45	5575	283	80
17-Aug-82	38.2	24	27.26			78.6
	38.2					
9-Sep-82	39.2	24	20	7825	285	80.5
	39.2					
15-Sep-82	39.6	10.5	0.6			
16-Sep-82	40.2	15	28.27	9333	300	79
17-Sep-82	41.2	24	37.61	9978	315	77.4
18-Sep-82	42.2	24	73.77	9600	318	79
19-Sep-82	43.2	24	33.86			79
20-Sep-82	44.2	24	34.1	9200	320	80.1

Table BIP2IC3

Primrose Cycle 3; IP2 Injection Data

Date d-mmm-yy	Days	Hours on Injection	Inj Rate m^3/d	Inj pressure kPa	Temperature Degree C	Quality Percent
1-May-83		PRODUCTION				
2-May-83		PRODUCTION				
3-May-83		PRODUCTION				
4-May-83		PRODUCTION				
5-May-83		PRODUCTION				
6-May-83		PRODUCTION				
7-May-83		PRODUCTION				
8-May-83		PRODUCTION				
9-May-83		PRODUCTION				
10-May-83		PRODUCTION				
11-May-83		PRODUCTION				
12-May-83		PRODUCTION				
13-May-83		PRODUCTION				
14-May-83		PRODUCTION				
15-May-83		PRODUCTION				
16-May-83		PRODUCTION				
17-May-83		PRODUCTION				
18-May-83		PRODUCTION				
19-May-83		SHUT IN				
20-May-83		SHUT IN				
21-May-83		SHUT IN				
22-May-83		SHUT IN				
23-May-83	1	6.5	-	800	112	80.00
24-May-83	2	24	-	600	175	80.40
25-May-83	3	24	90.40	5500	244	79.00
26-May-83	4	24	119.35	8000	330	79.70
27-May-83	5	24	112.65	9100	330	76.50
28-May-83	6	24	108.55	10500	330	75.00
29-May-83	7	24	103.21	11000	330	76.00
30-May-83	8	24	122.38	11250	330	81.50
31-May-83	9	24	124.62	11800	330	80.70
1-Jun-83	10	24	98.48	12000	243	80.95
2-Jun-83	11	24	96.81	12000	247	79.50
3-Jun-83	12	24	92.20	12000	290	79.00
4-Jun-83	13	24	97.02	12600	291	79.80
5-Jun-83	14	24	96.39	11900	273	79.60
6-Jun-83	15	24	94.79	12000	262	80.20
7-Jun-83	16	24	98.88	12000	330	80.30
8-Jun-83	17	24	141.22	13000	330	78.60
9-Jun-83	18	24	145.00	14000	330	76.40
10-Jun-83	19	24	154.70	13000	330	77.80
11-Jun-83	20	24	158.03	12900	330	79.20
12-Jun-83	21	24	171.02	12500	330	79.90

Table BIP2IC3

Primrose Cycle 3; IP2 Injection Data

Date d-mmm-yy	Days	Hours on Injection	Inj Rate m^3/d	Inj pressure kPa	Temperature Degree C	Quality Percent
13-Jun-83	22	24	179.01	12500	330	80.00
14-Jun-83	23	24	176.70	12900	330	78.50
15-Jun-83	24	24	171.50	12950	271	78.40
16-Jun-83	25	24	165.20	13000	250	80.70
17-Jun-83	26	24	160.70	13000	251	80.00
18-Jun-83	27	24	157.80	13000	258	80.00
19-Jun-83	28	24	159.80	13000	259	80.80
20-Jun-83	29	24	159.50	12900	250	80.60
21-Jun-83	30	24	146.47	12800	330	80.50
22-Jun-83	31	24	146.70	12500	330	76.80
23-Jun-83	32	24	145.90	12500	330	79.00
24-Jun-83	33	24	141.60	12500	330	80.30
25-Jun-83	34	24	137.10	12400	330	80.50
26-Jun-83	35	24	134.60	12300	330	80.00
27-Jun-83	36	24	143.20	12500	330	80.00
28-Jun-83	37	24	142.00	12400	330	80.20
29-Jun-83	38	9	27.60	12400	258	80.90
30-Jun-83	39	SOAK		6600		

Table BIP2IC4

Primrose Cycle 4; IP2 Injection Data

Date d-mmm-yy	Days	Hours on Injection	Inj Rate m^3/d	Inj pressure kPa	Temperature Degree C	Quality Percent
1-Nov-83		PRODUCTION				
2-Nov-83		PRODUCTION				
3-Nov-83		PRODUCTION				
4-Nov-83		PRODUCTION				
5-Nov-83		PRODUCTION				
6-Nov-83		PRODUCTION				
7-Nov-83		PRODUCTION				
8-Nov-83		PRODUCTION				
9-Nov-83		PRODUCTION				
10-Nov-83		PRODUCTION				
11-Nov-83		PRODUCTION				
12-Nov-83		PRODUCTION				
13-Nov-83		PRODUCTION				
14-Nov-83		PRODUCTION				
15-Nov-83		PRODUCTION				
16-Nov-83		PRODUCTION				
17-Nov-83		PRODUCTION				
18-Nov-83		PRODUCTION				
19-Nov-83		PRODUCTION				
20-Nov-83		SHUT IN				
21-Nov-83		SHUT IN				
22-Nov-83		SHUT IN				
23-Nov-83		SHUT IN				
24-Nov-83		SHUT IN				
25-Nov-83		SHUT IN				
26-Nov-83		SHUT IN				
27-Nov-83	1	24	WARM UP	650		
28-Nov-83	2	24	WARM UP	2500	245	
29-Nov-83	3	24	WARM UP	4750	302	
30-Nov-83	4	24	140*	6000	250	82.00
1-Dec-83	5	22	155*	7200	322	79.00
2-Dec-83	6	24	144.7*	9000	320	79.00
3-Dec-83	7	24	140*	10400	321	79.00
4-Dec-83	8	24	149.08	11600	318	79.00
5-Dec-83	9	24	142.03	12300	323	81.00
6-Dec-83	10	24	129.71	12300	325	81.00
7-Dec-83	11	24	144.46	12350	300	82.00
8-Dec-83	12	24	140.29	12200	330	82.00
9-Dec-83	13	24	180.83	12325	330	82.00
10-Dec-83	14	24	205.50	12150	330	81.00
11-Dec-83	15	24	184.36	12200	330	80.00
12-Dec-83	16	24	154.70	12350	315	67.00
13-Dec-83	17	24	158.56	12000	295	49.00

Table BIP2IC4

Primrose Cycle 4; IP2 Injection Data

Date d-mmm-yy	Days	Hours on Injection	Inj Rate m^3/d	Inj pressure kPa	Temperature Degree C	Quality Percent
14-Dec-83	18	24	149.06	12200	305	51.00
15-Dec-83	19	24	147.67	12200	304	52.00
16-Dec-83	20	24	140.20	11800	298	49.00
17-Dec-83	21	24	157.04	11200	295	50.00
18-Dec-83	22	24	149.04	10800	292	60.76
19-Dec-83	23	24	143.26	10500	296	69.60
20-Dec-83	24	24	135.66	10700	294	79.70
21-Dec-83	25	24	131.58	10450	288	79.00
22-Dec-83	26	24	133.05	11100	328	77.00
23-Dec-83	27	24	127.52	10700	330	77.00
24-Dec-83	28	24	132.31	10800	330	85.00
25-Dec-83	29	24	133.11	10900	330	77.40
26-Dec-83	30	24	133.78	11000	330	79.00
27-Dec-83	31	24	133.80	11000	330	78.20
28-Dec-83	32	24	136.40	11000	330	79.00
29-Dec-83	33	24	129.67	11100	295	81.30
30-Dec-83	34	24	131.39	11000	300	81.50
31-Dec-83	35	24	129.67	11200	300	80.50
1-Jan-84	36	24	128.28	11200	300	79.30
2-Jan-84	37	24	131.30	11300	305	82.70
3-Jan-84	38	24	130.50	11300	330	81.30
4-Jan-84	39	24	126.79	11400	330	82.00
5-Jan-84	40	24	120.46	12200	330	80.00
6-Jan-84	41	24	124.09	11400	330	82.75
7-Jan-84	42	SOAK				
8-Jan-84	43	SOAK				
9-Jan-84		PRODUCING				

Table BIP2IC5

Primrose Cycle 5; IP2 Injection Data

Date d-mmm-yy	Days	Hours on Injection	Inj Rate m^3/d	Inj pressure kPa	Temperature Degree C	Quality Percent
1-Sep-84	1	24	101.90	13000	330	76.00
2-Sep-84	2	24	119.90	13000	327	76.00
3-Sep-84	3	24	124.80	12800	330	73.00
4-Sep-84	4	24	140.00	13500	328	77.50
5-Sep-84	5	24	129.62	13600	329	73.00
6-Sep-84	6	24	125.04	13700	326	78.00
7-Sep-84	7	24	135.37	13550	329	79.30
8-Sep-84	8	24	118.15	13600	330	79.00
9-Sep-84	9	24	121.42	13250	330	79.10
10-Sep-84	10	24	126.14	13500	330	81.00
11-Sep-84	11	24	130.03	13500	330	78.60
12-Sep-84	12	24	139.20	13500	328	79.50
13-Sep-84	13	24	116.80	13000	329	77.00
14-Sep-84	14	24	136.10	13000	330	76.00
15-Sep-84	15	24	129.40	13000	330	80.00
16-Sep-84	16	24	125.30	13000	331	75.60
17-Sep-84	17	24	129.90	13000	330	77.00
18-Sep-84	18	24	126.10	13000	330	80.00
19-Sep-84	19	24	121.37	13000	330	78.00
20-Sep-84	20	24	128.04	13000	330	81.00
21-Sep-84	21	24	123.06	12850	327	81.80
22-Sep-84	22	24	76.60	12000	324	76.00
23-Sep-84	23	24	44.15	11250	325	79.00
24-Sep-84	24	24	45.95	10750	325	79.00
25-Sep-84	25	17	27.97	11000	325	79.00

Table BIP8IC1

Primrose Cycle 1; IP8 Injection Data

Date d-mmm-yy	Days	Hours on Injection	Inj Rate m^3/d	Inj pressure kPa	Temperature Degree C	Quality Percent
13-Mar-82	0.9	21	41.9	7800	275.8	58
14-Mar-82	1.8	21	72	9280	305.1	70.5
15-Mar-82	2.8	24	118.3	9800	295	74.6
16-Mar-82	3.8	24	117.6	9900	242	69.2
17-Mar-82	4.8	24	120	10300	320	74.3
18-Mar-82	5.8	24	168.5	10600	325	69.1
19-Mar-82	6.8	24	197.3	10700		64.8
20-Mar-82	7.6	20	204.4	10800	330	67.1
21-Mar-82	8.6	24	118.7	9800	320	54.5
22-Mar-82	9.6	24	114.2	9950	320	52
23-Mar-82	10.6	24	152.9	10825	264	62.9
24-Mar-82	11.6	24	182.6			83
25-Mar-82	12.6	24	192.2	11140	303	83
26-Mar-82	13.6	24	214.2	11500	300	83
27-Mar-82	14.6	24	204.8	11667		81
28-Mar-82	15.6	24	159.4	11526	280	79
29-Mar-82	16.6	24	159.6	11500	285	80
30-Mar-82	17.6	24	216	11508	220	74.5
31-Mar-82	18.6	24	207.8	12000	322	78
1-Apr-82	19.6	24	207.6	11633	321	80
2-Apr-82	20.6	24	185.2	11983	318.5	78.5
3-Apr-82	21.6	24	208	12258	322	81.9
4-Apr-82	22.6	24	195	12408	322	81.5
5-Apr-82	23.6	24	196.4	12241	322	81.3
6-Apr-82	24.6	24	194.6	12260	323	81.2
7-Apr-82	25.6	24	160.3	11900	325	76
8-Apr-82	26.6	24	224.4	12100	325	72
9-Apr-82	27.6	24	193.6	11825	325	79.4
10-Apr-82	28.6	24	191.1	11525	325	78.9
11-Apr-82	28.8	6	47.9	11500	325	79
2-Jul-82	29.8	22.5	136.08	10625	215	78.6
3-Jul-82	30.8	24	133.07	12250	320	80
4-Jul-82	31.5	17	23.46	12166	330	80

Table BIP8IC2

Primrose Cycle 2; IP8 Injection Data

Date d-mmm-yy	Days	Hours on Injection	Inj Rate m^3/d	Inj pressure kPa	Temperature Degree C	Quality Percent
25-Jul-82	1.0	24	174.63	6820	290	52.4
26-Jul-82	2.0	24	145.96	10500	297	80.2
27-Jul-82	3.0	24	86	12000	300	79.3
28-Jul-82	4.0	24	85	12000	300	79
29-Jul-82	5.0	24	126.31	13000	310	76
30-Jul-82	6.0	24	93.22	12700	310	78
31-Jul-82	7.0	24	104.29	12000	293	79
1-Aug-82	8.0	24	104	12000	290	81
2-Aug-82	9.0	24	118.3	12100	290	78
3-Aug-82	10.0	24	118	12320	290	78.2
4-Aug-82	11.0	24	117.31	12110	291	77.8
5-Aug-82	12.0	24	150.4	12490	300	78.3
6-Aug-82	13.0	24	103.9	12000	306	77.8
7-Aug-82	13.6	15	70.04	11600	305	80
8-Aug-82	14.6	24	98.58	11580	297	81.3
9-Aug-82	15.6	24	97.75	11920	308	79.6
10-Aug-82	16.6	24	112	11500	305	80
11-Aug-82	17.6	24	120	11750	310	79
12-Aug-82	18.6	24	128	11400	310	80
13-Aug-82	19.6	24	125	11400	310	79
14-Aug-82	20.6	24	98.17	11000	310	84
15-Aug-82	21.6	24	92.72	11475	305	79.5
16-Aug-82	22.6	24	74.83	10000	300	80
17-Aug-82	23.6	24	88.62	10240	300	73.6
18-Aug-82	24.6	24	109.7	10600	309	79.7
19-Aug-82	25.6	24	111.1	11370	311	78.6
20-Aug-82	26.5	20.5	101.62	11410	307	78.7
21-Aug-82	27.5	24	111.77	11490	310	80.6
22-Aug-82	28.5	24	104.26	11570	308	81.2
23-Aug-82	29.5	24	101.36	11430	308	80.3
24-Aug-82	30.5	24	99.65	11500	315	81
25-Aug-82	31.5	24	93.52	11600	320	80
26-Aug-82	32.5	24	99.52	11650	325	79
27-Aug-82	33.5	24	101.41	11600	323	77
28-Aug-82	34.5	24	96.45	11600	323	77
29-Aug-82	35.5	24	107.56	11700	325	78.6
30-Aug-82	36.5	24	114.52	11700	325	85
31-Aug-82	37.5	24	114.4	12050	326	77.4
1-Sep-82	38.5	24	104.05	12050	325	78.2
2-Sep-82	39.5	24	112.8	12180	326	80.4
3-Sep-82	40.5	24	113.94	12300	326	81.1
4-Sep-82	41.5	24	101.17	12240	327	77.6
5-Sep-82	42.5	24	115.91	12280	327	80.2
6-Sep-82	43.5	24	84	11260	304	81.5

Table BIP8IC2

Primrose Cycle 2; IP8 Injection Data

Date d-mmm-yy	Days	Hours on Injection	Inj Rate m^3/d	Inj pressure kPa	Temperature Degree C	Quality Percent
7-Sep-82	44.5	24	82	8900	300	82
8-Sep-82	45.5	24	80	8600	300	81
9-Sep-82	46.1	14	26.4	8600	303	80.5

Table BIP8IC3

Primrose Cycle 3; IP8 Injection Data

Date d-mmm-yy	Days	Hours on Injection	Inj Rate m^3/d	Inj pressure kPa	Temperature Degree C	Quality Percent
5-Mar-83	0.4	10.5		4350	237	
6-Mar-83	1.4	24	188.3	9400	282	60
7-Mar-83	2.0	14.5	90.23	9100	282	78.9
8-Mar-83	2.0	0	0			
9-Mar-83	2.5	12	114.71	12400		
10-Mar-83	3.5	24	190	13000	300	81
11-Mar-83	4.5	24	191.62	13200	320	79
12-Mar-83	5.5	24	184.2	13200	320	76.5
13-Mar-83	6.5	24	180.24	13200	320	72
14-Mar-83	7.5	24	140.11	13000	310	81
15-Mar-83	8.5	24	131	12000	300	79.4
16-Mar-83	9.5	24	152.62	12400	301	79.6
17-Mar-83	10.5	24	109.85	12400	301	79.8
18-Mar-83	11.5	24	137.51	11950	297	79.3
19-Mar-83	12.5	24	188.81	13000	300	78.2
20-Mar-83	13.5	24	195.05	13400	317	79.8
21-Mar-83	14.5	24	186.78	13300	319	80.1
22-Mar-83	15.5	24	186.08	13400	320	80
23-Mar-83	16.5	24	189.3	13200	320	82
24-Mar-83	17.5	24	190.5	13800	320	
25-Mar-83	18.5	24	187.21	13800	320	80
26-Mar-83	19.5	24	187.47	12750	320	81.5
27-Mar-83	20.5	24	185.21	12800	320	80
28-Mar-83	21.5	24	184	12750	315	80
29-Mar-83	22.5	24	171.1	12700	315	79.9
30-Mar-83	23.5	24	170.6	12600	316	78.7
31-Mar-83	24.5	24	173.10	12600	315	79.90
1-Apr-83	25.5	24	180.12	12300	315	
2-Apr-83	26.5	23	187.14	12200	300	
3-Apr-83	27.5	23.25	186.11	12200	285	80.20
4-Apr-83	28.5	24	179.24	12400	289	80.50
5-Apr-83	29.0	12.5	70.22	12500	286	80.00

Table BIP8IC4

Primrose Cycle 4; IP8 Injection Data

Date d-mmm-yy	Days	Hours on Injection	Inj Rate m^3/d	Inj pressure kPa	Temperature Degree C	Quality Percent
29-Jul-83	0.3	6.3	10.8		200	80
30-Jul-83	1.3	24	41		207	79.5
31-Jul-83	2.3	24	183.9		270	78.7
1-Aug-83	3.3	24	192.4		270	80
2-Aug-83	4.3	24	149.87	5800	269	81
3-Aug-83	5.3	24	156.09	6500	333	79.6
4-Aug-83	6.3	24	156.59	7600	333	77.2
5-Aug-83	7.3	24	151.49	9000	334	82.7
6-Aug-83	8.3	24	144.34	9800	335	81
7-Aug-83	9.3	24	164.16	12000	333	78
8-Aug-83	10.3	24	182	12500	334	81.8
9-Aug-83	11.3	24	169.95		336	80.6
10-Aug-83	12.3	24	159.3		337	81.9
11-Aug-83	13.3	24	129.36		337	81.4
12-Aug-83	14.3	24	167.74		335	80.8
13-Aug-83	15.3	24	167.1		335	80.1
14-Aug-83	16.3	24	159.9		335	81.1
15-Aug-83	17.3	24	167.54		334	81
16-Aug-83	18.3	24	160.4		334	80
17-Aug-83	19.3	24	158.48		333	81
18-Aug-83	20.3	24	159.6		333	79
19-Aug-83	21.3	24	177.9		333	81
20-Aug-83	22.3	24	197.2		332	79
21-Aug-83	23.3	24	206.7		333	79
22-Aug-83	24.3	24	224.5		333	79
23-Aug-83	25.3	24	229.5		335	78.6
24-A[illegible]-83	26.3	24	234.10		335	80.90
25-Aug-83	27.3	24	239.40		334	80.10
26-Aug-83	28.3	24	227.80		334	80.00
27-Aug-83	29.3	24	242.20		334	79.80
28-Aug-83	30.3	24	234.10		334	80.00
29-Aug-83	31.3	24	210.80		333	80.60
30-Aug-83	32.3	24	194.70		330	81.00
31-Aug-83	33.3	24	198.00		330	81.00

Table BIP8IC5

Primrose Cycle 5; IP8 Injection Data

Date d-mmm-yy	Days	Hours on Injection	Inj Rate m^3/d	Inj pressure kPa	Temperature Degree C	Quality Percent
22-Apr-84	1.0	24	288.59	8000	285	15
23-Apr-84	2.0	24	229.02	8400	281	75
24-Apr-84	3.0	24	207.51	9300	278	85
25-Apr-84	3.8	19.5	163.8	9400	325	81
26-Apr-84	4.8	24	181.46	8500	320	70
27-Apr-84	5.8	24	201.6	11300	320	78
28-Apr-84	6.8	24	194.29	12500	324	78
29-Apr-84	7.8	24	175.96	13000	317	78
30-Apr-84	8.8	24	190.63	12900	310	81
1-May-84	9.8	24	190.63	12500	315	80
2-May-84	10.8	24	194.3	12700	311	83
3-May-84	11.8	24	192.92	12700	305	67.5
4-May-84	12.8	24	195.82	12750	315	77
5-May-84	13.8	24	194.3	13600	315	74.5
6-May-84	14.8	24	192.46	12600	315	73
7-May-84	15.8	24	192.46	12800	315	73
8-May-84	16.8	24	182.38	12800	315	73
9-May-84	17.8	24	175.96	12750	315	74
10-May-84	18.8	24	177.8	12800	315	75.3
11-May-84	19.8	24	179.63	12700	315	75
12-May-84	20.8	24	179.84	12500	312	72
13-May-84	21.8	24	176.33	12500	312	71
14-May-84	22.8	24	177.51	12700	312	74.6
15-May-84	23.8	24	178.25	12600	312	78
16-May-84	24.8	24	172.3	12400	315	72
17-May-84	25.8	24	170.47	12400	315	71
18-May-84	26.8	24	169.55	12500	315	74
19-May-84	27.8	24	168.63	12500	315	75
20-May-84	28.8	24	168.63	12500	315	74
21-May-84	29.8	24	168.63	12500	314	73
22-May-84	30.8	24	168.63	12800	315	73
23-May-84	31.8	24	168.63	12600	312	75
24-May-84	32.8	24	164.97	12600	315	76
25-May-84	33.8	24	172.3	12600	315	79
26-May-84	34.8	24	168.63	12600	315	79
27-May-84	35.8	24	164.97	12700	315	79
28-May-84	36.8	24	168.6	12200	315	80
29-May-84	37.1	6	0	12200	0	0

Table BW1034IC1

Primrose Cycle 1; 10-34 Injection Data

Date d-mmm-yy	Days	Hours on Injection	Inj Rate m^3/d	Inj Pressure kPa	Temperature Degree C	Quality Percent
28-Feb-82	0	4	76.80	4720	240	10.00
1-Mar-82	1	24	252.00			10.00
2-Mar-82	2	24	157.00			10.00
3-Mar-82	2	2	29.00			10.00
4-Mar-82	3	24	160.00			9.00
5-Mar-82	4	24	252.00			48.00
6-Mar-82	5	24	252.00			63.00
7-Mar-82	5	1	13.80			66.00
8-Mar-82	5	3	42.60			50.00
9-Mar-82	6	4	67.50			50.00
10-Mar-82	6	4	43.70			25.00
11-Mar-82	6	3	98.20			34.00
12-Mar-82	6	2	38.00			45.00
13-Mar-82	6	3	45.00			40.00
14-Mar-82	7	24	124.40			
15-Mar-82	8	24	174.40	5283	227	66.00
16-Mar-82	9	24	172.00	5340	237	71.00
17-Mar-82	10	24	145.00	4440	234	69.00
18-Mar-82	11	24	174.00	4760	242	80.00
19-Mar-82	12	24	174.00			77.80
20-Mar-82	13	24	168.00	4750	242	78.00
21-Mar-82	14	24	167.00	4790	242	80.00
22-Mar-82	15	24	185.00	4720	240	78.00
23-Mar-82	16	24	155.00	4600	230	66.00
24-Mar-82	17	24	187.00			
25-Mar-82	18	24	197.00	3200	220	70.00
26-Mar-82	19	24	197.00	3300	228	79.00
27-Mar-82	20	24	201.00	3450	240	78.00
28-Mar-82	21	24	189.00	3400	230	70.00
29-Mar-82	22	24	197.00	3400	230	78.00
30-Mar-82	23	24	192.00	6620	220	80.00
31-Mar-82	24	24	184.00	4262	228	70.50
1-Apr-82	25	24	168.00	2600	220	70.00
2-Apr-82	26	24	184.00	3120	227	80.00
3-Apr-82	27	12	80.00	5500	230	80.00

Table BW1034IC2

Primrose Cycle 2; 10-34 Injection Data

Date d-mmm-yy	Days	Hours on Injection	Inj Rate m^3/d	Inj Pressure kPa	Temperature Degree C	Quality Percent
19-Nov-82	0	4	135.00	3000	250	30.00
20-Nov-82	1	24	168.00	2100	250	15.00
21-Nov-82	2	24	190.00	3000		65.00
22-Nov-82	3	24	190.00	3300	268.9	73.00
23-Nov-82	4	24	190.00	3700		74.00
24-Nov-82	5	24	189.00	4033	250	75.00
25-Nov-82	6	24	99.00	3800	250	66.00
26-Nov-82	6	0				
27-Nov-82	6	0				
28-Nov-82	6	0				
29-Nov-82	6	0				
30-Nov-82	6	0				
1-Dec-82	6	0				
2-Dec-82	6	0				
3-Dec-82	6	0				
4-Dec-82	6	0				
5-Dec-82	6	0				
6-Dec-82	6	0				
7-Dec-82	6	5	40.00	2600	260	65.00
8-Dec-82	7	24	199.00	2500		77.80
9-Dec-82	8	24	199.00	3150	265	77.10
10-Dec-82	9	24	200.00	3400		77.70
11-Dec-82	10	24	203.00	3500		75.80
12-Dec-82	11	24	193.00	3500		74.00
13-Dec-82	12	24	203.00	3433		76.00
14-Dec-82	13	24	203.00	3300		74.50
15-Dec-82	14	24	208.00	3200	250	75.00
16-Dec-82	15	24	208.00	3200	240	76.00
17-Dec-82	16	24	208.00	3200	240	76.00
18-Dec-82	17	24	208.00	3100	240	76.00
19-Dec-82	18	24	208.00	3100	240	76.00
20-Dec-82	19	24	218.00			
21-Dec-82	20	24	208.00	3100	240	77.00
22-Dec-82	21	24	208.00	3200	195	75.00
23-Dec-82	22	24	208.00	3000	195	74.00
24-Dec-82	23	24	208.00	3000	190	72.00
25-Dec-82	24	24	208.00	3100	190	78.00
26-Dec-82	25	23	200.00	2600		66.00
27-Dec-82	26	24	200.00	3000		73.00
28-Dec-82	27	24	200.00	3150		76.00
29-Dec-82	28	23	187.00	3200		73.00
30-Dec-82	29	24	200.00	3200		77.00
31-Dec-82	30	24	195.00	3200		77.00

Table BW1034IC2

Primrose Cycle 2; 10-34 Injection Data

Date d-mmm-yy	Days	Hours on Injection	Inj Rate m^3/d	Inj Pressure kPa	Temperature Degree C	Quality Percent
1-Jan-83	31	24	195.00	3300		78.00
2-Jan-83	32	24	200.00	3300		78.00
3-Jan-83	33	24	200.00	3300	241	78.00
4-Jan-83	34	24	195.00	3350	240	77.50
5-Jan-83	35	24	195.00	3300		77.00

Table BW1034IC3

Primrose Cycle 3; 10-34 Injection Data

Date d-mmm-yy	Days	Hours on Injection	Inj Rate m^3/d	Inj Pressure kPa	Temperature Degree C	Quality Percent
31-May-83	0.2	4	180.00	1700	224	60.00
1-Jun-83	1.2	24	178.79	2000	232	74.00
2-Jun-83	2.0	20	208.00	2000	238	78.00
3-Jun-83	3.0	24	222.00	2200	243	79.00
4-Jun-83	4.0	24	224.00	2338	245	76.00
5-Jun-83	5.0	24	216.00	2463	245	79.00
6-Jun-83	6.0	24	219.00	2608	246	80.00
7-Jun-83	7.0	24	221.00	2634	245	77.00
8-Jun-83	8.0	24	217.00	2716	247.5	80.50
9-Jun-83	9.0	24	210.00	2750	248	78.00
10-Jun-83	10.0	24	215.00	2800	248	77.00
11-Jun-83	11.0	24	215.00	2800	248	75.00
12-Jun-83	12.0	24	216.00	2800	250	75.00
13-Jun-83	12.4	9	76.00	2800	250	77.00
14-Jun-83	12.4	0				
15-Jun-83	13.0	15	135.45	2500	240	68.00
16-Jun-83	13.8	20	216.17	2720	244	80.00
17-Jun-83	14.8	24	216.72	2850	240	81.00
18-Jun-83	15.8	24	215.18	3016	241	81.00
19-Jun-83	16.8	24	216.72	3025	239	82.00
20-Jun-83	17.8	24	216.72	3091	240	81.00
21-Jun-83	18.8	24	214.00	3120	239	80.00
22-Jun-83	19.8	24	220.00	3125	243	80.30
23-Jun-83	20.8	24	228.00	3200	243	81.20
24-Jun-83	21.8	24	233.00	3200	243	79.50
25-Jun-83	22.8	24	233.00	3200	241	80.00
26-Jun-83	23.8	24	234.00	3200	242	80.00
27-Jun-83	24.8	24	234.00	3300	244	79.00
28-Jun-83	25.8	24	234.00	3350	244	78.00
29-Jun-83	26.8	24	230.00	3375	243	77.00
30-Jun-83	27.8	24	230.26	3360	241	76.00
1-Jul-83	28.8	24	230.00	3375	243	79.00
2-Jul-83	29.8	24	230.26	3400	244	80.00
3-Jul-83	30.8	24	230.26	3425	244	78.00
4-Jul-83	31.8	24	230.26	3458	244	79.00
5-Jul-83	32.8	24	230.26	3458	244	78.00
6-Jul-83	33.8	24	233.00	3500	245	78.00
7-Jul-83	34.8	24	233.00	3550	245	77.00
8-Jul-83	35.8	24	233.00	3450	244	72.00
9-Jul-83	36.8	24	215.47	3450	241	70.27
10-Jul-83	37.8	24	227.60	3450	241	74.00
11-Jul-83	38.8	24	229.20	3450	245	76.00
12-Jul-83	39.8	24	225.40	3500	244	77.50

Table BW1034IC3

Primrose Cycle 3; 10-34 Injection Data

Date d-mmm-yy	Days	Hours on Injection	Inj Rate m^3/d	Inj Pressure kPa	Temperature Degree C	Quality Percent
13-Jul-83	40.8	24	230.26	3575	243	78.00
14-Jul-83	41.8	24	230.26	3583	243	79.00
15-Jul-83	42.8	24	230.26	3596	243	80.00
16-Jul-83	43.8	24	230.26	3600	242	80.00
17-Jul-83	44.8	24	230.00	3600	240	81.00

Table BW1034IC4

Primrose Cycle 4; 10-34 Injection Data

Date d-mmm-yy	Days	Hours on Injection	Inj Rate m^3/d	Inj Pressure kPa	Temperature Degree C	Quality Percent
12-Mar-84	1	24	188.61	3200	210	39.30
13-Mar-84	2	24	159.30	4300	210	71.70
14-Mar-84	3	24	151.70		265	79.00
15-Mar-84	4	24	148.99	2300	265	81.30
16-Mar-84	5	24	173.37	2250	275	79.00
17-Mar-84	6	24	189.63	2250	275	79.00
18-Mar-84	7	24	223.89	2600	275	80.00
19-Mar-84	8	24	219.42	2600	282	78.00
20-Mar-84	9	24	219.42	2625	282	75.00
21-Mar-84	10	24	216.72	2700	282	76.20
22-Mar-84	11	24	216.72	2750	282	75.00
23-Mar-84	12	24	212.20	2820	280	74.00
24-Mar-84	13	24	207.69	2865	282	76.00
25-Mar-84	14	24	205.88		282	75.00
26-Mar-84	15	24	211.87		280	76.00
27-Mar-84	16	24	218.07			78.60
28-Mar-84	17	24	214.01	3200	282	79.00
29-Mar-84	18	24	211.30	3100	282	79.00
30-Mar-84	19	24	216.72	3100	285	80.00
31-Mar-84	20	24	222.13	3200	285	80.00
1-Apr-84	21	24	220.78	3200	284	80.00
2-Apr-84	22	24	219.42	3250	284	80.00
3-Apr-84	23	24	227.55	3250	284	78.00
4-Apr-84	24	24	227.56	3250	285	76.40
5-Apr-84	25	24	225.39	3400	285	
6-Apr-84	26	24	225.12	3400	285	77.00
7-Apr-84	27	24	224.85	3400	285	76.50
8-Apr-84	28	24	224.85	3550	285	77.00
9-Apr-84	29	24	224.85	3550	286	77.00
10-Apr-84	30	24	223.49	3550	286	77.00
11-Apr-84	31	24	223.49	3500	285	77.00
12-Apr-84	32	24	223.40	3600	285	77.00
13-Apr-84	33	24	220.80	3600	285	78.00
14-Apr-84	34	24	222.13	3600	285	79.00
15-Apr-84	35	24	223.40	3650	286	80.00
16-Apr-84	36	24	224.80	3700	285	73.00
17-Apr-84	37	24	223.50	3800	285	78.00
18-Apr-84	38	24	218.75	3750	265	78.00
19-Apr-84	39	24	221.60	3750	285	77.00
20-Apr-84	40	24	222.14	3750	286	78.00
21-Apr-84	41	24	221.46	3750	286	78.50
22-Apr-84	42	24	222.73	3750	286	78.50
23-Apr-84	43	24	221.46	3775	286	78.00

Table BW1034IC4

Primrose Cycle 4; 10-34 Injection Data

Date d-mmm-yy	Days	Hours on Injection	Inj Rate m^3/d	Inj Pressure kPa	Temperature Degree C	Quality Percent
24-Apr-84	44	24	221.32	3800	286	77.00
25-Apr-84	45	24	220.80	3850	286	80.00
26-Apr-84	46	24	219.40	3850	286	82.00
27-Apr-84	47	24	220.80	3850	286	80.40
28-Apr-84	48	24	219.40	3850	286	82.00
29-Apr-84	49	24	216.70	3850	286	80.00
30-Apr-84	50	24	216.70	3800	286	80.00
1-May-84	51	24	216.72	3800	286	80.00
2-May-84	52	12	104.23	3800	286	80.00

APPENDIX C

PHOP Pilot, Wells IP2 and IP8

and

Single Well Test 10-34

Daily Production Data

Note: In this appendix, The Table Heading denotes the production data for the individual well, for different cycles, as follows in the example:

Table CIP2PC1 for the PHOP Wells means:

Appendix "C", Well "IP2", "P"= production, "C1" Cycle number 1

Table BW1034PC1 for the Single Well Tests means:

Appendix "B", "W"Well "10-34", "P"= production, "C1" Cycle number 1

Table CIP2PC1

Primrose Cycle 1; IP2 Production Data

Date d-mmm-yy	Days	Hours on Production	Oil Produced m^3	Water Produced m^3	Fluid Level Joints	Casing Pressure kPa	Wellhead Temperature Deg C	Total Fluid Produced m^3
31-Mar-82	0.6	14	13.2	30.3				43.5
1-Apr-82	1.6	24	13.2	60.11				73.31
2-Apr-82	2.6	24	13.2	52.76				65.96
3-Apr-82	3.6	24	13.2	37.5				50.7
4-Apr-82	4.6	24	13.2	56.08				69.28
5-Apr-82	5.6	24	13.2	70.78				83.98
6-Apr-82	6.3	16	13.2	14.86				28.06
7-Apr-82	6.3	0	0	0				0
8-Apr-82	6.3	0	0	0				0
9-Apr-82	7.3	24	13.2	25.32				38.52
10-Apr-82	8.3	24	13.2	30.12				43.32
11-Apr-82	9.3	24	13.2	30.6				43.8
12-Apr-82	10.3	24	13.2	24.53				37.73
13-Apr-82	11.3	24	13.2	16.25				29.45
14-Apr-82	12.3	24	13.2	26.15				39.35
15-Apr-82	13.3	24	10.2	25.18				35.38
16-Apr-82	14.3	24	13	21.05				34.05
17-Apr-82	15.3	24	6.82	21.96				28.78
18-Apr-82	16.3	24	11	25.18				36.18
19-Apr-82	17.3	24	7	28.89				35.89
20-Apr-82	18.3	24	6.38	19.62				26
21-Apr-82	19.3	24	11	39.25				50.25
22-Apr-82	20.3	24	9	47.77				56.77
23-Apr-82	21.3	24	9	27.92				36.92
24-Apr-82	22.3	24	10.2	19.63				29.83
25-Apr-82	23.3	24	15	19.07				34.07

Table CIP2PC1

Primrose Cycle 1;   IP2 Production Data

Date d-mmm-yy	Days	Hours on Production	Oil Produced m^3	Water Produced m^3	Fluid Level Joints	Casing Pressure kPa	Wellhead Temperature Deg C	Total Fluid Produced m^3
26-Apr-82	24.3	24	9.57	24.36				33.93
27-Apr-82	25.3	24	4	23.2				27.2
28-Apr-82	26.3	24	3	23.53				26.53
29-Apr-82	27.3	24	3	23.32				26.32
30-Apr-82	28.3	24	3	23.28				26.28
1-May-82	29.3	24	1	50.24				51.24

Table CIP2PC2

Primrose Cycle 2; IP2 Production Data

Date d-mmm-yy	Days	Hours on Production	Oil Produced m^3	Water Produced m^3	Fluid Level Joints	Casing Pressure kPa	Wellhead Temperature Deg C	Total Fluid Produced m^3
4-Nov-82	0.3	8.0	8.4	17.1		3500.0	116.0	25.5
5-Nov-82	1.3	24.0	8.4	17.1		3200.0	122.0	25.5
6-Nov-82	2.3	24.0	8.4	17.1	full	1800.0	110.0	25.5
7-Nov-82	3.3	24.0	8.4	17.1		850.0	90.0	25.5
8-Nov-82	4.3	24.0	8.4	17.1		400.0	66.0	25.5
9-Nov-82	5.3	24.0	8.4	17.1		400.0	66.0	25.5
10-Nov-82	6.3	24.0	8.4	17.1		500.0	70.0	25.5
11-Nov-82	7.3	24.0	8.4	17.1		400.0	96.0	25.5
12-Nov-82	8.3	24.0	8.4	17.1		400.0	91.0	25.5
13-Nov-82	9.3	24.0	8.4	17.1		0.0	90.0	25.5
14-Nov-82	10.3	24.0	8.4	17.1		0.0	84.0	25.5
15-Nov-82	11.3	24.0	8.4	17.1		0.0	83.0	25.5
16-Nov-82	12.3	24.0	8.4	17.1		0.0	82.0	25.5
17-Nov-82	13.3	24.0	8.4	17.1		0.0	80.0	25.5
18-Nov-82	14.3	24.0	8.4	17.1	42.0	0.0	78.0	25.5
19-Nov-82	15.3	24.0	8.4	20.7	27.0	0.0	74.0	29.0
20-Nov-82	16.3	24.0	8.4	20.7	25.0	0.0	73.0	29.0
21-Nov-82	17.3	24.0	0.0	18.7		0.0	66.0	18.7
22-Nov-82	17.5	4.0	0.0	18.7	21.0	0.0	65.0	18.7
23-Nov-82	17.5	0.0			SHUT IN			
24-Nov-82	18.0	11.0	0.0	33.8	18.0	0.0	42.0	33.8
25-Nov-82	19.0	24.0	13.3	9.0	13.0	0.0	40.0	22.2
26-Nov-82	20.0	24.0	6.1	3.6	9.0	0.0	30.0	9.7
27-Nov-82	21.0	24.0	6.1	3.6	8.0	0.0	24.0	9.7
28-Nov-82	22.0	24.0	7.4	3.8	6.0	0.0	23.0	11.2
29-Nov-82	23.0	24.0	7.4	3.8	7.0	0.0	21.0	11.2

Table CIP2PC2

Primrose Cycle 2; IP2 Production Data

Date d-mmm-yy	Days	Hours on Production	Oil Produced m^3	Water Produced m^3	Fluid Level Joints	Casing Pressure kPa	Wellhead Temperature Deg C	Total Fluid Produced m^3
30-Nov-82	24.0	24.0	7.4	3.8	6.0	0.0	20.0	11.2
1-Dec-82	25.0	24.0	4.1	2.0	7.0	0.0	19.0	6.1
2-Dec-82	26.0	24.0	4.1	2.0		0.0	18.0	6.1
3-Dec-82	27.0	24.0	6.7	0.7		0.0	13.0	7.3
4-Dec-82	28.0	24.0	4.4	2.5	4.0	0.0	9.0	6.8
5-Dec-82	29.0	24.0	3.7	35.7		0.0	9.0	39.4
6-Dec-82	30.0	24.0	5.2	1.5	5.0	0.0	6.0	6.6
7-Dec-82	31.0	24.0	5.2	1.5	2.0	0.0	0.0	6.6
8-Dec-82	32.0	24.0	5.6	0.4	4.0	0.0	23.0	5.9
9-Dec-82	33.0	24.0	5.6	0.4	5.0	0.0	24.0	5.9
10-Dec-82	34.0	24.0	4.8	1.6	2.0	0.0	17.0	6.4
11-Dec-82	35.0	24.0	4.8	1.6	3.0	0.0	22.0	6.4
12-Dec-82	36.0	24.0	3.6	1.9	4.0	0.0	27.0	5.5
13-Dec-82	37.0	24.0	3.6	1.9	4.0	0.0	26.0	5.5
14-Dec-82	38.0	24.0	3.2	1.5	4.0	0.0	25.0	4.8
15-Dec-82	39.0	24.0	3.2	1.5	3.0	0.0	25.0	4.8
16-Dec-82	40.0	24.0	3.2	1.5	4.0	0.0	30.0	4.8
17-Dec-82	41.0	24.0	4.3	0.2	4.0	0.0	26.0	4.5
18-Dec-82	42.0	24.0	4.3	0.2	3.0	0.0	26.0	4.5
19-Dec-82	43.0	24.0	4.3	0.2	3.0	0.0	24.0	4.5
20-Dec-82	44.0	24.0	4.3	0.2	4.0	0.0	15.0	4.5
21-Dec-82	45.0	24.0	2.6	1.7		0.0	15.0	4.2
22-Dec-82	46.0	24.0	2.6	1.7		0.0	13.0	4.2
23-Dec-82	47.0	24.0	2.5	1.6	4.0	0.0	13.0	4.1
24-Dec-82	48.0	24.0	2.5	1.6	4.0	0.0	11.0	4.1
25-Dec-82	49.0	24.0	2.4	1.3	4.0	0.0	14.0	3.6

Table CIP2PC2

Primrose Cycle 2; IP2 Production Data

Date d-mmm-yy	Days	Hours on Production	Oil Produced m^3	Water Produced m^3	Fluid Level Joints	Casing Pressure kPa	Wellhead Temperature Deg C	Total Fluid Produced m^3
26-Dec-82	50.0	24.0	2.4	1.3	4.0	0.0	10.0	3.6
27-Dec-82	51.0	24.0	1.9	1.3	4.0	0.0	9.0	3.2
28-Dec-82	52.0	24.0	2.4	1.6	4.0	0.0	10.0	4.0
29-Dec-82	53.0	24.0	3.3	0.9	4.0	0.0	7.0	4.2
30-Dec-82	54.0	24.0	3.3	0.9			11.0	4.2
31-Dec-82	54.0	0.0			SHUT IN			
1-Jan-83	54.0	0.0			SHUT IN			
2-Jan-83	54.0	0.0			SHUT IN			
3-Jan-83	54.0	0.0			SHUT IN			
4-Jan-83	54.0	0.0			SHUT IN			
5-Jan-83	54.0	0.0			SHUT IN			
6-Jan-83	54.0	0.0			SHUT IN			
7-Jan-83	54.0	0.0			SHUT IN			
8-Jan-83	54.0	0.0			SHUT IN			
9-Jan-83	54.0	0.0			SHUT IN			
10-Jan-83	54.0	0.0			SHUT IN			
11-Jan-83	54.0	0.0			SHUT IN			
12-Jan-83	54.4	10.0	1.8	2.1	6.0	20.0	3.9	
13-Jan-83	55.4	24.0	5.3	6.4	4.0	20.0	11.6	
14-Jan-83	56.4	24.0	4.2	3.7	6.0	0.0	20.0	7.8
15-Jan-83	57.4	24.0	4.2	3.7	5.0	0.0	12.0	7.8
16-Jan-83	58.4	24.0	2.5	3.8	5.0	0.0	50*	6.3
17-Jan-83	59.4	24.0	2.5	3.8	4.0	0.0	50*	6.3
18-Jan-83	60.4	24.0	2.8	4.1	3.0	0.0	22.0	6.9
19-Jan-83	61.4	24.0	3.3	2.1	6.0	0.0	18.0	5.3
20-Jan-83	62.4	24.0	3.3	2.1	5.0	0.0	10.0	5.3

Table CIP2PC2

Primrose Cycle 2; IP2 Production Data

Date d-mmm-yy	Days	Hours on Production	Oil Produced m^3	Water Produced m^3	Fluid Level Joints	Casing Pressure kPa	Wellhead Temperature Deg C	Total Fluid Produced m^3
21-Jan-83	63.4	24.0	3.3	2.1	5.0	0.0	10.0	5.3
22-Jan-83	64.4	24.0	3.3	2.1	5.0	0.0	8.0	5.3
23-Jan-83	65.4	24.0	3.3	2.1	5.0	0.0	0.0	5.3
24-Jan-83	66.4	24.0	3.3	2.1	4.0	0.0	4.0	5.4
25-Jan-83	67.4	24.0	3.5	0.8		0.0	0.0	4.3
26-Jan-83	68.4	24.0	3.5	0.8		0.0	6.0	4.3
27-Jan-83	69.4	24.0	3.5	0.8	5.0	0.0	18.0	4.3
28-Jan-83	70.4	24.0	3.5	0.8		0.0	50.0	4.3
29-Jan-83	71.4	24.0	1.4	3.1	2.0	0.0	28.0	4.5
30-Jan-83	72.4	24.0	1.4	3.1	6.0	0.0	0.0	4.5
31-Jan-83	73.4	24.0	1.4	3.1	4.0	0.0	0.0	4.5
1-Feb-83	74.4	24.0	1.9	4.1	3.0	0.0	0.0	6.1
2-Feb-83	75.4	24.0	1.9	4.1	4.0	0.0	0.0	6.1
3-Feb-83	76.4	24.0	1.0	4.1	3.0	0.0	0.0	5.1
4-Feb-83	77.4	24.0	1.0	4.1	5.0	0.0	0.0	5.1
5-Feb-83	78.3	21.0	1.7	1.2	5.0	0.0	0.0	2.9
6-Feb-83	79.3	24.0	2.0	1.3	2.0	0.0	0.0	3.3
7-Feb-83	80.3	24.0	2.0	1.3	3.0	0.0	0.0	3.3
8-Feb-83	81.3	24.0	1.0	0.7	4.0	0.0	12.0	1.7
9-Feb-83	82.3	24.0	1.0	0.7	4.0	0.0	4.0	1.7
10-Feb-83	83.3	24.0	1.0	0.7	4.0	10.0	1.7	
11-Feb-83	84.3	24.0	2.2	1.3	4.0	4.0	3.4	
12-Feb-83	85.3	24.0	2.2	1.3	3.0	0.0	18.0	3.4
13-Feb-83	86.3	24.0	2.2	1.3	1.0	0.0	18.0	3.4
14-Feb-83	87.3	24.0	2.2	1.3	2.0	0.0	20.0	3.4
15-Feb-83	88.3	24.0	2.3	2.5	4.0	0.0	10.0	4.8

Table CIP2PC2

Primrose Cycle 2; IP2 Production Data

Date d-mmm-yy	Days	Hours on Production	Oil Produced m^3	Water Produced m^3	Fluid Level Joints	Casing Pressure kPa	Wellhead Temperature Deg C	Total Fluid Produced m^3
16-Feb-83	89.3	24.0	2.3	2.5		0.0	3.0	4.8
17-Feb-83	90.3	24.0	2.3	2.5	2.0	0.0	6.0	4.8
18-Feb-83	91.3	24.0	2.3	2.5	3.0	0.0	14.0	4.8
19-Feb-83	92.3	24.0	2.3	2.5	3.0	0.0	38.0	4.8
20-Feb-83	93.3	24.0	4.7	2.8	2.0	0.0	6.0	7.5
21-Feb-83	94.3	24.0	4.7	2.8	4.0	0.0	8.0	7.5
22-Feb-83	95.3	24.0	2.5	2.0	3.0	0.0	10.0	4.5
23-Feb-83	96.3	24.0	2.5	2.0	7.0	0.0	8.0	4.5
24-Feb-83	97.3	24.0	2.5	2.0	12.0	10.0	4.5	
25-Feb-83		SHUT IN						
26-Feb-83		SHUT IN						
27-Feb-83		SHUT IN						
28-Feb-83		SHUT IN						

Table CIP2P2B

Primrose Cycle 2B; IP2 Production Data

Date d-mmm-yy	Days	Hours on Production	Oil Produced m^3	Water Produced m^3	Fluid Level Joints	Casing Pressure kPa	Wellhead Temperature Deg C	Total Fluid Produced m^3
1-Mar-83		SHUT IN						
2-Mar-83		SHUT IN						
3-Mar-83		SHUT IN						
4-Mar-83		SHUT IN						
5-Mar-83		STEAM INJECTION TEST						
6-Mar-83		STEAM INJECTION TEST						
7-Mar-83		STEAM INJECTION TEST						
8-Mar-83		STEAM INJECTION TEST						
9-Mar-83		STEAM INJECTION TEST						
10-Mar-83		STEAM INJECTION TEST						
11-Mar-83		STEAM INJECTION TEST						
12-Mar-83		STEAM INJECTION TEST						
13-Mar-83		STEAM INJECTION TEST						
14-Mar-83		STEAM INJECTION TEST						
15-Mar-83		STEAM INJECTION TEST						
16-Mar-83		STEAM INJECTION TEST						
17-Mar-83		STEAM INJECTION TEST						
18-Mar-83		STEAM INJECTION TEST						
19-Mar-83		STEAM INJECTION TEST-542 17 m3 injected						
20-Mar-83		SOAK						
21-Mar-83		SOAK						
22-Mar-83		SOAK						
23-Mar-83		SOAK						
24-Mar-83	0.27	6.5	0.54	3.42	35	0	54	3.96
25-Mar-83	1.27	24	2.02	12.62	21	0	54	14.64

Table CIP2P2B

Primrose Cycle 2B; IP2 Production Data

Date d-mmm-yy	Days	Hours on Production	Oil Produced m^3	Water Produced m^3	Fluid Level Joints	Casing Pressure kPa	Wellhead Temperature Deg C	Total Fluid Produced m^3
26-Mar-83	2.27	24	2.07	12.75	23	0	56	14.82
27-Mar-83	3.27	24	2.49	16.82	19	0	54	19.31
28-Mar-83	4.27	24	2.49	16.82	21	0	54	19.31
29-Mar-83	5.27	24	3.81	15.48	20	0	55	19.29
30-Mar-83	6.27	24	3.81	15.48	19	0	52	19.29
31-Mar-83	7.27	24	2.66	14.04	16	0	49	16.7
1-Apr-83	8.27	24	2.66	14.04	16	0	49	16.7
2-Apr-83	9.27	24	5.26	10.61	16	0	46	15.87
3-Apr-83	10.27	24	5.26	10.61	14	0	43	15.87
4-Apr-83	11.27	24	6.49	8.35	15	0	40	14.84
5-Apr-83	12.27	24	5.23	6.74	14	0	46	11.97
6-Apr-83	13.27	24	5.23	6.74	12	0	38	11.97
7-Apr-83	14.27	24	6.43	3.68	14	0	34	10.49
8-Apr-83	15.27	24	5.41	4.25	13	0	32	9.66
9-Apr-83	16.27	24	5.41	4.25	12	0	26	9.66
10-Apr-83	17.27	24	4.36	6.04	13	0	26	10.4
11-Apr-83	18.27	24	3.63	7.09		0	32	10.72
12-Apr-83	19.27	24	3.86	7.53	12	0	28	11.37
13-Apr-83	20.27	24	3.86	7.53	10	0	36	11.37
14-Apr-83	21.27	24	4.52	9.66	10	0	31	14.18
15-Apr-83	22.27	24	5.97	7.51	11	0	32	13.48
16-Apr-83	23.27	24	5.97	7.51	12	0	34	13.48
17-Apr-83	24.27	24	4.53	8.67	12	0	34	13.2
18-Apr-83	25.27	24	5.71	10.23	15	0	46	15.94
19-Apr-83	26.27	24	3.61	7.38	8	0	38	10.99
20-Apr-83	27.27	24	3.61	7.38		0	36	10.99

Table CIP2P2B

Primrose Cycle 2B; IP2 Production Data

Date d-mmm-yy	Days	Hours on Production	Oil Produced m^3	Water Produced m^3	Fluid Level Joints	Casing Pressure kPa	Wellhead Temperature Deg C	Total Fluid Produced m^3
21-Apr-83	28.27	24	3.61	7.38	13	0	35	10.99
22-Apr-83	29.27	24	4.62	9.71	10	0	34	14.33
23-Apr-83	30.23	23	3.94	5.9	13	0	44*	9.84
24-Apr-83	31.23	24	4.1	6.15	13	0	82*	10.25
25-Apr-83	32.23	24	2.04	13.67	12	0	30	15.71
26-Apr-83	33.23	24	4.55	8.56	7	0	22	13.11
27-Apr-83	34.23	24	4.25	9.54	7	0	27	13.79
28-Apr-83	35.23	24	4.25	9.54	7	0	28	13.79
29-Apr-83	36.23	24	3.71	9.15	10	0	26	12.86
30-Apr-83	37.23	24	3.99	9.84	9	0	24	13.83
1-May-83	38.23	24	5.14	8.54	9	0	29	13.68
2-May-83	38.71	11.5	0.55	0.89	8	0	24	1.44
3-May-83	38.71	0		SHUT IN				
4-May-83	38.96	6	0	6.92	17	300	40	6.92
5-May-83	39.96	24	0	27.65	8	0	38	27.65
6-May-83	40.96	24	0	27.65	8	0	31	27.65
7-May-83	41.96	24	5.4	15.95	6	0	26	21.35
8-May-83	42.96	24	4.42	7.49	3	0	29	11.91
9-May-83	43.96	24	3.95	10.28	5	0	22	14.23
10-May-83	44.96	24	4.46	11.61	5.5	0	18	16.07
11-May-83	45.96	24	4.46	11.61	4	0	20	16.07
12-May-83	46.96	24	4.66	6.08	5	0	21	10.74
13-May-83	47.96	24	4.66	6.08	5	0	14	10.74
14-May-83	48.96	24	3.61	5.31	4	0	16	8.92
15-May-83	49.96	24	3.61	5.31	6	0	20	8.92
16-May-83	50.96	24	4.75	7.09	5	0	19	11.84

Table CIP2P2B

Primrose Cycle 2B; IP2 Production Data

Date d-mmm-yy	Days	Hours on Production	Oil Produced m^3	Water Produced m^3	Fluid Level Joints	Casing Pressure kPa	Wellhead Temperature Deg C	Total Fluid Produced m^3
17-May-83	51.96	24	1.59	4.91		0	18	6.5
18-May-83	52.15	4.5	0.15	0.41		0	12	0.56
19-May-83		SHUT IN				0		

Table CIP2PC3

Primrose Cycle 3; IP2 Production Data

Date d-mmm-yy	Days	Hours on Production	Oil Produced m^3	Water Produced m^3	Fluid Level Joints	Casing Pressure kPa	Wellhead Temperature Deg C	Total Fluid Produced m^3
1-Jul-83	0.42	10	1.01	32.89	FULL		135	33.9
2-Jul-83	1.42	24	2.43	78.93	FULL		138	81.36
3-Jul-83	2.42	24	2.43	78.93	FULL		139	81.36
4-Jul-83	3.42	24	2.39	93.54	FULL		132	95.93
5-Jul-83	4.42	24	2.41	94.3	FULL	5000	130	96.71
6-Jul-83	5.42	24	2.41	94.3	FULL	4500	140	96.71
7-Jul-83	6.42	24	2.41	94.3	FULL	3900	42	96.71
8-Jul-83	7.15	17.5	1.76	68.76	FULL	0	54	70.52
9-Jul-83	7.98	20	2.01	78.58	FULL	0	25	80.59
10-Jul-83	8.85	21	2.11	82.5	FULL	200	28	84.61
11-Jul-83	9.60	18	1.82	70.73	FULL	500	24	72.55
12-Jul-83	10.46	20.5	1.98	47.47	FULL	0	83	49.45
13-Jul-83	11.46	24	1.98	47.47	FULL	0	84	49.45
14-Jul-83	12.46	24	2.33	48.45	51	0	86	50.78
15-Jul-83	13.46	24	5.84	43.3	50	0	90	49.14
16-Jul-83	14.46	24	5.84	43.3	50	0	88	49.14
17-Jul-83	15.46	24	12.38	36.52	44	0	88	48.9
18-Jul-83	16.43	23.33	11.05	36.18	42	0	86	47.23
19-Jul-83	17.43	24	10.05	23.87	41	0	88	33.92
20-Jul-83	18.43	24	10.24	26.14	40	0	86	36.38
21-Jul-83	19.43	24	9.59	25.25	40	0	84	34.84
22-Jul-83	20.43	24	9.59	25.25	36	0	88	34.84
23-Jul-83	21.43	24	8.36	25.09	35	0	87	33.45
24-Jul-83	22.43	24	5.44	29.12	32	0	83	34.56
25-Jul-83	23.43	24	5.44	29.12	30	0	84	34.56

Table CIP2PC3

Primrose Cycle 3; IP2 Production Data

Date d-mmm-yy	Days	Hours on Production	Oil Produced m^3	Water Produced m^3	Fluid Level Joints	Casing Pressure kPa	Wellhead Temperature Deg C	Total Fluid Produced m^3
26-Jul-83	24.43	24	12.05	26.2	26	0	84	38.25
27-Jul-83	25.43	24	12.05	26.2	25	0	82	38.25
28-Jul-83	26.43	24	11.87	26.13	25	0	84	38
29-Jul-83	27.43	24	17.11	24.57	25	0	83	41.68
30-Jul-83	28.43	24	14.55	28.74	21	0	88	43.29
31-Jul-83	29.43	24	18.36	24.37	20	0	84	42.73
1-Aug-83	30.41	23.5	18.5	20.47	19	0	84	38.97
2-Aug-83	31.41	24	11.98	15.18	19	0	81	27.16
3-Aug-83	32.41	24	11.49	15.29	20	0	80	26.78
4-Aug-83	33.41	24	12.51	15.18	17	0	77	27.69
5-Aug-83	34.41	24	10.15	16.15	15	0	76	26.3
6-Aug-83	35.41	24	10.05	14.27	15	0	73	24.32
7-Aug-83	36.41	24	9.98	15.4	15	0	70	25.38
8-Aug-83	37.41	24	9.96	14.05	14	0	69	24.01
9-Aug-83	38.41	24	10.01	20.34	15	0	73	30.35
10-Aug-83	39.41	24	10.01	20.34	13	0	72	30.35
11-Aug-83	40.41	24	12.59	20.41	13	0	71	33
12-Aug-83	41.41	24	12.59	20.41	13	0	66	33
13-Aug-83	42.41	24	10.31	19.16	12	0	64	29.47
14-Aug-83	43.41	24	9.78	16.5	12	0	64	29.28
15-Aug-83	44.41	24	8.55	19.76	12	0	62	28.31
16-Aug-83	45.41	24	16.88	20.47	11	0	66	37.35
17-Aug-83	46.41	24	14.68	22.65	10	0	60	37.33
18-Aug-83	47.41	24	14.46	21.01	10	0	61	35.47
19-Aug-83	48.41	24	11.44	15.88	10	0	59	27.32
20-Aug-83	49.41	24	13.5	18.34	11	0	56	31.84

Table CIP2PC3

Primrose Cycle 3;   IP2 Production Data

Date d-mmm-yy	Days	Hours on Production	Oil Produced m^3	Water Produced m^3	Fluid Level Joints	Casing Pressure kPa	Wellhead Temperature Deg C	Total Fluid Produced m^3
21-Aug-83	50.41	24	13.31	19.48	10	0	58	32.79
22-Aug-83	51.41	24	13.94	17.31	10	0	60	31.25
23-Aug-83	52.41	24	9.25	11.48	10	0	60	20.73
24-Aug-83	53.41	24	9.1	12.82	10	0	60	21.92
25-Aug-83	54.41	24	8.06	12.66	10	0	59	20.72
26-Aug-83	55.41	24	8.34	11.66	10	0	58	20
27-Aug-83	56.41	24	7.7	11.73	10	0	58	19.43
28-Aug-83	57.41	24	8.08	10.31	10	0	56	18.39
29-Aug-83	58.41	24	7.43	11.15	10	0	56	18.58
30-Aug-83	59.41	24	7.96	11.95	10	0	57	19.91
31-Aug-83	60.41	24	8.31	11.24		0	54	19.55

Table CIP2PC3A

Primrose Cycle 3A; IP2 Production Data

Date d-mmm-yy	Days	Hours on Production	Oil Produced m^3	Water Produced m^3	Fluid Level Joints	Casing Pressure kPa	Wellhead Temperature Deg C	Total Fluid Produced m^3
1-Sep-83	1.00	24	7.91	10.3		0	54	18.21
2-Sep-83	2.00	24	7.91	10.3	8	0	50	18.21
3-Sep-83	3.00	24	8.67	9.39	8	0	50	18.06
4-Sep-83	4.00	24	9.83	7.16	8	0	50	16.99
5-Sep-83	5.00	24	9.84	7.16	7.5	0	50	17
6-Sep-83	6.00	24	5.39	14.62		0	50	20.01
7-Sep-83	7.00	24	5.39	14.62	7	0	50	20.01
8-Sep-83	8.00	24	5.82	13.76		0	50	19.58
9-Sep-83	9.00	24	8.19	11.07	6	0	50	19.26
10-Sep-83	10.00	24	8.19	11.07	7	0	48	19.26
11-Sep-83	10.21	5	0	0		0		0
12-Sep-83	10.85	15.5	5.29	7.16	8	0	53	12.45
13-Sep-83	11.85	24	6.33	7.36	5	0	44	13.69
14-Sep-83	12.85	24	6.33	7.36	6	0	44	13.69
15-Sep-83	13.85	24	8.25	5.98	6	0	47	14.23
16-Sep-83	14.85	24	8.25	5.98	4	0	45	14.23
17-Sep-83	15.85	24	7.1	7.1	4	0	42	14.2
18-Sep-83	16.85	24	7.1	7.1	4	0	38	14.2
19-Sep-83	17.85	24	7.57	5.04	5	0	42	12.61
20-Sep-83	18.85	24	7.77	5.18	5	0	42	12.95
21-Sep-83	19.85	24	6.31	5.15	4	0	42	11.46
22-Sep-83	20.85	24	6.31	5.15	2	0	38	11.46
23-Sep-83	21.85	24	5.85	3.9	3	0	37	9.75
24-Sep-83	22.85	24	5.85	3.9	2	0	36	9.75
25-Sep-83	23.85	24	6.38	4.26	2	0	37	10.64

Table CIP2PC3A

Primrose Cycle 3A; IP2 Production Data

Date d-mmm-yy	Days	Hours on Production	Oil Produced m^3	Water Produced m^3	Fluid Level Joints	Casing Pressure kPa	Wellhead Temperature Deg C	Total Fluid Produced m^3
26-Sep-83	24.85	24	6.39	4.26	2	0	40	10.65
27-Sep-83	25.85	24	6.87	4.58	4	0	32	11.45
28-Sep-83	26.85	24	4.29	7.45	1	0	36	11.74
29-Sep-83	27.85	24	4.29	7.45	8	0	38	11.74
30-Sep-83	28.85	24	5.52	5.87	9	0	36	11.39
1-Oct-83	29.85	24	5.52	5.87	7	0	36	11.39
2-Oct-83	30.85	24	5.7	5.7	6	0	42	11.4
3-Oct-83	31.85	24	5.69	5.7	9	0	40	11.39
4-Oct-83	32.85	24	5.69	5.7	12	0	40	11.39
5-Oct-83	33.85	24	5.69	5.7	10	0	38	11.39
6-Oct-83	34.85	24	4.79	6.63	10	0	38	11.42
7-Oct-83	35.85	24	4.79	6.63	9	0	38	11.42
8-Oct-83	36.85	24	4.65	6.21	12	0	36	10.86
9-Oct-83	37.85	24	4.65	6.21	11	0	36	10.86
10-Oct-83	38.85	24	4.75	6.65	8	0	34	11.4
11-Oct-83	39.85	24	4.1	6.95	5	0	38	11.05
12-Oct-83	40.85	24	4.09	6.95	3	0	37	11.04
13-Oct-83	41.85	24	3.98	6.76		0	37	10.74
14-Oct-83	42.85	24	3.99	6.76	7	0	34	10.75
15-Oct-83	43.85	24	5.21	4.6	8	0	30	9.81
16-Oct-83	44.85	24	5.21	4.6	5	0	31	9.81
17-Oct-83	45.85	24	5.21	4.6	6	0	32	9.81
18-Oct-83	46.85	24	5.21	4.6	8	0	30	9.81
19-Oct-83	47.85	24	5.21	4.6	9	0	30	9.81
20-Oct-83	48.85	24	3.02	4.52	8	0	32	7.54
21-Oct-83	49.85	24	3.02	4.52	5	0	30	7.54

Table CIP2PC3A

Primrose Cycle 3A; IP2 Production Data

Date d-mmm-yy	Days	Hours on Production	Oil Produced m^3	Water Produced m^3	Fluid Level Joints	Casing Pressure kPa	Wellhead Temperature Deg C	Total Fluid Produced m^3
22-Oct-83	50.85	24	2.93	4.31	2	0	30	7.24
23-Oct-83	51.85	24	3.19	4.7	6	0	28	7.89
24-Oct-83	52.85	24	2.85	5.69	6	0	26	8.54
25-Oct-83	53.85	24	2.85	5.69	9	0	23	8.54
26-Oct-83	54.85	24	3.92	6.34	6	0	25	10.26
27-Oct-83	55.85	24	5.08	7.33	7	0	30	12.41
28-Oct-83	56.85	24	5.08	7.33	6	0	30	14.41
29-Oct-83	57.85	24	4.59	5.2	10	0	32	9.79
30-Oct-83	58.85	24	4.59	5.2	9	0	32	
31-Oct-83	59.85	24	4.55	5.72	9	0		
1-Nov-83	60.85	24	4.54	5.72	[illegible]			
2-Nov-83	61.85	[illegible]	[illegible]	[illegible]				
3-Nov-83	62.85		[illegible]					
4-Nov-83	63.85							
5-Nov-83	64.85							
6-Nov-83	65.85							
7-Nov-83	66.85							
8-Nov-83	67.85							
9-Nov-83	68.85							
10-Nov-83	69.85							
[illegible]	[illegible]							
[illegible]	[illegible]							

	[illegible]
	[illegible]
[illegible] Nov [illegible]	[illegible]
20 Nov [illegible]	SHUT IN
21 Nov [illegible]	SHUT IN
22 Nov [illegible]	SHUT IN
23 Nov [illegible]	SHUT IN
24 Nov [illegible]	SHUT IN
25 Nov [illegible]	SHUT IN
26 Nov [illegible]	SHUT IN
27 Nov [illegible]	WARM [illegible]
	WARM [illegible]
	WARM [illegible]

Table CIP2PC4

Primrose Cycle 4; IP2 Production Data

Date d-mmm-yy	Days	Hours on Production	Oil Produced m^3	Water Produced m^3	Fluid Level Joints	Casing Pressure kPa	Wellhead Temperature Deg C	Total Fluid Produced m^3
22-Apr-84	51.60	24	7.2	3.15	0	0	48	10.35
23-Apr-84	52.60	24	9.4	4.6	0	0	45	14
24-Apr-84	53.60	24	9.4	4.6	0	0	45	14
25-Apr-84	54.60	24	9.4	4.6	6	0	42	14
26-Apr-84	55.60	24	14.07	1.27	6	0	41	15.34
27-Apr-84	56.60	24	14.07	1.27	0	0	42	15.34
28-Apr-84	57.60	24	9.36	3.85	6	0	40	13.21
29-Apr-84	58.60	24	9.38	3.85	0	0	38	13.23
30-Apr-84	59.60	24	5.3	2.18	0	0	40	7.48
1-May-84	60.60	24	5.3	2.18	7	0	40	7.48
2-May-84	61.60	24	4.81	2.07	2	0	40	6.88
3-May-84	62.60	24	4.81	2.07	0	0	43	6.88
4-May-84	63.60	24	4.81	2.07	6	0	40	6.88
5-May-84	64.60	24	4.9	2	2	0	40	6.9
6-May-84	65.60	24	4.9	2	0	0	39	6.9
7-May-84	66.60	24	4.92	2	0	0	40	6.92
8-May-84	67.60	24	5.42	4.49	0	0	38	9.91
9-May-84	68.60	24	5.42	4.49	0	0	40	9.91
10-May-84	69.60	24	5.42	4.49	0	0	40	9.91
11-May-84	70.60	24	5.14	5.2	0	0	39	10.34
12-May-84	71.60	24	5.14	5.2	0	0	39	10.34
13-May-84	72.60	24	5.14	5.2	0	0	36	10.34
14-May-84	73.60	24	8.17	2.03	0	0	38	10.2
15-May-84	74.60	24	8.17	2.03	0	0	38	10.2
16-May-84	75.60	24	8.17	2.03	0	0	37	10.2
17-May-84	76.60	24	8.17	2.03	0	0	35	10.2

Table CIP2PC4

Primrose Cycle 4; IP2 Production Data

Date d-mmm-yy	Days	Hours on Production	Oil Produced m^3	Water Produced m^3	Fluid Level Joints	Casing Pressure kPa	Wellhead Temperature Deg C	Total Fluid Produced m^3
18-May-84	77.60	24	4.32	4.68	0	0	38	9
19-May-84	78.60	24	4.5	4.52	1	0	38	9.02
20-May-84	79.60	24	4.5	4.52	0	0	37	9.02
21-May-84	80.60	24	6.33	6.36	0	0	38	12.69
22-May-84	81.60	24	2.58	12.46	1	0	37	15.04
23-May-84	82.60	24	2.58	12.46	1	0	37	15.04
24-May-84	83.60	24	9.25	3.07	1	0	38	12.32
25-May-84	84.60	24	9.25	3.07	0	0	37	12.32
26-May-84	85.60	24	7.88	4.63	0	0	37	12.51
27-May-84	86.60	24	7.88	4.63	0	0	37	12.51
28-May-84	87.60	24	8.13	4.38	1	0	37	12.51
29-May-84	88.60	24	8.14	4.38	2	0	38	12.52
30-May-84	89.60	24	7.54	7.54	7	0	38	15.08
31-May-84	90.60	24	7.54	7.54	0	0	32	15.08
1-Jun-84	91.60	24	6.91	6.89	5	0	32	13.8
2-Jun-84	92.60	24	6.91	6.89	0	0	36	13.8
3-Jun-84	93.60	24	7.21	6	6	0	36	13.21
4-Jun-84	94.60	24	7.23	6	0	0	39	13.23
5-Jun-84	95.60	24	5.83	4.85	0	0	43	10.68
6-Jun-84	96.60	24	5.83	4.85	0	0	38	10.68
7-Jun-84	97.60	24	7.07	4.15	2	0	34	11.22
8-Jun-84	98.60	24	7.07	4.15	0	0	36	11.22
9-Jun-84	99.60	24	5.04	5.79	2	0	38	10.83
10-Jun-84	100.60	24	5.04	5.79	2	0	38	10.83
11-Jun-84	101.60	24	5.04	5.79	0	0	38	10.83
12-Jun-84	102.60	24	5.04	5.79	0	0	39	10.83

Table CIP2PC4

Primrose Cycle 4; IP2 Production Data

Date d-mmm-yy	Days	Hours on Production	Oil Produced m^3	Water Produced m^3	Fluid Level Joints	Casing Pressure kPa	Wellhead Temperature Deg C	Total Fluid Produced m^3
13-Jun-84	103.60	24	5.4	4.74	2	0	39	10.14
14-Jun-84	104.60	24	5.4	4.74	0	0	38	10.14
15-Jun-84	105.60	24	5.4	4.74	0	0	38	10.14
16-Jun-84	106.60	24	6.33	4.75	0	0	38	11.08
17-Jun-84	107.60	24	6.33	4.75	0	0	37	11.08
18-Jun-84	108.60	24	5.39	5.81	0	0	38	11.2
19-Jun-84	109.60	24	5.38	5.81	0	0	37	11.19
20-Jun-84	110.60	24	4.21	4.55	0	0	34	8.76
21-Jun-84	111.60	24	4.21	4.21	2	0	33	8.42
22-Jun-84	112.60	24	4.6	2.59	1	0	34	7.19
23-Jun-84	113.60	24	4.6	2.59	1	0	39	7.19
24-Jun-84	114.60	24	4.6	2.59	1	0	34	7.19
25-Jun-84	115.60	24	3.38	4.06	1	0	30	7.44
26-Jun-84	116.60	24	3.38	4.06	1	0	32	7.44
27-Jun-84	117.60	24	3.38	4.06	0	0	35	7.44
28-Jun-84	118.60	24	3.38	4.06	0	0	35	7.44
29-Jun-84	119.60	24	4.02	3.1	2	0	35	7.12
30-Jun-84	120.60	24	4.09	3.1	0	0	35	7.19
1-Jul-84	121.60	24	4.25	3.27	0	0	34	7.52
2-Jul-84	122.60	24	3.98	2.68	2	0	35	6.66
3-Jul-84	123.60	24	3.75	11.34	2	0	38	15.09
4-Jul-84	124.60	24	3.75	11.34	2	0	40	15.09
5-Jul-84	125.60	24	3.76	11.34	0	0	40	15.1
6-Jul-84	126.60	24	3.32	3.03	0	0	34	6.35
7-Jul-84	127.60	24	3.32	3.03	0	0	30	6.35
8-Jul-84	128.60	24	3.32	3.03	0	0	34	6.35

Table CIP2PC4

Primrose Cycle 4; IP2 Production Data

Date d-mmm-yy	Days	Hours on Production	Oil Produced m^3	Water Produced m^3	Fluid Level Joints	Casing Pressure kPa	Wellhead Temperature Deg C	Total Fluid Produced m^3
9-Jul-84	129.60	24	3.32	3.03	3	0	36	6.35
10-Jul-84	130.60	24	2.77	4.43	3	0	35	7.2
11-Jul-84	131.60	24	2.77	4.43	0	0	46	7.2
12-Jul-84	132.60	24	3.91	3.43	3	0	47	7.34
13-Jul-84	133.60	24	3.91	3.43	0	0	46	7.34
14-Jul-84	134.60	24	2.8	4.41	0	0	37	7.21
15-Jul-84	135.60	24	2.8	4.41	0	0	34	7.21
16-Jul-84	136.60	24	3.03	4.78	0	0	36	7.81
17-Jul-84	137.60	24	1.98	3.14	0	0	40	5.12
18-Jul-84	138.60	24	3.03	4.78	0	0	42	7.81
19-Jul-84	139.60	24	3.03	4.78	0	0	39	7.81
20-Jul-84	140.60	24	4.37	4.46	1	0	36	8.83

Table CIP2PC4A

Primrose Cycle 4A; IP2 Production Data

Date d-mmm-yy	Days	Hours on Production	Oil Produced m^3	Water Produced m^3	Fluid Level Joints	Casing Pressure kPa	Wellhead Temperature Deg C	Total Fluid Produced m^3
1-Jan-84		INJECTION						
2-Jan-84		INJECTION						
3-Jan-84		INJECTION						
4-Jan-84		INJECTION						
5-Jan-84		INJECTION						
6-Jan-84		INJECTION						
7-Jan-84		SOAK						
8-Jan-84		SOAK						
9-Jan-84	1.00	24	0	43.5	FULL	8500	103	43.5
10-Jan-84	2.00	24	0	43.5	FULL	8500	132	43.5
11-Jan-84	3.00	24	0	43.5	FULL	5200	132	43.5
12-Jan-84	4.00	24	0	43.5	FULL	4300	135	43.5
13-Jan-84	5.00	24	0	28.4	FULL	3800	142	28.4
14-Jan-84	6.00	24	0	28.4	FULL	3400	142	28.4
15-Jan-84	7.00	24	0	28.4	FULL	2700	93	28.4
16-Jan-84	8.00	24	0	28.4	FULL	1600		28.4
17-Jan-84	9.00	24	0	28.4	FULL	100		28.4
18-Jan-84	10.00	24	0	28.4	FULL	120		28.4
19-Jan-84	11.00	24	0	28.4	FULL	120		28.4
20-Jan-84	11.00	0			SHUT IN			
21-Jan-84	11.00	0			SHUT IN			
22-Jan-84	11.00	0			SHUT IN			
23-Jan-84	11.58	14	0	17.92		0	58	17.92
24-Jan-84	12.58	24	0	35.84		0	62	35.84
25-Jan-84	13.58	24	5.48	35.84		0	60	41.32

Table CIP2PC4A

Primrose Cycle 4A; IP2 Production Data

Date d-mmm-yy	Days	Hours on Production	Oil Produced m^3	Water Produced m^3	Fluid Level Joints	Casing Pressure kPa	Wellhead Temperature Deg C	Total Fluid Produced m^3
26-Jan-84	14.58	24	5.49	35.84		1000	55	41.33
27-Jan-84	15.58	24	3.87	41.59		0	55	45.46
28-Jan-84	16.58	24	3.87	41.59		0	60	45.46
29-Jan-84	17.58	24	3.87	41.59		0	70	45.46
30-Jan-84	18.58	24	3.87	41.59		0	87	45.46
31-Jan-84	19.58	24	3.87	41.59	FULL	1100	100	45.46
1-Feb-84	20.58	24	3.87	41.59	FULL	0	105	45.46
2-Feb-84	21.58	24	3.87	41.59		700	105	45.46
3-Feb-84	22.58	24	3.87	41.59		700	102	45.46
4-Feb-84	23.58	24	7.74	41.6		700	93	45.47
5-Feb-84	24.58	24	3.95	41.6		600	95	45.55
6-Feb-84	25.58	24	5.06	54.28	FULL	500	89	59.34
7-Feb-84	26.58	24	5.06	54.28	FULL	500	94	59.34
8-Feb-84	27.58	24	5.06	54.28	FULL	500	75	59.34
9-Feb-84	28.56	23.5	12.85	30.78	25	0	55	43.63
10-Feb-84	29.56	24	12.85	30.78	25	0	57	43.63
11-Feb-84	30.56	24	12.85	30.78	26	0	50	43.63
12-Feb-84	31.56	24	23.72	18.53		0	56	42.25
13-Feb-84	32.56	24	17.36	13.57		0	57	30.93
14-Feb-84	33.56	24	17.36	13.57		0	59	30.93
15-Feb-84	34.56	24	17.36	13.57		0	60	30.93
16-Feb-84	35.56	24	18.8	15.5		0	58	34.3
17-Feb-84	36.56	24	18.8	15.5	20	0	55	34.3
18-Feb-84	37.56	24	18.8	15.5	20	0	55	34.3
19-Feb-84	38.56	24	17.16	15.98	18	0	45	33.14
20-Feb-84	39.56	24	15.15	14.13	18	0	55	29.28

Table CIP2PC4A

Primrose Cycle 4A; IP2 Production Data

Date d-mmm-yy	Days	Hours on Production	Oil Produced m^3	Water Produced m^3	Fluid Level Joints	Casing Pressure kPa	Wellhead Temperature Deg C	Total Fluid Produced m^3
21-Feb-84	40.56	24	15.15	14.13		0	48	29.28
22-Feb-84	41.56	24	15.15	14.13	14	0		29.28
23-Feb-84	42.56	24	8.19	14.85		0		23.04
24-Feb-84	43.56	24	8.19	14.85		0	80	23.04
25-Feb-84	44.56	24	11.43	14.68	FULL	0	74	26.11
26-Feb-84	45.56	24	11.45	14.68	FULL	0	72	26.13
27-Feb-84	46.56	24	13.56	17.41		0	69	30.97
28-Feb-84	47.56	24	13.56	17.41		0	68	30.97
29-Feb-84	48.56	24	13.56	17.41	FULL	0	72	30.97

Table CIP2PC5

Primrose Cycle 5; IP2 Production Data

Date d-mmm-yy	Days	Hours on Production	Oil Produced m^3	Water Produced m^3	Fluid Level Joints	Casing Pressure kPa	Wellhead Temperature Deg C	Total Fluid Produced m^3
3-Oct-84	0.3	7	0	0	0	2400	80	0
4-Oct-84	1.3	24	0	0	0	3400	100	0
5-Oct-84	2.3	24	0	0	0	3600	102	0
6-Oct-84	3.3	24	0	0	0	3600	106	0
7-Oct-84	4.3	24	0	0	0	3900	153	0
8-Oct-84	5.3	24	0	0	0	3020	122	0
9-Oct-84	6.3	24	0	0	0	3600	120	0
10-Oct-84	7.3	24	0	0	0	3200	125	0
11-Oct-84	8.3	24	0	0	0	3200	125	0
12-Oct-84	9.3	24	0	0	0	2600	110	0
13-Oct-84	10.3	24	0	0	0	2100	75	0
14-Oct-84	11.3	24	0	0	0	1000	120	0
15-Oct-84	12.3	24	0	0	0	1900	130	0
16-Oct-84	12.3	0	-	-	-	-	-	#VALUE!
17-Oct-84	12.3	0	-	-	-	-	-	#VALUE!
18-Oct-84	13.3	24	0	0	0	0	72	0
19-Oct-84	14.3	24	0	0	0	3700	102	0
20-Oct-84	15.3	24	12.5	36.46	0	3200	115	48.96
21-Oct-84	16.3	24	4.91	41.82	0	1600	117	46.73
22-Oct-84	17.3	24	4.91	41.82	0	1400	119	46.73
23-Oct-84	18.3	24	4.91	41.82	0	1100	115	46.73
24-Oct-84	19.3	24	3.78	32.21	0	0	117	35.99
25-Oct-84	20.3	24	3.78	32.21	0	0	120	35.99
26-Oct-84	21.3	24	3.78	32.21	0	0	137	35.99
27-Oct-84	22.3	24	3.78	32.21	0	0	0	35.99
28-Oct-84	23.3	24	3.78	32.21	0	0	135	35.99

Table CIP2PC5

Primrose Cycle 5; IP2 Production Data

Date d-mmm-yy	Days	Hours on Production	Oil Produced m^3	Water Produced m^3	Fluid Level Joints	Casing Pressure kPa	Wellhead Temperature Deg C	Total Fluid Produced m^3
29-Oct-84	24.3	24	3.78	32.21	0	0	135	35.99
30-Oct-84	25.3	24	3.78	32.21	0	0	110	35.99
31-Oct-84	26.3	24	3.78	32.21	0	0	125	35.99
1-Nov-84	27.3	24	4.21	35.87	0	1000	100	40.08
2-Nov-84	28.3	24	4.21	35.87	0	200	104	40.08
3-Nov-84	29.3	24	4.21	35.87	0	400	103	40.08
4-Nov-84	30.3	24	4.07	30.18	0	300	88	34.25
5-Nov-84	31.3	24	4.07	31.08	0	400	89	35.15
6-Nov-84	32.3	24	4.07	30.18	0	300	87	34.25
7-Nov-84	33.3	24	4.07	30.18	0	200	93	34.25
8-Nov-84	34.3	24	4.07	30.18	0	300	85	34.25
9-Nov-84	35.3	24	6.44	26.09	0	220	69	32.53
10-Nov-84	36.3	24	6.44	26.09	0	100	105	32.53
11-Nov-84	37.3	24	5.67	29.41	0	0	103	35.08
12-Nov-84	38.3	24	6.07	31.47	14	0	97	37.54
13-Nov-84	39.3	24	6.07	31.47	13	0	95	37.54
14-Nov-84	40.3	24	6.07	31.47	13	0	95	37.54
15-Nov-84	41.3	24	6.07	31.47	0	0	92	37.54
16-Nov-84	42.3	24	8.71	26.13	0	0	93	34.84
17-Nov-84	43.3	24	8.71	26.13	0	0	89	34.84
18-Nov-84	44.3	24	8.36	29.87	8	0	88	38.23
19-Nov-84	45.3	24	9.73	28.69	0	0	83	38.42
20-Nov-84	46.3	24	7.65	28.6	0	0	84	36.25
21-Nov-84	47.3	24	7.65	28.6	0	0	83	36.25
22-Nov-84	48.3	24	10.8	24.38	10	0	82	35.18
23-Nov-84	49.3	24	6.09	19.45	9	0	85	25.54

Table CIP2PC5

Primrose Cycle 5;   IP2 Production Data

Date d-mmm-yy	Days	Hours on Production	Oil Produced m^3	Water Produced m^3	Fluid Level Joints	Casing Pressure kPa	Wellhead Temperature Deg C	Total Fluid Produced m^3
24-Nov-84	50.3	24	6.09	19.45	9	0	82	25.54
25-Nov-84	51.3	24	6.09	19.45	9	0	85	25.54
26-Nov-84	52.3	24	6.09	19.45	0	0	80	25.54
27-Nov-84	53.3	24	7.11	19.94	9	0	80	27.05
28-Nov-84	54.3	24	7.11	19.94	0	0	75	27.05
29-Nov-84	55.3	24	5.65	19.94	0	0	72	25.59
30-Nov-84	56.3	24	7.15	19.77	8	0	75	26.92
1-Dec-84	57.3	24	11.03	30.51	0	0	0	41.54
2-Dec-84	58.3	24	10.52	30.56	19	0	72	41.08
3-Dec-84	59.3	24	10.52	30.56	0	0	71	41.08
4-Dec-84	60.3	24	10.52	30.56	0	0	63	41.08
5-Dec-84	61.3	24	10.52	30.56	0	0	65	41.08
6-Dec-84	62.3	24	14.35	28.12	8	0	71	42.47
7-Dec-84	63.3	24	11.06	21.68	0	0	74	32.74
8-Dec-84	64.3	24	11.06	21.68	0	0	71	32.74
9-Dec-84	65.3	24	11.06	21.68	0	0	76	32.74
10-Dec-84	66.3	24	11.06	21.68	0	0	70	32.74
11-Dec-84	67.3	24	9.91	18.42	8	0	72	28.33
12-Dec-84	68.3	24	9.91	18.42	0	0	65	28.33
13-Dec-84	69.3	24	9.6	22.09	17	0	68	31.69
14-Dec-84	70.3	24	9.6	22.09	0	0	68	31.69
15-Dec-84	71.3	24	9.51	22	8	0	66	31.51
16-Dec-84	72.3	24	9.51	22	0	0	66	31.51
17-Dec-84	73.3	24	9.62	22.64	0	0	64	32.26
18-Dec-84	74.3	24	8.58	20.22	7	0	66	28.8
19-Dec-84	75.3	24	8.58	20.22	7	0	60	28.8

Table CIP2PC5

Primrose Cycle 5; IP2 Production Data

Date d-mmm-yy	Days	Hours on Production	Oil Produced m^3	Water Produced m^3	Fluid Level Joints	Casing Pressure kPa	Wellhead Temperature Deg C	Total Fluid Produced m^3
20-Dec-84	76.3	24	11.61	19.13	4	0	65	30.74
21-Dec-84	77.3	24	11.61	19.21	0	0	60	30.82
22-Dec-84	78.3	24	11.84	22.04	6	0	58	33.88
23-Dec-84	79.3	24	11.84	22.04	0	0	67	33.88
24-Dec-84	80.3	24	11.84	22.04	3	0	65	33.88
25-Dec-84	81.3	24	11.84	22.04	3	0	60	33.88
26-Dec-84	82.3	24	7.33	20.41	3	0	66	27.74
27-Dec-84	83.3	24	7.33	20.41	0	0	64	27.74
28-Dec-84	84.3	24	7.33	20.41	3	0	63	27.74
29-Dec-84	85.3	24	8.32	20.62	4	0	61	28.94
30-Dec-84	86.3	24	8.32	20.62	6	0	66	28.94
31-Dec-84	87.3	24	8.32	20.21	2	0	65	28.53
1-Jan-85	88.3	24	8.47	20.58	0	0	65	29.05
2-Jan-85	89.3	24	10.09	18.43	7	0	66	28.52
3-Jan-85	90.3	24	10.09	18.43	7	0	65	28.52
4-Jan-85	91.3	24	10.09	18.43	7	0	64	28.52
5-Jan-85	92.3	24	10.09	18.43	5	0	65	28.52
6-Jan-85	93.3	24	10.09	18.43	5	0	60	28.52
7-Jan-85	94.3	24	10.09	18.43	5	0	59	28.52
8-Jan-85	95.3	24	10.09	18.43	5	0	61	28.52
9-Jan-85	96.3	24	10.09	18.43	0	0	60	28.52
10-Jan-85	97.3	24	7	18.52	7	0	60	25.52
11-Jan-85	98.3	24	7	18.52	0	0	60	25.52
12-Jan-85	99.3	24	4.52	19.87	7	0	60	24.39
13-Jan-85	100.3	24	7.09	21.79	0	0	63	28.88
14-Jan-85	101.3	24	7.09	19.55	7	0	65	26.64

Table CIP2PC5

Primrose Cycle 5; IP2 Production Data

Date d-mmm-yy	Days	Hours on Production	Oil Produced m^3	Water Produced m^3	Fluid Level Joints	Casing Pressure kPa	Wellhead Temperature Deg C	Total Fluid Produced m^3
15-Jan-85	102.3	24	7.09	19.55	0	0	64	26.64
16-Jan-85	103.3	24	7.09	19.55	6	0	63	26.64
17-Jan-85	104.3	24	7.09	19.55	4	0	59	26.64
18-Jan-85	105.3	24	7.09	19.55	3	0	60	26.64
19-Jan-85	106.3	24	12.27	15.59	4	0	60	27.86
20-Jan-85	107.3	24	12.27	15.59	3	0	57	27.86
21-Jan-85	108.3	24	12.27	15.59	7	0	60	27.86
22-Jan-85	109.3	24	12.27	15.59	2	0	60	27.86
23-Jan-85	110.3	24	12.27	15.59	1	0	60	27.86
24-Jan-85	111.3	24	5.72	18.29	5	0	57	24.01
25-Jan-85	112.3	24	5.72	18.29	5	0	57	24.01
26-Jan-85	113.3	24	6.75	17.53	5	0	58	24.28
27-Jan-85	114.3	24	6.75	17.53	5	0	55	24.28
28-Jan-85	115.3	24	6.75	17.53	6	0	53	24.28
29-Jan-85	116.3	24	4.56	18.79	6	0	52	23.35
30-Jan-85	117.3	24	4.56	18.79	4	0	50	23.35
31-Jan-85	118.3	24	4.56	18.79	4	0	50	23.35
1-Feb-85	119.3	24	8.55	14.83	6	0	50	23.38
2-Feb-85	120.3	24	8.55	14.83	6	0	50	23.38
3-Feb-85	121.3	24	8.55	14.83	5	0	50	23.38
4-Feb-85	122.3	24	8.55	14.83	5	0	50	23.38
5-Feb-85	123.3	24	8.55	14.83	5	0	51	23.38
6-Feb-85	124.3	24	5.57	14.45	5	0	51	20.02
7-Feb-85	125.3	24	5.57	14.45	0	0	50	20.02
8-Feb-85	126.3	24	5.57	14.45	0	0	48	20.02
9-Feb-85	127.3	24	5.57	14.45	0	0	48	20.02

Table CIP2PC5

Primrose Cycle 5; IP2 Production Data

Date d-mmm-yy	Days	Hours on Production	Oil Produced m^3	Water Produced m^3	Fluid Level Joints	Casing Pressure kPa	Wellhead Temperature Deg C	Total Fluid Produced m^3
10-Feb-85	128.3	24	4.23	16.03	7	0	49	20.26
11-Feb-85	129.3	24	5.14	15.45	7	0	48	20.59
12-Feb-85	130.3	24	5.14	15.45	0	0	49	20.59
13-Feb-85	131.3	24	5.14	15.45	0	0	49	20.59
14-Feb-85	132.3	24	3.77	16.32	5	0	45	20.09
15-Feb-85	133.3	24	3.77	16.32	4	0	49	20.09
16-Feb-85	134.3	24	3.77	16.32	6	0	50	20.09
17-Feb-85	135.3	24	3.77	16.32	4	0	50	20.09
18-Feb-85	136.3	24	3.81	16.51	5	0	50	20.32
19-Feb-85	137.3	24	3.81	16.51	6	0	0	20.32
20-Feb-85	138.3	24	3.81	16.51	0	0	48	20.32
21-Feb-85	139.3	24	4.19	16.43	9	0	47	20.62
22-Feb-85	140.3	24	4.19	16.43	8	0	47	20.62
23-Feb-85	141.3	24	4.38	15.66	5	0	48	20.04
24-Feb-85	142.3	24	4.38	15.66	6	0	46	20.04
25-Feb-85	143.3	24	4.38	15.66	7	0	47	20.04
26-Feb-85	144.3	24	4.23	16.61	6	0	47	20.84
27-Feb-85	145.3	24	4.23	16.61	0	0	48	20.84
28-Feb-85	146.3	24	4.23	16.61	3	0	49	20.84
1-Mar-85	147.3	24	4.82	18.93		0	48	23.75
2-Mar-85	148.3	24	6.16	17.69	4	0	47	23.85
3-Mar-85	149.3	24	6.16	17.69	4	0	45	23.85
4-Mar-85	150.3	24	6.16	17.69		0	45	23.85
5-Mar-85	151.3	24	6.16	17.69	5	0	45	23.85
6-Mar-85	152.3	24	6.16	17.69		0	46	23.85
7-Mar-85	153.3	24	6.16	17.69		0	46	23.85

Table CIP2PC5

Primrose Cycle 5; IP2 Production Data

Date d-mmm-yy	Days	Hours on Production	Oil Produced m^3	Water Produced m^3	Fluid Level Joints	Casing Pressure kPa	Wellhead Temperature Deg C	Total Fluid Produced m^3
8-Mar-85	154.3	24	3.99	17.3	8	0	48	21.29
9-Mar-85	155.3	24	3.99	17.3		0	47	21.29
10-Mar-85	156.3	24	4.33	17.18	8	0	44	21.51
11-Mar-85	157.3	24	4.33	17.18		0	46	21.51
12-Mar-85	158.3	24	4.33	17.18		0	46	21.51
13-Mar-85	159.3	24	4.33	17.18	7	0	46	21.51
14-Mar-85	160.3	24	4.33	17.18		0	47	21.51
15-Mar-85	161.3	24	6.8	15.41	7	0	45	22.21
16-Mar-85	162.3	24	6.8	15.41	7	0	45	22.21
17-Mar-85	163.3	24	6.8	15.41	8	0	45	22.21
18-Mar-85	164.3	24	6.8	15.41	8	0	44	22.21
19-Mar-85	165.3	24	3.28	19.97	8	0	46	23.25
20-Mar-85	166.3	24	3.28	19.97		0	47	23.25
21-Mar-85	167.3	24	3.28	19.97		0	46	23.25
22-Mar-85	168.3	24	4.26	17.54	7	0	45	21.8
23-Mar-85	169.3	24	4.26	17.54		0	46	21.8
24-Mar-85	170.3	24	4.26	17.54		0	45	21.8
25-Mar-85	171.3	24	4.84	17.31	8	0	45	22.15
26-Mar-85	172.3	24	4.84	17.31		0	45	22.15
27-Mar-85	173.3	24	4.84	17.31	6	0		22.15
28-Mar-85	174.3	24	4.84	17.31	6	0		22.15
29-Mar-85	174.6	7	1.41	5.05		0		6.46

Table IP8PC1

Primrose Cycle 1; IP8 Production Data

Date d-mmm-yy	Days	Hours on Production	Oil Produced m^3	Water Produced m^3	Fluid Level Joints	Casing Pressure kPa	Wellhead Temperature Deg C	Total Fluid Produced m^3
12-Apr-82	0.7	16	13.79	24.96				38.75
13-Apr-82	1.7	24	21.25	18.97				40.22
14-Apr-82	2.7	24	21.25	6.77				28.02
15-Apr-82	3.7	24	15.17	20.75				35.92
16-Apr-82	4.7	24	17.08	19.86				36.94
17-Apr-82	5.7	24	10	20.71				30.71
18-Apr-82	6.7	24	19.85	23.38				43.23
19-Apr-82	7.7	24	14.22	31.78				46
20-Apr-82	8.7	24	12	33.34				45.34
21-Apr-82	9.7	24	15.3	32.82				48.12
22-Apr-82	10.7	24	15	36.08				51.08
23-Apr-82	11.7	24	12.35	33.25				45.6
24-Apr-82	12.7	24	13	31.69				44.69
25-Apr-82	13.7	24	20	39.25				59.25
26-Apr-82	14.7	24	13	28.97				41.97
27-Apr-82	15.7	24	4	30.71				34.71
28-Apr-82	16.7	24	1	30.98				31.98
29-Apr-82	16.7	0		0				
30-Apr-82	16.7	0		0				
	16.7	0						
	16.7	0						
13-May-82	17.2	12	16.61	54.54				71.15
14-May-82	18.2	24	13.5	50.24				63.74
15-May-82	19.2	24	9.11	44.65				53.76
16-May-82	20.2	24	14.26	43.06				57.32
17-May-82	21.2	24	13.79	39.47				53.26

Table IP8PC1

Primrose Cycle 1; IP8 Production Data

Date d-mmm-yy	Days	Hours on Production	Oil Produced m^3	Water Produced m^3	Fluid Level Joints	Casing Pressure kPa	Wellhead Temperature Deg C	Total Fluid Produced m^3
18-May-82	22.2	24	10.36	19.64				30
19-May-82	23.2	24	7.21	25.12				32.33
20-May-82	24.2	24	7.83	46.88				54.71
21-May-82	25.2	24	7.83	35.88				43.71
22-May-82	26.2	24	7	24.81				31.81
23-May-82	27.2	24	6.5	24.94				31.44
24-May-82	28.2	24	7	23.32				30.32
25-May-82	29.2	24	8	21.53				29.53
26-May-82	30.2	24	7	19.74				26.74
27-May-82	31.2	24	7.14	17.94				25.08
28-May-82	32.2	24	6.3	16.69				22.99
29-May-82	33.2	24	4.07	18.34				22.41
30-May-82	33.8	15.5	5.75	19.73				25.48
31-May-82	33.8	0		0				
	33.8	0						
	33.8	0						
11-Jul-82	34.8	24	10	13.25				23.25
12-Jul-82	34.8	0		0				
13-Jul-82	34.8	0		0				
14-Jul-82	34.8	0		0				
15-Jul-82	35.8	24	2.79	8.72				11.51
16-Jul-82	36.8	24	0.11	14.08				14.19
17-Jul-82	37.8	24	10	16.22				26.22
18-Jul-82	38.8	24	5	22.66				27.66
19-Jul-82	39.8	24	10	18.6				28.6

Table CIP8PC2

Primrose Cycle 2; IP8 Production Data

Date d-mmm-yy	Days	Hours on Production	Oil Produced m^3	Water Produced m^3	Fluid Level Joints	Casing Pressure kPa	Wellhead Temperature Deg C	Total Fluid Produced m^3
10-Sep-82	0.6	14	4.05	3.75		4000	125	7.8
11-Sep-82	1.6	24	4.1	3.84		4200	132	7.94
12-Sep-82	2.6	24	4.5	4.58		5000	142	9.08
13-Sep-82	3.6	24	4.6	4.76		3400	157	9.36
14-Sep-82	4.6	24	5	5.49		2600	150	14.49
15-Sep-82	5.6	24	5.5	6.41	54	1100	100	11.91
16-Sep-82	6.6	24	5.5	6.59		1550	100	12.09
17-Sep-82	7.6	24	5	6.77		1800	101	11.77
18-Sep-82	8.6	24	7	9.15		1900	109	16.15
19-Sep-82	8.9	8.5	7.2	9.52		1650	109	16.72
20-Sep-82	9.5	14	7.4	9.88	47	70	89	17.28
21-Sep-82	10.5	24	7.5	10.07		2600	93	17.57
22-Sep-82	11.5	24	7.8	10.62		2600	92	17.42
23-Sep-82	12.5	24	7	9.15		600	70	16.15
24-Sep-82	12.5	0						
25-Sep-82	12.5	0						
26-Sep-82	12.9	8	3.4	2.56		0	67	5.96
27-Sep-82	13.9	24	7	9.15		0	70	16.15
28-Sep-82	14.9	24	7	9.15		0	66	16.15
29-Sep-82	15.9	24	7	9.15		0	69	16.15
30-Sep-82	16.9	24	6.41	11.74	33	0	60	18.15
1-Oct-82	17.9	24	0.61	19.48	28	0	62	20.09
2-Oct-82	18.9	24	5.88	16.87	13	200	65	22.75
3-Oct-82	19.9	24	8.7	16.47	21	600	65	25.17
4-Oct-82	20.9	24	6.93	16.85	12	800	68	23.78
5-Oct-82	20.9	0						

Table CIP8PC2

Primrose Cycle 2; IP8 Production Data

Date d-mmm-yy	Days	Hours on Production	Oil Produced m^3	Water Produced m^3	Fluid Level Joints	Casing Pressure kPa	Wellhead Temperature Deg C	Total Fluid Produced m^3
6-Oct-82	20.9	0						
7-Oct-82	21.9	24	0	18.84	39	600	65	28.84
8-Oct-82	22.9	24	19.57	20.99	39	0	65	40.56
9-Oct-82	23.9	24	6.66	19.24	20	0	65	25.9
10-Oct-82	24.9	24	9.37	16.76		200	70	26.13
11-Oct-82	25.9	24	5.62	12.63	30	0	70	18.25
12-Oct-82	26.9	24	5.8	13.03	28	200	84	18.83
13-Oct-82	27.9	24	10.77	8.48	23	50	84	19.25
14-Oct-82	28.9	24	12.07	9.51	20	100	86	21.58
15-Oct-82	29.9	24	19.46	15.32	17	150	86	34.78
16-Oct-82	30.9	24	21.36	16.85	15	200	85	48.24
17-Oct-82	31.1	6.5	12.29	17.75		2000	84	30.04
18-Oct-82	31.4	5.5	6.15	18.93	16	0	70	25.08
19-Oct-82	32.4	24	0.55	20.67	16	0	70	21.22
20-Oct-82	33.4	24	9.65	18.23	18	0	65	27.88
21-Oct-82	33.4	0						
22-Oct-82	33.4	0						
23-Oct-82	34.1	19	17.47	13.76	22	300	60	31.23
	34.1				18			
24-Oct-82	35.1	24	18.45	12.54	18	0	60	30.99
25-Oct-82	36.1	24	16.82	10.79	16	0	50	27.61
26-Oct-82	37.1	24	15.16	7.77	16	0	52	22.93
27-Oct-82	38.1	24	16.39	6.76	16	0	50	23.15
28-Oct-82	39.1	24	12.95	6.71	8	0	39	19.66
	39.1				12			
29-Oct-82	40.1	24	12.56	6.54	11	0	42	19.1

Table CIP8PC2

Primrose Cycle 2; IP8 Production Data

Date d-mmm-yy	Days	Hours on Production	Oil Produced m^3	Water Produced m^3	Fluid Level Joints	Casing Pressure kPa	Wellhead Temperature Deg C	Total Fluid Produced m^3
30-Oct-82	41.1	24	12.39	5.87	12	0	42	18.26
31-Oct-82	42.1	24	11.89	5.74	12	0	45	17.63
1-Nov-82	43.1	24	9.84	4.12	10	0	40	13.96
2-Nov-82	44.1	24	9.28	4.16	10	0	30	13.96
3-Nov-82	45.1	24	9.56	3.7	8	0	32	13.26
4-Nov-82	46.1	24	9.08	3.29		0	30	12.37
5-Nov-82	47.1	24	9.12	3.21	7	0	35	12.33
6-Nov-82	48.1	24	8.78	2.54		0	35	11.32
7-Nov-82	49.1	24	8.33	2.15	7	0	31	10.48
8-Nov-82	50.1	24	7.52	1.98		0	28	9.5
9-Nov-82	51.1	24	8.07	2.01	7	0	26	10.08
10-Nov-82	52.1	24	8.63	1.77		0	29	10.4
11-Nov-82	53.1	24	8.79	1.8		0	22	10.59
12-Nov-82	54.1	24	9.07	1.48		0	26	10.55
13-Nov-82	55.1	24	9.17	1.26		0	24	10.43
14-Nov-82	56.1	24	8.51	1.5		0	30	10.01
15-Nov-82	57.1	24	8.05	2.01		0	31	10.06
16-Nov-82	58.1	24	11.1	3.71		0	23	14.81
17-Nov-82	59.1	24	10.06	1.92		0	30	11.98
18-Nov-82	60.1	24	11.16	3.24	10	0	24	14.4
19-Nov-82	61.1	24	11.16	3.24	5	0	20	14.4
20-Nov-82	62.1	24	11.16	3.24	8	0	20	14.4
21-Nov-82	63.1	24	9.3	2.33		0	20	11.63
22-Nov-82	64.1	24	9.3	2.33	5	0	22	11.63
23-Nov-82	65.1	24	9.3	2.33		0	20	11.63
24-Nov-82	66.1	24	8.47	3.02		0		11.49

Table CIP8PC2

Primrose Cycle 2; IP8 Production Data

Date d-mmm-yy	Days	Hours on Production	Oil Produced m^3	Water Produced m^3	Fluid Level Joints	Casing Pressure kPa	Wellhead Temperature Deg C	Total Fluid Produced m^3
25-Nov-82	67.1	24	8.47	3.02	5	0	21	11.49
26-Nov-82	68.1	24	7.81	2.49	4	0	18	10.3
27-Nov-82	69.1	24	7.81	2.49	4	0	22	10.3
28-Nov-82	70.1	24	7.73	0.86		0	26	8.59
29-Nov-82	71.1	24	7.73	0.86	4	0	26	8.59
30-Nov-82	72.1	24	9.31	0.48	4	0	26	9.79
1-Dec-82	73.1	24	6.85	1.24	5	0	24	8.09
2-Dec-82	74.1	24	6.85	1.24		0	26	8.09
3-Dec-82	75.1	24	8.21	1.56		0	25	9.77
4-Dec-82	76.1	24	8.21	1.56	6	0	24	9.77
5-Dec-82	77.1	24	8.62	2.29		0	20	10.91
6-Dec-82	78.1	24	5.4	1.44	6	0	18	6.84
7-Dec-82	79.1	24	5.4	1.44	4	0	12	6.84
8-Dec-82	80.1	24	6.71	0.61	4	0	18	7.32
9-Dec-82	81.1	24	5.73	1.62	3	0	20	7.35
10-Dec-82	82.1	24	5.73	1.62	2	0	16	7.35
11-Dec-82	83.1	24	5.73	1.62	3	0	20	7.35
12-Dec-82	84.1	24	5.73	1.62	3	0	22	7.35
13-Dec-82	85.1	24	5.29	0.58	4	0	20	5.87
14-Dec-82	86.1	24	5.29	0.58	4	0	20	5.87
15-Dec-82	87.1	24	5.29	0.58	3	0	20	5.87
16-Dec-82	88.1	24	6.56	0.72	4	0	22	7.28
17-Dec-82	89.1	24	6.56	0.72	4	0	22	7.28
18-Dec-82	90.1	24	4.83	1.36	4	0	22	6.19
19-Dec-82	91.1	24	4.83	1.36	4	0	20	6.19
20-Dec-82	92.1	24	6.1	0.73	5	0	11	6.83

Table CIP8PC2

Primrose Cycle 2; IP8 Production Data

Date d-mmm-yy	Days	Hours on Production	Oil Produced m^3	Water Produced m^3	Fluid Level Joints	Casing Pressure kPa	Wellhead Temperature Deg C	Total Fluid Produced m^3
21-Dec-82	93.1	24	6.1	0.73		0	10	6.83
22-Dec-82	94.1	24	4.8	1.35	5	0	12	5.15
23-Dec-82	95.1	24	4.8	1.35	4	0	14	5.15
24-Dec-82	96.1	24	4.67	1.47	4	0	10	6.14
25-Dec-82	97.1	24	4.67	1.47	4	0	17	6.14
26-Dec-82	98.1	24	4.43	0.66	4	0	10	5.09
27-Dec-82	99.1	24	4.43	0.66	3	0	14	5.09
28-Dec-82	100.1	24	6.53	0.2	4	0	14	6.73
29-Dec-82	101.1	24	6.53	0.2		0	12	6.73
30-Dec-82	101.1							
31-Dec-82	102.1	24	5.71	7.15	7	0	18	12.86
1-Jan-83	103.1	24	5.71	1.25	5	0	15	6.96
2-Jan-83	104.1	24	5.76	1.81		0	18	7.57
3-Jan-83	105.1	24	5.76	1.81	6	0	14	7.57
4-Jan-83	106.1	24	6.32	1.68	5	0	18	8
5-Jan-83	107.1	24	6.31	1.68	5	0	14	7.99
6-Jan-83	108.1	24	6.31	1.68				7.99
7-Jan-83	109.1	24	7.19	0.79	5	0	12	7.98
8-Jan-83	110.1	24	7.19	0.79	5	0	16	7.98
9-Jan-83	111.1	24	7.19	0.79	4	0	20	7.98
10-Jan-83	112.1	24	7.19	0.79	3	0	2	7.98
11-Jan-83	113.1	24	5.64	0.63		0	10	6.27
12-Jan-83	114.1	24	4.69	1.48	6	0	14	6.17
13-Jan-83	115.1	24	4.69	1.48	16	0	14	6.17
14-Jan-83	116.1	24	4.69	1.48	4	0	12	6.17
15-Jan-83	117.1	24	5.58	0.85	5	0	14	6.43

Table CIP8PC2

Primrose Cycle 2; IP8 Production Data

Date d-mmm-yy	Days	Hours on Production	Oil Produced m^3	Water Produced m^3	Fluid Level Joints	Casing Pressure kPa	Wellhead Temperature Deg C	Total Fluid Produced m^3
16-Jan-83	118.1	24	5.58	0.85	3	0	10	6.43
17-Jan-83	119.1	24	5.71	0.46	6	0	7	6.17
18-Jan-83	120.1	24	6.28	0.51	4	0	17	6.79
19-Jan-83	121.1	24	6.28	0.51	5	0	14	6.79
20-Jan-83	122.1	24	6.28	0.51	5	0	12	6.79
21-Jan-83	123.1	24	6.28	0.51	5	0	13	6.79
22-Jan-83	124.1	24	6.28	0.51		0	10	6.79
23-Jan-83	125.1	24	6.28	0.51	5	0	4	6.79
24-Jan-83	126.1	24	6.27	0.51	5	0	6	6.78
25-Jan-83	127.1	24	5.61	0.45		0	0	6.06
26-Jan-83	128.1	24	5.61	0.45		0	8	6.06
27-Jan-83	129.1	24	4.04	1.42	5	0	18	5.46
28-Jan-83	130.1	24	4.04	1.42		0	12	5.46
29-Jan-83	131.1	24	4.04	1.42	5	0	15	5.46
30-Jan-83	132.1	24	4.7	0.47	5	0	15	5.17
31-Jan-83	133.1	24	4.71	0.47	5	0	12	5.18
1-Feb-83	134.1	24	6.29	0.99	5	0	12	7.28
2-Feb-83	135.1	24	6.19	0.69	6	0	10	6.88
3-Feb-83	136.1	24	6.19	0.69	5	0	11	6.88
4-Feb-83	137.1	24	6.19	0.69	5	0	8	6.88
5-Feb-83	138.1	24	6.19	0.69	5	0	11	6.88
6-Feb-83	139.1	24	6.19	0.69	6	0	12	6.88
7-Feb-83	140.1	24	5.14	2	6	0	18	7.14
8-Feb-83	141.1	24	2.65	1.03	6	0	16	3.68
9-Feb-83	142.1	24	2.65	1.03	5	0	24	3.68
10-Feb-83	143.1	24	3.12	0.46	9	0	24	3.58

Table CIP8PC2

Primrose Cycle 2; IP8 Production Data

Date d-mmm-yy	Days	Hours on Production	Oil Produced m^3	Water Produced m^3	Fluid Level Joints	Casing Pressure kPa	Wellhead Temperature Deg C	Total Fluid Produced m^3
11-Feb-83	144.1	24	3.12	0.46	8	0	18	3.58
12-Feb-83	145.1	24	3.12	0.46	7	0	24	3.58
13-Feb-83	146.1	24	3.12	0.46	6	0	25	3.58
14-Feb-83	147.1	24	3.11	0.46	7	0	24	3.57
15-Feb-83	148.1	24	6.79	1.01	6	0	22	7.8
16-Feb-83	149.1	24	6.79	1.01		0	13	7.8
17-Feb-83	150.1	24	6.79	1.01	8	0	15	7.8
18-Feb-83	151.1	24	6.79	1.01	7	0	18	7.8
19-Feb-83	152.1	24	6.78	1.01	7	0	20	7.79
20-Feb-83	153.1	24	6.78	1.01	8	0	27	7.79
21-Feb-83	154.1	24	6.78	1.01	5	0	25	7.79
22-Feb-83	155.1	24	6.33	0.94	7	0	30	7.27
23-Feb-83	156.1	24	6.33	0.94	7	0	26	7.27
24-Feb-83	157.1	24	6.33	0.94	6	0	24	7.27
25-Feb-83	158.1	24	6.33	0.94	6	0	22	7.27
26-Feb-83	158.5	9	2.38	0.35		0	24	2.73
27-Feb-83		SHUT IN				0		
28-Feb-83		SHUT IN				0		

Table CIP8PC3

Primrose Cycle 3; IP8 Production Data

Date d-mmm-yy	Days	Hours on Production	Oil Produced m^3	Water Produced m^3	Fluid Level Joints	Casing Pressure kPa	Wellhead Temperature Deg C	Total Fluid Produced m^3
1-Apr-83		ON INJECTION						
2-Apr-83		ON INJECTION						
3-Apr-83		ON INJECTION						
4-Apr-83		ON INJECTION						
5-Apr-83		ON INJECTION						
6-Apr-83		SOAK						
7-Apr-83	0.6	14	0	5.3	FULL	0	120	5.3
8-Apr-83	1.6	24	0	9.13	FULL	0	165	9.13
9-Apr-83	2.6	24	0	9.13	FULL	0	155	9.13
10-Apr-83	3.6	24	0	7.3	FULL	0	135	7.3
11-Apr-83	4.6	24	0	7.3	FULL	0	185	7.3
12-Apr-83	5.6	24	0	9.66	FULL	0	168	9.66
13-Apr-83	6.6	24	0	14.5	FULL	0	154	14.5
14-Apr-83	7.6	24	0	19.33	FULL	0	155	19.33
15-Apr-83	8.6	24	5.62	42.2	FULL	0	170	47.82
16-Apr-83	9.6	24	5.62	42.2	FULL	0	165	47.82
17-Apr-83	10.6	24	5.62	42.2	FULL	0	150	47.82
18-Apr-83	11.6	24	19.55	86.05	FULL	0	145	105.6
19-Apr-83	12.6	24	18.73	82.38	FULL	0	135	101.11
20-Apr-83	12.6	1	18.73	82.38	FULL	0		101.11
21-Apr-83	12.6	0	- STOPPED FLOWING		31			
22-Apr-83	12.6	0						
23-Apr-83	12.6	0						
24-Apr-83	12.6	0						
25-Apr-83	13.2	14	2.52	18.97	35	0	65	21.49
26-Apr-83	14.2	24	3.04	22.93	28	0	70	25.97

Table CIP8PC3

Primrose Cycle 3; IP8 Production Data

Date d-mmm-yy	Days	Hours on Production	Oil Produced m^3	Water Produced m^3	Fluid Level Joints	Casing Pressure kPa	Wellhead Temperature Deg C	Total Fluid Produced m^3
27-Apr-83	15.2	24	0	26.06	26	0	70	26.06
28-Apr-83	16.2	24	4.04	24.73	30	0	66	28.77
29-Apr-83	17.2	24	5.13	22.5	30	0	62	27.63
30-Apr-83	18.2	24	4.63	18.9	31	0	52	23.53
1-May-83	19.2	24	4.63	18.9	31	0	60	23.53
2-May-83	20.2	24	6.77	14.96	30	0	42	21.73
3-May-83	21.2	24	4.26	19.01	29	0	60	23.27
4-May-83	22.2	24	4.63	18.64	27	0	64	23.27
5-May-83	23.2	24	4.86	18.61	27	0	60	23.47
6-May-83	24.2	24	6.82	21.85	24	0	75	28.67
7-May-83	25.2	24	7.01	17.22	17	34	70	24.23
8-May-83	26.0	20	7.32	17.9	19	6	62	25.22
9-May-83	27.0	23	7.32	17.9	27	0	56	25.22
10-May-83	28.0	24	9.54	21.52	27	0	70	31.06
11-May-83	29.0	24	9.54	21.52		0	63	31.06
12-May-83	30.0	24	9.54	21.52	12	0	65	31.06
13-May-83	31.0	24	15.08	14.51	19	0	60	29.59
14-May-83	32.0	24	15.08	14.51		0	64	29.59
15-May-83	33.0	24	17.67	12.44	13	0	58	30.11
16-May-83	34.0	24	16.86	12.44	12	0	60	29.3
17-May-83	35.0	24	8.5	9.34		0	62	17.84
18-May-83	36.0	24	8.64	8.65	14	0	63	17.29
19-May-83	37.0	24	8.64	8.65	19	0	62	17.29
20-May-83	38.0	24	6.46	9.96	30	0	62	16.42
21-May-83	39.0	24	10.56	5.26	30	0	56	15.82
22-May-83	40.0	24	11.3	4.96	30	0	58	16.26

Table CIP8PC3

Primrose Cycle 3; IP8 Production Data

Date d-mmm-yy	Days	Hours on Production	Oil Produced m^3	Water Produced m^3	Fluid Level Joints	Casing Pressure kPa	Wellhead Temperature Deg C	Total Fluid Produced m^3
23-May-83	41.0	24	11.34	4.64	30	0	52	15.98
24-May-83	42.0	24	12.9	10.74	30	0	58	23.64
25-May-83	43.0	24	11.14	9.5	9	0	54	20.64
26-May-83	44.0	24	13.5	13.5	9	0	51	27
27-May-83	45.0	24	11.04	12.37	9	0	54	23.41
28-May-83	46.0	24	12.28	10.05	12	0	54	22.33
29-May-83	47.0	24	10.68	10.68	7	0	56	21.36
30-May-83	48.0	24	10.01	11.07	7	0	51	21.08
31-May-83	49.0	24	11.99	14.66	7	0	48	26.65
1-Jun-83	50.0	24	11.22	12.16	7	0	39	23.38
2-Jun-83	51.0	24	11.22	12.16	5	0	34	23.38
3-Jun-83	52.0	24	12.06	8.72	8	0	42	20.78
4-Jun-83	53.0	24	10.91	10.91	6	0	48	21.82
5-Jun-83	54.0	24	13.93	9.49	5	0	50	23.42
6-Jun-83	55.0	24	13.29	8.86	7	0	42	22.15
7-Jun-83	56.0	24	11.96	8.75	5	0	40	20.71
8-Jun-83	57.0	24	11.96	8.75	5	0	42	20.71
9-Jun-83	58.0	24	11.96	8.75	5	0	42	20.71
10-Jun-83	59.0	24	7.61	11.4	5	0	46	19.01
11-Jun-83	60.0	24	11.48	7.65	1	0	38	19.13
12-Jun-83	61.0	24	11.48	7.65	5	0	40	19.13
13-Jun-83	62.0	24	9.44	8.36	5	0	32	17.8
14-Jun-83	63.0	24	9.2	7.53	5	0	42	16.73
15-Jun-83	64.0	24	9.2	7.53	5	0	40	16.73
16-Jun-83	65.0	24	8.75	8.41	5	0	41	17.16
17-Jun-83	66.0	24	10.47	6.29	5	0	40	16.76

Table CIP8PC3

Primrose Cycle 3; IP8 Production Data

Date d-mmm-yy	Days	Hours on Production	Oil Produced m^3	Water Produced m^3	Fluid Level Joints	Casing Pressure kPa	Wellhead Temperature Deg C	Total Fluid Produced m^3
18-Jun-83	67.0	24	10.35	6.55	5	0	39	16.9
19-Jun-83	68.0	24	10.16	6.77	4	0	32	16.93
20-Jun-83	69.0	24	10.16	6.77	4	0	37	16.93
21-Jun-83	70.0	24	9.04	6.82	5	0	31	15.86
22-Jun-83	71.0	24	9.76	5.26	4	0	34	15.02
23-Jun-83	72.0	24	9.72	6.48	4	0	39	16.2
24-Jun-83	73.0	24	9.72	6.48	4	0	38	16.2
25-Jun-83	74.0	24	8.35	6.84	4	0	30	15.19
26-Jun-83	75.0	24	8.13	7.52	4	0	36	15.65
27-Jun-83	76.0	24	7.18	7.18	4	0	34	14.36
28-Jun-83	77.0	24	11.51	12.47	3	0	36	23.98
29-Jun-83	78.0	24	11.51	12.47	3	0	39	23.98
30-Jun-83	79.0	24	13.37	9	3	0	39	22.37
1-Jul-83	80.0	24	12.61	9.91	3	0	40	22.52
2-Jul-83	81.0	24	12.61	9.91	3	0	38	22.52
3-Jul-83	82.0	24	12.06	10.29				22.35
4-Jul-83	83.0	24	12.06	10.29				22.35
5-Jul-83	84.0	24	12.16	10.38	3	0	38	22.54
6-Jul-83	85.0	24	17.65	4.86	3	0	38	22.51
7-Jul-83	86.0	24	12.31	8.19	3	0	37	20.5
8-Jul-83	87.0	24	11.72	8.83	2	0	34	20.55
9-Jul-83	88.0	24	10.26	10.26	3	0	34	20.52
10-Jul-83	89.0	24	10.74	10.74		0	37	21.48
11-Jul-83	90.0	24	11.38	9.3	3	0	34	20.68
12-Jul-83	91.0	24	9.38	7.29	2	0	31	16.67
13-Jul-83	92.0	24	9.09	7.74	2	0	36	16.83

Table CIP8PC3

Primrose Cycle 3; IP8 Production Data

Date d-mmm-yy	Days	Hours on Production	Oil Produced m^3	Water Produced m^3	Fluid Level Joints	Casing Pressure kPa	Wellhead Temperature Deg C	Total Fluid Produced m^3
14-Jul-83	93.0	24	9.09	7.74	2	0	33	16.83
15-Jul-83	94.0	24	9.27	7.15	2	0	30	16.42
16-Jul-83	95.0	24	8.56	6.97	3	0	32	15.53
17-Jul-83	96.0	24	8.56	6.97	2	0	30	15.53
18-Jul-83	97.0	24	9.7	5.83	2	0	34	15.53
19-Jul-83	98.0	24	5.98	4.72	2	0	36	10.7
20-Jul-83	99.0	24	5.73	4.89	1	0	38	10.62
21-Jul-83	100.0	24	5.32	5.32	1	0	30	10.64
22-Jul-83	101.0	23	5.95	5.28	2	0	34	11.23

Table CIP8PC4A

Primrose Cycle 4A; IP8 Production Data

Date d-mmm-yy	Days	Hours on Production	Oil Produced m^3	Water Produced m^3	Fluid Level Joints	Casing Pressure kPa	Wellhead Temperature Deg C	Total Fluid Produced m^3
1-Sep-83		INJECTION/SOAK						
2-Sep-83		SOAK				9500		
3-Sep-83		17	0	17.84	FULL	8964	135	17.84
4-Sep-83		24	0	25.18	FULL	8100	135	25.18
5-Sep-83		24	0	25.18	FULL	7500	167	25.18
6-Sep-83		24	0	31.45	FULL	9000	155	31.45
7-Sep-83		24	0	31.45	FULL	6500	190	31.45
8-Sep-83		24	0	31.45	FULL	6200	165	31.45
9-Sep-83		24	1.34	31.96	FULL	5000	165	33.3
10-Sep-83		24	1.34	31.96	FULL	4000	149	33.3
11-Sep-83		24	1.34	31.96	FULL	3250	149	33.3
12-Sep-83		24	4.48	31.9	FULL	2800	152	36.38
13-Sep-83		24	3.42	24.25	FULL	2500	152	27.67
14-Sep-83		24	3.42	24.25	FULL	2200	144	27.67
15-Sep-83		24	3.42	24.25	FULL	2200	170	27.67
16-Sep-83		23	3.28	23.25	FULL	2200	163	26.53
17-Sep-83		SHUT IN						
18-Sep-83		SHUT IN			43			
19-Sep-83		8	3.4	24.25	43	0	78	27.65
20-Sep-83		24	0	25.62	41	0	91	25.62
21-Sep-83		24	0	25.62	49	0	110	25.62
22-Sep-83		24	3.22	13.08	48	780	130	16.3
23-Sep-83		24	3.22	13.08	41	380	130	16.3
24-Sep-83		24	3.22	13.08	47	280	106	16.3
25-Sep-83		24	3.22	13.08	44	310	127	16.3
26-Sep-83		24	3.24	13.08	44	300	120	16.32

Table CIP8PC4A

Primrose Cycle 4A; IP8 Production Data

Date d-mmm-yy	Days	Hours on Production	Oil Produced m^3	Water Produced m^3	Fluid Level Joints	Casing Pressure kPa	Wellhead Temperature Deg C	Total Fluid Produced m^3
27-Sep-83		24	3.02	15.61	40	260	110	18.63
28-Sep-83		24	3.02	15.61	33	260	108	18.63
29-Sep-83		24	3.02	15.61	34	320	118	18.63
30-Sep-83		24	3.02	15.61	32	110	100	18.63
1-Oct-83		24	3.02	15.61	33	100	98	18.63
2-Oct-83		24	2.03	24.09	25	95	92	26.12
3-Oct-83		24	2.02	24.09	24	0	82	26.11
4-Oct-83		24	0	26.87	20	0	78	26.87
5-Oct-83		24	0	26.87	20	0	78	26.87
6-Oct-83		24	0	25.99	22	0	75	25.99
7-Oct-83		24	1.87	25.83	19	0	68	27.7
8-Oct-83		24	1.87	25.83	19	0	69	27.7
9-Oct-83		24	1.87	25.83	11	0	68	27.7
10-Oct-83		24	1.02	22.55	21	0	54	23.57
11-Oct-83		24	1.45	22.8	20	0	65	24.25
12-Oct-83		24	1.28	19.42	20	0	68	20.7
13-Oct-83		24	1.29	17.73	-	0	66	19.02
14-Oct-83		24	0	19.64	21	0	64	19.64
15-Oct-83		24	0	19.64	21	0	55	19.64
16-Oct-83		24	0.87	16.3	21	0	61	17.17
17-Oct-83		24	0.87	16.3	22	0	55	17.17
18-Oct-83		24	1.39	15.3	23	0	60	16.69
19-Oct-83		24	1.74	26.76	19	0	64	28.5
20-Oct-83		24	1.46	22.59				24.05
21-Oct-83		24	1.83	21.9				23.73
22-Oct-83		24	1.73	25.4	18	0	70	27.13

Table CIP8PC4A

Primrose Cycle 4A; IP8 Production Data

Date d-mmm-yy	Days	Hours on Production	Oil Produced m^3	Water Produced m^3	Fluid Level Joints	Casing Pressure kPa	Wellhead Temperature Deg C	Total Fluid Produced m^3
23-Oct-83		24	1.73	25.4	20	0	75	27.13
24-Oct-83		24	2.13	31.16	19	0	70	33.29
25-Oct-83		24	4.09	30.35	19	0	72	34.44
26-Oct-83		24	4.09	30.35	15	0	76	34.44
27-Oct-83		24	5.3	35	15	0	70	40.3
28-Oct-83		24	5.12	33	18	0	70	38.94
29-Oct-83		24	5.12	33.82	18	0	68	38.94
30-Oct-83		24	5.12	33.82	17	0	67	38.94
31-Oct-83		24	5.12	33.82	17	0	70	38.94
1-Nov-83		24	6.34	31.46	15	0	70	37.8
2-Nov-83		24	6.31	31.46	13	0	64	37.77
3-Nov-83		24	4.65	43.44	13	0	67	48.09
4-Nov-83		24	4.56	43.44	13	0	66	48.09
5-Nov-83		24	4.56	43.44	15	0	70	48.09
6-Nov-83		24	6.2	47.89	15	0	71	54.09
7-Nov-83		24	6.2	47.89	17	0	62	54.09
8-Nov-83		24	9.16	45.01	17	0	65	54.17
9-Nov-83		24	6.65	47.84	12	0	62	54.49
10-Nov-83		24	6.15	39.18		0	61	45.33
11-Nov-83		24	8.37	37.59		0	54	45.96
12-Nov-83		24	8.37	37.59	12	0	57	45.96
13-Nov-83		24	8.37	37.59		0	59	45.96
14-Nov-83		24	9.08	32.19	12	0	54	41.27
15-Nov-83		24	9.08	32.19		0	50	41.27
16-Nov-83		24	8.46	33.92	13	0	53	42.38
17-Nov-83		24	3.93	35.81	13	0	50	39.74

Table CIP8PC4A

Primrose Cycle 4A; IP8 Production Data

Date d-mmm-yy	Days	Hours on Production	Oil Produced m^3	Water Produced m^3	Fluid Level Joints	Casing Pressure kPa	Wellhead Temperature Deg C	Total Fluid Produced m^3
18-Nov-83		24	5.51	33.05	12	0	50	38.56
19-Nov-83		24	5.51	33.05	12	0	51	38.56
20-Nov-83		24	5.03	32.23		0	46	37.26
21-Nov-83		24	5.03	32.23		0	50	37.26
22-Nov-83		24	4.91	29.71				34.62
23-Nov-83		24	4.71	28.08		0	45	32.79
24-Nov-83		24	4.71	28.08		0	45	32.79
25-Nov-83		24	4.06	28.03	13	0	42	32.09
26-Nov-83		24	4.06	28.03		0	38	32.09
27-Nov-83		24	4.06	28.03		0	49	32.09
28-Nov-83		24	4.07	28.03	14	0	46	32.1
29-Nov-83		24	3.31	22.89				26.2
30-Nov-83		24	3.44	20.8	14	0	46	24.24
1-Dec-83		23	3.44	20.8	15	0	40	24.24
2-Dec-83		13	1.87	11.27	15	0	33	13.14
3-Dec-83		SHUT IN						
4-Dec-83		12.25	1.25	14	14	0	35	15.25
5-Dec-83		24	2.45	27.44		0	40	29.89
6-Dec-83		24	3.12	35.18	14	0	40	38.3
7-Dec-83		24	0	35.15		0	39	35.15
8-Dec-83		20.5	0	35.15		0	41	35.15
9-Dec-83		24	4.02	31.98		0	43	36
10-Dec-83		24	4.02	31.98		0	39	36
11-Dec-83		24	4.04	31.79		0		35.83
12-Dec-83		24	4.04	31.79		0		35.83
13-Dec-83		24	6.62	28.23	12		38	34.85

Table CIP8PC4A

Primrose Cycle 4A; IP8 Production Data

Date d-mmm-yy	Days	Hours on Production	Oil Produced m^3	Water Produced m^3	Fluid Level Joints	Casing Pressure kPa	Wellhead Temperature Deg C	Total Fluid Produced m^3
14-Dec-83		24	6.62	28.23		0	42	34.85
15-Dec-83		24	6.62	28.23		0	42	34.85
16-Dec-83		24	6.62	28.23		0	34	34.85
17-Dec-83		24	3.89	34.03			45	37.92
18-Dec-83		24	3.9	34.03		0	41	37.93
19-Dec-83		24	5.2	45.44		0	40	50.64
20-Dec-83		24	5.2	41.34	10	0	43	46.54
21-Dec-83		24	5.2	41.34	10	0	35	46.54
22-Dec-83		24	7.98	43.31		0	38	51.29
23-Dec-83		24	7.98	43.31			35	51.29
24-Dec-83		24	8.24	41.86		0		50.1
25-Dec-83		24	8.75	39.4		0		48.15
26-Dec-83		24	5.29	23.82		0	41	29.11
27-Dec-83		24	4.93	25.06	11	0	40	29.99
28-Dec-83		24	4.93	25.06	11	0	40	29.99
29-Dec-83		24	6.61	25.04	11	0	42	31.65
30-Dec-83		24	6.61	25.04	11	0	38	31.65
31-Dec-83		24	6.61	25.04	11	0	42	31.65
1-Jan-84		24	6.63	25.04	11	0	44	31.67
2-Jan-84		24	13.18	50.98	11	0	44	64.16
3-Jan-84		24	13.18	50.98	9	0	44	64.16
4-Jan-84		24	7.2	57.44	9	0	43	64.64
5-Jan-84		24	7.55	56.72	11	0	44	64.27
6-Jan-84		24	8.15	56.12		0	43	64.27
7-Jan-84		24	13.21	50.76		0	42	63.97
8-Jan-84		24	13.21	50.76	11	0	41	63.97

Table CIP8PC4A

Primrose Cycle 4A; IP8 Production Data

Date d-mmm-yy	Days	Hours on Production	Oil Produced m^3	Water Produced m^3	Fluid Level Joints	Casing Pressure kPa	Wellhead Temperature Deg C	Total Fluid Produced m^3
9-Jan-84		24	12.98	50.55		0	44	63.53
10-Jan-84		24	12.99	50.55	9	0	43	63.54
11-Jan-84		24	12.98	50.55	9	0	46	63.53
12-Jan-84		24	12.99	50.55	8	0	38	63.54
13-Jan-84		24	11.21	43.98	6	0	38	55.19
14-Jan-84		24	11.21	43.98	6	0	45	55.19
15-Jan-84		24	11.21	43.98	5	0	38	55.19
16-Jan-84		24	11.21	43.98	5	0	44	55.19
17-Jan-84		24	11.21	43.98	5	0	41	55.19
18-Jan-84		24	13.71	39.86	5	0	43	53.57
19-Jan-84		24	13.71	39.86		0	38	53.57
20-Jan-84		24	15.48	40.3	6	0	38	55.78
21-Jan-84		24	15.48	40.3		0	40	55.78
22-Jan-84		24	10.83	44.4		0	39	55.23
23-Jan-84		24	10.83	44.4		0	38	55.23
24-Jan-84		24	10.83	44.4			42	55.23
25-Jan-84		24	10.83	44.4		0	40	55.23
26-Jan-84		24	10.89	44.4		0	38	55.29
27-Jan-84		24	7.66	31.4		0	46	39.06
28-Jan-84		24	7.66	31.4		0	44	39.06
29-Jan-84		24	7.66	31.4		0	42	39.06
30-Jan-84		24	5.42	35.07		0	44	40.49
31-Jan-84		24	5.42	35.07	3	0	45	40.49
1-Feb-84		24	5.42	35.07	3	0	72	40.49
2-Feb-84		24	6.84	29.14		0	43	35.98
3-Feb-84		24	5.51	30.64		0	39	36.15

Table CIP8PC4A

Primrose Cycle 4A; IP8 Production Data

Date d-mmm-yy	Days	Hours on Production	Oil Produced m^3	Water Produced m^3	Fluid Level Joints	Casing Pressure kPa	Wellhead Temperature Deg C	Total Fluid Produced m^3
4-Feb-84		24	5.51	30.64		0	34	36.15
5-Feb-84		24	5.53	30.64		0	42	36.17
6-Feb-84		24	12.12	37.83	0	0	39	49.95
7-Feb-84		24	12.12	37.83	5	0	41	49.95
8-Feb-84		24	7.28	39.82	5	0	40	47.1
9-Feb-84		24	7.28	39.82	3	0	40	47.1
10-Feb-84		24	7.28	39.82	3	0	40	47.1
11-Feb-84		24	10.84	37.62	3	0	40	48.46
12-Feb-84		24	10.86	37.62		0	42	48.46
13-Feb-84		24	7.94	27.56		0	43	35.5
14-Feb-84		24	7.94	27.56	6	0	42	35.5
15-Feb-84		24	9.11	25.29		0	42	34.4
16-Feb-84		24	9.11	25.29	2	0	40	34.4
17-Feb-84		24	9.11	25.29	2	0	38	34.4
18-Feb-84		24	5.96	25.96	2	0	40	31.92
19-Feb-84		24	6	25.96	2	0	38	31.96
20-Feb-84		24	5.27	22.95	2	0	40	28.22
21-Feb-84		24	6.38	25.05	2	0	37	31.43
22-Feb-84		24	6.38	25.05		0	40	31.43
23-Feb-84		24	6.38	25.05		0	41	31.43
24-Feb-84		24	4.72	22.63		0	42	27.35
25-Feb-84		24	4.72	22.63	0	0	38	27.35
26-Feb-84		24	4.76	22.63		0	36	27.39
27-Feb-84		24	5	20.05		0	31	25.05
28-Feb-84		24	5	20.05	0	0	35	25.05
29-Feb-84		24	1.83	23.49	8	0	40	25.32

Table CIP8PC4

Primrose Cycle 4; IP8 Production Data

Date d-mmm-yy	Days	Hours on Production	Oil Produced m^3	Water Produced m^3	Fluid Level Joints	Casing Pressure kPa	Wellhead Temperature Deg C	Total Fluid Produced m^3
1-Mar-84	1.0	24	1.83	23.49	7	0	38	25.32
2-Mar-84	2.0	24	1.83	23.49	7	0	34	25.32
3-Mar-84	3.0	24	1.83	23.49	7	0	34	25.32
4-Mar-84	4.0	24	1.83	23.49	7	0	37	25.32
5-Mar-84	5.0	24	8.37	16.5	6	0	34	24.87
6-Mar-84	6.0	24	8.38	16.5	6	0	30	24.88
7-Mar-84	7.0	24	7.52	14.84	6	0	32	22.36
8-Mar-84	8.0	24	4.22	18.23	6	0	40	22.45
9-Mar-84	9.0	24	4.22	18.35	0	0	35	22.57
10-Mar-84	10.0	24	4.04	18.6	6	0	35	22.64
11-Mar-84	11.0	24	4.04	18.6	0	0	0	22.64
12-Mar-84	12.0	24	5.51	17.27	5	0	35	22.78
13-Mar-84	13.0	24	5.5	17.26	0	0	35	22.76
14-Mar-84	14.0	24	5.5	17.26	0	0	34	22.76
15-Mar-84	15.0	24	5	16.95	2	0	32	21.95
16-Mar-84	16.0	24	5	16.95	2	0	35	21.95
17-Mar-84	17.0	24	5	16.95	4	0	38	21.95
18-Mar-84	18.0	24	4.67	17.35	4	0	34	22.02
19-Mar-84	19.0	24	4.67	17.35	4	0	35	22.02
20-Mar-84	20.0	24	3.71	13.8	5	0	38	17.51
21-Mar-84	21.0	24	3.71	13.8	5	0	36	17.51
22-Mar-84	22.0	24	4.9	12.35	6	0	34	17.25
23-Mar-84	23.0	24	4.9	12.35	6	0	38	17.25
24-Mar-84	24.0	24	4.9	12.35	0	0	36	17.25
25-Mar-84	25.0	24	3.5	13.23	3	0	39	16.73
26-Mar-84	26.0	24	3.5	13.23	0	0	36	16.73

Table CIP8PC4

Primrose Cycle 4; IP8 Production Data

Date d-mmm-yy	Days	Hours on Production	Oil Produced m^3	Water Produced m^3	Fluid Level Joints	Casing Pressure kPa	Wellhead Temperature Deg C	Total Fluid Produced m^3
27-Mar-84	27.0	24	3.5	13.23	0	0	37	16.73
28-Mar-84	28.0	24	2.54	13.99	0	0	38	16.53
29-Mar-84	29.0	24	2.54	13.99	3	0	36	16.53
30-Mar-84	30.0	24	3.04	12.92	3	0	37	15.96
31-Mar-84	31.0	24	3.04	12.92	4	0	36	15.96
1-Apr-84	32.0	24	3.45	14.4	0	0	32	17.85
2-Apr-84	33.0	24	3.45	14.4	4	0	33	17.85
3-Apr-84	34.0	24	3.45	14.4	4	0	38	17.85
4-Apr-84	35.0	24	5.71	12.93	4	0	35	18.64
5-Apr-84	36.0	24	5.71	12.93	0	0	39	18.64
6-Apr-84	37.0	24	5.71	12.93	0	0	47	18.64
7-Apr-84	38.0	24	5.71	12.93	0	0	35	18.64
8-Apr-84	39.0	24	3.56	15.31	6	0	37	18.87
9-Apr-84	40.0	24	3.3	14.23	0	0	34	17.53
10-Apr-84	41.0	24	3.3	14.23	0	0	35	17.53
11-Apr-84	42.0	24	3.3	14.23	11	0	37	17.53
12-Apr-84	43.0	24	2.18	16.15	6	0	36	18.33
13-Apr-84	44.0	24	2.18	16.15	6	0	20	18.33
14-Apr-84	45.0	24	2.18	16.15	0	0	37	18.33
15-Apr-84	46.0	24	2.19	16.15	6	0	38	18.34
16-Apr-84	47.0	24	1.06	13.74	6	0	39	14.8
17-Apr-84	48.0	24	1.07	13.74	6	0	35	14.81
18-Apr-84	49.0	24	1.07	13.74	0	0	34	14.81
19-Apr-84	49.5	11	0.34	4.29	0	0	30	4.63

Table CIP8PC5

Primrose Cycle 5; IP8 Production Data

Date d-mmm-yy	Days	Hours on Production	Oil Produced m^3	Water Produced m^3	Fluid Level Joints	Casing Pressure kPa	Wellhead Temperature Deg C	Total Fluid Produced m^3
1-Jun-84	0.6	15	0	10	0	0	0	10
2-Jun-84	1.6	24	0	19	0	0	142	19
3-Jun-84	2.6	24	0	19	0	0	132	19
4-Jun-84	3.6	24	0	19	0	0	138	19
5-Jun-84	4.6	24	0	19	0	0	143	19
6-Jun-84	5.6	24	0	19	0	5700	120	19
7-Jun-84	6.6	24	0	19	0	5100	135	19
8-Jun-84	7.6	24	0	19	0	5000	155	19
9-Jun-84	8.6	24	0	19	0	4800	140	19
10-Jun-84	9.6	24	0	19	0	4500	146	19
11-Jun-84	10.6	24	0	19	0	0	146	19
12-Jun-84	11.6	24	0	19	0	1500	160	19
13-Jun-84	12.6	24	0	19	0	1300	157	19
14-Jun-84	13.6	24	0	19	0	0	0	19
15-Jun-84	14.6	24	0	19	0	0	0	19
16-Jun-84	15.6	24	0	19	0	0	94	19
17-Jun-84	16.6	24	0	19	0	0	137	19
18-Jun-84	17.6	24	3.83	23.63	0	0	147	27.46
19-Jun-84	18.6	24	4.54	23.63	0	0	150	28.17
20-Jun-84	19.6	24	7.26	18.62	0	960	144	25.88
21-Jun-84	20.6	24	7.26	18.62	0	825	118	25.88
22-Jun-84	21.6	24	7.26	18.62	0	700	115	25.88
23-Jun-84	22.6	24	8.84	18.62	0	820	142	27.46
24-Jun-84	23.6	24	3.55	18.62	0	850	137	22.17
25-Jun-84	24.6	24	3.95	18.62	0	650	135	22.57
26-Jun-84	25.6	24	7.93	18.62	0	640	128	26.55

Table CIP8PC5

Primrose Cycle 5; IP8 Production Data

Date d-mmm-yy	Days	Hours on Production	Oil Produced m^3	Water Produced m^3	Fluid Level Joints	Casing Pressure kPa	Wellhead Temperature Deg C	Total Fluid Produced m^3
27-Jun-84	26.6	24	7.93	18.62	0	550	108	26.55
28-Jun-84	27.6	24	7.93	18.62	0	580	120	26.55
29-Jun-84	28.6	24	5.61	21.77	0	650	125	27.38
30-Jun-84	29.6	24	5.61	21.77	0	620	112	27.38
1-Jul-84	30.6	24	5.92	22.96	0	720	120	28.88
2-Jul-84	31.6	24	8.53	19.27	0	620	118	27.8
3-Jul-84	32.6	24	8.53	19.27	0	480	112	27.8
4-Jul-84	33.6	24	8.53	19.27	0	400	112	27.8
5-Jul-84	34.6	24	16.38	10.3	0	360	108	26.68
6-Jul-84	35.6	24	16.38	10.3	0	380	90	26.68
7-Jul-84	36.6	24	10.64	17.49	0	360	92	28.13
8-Jul-84	37.6	24	10.64	17.49	0	310	95	28.13
9-Jul-84	38.6	24	10.64	17.49	0	300	100	28.13
10-Jul-84	39.6	24	10.64	17.49	0	275	94	28.13
11-Jul-84	40.6	24	10.38	20.5	0	200	96	30.88
12-Jul-84	41.6	24	10.38	20.5	0	200	94	30.88
13-Jul-84	42.6	24	12.71	19.07	0	150	90	31.78
14-Jul-84	43.6	24	12.71	19.07	0	70	78	31.78
15-Jul-84	44.6	24	12.71	19.07	0	50	72	31.78
16-Jul-84	45.6	24	12.79	20.25	21	22	75	33.04
17-Jul-84	46.6	24	11.85	18.77	0	20	76	30.62
18-Jul-84	47.6	24	12.79	20.25	0	20	75	33.04
19-Jul-84	48.6	24	13.74	19.74	0	10	76	33.48
20-Jul-84	49.6	24	13.74	19.74	0	0	72	33.48
21-Jul-84	50.6	24	13.74	19.74	16	0	60	33.48
22-Jul-84	51.6	24	14.58	18.9	16	0	64	33.48

Table CIP8PC5

Primrose Cycle 5; IP8 Production Data

Date d-mmm-yy	Days	Hours on Production	Oil Produced m^3	Water Produced m^3	Fluid Level Joints	Casing Pressure kPa	Wellhead Temperature Deg C	Total Fluid Produced m^3
23-Jul-84	52.6	24	14.58	18.9	16	0	64	33.48
24-Jul-84	53.6	24	14.58	18.9	16	0	66	33.48
25-Jul-84	54.6	24	16	20.75	0	0	70	36.75
26-Jul-84	55.6	24	16	20.75	0	0	63	36.75
27-Jul-84	56.6	24	15.88	19.91	21	0	62	35.79
28-Jul-84	57.6	24	16.44	17.59	0	0	70	34.03
29-Jul-84	58.6	24	16.44	17.59	0	0	65	34.03
30-Jul-84	59.6	24	14.14	18.79	0	0	66	32.93
31-Jul-84	60.6	24	14.14	18.79	0	0	64	32.93
1-Aug-84	61.6	24	17.25	22.93	0	0	62	40.18
2-Aug-84	62.6	24	17.25	22.93	0	0	64	40.18
3-Aug-84	63.6	24	17.25	22.93	0	0	67	40.18
4-Aug-84	64.6	24	17.25	22.93	0	0	64	40.18
5-Aug-84	65.6	24	17.25	22.93	0	0	62	40.18
6-Aug-84	66.6	24	17.25	22.93	0	0	65	40.18
7-Aug-84	67.6	24	17.25	22.93	0	0	50	40.18
8-Aug-84	68.6	24	17.25	22.93	0	0	57	40.18
9-Aug-84	69.6	24	17.25	22.93	0	0	58	40.18
10-Aug-84	70.6	24	17.61	21.21	0	0	61	38.82
11-Aug-84	71.6	24	14.2	15.2	0	0	53	29.4
12-Aug-84	72.6	24	12.47	15.02	0	0	56	27.49
13-Aug-84	73.6	24	12.47	15.02	0	0	49	27.49
14-Aug-84	74.6	24	12.47	15.02	11	0	52	27.49
15-Aug-84	75.6	24	12.47	15.02	0	0	50	27.49
16-Aug-84	76.6	24	12.47	15.02	0	0	54	27.49
17-Aug-84	77.6	24	8.7	15.34	18	0	54	24.04

Table CIP8PC5

Primrose Cycle 5; IP8 Production Data

Date d-mmm-yy	Days	Hours on Production	Oil Produced m^3	Water Produced m^3	Fluid Level Joints	Casing Pressure kPa	Wellhead Temperature Deg C	Total Fluid Produced m^3
18-Aug-84	78.6	24	8.7	15.34	18	0	50	24.04
19-Aug-84	79.6	24	8.7	15.34	18	0	45	24.04
20-Aug-84	80.6	24	6.96	12.27	0	0	44	19.23
21-Aug-84	81.6	24	6.96	12.27	0	0	48	19.23
22-Aug-84	82.6	24	6.82	11.3	0	0	45	18.12
23-Aug-84	83.6	24	6.82	11.3	0	0	43	18.12
24-Aug-84	84.6	24	4.2	6.95	0	0	41	11.15
25-Aug-84	85.6	24	3.26	13.24	0	0	36	16.5
26-Aug-84	86.6	24	3.26	13.24	0	0	42	16.5
27-Aug-84	87.6	24	3.26	13.24	0	0	30	16.5
28-Aug-84	88.6	24	3.26	13.24	0	0	21	16.5
29-Aug-84	89.6	24	2.71	10.65	4	0	28	13.36
30-Aug-84	90.6	24	2.71	10.65	4	0	38	13.36
31-Aug-84	91.6	24	2.71	10.65	4	0	28	13.36

Table CIP8PC5A

Primrose Cycle 5A; IP8 Production Data

Date d-mmm-yy	Days	Hours on Production	Oil Produced m^3	Water Produced m^3	Fluid Level Joints	Casing Pressure kPa	Wellhead Temperature Deg C	Total Fluid Produced m^3
1-Sep-84	1.0	24	2.71	10.67	0	0	22	13.38
2-Sep-84	2.0	24	2.71	10.67	4	0	26	13.38
3-Sep-84	3.0	24	2.71	10.67	4	0	35	13.38
4-Sep-84	4.0	24	3.47	8.89	4	0	34	12.36
5-Sep-84	5.0	24	3.47	8.9	0	0	36	12.37
6-Sep-84	6.0	24	3.47	8.9	0	0	23	12.37
7-Sep-84	7.0	24	4.35	8.85	0	0	30	13.2
8-Sep-84	8.0	24	4.35	8.85	0	0	35	13.2
9-Sep-84	9.0	24	4.35	8.85	0	0	30	13.2
10-Sep-84	10.0	24	4.35	8.85	0	0	38	13.2
11-Sep-84	11.0	24	8.89	10.81	55	0	33	19.7
12-Sep-84	12.0	24	8.89	10.81	0	0	39	19.7
13-Sep-84	12.9	22.5	10.07	12.21	9	0	32	22.28
14-Sep-84	13.9	24	4.84	9.61	9	0	32	14.45
15-Sep-84	14.9	24	4.84	9.61	6	0	27	14.45
16-Sep-84	15.9	24	4.84	9.61	6	0	30	14.45
17-Sep-84	16.9	24	4.84	9.61	6	0	28	14.45
18-Sep-84	17.9	24	4.84	9.61	6	0	24	14.45
19-Sep-84	18.9	24	4.84	9.61	0	0	30	14.45
20-Sep-84	19.9	24	4.84	9.63	0	0	30	14.47
21-Sep-84	20.9	24	5.88	9.73	7	0	19	15.61
22-Sep-84	21.9	24	3.92	16.99	6	0	26	20.91
23-Sep-84	22.9	24	9.36	11.9	8	0	29	21.26
24-Sep-84	23.9	24	6.88	13.96	15	0	30	20.84
25-Sep-84	24.9	24	6.08	14.11	21	0	35	20.19
26-Sep-84	25.9	24	3.92	9.1	1	0	48	13.02

Table CIP8PC5A

Primrose Cycle 5A; IP8 Production Data

Date d-mmm-yy	Days	Hours on Production	Oil Produced m^3	Water Produced m^3	Fluid Level Joints	Casing Pressure kPa	Wellhead Temperature Deg C	Total Fluid Produced m^3
27-Sep-84	26.9	24	3.92	9.1	1	0	36	13.02
28-Sep-84	27.9	24	3.92	9.1	1	0	38	13.02
29-Sep-84	28.9	24	3.92	9.1	1	0	38	13.02
30-Sep-84	29.9	24	4	7.58	1	0	38	11.58
1-Oct-84	30.9	24	4	7.58	1	0	36	11.58
2-Oct-84	31.9	24	4	7.58	1	0	38	11.58
3-Oct-84	32.9	24	4	7.58	0	0	38	11.58
4-Oct-84	33.9	24	4	7.58	0	0	35	11.58
5-Oct-84	34.9	24	4	7.58	0	0	32	11.58
6-Oct-84	35.9	24	4	7.58	0	0	37	11.58
7-Oct-84	36.9	24	3.8	6.28	5	0	37	10.08
8-Oct-84	37.9	24	3.8	6.28	0	0	38	10.08
9-Oct-84	38.9	24	3.8	6.28	0	0	41	10.08
10-Oct-84	39.9	24	6.26	10.34	0	0	36	16.6
11-Oct-84	40.9	24	6.26	10.34	0	0	32	16.6
12-Oct-84	41.9	24	6.26	10.34	0	0	30	16.6
13-Oct-84	42.9	24	6.26	10.34	0	0	30	16.6
14-Oct-84	43.9	24	6.26	10.34	0	0	28	16.6
15-Oct-84	44.9	24	6.26	10.34	0	0	30	16.6
16-Oct-84	45.9	24	6.26	10.34	0	0	30	16.6
17-Oct-84	46.9	24	6.26	10.34	0	0	30	16.6
18-Oct-84	47.9	24	6.12	9.51	0	0	30	15.63
19-Oct-84	48.9	24	6.12	9.51	0	0	35	15.63
20-Oct-84	49.9	24	6.12	9.51	0	0	35	15.63
21-Oct-84	50.9	24	6.12	9.51	0	0	31	15.63
22-Oct-84	51.9	24	6.12	9.51	0	0	34	15.63

Table CIP8PC5A

Primrose Cycle 5A;   IP8 Production Data

Date d-mmm-yy	Days	Hours on Production	Oil Produced m^3	Water Produced m^3	Fluid Level Joints	Casing Pressure kPa	Wellhead Temperature Deg C	Total Fluid Produced m^3
23-Oct-84	52.9	24	6.12	9.51	0	0	29	15.63
24-Oct-84	53.9	24	4.72	7.32	0	0	18	12.04
25-Oct-84	54.9	24	4.72	7.32	0	0	22	12.04
26-Oct-84	55.9	24	4.72	7.32	0	0	18	12.04
27-Oct-84	56.9	24	4.72	7.32	0	0	0	12.04
28-Oct-84	57.9	24	5.3	6.73	0	0	15	12.03
29-Oct-84	58.9	24	5.3	6.73	0	0	20	12.03
30-Oct-84	59.9	24	5.3	6.73	0	0	15	12.03
31-Oct-84	60.9	24	5.3	6.73	0	0	20	12.03
1-Nov-84	61.9	24	5.91	7.49	0	0	22	13.4
2-Nov-84	62.9	24	7.92	4.66	0	0	28	12.58
3-Nov-84	63.9	24	4.32	7.78	1	0	25	12.1
4-Nov-84	64.9	24	4.32	7.78	0	0	19	12.1
5-Nov-84	65.9	24	4.32	7.78	0	0	24	12.1
6-Nov-84	66.9	24	4.32	7.78	0	0	23	12.1
7-Nov-84	67.9	24	4.32	7.78	0	0	20	12.1
8-Nov-84	68.9	24	4.32	7.78	0	0	22	12.1
9-Nov-84	69.9	24	7.67	6.02	0	0	20	13.69
10-Nov-84	70.9	24	7.67	6.02	0	0	20	13.69
11-Nov-84	71.9	24	7.08	5.56	0	0	21	12.64
12-Nov-84	72.9	24	7.58	5.95	0	0	18	13.53
13-Nov-84	73.9	24	7.58	5.95	0	0	19	13.53
14-Nov-84	74.9	24	7.58	5.95	0	0	19	13.53
15-Nov-84	75.9	24	7.58	5.95	0	0	21	13.53
16-Nov-84	76.9	24	4.1	7.89	0	0	24	11.99
17-Nov-84	77.9	24	4.1	7.89	0	0	22	11.99

Table CIP8PC5A

Primrose Cycle 5A; IP8 Production Data

Date d-mmm-yy	Days	Hours on Production	Oil Produced m^3	Water Produced m^3	Fluid Level Joints	Casing Pressure kPa	Wellhead Temperature Deg C	Total Fluid Produced m^3
18-Nov-84	78.9	24	4.1	7.89	0	0	19	11.99
19-Nov-84	79.9	24	4.1	7.89	0	0	20	11.99
20-Nov-84	80.9	24	4.1	7.89	0	0	24	11.99
21-Nov-84	81.9	24	4.1	7.89	0	0	21	11.99
22-Nov-84	82.9	24	6.73	4.61	0	0	23	11.34
23-Nov-84	83.9	24	5.29	3.62	0	0	30	8.91
24-Nov-84	84.9	24	5.29	3.62	0	0	28	8.91
25-Nov-84	85.9	24	3.97	5.06	0	0	25	9.03
26-Nov-84	86.9	24	3.97	5.06	0	0	0	9.03
27-Nov-84	87.9	24	7.94	5.06	0	0	22	9.03
28-Nov-84	88.9	24	3.97	5.06	0	0	25	9.03
29-Nov-84	89.9	24	3.14	5.44	0	0	26	8.58
30-Nov-84	90.9	24	3.14	5.44	0	0	24	8.58
1-Dec-84	91.9	24	4.84	8.4	0	0	0	13.24
2-Dec-84	92.9	24	4.84	8.4	0	0	20	13.24
3-Dec-84	93.9	24	4.84	8.4	0	0	22	13.24
4-Dec-84	94.9	24	4.66	8.49	0	0	17	13.15
5-Dec-84	95.9	24	4.66	8.49	0	0	17	13.15
6-Dec-84	96.9	24	4.66	8.49	0	0	27	13.15
7-Dec-84	97.9	24	3.59	6.54	0	0	29	10.13
8-Dec-84	98.9	24	3.59	6.54	0	0	23	10.13
9-Dec-84	99.9	24	3.59	6.54	0	0	23	10.13
10-Dec-84	100.9	24	3.59	6.54	0	0	20	10.13
11-Dec-84	101.9	24	3.59	6.54	0	0	16	10.13
12-Dec-84	102.9	24	3.91	6.19	0	0	19	10.1
13-Dec-84	103.9	24	3.91	6.19	0	0	18	10.1

Table CIP8PC5A

Primrose Cycle 5A; IP8 Production Data

Date d-mmm-yy	Days	Hours on Production	Oil Produced m^3	Water Produced m^3	Fluid Level Joints	Casing Pressure kPa	Wellhead Temperature Deg C	Total Fluid Produced m^3
14-Dec-84	104.9	24	3.91	6.19	0	0	20	10.1
15-Dec-84	105.9	24	3.91	6.19	0	0	16	10.1
16-Dec-84	106.9	24	3.91	6.19	0	0	13	10.1
17-Dec-84	107.9	24	3.95	6.27	0	0	14	10.22
18-Dec-84	108.9	24	3.95	6.27	0	0	19	10.22
19-Dec-84	109.9	24	3.95	6.27	0	0	21	10.22
20-Dec-84	110.9	24	5.83	4.78	0	0	22	10.61
21-Dec-84	111.9	24	5.83	4.78	0	0	16	10.61
22-Dec-84	112.9	24	5.83	4.78	0	0	18	10.61
23-Dec-84	113.9	24	5.83	4.78	0	0	19	10.61
24-Dec-84	114.9	24	3.91	6.67	0	0	18	10.58
25-Dec-84	115.9	24	3.91	6.67	0	0	20	10.58
26-Dec-84	116.9	24	3.92	6.67	0	0	21	10.59
27-Dec-84	117.9	24	3.92	6.67	0	0	18	10.59
28-Dec-84	118.9	24	3.92	6.67	2	0	25	10.59
29-Dec-84	119.9	24	3.92	6.67	2	0	25	10.59
30-Dec-84	120.9	24	3.92	6.67	0	0	23	10.59
31-Dec-84	121.9	24	4.3	5.24	0	0	20	9.54
1-Jan-85	122.9	24	4.38	5.34	0	0	23	9.72
2-Jan-85	123.9	24	4.38	5.34	0	0	28	9.72
3-Jan-85	124.9	24	4.38	5.34	0	0	22	9.72
4-Jan-85	125.9	24	2.92	7.7	0	0	23	10.62
5-Jan-85	126.9	24	2.92	7.7	0	0	21	10.62
6-Jan-85	127.9	24	2.92	7.7	0	0	19	10.62
7-Jan-85	128.9	24	2.92	7.7	0	0	20	10.62
8-Jan-85	129.9	24	4.44	4.96	0	0	19	9.4

Table CIP8PC5A

Primrose Cycle 5A; IP8 Production Data

Date d-mmm-yy	Days	Hours on Production	Oil Produced m^3	Water Produced m^3	Fluid Level Joints	Casing Pressure kPa	Wellhead Temperature Deg C	Total Fluid Produced m^3
9-Jan-85	130.9	24	4.44	4.96	0	0	16	9.4
10-Jan-85	131.9	24	4.44	4.96	0	0	20	9.4
11-Jan-85	132.9	24	4.44	4.96	0	0	24	9.4
12-Jan-85	133.9	24	1.7	7.34	0	0	27	9.04
13-Jan-85	134.9	24	1.7	7.34	0	0	21	9.04
14-Jan-85	135.9	24	1.7	7.34	13	0	24	9.04
15-Jan-85	136.9	24	1.7	7.34	0	0	23	9.04
16-Jan-85	137.9	24	1.44	7.63	0	0	23	9.07
17-Jan-85	138.9	24	1.44	7.63	0	0	18	9.07
18-Jan-85	139.9	24	1.44	7.63	0	0	10	9.07
19-Jan-85	140.9	24	1.44	7.63	0	0	12	9.07
20-Jan-85	141.9	24	1.44	7.63	0	0	20	9.07
21-Jan-85	142.9	24	2.64	6.71	0	0	27	9.35
22-Jan-85	143.4	10	0.88	2.23	0	0	20	3.11

Table CW1034PC1

Primrose SWT 10-34 , Cycle 1 Production Data

Date d-mmm-yy	Days	Hours on Production	Oil Produced m^3	Water Produced m^3	Fluid Level Joints	Casing Pressure kPa	Wellhead Temperature Deg C	Total Fluid Produced m^3
8-Jun-82	1.0	24	0	3.5				3.5
9-Jun-82	2.0	24	0.57	27.73				28.3
10-Jun-82	3.0	24	0	3.01				3.01
11-Jun-82	4.0	24	0	52.75				52.75
12-Jun-82	5.0	24	0	38.2				38.2
13-Jun-82	6.0	24	0	46.7				46.7
14-Jun-82	7.0	24	0	37.64				37.64
15-Jun-82	8.0	24	2.85	25.73				28.58
16-Jun-82	9.0	24	1.94	23.9				25.84
17-Jun-82	10.0	24	2.45	22.03				24.48
18-Jun-82	11.0	24	2.7	24.6				27.3
19-Jun-82	12.0	24	1.5	28.45				29.95
20-Jun-82	13.0	24	1.14	27.48				28.62
21-Jun-82	14.0	24	1.28	32.05				33.33
22-Jun-82	15.0	24	1	24.57				25.57
23-Jun-82	16.0	24	0.65	23.74				24.39
24-Jun-82	17.0	24	1.26	21.52				22.78
25-Jun-82	18.0	24	1.67	18.48				20.15
26-Jun-82	19.0	24	4.95	23.48				28.43
27-Jun-82	20.0	24	1.39	32.37				33.76
28-Jun-82	21.0	24	4.25	31.77				36.02
29-Jun-82	22.0	24	0.12	22.23				22.35
30-Jun-82	23.0	24	2.35	27.07				29.42
1-Jul-82	24.0	24	5.86	20.81				26.67
2-Jul-82	25.0	24	4.18	28.02				32.2

Table CW1034PC1

Primrose SWT 10-34 , Cycle 1 Production Data

Date d-mmm-yy	Days	Hours on Production	Oil Produced m^3	Water Produced m^3	Fluid Level Joints	Casing Pressure kPa	Wellhead Temperature Deg C	Total Fluid Produced m^3
3-Jul-82	26.0	24	5.28	23.89				29.17
4-Jul-82	27.0	24	5.39	23.66				29.05
5-Jul-82	28.0	24	6	17.5				23.5
6-Jul-82	29.0	24	5.5	20.61				26.11
7-Jul-82	30.0	24	4	20.91				24.91
8-Jul-82	31.0	24	3.8	26.17				29.97
9-Jul-82	32.0	24	3.8	21.96				25.76
10-Jul-82	33.0	24	3.89	16.33				20.22
11-Jul-82	34.0	24	0.25	24.53				24.78
12-Jul-82	35.0	24	0.3	29.73				30.03
13-Jul-82	36.0	24	2.4	35.11				37.51
14-Jul-82	37.0	24	3.09	31.28				34.37
15-Jul-82	38.0	24	5.32	21.32				26.64
16-Jul-82	39.0	24	6.65	23.6				30.25
17-Jul-82	40.0	24	6.13	24.52				30.65
18-Jul-82	41.0	24	7.93	31.71				39.64
19-Jul-82	42.0	24	3.39	44.99				48.38
20-Jul-82	43.0	24	2.52	39.44				41.96
21-Jul-82	44.0	24	6.52	24.65	32	150		31.17
22-Jul-82	45.0	24	6.6	36.09				42.69
23-Jul-82	46.0	24	6.97	33.91				40.88
24-Jul-82	47.0	24	6.13	36.94	40	150		43.07
25-Jul-82	48.0	24	6.1	32.11				38.21
26-Jul-82	49.0	24	6.86	34.42	32	150		41.28
27-Jul-82	50.0	24	7.86	35.07	39	150		42.93
28-Jul-82	51.0	24	7.3	34.72	32	150		42.02

Table CW1034PC1

Primrose SWT 10-34 , Cycle 1 Production Data

Date d-mmm-yy	Days	Hours on Production	Oil Produced m^3	Water Produced m^3	Fluid Level Joints	Casing Pressure kPa	Wellhead Temperature Deg C	Total Fluid Produced m^3
29-Jul-82	52.0	24	7.88	32.57	34	150		40.45
30-Jul-82	53.0	24	8.16	32.68	31	150		40.84
31-Jul-82	54.0	24	8.1	35.05	37	150		43.15
1-Aug-82	55.0	24	8.1	34.74	31	150		42.84
2-Aug-82	56.0	24	8.05	21.56	30	150		29.61
3-Aug-82	57.0	24	8.05	29.38				37.43
4-Aug-82	58.0	24	8.07	32.66	40	150		40.73
5-Aug-82	59.0	24	7.9	33.72				41.62
6-Aug-82	60.0	24	7.95	30.88				38.83
7-Aug-82	61.0	24	8.1	29.3				37.4
8-Aug-82	62.0	24	8.05	31.02	39	150		39.07
9-Aug-82	63.0	24	7.77	30.57				38.34
10-Aug-82	64.0	24	7.76	31.48				39.24
11-Aug-82	65.0	24	8.9	23.83	32	150		32.73
12-Aug-82	66.0	24	9.5	26.85	32	150		36.35
13-Aug-82	67.0	24	10.5	26.62	32	150		37.12
14-Aug-82	68.0	24	10	27.22	37	150		37.22
15-Aug-82	69.0	24	10	27.53	36	150		37.53
16-Aug-82	70.0	24	11.27	24.15				35.42
17-Aug-82	70.4	10	6	16.43				22.43
18-Aug-82	70.4	0		0				
19-Aug-82	70.7	6	8.82	0	31	150		8.82
20-Aug-82	71.7	24	2.17	34.58				36.75
21-Aug-82	72.7	24	1.29	24.54				25.83
22-Aug-82	73.7	24	2.17	41.32	33	150		43.49
23-Aug-82	74.7	24	1.79	34.15				35.94

Table CW1034PC1

Primrose SWT 10-34 , Cycle 1 Production Data

Date d-mmm-yy	Days	Hours on Production	Oil Produced m^3	Water Produced m^3	Fluid Level Joints	Casing Pressure kPa	Wellhead Temperature Deg C	Total Fluid Produced m^3
24-Aug-82	75.7	24	3.36	30.28				33.64
25-Aug-82	76.7	24	5.29	28.41				33.7
26-Aug-82	77.7	24	3.33	29.99				33.32
27-Aug-82	78.7	24	4.17	32.36				36.53
28-Aug-82	79.7	24	4.35	31.91	33	150		36.26
29-Aug-82	80.7	24	4.91	34.38	34	150		39.29
30-Aug-82	81.7	24	3.46	27.97				31.43
31-Aug-82	82.7	24	3.81	34.31	35	150		38.12
1-Sep-82	83.7	24.0	2.5	38.7	35	200	58	41.2
2-Sep-82	84.7	24.0	2.7	36.9	35	240	56	39.7
3-Sep-82	85.7	24.0	3.0	36.2	37	240	56	39.2
4-Sep-82	86.7	24.0	4.4	36.0		170	56	40.4
5-Sep-82	87.7	24.0	3.6	32.3	35	160	55	35.8
6-Sep-82	88.7	24.0	4.2	34.5		170	56	38.7
7-Sep-82	89.7	24.0	3.9	34.8		165	54	38.6
8-Sep-82	90.7	24.0	3.4	33.3		171	58	36.7
9-Sep-82	91.7	24.0	4.3	32.7	32	172	57	37.0
10-Sep-82	92.7	24.0	4.2	32.1		175	52	36.3
11-Sep-82	93.7	24.0	4.4	36.3	33	174	51	40.7
12-Sep-82	94.7	24.0	3.4	30.5		174	53	33.9
13-Sep-82	95.7	24.0	4.2	31.7		175	55	35.8
14-Sep-82	96.7	24.0	3.0	35.3		166	56	38.4
15-Sep-82	97.7	24.0	2.0	34.8		175	55	36.8
16-Sep-82	98.7	24.0	1.3	34.1	20	177	53	35.4
17-Sep-82	99.7	24.0	1.5	32.8	20	174	53	34.3
18-Sep-82	100.7	24.0	2.0	35.5	21	175	51	37.6

Table CW1034PC1

Primrose SWT 10-34 , Cycle 1 Production Data

Date d-mmm-yy	Days	Hours on Production	Oil Produced m^3	Water Produced m^3	Fluid Level Joints	Casing Pressure kPa	Wellhead Temperature Deg C	Total Fluid Produced m^3
19-Sep-82	101.7	24.0	2.1	35.8	24	171	51	37.9
20-Sep-82	102.7	24.0	1.3	32.8	22	173	50	34.1
21-Sep-82	103.7	24.0	1.1	33.4		172	52	34.5
22-Sep-82	104.7	24.0	2.3	33.3	22	175	53	35.6
23-Sep-82	105.7	24.0	2.8	34.0	22	175	48	36.8
24-Sep-82	106.7	24.0	2.7	33.8		175	48	36.4
25-Sep-82	107.7	24.0	3.8	33.6	27	175	51	37.4
26-Sep-82	108.7	24.0	4.0	29.9		176	49	33.9
27-Sep-82	109.7	24.0	4.2	31.0	23	175	54	35.2
28-Sep-82	110.7	24.0	3.5	32.7	21	175	60	36.2
29-Sep-82	111.7	24.0	4.0	30.1	21	183	58	34.1
30-Sep-82	112.7	24.0	4.4	33.8	21	181	56	38.2
1-Oct-82	113.7	24.0	4.2	31.6	24	175	57	35.8
2-Oct-82	114.7	24.0	4.3	32.1	23	171	57	36.4
3-Oct-82	115.7	24.0	4.1	31.3		178	57	35.4
4-Oct-82	116.7	24.0	4.3	32.9	23	176	57	37.2
5-Oct-82	117.7	24.0	3.0	33.0	23	175	57	36.0
6-Oct-82	118.7	24.0	3.4	33.3		175	54	36.7
7-Oct-82	119.7	24.0	2.7	26.9		171	53	29.6
8-Oct-82	120.7	24.0	3.4	31.0		180	57	34.4
9-Oct-82	121.7	24.0	1.5	18.2				19.7
10-Oct-82	122.7	24.0	2.9	28.9		50	59	31.8
11-Oct-82	123.7	24.0	3.7	30.2		175	58	33.9
12-Oct-82	124.7	24.0	3.8	31.5	23	180	58	35.3
13-Oct-82	125.7	24.0	1.7	30.5		170	57	32.2
14-Oct-82	126.7	24.0	3.9	31.4		175	58	35.3

Table CW1034PC1

Primrose SWT 10-34 , Cycle 1 Production Data

Date d-mmm-yy	Days	Hours on Production	Oil Produced m³	Water Produced m³	Fluid Level Joints	Casing Pressure kPa	Wellhead Temperature Deg C	Total Fluid Produced m³
15-Oct-82	127.7	24.0	2.2	30.2		175	58	32.4
16-Oct-82	128.7	24.0	1.4	30.5		175	57	31.9
17-Oct-82	129.7	24.0	1.9	31.1		175	54	32.9
18-Oct-82	130.7	24.0	1.9	35.6		171	54	37.5
19-Oct-82	131.7	24.0	1.3	34.3		173	56	35.6
20-Oct-82	132.7	24.0	1.9	29.5		179	55	31.4
21-Oct-82	133.7	24.0	2.4	32.5	22	120	55	34.9
22-Oct-82	134.7	24.0	2.4	28.7		180	50	31.1
23-Oct-82	135.7	24.0	2.3	29.7		175	51.6	32.0
24-Oct-82	136.7	24.0	3.7	27.8		180	54	31.5
25-Oct-82	137.7	24.0	3.3	26.5		175	54	29.7
26-Oct-82	138.7	24.0	3.2	26.0		176	54	29.2
27-Oct-82	139.7	24.0	3.4	33.8		174	54	37.3
28-Oct-82	140.7	24.0	3.0	26.9		182	54	29.8
29-Oct-82	141.7	24.0	3.5	28.8		180	51	32.3
30-Oct-82	142.7	24.0	2.2	34.2		177	51	36.5
31-Oct-82	143.7	24.0	1.8	27.9		174	51	36.0
1-Nov-82	144.7	24.0	1.9	33.7		175	50	29.8
2-Nov-82	145.7	24.0	2.6	35.7				36.3
3-Nov-82	146.7	24.0	1.6	28.2				37.3
4-Nov-82	147.7	24.0	1.6	41.9				29.9
5-Nov-82	148.7	24.0	2.4	25.5				44.2
6-No[illegible]	149.7	24.0	6.7	35.8				32.2
7-Nov-82	150.7	24.0	1.6	24.0	24			37.4
8-Nov-82	151.7	24.0	0.0	18.9				24.0
9-Nov-82	152.7	24.0	2.0	28.8				20.9

Table CW1034PC1

Primrose SWT 10-34 , Cycle 1 Production Data

Date d-mmm-yy	Days	Hours on Production	Oil Produced m^3	Water Produced m^3	Fluid Level Joints	Casing Pressure kPa	Wellhead Temperature Deg C	Total Fluid Produced m^3
10-Nov-82	153.7	24.0	1.7	27.8		169	44	30.5
11-Nov-82	154.7	24.0	0.9	24.7	23	180	48	28.7
12-Nov-82	155.7	24.0	1.8	24.7		168	47	26.5
13-Nov-82	156.7	24.0	1.7	26.9		176	41	26.4
14-Nov-82	156.7	1.0	0.2	3.57				27.1

Table CW1034PC2

Primrose SWT 10-34 , Cycle 2 Production Data

Date d-mmm-yy	Days	Hours on Production	Oil Produced m^3	Water Produced m^3	Fluid Level Joints	Casing Pressure kPa	Wellhead Temperature Deg C	Total Fluid Produced m^3
6-Jan-83	0.7	16.0	0.0	25.9		2000	183	25.9
7-Jan-83	1.4	18.0	0.0	10.6		2000	149	10.6
8-Jan-83	1.4	0.0	0.0	0.0				0.0
9-Jan-83	1.7	7.0	0.3	9.6		125	71	9.9
10-Jan-83	2.7	24.0	0.3	8.7			53	9.0
11-Jan-83	3.7	24.0	2.3	4.6	33	47	56	6.9
12-Jan-83	4.7	24.0	2.0	6.0	25	113	54	7.9
13-Jan-83	5.7	24.0	1.2	8.7	31	144	57	9.9
14-Jan-83	6.7	24.0	1.7	12.2	31	162	64	13.9
15-Jan-83	7.4	17.0	3.0	9.1		164	56	12.1
16-Jan-83	8.4	22.5	7.3	9.1	30	160	45	16.4
17-Jan-83	9.4	24.0	8.2	10.3	33	352	62	18.5
18-Jan-83	10.4	24.0	7.1	9.4	32	615	69	16.5
19-Jan-83	11.4	24.0	15.2	6.6	31			21.7
20-Jan-83	12.4	24.0	17.6	4.0	19	339	76	21.6
21-Jan-83	13.4	24.0	18.9	2.1	31	434	82	21.0
22-Jan-83	14.4	24.0	15.5	2.3	21	428	80	17.8
23-Jan-83	15.2	21.0	12.3	3.9	25	825	70	16.1
24-Jan-83	16.2	24.0	20.8	4.3		770	76	25.1
25-Jan-83	17.2	24.0	8.4	4.2		1000	58	12.5
26-Jan-83	18.2	24.0	8.7	6.3		835	60	15.0
27-Jan-83	19.2	24.0	9.6	10.2		530	72	19.8
28-Jan-83	20.2	24.0	8.2	9.1		177.1	9.13	17.3
29-Jan-83	21.2	24.0	10.1	11.7	32	188.8	11.7	21.8
30-Jan-83	22.2	24.0	9.9	11.0	30	525	75	20.9

Table CW1034PC2

Primrose SWT 10-34 , Cycle 2 Production Data

Date d-mmm-yy	Days	Hours on Production	Oil Produced m^3	Water Produced m^3	Fluid Level Joints	Casing Pressure kPa	Wellhead Temperature Deg C	Total Fluid Produced m^3
31-Jan-83	23.2	24.0	10.0	12.1	32	577	73	22.2
1-Feb-83	24.2	24.0	10.5	9.2		421	77	19.7
2-Feb-83	25.2	24.0	11.4	8.2		500	71	19.6
3-Feb-83	26.2	24.0	14.4	8.5	27	399	78	22.9
4-Feb-83	27.2	24.0	14.3	9.2	27	433	78	23.5
5-Feb-83	28.2	24.0	13.3	9.2	21	426	76	22.5
6-Feb-83	29.2	24.0	12.1	9.6	36	434	75	21.7
7-Feb-83	30.2	24.0	14.3	12.6	32	408	76	27.0
8-Feb-83	31.2	24.0	19.3	3.6	29		76	22.9
9-Feb-83	32.2	24.0	17.8	4.4	32	404	75	22.2
10-Feb-83	33.2	24.0	15.5	4.6	31	420	75	20.2
11-Feb-83	34.2	24.0	20.0	6.6		392	76	26.6
12-Feb-83	35.2	24.0	13.0	4.7		350	83	17.6
13-Feb-83	36.2	24.0	12.8	4.2		400	83	17.0
14-Feb-83	37.2	24.0	16.7	6.3		400	83	23.0
15-Feb-83	38.2	24.0	13.1	6.1	33	400	80	19.3
16-Feb-83	39.2	24.0	19.4	7.1	35	452	79	26.5
17-Feb-83	40.2	24.0	20.1	5.4	39	430	78.8	25.4
18-Feb-83	41.2	24.0	15.4	4.0	37	446	78.6	19.5
19-Feb-83	42.2	24.0	15.8	5.5	37	489	73.6	21.3
20-Feb-83	42.6	10.0	7.0	8.5		275	97	15.5
21-Feb-83	43.6	24.0	29.2	11.2	32	219	98.5	40.4
22-Feb-83	44.6	24.0	23.6	14.0	32	250	100	37.5
23-Feb-83	45.6	24.0	31.8	18.9	32	220	112.5	50.7
24-Feb-83	46.6	24.0	25.5	22.9		150	111	48.4
25-Feb-83	47.6	24.0	25.6	23.0	34	150	111	48.6

Table CW1034PC2

Primrose SWT 10-34 , Cycle 2 Production Data

Date d-mmm-yy	Days	Hours on Production	Oil Produced m^3	Water Produced m^3	Fluid Level Joints	Casing Pressure kPa	Wellhead Temperature Deg C	Total Fluid Produced m^3
26-Feb-83	48.6	24.0	27.7	29.6		162	110	57.4
27-Feb-83	49.6	24.0	23.9	21.5		173	112	45.4
28-Feb-83	50.6	24.0	25.1	24.6		170	109	49.7
1-Mar-83	51.6	24.0	29.0	16.7	29	170	110	45.7
2-Mar-83	52.6	24.0	27.12	19.22		137	111	46.3
3-Mar-83	53.6	24.0	20.72	12.46		167	112	33.2
4-Mar-83	54.6	23.5	26.26	15.15				41.4
5-Mar-83	55.6	24.0	21.73	19.6		217	110	41.3
6-Mar-83	56.6	24.0	27.81	24.11		203	106	51.9
7-Mar-83	57.6	24.0	23.04	17.71	32	420	110	40.8
8-Mar-83	58.6	24.0	20.59	25.28		258	109	45.9
9-Mar-83	59.6	24.0	35.41	18.63				54.0
10-Mar-83	60.6	24.0	35.05	16.74		285	120.6	51.8
11-Mar-83	61.6	24.0	27.2	27.32		305	119	54.5
12-Mar-83	62.6	24.0	27.01	30.61		233	115	57.6
13-Mar-83	63.6	24.0	28.65	35.18		246	114	63.8
14-Mar-83	64.6	24.0	32.84	32.98		212	112	65.8
15-Mar-83	65.6	24.0	34.29	27.36	20	188	95	61.7
16-Mar-83	66.6	24.0	45.41	22.15		182	110	67.6
17-Mar-83	67.6	24.0	42.07	23.29		178	104	65.4
18-Mar-83	68.6	23.0	36.18	27.18	20	180	102	63.4
19-Mar-83	69.6	24.0	41.29	35.68		182	102	77.0
20-Mar-83	70.6	24.0	40.92	38.31		194	103	79.2
21-Mar-83	71.6	24.0	27.91	43.04	28	188	103	71.0
22-Mar-83	72.6	24.0	39.57	38.33		196	102	77.9
23-Mar-83	73.6	24.0	36.73	45.48		180	104	82.2

Table CW1034PC2

Primrose SWT 10-34 , Cycle 2 Production Data

Date d-mmm-yy	Days	Hours on Production	Oil Produced m^3	Water Produced m^3	Fluid Level Joints	Casing Pressure kPa	Wellhead Temperature Deg C	Total Fluid Produced m^3
24-Mar-83	74.6	24.0	33.19	44.64		168	103	77.8
25-Mar-83	75.6	24.0	28.03	48.78		157	103	76.8
26-Mar-83	76.6	24.0	13.99	50.15		130	101	64.1
27-Mar-83	77.6	24.0	21.86	45.71	26	133	96	67.6
28-Mar-83	78.6	24.0	23.1	42.07	27	122	98	65.2
29-Mar-83	79.6	24.0	21.01	43.92		150	99	64.9
30-Mar-83	80.6	24.0	22.74	47.52		175	100	70.3
31-Mar-83	81.6	24.0	21.6	42.93	24	125	98	64.5
1-Apr-83	82.6	24.0	21.88	45.74		157	98	67.6
2-Apr-83	83.6	24.0	20.69	47.97		177	98	68.7
3-Apr-83	84.6	24.0	21.5	49.85		180	99	71.4
4-Apr-83	85.6	24.0	18.47	47.8		165	85	66.3
5-Apr-83	86.6	24.0	23.23	49.29	30	180	99	72.5
6-Apr-83	87.6	24.0	20.87	49.09	24	155	99	70.0
7-Apr-83	88.6	24.0	22.26	49.69	25	129	97	72.0
8-Apr-83	89.6	24.0	22.25	52.36		155	102	74.6
9-Apr-83	90.6	24.0	20.11	52.78		135	101	72.9
10-Apr-83	91.6	24.0	21.86	54.25	26	146	101	76.1
11-Apr-83	92.6	24.0	10.69	56.09		135	96	66.8
12-Apr-83	93.6	24.0	12.21	59.74		130	94	72.0
13-Apr-83	94.6	24.0	12.44	60.91		138	94	73.4
14-Apr-83	95.6	23.5	11.78	61.66	18	129	98	73.4
15-Apr-83	96.6	24.0	15.35	66.29	17	136	101	81.6
16-Apr-83	97.6	24.0	20.79	55.68	18	131	100	76.5
17-Apr-83	98.6	24.0	20.36	60.09	20	125	102	80.5
18-Apr-83	99.6	24.0	22.47	63.07	20	125	101	85.5

Table CW1034PC2

Primrose SWT 10-34 , Cycle 2 Production Data

Date d-mmm-yy	Days	Hours on Production	Oil Produced m^3	Water Produced m^3	Fluid Level Joints	Casing Pressure kPa	Wellhead Temperature Deg C	Total Fluid Produced m^3
19-Apr-83	100.6	24.0	20.87	52.7		122	101	73.6
20-Apr-83	101.6	24.0	17.77	56.26		118	98	74.0
21-Apr-83	102.4	19.0	13.84	41.3		116	96	55.1
22-Apr-83	103.4	24.0	18.87	63.54	16	118	102	82.4
23-Apr-83	104.4	24.0	18.32	58.02	20	120	98	76.3
24-Apr-83	105.4	24.0	21.46	60.48	16	121	98	81.9
25-Apr-83	106.4	24.0	20.94	66.33	20	120	92	87.3
26-Apr-83	107.4	24.0	14.82	89.25	14	113	93	104.1
27-Apr-83	108.4	24.0	14.82	60.33		126	97	75.2
28-Apr-83	109.4	24.0	17.15	73.98	30	123	98	91.1
29-Apr-83	110.4	24.0	17.67	71.85	22	120	98	89.5
30-Apr-83	111.4	24.0	15.88	68.54	30	124	98	84.4
1-May-83	112.4	24.0	17.12	69.63	30	125	98	86.8
2-May-83	113.4	24.0	16.1	73.89	30	125	95	90.0
3-May-83	114.4	24.0	14.43	72.65		125	95	87.1
4-May-83	115.4	24.0	18.95	69.37	15	138	96	88.3
5-May-83	116.4	24.0	18.6	74.22		150	96	92.8
6-May-83	117.2	19.5	15.09	67.32	17	150	92	82.4
7-May-83	118.2	24.0	16.59	78.69		142	94	95.3
8-May-83	119.2	24.0	21.51	81.28	16	154	95	102.8
9-May-83	120.2	24.0	20.21	76.28		150	95	96.5
10-May-83	121.2	24.0	15.75	80.46	14	150	96	96.2
11-May-83	122.2	24.0	13	73.4	18			88.4
12-May-83	123.1	22.0	11.94	84.03	16	124	89	96.0
13-May-83	124.1	24.0	12.77	83.79	16	130	92	96.6
14-May-83	125.1	24.0	9.91	87.7		123	91	97.6

Table CW1034PC2

Primrose SWT 10-34 , Cycle 2 Production Data

Date d-mmm-yy	Days	Hours on Production	Oil Produced m^3	Water Produced m^3	Fluid Level Joints	Casing Pressure kPa	Wellhead Temperature Deg C	Total Fluid Produced m^3
15-May-83	126.1	24.0	10.99	89.72	16	133	87	100.7
16-May-83	127.1	24.0	10.66	86.95	16	131	87	97.6
17-May-83	128.1	24.0	9.86	90.03		128	87	99.9
18-May-83	129.1	24.0	6.13	96.15	13	124	86	102.3
19-May-83	130.1	24.0	6.96	105.61	14	135	87	112.6
20-May-83	131.0	22.5	7.51	92.23	15	136	90	99.7
21-May-83	132.0	24.0	6.85	84.09	13	130	91	90.9
22-May-83	133.0	24.0	4.54	97.03	14	122	87	101.6
23-May-83	134.0	24.0	4.89	104.37	17	124	89	109.3
24-May-83	135.0	24.0	4.22	94.91	17	119	85	99.1
25-May-83	136.0	23.0	5.43	89.55		135	86	95.0
26-May-83	137.0	24.0	7.05	81.74		141	86	88.8
27-May-83	137.4	11.0	1.67	27.66	15	135	85	29.3
28-May-83	137.4				29			

Table CW1034PC3

Primrose SWT 10-34 , Cycle 3 Production Data

Date d-mmm-yy	Days	Hours on Production	Oil Produced m^3	Water Produced m^3	Fluid Level Joints	Casing Pressure kPa	Wellhead Temperature Deg C	Total Fluid Produced m^3
21-Jul-83	0.5	12	0	7.96	38		72	7.96
22-Jul-83	1.5	23	0	11.65	36	122	77	11.65
23-Jul-83	2.5	24	0	9.37	33	100	72	9.37
24-Jul-83	3.0	12	0	5.88	31		66	5.88
25-Jul-83	3.6	15.5	0	10.13	32	120	82	10.13
26-Jul-83	4.6	24	0	18.75	32	130	86	18.75
27-Jul-83	5.6	24	0	17.08	32	148	81	17.08
28-Jul-83	6.6	24	5.83	21.12	37	152	88	26.95
29-Jul-83	7.6	24	18.3	17.8	33	165	84	36.1
30-Jul-83	8.6	24	14.25	10.22	33	162	81	24.47
31-Jul-83	9.4	20	12.2	11.72	31	165	80	23.92
1-Aug-83	10.4	24	17.65	8.85	32	190	76	26.5
2-Aug-83	11.4	24	16.49	8.99	32	422	78	25.48
3-Aug-83	12.4	24	14.14	10.68	32	462	77	24.82
4-Aug-83	13.4	24	16.12	10.8	29	400	76	26.92
5-Aug-83	14.4	24	16.05	12.63	30	436	78	28.68
6-Aug-83	15.4	24	16.64	12.56	30	386	79	29.2
7-Aug-83	16.4	23	13.06	8.75	30	389	75	21.81
8-Aug-83	17.4	24	19.21	12.86	30	305	81	32.07
9-Aug-83	18.4	24	17.84	11.95	28	268	84	29.79
10-Aug-83	19.4	24	18.3	14.38	27	185	89	32.68
11-Aug-83	20.4	24	24.12	16.83	24	202	101	40.95
12-Aug-83	21.4	24	21.32	18.17	23	202	102	39.49
13-Aug-83	22.4	24	22.37	14.99	23	215	101	37.36
14-Aug-83	23.4	24	26.18	17.55	18	232	101	43.73

Table CW1034PC3

Primrose SWT 10-34 , Cycle 3 Production Data

Date d-mmm-yy	Days	Hours on Production	Oil Produced m^3	Water Produced m^3	Fluid Level Joints	Casing Pressure kPa	Wellhead Temperature Deg C	Total Fluid Produced m^3
15-Aug-83	24.4	23	25.83	18.02	15	270	102	43.85
16-Aug-83	25.4	24	15.38	32.02	14	388	107	47.4
17-Aug-83	26.4	24	17.13	28.83	16	388	103	45.96
18-Aug-83	27.4	24	14.08	27.92	16.5	361	100	42
19-Aug-83	28.4	24	16.21	26.33	17	379	102	42.54
20-Aug-83	29.4	24	15.85	29.45	17	401	102	45.3
21-Aug-83	30.4	24	17.99	20.73	22	442	91	38.72
22-Aug-83	31.4	24	13.69	24.28		701	87	37.97
23-Aug-83	32.4	24	27.15	13.51		880	90	40.66
24-Aug-83	33.4	24	33.13	12.76	30	987	91	45.89
25-Aug-83	34.4	24	29.9	12.52	30	1000	91	42.42
26-Aug-83	35.4	24	27.75	13.16		1050	91	40.91
27-Aug-83	36.4	24	29.23	16.96		1033	92	46.19
28-Aug-83	37.4	24	30.26	16.87		1042	89	47.13
29-Aug-83	38.4	24	25.74	16.18		1050	86	41.92
30-Aug-83	39.4	24	16.53	29.18		942	86	45.71
31-Aug-83	40.4	24	18.37	31.05		779	88	49.42
1-Sep-83	41.4	24.0	18.1	34.7		10.0	90.0	52.8
2-Sep-83	42.4	24.0	17.6	26.1		15.0	87.0	43.7
3-Sep-83	43.4	24.0	21.5	20.4		20.0	88.0	41.9
4-Sep-83	44.4	24.0	21.0	25.8		20.0	100.0	46.9
5-Sep-83	45.4	24.0	17.4	37.8		20.0	112.0	55.2
6-Sep-83	46.4	24.0	31.7	25.5		20.0	112.0	57.3
7-Sep-83	47.4	24.0	30.7	26.9		20.0	112.0	57.6
8-Sep-83	48.4	24.0	26.4	26.1		20.0	111.0	52.5
9-Sep-83	49.4	24.0	31.9	26.7		25.0	116.0	58.7

Table CW1034PC3

Primrose SWT 10-34 , Cycle 3 Production Data

Date d-mmm-yy	Days	Hours on Production	Oil Produced m^3	Water Produced m^3	Fluid Level Joints	Casing Pressure kPa	Wellhead Temperature Deg C	Total Fluid Produced m^3
10-Sep-83	50.4	24.0	26.8	31.3		20.0	122.0	58.1
11-Sep-83	51.4	24.0	27.9	25.4		20.0	122.0	53.3
12-Sep-83	52.4	24.0	30.1	29.8		20.0	126.0	59.9
13-Sep-83	53.4	24.0	16.1	49.8		20.0	126.0	65.9
14-Sep-83	54.4	24.0	16.6	38.5		20.0	121.0	55.1
15-Sep-83	55.4	24.0	17.9	38.4		20.0	124.0	56.3
16-Sep-83	56.4	24.0	10.0	42.4		20.0	127.0	52.4
17-Sep-83	57.4	24.0	18.0	43.4		20.0	124.0	61.4
18-Sep-83	58.3	23.0	16.3	44.4		20.0	125.0	60.7
19-Sep-83	59.3	24.0	17.9	39.8	29.0	20.0		57.7
20-Sep-83	60.3	24.0	21.6	26.3		0.0	106.0	47.9
21-Sep-83	61.3	24.0	28.3	29.4		0.0	122.0	57.7
22-Sep-83	62.3	24.0	26.1	46.1		0.0	128.0	72.1
23-Sep-83	63.3	24.0	24.7	38.5		0.0	128.0	63.3
24-Sep-83	64.3	24.0	24.2	32.0		0.0	125.0	56.2
25-Sep-83	65.3	23.0	29.6	32.0		0.0	110.0	61.6
26-Sep-83	66.3	24.0	25.6	36.7		0.0	118.0	62.3
27-Sep-83	67.3	24.0	24.0	41.3		0.0	128.0	65.3
28-Sep-83	68.3	24.0	25.1	46.8		0.0	129.0	71.8
29-Sep-83	69.3	24.0	26.5	40.3		0.0	129.0	66.9
30-Sep-83	70.3	24.0	23.2	38.3		0.0	126.0	61.6
1-Oct-83	71.3	24.0	17.3	29.7	23.0	0.0	108.0	47.0
2-Oct-83	72.3	24.0	13.6	22.8		0.0	85.0	36.4
3-Oct-83	73.1	21.0	17.8	29.9		0.0	97.0	47.7
4-Oct-83	74.0	21.0	20.1	31.8		0.0	98.0	51.9
5-Oct-83	74.9	21.0	19.7	27.7		0.0	84.0	47.4

Table CW1034PC3

Primrose SWT 10-34 , Cycle 3 Production Data

Date d-mmm-yy	Days	Hours on Production	Oil Produced m^3	Water Produced m^3	Fluid Level Joints	Casing Pressure kPa	Wellhead Temperature Deg C	Total Fluid Produced m^3
6-Oct-83	75.7	19.0	15.8	27.0	22.0	0.0	82.0	42.8
7-Oct-83	76.5	20.0	20.5	32.4		0.0	96.0	52.9
8-Oct-83	77.5	24.0	26.8	34.6		0.0	102.0	61.4
9-Oct-83	78.5	24.0	18.6	40.6		0.0	101.0	59.2
10-Oct-83	79.5	24.0	20.0	56.5		0.0	99.0	76.5
11-Oct-83	80.5	24.0	15.2	39.4		0.0	101.0	54.7
12-Oct-83	81.5	23.0	19.8	43.3		0.0	102.0	63.1
13-Oct-83	82.5	24.0	18.7	43.3		0.0	103.0	61.9
14-Oct-83	83.4	22.0	17.5	42.3		0.0	101.0	59.8
15-Oct-83	84.4	24.0	19.7	51.6		0.0	102.0	71.2
16-Oct-83	85.4	23.0	18.5	41.1		0.0	104.0	59.6
17-Oct-83	86.4	24.0	18.7	38.4		0.0	104.0	57.1
18-Oct-83	87.4	24.0	16.0	47.6		0.0	103.0	63.6
19-Oct-83	88.3	23.0	28.0	26.4		0.0	106.0	54.5
20-Oct-83	89.3	24.0	12.4	52.6		0.0	105.0	65.0
21-Oct-83	90.3	24.0	28.2	36.6		0.0	104.0	64.8
22-Oct-83	91.3	24.0	14.4	29.7		0.0	104.0	44.1
23-Oct-83	92.3	24.0	25.5	46.5		0.0	102.0	72.0
24-Oct-83	93.3	23.0	4.0	36.9		0.0	102.0	40.9
25-Oct-83	94.3	24.0	4.0	19.0		0.0	102.0	22.9
26-Oct-83	95.3	24.0	4.0	45.4		0.0	104.0	49.4
27-Oct-83	96.3	24.0	13.8	58.1		0.0	110.0	71.8
28-Oct-83	97.3	24.0	6.6	64.1		0.0	112.0	70.7
29-Oct-83	98.3	24.0	20.0	40.8		0.0	110.0	60.8
30-Oct-83	99.3	24.0	7.8	58.5	24.0	0.0	120.0	66.3
31-Oct-83	100.3	24.0	13.0	45.2	24.0	0.0	120.0	58.2

Table CW1034PC3

Primrose SWT 10-34 , Cycle 3 Production Data

Date d-mmm-yy	Days	Hours on Production	Oil Produced m^3	Water Produced m^3	Fluid Level Joints	Casing Pressure kPa	Wellhead Temperature Deg C	Total Fluid Produced m^3
1-Nov-83	101.3	24.0	19.3	49.3		0.0	119.0	68.6
2-Nov-83	102.3	24.0	34.9	30.4		0.0	116.0	65.3
3-Nov-83	103.3	24.0	15.5	51.8	25.0	0.0	118.0	67.3
4-Nov-83	104.2	23.0	15.1	51.9	25.0	0.0	116.0	67.0
5-Nov-83	105.2	24.0	13.0	57.6	25.0	0.0	118.0	70.6
6-Nov-83	106.2	24.0	29.9	44.8	25.0	0.0	115.0	74.7
7-Nov-83	107.2	24.0	16.1	51.2	21.0	0.0	110.0	67.3
8-Nov-83	108.2	24.0	23.5	49.9	21.0	0.0	108.0	73.4
9-Nov-83	109.2	24.0	6.2	67.3	21.0	0.0	104.0	73.6
10-Nov-83	110.2	24.0	21.5	45.1		0.0	104.0	66.7
11-Nov-83	111.2	24.0	20.4	51.7		0.0	107.0	72.1
12-Nov-83	112.2	24.0	13.0	58.8	21.0	0.0	109.0	71.8
13-Nov-83	113.2	24.0	10.6	59.1		0.0	109.0	69.7
14-Nov-83	114.2	24.0	12.1	58.1	21.0	0.0	108.0	70.2
15-Nov-83	115.2	24.0	14.2	52.8	21.0	0.0	106.0	67.0
16-Nov-83	116.2	24.0	14.8	61.1	21.0	0.0	110.0	75.9
17-Nov-83	117.2	24.0	17.4	53.7		0.0	110.0	71.1
18-Nov-83	118.2	24.0	21.1	49.5		0.0	110.0	70.7
19-Nov-83	119.2	24.0	20.9	57.3		0.0	110.0	78.2
20-Nov-83	120.2	24.0	14.7	50.7		0.0	108.0	65.3
21-Nov-83	121.2	24.0	15.4	56.6		0.0	100.0	72.0
22-Nov-83	122.2	24.0	14.8	51.3		0.0	100.0	66.0
23-Nov-83	123.2	24.0	15.3	51.5		0.0	100.0	66.8
24-Nov-83	124.0	18.5	12.0	36.7		0.0	101.0	48.6
25-Nov-83	124.0	0.0	0.0	0.0	shut-in	0.0		0.0
26-Nov-83	124.5	11.5	6.2	33.1		0.0	104.0	39.3

Table CW1034PC3

Primrose SWT 10-34 , Cycle 3 Production Data

Date d-mmm-yy	Days	Hours on Production	Oil Produced m^3	Water Produced m^3	Fluid Level Joints	Casing Pressure kPa	Wellhead Temperature Deg C	Total Fluid Produced m^3
27-Nov-83	125.5	24.0	5.2	35.7		0.0	105.0	40.9
28-Nov-83	126.5	24.0	5.2	35.7		0.0	103.0	40.9
29-Nov-83	126.8	7.0	0.1	26.0		0.0	104.0	26.1
30-Nov-83	127.8	24.0	8.8	76.4		0.0	98.0	85.2
1-Dec-83	128.8	24.0	15.7	78.9		0.0	96.0	94.6
2-Dec-83	129.8	24.0	8.2	77.8		0.0	97.0	86.0
3-Dec-83	130.8	24.0	21.3	75.4		0.0	100.0	96.6
4-Dec-83	131.8	24.0	14.2	78.1		0.0	98.0	92.2
5-Dec-83	132.8	24.0	16.6	76.1		0.0	100.0	92.8
6-Dec-83	133.8	24.0	18.1	75.9		0.0	100.0	94.0
7-Dec-83	134.7	22.5	14.1	73.9		0.0	100.0	88.0
8-Dec-83	134.9	4.0	0.0	19.1		0.0	94.0	19.1
9-Dec-83	135.9	24.0	4.8	69.8		0.0	100.0	74.6
10-Dec-83	136.9	24.0	15.8	69.5		0.0	102.0	85.2
11-Dec-83	137.9	24.0	13.7	62.2		0.0	103.0	76.0
12-Dec-83	138.9	24.0	16.3	78.1		0.0	104.0	94.4
13-Dec-83	139.9	24.0	11.9	74.8		0.0	102.0	86.7
14-Dec-83	140.9	24.0	5.5	83.2		0.0	98.0	88.7
15-Dec-83	141.9	24.0	4.8	85.4		0.0	99.0	90.3
16-Dec-83	142.9	24.0	17.3	91.5		0.0	100.0	108.8
17-Dec-83	143.9	24.0	10.5	78.9		0.0	100.0	89.3
18-Dec-83	144.9	24.0	10.5	78.9		0.0	100.0	89.3
19-Dec-83	145.9	24.0	4.6	74.4		0.0	100.0	79.0
20-Dec-83	146.9	24.0	4.6	74.4		0.0	100.0	79.0
21-Dec-83	147.9	24.0	13.0	74.8		0.0	100.0	87.8
22-Dec-83	148.9	24.0	12.4	75.6		0.0	100.0	88.0

Table CW1034PC3

Primrose SWT 10-34 , Cycle 3 Production Data

Date d-mmm-yy	Days	Hours on Production	Oil Produced m^3	Water Produced m^3	Fluid Level Joints	Casing Pressure kPa	Wellhead Temperature Deg C	Total Fluid Produced m^3
23-Dec-83	149.9	24.0	11.3	86.0		0.0	100.0	97.3
24-Dec-83	150.9	24.0	14.9	79.5		0.0	32.0	94.4
25-Dec-83	151.9	24.0	19.2	77.2		0.0	103.0	96.4
26-Dec-83	152.9	24.0	23.4	69.1		0.0	100.0	92.5
27-Dec-83	153.9	24.0	17.8	74.0	22.0	0.0	100.0	91.9
28-Dec-83	154.9	24.0	3.9	77.2	22.0	0.0	98.0	81.2
29-Dec-83	155.9	24.0	6.2	78.0		0.0	98.0	84.2
30-Dec-83	156.9	24.0	15.6	73.7		0.0	98.0	89.3
31-Dec-83	157.9	24.0	10.7	75.0		0.0	98.0	85.6
1-Jan-84	158.9	24.0	10.4	77.8		0.0	98.0	88.2
2-Jan-84	159.9	24.0	24.3	72.7	16.0	0.0	99.0	97.0
3-Jan-84	160.9	24.0	28.1	51.3	16.0	0.0	100.0	79.4
4-Jan-84	161.9	24.0	20.6	70.7		0.0	102.0	91.2
5-Jan-84	162.9	24.0	19.8	76.4	16.0	0.0	100.0	96.2
6-Jan-84	163.9	24.0	19.8	76.4	22.0	0.0	100.0	96.2
7-Jan-84	164.9	24.0	15.4	69.6	22.0	0.0	100.0	85.1
8-Jan-84	165.9	24.0	18.6	77.0	22.0	0.0	100.0	95.7
9-Jan-84	166.9	24.0	5.2	75.3	23.0	0.0	100.0	80.5
10-Jan-84	167.9	24.0	13.3	80.0	22.0	0.0	100.0	93.3
11-Jan-84	168.9	24.0	12.0	85.3	22.0	0.0	100.0	97.3
12-Jan-84	169.9	24.0	23.0	66.0	22.0	0.0	100.0	89.0
13-Jan-84	170.9	24.0	2.6	110.3	22.0	0.0	100.0	112.9
14-Jan-84	171.9	24.0	2.6	76.0	22.0	0.0	100.0	78.6
15-Jan-84	172.9	24.0	2.6	78.9	22.0	0.0	100.0	81.5
16-Jan-84	173.9	24.0	16.5	79.2	22.0	0.0	100.0	95.7
17-Jan-84	174.9	24.0	8.6	85.7	19.0	0.0	100.0	94.3

Table CW1034PC3

Primrose SWT 10-34 , Cycle 3 Production Data

Date d-mmm-yy	Days	Hours on Production	Oil Produced m^3	Water Produced m^3	Fluid Level Joints	Casing Pressure kPa	Wellhead Temperature Deg C	Total Fluid Produced m^3
18-Jan-84	175.9	24.0	8.3	88.2	19.0	0.0	101.0	96.5
19-Jan-84	176.9	24.0	8.3	88.2	19.0	0.0	101.0	96.5
20-Jan-84	177.9	24.0	14.0	79.9	19.0	0.0	101.0	93.8
21-Jan-84	178.9	24.0	5.8	87.6		0.0	101.0	93.4
22-Jan-84	179.9	24.0	10.74	82.99		0.0	101	93.7
23-Jan-84	180.9	24.0	6.06	88.47		0.0	100	94.5
24-Jan-84	181.9	24.0	3.38	93.4	19	0.0	99	96.8
25-Jan-84	182.9	24.0	16.72	76.65		0.0	99	93.4
26-Jan-84	183.9	24.0	1.05	95.37		0.0	99	96.4
27-Jan-84	184.9	24.0	10.19	87.85		0.0	100	98.0
28-Jan-84	185.9	24.0	4.2	88.93		0.0	100	93.1
29-Jan-84	186.9	24.0	8.6	94.78		0.0	98	103.4
30-Jan-84	187.9	24.0	3.52	87.3		0.0	98	90.8
31-Jan-84	188.9	24.0	3.52	88.25		0.0	99	91.8
1-Feb-84	189.9	24.0	5.74	84.94		0.0	98	90.7
2-Feb-84	190.9	24.0	11.11	87.38		0.0	98	98.5
3-Feb-84	191.9	24.0	4.37	84.69		0.0	97	89.1
4-Feb-84	192.9	24.0	10.81	84.03		0.0	96	94.8
5-Feb-84	193.9	24.0	10.52	84.28		0.0	96	94.8
6-Feb-84	194.9	24.0	9.98	82.08		0.0	96	92.1
7-Feb-84	195.9	24.0	9.36	82.24		0.0	96	91.6
8-Feb-84	196.9	24.0	10.52	80.8		0.0	94	91.3
9-Feb-84	197.9	24.0	7.77	89.95		0.0		97.7
10-Feb-84	198.9	24.0	7.98	77.17		0.0	96	85.2
11-Feb-84	199.9	24.0	10.94	92	17	0.0	95	102.9
12-Feb-84	200.9	24.0	7.65	80.8		0.0	95	88.5

Table CW1034PC3

Primrose SWT 10-34 , Cycle 3 Production Data

Date d-mmm-yy	Days	Hours on Production	Oil Produced m^3	Water Produced m^3	Fluid Level Joints	Casing Pressure kPa	Wellhead Temperature Deg C	Total Fluid Produced m^3
13-Feb-84	201.9	24.0	9.53	88.81		0.0	96	98.3
14-Feb-84	202.9	24.0	10.11	83.61		0.0	96	93.7
15-Feb-84	203.9	24.0	12.4	76.96		0.0	94	89.4
16-Feb-84	204.9	24.0	0.25	90.59	18	0.0	94	90.8
17-Feb-84	205.9	24.0	10.08	89.61	18	0.0	96	99.7
18-Feb-84	206.9	24.0	1.58	86.45	17	0.0	94	88.0
19-Feb-84	207.9	24.0	9.77	98.23	17	0.0	94	108.0
20-Feb-84	208.9	24.0	[illegible].63	81.55	19	0.0	94	95.2
21-Feb-84	209.9	24.0	13.63	81.55	20	0.0	94	95.2
22-Feb-84	210.9	24.0	13.63	81.55		0.0		95.2
23-Feb-84	211.9	24.0	7.55	85.63		0.0	92	93.2
24-Feb-84	212.9	24.0	7.55	85.63		0.0	92	93.2
25-Feb-84	213.9	24.0	7.55	85.63		0.0	91	93.2
26-Feb-84	214.9	24.0	7.55	85.63		0.0	92	93.2
27-Feb-84	215.9	24.0	5.21	86.53		0.0	90	91.7
28-Feb-84	216.9	24.0	5.21	86.53		0.0	90	91.7
29-Feb-84	217.9	24.0	5.21	86.53		0.0	90	91.7
1-Mar-84	218.9	24.0	6.76	88.78	18	0.0		95.5
2-Mar-84	219.9	24.0	6.76	88.78	18	0.0		95.5
3-Mar-84	220.9	24.0	6.76	88.78	18	0.0		95.5
4-Mar-84	221.9	24.0	6.76	88.78	18	0.0		95.5
5-Mar-84	222.9	24.0	6.76	88.77	18	0.0		95.5
6-Mar-84	223.9	24.0	6.76	88.77	18	0.0		95.5
7-Mar-84	224.9	24.0	6.76	88.77		0.0		95.5
8-Mar-84	225.9	24.0	6.76	88.77		0.0		95.5
9-Mar-84	226.9	24.0	6.76	88.77		0.0		95.5

Table CW1034PC3

Primrose SWT 10-34 , Cycle 3 Production Data

Date d-mmm-yy	Days	Hours on Production	Oil Produced m^3	Water Produced m^3	Fluid Level Joints	Casing Pressure kPa	Wellhead Temperature Deg C	Total Fluid Produced m^3
10-Mar-84	227.1	6	1.69	22.19		0.0		23.9

Table CW1034PC4

Primrose SWT 10-34 , Cycle 4 Production Data

Date d-mmm-yy	Days	Hours on Production	Oil Produced m^3	Water Produced m^3	Fluid Level Joints	Casing Pressure kPa	Wellhead Temperature Deg C	Total Fluid Produced m^3
4-May-84	0.5	11.5	0.0	0.0		0.0	0.0	0.0
5-May-84	1.5	24.0	0.0	0.0		0.0	82.0	0.0
6-May-84	2.5	24.0	0.0	22.3		0.0	82.0	22.3
7-May-84	2.8	7.0	0.0	32.3		0.0		32.3
8-May-84	3.8	24.0	0.0	18.7		0.0	83.0	18.7
9-May-84	4.8	24.0	0.0	14.7		0.0	80.0	14.7
10-May-84	5.8	24.0	0.0	37.3		0.0		37.3
11-May-84	6.8	23.5	0.0	27.2		0.0	0.0	27.2
12-May-84	7.8	24.0	0.0	32.6		0.0	0.0	32.6
13-May-84	8.3	13.0	0.0	15.9		0.0	94.0	15.9
14-May-84		0.0	0.0	0.0		0.0		
15-May-84		0.0	0.0	0.0		0.0		
16-May-84	8.7	10.0	0.0	19.1		0.0	79.0	19.1
17-May-84	9.7	24.0	0.0	33.6		0.0	82.0	33.6
18-May-84	10.7	24.0	0.0	35.9		0.0	88.0	35.9
19-May-84	11.7	24.0	0.0	37.5		0.0	84.0	37.5
20-May-84	12.7	24.0	0.0	39.3		0.0	88.0	39.3
21-May-84	13.7	24.0	0.0	34.5		0.0	90.0	34.5
22-May-84	14.7	24.0	0.0	37.2		0.0	89.0	37.2
23-May-84	15.7	23.0	0.0	31.3		0.0		31.3
24-May-84	16.7	24.0	0.0	32.0		0.0	87.0	32.0
25-May-84	17.7	24.0	0.0	26.7		0.0	88.0	26.7
26-May-84	18.7	24.0	0.0	26.7		0.0	86.0	26.7
27-May-84	19.7	24.0	0.0	24.4		0.0	89.0	24.4
28-May-84	20.7	24.0	0.0	34.2		0.0	84.0	34.2

Table CW1034PC4

Primrose SWT 10-34 , Cycle 4 Production Data

Date d-mmm-yy	Days	Hours on Production	Oil Produced m^3	Water Produced m^3	Fluid Level Joints	Casing Pressure kPa	Wellhead Temperature Deg C	Total Fluid Produced m^3
29-May-84	21.7	24.0	0.0	23.2		0.0	86.0	23.2
30-May-84	22.6	23.0	0.0	25.4		0.0		25.4
31-May-84	23.6	24.0	0.0	39.0		0.0	80.0	39.0
1-Jun-84	24.6	24.0	4.4	22.1		0.0		26.5
2-Jun-84	25.6	24.0	4.4	35.7		0.0	81.0	40.1
3-Jun-84	26.6	24.0	4.4	32.1		0.0	84.0	36.5
4-Jun-84	27.6	24.0	10.7	14.1		0.0	83.5	24.8
5-Jun-84	28.6	24.0	5.2	23.0		0.0	81.0	28.2
6-Jun-84	29.6	24.0	3.3	30.8		0.0	86.0	34.1
7-Jun-84	30.6	24.0	9.8	20.3		0.0	85.0	30.0
8-Jun-84	31.6	24.0	6.7	26.3		0.0	86.0	33.0
9-Jun-84	32.6	24.0	6.7	26.3		0.0	89.0	33.0
10-Jun-84	33.6	24.0	6.7	25.5		0.0	86.0	32.3
11-Jun-84	34.6	24.0	6.7	25.5		0.0	82.0	32.3
12-Jun-84	35.6	24.0	6.7	25.5		0.0	90.0	32.3
13-Jun-84	36.6	24.0	5.4	28.1		0.0	84.0	33.5
14-Jun-84	37.6	24.0	5.4	28.1		0.0	88.0	33.5
15-Jun-84	38.6	24.0	5.4	28.1		0.0	88.0	33.5
16-Jun-84	39.6	24.0	5.2	37.6		0.0	87.0	42.8
17-Jun-84	40.6	24.0	9.5	27.7		0.0	86.0	37.2
18-Jun-84	41.6	24.0	9.5	27.7		0.0	86.0	37.2
19-Jun-84	42.6	24.0	10.5	24.9		0.0	87.0	35.4
20-Jun-84	43.6	24.0	10.5	24.9		0.0		35.4
21-Jun-84	44.6	24.0	10.5	24.9		0.0	86.0	35.4
22-Jun-84	45.6	24.0	10.2	27.4		0.0	87.0	37.6
23-Jun-84	46.6	24.0	5.7	44.7		0.0	87.0	50.4

Table CW1034PC4

Primrose SWT 10-34 , Cycle 4 Production Data

Date d-mmm-yy	Days	Hours on Production	Oil Produced m^3	Water Produced m^3	Fluid Level Joints	Casing Pressure kPa	Wellhead Temperature Deg C	Total Fluid Produced m^3
24-Jun-84	47.6	24.0	10.0	8.0		0.0	87.0	17.9
25-Jun-84	48.6	24.0	26.3	10.8		0.0	86.0	37.1
26-Jun-84	49.6	24.0	11.0	23.8		0.0	86.0	34.8
27-Jun-84	50.6	24.0	16.1	27.1		0.0	85.0	43.3
28-Jun-84	51.6	24.0	16.1	27.1		0.0	86.0	43.3
29-Jun-84	52.6	24.0	12.6	20.7		0.0	82.0	33.3
30-Jun-84	53.6	24.0	19.7	20.1		0.0	78.0	39.8
1-Jul-84	54.6	24.0	19.5	19.9		0.0	80.0	39.4
2-Jul-84	55.6	24.0	13.6	22.5		0.0	81.0	36.0
3-Jul-84	56.6	24.0	13.6	22.5		0.0	83.0	36.0
4-Jul-84	57.6	24.0	13.6	22.5		0.0	87.0	36.0
5-Jul-84	58.6	24.0	16.8	21.8		0.0	80.0	38.6
6-Jul-84	59.6	24.0	16.8	21.8		0.0	85.0	38.6
7-Jul-84	60.6	24.0	13.7	23.9		0.0	81.0	37.7
8-Jul-84	61.6	24.0	13.7	23.9		0.0	81.0	37.7
9-Jul-84	62.6	24.0	13.7	23.9		0.0	85.0	37.7
10-Jul-84	63.6	24.0	15.7	17.3		0.0	83.0	33.0
11-Jul-84	64.6	24.0	15.7	17.3		0.0	85.0	33.0
12-Jul-84	65.6	24.0	19.3	28.8		0.0	83.0	48.0
13-Jul-84	66.6	24.0	19.3	28.8		0.0	83.0	48.0
14-Jul-84	67.6	24.0	19.3	28.8		0.0	81.0	48.0
15-Jul-84	68.6	24.0	19.3	28.8		0.0	81.0	48.0
16-Jul-84	69.6	24.0	19.2	24.9		0.0	85.0	44.1
17-Jul-84	70.6	24.0	19.2	24.9		0.0	92.5	44.1
18-Jul-84	71.6	24.0	19.2	24.9		0.0	104.0	44.1
19-Jul-84	72.6	24.0	15.6	28.3		0.0	112.0	43.9

Table CW1034PC4

Primrose SWT 10-34 , Cycle 4 Production Data

Date d-mmm-yy	Days	Hours on Production	Oil Produced m^3	Water Produced m^3	Fluid Level Joints	Casing Pressure kPa	Wellhead Temperature Deg C	Total Fluid Produced m^3
20-Jul-84	73.6	24.0	18.3	28.7	30.0	0.0	114.0	47.1
21-Jul-84	74.6	24.0	18.3	28.7	29.0	0.0	116.0	47.1
22-Jul-84	75.6	24.0	22.9	25.2	27.0	0.0	117.0	48.0
23-Jul-84	76.6	24.0	22.9	25.2	27.0	0.0	114.0	48.0
24-Jul-84	77.6	23.0	21.9	24.1	27.0	0.0	120.0	46.0
25-Jul-84	78.6	24.0	21.9	24.1		0.0	120.0	46.0
26-Jul-84	79.6	24.0	21.9	24.1		0.0	114.0	46.0
27-Jul-84	80.6	24.0	22.1	34.2		0.0	114.0	56.3
28-Jul-84	81.6	24.0	22.1	34.2		0.0	110.0	56.3
29-Jul-84	82.6	24.0	25.1	35.9		0.0	121.0	61.0
30-Jul-84	83.6	24.0	25.1	35.9		0.0	117.0	61.0
31-Jul-84	84.6	24.0	25.1	35.9		0.0	115.0	61.0
1-Aug-84	85.6	24.0	26.0	35.5		0.0	105.0	61.5
2-Aug-84	86.6	24.0	26.0	35.5		0.0	108.0	61.5
3-Aug-84	87.6	24.0	26.0	35.5		0.0	112.0	61.5
4-Aug-84	88.6	24.0	26.0	35.5		0.0	118.0	61.5
5-Aug-84	89.6	24.0	32.1	28.3		0.0	117.0	60.4
6-Aug-84	90.6	24.0	32.1	28.3		0.0	115.0	60.4
7-Aug-84	91.6	24.0	17.4	44.7		0.0		62.0
8-Aug-84	92.6	24.0	22.3	43.0		0.0		65.3
9-Aug-84	93.6	24.0	16.7	50.6		0.0		67.3
10-Aug-84	94.6	24.0	19.5	44.8		0.0		64.3
11-Aug-84	95.6	24.0	20.8	50.0		0.0		70.7
12-Aug-84	96.6	24.0	21.8	44.8		0.0	128.0	66.7
13-Aug-84	97.6	24.0	23.2	47.0		0.0	127.0	70.2
14-Aug-84	98.6	24.0	23.8	44.9		0.0		68.7

Table CW1034PC4

Primrose SWT 10-34 , Cycle 4 Production Data

Date d-mmm-yy	Days	Hours on Production	Oil Produced m^3	Water Produced m^3	Fluid Level Joints	Casing Pressure kPa	Wellhead Temperature Deg C	Total Fluid Produced m^3
15-Aug-84	99.6	24.0	23.8	44.9		0.0	100.0	68.7
16-Aug-84	100.6	24.0	19.6	36.0		0.0	92.0	55.6
17-Aug-84	101.6	24.0	10.9	29.6		0.0	92.0	40.5
18-Aug-84	102.6	24.0	10.9	29.6		0.0	88.0	40.5
19-Aug-84	103.6	24.0	10.9	29.6		0.0	90.0	40.5
20-Aug-84	104.6	24.0	10.0	75.8		0.0	96.0	85.8
21-Aug-84	105.6	24.0	10.0	75.8		0.0	101.0	85.8
22-Aug-84	106.6	24.0	20.2	52.8		0.0	100.0	73.0
23-Aug-84	107.6	24.0	16.4	62.1		0.0	110.0	78.4
24-Aug-84	108.6	24.0	28.6	64.4		0.0	113.0	93.0
25-Aug-84	109.6	24.0	19.6	74.6		0.0	112.0	94.2
26-Aug-84	110.6	24.0	18.9	76.9		0.0	115.0	95.8
27-Aug-84	111.6	24.0	18.9	76.9		0.0	121.0	95.8
28-Aug-84	112.6	24.0	20.7	72.3		0.0	114.0	93.0
29-Aug-84	113.6	24.0	20.7	72.3		0.0	112.0	93.0
30-Aug-84	114.6	24.0	20.7	72.3		0.0	110.0	93.0
31-Aug-84	115.6	24.0	20.7	72.3		0.0	110.0	93.0
1-Sep-84	116.6	24.0	16.9	70.54		0.0	106.0	87.4
2-Sep-84	117.6	24.0	16.9	70.54		0.0	108.0	87.4
3-Sep-84	118.6	24.0	16.9	70.54		0.0		87.4
4-Sep-84	119.6	24.0	16.9	70.54		0.0	107.0	87.4
5-Sep-84	120.6	24.0	22.63	62.44		0.0	109.0	85.1
6-Sep-84	121.6	24.0	22.63	62.44		0.0	108.0	85.1
7-Sep-84	122.6	24.0	14.16	69.77		0.0	106.0	83.9
8-Sep-84	123.6	24.0	15.68	65.98		0.0	107.0	81.7
9-Sep-84	124.6	24.0	18.71	65.44		0.0	110.0	84.2

Table CW1034PC4

Primrose SWT 10-34 , Cycle 4 Production Data

Date d-mmm-yy	Days	Hours on Production	Oil Produced m^3	Water Produced m^3	Fluid Level Joints	Casing Pressure kPa	Wellhead Temperature Deg C	Total Fluid Produced m^3
10-Sep-84	125.6	24.0	16.97	66.97		0.0	112.0	83.9
11-Sep-84	126.6	24.0	16.97	66.97		0.0	113.0	83.9
12-Sep-84	127.6	24.0	16.97	66.97		0.0	120.0	83.9
13-Sep-84	128.6	24.0	12.92	50.99	25	0.0	119.0	63.9
14-Sep-84	129.6	24.0	12.92	50.99	25	0.0	120.0	63.9
15-Sep-84	130.6	24.0	20.94	42.97	26	0.0	120.0	63.9
16-Sep-84	131.6	24.0	20.94	42.97	26	0.0	120.0	63.9
17-Sep-84	132.6	24.0	11.76	47.19	26	0.0	117.0	59.0
18-Sep-84	133.6	24.0	11.76	47.19	26	0.0	119.0	59.0
19-Sep-84	134.6	24.0	11.76	47.19		0.0	116.0	59.0
20-Sep-84	135.6	24.0	16.33	47.56		0.0	119.0	63.9
21-Sep-84	136.6	24.0	16.33	47.56		0.0	116.0	63.9
22-Sep-84	137.6	24.0	16.67	49.22		0.0	117.0	65.9
23-Sep-84	138.6	24.0	16.67	49.22		0.0	117.0	65.9
24-Sep-84	139.6	24.0	14.44	49.37		0.0	116.0	63.8
25-Sep-84	140.6	24.0	14.44	49.46		0.0	116.0	63.9
26-Sep-84	141.6	24.0	19.1	65.43		0.0	116.0	84.5
27-Sep-84	142.6	24.0	12.93	71.62	21	0.0	116.0	84.6
28-Sep-84	143.6	24.0	12.93	71.62	21	0.0	116.0	84.6
29-Sep-84	144.6	24.0	24.38	53.61	21	0.0	116.0	78.0
30-Sep-84	145.6	24.0	24.38	53.61	17	0.0	112.0	78.0
1-Oct-84	146.6	24.0	11	73.56	23	0.0	112.0	84.6
2-Oct-84	147.6	24.0	10.67	78.32	23	0.0	112.0	89.0
3-Oct-84	148.6	24.0	10.67	78.32		0.0	114.0	89.0
4-Oct-84	149.6	24.0	10.67	78.32		0.0	110.0	89.0
5-Oct-84	150.6	24.0	11.14	72.57	35	0.0	113.0	83.7

Table CW1034PC4

Primrose SWT 10-34 , Cycle 4 Production Data

Date d-mmm-yy	Days	Hours on Production	Oil Produced m^3	Water Produced m^3	Fluid Level Joints	Casing Pressure kPa	Wellhead Temperature Deg C	Total Fluid Produced m^3
6-Oct-84	151.6	24.0	11.14	72.57		0.0	110.0	83.7
7-Oct-84	152.6	24.0	11.14	72.57		0.0	109.0	83.7
8-Oct-84	153.6	24.0	11.14	72.57		0.0	110.0	83.7
9-Oct-84	154.6	24.0	11.14	72.57		0.0	109.0	83.7
10-Oct-84	155.6	24.0	11.53	75.14	32	0.0	107.0	86.7
11-Oct-84	156.6	24.0	8.23	86.46	24	0.0	109.0	94.7
12-Oct-84	157.6	24.0	8.23	86.46	24	0.0	108.0	94.7
13-Oct-84	158.6	24.0	8.23	86.46	24	0.0	109.0	94.7
14-Oct-84	159.6	24.0	8.23	86.46	24	0.0	110.0	94.7
15-Oct-84	160.6	24.0	8.23	86.46	24	0.0	106.0	94.7
16-Oct-84	161.6	24.0	23.21	83.03	23	0.0	105.0	106.2
17-Oct-84	162.6	24.0	10.02	77.88	23	0.0	105.0	87.9
18-Oct-84	163.6	24.0	10.02	77.88		0.0	102.0	87.9
19-Oct-84	164.6	24.0	9.41	83.83	25	0.0	102.0	93.2
20-Oct-84	165.6	24.0	9.41	83.83		0.0	102.0	93.2
21-Oct-84	166.6	24.0	9.41	83.83		0.0	103.0	93.2
22-Oct-84	167.6	24.0	9.41	83.83		0.0	102.0	93.2
23-Oct-84	168.6	24.0	12.78	80.45	24	0.0	103.0	93.2
24-Oct-84	169.6	24.0	15.52	97.74		0.0	93.0	113.3
25-Oct-84	170.6	24.0	15.52	97.74	26	0.0	120.0	113.3
26-Oct-84	171.6	24.0	6.24	93.47		0.0	100.0	99.7
27-Oct-84	172.6	24.0	6.24	93.47		0.0	99.0	99.7
28-Oct-84	173.6	24.0	6.24	93.47		0.0	99.0	99.7
29-Oct-84	174.6	24.0	6.24	93.47		0.0	99.0	99.7
30-Oct-84	175.6	24.0	15.42	89.72		0.0	98.0	105.1
31-Oct-84	176.6	24.0	15.42	89.72		0.0	99.0	105.1

Table CW1034PC4

Primrose SWT 10-34 , Cycle 4 Production Data

Date d-mmm-yy	Days	Hours on Production	Oil Produced m^3	Water Produced m^3	Fluid Level Joints	Casing Pressure kPa	Wellhead Temperature Deg C	Total Fluid Produced m^3
1-Nov-84	177.6	24.0	7.57	52.15		0.0	99.0	59.7
2-Nov-84	178.6	24.0	7.57	52.15		0.0	103.0	59.7
3-Nov-84	179.6	24.0	7.57	52.15		0.0	104.0	59.7
4-Nov-84	180.6	24.0	7.57	52.15		0.0	102.0	59.7
5-Nov-84	181.6	24.0	7.57	52.15		0.0	102.0	59.7
6-Nov-84	182.6	24.0	7.57	52.15		0.0	104.0	59.7
7-Nov-84	183.6	24.0	6.97	61.71	20	0.0	102.0	68.7
8-Nov-84	184.6	24.0	6.97	61.71		0.0	100.0	68.7
9-Nov-84	185.6	24.0	6.97	61.71	20	0.0	100.0	68.7
10-Nov-84	186.6	24.0	6.62	54.74	20	0.0	100.0	61.4
11-Nov-84	187.6	24.0	6.62	54.74		0.0	101.0	61.4
12-Nov-84	188.6	24.0	11.57	95.72	21	0.0	101.0	107.3
13-Nov-84	189.6	24.0	11.57	95.72	21	0.0	101.0	107.3
14-Nov-84	190.6	24.0	11.57	95.72	21	0.0		107.3
15-Nov-84	191.6	24.0	11.57	95.72		0.0	100.0	107.3
16-Nov-84	192.6	24.0	11.57	95.72		0.0	99.0	107.3
17-Nov-84	193.6	24.0	11.57	95.72		0.0	94.0	107.3
18-Nov-84	194.6	24.0	11.57	95.72		0.0	96.0	107.3
19-Nov-84	195.6	24.0	11.57	95.72		0.0	97.0	107.3
20-Nov-84	196.6	24.0	6.61	113.67	23	0.0	98.0	120.3
21-Nov-84	197.6	24.0	6.61	113.67		0.0	99.0	120.3
22-Nov-84	198.6	24.0	6.61	113.67	23	0.0	98.0	120.3
23-Nov-84	199.6	24.0	6.53	112.25		0.0	100.0	118.8
24-Nov-84	200.6	24.0	6.85	93.61		0.0	100.0	100.5
25-Nov-84	201.6	24.0	6.85	93.61		0.0	99.0	100.5
26-Nov-84	202.6	24.0	11.19	94.68		0.0	99.0	105.9

Table CW1034PC4

Primrose SWT 10-34 , Cycle 4 Production Data

Date d-mmm-yy	Days	Hours on Production	Oil Produced m^3	Water Produced m^3	Fluid Level Joints	Casing Pressure kPa	Wellhead Temperature Deg C	Total Fluid Produced m^3
27-Nov-84	203.6	24.0	11.19	94.68	22	0.0	92.0	105.9
28-Nov-84	204.6	24.0	11.19	94.68		0.0	100.0	105.9
29-Nov-84	205.6	24.0	8.4	98.36	18	0.0	100.0	106.8
30-Nov-84	206.6	24.0	8.4	98.36		0.0	100.0	106.8
1-Dec-84	207.6	24.0	5.01	58.65		0.0	98.0	63.7
2-Dec-84	208.6	24.0	5.01	58.65		0.0	98.0	63.7
3-Dec-84	209.6	24.0	5.34	59.88	20	0.0	96.0	65.2
4-Dec-84	210.6	24.0	5.34	59.88		0.0	99.0	65.2
5-Dec-84	211.6	24.0	5.34	59.88		0.0	98.0	65.2
6-Dec-84	212.6	24.0	5.34	59.88	18	0.0	98.0	65.2
7-Dec-84	213.6	24.0	5.99	87.73		0.0	98.0	93.7
8-Dec-84	214.6	24.0	5.99	87.73		0.0	98.0	93.7
9-Dec-84	215.6	24.0	5.99	87.73	20	0.0	98.0	93.7
10-Dec-84	216.6	24.0	5.96	91.67		0.0	98.0	97.6
11-Dec-84	217.3	18.0	4.47	68.75		0.0	91.0	73.2
12-Dec-84	218.3	24.0	5.96	91.67		0.0	95.0	97.6
13-Dec-84	219.3	24.0	5.96	91.67		0.0	90.0	97.6
14-Dec-84	220.3	24.0	5.76	71.28		0.0	95.0	77.0
15-Dec-84	221.3	24.0	5.76	71.28		0.0	95.0	77.0
16-Dec-84	222.3	24.0	5.76	71.28		0.0	95.0	77.0
17-Dec-84	223.3	24.0	5.99	71.6		0.0	92.0	77.6
18-Dec-84	224.3	24.0	5.99	71.6	20	0.0	92.0	77.6
19-Dec-84	225.3	24.0	5.99	71.6	20	0.0	60.0	77.6
20-Dec-84	226.3	24.0	5.99	71.6	16	0.0	96.0	77.6
21-Dec-84	227.3	24.0	6.58	72.47		0.0	94.0	79.1
22-Dec-84	228.3	24.0	6.58	72.47		0.0	94.0	79.1

Table CW1034PC4

Primrose SWT 10-34 , Cycle 4 Production Data

Date d-mmm-yy	Days	Hours on Production	Oil Produced m^3	Water Produced m^3	Fluid Level Joints	Casing Pressure kPa	Wellhead Temperature Deg C	Total Fluid Produced m^3
23-Dec-84	229.3	24.0	6.58	72.47		0.0	96.0	79.1
24-Dec-84	230.3	24.0	6.58	72.47		0.0	96.0	79.1
25-Dec-84	231.3	24.0	3.67	81.89		0.0	94.0	85.6
26-Dec-84	232.3	24.0	3.67	81.89		0.0	95.0	85.6
27-Dec-84	233.3	24.0	3.67	81.89		0.0	94.0	85.6
28-Dec-84	234.3	24.0	7.59	75.32	17	0.0	93.0	82.9
29-Dec-84	235.3	24.0	7.59	75.32		0.0	91.0	82.9
30-Dec-84	236.3	24.0	7.59	75.32		0.0	93.0	82.9
31-Dec-84	237.3	24.0	7.59	75.32		0.0		82.9
1-Jan-85	238.3	24.0	9.41	93.41		0.0	93.0	102.8
2-Jan-85	239.3	24.0	5.49	96.18	19	0.0	93.0	101.7
3-Jan-85	240.3	24.0	5.5	91.77	19	0.0	95.0	97.3
4-Jan-85	241.3	24.0	10.13	92.25	19	0.0	95.0	102.4
5-Jan-85	242.3	24.0	8.22	94.44	19	0.0	93.0	102.7
6-Jan-85	243.3	24.0	7.8	93.08	19	0.0	93.0	100.9
7-Jan-85	244.3	24.0	3.69	94.81	19	0.0	92.0	98.5
8-Jan-85	245.3	24.0	5.53	92.48	19	0.0	89.0	98.0
9-Jan-85	246.3	24.0	6.78	92.94	19	0.0	89.0	99.7
10-Jan-85	247.3	24.0	6.78	92.94	19	0.0	90.0	99.7
11-Jan-85	248.3	24.0	5.73	94.15		0.0	90.0	99.9
12-Jan-85	249.3	24.0	5.73	94.15		0.0	91.0	99.9
13-Jan-85	250.3	24.0	5.73	94.15		0.0	92.0	99.9

APPENDIX D

Example of Correlation of Weight Percent Bitumen Between Logs and Cores

PCEJ Area 1, McMurray Formation

Example of Correlation of Weight Percent Bitumen Between Logs and Cores

PCEJ Area 1, McMurray Formation

Calculations For Core and Log Analysis

(Explanations are given in the same order as shown in the example tables AD1 and AD2: Well 13-27-84-11W4, which is the first cyclically steamed well at Hangingstone 35 km south of Fort McMurray; well 16-26-84-11W4 is an exploration well.)

1. **"Corr. to Core"**

   The correction in metres added to core depths to match log depths.

2. **"Interval"**

   Interval of oil sand greater than 8 wt% bitumen as analyzed by Dean and Stark on core samples and substantiated by resistivity and porosity logs. The interval is given in mKB and corresponds to log depths. The top of the Devonian Formation is also noted.

3. **"Ht"**

   The thickness of the rich oil sand interval in metres.

4. **"Core Analysis"**

   a) **"wt% bitumen"**

      The wt% bitumen as analyzed from cores by Dean & Stark and calculated as a weighted average over the interval selected.

b) **"Grain wt%"**

Grain wt% eliminates the affect of invasion of water into cores by drilling muds and can be used for a more accurate determination of So if the porosity is known.

Grain wt% = (wt% bit)/(1-(wt% bit+wt% H_2O)) = wt Bit/wt sand

= $(So \cdot \varnothing_{core})/((1- \varnothing_{core})\rho_{sand})$

= Gw

Corrected wt% bitumen = (wt bit)/(wt sand + wt bit + corrected wt H_2O)

= $(So \cdot \varnothing_{log})/((1-\varnothing_{log})^{*}\rho_{sand} + \varnothing_{log})$

= Bw

or Bw = $(Gw)/(1+\varnothing_{log}/(1-\varnothing_{log})\rho_{sand}$

Invasion of water in Area 1 cores is not significant due to the richness of the oil sand. For calculation of corrected water using tracers in the drilling mud see Leshchyshyn (1991).

c) **"Porosity"**

Porosity is calculated by the service labs from regular Dean & Stark analysis and assumes the density of oil = 1.00 gm/cc and the density of sand = 2.65 gm/cc.

$\varnothing$ =((wt bit/ρ_{bit}) + (wt H_2O/ρ_{H2O}))/((wt bit/ρ_{bit})+(wt H_2O/ρ_{H20})+(wt sand/ρ_{sand}))

=(wt bit + wt H_2O)/((wt bit + wt H_2O + ((1-(wt bit + wt H_20))/2.65)))

5. **"Log Analysis"**

a) **"Resistivity"** (ohm-metres)

R_t is measured over the interval, giving both average and maximum values over the interval being examined. Deep, medium, and shallow induction resistivities are examined.

b) **"Porosity"**

The average and maximum porosities (Neutron and Density) are measured. A total porosity is then calculated.

$$\text{Total } \varnothing = (\varnothing_N + \varnothing_D)/2$$

Effective porosity is calculated using Gamma Ray analysis.

Effective $\varnothing = (1 - V_f)\, \varnothing_{total}$, where V_f = volume of fines or shales as calculated from gamma ray.

c) **"Gamma Ray"**

A maximum (100% shale) and a minimum (0% shale) value of GR is determined from the log, over the McMurray Formation. Average and minimum values of GR are read over each interval. Typical values are $GR_{max} = 100$, $GR_{min} = 25$ API.

RGRD is then calculated: $RGRD = (GR - GR_{min})/(GR_{max} - G_{min})$

and $Vf = 0.83(RGRD)^2 + 0.17(RGRD)$

d) **"Sonic Log"**

The average and minimum values of sonic time (μs/m) are measured and can be used in further porosity determinations using:

$\varnothing_s = ((t - 182)/438)\cdot(1/B_{cp})$, where B_{cp} = compaction factor.

Back calculation of B_{cp} with depth gives values from 1.2 to 1.55 with an average of 1.4. Also, B_{cp} decreased with increasing depth in each particular well analyzed. Therefore, without knowing B_{cp} beforehand, it is difficult to calculate porosities from sonic logs.

e) **"S_w Calculation"**

Prior to S_w calculations, a value for Rw for each well must be obtained. Required information is obtained from the "Dual Induction SFL" log.

ESSP = delta SP = deflection of the SP signal over the range of the Grand Rapids, Clearwater, and McMurray formations. This value is normally negative.

R_{mf} = resistivity of the mud filtrate at bottomhole temperature

T_{mf} = temperature of mud filtrate at bottomhole.

ESSP = $-K_c \log (R_{mf}/R_w)$, where $K_c = 65 + 0.24T$ (°C). Solve for R_w

More than one value for R_w may be required for a well if lithology changes are significant.

To calculate R_w at any temperature, if required,

$$R_{w(T)} = R_w(T_{mf} + 21.5)/(T + 21.5)$$

To calculate salinity at any temperature, if required,

$$\text{Salinity (ppm)} = 10^x, \text{ where } x = (3.562 - \log(Rw - 0.0123))/0.955$$

Once R_w is known,

$$Sw = ((1 \cdot R_w)/\varnothing^{1.45} \cdot Rt)^{1/1.6}$$

The “a”, “m”, and “n” values for the Archie equation were derived from previous correlations with the McMurray Formation log and core analyses.

$a^* = 1$ = empirical constant (see end of section 5.)
$m^* = 1.45$ = cementation factor
$n^* = 1.60$ = saturation exponent

R_t and $\varnothing$ used here is dependent upon thickness of the oil sand bed and is obtained from Table AD1:

Deep induction resistivity appears to be affected substantially by the nature of material up to 2 metres vertical distance from the reference point of the induction tool. This results in inaccurate determinations of Sw for homogeneous beds less than 4 m in thickness. Corrections can be made using the medium resistivity (30% less vertical resolution than deep resistivity) or the shallow resistivity (70% less vertical resolution than deep resistivity) as long as no mud invasion has occured. For rich oil sands, invasion appears to be slight. The McMurray Formation in Area 1 is a combination of rich oil sand and shale streaks. A 30 ohm-m deep resistivity cutoff (8 wt% bitumen) seems to give the point at which shale ends and rich oil sand begins and vice versa. For less than 4 m thick oil sand intervals, a 40 ohm-m shallow resistivity is more accurate.

The overall effect shows that analyzing logs in heterogeneous oil sands as encountered in the McMurray formation on a metre by metre basis will give erroneous results. For this reason, the logs have been analyzed mostly as larger intervals (up to about 10 m) as long as R_t does not drop below 30 ohm-m or the lithology does not change within this interval. The thicker the interval, the more accurate this method appears to be.

One must remember that core analysis is not completly accurate over the full range of 0.0 wt% bitumen to 16% wt bitumen. The best Dean & Stark analysis has an error of ± 1.0 wt% bitumen. 0.0 to 6 wt% bitumen may have invasion due to drilling mud. 12 to 16 wt% bitumen may have significant errors in water measurements or loss of light ends.

Core samples taken for Dean & Stark in rich oil sands containing shale streaks (less than 1 inch shale) could giveerroneously high water saturations. One must differentiate between this type of oil sand and water sand.

* These calculations were performed prior to special core analysis from which new values for "m" and "n" were derived. These new values are: a = 1, m = 1.4, and n = 1.77. On the average, this would lower wt% bitumen by about 0.5 wt% or increase S_w by about 0.03. Overall, this would provide better correlation between log and core analyses.

6. Well average values

Average values are given in the row marked "Total" and are:
- total oil sand thickness above 8 wt% bitumen cutoff.
- ave. wt% bitumen as calculated from cores (weighted).
- ave. wt% bitumen corrected for invasion.
- ave. porosity as calculated from cores (weighted).
- ave. porosity as calculated from logs (weighted).
- ave. S_w as calculated from logs (weighted).

- ave. S_o as calculated from logs (weighted).
- ave. W_o as calculated from logs (weighted).

7. **6, 8, and 10 wt% bitumen cutoffs**

Given are the oil sand intervals as shown by R_t log analysis:

6 wt% bitumen = 20 ohm-m cutoff
8 wt% bitumen = 30 ohm-m cutoff
10 wt% bitumen = 40 ohm-m cutoff

These values were approximated from a cutoff curve as plotted from PCEJ Area 1 wells as Rt (deep, average from logs) versus wt% bitumen (from cores), see Figure 11.3.6.1 in chapter 11.

The best cutoffs (as compared to core analysis of oil sand) for > 8 wt% bitumen appear to be 30 ohm-m (deep induction) or 40 ohm-m (shallow induction).

General observations comparing log and core analysis

Averaging wt% bitumen values from all wells analyzed, values of 12.2 wt% bitumen (cores) and 12.6 wt% bitumen (logs) are obtained. Sw is 0.20 (logs) to 0.22 (cores). Average porosity is 0.33 (logs).

Generally, core porosities are equivalent to calculated total porosities from logs, thus giving similar effective porosities.

Table AD 1: Values to use for R_t and ∅

Bed Thickness	**Value for Rt**	**Value for ∅** (marked as ∅ on core and log analysis sheet)
0.2 - 1 m	shallow, max.	*Total ∅, ($\varnothing_t$)
1 - 2 m	shallow, avg .	**($\varnothing_t + \varnothing_e$)/2
2 - 4 m	medium, avg.	($\varnothing_t + \varnothing_e$)/2
4 m and upwards	deep, avg.	($\varnothing_t + \varnothing_e$)/2 if $R_t < 50$ ohm-m, use $\varnothing_t$ (shale streaks)

$S_w = ((1 \cdot R_w)/(\varnothing^{1.45} \cdot R_t))^{1/1.6}$

f) **So**

So = 1 - Sw

g) Wo (wt% bitumen)

$$W_o = S_o \cdot \varnothing / (\varnothing + (1 - \varnothing)2.65)$$

Some values of $\varnothing + (1 - \varnothing)2.65$ (density of oil sand) for various porosities are provided:

$\varnothing$	$\varnothing + (1 - \varnothing)2.65$
23	2.2705
24	2.2540
25	2.2375
26	2.2210
27	2.2045
28	2.1880
29	2.1715
30	2.1550
31	2.1385
32	2.1220
33	2.1055
34	2.0890
35	2.0725
36	2.0560
37	2.0395

* $\varnothing e$ is not considered here since the gamma ray signal is influenced by the shaliness on either side of the oil sand streak and does not give the true signal.

** compensates for gamma ray signal affected by boundary shales or thin shale streaks.

Well # 13-27-84-11W4 PCEJ Area 1 - Core and Log Analysis

Table AD 1: PCEJ Area 1 - Core and Log Analysis

Date 4/27/1984

Corr to Core m	Inter-val mKB	Ht m	Core Analysis Wt% Bit.	Core Analysis Grain Wt%	Core Analysis Wt% Bit. Corr.	Core Analysis Poro-sity	Log Analysis Resistivity, ohm-m Deep Ave./Max.	Resistivity, ohm-m Med. Ave./Max.	Resistivity, ohm-m Shal. Ave./Max.	Porosity Neut Ave./Max.	Porosity Dens Ave./Max.	Porosity Total Ave./Max.	Porosity Effect Ave./Min.	Gamma Ray Phi Ave./Min.	Gamma Ray GR Ave./Min.	Gamma Ray RGRD Ave./Min.	Vf Ave./Min.	Sonic Ds/m Ave./Min.	Sw Deep Ave./Max.	Sw Med Ave./Max.	Sw Shal Ave./Max.	So Deep Ave./Max.	So Med Ave./Max.	So Shal Ave./Max.	Wo(Wt% Bit) Deep Ave./Max.	Wo(Wt% Bit) Med Ave./Max.	Wo(Wt% Bit) Shal Ave./Max.
0	268.0-271.6	3.6	10.2	12.1	10.6	0.33	60/85	65/95	140/ 220	34/36	29/31	31/34	23/26	27	57/48	.4333/	24.8/	376/ 366		.19/			.8/			9.9/	
	271.9-275.0	3.1	9.8	11.3	10.2	0.32	68/90	63/80	100/ 160	33/39	28/30	31/34	20/22	26	65/55	0.5600/	35.6/	382/ 376		0.20			0.80			9.3	
	275.0-276.7	1.7	10.1	12.1	10.4	0.34	110/ 120	95/ 110	140/ 195	37/39	31/32	34/35	25/25	30	59/43	.4800/	27.3	386/ 384		.11/			.89/			12.4/	
	276.7-285.4	8.7	11.0	13.1	11.1	0.34	265/ 500	180/ 310	285/ 600	37/40	31/33	34/38	30/32	32	45/29	0.2933	12.1/	382/ 370		.09/			.91/			13.8/	
	286.0-288.6	2.6	9.3	10.9	9.5	0.32	48/70	32/85	158/ 440	37/41	28/31	32/38	25/28	28	55/41	.4267/	22.4/	370/ 358		.21/			.79/			10.1/	
	289.6-292.0	2.4	13.3	16.0	13.7	0.35	250/ 800	175/ 400	420/ 1000	37/38	30/32	33/35	30/32	31	40/33	.2267/	8.1/	378/ 374		.09/			.91/			13.2/	
	292.2-295.0	2.8	13.8	16.6	14.0	0.34	340/ 550	180/ 250	390/ 1010	36/41	32/32	34/36	32/34	33	38/32	.2000/	6.7/	381/ 372		.09/			.91/			14.3/	
	295.0-301.0	6.0	12.6	15.1	12.7	0.35	390/ 520	220/ 270	350/ 500	37/41	31/33	34/37	33/36	33	33/26	.1333/	3.7/	379/ 374		.08/			.92/			14.5/	
	301.0-304.0	3.0	13.3	15.9	13.4	0.34	310/ 430	200/ 280	290/ 550	37/41	32/33	34/37	33/36	33	37/27	.1333/	3.7/	380/ 376		.08/			.92/			14.4/	
	304.0-308.0	4.0	13.8	16.5	13.7	0.34	195/ 280	150/ 200	215/ 460	39/40	33/34	36/37	35/36	33	32/26	.1200/	3.2/	388/ 376		0.09			0.91			13.4/	
	308.0-312.2	4.2	12.5	15.1	12.5	0.35	100/ 150	100/ 150	145/ 230	40/47	33/38	36/42	36/42	36	27/23	.0533/	1.1/	388/ 376		.11/			.89/			13.3/	
	312.2 Total	Dev 42.1	11.8		12.0	0.34								32						0.11			0.89			13.3	

GRmax = 98
GRmin = 23

delta SP = - 66

RMF = 6.390
TMF = 16 C

Rw = 0.70

Core thickness greater than 8 wt% = 41 - 42 m

a=1 m = 1.45 n = 1.6
Deep Resistivity not used (inconsistent signal)

	30 ohm-m Cutoff	40 ohm-m Cutoff
Deep	268.3-285.3, 286.4-312.1 = 42.7 m	268.9-285.1, 286.7- 288.5, 289.3-311.8 = 40.5 m
Med	268.2-285.3, 286.4-288.9, 289.2-312.1 = 42.0 m	268.9-285.1, 287.0-288.3, 289.5-311.8 = 39.8 m
Shal	267.9-285.4, 285.9-288.7, 289.5-312.2 = 43.0 m	268.0-268.7, 268.9-271.7, 271.8-285.4, 286.0-286.7, 287.0-288.5, 289.5-312.1 = 41.9 m

Table AD 2: PCEJ Area 1 - Core and Log Analysis
Date 4/27/1984

Well # 16-26-84-11W4 PCEJ Area 1 - Core and Log Analysis

Corr to Core m	Inter-val mKB	Ht m	Core Analysis				Log Analysis																				
			Wt% Bit.	Grain Wt%	Wt% Bit. Corr.	Poro-sity	Resistivity, ohm-m Deep Ave./Max.	Med. Ave./Max.	Shal. Ave./Max.	Porosity Neut Ave./Max.	Dens Ave./Max.	Total Ave./Max.	Effect Ave./Min.	Phi Ave./Min.	Gamma Ray GR Ave./Min.	RGRD Ave./Min.	Vf Ave./Min.	Sonic Ds/m Ave./Min.	Deep Ave./Max.	Sw Med Ave./Max.	Shal Ave./Max.	Deep Ave./Max.	So Med Ave./Max.	Shal Ave./Max.	Wo(Wt% Bit) Deep Ave./Max.	Med Ave./Max.	Shal Ave./Max.
+2.2	271.6-271.9	0.3	8.9	10.7	9.1	0.33	13/13	15/15	25/28	35/36	29/30	32/33	19/20	32	83/83	.6029/	40.4/	408/404			/.45			/.55			/8.3
	296.0-296.8	0.8	10.9	12.9	11.0	0.32	22/23	26/28	50/75	35/37	26/28	31/33	26/31	31	66/56	.3529/0.2059	16.3/7.0	392/380			/.25			/.75			/10.9
+2.8	302.2-302.5	0.3	16.4	20.0	16.9	0.37	27/30	30/31	60/70	39/40	26/28	33/34	30/32	33	57/54	.2206/0.1765	7.8/5.6	380/374			/.24			/.76			/11.9
+3.2	303.2-305.1	1.9	13.7	16.7	14.0	0.35	37/42	42/49	80/130	39/39	28/29	34/34	34/34	34	45/42	.0441/0.0000	0.9/0.0	390/376			.22/			.78/			12.7/
	305.6-306.0	0.4	8.3	9.6	8.2	0.29	22/22	23/24	32/37	36/36	25/25	31/31	27/28	31	63/60	.3088/0.2647	13.2/10.3	384/380			/.38			/.62			/9.0
	308.2-308.5	0.3	12.3	14.7	12.5	0.34	30/30	32/33	47/50	37/38	26/26	32/32	30/30	32	57/56	.2206/0.2059	7.8/7.0	384/380			/.31			/.69			/10.4
	308.7-308.9	0.2	16.5	20.2	17.4	0.37	28/30	28/30	36/40	35/35	25/26	30/31	26/28	30	63/60	.3088/0.2647	13.2/10.3	376/374			/.38			/.62			/8.6
	309.3-309.5	0.2	9.5	11.1	9.7	0.31	27/30	27/30	27/30	32/33	21/26	27/30	19/22	27	77/75	.5147/0.4853	30.7/27.8	366/360			/.50			/.50			/6.1
	311.5-311.7	0.2	13.0	15.5	13.6	0.34	22/25	22/25	30/31	33/33	21/22	27/28	18/19	27	78/78	.5294/0.5294	32.3 32.3	368/360			/.49			/.51			/6.3
	311.9-312.1	0.2	10.4	12.3	10.5	0.33	31/32	37/40	40/50	37/37	24/24	31/31	29/29	31	57/57	.2206/0.2206	7.8/7.8	300/280			/.32			/.68			/9.9
	312.1 Total	Dev 4.8	12.3		12.6	0.34								32							0.29			0.71			10.8

GRmax = 110
GRmin = 42

delta SP = - 50

RMF = 7.7772
TMF = 17 C

Rw = 1.47

Core thickness greater than 8 wt% = 5 - 6 m

a=1 m = 1.45 n = 1.8

	30 ohm-m Cutoff	40 ohm-m Cutoff
Deep	302.5-304.7, 307.9-308.7 = 3.0 m	303.6-304.2 = 0.6m
Med	292.2-299.4, 302.0-304.8, 307.7-308.7 = 4.0 m	303.0-304.5 = 1.5m
Shal	296.0-296.8, 299.1-300.0, 302.0-305.0, 305.5-306.0, 307.3-308.9 = 6.8 m	296.2-296.8, 299.2-299.9, 302.1-302.6, 303.0-304.9, 307.0-307.6 = 4.3 m

APPENDIX E

Effects of Various Parameters on Creation of Multiple Fractures and Fracture Length

Table E1

Factors Affecting Multiple Fracture Generation

Multiple radial fracture stimulations around a wellbore have been well summarized by GRI (Prediction and Interpretation of Multiple Radial Fracture Stimulations, Final Report August 1985 - March 1987, Gas Research Institute, GRI -87/0199).

Below is a list of **factors** (in order of importance) **which appear to increase multiple fracture growth** and if these factors directly affect cyclic steaming of oilsands wells.

Factors encouraging multiple fracs	Approximate effect	Affect oil sands?
1. Lower fluid viscosity	higher pore pressure	yes+
2. Lower horizontal stress ratio	longer cross-fractures	yes+
3. Higher press frac	higher pore pressure due to oil banking	yes+
4. Lower wellbore confining stress Less depth of burial	shorter fractures	yes+
5. Stiffer/less perm rock	high%quartz + high visc oil	yes-
6. Increase perf height	less length near wellbore	yes-
7. Higher charge perf	higher pore pressure/pulverize better main frac orientation	no
8. Liquid filled wellbore on perf	longer fractures/high press	no
9. Open hole completion	more sites for fracturing	no
10. Less repeat perf firing	shorter fracs	no

Table E2

Factors Affecting Fracture Length Growth

Below is a list of **factors** (in order of importance) **which appear to decrease fracture length** and if these factors directly affect cyclic steaming of oilsands wells.

Factors reducing fracture length	Approximate effect	Affect oil sands?
1. Multiple fracs	doubling reduces length 50%	yes+
2. Increasing permeability	from 0.1- 50 md increase reduce length 1/2, but wider from 0.1 - 1 md increase not much effect	yes+
3. High porosity	2% phi - 20% phi increase decreases length 50%, function of increased perm	yes- but later cycles
4. Softer rock	reduce length 20 - 40%	yes+
5. Lower tensile strength	decreasing strength 10x decreases length 20%	yes- sand production
6. High fracture roughness/tortuosity	no effect for pads increasing two fold decreases length 50% due to leak-off	no
7. Lower Young's Modulus	halving modulus decreases length 5%	no
8. High fracture toughness	only slight length decrease	no

APPENDIX F

Rule of Eight Derivation

Appendix F

THE RULE OF EIGHT

- The Rule of Eight is an equation which estimates expected production for a well, gas of oil, after stimulation, knowing only the production rate and skin prior to stimulation.
- The rule has been applied successfully for the last 10 - 15 years. Credit has to be given to **Dave Pridie** of **Crestar Energy Inc.** (formerly of Chevron Canada) who formulated the rule and has repeatedly proven the equation works.
- Derivation is simple, therefore has not been presented in any technical paper.
- The equation for Darcy radial flow from a reservoir into a well bore is given as:

Before Stimulation

$$Q_1 = \frac{kh\Delta P}{\mu(\ln(r_e/r_w)+s_1)}$$

After Stimulation

$$Q_2 = \frac{kh\Delta P}{\mu(\ln(r_e/r_w)+s_2)}$$

Where

Q_1 = flow rate prior to stimulation
Q_2 = calculated flow rate after stimulation
k = effective permeability to flow
h = net pay
ΔP = Pressure drop between reservoir and the flowing wellbore, assuming bottomhole flowing pressure remains the same just before and after fracturing
μ = reservoir fluid/gas viscosity
r_e = drainage radius
r_w = wellbore radius
s_1 = near-wellbore skin prior to fracturing
s_s = estimated near-wellbore skin after fracturing, usually = -4 (-1 for acid frac)

Units are not required as they cancel, but Q can have any units as long as it is consistent.

Rationing the two equations cancels $\frac{kh\Delta P}{\mu}$, leaving

$$Q_2 = \frac{\ln(r_e/r_w)+s_1}{\ln(r_e r_w)+s_2} \times Q_1$$

Assuming $r_e = 800$ ft and $r_w = 0.328$ ft, $\ln(r_e/r_w) = 7.8$
Assuming $r_e = 1000$ ft and $r_w = 0.328$ ft, $\ln(r_e/r_w) = 8.02$
Assuming $r_e = 1500$ ft and $r_w = 0.328$ ft, $\ln(r_e/r_w) = 8.42$

The value we used here is 8.0 (some people use 7.0 and some use 9.0)

The general equation then becomes:

$$Q_2 = \frac{8+s_1}{8+s_2} \times Q_1 \quad \text{or} \quad Q_{new} = \frac{8+s_{old}}{8+s_{new}} \times Q_{old}$$

As an example, if oil flow rate was 2 m^3/day with skin = + 3 prior to fracturing, the rate after should be:

$$Q_2 = \frac{8+(+3)}{8+(-4)} \times 2m^3/day = 5.5m^3/day$$

APPENDIX G

Mandel-Volek Steam Volume Calculations for PHOP Wells IP4 and IP5

Appendix G

Mandel-Volek Steam-Volume Calculations fornPHOP Wells IP4 andIP5

Below is an example of the use of the material balance Mandl-Volek steam volume calculations and its use in determining whether an observation well , OBS3, showed an increase in temperature due to cyclic steaming of PHOP wells IP4 or IP5. OBS3 is located about 30 m northwest of IP4 and 75 m southwest of IP5 (See Figure 1.1.2 in the Introduction). Analysis showed neither well could heat OBS3 if the injected steam followed the NE-SW fracture trend. It was determined that the increased temperature was due to a recalibration of the temperature tool, so no increase in temperature was seen at OBS3 as of August/83.

Two types of calculations were performed using Mandl-Volek. The first used total heat injected for individual cycles, while the second used cumulative heat injected minus heat lost from produced fluids.

A) An example calculation for IP4, first cycle injection is presented below:

i = steam injection rate (***CWE***) = 173.7 m^3/d = 1093 BBL/d

t = injection time = 29 days = 696 hrs

BHP_{inj} = bottomhole injection pressure = 108.1 atm

$BHTinj$ = bottomhole injection temperature = 317 °C = 603 °F = T_S

T_{res} = reservoir temperature = 13 °C = 56 °F = T_R

H_W = latent heat of water = 624 Btu/lb

L_V = latent heat of steam = 541 Btu/lb

h_V = enthalpy = $H_W + fst \bullet L_V$ = 895 Btu/lb

fst = BH steam quality = 0.5

$$Q_i = \text{heat injection rate} = \frac{350i \cdot h_V}{24} \text{ Btu/hr} = 14.27 \times 10^6 \text{ Btu/hr}$$

$$B = \frac{fst \cdot L_V}{C_W(T_S - T_R)}$$ where **C_W** = specific heat of water = 1 Btu/lb °F

= 0.495

h_t = perforated interval = 8 m = 26.25 ft

$$t_D = \text{dimensionless time} = \frac{4K_{hob} \cdot M_{ob}}{Ms^2} \frac{t}{h_t^2}$$

K_{hob} = thermal conductivity overburden = 1.125 Btu/hr.ft.°F

M_{ob} = heat capacity overburden = 40 Btu/ft^3. °F

M_s = heat capacity of oil sand = 35 Btu/ ft^3. °F

$t_D = 0.148$

$$F_3 = e^{t_D} \cdot erfc\, t_D + 2\sqrt{\frac{T_D}{\pi}} - 1 - \sqrt{\frac{T_D - T_{DC}}{\pi}} \cdot \frac{1 + fst \cdot L_V}{C_W(T_S - T_R)}^{-1}$$

$$+\frac{t_D^{-1} \cdot t_{DC}^{-3}}{3} \cdot e^{t_D} \cdot erfc\sqrt{t_D} - \frac{t_D - t_{DC}}{3\pi t_D} \qquad \text{(AG1)}$$

For F_3 it is easier to use Figure AG1 instead of equation (AG1).

$F_3 = 0.12$

$$V_s = \text{volume steam} = \frac{Q_i M_s h_t^2 F_3}{4K_{hob} M_{ob}(T_S - T_R)} \qquad \text{(AG2)}$$

$= 4.194 \times 10^5$ ft^3 = 11,879 m^3

$$r = \text{radius} = \sqrt{\frac{V_s}{\pi h_t}} = 21.74 \text{ m}$$

A_s = area steam = πr^2 = 1485 m^2

If the area is elliptical, then $A_e = \pi ab$,

For $a = 1/2\ b$

$$b = \sqrt{\frac{2A_s}{\pi}} = 30.75 \text{ m}, \qquad a = 15.4 \text{ m}$$

For a = 1/5 b

$$b = \sqrt{\frac{5A_s}{\pi}} = 48.6 \text{ m}, \qquad a = 9.7 \text{ m}$$

B) For subsequent cycles, production heat loss calculations are required. A simplified version is used where only the heat of produced fluids is considered, not heat losses to the overburden and underburden during production. The example provided here is for IP4 first cycle production:

Total bottomhole heat injected = 14.27×10^6 Btu/hr x 696 hrs = 9.932×10^9 Btu

$F_3/t_D \times 9.932 \times 10^9$ Btu = heat retained at end of injection

Assume the average production temperature = 250 °C = 482 °F

$\Delta T = (482\ °F - 56\ °F) = 426\ °F$

a) Heat loss oil

600 m^3 oil was produced

Heat from oil production = $C_o V_o \rho_o \Delta T$

where C_o = specific heat oil = 0.501 Btu/lb°F

ρ_o = density oil = 62.91 lb/ft^3

= 0.2845×10^9 Btu

b) Heat loss water

1990 m^3 water was produced.

Heat from oil production = $C_w V_w \rho_w \Delta T$

where C_w = specific heat water = 1.0 Btu/lb°F

ρ_w = density water = 62.37 lb/ft^3

= 1.867×10^9 Btu

Total heat loss = 2.15 x 109 Btu = 20% of heat injected

Results

Results for the calculations of steam volumes for 3 cycles of IP4 and IP5 are given in Table AG1 and Figure AG2. Radii of steam fronts are calculated using:

i) radial coordinates (circle)

ii) areal elliptic coordinates

$A = \pi ab$ where a = 1/2 b

iii) areal elliptical coordinates

$A = \pi ab$ where a = 1/5 b

Steam volumes are presented as:

a) individual cycles

b) combined cycles, total heat input minus production fluid heat losses

Discussion of results:

Steam volumes were calculated as in the examples above and also as cumulative injection minus production.

The maximum calculated radii with respect to OBS3 is the ***radial*** mode. For IP5, after 3 cycles (see Table AG2 and Figure AG3), the steam front is at least 76-28 = 28 m away from OBS3. For IP4 (see Table AG1 and Figure AG3), after 3 cycles, the steam front is at least 30-27 = 3 m away from OBS3.

For a 1:5 radii ratio, 5 times greater in the direction of wells IP3 and IP6 as in the direction of well IP5, the steam front is 30-12 = 18 m away from OBS3. After only 1 cycle of injection, using the 1:5 ratio, the steam front is 50-48.5 = 1.5 m away from OBS4 or OBS2. This shows the possibility of a temperature rise at either well OBS2 or OBS4. In the field a temperature rise was noted at OBS4 just after first cycle injection into IP4 at OBS4. OBS2 and OBS3 also showed a slight increase in temperature (few °C), but may have been due to the change in logging tool or logging tool calibration.

Conclusions:

1. OBS3 should not have any temperature response from 3 cycles of injection into IP4, especially at a radii ratio of 1:5.

2. IP5 injection is not likely to affect OBS3 unless secondary fracturing becomes significant.

3. A elliptical areal ratio of 1:5 is sufficient to cause a temperature rise at OBS2 or OBS4 after only 1 cycle of steam injection into IP4 (5,000 m^3 slug).

Table AG1

IP4 Steam Volume Calculations - Summary of Results

Computation for total heat					
Event	**Steam Volume, VS (m3)**	**$r_{cylinder}$ (m)**	**$r_{ellipse}$ a = 1/2b (m)**	**$r_{ellipse}$ a=1/5b (m)**	**Remarks**
End of 1st cycle injection	11,879	21.7	a=15.3 b=30.7	a=9.7 b=48.5	Cycles
End of 2nd cycle injection	7,759	17.6	a=12.4 b=24.9	a=7.9 b=39.4	Treated
End of 3rd cycle injection					Independently
End of 1st cycle injection	11,879	21.7	a=15.3 b=30.7	a=9.7 b=48.5	Cycles Combined minus Production Losses
End of 2nd cycle injection	11,931	21.8	a=15.4 b=30.8	a=9.7 b=48.7	
End of 3rd cycle injection	18,739	27.3	a=19.3 b=38.6	a=12.2 b=61.0	

Table AG2

IP5 Steam Volume Calculations - Summary of Results

Computation for total heat					
Event	**Steam Volume, VS (m3)**	**$r_{cylinder}$ (m)**	**$r_{ellipse}$ a = 1/2b (m)**	**$r_{ellipse}$ a=1/5b (m)**	**Remarks**
End of 1st cycle injection	14,413	24	a=17.0 b=33.9	a=10.7 b=53.7	Cycles
End of 2nd cycle injection	9,279	19.2	a=13.6 b=27.2	a=8.6 b=42.9	Treated
End of 3rd cycle injection	9,316	19.3	a=13.6 b=27.3	a=8.6 b=43.2	Independently
End of 1st cycle injection	14,413	24	a=17.0 b=33.9	a=10.7 b=53.7	Cycles Combined minus Production Losses
End of 2nd cycle injection	17,245	26.2	a=18.5 b=37.1	a=11.7 b=58.6	
End of 3rd cycle injection	19,180	27.6	a=19.5 b=39.0	a=12.3 b=61.7	

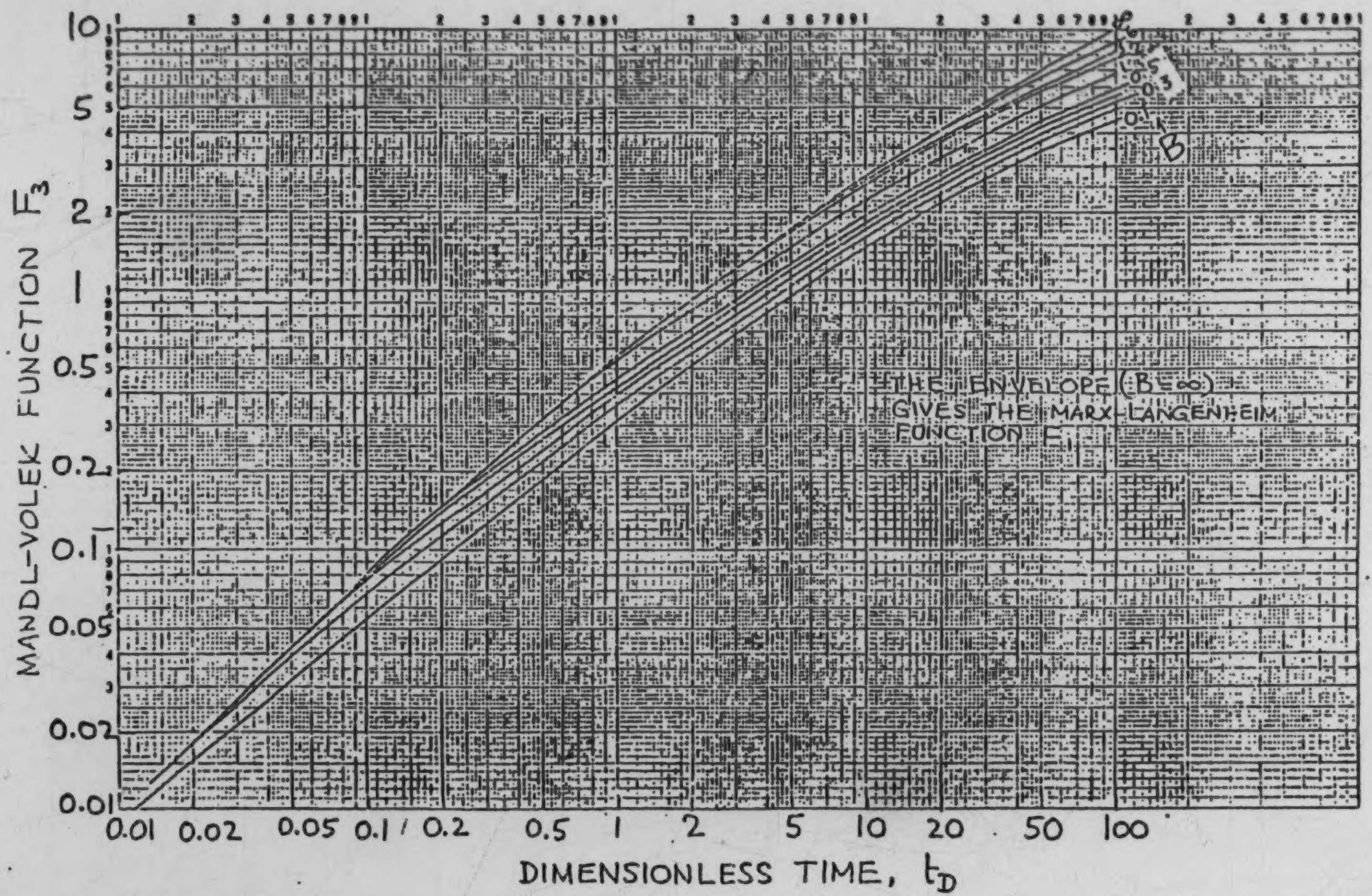

Figure AG1: Mandl-Volek Function F_3 as a function of t_D

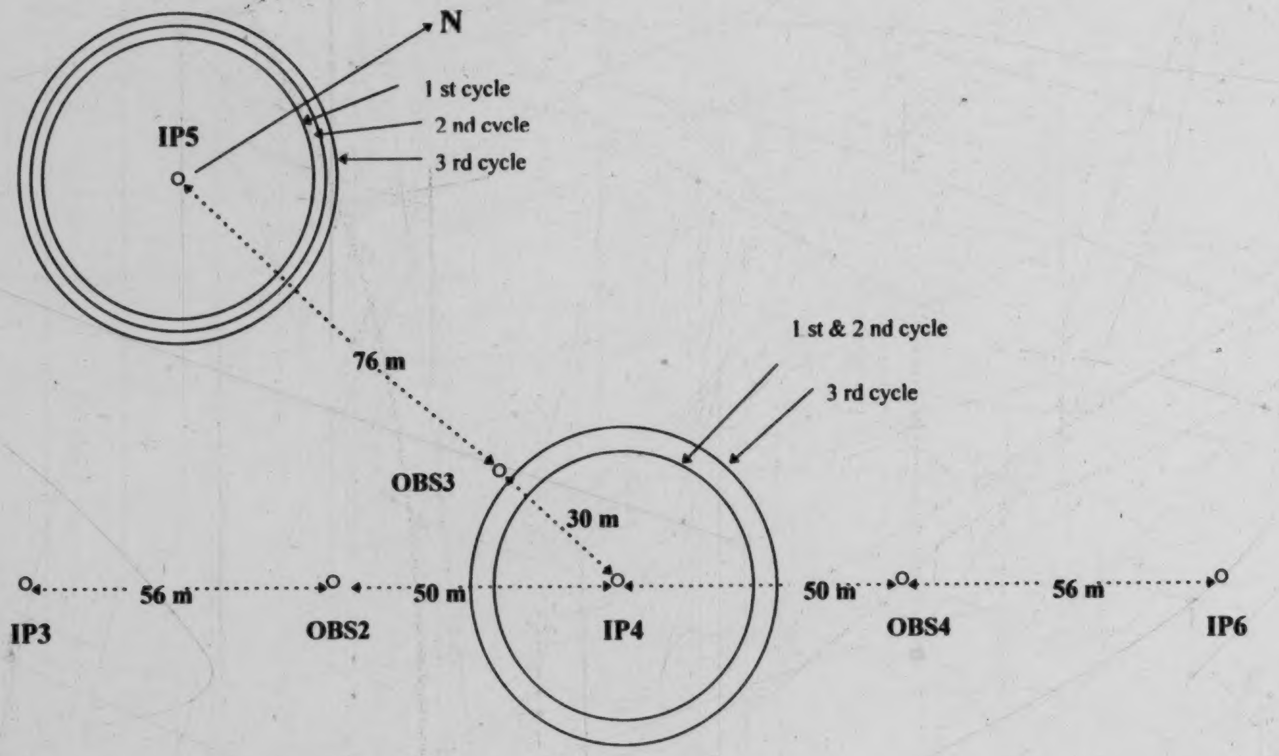
N
IP5
1 st cycle
2 nd cycle
3 rd cycle
76 m
1 st & 2 nd cycle
3 rd cycle
OBS3
30 m
IP3
56 m
OBS2
50 m
IP4
50 m
OBS4
56 m
IP6

Figure AG2: Mandl-Volek steam front, radial mode, 3 cycles

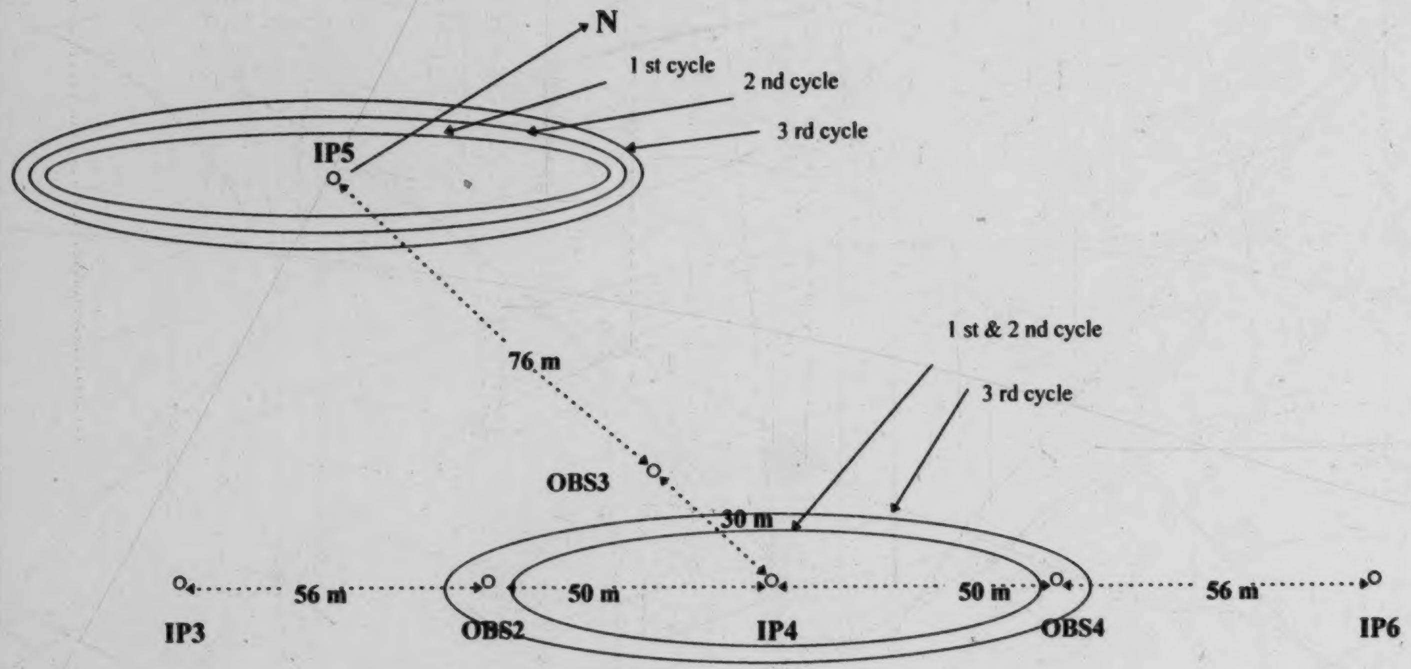
N
1 st cycle
2 nd cycle
3 rd cycle
IP5
76 m
1 st & 2 nd cycle
3 rd cycle
OBS3
30 m
56 m
50 m
50 m
56 m
IP3
OBS2
IP4
OBS4
IP6

Figure AG3: Mandl-Volek steam front, elipse, a = 1/5b, 3 cycles

APPENDIX H

Letter of Permission from Petro-Canada to use PHOP and PCEJ Data

Petro-Canada Resources

P.O. Box 2844
Calgary, Alberta T2P 3E3
Telephone (403) 296-8000
Telex 03-821524

Ressources Petro-Canada

C.P. 2844
Calgary (Alberta) T2P 3E3
Téléphone (403) 296-8000
Télex 03-821524

PETRO-CANADA

June 23, 1992

File PCJ 0525.06

Petro-Canada hereby gives permission to Ted Leshchyshyn to use PCEJ Phase II and Phase III data solely, and Primrose (PHOP) data for educational purposes, either for published papers or as part of a PhD thesis, provided that the following conditions are met:

1. All data to be published must be approved by Petro-Canada prior to publishing and a copy supplied to Petro-Canada thereafter.
2. Petro-Canada will be acknowledged for supplying the data.
3. The publication of PCEJ data must first be approved by all PCEJ participants.
4. The publication of Primrose data must first be approved by all Primrose participants.

Except as specifically set out above, all such data shall be guarded and kept confidential.

Petro-Canada per:

Acknowledged and agreed
June 23, 1992:

G. W. Sinclair
Manager,
Oil Sands Development

Ted Leshchyshyn
T. Leshchyshyn

Witness

c:\word\OSE\AGREE-TL